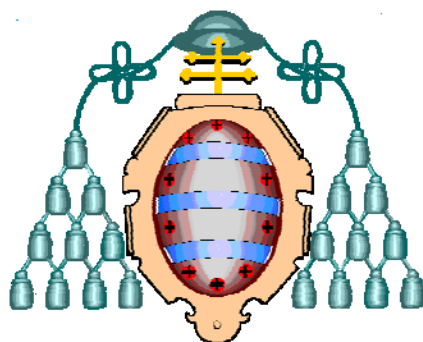


UNIVERSIDAD DE OVIEDO



Departamento de Química Física y Analítica

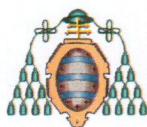
Programa de Doctorado Análisis químico, bioquímico y estructural
avanzado (Mención de Calidad)

**DESARROLLO DE METODOLOGÍAS ANALÍTICAS
PARA EL ESTUDIO DEL METABOLISMO DEL AZUFRE
UTILIZANDO ISÓTOPOS ESTABLES ENRIQUECIDOS**

TESIS DOCTORAL

Justo Giner Martínez-Sierra

Oviedo, 2012



RESUMEN DEL CONTENIDO DE TESIS DOCTORAL

1.- Título de la Tesis	
Español: Desarrollo de metodologías analíticas para el estudio del metabolismo del azufre utilizando isótopos estables enriquecidos	Inglés: Development of analytical methodologies for the study of sulfur metabolism using enriched stable isotopes
2.- Autor	
Nombre: Justo Giner Martínez-Sierra	
Programa de Doctorado: Análisis Químico, Bioquímico y Estructural Avanzados (Mención de Calidad)	
Órgano responsable: Departamento de Química Física y Analítica	

RESUMEN (en español)

La alteración intencionada de la composición isotópica de un elemento dado en un organismo vivo permite obtener información metabólica del elemento. La composición isotópica del azufre varía en la naturaleza por lo que para seguir la pista del azufre en un ser vivo utilizando un trazador marcado isotópicamente, la cantidad de trazador metabólico utilizada debe ser lo suficientemente elevada como para alterar la composición isotópica del azufre por encima de los límites de variabilidad natural. Los equipos ICP-MS multicolectores permiten realizar medidas de relaciones isotópicas de azufre con excelentes precisiones instrumentales, necesarias para la determinación de variaciones isotópicas naturales.

Tradicionalmente, los estudios de metabolismo con trazadores de azufre se han llevado a cabo utilizando el isótopo radiactivo de azufre-35. En los últimos años, la creciente popularidad del ICP-MS ha acelerado el uso de isótopos estables para estudios de metabolismo. En este sentido, la baja abundancia isotópica que presentan los isótopos estables azufre-33 y azufre-34 en el azufre natural, los hace muy adecuados para su uso como trazadores. Sin embargo, hasta el comienzo de la presente Tesis Doctoral, el número de estudios de metabolismo utilizando isótopos estables de azufre que empleasen ICP-MS era muy escaso. Además, no se había descrito ninguna aplicación con trazadores múltiples de azufre.

La determinación de azufre por ICP-MS puede ser usada como una herramienta genérica para la detección y cuantificación de péptidos y proteínas. Ningún estudio de metabolismo de proteínas en mamíferos utilizando isótopos estables enriquecidos de azufre había sido descrito con anterioridad. Estos estudios requieren la síntesis previa de cisteína y/o metionina marcada con el isótopo enriquecido dado que los mamíferos no son capaces de sintetizar estos aminoácidos y necesitan obtenerlos a través de la alimentación. Particularmente, se podría administrar levadura marcada con isótopos estables de azufre como alimento por vía oral para realizar estudios de metabolismo del azufre evitando los riesgos derivados de la exposición a la radiación.

En este contexto, la presente Tesis Doctoral se centró en el desarrollo de metodologías analíticas para el estudio del metabolismo del azufre utilizando isótopos estables enriquecidos. Este objetivo general se abordó a través de las investigaciones que se resumen a continuación:

1. **Estudios de variabilidad natural de la composición isotópica de azufre mediante ICP-MS multicolector.** En primer lugar, se desarrolló un procedimiento directo para la medida de la variabilidad natural de la composición isotópica de azufre en muestras de cerveza mediante ICP-MS multicolector. Asimismo, se desarrolló una metodología analítica que permite realizar la medida de variaciones naturales en la composición isotópica de azufre a lo largo de un pelo mediante un sistema de ablación láser acoplado a un ICP-MS multicolector.



2. **Preparación y caracterización de levadura marcada con azufre-34.** Se preparó levadura marcada isotópicamente con azufre-34 en un medio de cultivo exento de azufre de abundancia natural. La levadura marcada se caracterizó tanto en composición isotópica como en concentración total de azufre mediante ICP-MS multicollector. A continuación, se evaluaron diferentes estrategias analíticas para la cuantificación de biomoléculas que contienen azufre mediante HPLC-ICP-MS. Se desarrolló un procedimiento basado en la deconvolución de perfiles isotópicos y el análisis por dilución isotópica inespecífica para la determinación simultánea de concentración y composición isotópica de azufre en especies individuales y se aplicó a la caracterización de la levadura marcada con azufre-34.
3. **Estudios *in vitro* e *in vivo* del metabolismo del azufre utilizando isótopos estables enriquecidos.** Se simuló *in vitro* una digestión gastrointestinal de la levadura marcada con azufre-34 y el hidrolizado se caracterizó mediante SDS-PAGE y HPLC-ICP-MS. Finalmente, se realizaron estudios con trazadores estables de azufre en animales de laboratorio utilizando levadura marcada con azufre-34. Se puede concluir que a lo largo de la presente Tesis Doctoral se han desarrollado metodologías analíticas novedosas para el estudio del metabolismo del azufre utilizando isótopos estables enriquecidos. En particular, la combinación del enriquecimiento isotópico en azufre-34 (utilizando azufre-34 como trazador metabólico) y la cuantificación absoluta de biomoléculas (utilizando azufre-33 como trazador de cuantificación) mediante HPLC-ICP-MS se podría establecer como una estrategia alternativa en estudios metabólicos de compuestos que contengan azufre en su estructura.

RESUMEN (en Inglés)

The intentional alteration of the isotopic composition of a certain element in a living organism allows to obtain metabolic information of the element. The stable isotope composition of sulfur varies in nature and hence to follow the metabolic pathway of sulfur by using an isotopically enriched tracer, the amount of tracer to be used should be enough to change the isotopic composition of sulfur above the natural variability limits. Multicollector ICP-MS instruments can be applied to perform the highly precise and accurate sulfur isotope ratio measurements needed for the determination of natural differences.

Fundamental studies on the metabolism of sulfur have been traditionally carried out using radioactive sulfur-35 as tracer. The increasing popularity of ICP-MS has boosted the use of stable isotopes for metabolism studies in recent years. In this regard, both sulfur-33 and sulfur-34 could be used for tracer studies due to their low isotope abundance in natural sulfur. However, at the beginning of the present Ph.D. Thesis the number of metabolism studies reported using stable sulfur isotopes and ICP-MS detection were very scarce. Moreover, the application of multiple tracers for sulfur metabolism studies had not been described before.

The determination of sulfur by ICP-MS can be considered as an universal tool for the detection and quantification of peptides and proteins. Tracer experiments on protein synthesis and breakdown using sulfur enriched stable isotopes in mammals had not been described before. These studies require the previous synthesis of methionine and/or cysteine labelled with the enriched isotope as mammals cannot synthesise those amino acids and need to obtain them from their food. In particular, (stable)sulfur-labelled yeast could be administered orally to the test subjects in order to perform sulfur metabolism studies without use of radioactivity.

Therefore, the general aim of this Ph.D. Thesis was the development of analytical methodologies for the study of sulfur metabolism using enriched stable isotopes. The research developed in the present Ph.D. Thesis can be summarized through the following stages:

1. **Studies of natural variability of sulfur isotope composition by multicollector ICP-MS.** Firstly, a direct procedure for the measurement of sulfur isotope variability in beer samples by multicollector ICP-MS has been developed. In a similar vein, a method for the measurement of longitudinal variations of sulfur isotope ratios in single hair strands



using a laser ablation system coupled to a multicollector ICP-MS has been developed.

2. **Preparation and characterisation of sulfur-34 labelled yeast.** Yeast labelled with sulfur-34 has been prepared by yeast growth on a ^{34}S -enriched, specially prepared, culture medium in the absence of natural abundance sulfur. The final product has been characterised both in isotope composition and total sulfur concentration by multicollector ICP-MS. Afterwards, different analytical strategies for the quantification of sulfur-containing biomolecules by HPLC-ICP-MS have been evaluated. A procedure based on post-column isotope pattern deconvolution was developed for the simultaneous determination of concentration and isotope composition of sulfur in single compounds rather than in the total element and it has been applied to the characterisation of ^{34}S -labelled yeast.
3. **In vitro and in vivo studies of sulfur metabolism using enriched stable isotopes.** An *in vitro* gastrointestinal digestion of the ^{34}S -labelled yeast has been simulated and the corresponding hydrolysate has been characterised by SDS-PAGE and HPLC-ICP-MS techniques. Finally, sulfur stable tracer experiments in laboratory animals using ^{34}S -labelled yeast have been performed. It can be concluded that novel analytical methodologies for the study of sulfur metabolism using enriched stable isotopes have been developed throughout the present Ph.D. Thesis. In particular, the combination of ^{34}S -isotopic enrichment (using sulfur-34 as metabolic tracer) and absolute quantification (using sulfur-33 as quantification tracer) after HPLC-ICP-MS could be an alternative strategy for protein turnover or other sulfur-related metabolism studies.

SR. DIRECTOR DE DEPARTAMENTO DE QUÍMICA FÍSICA Y ANALÍTICA
SR. PRESIDENTE DE LA COMISIÓN ACADÉMICA DEL PROGRAMA DE DOCTORADO EN ANÁLISIS QUÍMICO,
BIOQUÍMICO Y ESTRUCTURAL AVANZADOS (Mención de Calidad)



INFORME PARA LA PRESENTACIÓN DE TESIS DOCTORAL COMO COMPENDIO DE PUBLICACIONES

Año Académico: 2012/2013

1.- Datos personales del autor de la Tesis		
Apellidos: GINER MARTÍNEZ-SIERRA	Nombre: JUSTO	
DNI/Pasaporte/NIE:	Teléfono:	Correo electrónico:

2.- Datos académicos	
Programa de Doctorado cursado: ANÁLISIS QUÍMICO, BIOQUÍMICO Y ESTRUCTURAL AVANZADOS (Mención de Calidad)	
Órgano responsable: DEPARTAMENTO DE QUÍMICA FÍSICA Y ANALÍTICA	
Departamento/Instituto en el que presenta la Tesis Doctoral: QUÍMICA FÍSICA Y ANALÍTICA	
Título definitivo de la Tesis	
Español: DESARROLLO DE METODOLOGÍAS ANALÍTICAS PARA EL ESTUDIO DEL METABOLISMO DEL AZUFRE UTILIZANDO ISÓTOPOS ESTABLES ENRIQUECIDOS	Inglés: DEVELOPMENT OF ANALYTICAL METHODOLOGIES FOR THE STUDY OF SULFUR METABOLISM USING ENRICHED STABLE ISOTOPES
Rama de conocimiento: CIENCIAS	

3.- Director/es de la Tesis	
D: JOSÉ IGNACIO GARCÍA ALONSO	DNI/Pasaporte/NIE:
Departamento/Instituto: QUÍMICA FÍSICA Y ANALÍTICA	
D: JUAN MANUEL MARCHANTE GAYÓN	DNI/Pasaporte/NIE:
Departamento/Instituto/Institución: QUÍMICA FÍSICA Y ANALÍTICA	

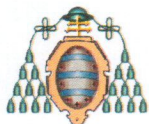
4.- Informe
La calidad de esta Tesis Doctoral queda reflejada tanto en el número como en el impacto de las publicaciones en revistas internacionales derivadas de los principales resultados de la misma, encontrándose todas ellas entre las diez mejores de su especialidad clasificadas de acuerdo a su índice de impacto. Consecuentemente, los directores abajo firmantes informan favorablemente sobre esta Tesis Doctoral.

Oviedo, 15 de octubre de 2012,

Director/es de la Tesis Doctoral

Fdo.: José Ignacio García Alonso

Fdo.: Juan Manuel Marchante Gayón

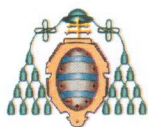


ACEPTACIÓN COAUTORES PRESENTACIÓN TRABAJOS FORMANDO PARTE DE TESIS DOCTORAL COMO COMPENDIO DE PUBLICACIONES

1.- Datos personales del coautor		
Apellidos: GARCÍA ALONSO	Nombre: JOSÉ IGNACIO	
DNI/Pasaporte/NIE	Teléfono	Correo electrónico

2.- Publicaciones que formarán parte de la tesis y de las que es coautor
<ol style="list-style-type: none"> 1. Development of a direct procedure for the measurement of sulfur isotope variability in beers by MC-ICP-MS. <i>Journal of Agricultural and Food Chemistry</i>, 2010, 58, 4043-4050. 2. Measurement of longitudinal sulfur isotopic variations by laser ablation MC-ICP-MS in single human hair strands. <i>Analytical and Bioanalytical Chemistry</i>, 2009, 394, 225-233. 3. Biosynthesis of ³⁴S-labelled yeast and its characterisation by multicollector-ICP-MS. <i>Journal of Analytical Atomic Spectrometry</i>, 2007, 22, 1105-1112. 4. Evaluation of different analytical strategies for the quantification of sulfur-containing biomolecules by HPLC-ICP-MS: application to the characterisation of ³⁴S-labelled yeast. <i>Journal of Analytical Atomic Spectrometry</i>, 2010, 25, 989-997. 5. Sulphur tracer experiments in laboratory animals using ³⁴S-labelled yeast. <i>Analytical and Bioanalytical Chemistry</i>, DOI 10.1007/s00216-012-6420-x.

ACEPTACIÓN:
<p>Acepto que las publicaciones anteriores formen parte de la Tesis Doctoral titulada "Desarrollo de metodologías analíticas para el estudio del metabolismo del azufre utilizando isótopos estables enriquecidos"</p> <p>Y elaborada por D. Justo Giner Martínez-Sierra</p> <p style="text-align: center;">Oviedo, 15 de octubre de 2012</p> <p style="text-align: center;">Fdo.: José Ignacio García Alonso</p>

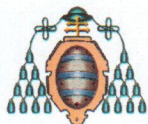


ACEPTACIÓN COAUTORES PRESENTACIÓN TRABAJOS FORMANDO PARTE DE TESIS DOCTORAL COMO COMPENDIO DE PUBLICACIONES

1.- Datos personales del coautor		
Apellidos: MARCHANTE GAYÓN	Nombre: JUAN MANUEL	
DNI/Pasaporte/NIE	Teléfono	Correo electrónico

2.- Publicaciones que formarán parte de la tesis y de las que es coautor
<ol style="list-style-type: none"> 1. Development of a direct procedure for the measurement of sulfur isotope variability in beers by MC-ICP-MS. <i>Journal of Agricultural and Food Chemistry</i>, 2010, 58, 4043-4050. 2. Measurement of longitudinal sulfur isotopic variations by laser ablation MC-ICP-MS in single human hair strands. <i>Analytical and Bioanalytical Chemistry</i>, 2009, 394, 225-233. 3. Biosynthesis of ³⁴S-labelled yeast and its characterisation by multicollector-ICP-MS. <i>Journal of Analytical Atomic Spectrometry</i>, 2007, 22, 1105-1112. 4. Evaluation of different analytical strategies for the quantification of sulfur-containing biomolecules by HPLC-ICP-MS: application to the characterisation of ³⁴S-labelled yeast. <i>Journal of Analytical Atomic Spectrometry</i>, 2010, 25, 989-997. 5. Sulphur tracer experiments in laboratory animals using ³⁴S-labelled yeast. <i>Analytical and Bioanalytical Chemistry</i>, DOI 10.1007/s00216-012-6420-x.

ACEPTACIÓN:
<p>Acepto que las publicaciones anteriores formen parte de la Tesis Doctoral titulada "Desarrollo de metodologías analíticas para el estudio del metabolismo del azufre utilizando isótopos estables enriquecidos"</p> <p>Y elaborada por D. Justo Giner Martínez-Sierra</p> <p style="text-align: center;">Oviedo, 15 de octubre de 2012</p> <p style="text-align: center;">Fdo.: Juan Manuel Marchante Gayón</p>

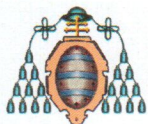


ACEPTACIÓN COAUTORES PRESENTACIÓN TRABAJOS FORMANDO PARTE DE TESIS DOCTORAL COMO COMPENDIO DE PUBLICACIONES

1.- Datos personales del coautor		
Apellidos: SANTAMARÍA FERNÁNDEZ	Nombre: REBECA	
DNI/Pasaporte/NIE	Teléfono	Correo electrónico

2.- Publicaciones que formarán parte de la tesis y de las que es coautor
<ol style="list-style-type: none">1. Development of a direct procedure for the measurement of sulfur isotope variability in beers by MC-ICP-MS. <i>Journal of Agricultural and Food Chemistry</i>, 2010, 58, 4043-4050.2. Measurement of longitudinal sulfur isotopic variations by laser ablation MC-ICP-MS in single human hair strands. <i>Analytical and Bioanalytical Chemistry</i>, 2009, 394, 225-233.3. Evaluation of different analytical strategies for the quantification of sulfur-containing biomolecules by HPLC-ICP-MS: application to the characterisation of ³⁴S-labelled yeast. <i>Journal of Analytical Atomic Spectrometry</i>, 2010, 25, 989-997.

ACEPTACIÓN:
<p>Acepto que las publicaciones anteriores formen parte de la Tesis Doctoral titulada "Desarrollo de metodologías analíticas para el estudio del metabolismo del azufre utilizando isótopos estables enriquecidos"</p> <p>Y elaborada por D. Justo Giner Martínez-Sierra</p> <p>Oviedo, 15 de noviembre de 2012</p> <p>Fdo.: Rebeca Santamaría Fernández</p>



ACEPTACIÓN COAUTORES PRESENTACIÓN TRABAJOS FORMANDO PARTE DE TESIS DOCTORAL COMO COMPENDIO DE PUBLICACIONES

1.- Datos personales del coautor		
Apellidos: HEARN	Nombre: RUTH	
DNI/Pasaporte/NIE	Teléfono	Correo electrónico

2.- Publicaciones que formarán parte de la tesis y de las que es coautor
<ol style="list-style-type: none">1. Development of a direct procedure for the measurement of sulfur isotope variability in beers by MC-ICP-MS. <i>Journal of Agricultural and Food Chemistry</i>, 2010, 58, 4043-4050.2. Measurement of longitudinal sulfur isotopic variations by laser ablation MC-ICP-MS in single human hair strands. <i>Analytical and Bioanalytical Chemistry</i>, 2009, 394, 225-233.

ACEPTACIÓN:
<p>Acepto que las publicaciones anteriores formen parte de la Tesis Doctoral titulada "Desarrollo de metodologías analíticas para el estudio del metabolismo del azufre utilizando isótopos estables enriquecidos"</p> <p>Y elaborada por D. Justo Giner Martínez-Sierra</p> <p>Oviedo, 15 de noviembre de 2012</p> <p>Fdo.: Ruth Hearn</p>

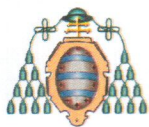


ACEPTACIÓN COAUTORES PRESENTACIÓN TRABAJOS FORMANDO PARTE DE TESIS DOCTORAL COMO COMPENDIO DE PUBLICACIONES

1.- Datos personales del coautor		
Apellidos: MORENO SANZ	Nombre: FERNANDO	
DNI/Pasaporte/NIE	Teléfono	Correo electrónico

2.- Publicaciones que formarán parte de la tesis y de las que es coautor
<ol style="list-style-type: none">1. Biosynthesis of ^{34}S-labelled yeast and its characterisation by multicollector-ICP-MS. <i>Journal of Analytical Atomic Spectrometry</i>, 2007, 22, 1105-1112.2. Evaluation of different analytical strategies for the quantification of sulfur-containing biomolecules by HPLC-ICP-MS: application to the characterisation of ^{34}S-labelled yeast. <i>Journal of Analytical Atomic Spectrometry</i>, 2010, 25, 989-997.3. Sulphur tracer experiments in laboratory animals using ^{34}S-labelled yeast. <i>Analytical and Bioanalytical Chemistry</i>, DOI 10.1007/s00216-012-6420-x.

ACEPTACIÓN:
<p>Acepto que las publicaciones anteriores formen parte de la Tesis Doctoral titulada "Desarrollo de metodologías analíticas para el estudio del metabolismo del azufre utilizando isótopos estables enriquecidos"</p> <p>Y elaborada por D. Justo Giner Martínez-Sierra</p> <p>Oviedo, 15 de octubre de 2012</p> <p>Fdo.: Fernando Moreno Sanz</p>

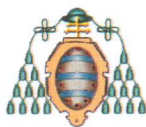


ACEPTACIÓN COAUTORES PRESENTACIÓN TRABAJOS FORMANDO PARTE DE TESIS DOCTORAL COMO COMPENDIO DE PUBLICACIONES

1.- Datos personales del coautor		
Apellidos: HERRERO ESPÍLEZ	Nombre: PILAR	
DNI/Pasaporte/NIE	Teléfono	Correo electrónico

2.- Publicaciones que formarán parte de la tesis y de las que es coautor
<ol style="list-style-type: none">1. Biosynthesis of ^{34}S-labelled yeast and its characterisation by multicollector-ICP-MS. <i>Journal of Analytical Atomic Spectrometry</i>, 2007, 22, 1105-1112.2. Evaluation of different analytical strategies for the quantification of sulfur-containing biomolecules by HPLC-ICP-MS: application to the characterisation of ^{34}S-labelled yeast. <i>Journal of Analytical Atomic Spectrometry</i>, 2010, 25, 989-997.3. Sulphur tracer experiments in laboratory animals using ^{34}S-labelled yeast. <i>Analytical and Bioanalytical Chemistry</i>, DOI 10.1007/s00216-012-6420-x.

ACEPTACIÓN:
<p>Acepto que las publicaciones anteriores formen parte de la Tesis Doctoral titulada "Desarrollo de metodologías analíticas para el estudio del metabolismo del azufre utilizando isótopos estables enriquecidos"</p> <p>Y elaborada por D. Justo Giner Martínez-Sierra</p> <p>Oviedo, 15 de octubre de 2012</p> <p>Fdo.: Pilar Herrero Espílez</p>



ACEPTACIÓN COAUTORES PRESENTACIÓN TRABAJOS FORMANDO PARTE DE TESIS DOCTORAL COMO COMPENDIO DE PUBLICACIONES

1.- Datos personales del coautor		
Apellidos: RODRÍGUEZ FERNÁNDEZ	Nombre: JULIO	
DNI/Pasaporte/NIE	Teléfono	Correo electrónico

2.- Publicaciones que formarán parte de la tesis y de las que es coautor
1. Sulphur tracer experiments in laboratory animals using ³⁴ S-labelled yeast. <i>Analytical and Bioanalytical Chemistry</i> , DOI 10.1007/s00216-012-6420-x.

ACEPTACIÓN:
Accepto que las publicaciones anteriores formen parte de la Tesis Doctoral titulada " Desarrollo de metodologías analíticas para el estudio del metabolismo del azufre utilizando isótopos estables enriquecidos " Y elaborada por D. Justo Giner Martínez-Sierra Oviedo, 15 de octubre de 2012 Fdo.: Julio Rodríguez Fernández

AGRADECIMIENTOS

Tras más de siete años de investigación y convivencia, desearía expresar mi más sincero agradecimiento a todas las personas, instituciones y organismos que de una u otra forma han hecho posible el haber llegado con éxito hasta aquí. Mi doctorado ha sido un camino largo, bonito y enriquecedor, difícil y precario... de sentimientos encontrados. Por ello, antes de comenzar quisiera agradecer a todos aquellos que durante este tiempo han compartido conmigo trabajo y diversión, éxitos y fracasos, penas y alegrías, dentro y fuera del laboratorio. De igual forma pido disculpas a quienes de modo involuntario pueda haberme dejado en el tintero.

En primer lugar, quisiera expresar mi agradecimiento al Dr. José Ignacio García Alonso, Catedrático del Departamento de Química Física y Analítica de la Universidad de Oviedo y co-director de esta Tesis Doctoral. *Gracias Nacho por recibirme con los brazos abiertos y brindarme la oportunidad de entrar a formar parte de tu Grupo de Investigación de Isótopos Estables Enriquecidos, del que siempre me sentiré orgulloso de haber sido miembro desde sus inicios. Tu brillante impulso y criterio científico nos han llevado de la mano hoy hasta aquí, ofreciéndome en todo momento tu apoyo y orientación.*

Al Dr. Juan Manuel Marchante Gayón, Profesor Titular del Departamento de Química Física y Analítica de la Universidad de Oviedo y co-director de esta Tesis Doctoral. *Gracias Juanma por la confianza depositada en mí desde los comienzos de este trabajo, y muy especialmente por la dedicación y las críticas constructivas durante la escritura de esta Memoria. Tu asesoramiento ha sido determinante para presentar esta Tesis Doctoral "como una novela, con un principio y un fin y no como historias paralelas".*

Al Dr. Fernando Moreno Sanz y a la Dra. Pilar Herrero Espílez del Departamento de Bioquímica y Biología Molecular de la Universidad de Oviedo, por abrirme las puertas de su laboratorio e integrarme en su Grupo de Investigación de Biología Molecular y Biotecnología de Levaduras. *Muchas gracias a los dos por vuestro apoyo y dedicación desde el primer día.*

A la Dra. Ruth Hearn y muy especialmente a la Dra. Rebeca Santamaría Fernández del Grupo de Investigación de Espectrometría de Masas Inorgánica del Laboratorio Nacional de Metrología Química del Reino Unido (LGC Ltd.), donde realicé dos estancias predoctorales en los años 2007 y 2008. *Gracias Rebe por toda tu ayuda más allá de los trabajos publicados. Para ti, mi admiración y mi más sincero agradecimiento y amistad.*

AGRADECIMIENTOS

Al Dr. Rubén Rellán Álvarez del Departamento de Nutrición Vegetal del Instituto de Ciencias Agrarias del CSIC de Zaragoza y al Dr. Kristoffer Lunøe del Departamento de Farmacología y Química Analítica de la Universidad de Ciencias Farmacéuticas de Copenhague (Dinamarca) con quienes trabajé estrechamente durante sus respectivas estancias predoctorales en Oviedo y de quienes además de haber aprendido muchas cosas a su lado, he ganado una buena amistad a pesar de la distancia.

A D^a. Teresa Fernández y D. Agustín Brea responsables de la Unidad de Bioterio de la Universidad de Oviedo, por su colaboración en todas las actividades que implicaron el uso de animales de experimentación.

Quisiera mostrar mi agradecimiento a la Comisión Interministerial de Ciencia y Tecnología (CICYT) por su apoyo económico a través de dos proyectos de investigación (BQU2003-03438 y CTQ2006-05722) entre los años 2006 y 2007 en los que estuve contratado como Personal Científico - Técnico, y a la Fundación para el Fomento en Asturias de la Investigación Científica Aplicada y la Tecnología (FICYT) por la concesión de una beca predoctoral bajo el programa "Severo Ochoa" (BP07-059) que me permitió continuar durante cuatro años más con mi actividad investigadora. Asimismo, parte del trabajo presentado en esta Tesis Doctoral ha ido galardonado con el 1^{er} Premio de Espectrometría de Masas otorgado por la Sociedad Española de Espectrometría de Masas (SEEM) en 2009 y con el XXII Premio San Alberto Magno para Trabajos de Investigación y Desarrollo Tecnológico otorgado por el Ilustre Colegio de Químicos de Asturias y León y la Asociación de Químicos del Principado de Asturias en 2010. Para ellos, por el fuerte incentivo y apoyo que supuso la concesión de ambos premios, mi más sincero agradecimiento. *Gracias Nacho y Juanma por haberme donado generosamente vuestra parte económica de los premios.*

Después de todo este tiempo trabajando en la Facultad de Química, quisiera agradecer a todos los integrantes del Departamento de Química Física y Analítica, que en su medida y posibilidades me han hecho más fácil la realización de esta Tesis Doctoral. A los profesores Dr. Alfredo Sanz Medel, Dr. José Manuel Costa Fernández, Dr. Jorge Ruiz Encinar, Dra. Rosario Pereiro, Dra. Charo Fernández, Dra. Marisa Fernández, Dra. Elisa Blanco, Dra. María Montes, Dr. Jörg Bettmer, Dr. Jorge Pisonero, Dr. Pablo Rodríguez y Dra. Mariella Moldován; por su buen talante y cercanía.

En especial quiero mencionar a mis compañeros del Grupo de Investigación y de la sala de becarios del Departamento, los actuales y los que ya no están, por los buenos momentos que han hecho más sencillo el día a día y porque siempre han estado dispuestos a ofrecer una mano. Los buenos consejos de la Dra. Cristina Sariego, Dra. Natalia Fidalgo, Dr. Oscar Palacios, Dr. Israel Sánchez, Dr. Antonio Martín y del Dr. Giuseppe Centineo. Las horas de trabajo y risas compartidas en el despacho con la Dra. Maite Fernández, Dra. Cristina Sánchez, Dr. Silvia García Ruiz,

AGRADECIMIENTOS

Dra. Adriana González Gago, Dr. Alejandro Sarmiento, Ioana y Tobias Konz (*gute Freunde!*), Alberto Mudarra, Isabel Caramés, Laura Trapiella (*¡gracias por las correcciones!*), Dr. Daniel Kutscher, Dra. Auristela Solà, Dra. Ana Coto, Lourdes Somoano (*esas gominolas...*), Mario Fernández (*que cogerá el relevo del “científico de calidad”*), Emma... Los congresos, confidencias y cafés con Sergio Cueto, Gonzalo Huelga, Antonio Montoro, José Ángel y Ana González-Antuña. *Mucha suerte, paciencia y ánimo con vuestras Tesis Doctorales que seguro defenderéis en breve.*

A mis compañeros de generación de cursos de doctorado, el Dr. Hector González-Iglesias, Azucena, Carmen y Alberto.

A mis compañeros Bioquímicos el Dr. Alberto Riera, Dra. Alejandra Fernández-Cid, Dra. Paula Fernández y muy especialmente al Dr. Rafael Peláez, por haber compartido conmigo su experiencia y sus conocimientos desinteresadamente. *Muchas gracias Rafa, además de un gran compañero de trabajo, he ganado un amigo en tu persona.*

A mi gran amigo con mayúsculas el Dr. Daniel Garcia Sar. *Por tantas y tantas vivencias juntos que no se pueden describir en pocas líneas. Los mejores momentos de esta Tesis Doctoral son nuestros. Sin duda, en mí tienes a un hermano. Gracias por todo Dani.*

A todo aquel a quien le sea útil esta memoria de Tesis Doctoral para seguir profundizando en el conocimiento científico y que sin saberlo, me habrá compensado las incontables, y *digo bien*, incontables horas de esfuerzo y dedicación.

Finalmente, pero ocupando el primer lugar en mi corazón, he reservado el agradecimiento más especial a mi familia.

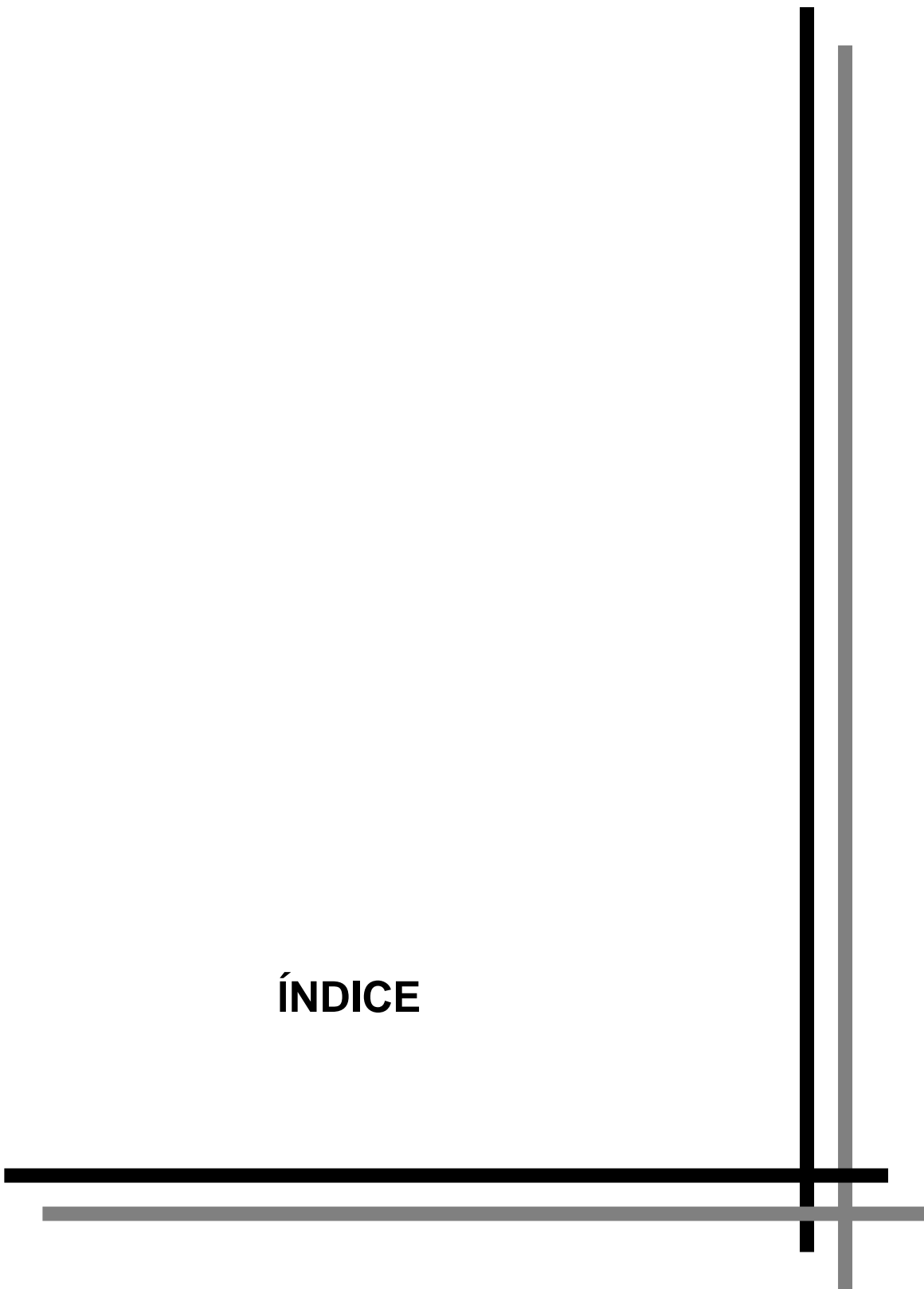
A Paula, *si bien siempre he intentado mantenerte al margen de mi vida profesional, sin duda, no podría agradecer suficientemente con palabras todo lo que te debo. Siempre has estado muy cerca para animarme y ayudarme sin la menor vacilación, haciendo sacrificios y mostrándome tu ilusión para que acabara mi Tesis Doctoral. Por tu amor y apoyo incondicionales en los momentos dulces y en los que no lo han sido tanto... a lo largo de todos estos años. Por ser el motor y lo que da sentido a mi vida. Esta Tesis Doctoral es lo que es, en gran medida, gracias a ti.*

A Jose y Marieli, *para vosotros también es el mayor de mis agradecimientos y mi cariño. Por toda vuestra ayuda y colaboración, sin la cual habría sido mucho más difícil llegar hasta aquí. Por vuestra dedicación y cariño en el cuidado y educación de mis hijos, vuestros nietos. Porque con vosotros aprendo casi a diario clases magistrales que no se encuentran en los libros. Por supuesto, en mí tenéis a un hijo.*

A mi hija Claudia y a mi hijo Sergio, *porque sin saberlo me habéis convertido en la persona más feliz del mundo.*

A todos vosotros, muchísimas gracias.

ÍNDICE



A. INTRODUCCIÓN	11
A.1. IMPORTANCIA BIOLÓGICA DEL AZUFRE	13
A.1.1. Introducción	13
A.1.2. Aminoácidos proteínogénicos que contienen azufre	15
A.1.3. Síntesis química de metionina.....	16
A.1.4. Biosíntesis de metionina y cisteína en <i>Saccharomyces cerevisiae</i>	17
A.2. EMPLEO DE ISÓTOPOS ESTABLES EN QUÍMICA ANALÍTICA....	19
A.2.1. Isótopos de azufre	19
A.2.2. Abundancias isotópicas naturales	19
A.2.2.1. Introducción	19
A.2.2.2. La notación delta	20
A.2.2.3. Técnicas analíticas más utilizadas para la medida de relaciones isotópicas	24
A.2.3. Obtención y principales aplicaciones de los isótopos estables enriquecidos.....	25
A.2.4. Isótopos estables en estudios metabólicos	26
A.2.5. Análisis por dilución isotópica (IDA)	27
A.2.5.1. Introducción	27
A.2.5.2. Determinación total elemental mediante IDA.....	29
A.2.5.2.1. Cantidad de trazador añadida a la muestra	33
A.2.5.2.2. Exactitud de la medida de relaciones isotópicas.....	35
A.2.5.2.2.1 Interferencias espectrales.....	36
A.2.5.2.2.2 Discriminación de masas.....	37
A.2.5.2.2.3 Tiempo muerto del detector.....	38
A.2.5.3. Especiación elemental mediante IDA	39
A.2.5.3.1. La dilución isotópica específica.....	39
A.2.5.3.2. La dilución isotópica inespecífica o post-columna.....	40
A.2.5.4. Deconvolución de perfiles isotópicos (IPD).....	42
A.2.5.4.1. Introducción.....	42
A.2.5.4.2. Fundamento de la metodología de cálculo.....	43
A.2.5.4.3. Resolución matemática	44

A.3. ESPECTROMETRÍA DE MASAS CON FUENTE DE PLASMA DE ACOPLAMIENTO INDUCTIVO (ICP-MS)	46
A.3.1. Introducción	46
A.3.2. Monitorización de azufre por ICP-MS	49
A.3.2.1. ICP-MS de tipo cuadrupolo.....	49
A.3.2.2. ICP-MS con celda de colisión/reacción	50
A.3.2.3. ICP-MS de doble enfoque (DF)	51
A.3.2.3.1. <i>DF-ICP-MS con detección simple</i>	52
A.3.2.3.2. <i>DF-ICP-MS multicolector</i>	54
A.3.3. El ICP-MS en metodologías híbridas	59
A.3.3.1. Determinación de azufre por HPLC-ICP-MS	60
A.3.3.2. Determinación de azufre por LA-ICP-MS	62
A.3.4. Revisión bibliográfica sobre la medida de azufre por ICP-MS y sus aplicaciones	63
B. OBJETIVOS	97
C. EXPERIMENTAL	103
C.1. INSTRUMENTACIÓN	105
C.1.1. Espectrómetros de masas con fuente de plasma de acoplamiento inductivo (ICP-MS)	105
C.1.1.1. ICP-MS de cuadrupolo	105
C.1.1.2. ICP-MS de cuadrupolo equipado con celda de colisión/reacción	107
C.1.1.3. ICP-MS de doble enfoque con detección simple	107
C.1.1.4. ICP-MS de doble enfoque multicolector	108
C.1.2. Instrumentación utilizada para las separaciones por cromatografía líquida de alta resolución (HPLC)	110
C.1.3. Sistema de ablación láser	111
C.1.4. Otra instrumentación	112
C.2. MATERIALES Y REACTIVOS	113
C.3. PROCEDIMIENTOS EXPERIMENTALES	115
C.3.1. Corrección del efecto de discriminación de masas	115
C.3.2. Cálculo del tiempo muerto del detector	116
C.3.3. HPLC-ICP-MS con dilución isotópica inespecífica	117

C.3.4.	Estudios con muestras de cerveza	118
C.3.5.	Estudios con muestras de pelo	119
C.3.6.	Caracterización de los trazadores isotópicos mediante ICP-MS multicolector	120
C.3.7.	Preparación de levadura marcada con azufre-34.....	122
C.3.8.	Digestión de las muestras sólidas	131
C.3.9.	Deconvolución de perfiles isotópicos (IPD)	132
C.3.10.	Estudios con ratas Wistar	135
D.	RESULTADOS.....	139
D.1.	ESTUDIOS DE VARIABILIDAD NATURAL DE LA COMPOSICIÓN ISOTÓPICA DE AZUFRE MEDIANTE ICP-MS MULTICOLECTOR	141
D.1.1.	Desarrollo de un procedimiento directo para la medida de la variabilidad isotópica de azufre en muestras de cerveza mediante ICP-MS multicolector	141
D.1.1.1.	Artículo científico I: J. Agr. Food Chem., 2010, 58, 4043-4050 141	
D.1.2.	Medida de variaciones isotópicas de azufre en cabello humano mediante ablación láser acoplada a ICP-MS multicolector	153
D.1.2.1.	Artículo científico II: Anal. Bioanal. Chem., 2009, 394, 225-233 153	
D.2.	PREPARACIÓN Y CARACTERIZACIÓN DE LEVADURA MARCADA CON AZUFRE-34	165
D.2.1.	Preparación de levadura marcada con azufre-34 y su caracterización mediante ICP-MS multicolector	165
D.2.1.1.	Artículo científico III: J. Anal. At. Spectrom., 2007, 22, 1105-1112 165	
D.2.2.	Evaluación de diferentes estrategias analíticas para la cuantificación de biomoléculas que contienen azufre mediante HPLC-ICP-MS: aplicación a la caracterización de levadura marcada con azufre-34	177
D.2.2.1.	Artículo científico IV: J. Anal. At. Spectrom., 2010, 25, 989-997 177	
D.2.2.2.	Información suplementaria del artículo científico IV.....	187

D.3. ESTUDIOS <i>IN VITRO</i> E <i>IN VIVO</i> DEL METABOLISMO DEL AZUFRE UTILIZANDO ISÓTOPOS ESTABLES ENRIQUECIDOS.....	193
D.3.1. Estudios con trazadores estables de azufre en animales de laboratorio utilizando levadura marcada con azufre-34	193
D.3.1.1. Artículo científico V. Anal. Bioanal. Chem., DOI 10.1007/s00216-012-6420-x.....	193
D.3.1.2. Información suplementaria del artículo científico V.....	206
E. DISCUSIÓN INTEGRADORA	217
F. CONCLUSIONES / CONCLUSIONS	241
G. SUGERENCIAS PARA TRABAJOS FUTUROS.....	251
H. PUBLICACIONES RELACIONADAS CON LA TESIS DOCTORAL	257
H.1. ESTUDIOS DEL METABOLISMO DEL HIERRO UTILIZANDO ISÓTOPOS ESTABLES ENRIQUECIDOS	259
H.1.1. Artículo científico VI: Plant Cell Physiol., 2010, 58, 91-102 .	259
H.1.2. Información suplementaria del artículo científico VI.....	273
H.2. ESTUDIOS DEL METABOLISMO DEL SELENIO UTILIZANDO ISÓTOPOS ESTABLES ENRIQUECIDOS	289
H.2.1. Artículo científico VII: Anal. Bioanal. Chem., 2012, 402, 2749-2763	289
I. INFORME CON EL FACTOR DE IMPACTO DE LAS PUBLICACIONES PRESENTADAS	307
J. REFERENCIAS BIBLIOGRÁFICAS	315

ÍNDICE DE TABLAS

Tabla 1. Algunos compuestos de interés biológico que contienen azufre.....	14
Tabla 2. Principales interferencias espectrales en la determinación de azufre por ICP-MS.....	36
Tabla 3. Concentración, composición isotópica y peso atómico de las disoluciones enriquecidas isotópicamente en azufre-33 y azufre-34 utilizadas como trazadores.....	121
Tabla 4. Composición del medio de cultivo para el crecimiento de la levadura (por litro).....	125
Tabla 5. Composición isotópica (%) del azufre de abundancia isotópica natural (Snat) y de los trazadores de azufre utilizados (S33 y S34).	225

Figura 1. Metabolismo del aminoácido azufrado metionina en mamíferos.	16
Figura 2. Biosíntesis de aminoácidos de azufre en <i>Saccharomyces cerevisiae</i>	18
Figura 3. Composición isotópica de algunos materiales que contienen azufre seleccionados de la referencia [44].	23
Figura 4. Ilustración del fundamento de la dilución isotópica para un elemento que contiene dos isótopos (a y b).	29
Figura 5. Curvas de magnificación del error para los trazadores isotópicos enriquecidos en azufre-34 y azufre-33.	35
Figura 6. Crecimiento exponencial del número de publicaciones científicas utilizando ICP-MS en los últimos 25 años. Fuente Web of Science®.	46
Figura 7. Esquema de una fuente de plasma de acoplamiento inductivo (ICP).	47
Figura 8. Esquema de un analizador de masas de tipo cuadrupolo.	50
Figura 9. Esquema del equipo ICP-MS de tipo cuadrupolo equipado con celda de colisión/reacción modelo X Series 2.	51
Figura 10. Esquema del equipo DF-ICP-MS modelo Element 2.	52
Figura 11. Espectro de masas de los isótopos de azufre ³² S, ³³ S y ³⁴ S obtenidos en el Element 2, donde se puede apreciar la resolución de las principales interferencias poliatómicas.	54
Figura 12. Esquema del equipo ICP-MS multicolector modelo Neptune.	55
Figura 13. Pseudo-resolución de interferencias poliatómicas en el ICP-MS multicolector.	57
Figura 14. Espectro de masas obtenido en el ICP-MS multicolector para los isótopos de azufre ³² S, ³³ S y ³⁴ S.	58
Figura 15. Modelos de ICP-MS empleados en la presente Tesis Doctoral.	105
Figura 16. Esquema del equipo ICP-MS de tipo cuadrupolo modelo HP 4500.	106
Figura 17. Configuraciones de copas de Faraday empleadas a lo largo de la Tesis Doctoral para la medida de relaciones isotópicas de azufre en el ICP-MS multicolector.	109
Figura 18. Espectro de masas obtenido para la medida simultánea de relaciones isotópicas de azufre y silicio en el equipo ICP-MS multicolector.	110
Figura 19. Relación isotópica normalizada ³⁴ S/ ³² S a diferentes concentraciones de azufre para el cálculo del tiempo muerto del detector en el equipo DF-ICP-MS.	117
Figura 20. Esquema del acoplamiento HPLC-ICP-MS utilizado en el análisis por dilución isotópica inespecífica.	118
Figura 21. Detalle del soporte utilizado para fijar las muestras de pelo (A) e imagen de una hebra de pelo tras la ablación (B).	119
Figura 22. Crecimiento típico de la levadura en medio de cultivo YNB tras la adición de cantidades crecientes de azufre (como sulfato) (0 [■], 30 μM [■], 300 μM [■] y 10mM [■]). ..	123
Figura 23. Resumen del procedimiento de preparación del medio de cultivo para el crecimiento de levaduras “exento” de azufre de abundancia natural.	126
Figura 24. Efecto de la concentración adicionada de sulfato al nuevo medio de cultivo, sobre el crecimiento de la levadura (0 [■], 10 μM [■], 50 μM [■] y 100 μM [■]).	127

Figura 25. Recursos utilizados para el crecimiento de las células de levadura en medio sólido.	128
Figura 26. Cámara termostatazada y agitador circular utilizado para el crecimiento de los medios líquidos.	129
Figura 27. Seguimiento del crecimiento celular y evolución del medio de cultivo enriquecido con azufre-34 mediante medidas de turbidez a 600 nm.	130
Figura 28. Etapas del proceso de preparación de levadura marcada con azufre-34.	131
Figura 29. Esquema general del análisis por ICP-MS utilizando isótopos estables enriquecidos de azufre y Deconvolución de Perfiles Isotópicos (IPD).	133
Figura 30. Esquema representativo del procedimiento experimental <i>in vivo</i> realizado con ratas Wistar.	136
Figura 31. Países de elaboración (A) de las muestras de cerveza (B) analizadas mediante ICP-MS multicolector.	221
Figura 32. Variaciones isotópicas longitudinales de azufre en cabello humano determinadas mediante LA-MC-ICP-MS.	224
Figura 33. Resumen del procedimiento de preparación de levadura marcada con azufre-34.	226
Figura 34. Separación cromatográfica en modo isocrático de los compuestos de azufre sulfato, cisteína, glutatión y metionina detectados por ICP-MS multicolector.	228
Figura 35. Análisis de un extracto proteico de levadura marcada isotópicamente con azufre-34 mediante HPLC-ICP-MS.	231
Figura 36. Estudios <i>in vitro</i> de digestión gastrointestinal de la levadura marcada con azufre-34 mediante SDS-PAGE y HPLC-ICP-MS.	233
Figura 37. Valores de la relación X_{S34}/X_{Snat} en los tejidos de las ratas Wistar alimentadas con levadura marcada con azufre-34 obtenidos mediante DF-ICP-MS con detección simple.	235
Figura 38. Valores de la relación X_{S34}/X_{Snat} en los productos de desecho (heces y orina) de las ratas Wistar alimentadas con levadura marcada con azufre-34 obtenidos mediante DF-ICP-MS con detección simple.	236
Figura 39. Análisis de orina de una rata Wistar alimentada con levadura marcada con azufre-34 mediante HPLC-ICP-MS (fase reversa).	238
Figura 40. Diagrama de barras de la relación X_{S34}/X_{Snat} detectada en las muestras de orina de ratas Wistar sanas alimentadas con levadura marcada con azufre-34.	239

BIPM: oficina internacional de pesos y medidas (*bureau international des poids et mesures*).

CA 125: antígeno carbohidrato125 (*carbohydrate antigen 125*).

CAWIA: comisión de pesos atómicos y abundancias isotópicas (*commission on atomic weights and isotopic abundances*).

CDT: troilita del cañón del diablo (*canyon diablo troilite*).

CE: electroforesis capilar (*capillary electrophoresis*).

CIC: calibración independiente del compuesto (*compound independent calibration*).

DAD: detector de diodos en línea (*diode array detector*).

DC: corriente continua (*direct current*).

DF: doble enfoque (*double focusing*).

d.i.: diámetro interno.

FDA: agencia de alimentos y medicamentos (*food and drug administration*).

GC: cromatografía de gases (*gas chromatography*).

GRAS: reconocido como seguro para la salud (*generally regarded as safe*).

GS: fuente gaseosa (*gas source*).

HFBA: ácido heptafluorobutírico (*heptafluorobutyric acid*).

HMW: alto peso molecular (*high molecular weight*).

HPLC: cromatografía líquida de alta resolución (*high performance liquid chromatography*).

i.e.: es decir (*id est*).

IAEA: agencia internacional de energía atómica (*international atomic energy agency*).

ICP-MS: espectrometría de masas con fuente de plasma de acoplamiento inductivo (*inductively coupled plasma mass spectrometry*).

IDA: análisis por dilución isotópica (*isotope dilution analysis*).

IPD: deconvolución de perfiles isotópicos (*isotope pattern deconvolution*).

IRMS: espectrometría de masas de relaciones isotópicas (*isotope ratio mass spectrometry*).

JCR: informe sobre el factor de impacto y número de citas de las revistas (*journal citation reports*).

LA: ablación por láser (*laser ablation*).

LMW: bajo peso molecular (*low molecular weight*).

m/z: relación masa-carga (*mass-to-charge ratio*).

MC: multicollector (*multicollector*).

MS: espectrometría de masas (*mass spectrometry*).

NIST: instituto nacional de estándares y tecnología de los Estados Unidos (*national institute of standards and technology*).

p.e.: por ejemplo.

ppb: partes por billón (*parts per billion*).

ppm: partes por millón (*parts per million*).

ppq: partes por cuatrillón (*parts per quadrillion*).

ppt: partes por trillón (*parts per trillion*).

PSA: antígeno prostático específico (*prostate-specific antigen*).

RF: radiofrecuencia (*radio frequency*).

RM: material de referencia (*reference material*).

RDA: cantidad diaria recomendada (*recommended dietary allowance*).

RSD: desviación estándar relativa (*relative standard deviation*).

SDS-PAGE: electroforesis en gel de poliacrilamida con dodecilsulfato sódico (*sodium dodecyl sulfate polyacrylamide gel electrophoresis*).

SEC: cromatografía de exclusión por tamaños (*size exclusion chromatography*).

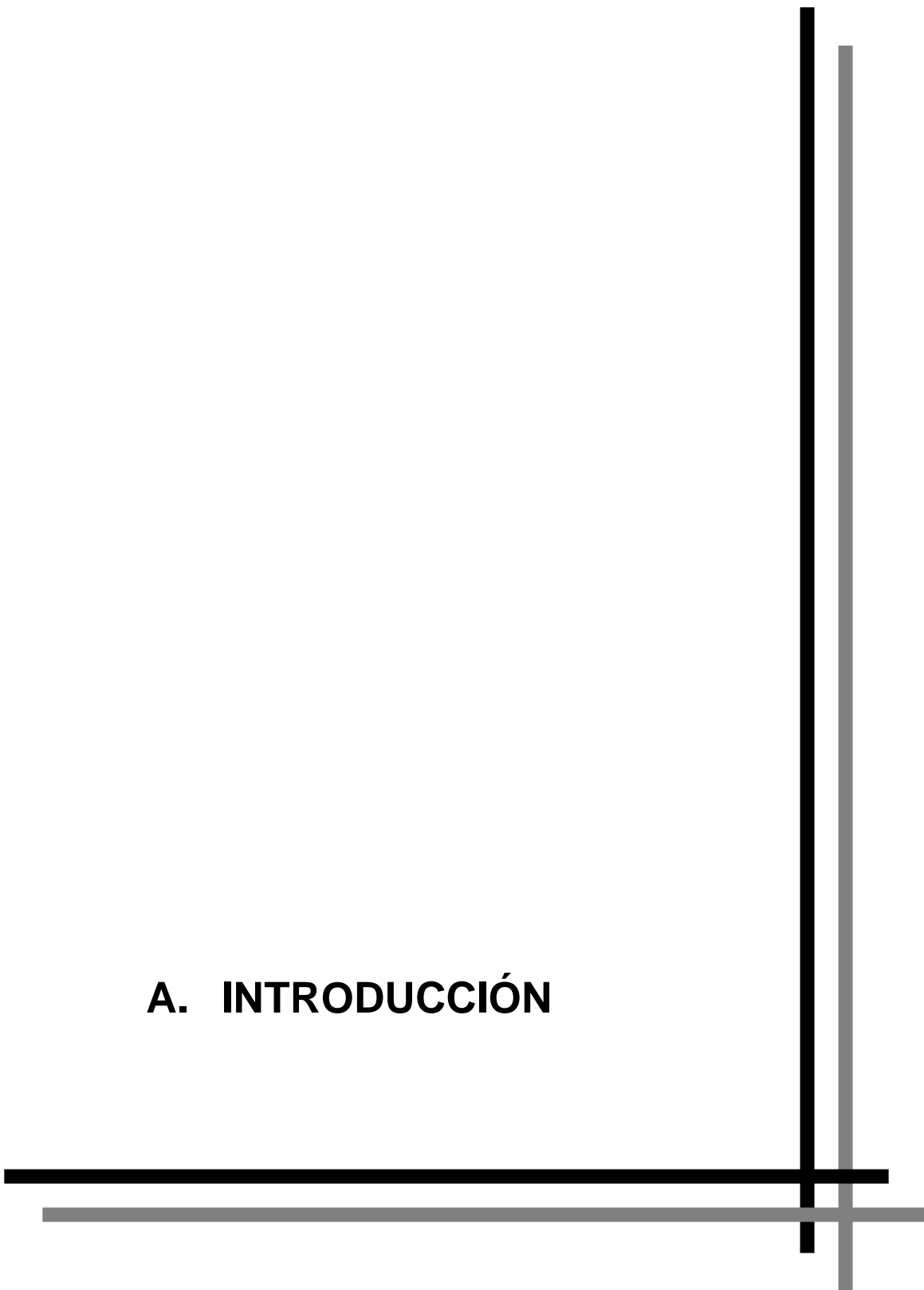
SEM: multiplicador de electrones secundarios (*secondary electron multiplier*).

TIMS: espectrometría de masas con fuente de ionización térmica (*thermal ionisation mass spectrometry*).

V-CDT: valor de la troilita del cañón del diablo establecido en Viena (*Vienna-canyon diablo troilite*).

YNB: base de nitrógeno para levaduras (*yeast nitrogen base*).

A. INTRODUCCIÓN



A.1. IMPORTANCIA BIOLÓGICA DEL AZUFRE

A.1.1. Introducción

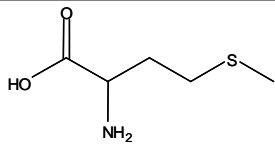
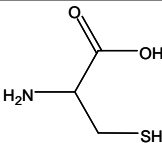
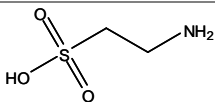
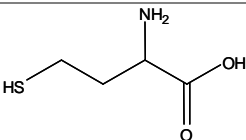
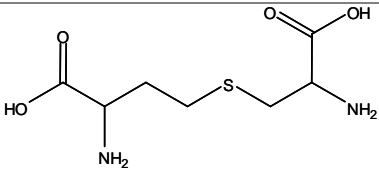
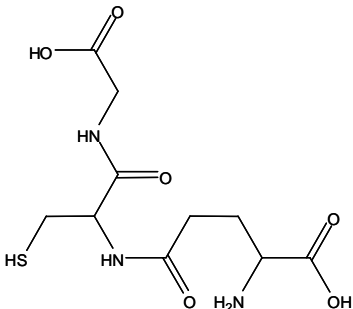
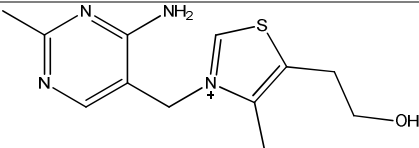
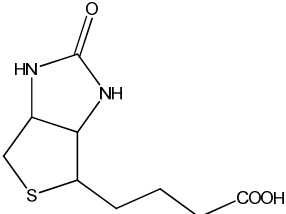
El azufre (S) es un elemento traza esencial para todos los organismos vivos y está presente en multitud de compuestos biológicamente importantes, como aminoácidos, péptidos y proteínas, vitaminas, etc. [1,2]. En la Tabla 1 se muestran algunos compuestos de interés biológico que contienen azufre en su estructura.

Los aminoácidos azufrados cisteína, metionina, taurina y homocisteína tienen numerosas funciones biológicas [3-7], entre las que destacan ser precursores de moléculas esenciales y su rol como mediadores en el metabolismo [8] y en diversas funciones celulares [9]. La cisteína es muy importante en el mantenimiento de la estructura terciaria y cuaternaria de la mayoría de las proteínas mediante la formación de puentes disulfuro. Al oxidarse da lugar a la cistina (dímero de la cisteína) y también actúa como antioxidante [10] al ser precursor del glutatión (cisteína, ácido glutámico y glicina). El tripéptido glutatión (GSH), es un péptido muy abundante a nivel intracelular con numerosas funciones biológicas, entre las que destacan su papel antioxidante ayudando a proteger las células de especies reactivas de oxígeno como los radicales libres y los peróxidos [11], desempeñar una tarea clave en la detoxificación de xenobióticos [12] y actuar como almacén de azufre [13]. De hecho, cualquier exceso en la dieta de cisteína y metionina no es almacenado como tales especies en el organismo, sino que se excreta en forma de sulfato a través de la orina o se almacena en forma de GSH [14]. La presencia de azufre en péptidos y proteínas se discutirá más adelante.

El azufre está presente en la vitamina B1 (tiamina) que juega un papel importante en el metabolismo de carbohidratos, principalmente para producir energía; además de participar en el metabolismo de grasas, proteínas y ácidos nucleicos (ADN, ARN). Es esencial para el crecimiento y desarrollo normal de la mayor parte de los vertebrados y ayuda a mantener el funcionamiento propio del corazón, sistema nervioso y digestivo. Asimismo, el azufre forma parte de la vitamina B7 (biotina) la cual actúa como un cofactor de las enzimas que intervienen en la catálisis de reacciones metabólicas esenciales para sintetizar ácidos grasos, en la gluconeogénesis y en el metabolismo de la leucina. La coenzima A contiene también azufre. Esta coenzima desempeña un papel clave en la biosíntesis y la oxidación de ácidos grasos, así como en la descarboxilación oxidativa del ácido pirúvico, paso previo al ciclo de Krebs.

A. INTRODUCCIÓN

Tabla 1. Algunos compuestos de interés biológico que contienen azufre.

Aminoácidos proteínogénicos	Metionina	
	Cisteína	
Aminoácidos no proteínogénicos	Taurina	
	Homocisteína	
	Cistatión	
Péptidos	Glutatión (GSH)	
Vitaminas	Tiamina (B1)	
	Biotina (B7)	

A.1. IMPORTANCIA BIOLÓGICA DEL AZUFRE

A.1.2. Aminoácidos proteínogénicos que contienen azufre

El azufre se encuentra presente en los aminoácidos proteínogénicos cisteína y metionina, es decir, en dos aminoácidos del exclusivo grupo de veinte que pueden participar en la formación de proteínas. A pesar de que ninguno de los dos se encuentra en gran abundancia en las proteínas, si aparecen en la gran mayoría de ellas. Juntos exhiben una abundancia próxima al 3-4% en proteomas eucarióticos, lo que significa que estadísticamente todos los péptidos/proteínas con una longitud de al menos 30 residuos de aminoácidos contienen azufre. Esto supone que aproximadamente el 93% de las proteínas conocidas contienen azufre en su secuencia [15]. Así pues, la determinación de azufre podría ser usada como herramienta genérica para la detección y cuantificación de la mayoría de péptidos y proteínas.

La metionina es un aminoácido esencial, ya que los animales no son capaces de sintetizar este aminoácido azufrado y necesitan incorporarlo a través de la alimentación (p.e. carnes, pescados, lácteos, huevos, frutos secos, etc.). Las principales rutas metabólicas de la metionina en mamíferos se recogen en la Figura 1. La cisteína se puede producir a través del metabolismo de la metionina (nunca al revés) [16]. Al igual que en el caso de la metionina, el organismo puede obtener la cisteína mediante la degradación de proteínas que contengan este aminoácido. Por lo tanto, si se pretende realizar estudios de metabolismo de péptidos y proteínas en mamíferos utilizando isótopos enriquecidos de azufre, se debe utilizar metionina, cisteína o péptidos o proteínas que las contengan marcadas con el isótopo de interés.

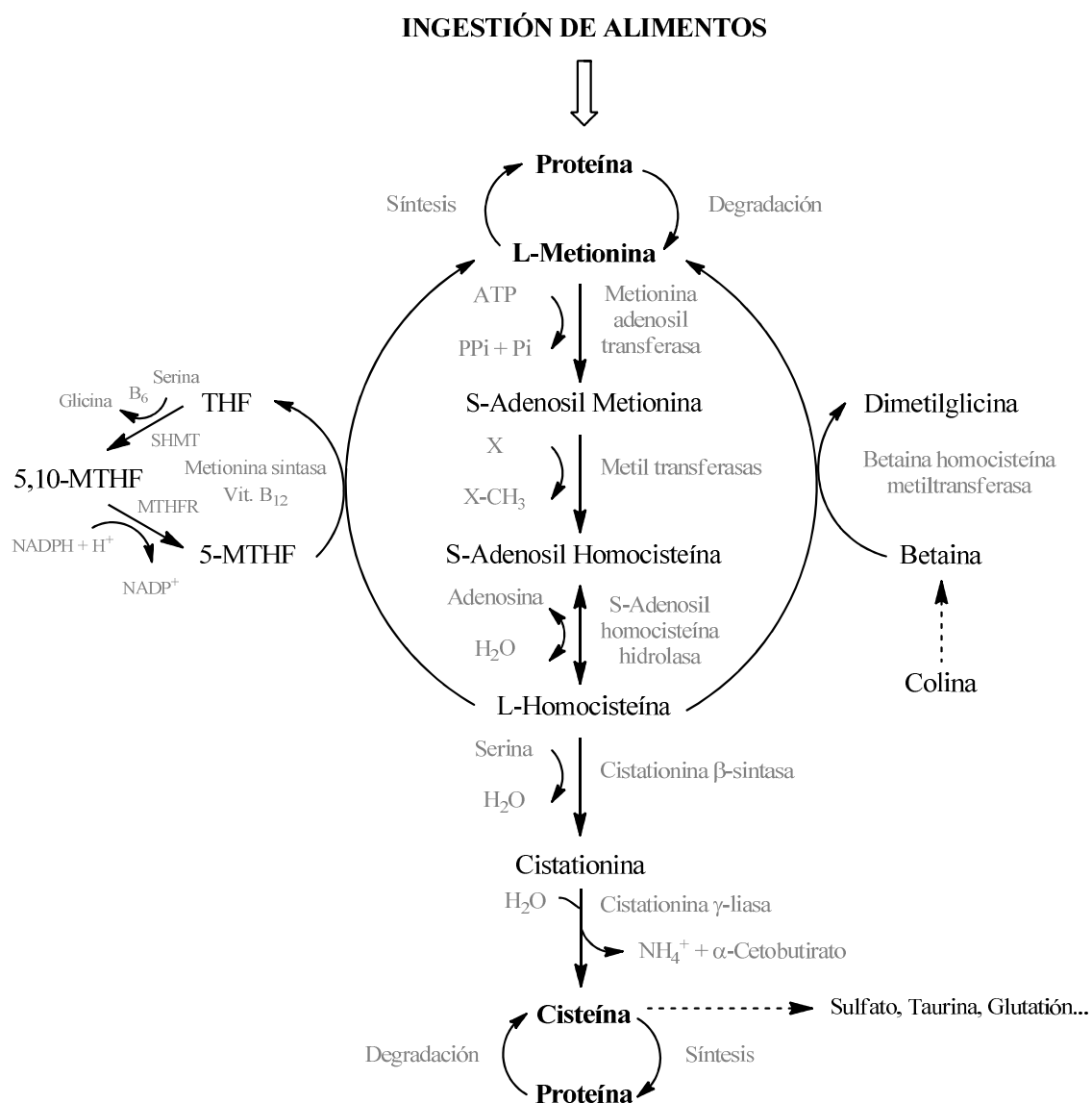


Figura 1. Metabolismo del aminoácido azufrado metionina en mamíferos.

A.1.3. Síntesis química de metionina

Todos los aminoácidos, a excepción de la glicina, tienen dos formas estructurales o estereoisómeros: L y D. En las proteínas animales todos los aminoácidos presentes pertenecen a la serie L. Sin embargo, en ciertos casos, el animal dispone de la capacidad enzimática precisa para aprovechar la forma D, previa transformación a la forma L correspondiente. Este es el caso de la metionina, donde ambas formas se encuentran totalmente disponibles.

Desde el punto de vista de la dieta humana, la alimentación únicamente con metionina proporcionaría todo el azufre necesario para el organismo, con la excepción

de las vitaminas tiamina y biotina. La cantidad diaria recomendada (RDA) en adultos para la metionina está establecida en 14 mg/kg/día [14], mientras que la cantidad de metionina a partir de la cual comienza a ser tóxica en humanos se estima por encima de los 100 mg/kg/día [17], cantidad muy superior a la necesaria para realizar experimentos con trazadores.

El producto sólido comercial DL-metionina tiene una riqueza superior al 99% y se obtiene por síntesis química a partir del propileno, metiltiol, metano y amoníaco. Una posibilidad no explorada en la presente Tesis Doctoral es la preparación de DL-metionina marcada con azufre-34 obtenida por síntesis química para su uso posterior como trazador metabólico. En este sentido, se ha optado por realizar la síntesis de metionina a partir de organismos vivos (biosíntesis) teniendo en cuenta además la ventajosa posibilidad de acceder a otros compuestos marcados con azufre-34 (péptidos, proteínas, etc.) que por síntesis química presentarían una mayor dificultad.

A.1.4. Biosíntesis de metionina y cisteína en *Saccharomyces cerevisiae*

Teniendo en cuenta todo lo comentado hasta ahora, los estudios de metabolismo de proteínas en mamíferos utilizando isótopos estables enriquecidos de azufre requieren la síntesis previa de los aminoácidos proteinogénicos cisteína y/o metionina marcados con un isótopo enriquecido de azufre, dado que los mamíferos no son capaces de sintetizar estos aminoácidos esenciales y necesitan obtenerlos a través de la alimentación [18]. Es decir, no se pueden utilizar como trazadores metabólicos en mamíferos especies químicas de azufre diferentes a la metionina, la cisteína o un péptido/proteína que las contengan, ya que el trazador no se incorporaría a las proteínas del organismo. Por el contrario, otros seres vivos pueden reducir el sulfato inorgánico a sulfuro y sintetizar a partir de él compuestos orgánicos de azufre [19]. La Figura 2 recoge las rutas de biosíntesis de los aminoácidos azufrados a partir de azufre inorgánico en la levadura *Saccharomyces cerevisiae* utilizada a lo largo de la presente Tesis Doctoral. Algunos microorganismos procariota (p.e. *Escherichia coli*) así como microorganismos eucariota (p.e. levaduras) [20] son una elección ventajosa para este tipo de estudios debido a las elevadas tasas de crecimiento celular que pueden alcanzar [21]. En este sentido, la levadura *Saccharomyces cerevisiae* es considerada una sustancia ideal para su uso en experimentos con trazadores metabólicos en animales o humanos.

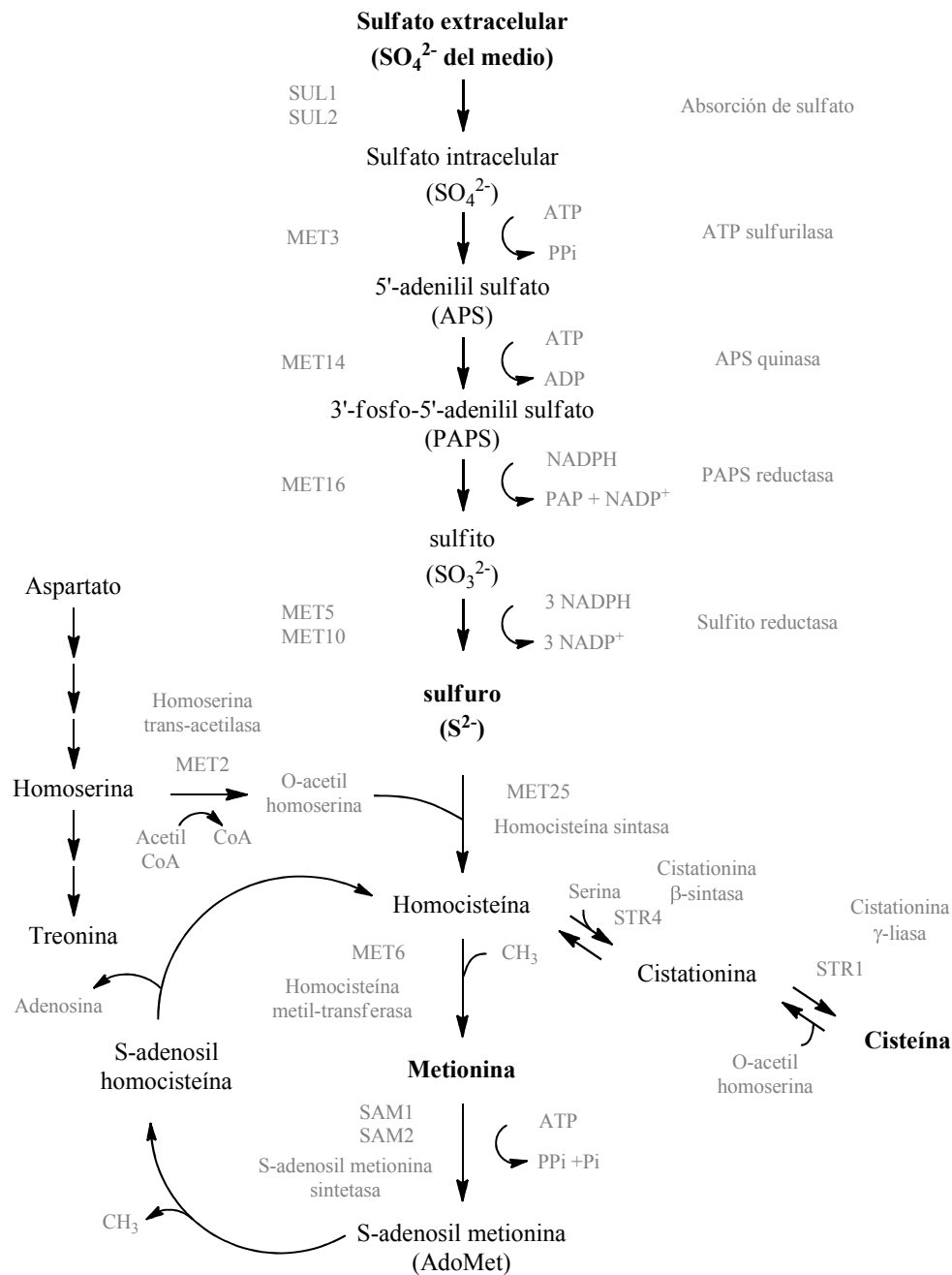


Figura 2. Biosíntesis de aminoácidos de azufre en *Saccharomyces cerevisiae*.

Este hecho se debe a su clasificación como organismo reconocido como seguro para la salud (GRAS) por la agencia de alimentos y medicamentos (FDA) de los Estados Unidos, debido a su inocuidad y a la posibilidad de administrarla como alimento por vía oral.

A.2. EMPLEO DE ISÓTOPOS ESTABLES EN QUÍMICA ANALÍTICA

A.2.1. Isótopos de azufre

Se conocen al menos 25 isótopos de azufre, tanto estables como radiactivos, la mayoría de los cuales han sido creados artificialmente.

Casi todos los isótopos de azufre radiactivos (naturales o artificiales) poseen vidas medias del orden de segundos o incluso milisegundos, lo que limita enormemente su aplicabilidad analítica. Sin embargo, el isótopo radiactivo natural de azufre-35 (^{35}S), formado al incidir la radiación cósmica sobre el argón-40 atmosférico, posee una vida media de 87 días y experimenta un decaimiento beta según $^{35}_{16}\text{S} \rightarrow ^0_{-1}e + ^{35}_{17}\text{Cl}$. La radiación emitida en este proceso ha sido utilizada para la medida de azufre-35 empleando diferentes técnicas analíticas [22]. De esta manera, el ^{35}S se ha utilizado como trazador en la mayoría de estudios fundamentales del metabolismo básico de azufre y sus aminoácidos [23,24], en estudios de síntesis y degradación de proteínas (recambio proteico) [25,26] y en estudios farmacocinéticos y del metabolismo de drogas y medicamentos que contienen azufre en su estructura [27-29], por citar algunas áreas.

Únicamente cuatro de los isótopos naturales de azufre son estables (^{32}S , ^{33}S , ^{34}S y ^{36}S). El isótopo mayoritario es el azufre-32 con una abundancia del 94,93%. Es de destacar la baja abundancia isotópica que presentan los isótopos ^{33}S (0,76%), ^{34}S (4,29%) y ^{36}S (0,02%), lo que los hace muy adecuados para su uso como trazadores.

A.2.2. Abundancias isotópicas naturales

A.2.2.1. Introducción

La composición isotópica promedio de cada elemento terrestre se fijó hace millones de años durante la formación del planeta, siendo los isótopos con configuraciones de núcleo más estables los que presentan una mayor abundancia relativa. La variabilidad de las abundancias isotópicas de la mayoría de los elementos en la naturaleza es muy pequeña por lo que se considera que las abundancias isotópicas de los elementos son invariables. Sin embargo, si se estudia con atención la composición isotópica de los elementos terrestres, se puede observar que determinados elementos químicos presentan variaciones significativas en las

abundancias isotópicas basadas en un enriquecimiento/empobrecimiento de unos isótopos con respecto a otros. Por tanto, la composición isotópica de algunos elementos químicos, tradicionalmente ligeros (p.e. H, C, N, O y S), aunque en la actualidad se estudian también elementos pesados (p.e. Sr, Pb, etc.), se puede utilizar en estudios de trazabilidad, dado que su composición isotópica varía en la naturaleza (variaciones naturales). De hecho, en la literatura actual se pueden encontrar libros especializados [30,31] y numerosas revisiones bibliográficas que describen la utilización de la medida de variaciones naturales en la composición isotópica de los elementos, en campos tan variados como la autenticidad y trazabilidad de alimentos [32-36], arqueología [37-39], geoquímica [40], biología [41] y ciencia forense [42].

El origen de las variaciones naturales en las abundancias isotópicas se atribuye al fraccionamiento isotópico [43]. Se conoce como fraccionamiento isotópico a cualquier proceso (bien sea químico, físico o biológico) que cambia la abundancia relativa de los isótopos estables de un elemento [44]. Aunque las causas no se saben con exactitud, el hecho es que la materia viva prefiere las moléculas con isótopos ligeros. Así, por ejemplo, el mecanismo dominante del fraccionamiento isotópico del azufre es la reducción bacteriana de sulfato, ya que la especie con azufre-32 puede reaccionar hasta 1,07 veces más rápido que su homólogo con azufre-34 [44]. Por el contrario, otros procesos como la evaporación y condensación, cristalización y fusión, absorción y desorción, etc., pueden conducir a un enriquecimiento preferente del isótopo más pesado [44].

En cualquier caso, como consecuencia de estos efectos de fraccionamiento isotópico, se puede afirmar que el perfil isotópico de una sustancia está ligado a su origen y a su historia y que los procesos de fabricación y/o los procesos biológicos pueden conducir a la formación de productos cuya composición isotópica sea característica de dicho proceso (huella dactilar). De hecho, cuando dos muestras diferentes del mismo producto son químicamente idénticas y tienen el mismo perfil isotópico, se puede concluir con un alto grado de certeza que ambas muestras provienen de la misma fuente.

A.2.2.2. La notación delta

Las variaciones naturales se suelen expresar utilizando la notación delta, que proporciona una información manejable de la diferencia relativa entre las relaciones isotópicas medidas de un elemento. Las variaciones naturales son típicamente del orden de décimas de tanto por ciento y se suelen expresar en tanto por mil, donde un

A. INTRODUCCIÓN

1‰ significa un cambio del 0,1%. Esto significa que los cambios en las relaciones isotópicas naturales ocurren alrededor de la tercera o cuarta cifra significativa. Indiscutiblemente es más cómodo e intuitivo expresar una variación del 4‰ que de 0,004. Obviamente para poder ver estos cambios tan pequeños, se necesitan equipos que permitan realizar medidas de relaciones isotópicas de elevada precisión.

En la notación delta (δ), lo que se hace es expresar como tanto por mil la relación isotópica de interés medida en la muestra ($R_{muestra}$) con respecto a una relación isotópica de referencia internacionalmente reconocida (R_{ref}), de acuerdo con la siguiente ecuación:

$$\delta_{ref} = \left(\frac{R_{muestra} - R_{ref}}{R_{ref}} \right) \cdot 1000 \quad \text{Ecuación 1}$$

que se puede expresar también de la siguiente manera:

$$\delta_{ref} = \left(\frac{R_{muestra}}{R_{ref}} - 1 \right) \cdot 1000 \quad \text{Ecuación 2}$$

Las variaciones naturales en la composición isotópica de azufre se basan en la medida relativa de la relación isotópica $^{34}\text{S}/^{32}\text{S}$. El material de referencia histórico para realizar estas medidas es el azufre de un meteorito, el CDT (Canyon Diablo Troilite meteorite, Arizona, USA). Este material (FeS) ha sido utilizado desde 1962 como estándar de referencia internacional para las medidas de la composición isotópica de azufre [45]. Sin embargo, el CDT ya no es tan fácilmente accesible y además se demostró que su composición isotópica expresada en términos de $\delta^{34}\text{S}$ podía variar tanto como un 0,4‰ [46]. Consecuentemente, en 1993 el grupo asesor de la Agencia Internacional de Energía Atómica (IAEA) recomendó en Viena que al material de referencia IAEA-S-1 (Ag_2S) se le asignara un valor $\delta^{34}\text{S}$ exacto de -0,3‰; estableciendo por tanto una escala V-CDT [47]. La propuesta fue aceptada en 1995 por la Comisión de Pesos Atómicos y Abundancias Isotópicas (CAWIA) y desde entonces está internacionalmente aceptado que todos los datos de composición isotópica de azufre se documenten como $\delta^{34}\text{S}$ en la escala V-CDT [48], de acuerdo a la siguiente ecuación:

A.2. EMPLEO DE ISÓTOPOS ESTABLES EN QUÍMICA ANALÍTICA

$$\delta^{34}\text{S}_{V\text{-CDT}} = \left(\frac{(^{34}\text{S}/^{32}\text{S})_{\text{muestra}}}{(^{34}\text{S}/^{32}\text{S})_{V\text{-CDT}}} - 1 \right) \cdot 1000 \quad \text{Ecuación 3}$$

De esta manera se habla de delta de azufre en la escala V-CDT ($\delta_{V\text{-CDT}}$) porque éste es el material de referencia que se utiliza para normalizar esta relación isotópica. El valor asignado para la relación isotópica $^{34}\text{S}/^{32}\text{S}$ en este material de referencia es de 0,0441626 [47]. Por tanto, cuando la relación $^{34}\text{S}/^{32}\text{S}$ en la muestra es mayor que la de referencia tendremos valores positivos de delta y en caso contrario valores de delta negativos. De una manera arbitraria, por la propia definición, los valores de delta para estos estándares se fijan en 0‰. Como el estándar V-CDT es escaso y caro, lo más común es utilizar un segundo estándar de referencia certificado en delta respecto al V-CDT. De esta manera:

$$\delta^{34}\text{S}_{V\text{-CDT ref}} = \left(\frac{(^{34}\text{S}/^{32}\text{S})_{\text{ref}}}{(^{34}\text{S}/^{32}\text{S})_{V\text{-CDT}}} - 1 \right) \cdot 1000 \quad \text{Ecuación 4}$$

Si despejamos la relación isotópica $^{34}\text{S}/^{32}\text{S}$ en el material de referencia V-CDT se obtiene:

$$(^{34}\text{S}/^{32}\text{S})_{V\text{-CDT}} = \frac{(^{34}\text{S}/^{32}\text{S})_{\text{ref}}}{\frac{\delta^{34}\text{S}_{V\text{-CDT ref}}}{1000} + 1} \quad \text{Ecuación 5}$$

Y sustituyendo este valor en la ecuación 3, se encuentra finalmente la ecuación utilizada en la presente Tesis Doctoral para el cálculo de variaciones naturales en la composición isotópica de azufre utilizando la notación delta:

$$\delta^{34}\text{S}_{V\text{-CDT}} = \left(\left(\frac{(^{34}\text{S}/^{32}\text{S})_{\text{muestra}}}{(^{34}\text{S}/^{32}\text{S})_{\text{ref}}} \cdot \left(\frac{\delta^{34}\text{S}_{V\text{-CDT ref}}}{1000} + 1 \right) \right) - 1 \right) \cdot 1000 \quad \text{Ecuación 6}$$

Existen diferentes estándares certificados en delta, cubriendo el rango desde +34 hasta -32‰. En los estudios realizados en la presente Tesis Doctoral relacionados con la medida de variaciones naturales en la composición isotópica de azufre (**artículos científicos I y II**), se utilizaron tres materiales de referencia certificados en delta. El primero de ellos, NIST RM8553 ($\delta^{34}\text{S}_{V\text{-CDT}} = 16 \pm 0,3\text{‰}$) se utilizó como estándar

A. INTRODUCCIÓN

secundario para poder expresar los resultados de acuerdo a la notación $\delta_{V\text{-CDT}}$ y los otros dos, NIST RM8554 ($\delta^{34}\text{S}_{V\text{-CDT}} = -0,3 \pm 0,3\%$) y NIST RM8556 ($\delta^{34}\text{S}_{V\text{-CDT}} = 17,44 \pm 0,3\%$) se utilizaron como controles de calidad de la metodología utilizada.

La composición isotópica de azufre ($\delta^{34}\text{S}_{V\text{-CDT}}$) de algunos materiales seleccionados de la referencia [44] que contienen este elemento, así como de los materiales de referencia utilizados en la presente Tesis Doctoral se recoge en la Figura 3.

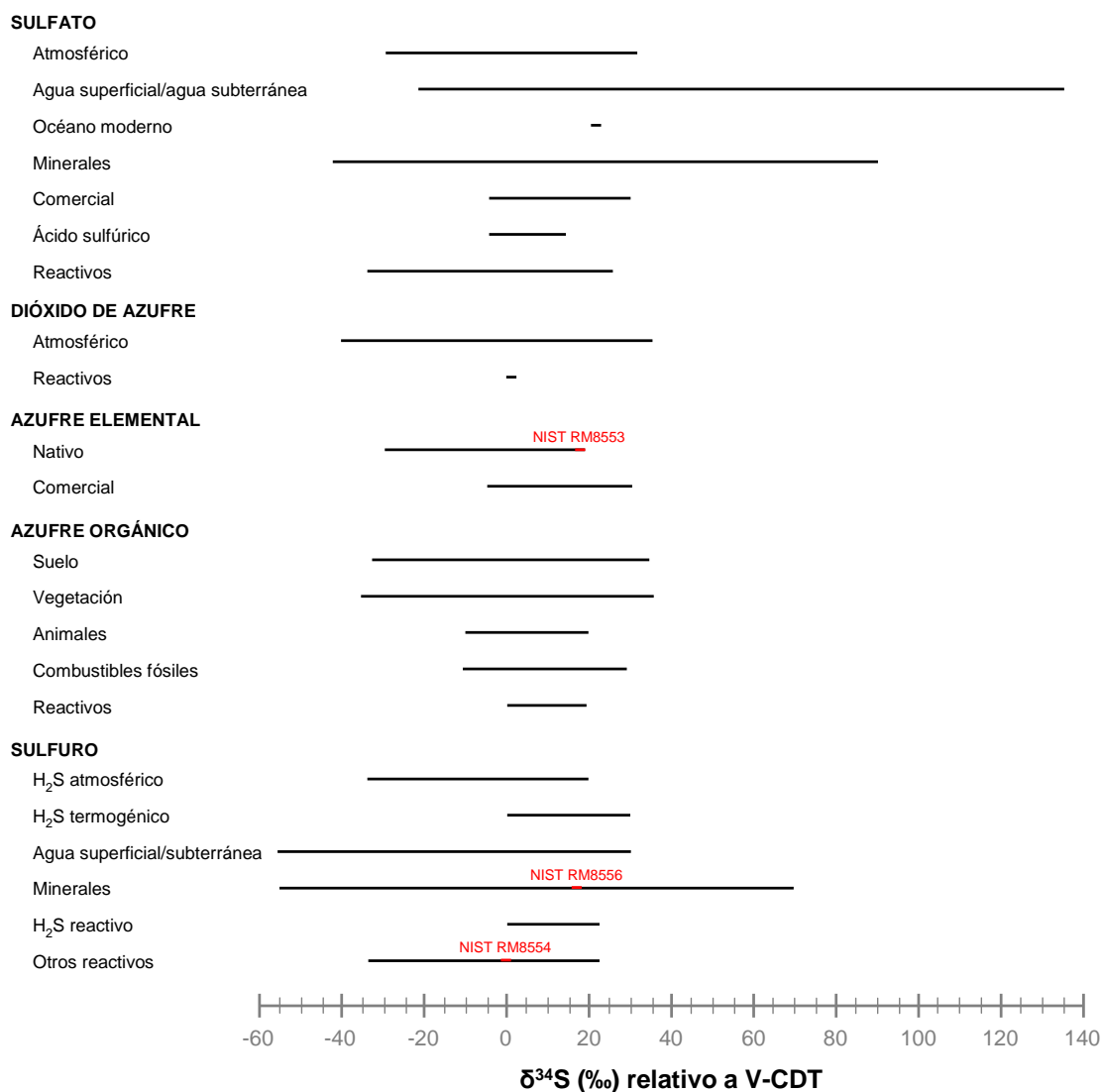


Figura 3. Composición isotópica de algunos materiales que contienen azufre seleccionados de la referencia [44].

A.2. EMPLEO DE ISÓTOPOS ESTABLES EN QUÍMICA ANALÍTICA

A.2.2.3. Técnicas analíticas más utilizadas para la medida de relaciones isotópicas

La medida de las variaciones isotópicas naturales requiere el uso de instrumentación especializada, ya que, como se comentó anteriormente, para poder ver cambios tan pequeños en la composición isotópica se necesitan medidas de relaciones isotópicas de elevada precisión. Las técnicas analíticas más comúnmente utilizadas para medir estas variaciones naturales en la composición isotópica de los elementos son la espectrometría de masas de relaciones isotópicas (IRMS) [49-51] y la espectrometría de masas con fuente de ionización térmica (TIMS) [52].

En el caso particular del azufre, para la medida de variaciones naturales en su composición isotópica, generalmente se utiliza la técnica IRMS con fuente gaseosa (GS), en la que previamente hay que transformar el azufre en SO_2 o SF_6 . Así, en la literatura se encuentran numerosas publicaciones relacionadas con estudios biogeoquímicos [53-60] y estudios de autenticidad y trazabilidad de alimentos [61-63]. Sin embargo, esta técnica presenta una serie de inconvenientes. La preparación de muestra para transformar las diferentes especies de azufre presentes en matrices geológicas, biológicas o medioambientales en SO_2 o SF_6 es compleja, tediosa, puede conducir a un adicional fraccionamiento isotópico o incluso contaminación procedente de los reactivos empleados. Además, se han obtenido diferentes valores de delta para el mismo material dependiendo que especie (SO_2 o SF_6) se introduzca en el equipo [64]. Por otro lado, cuando se utiliza SO_2 son necesarias correcciones matemáticas para eliminar la contribución isotópica del oxígeno [65]. Por todo ello, en la presente Tesis Doctoral se ha propuesto el uso de una instrumentación alternativa al IRMS para la medida de variaciones naturales en la composición isotópica de azufre.

El uso del ICP-MS para la medida de relaciones isotópicas de azufre está relativamente extendido. En los últimos años, se han utilizado equipos ICP-MS de tipo cuadrupolo equipados con celda de colisión/reacción [66-68] y equipos de doble enfoque con detección simple [69,70] para este fin. Sin embargo, debido a que la adquisición de los datos se lleva a cabo de un modo secuencial, la precisión que se obtiene en estos estudios únicamente permite detectar variaciones relativamente grandes en la composición isotópica de azufre (*i.e.* variaciones isotópicas inducidas). En este sentido, la aparición de los equipos ICP-MS multicolectores ha resultado clave para poder realizar medidas de variaciones naturales en la composición isotópica de la mayoría de elementos de la tabla periódica [71-73]. Así, para el azufre, el uso de equipos ICP-MS multicolectores permite la determinación en continuo, rápida y simultánea de varios isótopos [74-77], evitando el procedimiento largo y tedioso de

preparación de muestra de la técnica IRMS y con excelentes precisiones instrumentales (desde 0,1% a <0,005%) dependiendo de la concentración de azufre [60,78,79].

A.2.3. Obtención y principales aplicaciones de los isótopos estables enriquecidos

Hoy en día, es posible obtener un elemento enriquecido isotópicamente, donde un isótopo natural de baja abundancia (por ejemplo, el ^{34}S que posee una abundancia isotópica natural del 4,29%) se encuentra enriquecido en más del 90%, mientras el resto de isótopos de ese mismo elemento se encuentran en forma minoritaria.

Los métodos de obtención de isótopos enriquecidos se basan en la separación de los isótopos de un mismo elemento. Dada la similitud de sus propiedades químicas, están fundamentados en las diferencias entre sus propiedades físicas y en concreto en las pequeñas diferencias en sus pesos atómicos. Entre los métodos de producción de isótopos enriquecidos destacan la separación electromagnética, la difusión gaseosa y la centrifugación gaseosa. El resultado de todos ellos es la separación de la mezcla isotópica original en dos fracciones: una con un mayor porcentaje del isótopo más pesado y la otra con un mayor porcentaje del isótopo más ligero. La separación isotópica es más efectiva cuanto mayor sea la diferencia de masa entre los isótopos a separar. Por ejemplo, la diferencia de masa entre los isótopos de azufre ^{34}S y ^{33}S frente a ^{32}S es un poco mayor del 6 y 3% respectivamente. Por tanto, la separación isotópica será 2 veces más difícil para el isótopo ^{33}S que para el isótopo ^{34}S . Este hecho, junto con la menor abundancia natural del isótopo ^{33}S (0,76 frente a 4,29%) justifican la diferencia económica del precio del isótopo enriquecido ^{33}S frente al ^{34}S (unas cinco veces más caro el ^{33}S).

Los isótopos estables enriquecidos destacan como productos de partida en la preparación de radioisótopos, mediante el uso de aceleradores de partículas y/o reactores nucleares. Estos radioisótopos son utilizados principalmente en dos tipos de aplicaciones: como fármacos contra enfermedades y como trazadores en técnicas diagnósticas.

Asimismo, los isótopos estables enriquecidos se utilizan en estudios metabólicos y para realizar el análisis por dilución isotópica, que se explicará en detalle en apartados posteriores.

A.2.4. Isótopos estables en estudios metabólicos

Los primeros trabajos con trazadores isotópicos se realizaron empleando radioisótopos, primero en animales y después en humanos. Los isótopos radioactivos comenzaron a ser muy populares para el estudio de la absorción y metabolismo de minerales en los años 40 del siglo pasado, pero esta popularidad ha decrecido en los últimos años debido a los riesgos de la radioactividad [80].

Desde una perspectiva de investigación y desarrollo, los radioisótopos presentan varias ventajas como trazadores frente al uso de isótopos estables. En primer lugar, la cantidad de radioisótopo necesaria para poder monitorizarlo suele ser muy pequeña, con lo que la perturbación que el trazador produce en el sistema investigado es también pequeña. Además, la cantidad de trazador absorbido y remanente en el organismo se puede determinar de modo inequívoco. Generalmente son más baratos y el sistema de detección empleado más simple. Sin embargo, la desventaja principal de los radioisótopos frente a los isótopos estables es el problema de seguridad que plantean debido a la exposición a la radiación. Además, no se pueden utilizar en estudios en recién nacidos ni en mujeres embarazadas o lactantes. El análisis con radioisótopos es dependiente de su vida media (tiempo de decaimiento). Por otra parte, sólo se puede suministrar un elemento radiactivo por análisis y se genera un costoso problema con los residuos [81].

R. Schoenheimer y D. Rittenberg introdujeron en 1935 el uso de isótopos estables enriquecidos en estudios metabólicos tal como se conocen actualmente [82]. Estos autores abrieron con sus trabajos la puerta a una nueva concepción de las actividades metabólicas del organismo, poniendo de manifiesto que los componentes estructurales del organismo, considerados hasta entonces como estables, están sujetos a un recambio continuo [83]. El enfoque general para estudios metabólicos utilizando isótopos estables es el mismo que con el empleo de isótopos radiactivos. Sin embargo, el empleo de isótopos estables enriquecidos, dado que no existe radiación emitida, presenta ciertas ventajas, entre las que destacan: efectos mínimos sobre la salud de los individuos, pudiéndose aplicar a mujeres embarazadas y a recién nacidos; las muestras se pueden conservar sin la pérdida del trazador; se puede seguir la marca durante largos periodos; posibilidad de re-análisis; etc. Además, los métodos de análisis empleados se basan en la determinación por espectrometría de masas, lo que abre la puerta a procedimientos multielementales y multiisotópicos [84-88].

Tradicionalmente, los estudios de metabolismo utilizando trazadores de azufre se han llevado a cabo usando ^{35}S radiactivo [89,90], encontrándose muy pocas publicaciones en las que se empleen isótopos estables [91,92]. Recientemente se ha indicado que el marcaje metabólico con azufre-35 radiactivo puede inhibir el ciclo de progresión, proliferación y supervivencia celular [93], poniendo de relieve la adecuación del uso de isótopos estables de azufre para realizar este tipo de estudios. En los últimos años, la creciente popularidad del ICP-MS ha acelerado el uso de isótopos estables para estudios de metabolismo [94-96]. Sin embargo, hasta el comienzo de la presente Tesis Doctoral, el número de estudios de metabolismo utilizando isótopos estables de azufre que empleasen ICP-MS era muy escaso [92]. Además, no se había descrito ninguna aplicación con trazadores múltiples de azufre.

A.2.5. Análisis por dilución isotópica (IDA)

A.2.5.1. Introducción

Los métodos de medida químico-analítica cuyo resultado es trazable directamente al sistema internacional de unidades (kilogramo, mol, amperio, segundo, etc.) y que no requieren calibrado metodológico, es decir, la obtención de una relación biunívoca entre señal y concentración, se denominan métodos primarios. Estos se utilizan generalmente para la preparación de materiales de referencia y para la validación de otros métodos analíticos. La inmensa mayoría de las metodologías analíticas utilizadas en el análisis de trazas y/o ultratrazas requieren el uso de calibrados metodológicos y, por tanto, no se pueden considerar métodos primarios. Por otro lado, métodos primarios como la gravimetría o la volumetría no se pueden utilizar para el análisis de trazas por su falta de sensibilidad. La coulombimetría, a su vez, es una técnica muy poco selectiva y se emplea únicamente para aplicaciones analíticas muy concretas.

El análisis por dilución isotópica (IDA) es considerado desde el año 1997 como el método definitivo para el análisis de elementos traza, siendo clasificado por la oficina internacional de pesos y medidas (BIPM) como método primario debido a su alta calidad metrológica [97]. El concepto de dilución isotópica es similar al utilizado para determinar poblaciones de especies raras de pájaros en islas [81]. Para ello, se colocan anillas en las patas de un número dado de pájaros a los que posteriormente se les permite mezclarse libremente con los demás pájaros no marcados de la isla durante un tiempo suficientemente largo. Más tarde se capturan al azar otro grupo de pájaros y la relación de no marcados frente a marcados proporciona la población total

A. INTRODUCCIÓN

de pájaros en la isla. Hoy en día se aplica este mismo principio para la cuantificación de elementos y compuestos (bio)químicos mediante la medida de relaciones isotópicas por técnicas de espectrometría de masas utilizando isótopos estables enriquecidos como marca.

El análisis por dilución isotópica es una técnica analítica que se basa en la medida de relaciones isotópicas de un elemento en muestras donde su composición isotópica ha sido previamente alterada por la adición de una cantidad conocida del elemento o compuesto que contiene el elemento enriquecido isotópicamente. Se emplea principalmente en la certificación de patrones y/o materiales de referencia [98,99] así como en la validación de otros métodos analíticos [100]. Sin embargo, en los últimos años, debido al coste relativamente bajo de los isótopos enriquecidos, la facilidad de manejo, rapidez y robustez analítica de las metodologías basadas en la dilución isotópica y a la comercialización cada vez más extendida de compuestos marcados isotópicamente, se está popularizando su uso en análisis de rutina [101].

La espectrometría de masas con fuente de ionización térmica (TIMS) ha sido la técnica empleada tradicionalmente en el análisis elemental por dilución isotópica debido a la alta precisión de las medidas. Sin embargo, el tratamiento de la muestra para llevar a cabo la medida por TIMS es largo y tedioso. Por ello, y dado que en la mayoría de los casos se pueden conseguir precisiones similares en la medida de las relaciones isotópicas con los equipos ICP-MS convencionales, en los últimos años han aparecido un gran número de aplicaciones en las que se utiliza este detector para tales propósitos. De hecho, hoy en día, el uso de IDA para el análisis elemental se realiza de forma casi exclusiva mediante ICP-MS [102-104].

El análisis por dilución isotópica también se puede aplicar a la determinación de compuestos. En el campo de la química clínica, la necesidad de una correcta determinación de fármacos, drogas, etc., junto con la disponibilidad de diferentes compuestos marcados con ^2H ó ^{13}C , ha acelerado el uso esta técnica y generalmente se utiliza como referencia para validar otras metodologías más rápidas utilizadas en rutina [105,106].

Las metodologías basadas en el análisis por dilución isotópica utilizando ICP-MS se han extendido a nuevos campos analíticos. Uno de estos nuevos campos es la especiación elemental, revisada con detalle a lo largo de los últimos años [107-117], donde el objetivo es la determinación de las especies químicas individuales en las que un elemento se distribuye en una muestra dada.

A.2. EMPLEO DE ISÓTOPOS ESTABLES EN QUÍMICA ANALÍTICA

A.2.5.2. Determinación total elemental mediante IDA

En análisis elemental, la dilución isotópica se basa en la alteración intencionada de las abundancias isotópicas del elemento a determinar en la muestra mediante la adición a la misma de una cantidad conocida de un isótopo enriquecido del mismo elemento (trazador). La mayor parte de los elementos de la tabla periódica poseen más de un isótopo estable y se pueden determinar, por tanto, mediante análisis por dilución isotópica.

El principio básico de un análisis elemental mediante IDA para el caso de un elemento que contiene dos isótopos diferentes a y b, se ilustra en la Figura 4.

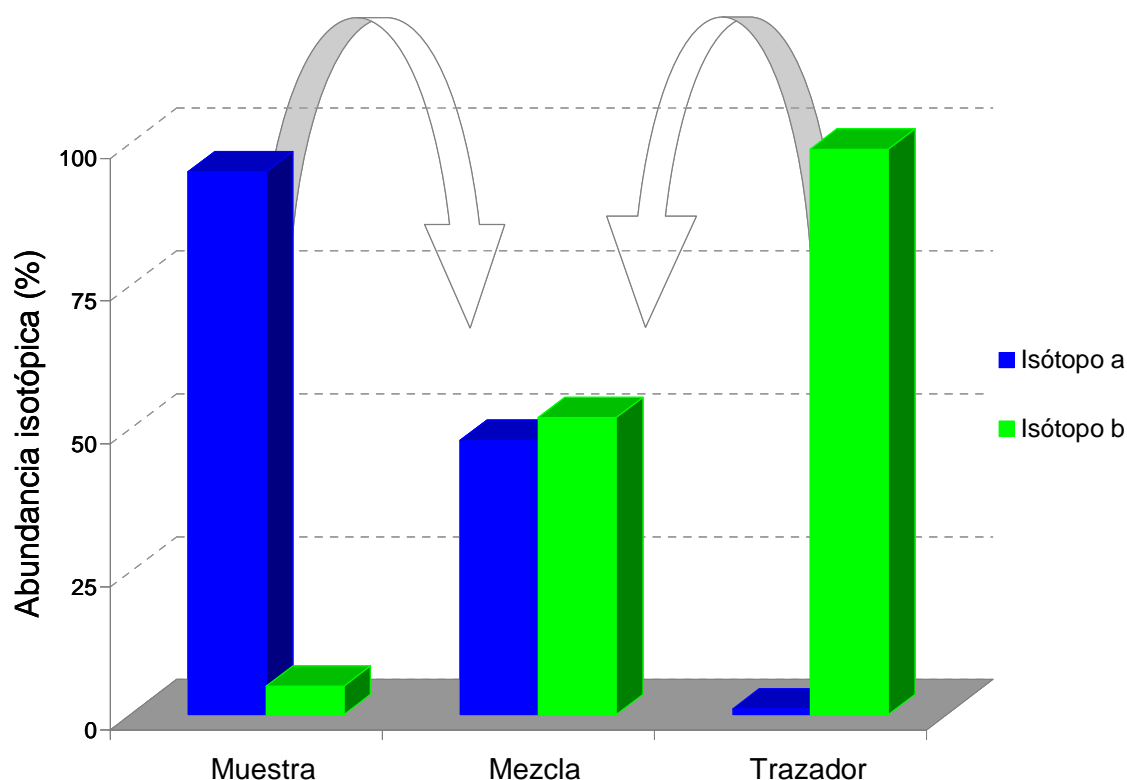


Figura 4. Ilustración del fundamento de la dilución isotópica para un elemento que contiene dos isótopos (a y b).

Como se puede observar, el isótopo a es el más abundante en la muestra, mientras que el trazador está claramente enriquecido en el isótopo b. Las abundancias isotópicas de la mezcla de ambos, y por tanto las relaciones isotópicas, serán intermedias entre las de la muestra y el trazador, y dependerán tanto de la cantidad adicionada de trazador como de la cantidad original del elemento en la muestra. A partir de la medida de la relación isotópica en la mezcla, se puede calcular la

A. INTRODUCCIÓN

concentración del elemento en la muestra original utilizando la ecuación de la dilución isotópica, cuyo desarrollo matemático [113] se expone a continuación.

Si se denomina N_S al número de moles de un elemento poli-isotópico presente en la muestra y N_{Sp} al número de moles del mismo elemento en el trazador, el número de moles del elemento en la mezcla resultante N_m vendrá dado por:

$$N_m = N_S + N_{Sp} \quad \text{Ecuación 7}$$

De modo similar para los isótopos a y b podemos establecer los siguientes balances de masas:

$$N_m^a = N_S^a + N_{Sp}^a \quad \text{Ecuación 8}$$

$$N_m^b = N_S^b + N_{Sp}^b \quad \text{Ecuación 9}$$

Si se divide la Ecuación 8 entre la Ecuación 9 se obtiene la relación isotópica de ambos isótopos (a/b) en la mezcla (R_m), la cual puede expresarse de la siguiente manera:

$$R_m = \frac{N_m^a}{N_m^b} = \frac{N_S^a + N_{Sp}^a}{N_S^b + N_{Sp}^b} = \frac{N_S A_S^a + N_{Sp} A_{Sp}^a}{N_S A_S^b + N_{Sp} A_{Sp}^b} \quad \text{Ecuación 10}$$

Donde $N_S^a = N_S A_S^a$; $N_{Sp}^a = N_{Sp} A_{Sp}^a$; $N_S^b = N_S A_S^b$; $N_{Sp}^b = N_{Sp} A_{Sp}^b$ si se tienen en cuenta las abundancias de los isótopos a y b en la muestra (A_S^a y A_S^b) y en el trazador (A_{Sp}^a y A_{Sp}^b) respectivamente. Despejando N_S en la Ecuación 10 se obtiene:

$$N_S = N_{Sp} \frac{R_m A_{Sp}^b - A_{Sp}^a}{A_S^a - R_m A_S^b} \quad \text{Ecuación 11}$$

La Ecuación 11 es la forma más básica de la ecuación de la Dilución Isotópica y en ella se puede observar que conociendo la composición isotópica del trazador y la muestra y el número de moles añadidos de trazador se puede calcular el número de moles del elemento en la muestra solamente con la medida de la relación isotópica R_m en la mezcla. Esta ecuación se puede adaptar para expresar concentraciones en

A.2. EMPLEO DE ISÓTOPOS ESTABLES EN QUÍMICA ANALÍTICA

lugar de número de moles. Si se define $R_s = \frac{A_s^b}{A_s^a}$ como la relación isotópica (b/a) en la

muestra y $R_{sp} = \frac{A_{sp}^a}{A_{sp}^b}$ como la relación isotópica (a/b) en el trazador se puede expresar

la Ecuación 11 como:

$$N_s = N_{sp} \frac{A_{sp}^b}{A_s^a} \left(\frac{R_m - R_{sp}}{1 - R_m R_s} \right) \quad \text{Ecuación 12}$$

Utilizando las expresiones $N_s = \frac{C_s \cdot m_s}{M_s}$ y $N_{sp} = \frac{C_{sp} \cdot m_{sp}}{M_{sp}}$ donde C_s y C_{sp} son

las concentraciones del elemento en la muestra y en el trazador, respectivamente; m_s y m_{sp} son el peso de muestra tomada y el peso de trazador añadido, respectivamente; y M_s y M_{sp} son los pesos atómicos del elemento en la muestra y en el trazador, respectivamente, se obtiene la ecuación final de la dilución isotópica utilizada en la presente Tesis Doctoral:

$$C_s = C_{sp} \frac{m_{sp}}{m_s} \frac{M_s}{M_{sp}} \frac{A_{sp}^b}{A_s^a} \left(\frac{R_m - R_{sp}}{1 - R_m R_s} \right) \quad \text{Ecuación 13}$$

Como se puede observar, todos los parámetros de esta ecuación son conocidos o medibles, por lo que la concentración del elemento en la muestra C_s se calcula simplemente a partir de la medida de la relación isotópica R_m mediante espectrometría de masas.

En la Ecuación 13 no aparece ningún parámetro relacionado con la sensibilidad instrumental, al contrario de lo que sucede con otras técnicas de calibración como las adiciones estándar o la calibración externa. Por tanto, la primera ventaja de IDA es que cualquier variación de este parámetro debida a inestabilidades instrumentales como la deriva de la señal o los efectos de matriz no tendrá ninguna influencia en el valor final de la concentración del elemento en la muestra (C_s). Es decir, un isótopo actúa como “patrón interno” ideal del otro.

A. INTRODUCCIÓN

Por otra parte, la incertidumbre en la medida de la concentración depende prácticamente sólo de la incertidumbre de la medida de las relaciones isotópicas R_S , R_{Sp} y R_m , ya que los pesos atómicos de la muestra y del trazador (M_S y M_{Sp}) son conocidos y los pesos de muestra y trazador (m_S y m_{Sp}) pueden determinarse gravimétricamente (muy baja incertidumbre). En la mayoría de los casos (a excepción de unos pocos elementos que muestran variaciones naturales en sus abundancias isotópicas) R_S es conocida, mientras que el valor de R_{Sp} se puede determinar previamente o puede ser conocido de antemano empleando un trazador certificado. Por tanto, el único parámetro que tiene que ser determinado experimentalmente es R_m y esta determinación se puede realizar con una elevada exactitud y precisión utilizando un espectrómetro de masas adecuado.

La tercera ventaja del IDA es que una vez añadido el isótopo enriquecido y alcanzada la homogeneización entre éste y la muestra, cualquier pérdida de analito de la mezcla no va a tener ninguna influencia en el resultado final. Esto es debido a que cualquier alícuota de la muestra diluida isotópicamente contendrá la misma R_m (permanece invariable) y, por tanto, no será necesario conocer los factores de dilución o preconcentración utilizados, ni tener en cuenta las separaciones no cuantitativas o procesos de evaporación. Además, debido a que la medida de R_m proporciona directamente la concentración inicial del elemento en la muestra (Ecuación 13), no es necesario recurrir a la calibración externa instrumental ni a métodos de adiciones estándar, lo que supone un ahorro considerable del tiempo de análisis respecto a los métodos analíticos convencionales. Por todas estas ventajas, el análisis por dilución isotópica está considerado internacionalmente como un método de referencia o absoluto, análogo a la gravimetría, volumetría o coulombimetría.

Sin embargo, para que todas estas ventajas tengan lugar, se han de cumplir algunos requisitos. En primer lugar, se tiene que tener en cuenta que cualquier pérdida de analito (ya sea de muestra o de trazador) antes de que se produzca la homogeneización de la mezcla va a suponer una fuente de error considerable. Además, una vez alcanzada dicha homogeneización, el isótopo enriquecido añadido a la muestra deberá comportarse de manera idéntica al elemento natural a lo largo de todo el proceso analítico. Por ejemplo, si el método incluye una etapa de extracción y el trazador resultase extraído con una mayor eficacia que el analito de la muestra, los resultados obtenidos serían erróneos. Por otra parte, la medida de las intensidades de los isótopos a y b debe estar libre de interferencias espectrales y los factores que

A.2. EMPLEO DE ISÓTOPOS ESTABLES EN QUÍMICA ANALÍTICA

afectan a la exactitud de la medida de relaciones isotópicas (como la discriminación de masas o el tiempo muerto del detector) deben ser debidamente corregidos. Finalmente, también se han de controlar los valores del blanco ya que cualquier tipo de contaminación que afecte a la muestra isotópicamente diluida conducirá a valores erróneos de R_m . En el caso de que cualquiera de los requisitos expuestos no se cumpla, la relación isotópica medida R_m que se introduce en la Ecuación 13 no es exacta y por ello no proporcionará la concentración real del elemento en la muestra (C_s).

A.2.5.2.1. Cantidad de trazador añadida a la muestra

Uno de los parámetros que puede tener una influencia significativa en el resultado final de un análisis por dilución isotópica es la cantidad de trazador añadida a la muestra. Esta cantidad se puede optimizar calculando el rango óptimo de la relación muestra / trazador en el que se minimicen los errores aleatorios [118]. Aplicando la teoría de propagación de los errores aleatorios en la ecuación final de la dilución isotópica (Ecuación 13), se obtiene la siguiente expresión para la varianza de la concentración en la muestra, $s(c_s)^2$:

$$s(c_s)^2 = \left[\frac{\partial c_s}{\partial m_{sp}} \right]^2 s(m_{sp})^2 + \left[\frac{\partial c_s}{\partial m_s} \right]^2 s(m_s)^2 + \left[\frac{\partial c_s}{\partial M_{sp}} \right]^2 s(M_{sp})^2 + \left[\frac{\partial c_s}{\partial M_s} \right]^2 s(M_s)^2 + \left[\frac{\partial c_s}{\partial A_{sp}^b} \right]^2 s(A_{sp}^b)^2 + \left[\frac{\partial c_s}{\partial A_s^a} \right]^2 s(A_s^a)^2 + \left[\frac{\partial c_s}{\partial R_s} \right]^2 s(R_s)^2 + \left[\frac{\partial c_s}{\partial R_{sp}} \right]^2 s(R_{sp})^2 + \left[\frac{\partial c_s}{\partial R_m} \right]^2 s(R_m)^2$$

Ecuación 14

Tomando derivadas parciales ∂c_s y agrupando la expresión se obtiene:

$$\left[\frac{s(c_s)}{c_s} \right]^2 = \left[\frac{s(m_{sp})}{m_{sp}} \right]^2 + \left[\frac{s(m_s)}{m_s} \right]^2 + \left[\frac{s(M_{sp})}{M_{sp}} \right]^2 + \left[\frac{s(M_s)}{M_s} \right]^2 + \left[\frac{s(A_{sp}^b)}{A_{sp}^b} \right]^2 + \left[\frac{s(A_s^a)}{A_s^a} \right]^2 + \left[\frac{R_m R_s}{1 - R_m R_s} \right]^2 \left[\frac{s(R_s)}{R_s} \right]^2 + \left[\frac{-R_{sp}}{R_m - R_{sp}} \right]^2 \left[\frac{s(R_{sp})}{R_{sp}} \right]^2 + \left[\frac{R_m (1 - R_{sp} R_s)}{(R_m - R_{sp})(1 - R_m R_s)} \right]^2 \left[\frac{s(R_m)}{R_m} \right]^2$$

Ecuación 15

Si se asume que tanto la medida de la relación isotópica en la muestra como en el trazador no influyen significativamente en el resultado final, podemos definir el factor de magnificación del error $f(R)$ como:

$$f(R) = \left[\frac{R_m (1 - R_{Sp} R_S)}{(R_m - R_{Sp}) (1 - R_m R_S)} \right] \quad \text{Ecuación 16}$$

Como se puede observar en esta expresión, $f(R)$ depende de R_m , R_{Sp} y R_S . Como R_S y R_{Sp} no pueden ser optimizadas, los valores de $f(R)$ se pueden representar frente a R_m para obtener el rango en el que la magnificación del error sea mínimo. Una vez conocido este intervalo, la cantidad de trazador que se añade a la muestra puede ser fácilmente optimizada. Ésta es la razón por la que, en el análisis por dilución isotópica, es necesario tener una idea aproximada del nivel de concentración del analito en la muestra. A partir de este conocimiento, se deberán calcular los pesos de muestra y trazador a mezclar para obtener un R_m próximo al valor óptimo.

La Figura 5 muestra la variación de $f(R)$ obtenida frente a las relaciones isotópicas $^{32}\text{S}/^{34}\text{S}$ y $^{32}\text{S}/^{33}\text{S}$ para los dos trazadores isotópicos utilizados enriquecidos en azufre-34 al 99,37% y en azufre-33 al 99,70% respectivamente.

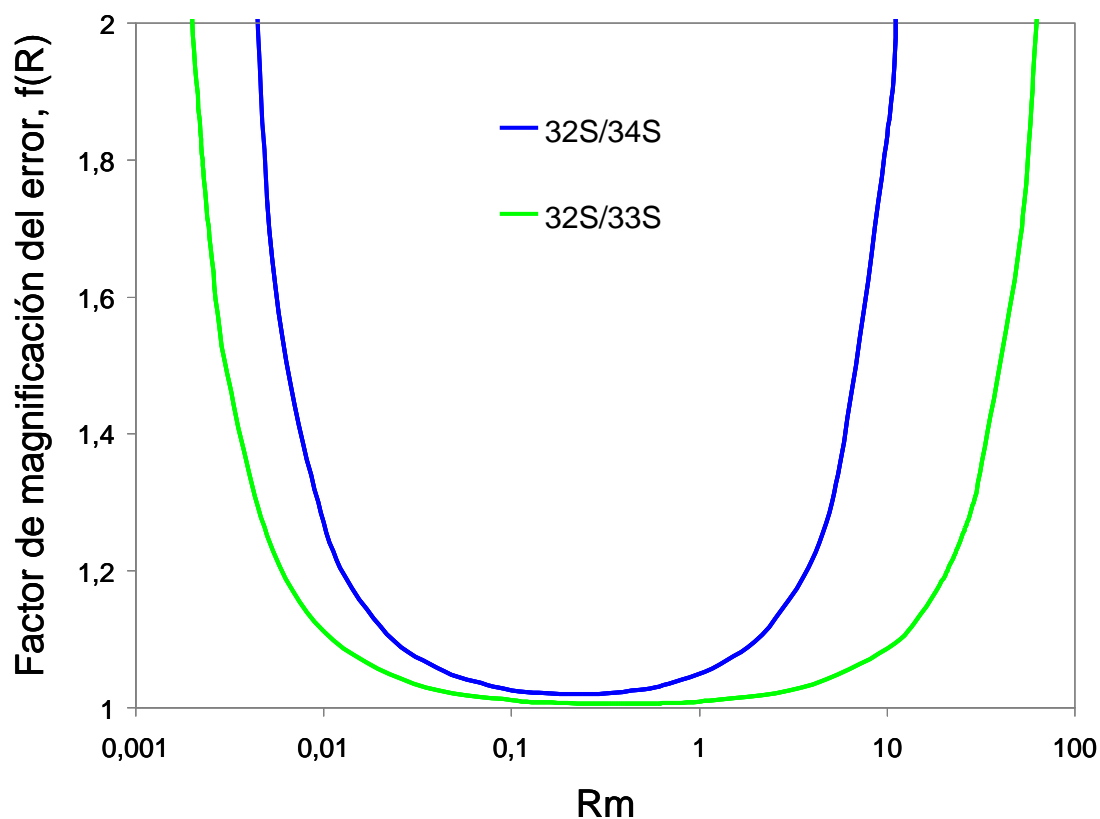


Figura 5. Curvas de magnificación del error para los trazadores isotópicos enriquecidos en azufre-34 y azufre-33.

Como se puede observar la relación isotópica en la mezcla (R_m) presenta un mínimo plano, es decir, un intervalo óptimo entre 0,04 y 2,5 para el trazador de azufre-34 y 0,01 y 10 para el de azufre-33. Siempre que R_m se encuentre dentro de estos intervalos, la incertidumbre en el cálculo de la concentración dependerá sólo de la incertidumbre en la medida de la relación isotópica, ya que $f(R)$ en estos intervalos es muy próximo a la unidad. Por tanto, todas las mezclas de muestra con isótopo enriquecido se prepararon tratando de que la relación final medida se encontrase dentro de estos valores. En caso contrario, la medida no se consideraba como válida y se preparaba de nuevo la mezcla con una proporción de muestra / trazador adecuada.

A.2.5.2.2. Exactitud de la medida de relaciones isotópicas

La medida de relaciones isotópicas en ICP-MS está sujeta a una serie de errores sistemáticos que se deben conocer y corregir: interferencias espectrales, discriminación de masas y tiempo muerto del detector.

A.2.5.2.2.1 Interferencias espectrales

El análisis elemental por dilución isotópica sólo se puede llevar a cabo si al menos dos isótopos del elemento a analizar (isótopos a y b) están libres de interferencias espectrales. Por tanto, para una medida exacta de relaciones isotópicas, se debe evitar la presencia de iones (mono- y/o poliatómicos) que tengan la misma relación m/z que los isótopos del elemento a monitorizar.

La determinación de azufre por ICP-MS está dificultada por las interferencias espectrales que afectan a todos sus isótopos estables. Estas interferencias espectrales están originadas por iones atómicos (interferencias isobáricas) o iones moleculares (interferencias poliatómicas, formadas a partir del argón, disolvente y/o matriz de la muestra, así como por la entrada de gases atmosféricos en la región de la interfase del ICP-MS) que tienen la misma relación m/z que el analito de interés, lo que ocasiona que a la señal del analito se sume la señal del ión interferente. Las principales interferencias espectrales que afectan a los isótopos de azufre, junto con el poder de resolución necesario para resolver dichas interferencias, se recogen en la Tabla 2.

Tabla 2. Principales interferencias espectrales en la determinación de azufre por ICP-MS.

Isótopo	Abundancia (%)	Interferencia	Resolución m/ Δ m
³² S	94,93	¹⁶ O ¹⁶ O ⁺	1.801
		¹⁴ N ¹⁸ O ⁺	1.061
		¹⁵ N ¹⁶ O ¹ H ⁺	1.040
		¹⁴ N ¹⁶ O ¹ H ₂ ⁺	770
³³ S	0,76	³² S ¹ H ⁺	3.907
		¹⁶ O ¹⁶ O ¹ H ⁺	1.259
		¹⁴ N ¹⁸ O ¹ H ⁺	854
		¹⁵ N ¹⁸ O ⁺	1.186
³⁴ S	4,29	³³ S ¹ H ⁺	2.977
		³² S ¹ H ₂ ⁺	1.711
		¹⁶ O ¹⁸ O ⁺	1.297
		¹⁶ O ¹⁷ O ¹ H ⁺	1.000
		¹⁶ O ¹⁶ O ¹ H ₂ ⁺	904
		¹⁵ N ¹⁸ O ¹ H ⁺	866
³⁶ S	0,02	³⁶ Ar ⁺	77.350

Con la tecnología actual no es posible resolver la interferencia isobárica del argón-36 sobre el azufre-36, ya que el poder de resolución necesario para separar ambos isótopos es tremendamente elevado (>75.000). Consecuentemente, el isótopo ^{36}S no se puede monitorizar mediante ICP-MS utilizando plasmas de argón.

Los tres restantes isótopos estables de azufre (^{32}S , ^{33}S y ^{34}S) están interferidos por especies poliatómicas generadas a partir de los gases del plasma, agua y del propio azufre (formación de SH^+), si bien en todos los casos el poder de resolución necesario para evitar estas interferencias es inferior a 4.000 (ver Tabla 2). Como norma general, con los equipos ICP-MS de tipo cuadrupolo (poder de resolución próximo a 300) no es posible monitorizar ninguno de estos isótopos. La eliminación de las interferencias espectrales poliatómicas que afectan a los isótopos de azufre ^{32}S , ^{33}S y ^{34}S exige el uso de instrumentos cuadrupolares equipados con celdas de colisión-reacción [119-123] o equipos de alta resolución [124-126].

A.2.5.2.2 Discriminación de masas

La discriminación de masas es otro efecto que provoca desviaciones en la exactitud de las relaciones isotópicas medidas. Se ha demostrado que la respuesta molar observada en el ICP-MS se incrementa al aumentar la masa del isótopo medido [127]. En otras palabras, los isótopos más pesados se transmiten preferentemente con respecto a los más ligeros y por tanto existe un efecto de discriminación de masas.

La discriminación de masas en ICP-MS se origina tanto en el vacío de la interfase de extracción (efecto "orificio") como en el sistema de lentes iónicas (efectos "espacio-carga"). El efecto "espacio-carga" consiste en la repulsión mutua que sufren los iones del haz al abandonar el cono separador ("skimmer"). Por tanto, el número de iones que son transmitidos por la óptica iónica disminuye debido a que los iones más ligeros son deflectados en un mayor grado mientras que los más pesados permanecen en el centro del haz iónico. El efecto "orificio" también produce enriquecimiento en los iones más pesados. En la región situada en la interfase de extracción, entre el cono de muestreo y el cono separador, se produce un chorro supersónico de iones, átomos y moléculas que se expande en función de su energía cinética. Los iones más ligeros, con menor energía cinética, se expanden en mayor proporción que los más pesados por lo que serán absorbidos preferentemente por el sistema de vacío.

El efecto de discriminación de masas en la medida de relaciones isotópicas de un elemento por ICP-MS se suele corregir utilizando un estándar de ese elemento de composición isotópica conocida o certificada [128] u otro elemento de m/z similar

[129,130]. En todos los casos esta corrección implica el cálculo del llamado factor de discriminación de masas (K) utilizando una ecuación matemática adecuada.

A.2.5.2.2.3 Tiempo muerto del detector

El detector multiplicador de electrones secundarios (SEM) que utilizan la mayoría de equipos ICP-MS opera normalmente como contador de iones. En este modo, el pulso individual de electricidad producido por la llegada al detector de cada ión es contado y la intensidad del haz de iones se registra digitalmente en términos de cuentas por unidad de tiempo. Este tipo de operación requiere tiempos de respuesta rápidos del detector y del procesador de señal respecto a la velocidad con la que llegan los iones al detector.

Se denomina tiempo muerto del detector al tiempo que necesita el instrumento para la detección y posterior manejo electrónico de la señal. En este tiempo (en torno a unos pocos nanosegundos), el detector no es capaz de registrar nuevos iones que eventualmente alcancen al detector. Cuando la concentración del elemento medido es elevada (típicamente $> 10^6$ cuentas/s) llegarán al detector muchos iones en un intervalo de tiempo menor que el tiempo muerto, registrándose en el sistema de conteo de pulsos menos iones de los que realmente han llegado. Esto provoca pérdidas de linealidad en el detector a concentraciones elevadas de analito, que se conocen como pérdidas por tiempo muerto del detector. Este problema se agrava cuando se miden relaciones isotópicas donde las abundancias isotópicas de ambos isótopos difieren considerablemente. En estos casos, se intenta aumentar la sensibilidad instrumental para obtener buenas estadísticas de conteo para el isótopo menos abundante, y ello hace que el isótopo más abundante se vea afectado por el tiempo muerto del detector. Dado que la pérdida de cuentas es una función del número de iones que llegan al detector por unidad de tiempo, cuando se mide una relación isotópica distinta de la unidad, la pérdida de cuentas para los dos isótopos será de distinta magnitud (mayor cuanto mayor sea la diferencia entre sus abundancias isotópicas) y, por tanto, la relación isotópica medida será diferente de la real. En consecuencia, este error sistemático provoca desviaciones en la exactitud de las relaciones isotópicas obtenidas experimentalmente y por tanto este parámetro debe ser evaluado para corregir las intensidades y por consiguiente las relaciones isotópicas [131,132].

Los detectores que se utilizan en el equipo multicolector Neptune (copas de Faraday) no funcionan por conteo de iones. En este caso, cada copa está conectada

al potencial base a través de una resistencia elevada. La carga de iones positivos que alcanza la placa es neutralizada por un flujo de electrones a través de la resistencia y el potencial resultante, una vez amplificado, es la señal que se registra. Como consecuencia, dado que no se trata de una señal digital sino analógica, este tipo de detectores no presentan efecto de tiempo muerto.

A.2.5.3. Especiación elemental mediante IDA

Los equipos ICP-MS no son capaces de proporcionar información sobre las diferentes formas químicas, físicas o morfológicas en las que el elemento de interés se encuentra en una muestra determinada. Por tanto, a la hora de aplicar el análisis por dilución isotópica en el campo de la especiación elemental se necesita una separación previa de las distintas especies a determinar antes de la medida con el espectrómetro de masas.

El análisis de especiación de elementos traza se realiza normalmente recurriendo a las metodologías híbridas que acoplan una técnica de separación potente (GC, HPLC, CE, etc.) con un detector sensible y específico al elemento a determinar. El papel del ICP-MS como sistema de detección en metodologías híbridas será comentado con más detalle posteriormente.

Existen dos modalidades de dilución isotópica en el campo de la especiación: (i) dilución isotópica específica y (ii) dilución isotópica inespecífica o post-columna. Ambos modos se diferencian en el momento en el que se añade el trazador isotópico y en la forma química de este último.

A.2.5.3.1. La dilución isotópica específica

Este modo de dilución isotópica para la especiación elemental requiere el uso de un trazador que contenga la especie a analizar marcada isotópicamente. Por tanto, es necesario conocer *a priori* la composición y estructura de la especie a determinar. Existen pocas especies enriquecidas isotópicamente disponibles en el mercado y las que hay son muy caras, lo que obliga generalmente a sintetizar el compuesto de interés enriquecido isotópicamente como paso previo. En esta modalidad, la especie enriquecida se añade a la muestra al principio del proceso analítico y una vez alcanzada la mezcla total entre la especie enriquecida añadida y la especie endógena de la muestra, se consiguen todas las ventajas ofrecidas por la dilución isotópica elemental convencional.

Utilizando esta estrategia se ha desarrollado una metodología analítica que emplea compuestos enriquecidos isotópicamente en azufre para la determinación por GC-ICP-MS de compuestos de la familia del tiofeno en productos derivados del petróleo [133].

A.2.5.3.2. La dilución isotópica inespecífica o post-columna

La primera aplicación de este modo de dilución isotópica para especiación elemental fue desarrollada en 1994 para la determinación mediante HPLC-ICP-MS de complejos metálicos de cobre y molibdeno en sustancias húmicas de aguas de río [134]. La adición del trazador isotópico se realiza tras la completa separación de las diferentes especies presentes en la muestra. En este modo inespecífico, el trazador se suele añadir en una forma química distinta a las presentes en la muestra a analizar.

Esta metodología es especialmente útil cuando no se conoce con exactitud la estructura y la composición de las especies a analizar y también cuando las correspondientes especies isotópicamente enriquecidas no están disponibles comercialmente o no se pueden sintetizar. Sin embargo, mediante esta modalidad no es posible aprovechar todas las ventajas que ofrece la dilución isotópica elemental convencional. Así, cualquier pérdida de analito que ocurra antes de la mezcla con el trazador no podrá ser corregida, lo que incluye las etapas de preparación de muestra y las recuperaciones no cuantitativas en la columna cromatográfica. Además, sólo se puede aplicar cuando la eficacia de la ionización es independiente de la forma química del elemento.

En el modo inespecífico de la dilución isotópica para especiación elemental, el aporte del elemento de la muestra a la mezcla varía con el tiempo (señal transitoria) debido a la separación cromatográfica. Por tanto se ha de modificar la ecuación de la Dilución Isotópica (Ecuación 13) introduciendo el flujo másico del elemento como variable. Tras una separación cromatográfica, el eluato de la columna que contiene N_s moles de un elemento por gramo de disolución, y cuya densidad es d_s (en $\text{g}\cdot\text{mL}^{-1}$) y flujo f_s (en $\text{mL}\cdot\text{min}^{-1}$), se mezcla con un flujo adicional que contiene al trazador. Este flujo adicional f_{sp} ($\text{mL}\cdot\text{min}^{-1}$) contiene N_{sp} moles del mismo elemento por gramo de disolución. La densidad de esta disolución es d_{sp} ($\text{g}\cdot\text{mL}^{-1}$). El flujo másico total ($\text{mol}\cdot\text{min}^{-1}$) para dos isótopos a y b del elemento en la mezcla será:

$$N_S^a d_S f_S + N_{Sp}^a d_{Sp} f_{Sp} = N_m^a d_m f_m \quad \text{Ecuación 17}$$

$$N_S^b d_S f_S + N_{Sp}^b d_{Sp} f_{Sp} = N_m^b d_m f_m \quad \text{Ecuación 18}$$

Donde a es el isótopo de referencia en el eluato cromatográfico (isótopo 32) y b el isótopo más abundante en el trazador (isótopo 33). Igualmente, d_m será la densidad de la mezcla y f_m su flujo. Si dividimos la Ecuación 17 entre la Ecuación 18 obtenemos la expresión de la relación isotópica en la mezcla en cada punto del cromatograma:

$$R_m = \frac{N_S^a d_S f_S + N_{Sp}^a d_{Sp} f_{Sp}}{N_S^b d_S f_S + N_{Sp}^b d_{Sp} f_{Sp}} = \frac{N_S A_S^a d_S f_S + N_{Sp} A_{Sp}^a d_{Sp} f_{Sp}}{N_S A_S^b d_S f_S + N_{Sp} A_{Sp}^b d_{Sp} f_{Sp}} \quad \text{Ecuación 19}$$

Donde $R_m = \frac{N_m^a}{N_m^b}$ es la relación isotópica (a/b) en la mezcla, que variará con el tiempo, y $N_S^a = N_S A_S^a$, $N_{Sp}^a = N_{Sp} A_{Sp}^a$, $N_S^b = N_S A_S^b$ y $N_{Sp}^b = N_{Sp} A_{Sp}^b$; teniendo en cuenta las abundancias isotópicas de los isótopos a y b en el azufre natural (A_S^a y A_S^b) y en el trazador (A_{Sp}^a y A_{Sp}^b) respectivamente. Despejando N_S obtenemos:

$$N_S d_S f_S = N_{Sp} d_{Sp} f_{Sp} \frac{R_m A_{Sp}^b - A_{Sp}^a}{A_S^a - R_m A_S^b} \quad \text{Ecuación 20}$$

Las concentraciones N_S y N_{Sp} ($\text{mol}\cdot\text{g}^{-1}$) se pueden convertir en concentraciones en peso ($\text{g}\cdot\text{g}^{-1}$) usando las expresiones $N_S = \frac{C_S}{M_S}$ y $N_{Sp} = \frac{C_{Sp}}{M_{Sp}}$, donde C_S y C_{Sp} son las concentraciones del elemento en la muestra y trazador respectivamente (en $\text{g}\cdot\text{g}^{-1}$) y M_S y M_{Sp} son los pesos atómicos del elemento en la muestra y en el trazador respectivamente. Sustituyendo en la Ecuación 20 obtenemos:

$$C_S d_S f_S = C_{Sp} d_{Sp} f_{Sp} \frac{M_S}{M_{Sp}} \frac{A_{Sp}^b}{A_S^a} \left(\frac{R_m - R_{Sp}}{1 - R_m R_S} \right) \quad \text{Ecuación 21}$$

Si las concentraciones que aparecen en la Ecuación 21 se expresan en $\text{ng}\cdot\text{g}^{-1}$, la expresión $C_S d_S f_S$ tiene las unidades de $\text{ng}\cdot\text{min}^{-1}$ y corresponde al flujo másico del elemento que eluye de la columna, MF_S . Entonces el flujo másico puede calcularse según la ecuación:

$$MF_S = C_{Sp} d_{Sp} f_{Sp} \frac{M_S}{M_{Sp}} \frac{A_{Sp}^b}{A_S^a} \left(\frac{R_m - R_{Sp}}{1 - R_m R_S} \right) \quad \text{Ecuación 22}$$

Esta ecuación indica que si la relación isotópica en la mezcla (R_m) varía con el tiempo (por ejemplo, al eluir un compuesto de la columna cromatográfica), MF_S también variará con el tiempo. La representación de MF_S en función del tiempo será el denominado cromatograma de flujo másico. Si el flujo másico viene expresado en $\text{ng}\cdot\text{min}^{-1}$ y el tiempo en min la integración de cada pico cromatográfico nos proporcionará la masa del elemento eluída en dicho pico (en ng). La concentración en la muestra original podrá calcularse conociendo la masa (o el volumen y la densidad) de la muestra inyectada en el sistema cromatográfico.

A.2.5.4. Deconvolución de perfiles isotópicos (IPD)

A.2.5.4.1. Introducción

La metodología general de cálculo denominada “Deconvolución de Perfiles Isotópicos” se puede considerar como una plataforma común y transparente para asegurar, en todas aquellas aplicaciones que empleen isótopos estables enriquecidos, la trazabilidad de las medidas al sistema internacional de unidades y el cálculo de la incertidumbre de todo el proceso.

Esta forma de calcular en análisis por dilución isotópica presenta una serie de ventajas respecto a las ecuaciones usadas tradicionalmente. Por un lado, es una metodología general que se puede aplicar a cualquier sistema en el que se utilicen elementos o compuestos marcados isotópicamente, tanto para dilución isotópica elemental como orgánica o bioquímica. Por otro lado, permite el trabajo con múltiples perfiles isotópicos lo cual es necesario cuando se pretenden realizar estudios fundamentales de metabolismo mineral y de especiación como los llevados a cabo en la presente Tesis Doctoral. Esta metodología permite, por ejemplo, utilizar un isótopo enriquecido metabólico (añadido al organismo en estudio) y otro isótopo distinto para

la cuantificación final por dilución isotópica (**artículos científicos III, IV y V**). Asimismo, en el caso de especiación metálica se pueden corregir reacciones de interconversión de especies de una forma sencilla y elegante [135,136].

Finalmente, para el análisis de aquellos elementos que permitan trabajar con más isótopos de los estrictamente necesarios para realizar un análisis por dilución isotópica (p.e. Fe, Se, etc.), existe la posibilidad de corregir automáticamente errores sistemáticos. Así, se pueden corregir la discriminación de masas y las interferencias espectrales en ICP-MS sin necesidad de utilizar patrones certificados isotópicamente, mediante el proceso de minimización de la suma cuadrática de residuales utilizando la herramienta “Solver” en EXCEL (**artículos científicos VI y VII**).

A.2.5.4.2. Fundamento de la metodología de cálculo

En general, cuando se quiere determinar mediante análisis por dilución isotópica, en cualquiera de sus modalidades la cantidad de materia de un elemento o compuesto químico de abundancia isotópica natural (en moles, N_{nat}) presente en una determinada alícuota de la muestra, se añade a dicha alícuota una cantidad conocida de materia enriquecida isotópicamente (en moles, N_{enr}) del elemento o compuesto a determinar. La mezcla (N_m) entre el elemento o compuesto de abundancia isotópica natural y el enriquecido isotópicamente, cumplirá el balance de masas:

$$N_m = N_{nat} + N_{enr} \quad \text{Ecuación 23}$$

El balance de masas de la ecuación 23 se puede hacer también para todas y cada una de las masas que configuran el perfil isotópico del elemento o compuesto determinado. Por ejemplo, para un isótopo cualquiera i de un elemento el balance de masas sería:

$$N_m^i = N_{nat}^i + N_{enr}^i \quad \text{Ecuación 24}$$

Si se tratase de un compuesto químico, la ecuación 24 representaría el balance de masas para una masa determinada de su perfil isotópico molecular. Ya sea para un elemento o un compuesto, la ecuación 24 se puede expresar como una combinación lineal de la cantidad total del elemento o compuesto en cada uno de los perfiles

isotópicos (natural o enriquecido) y de las abundancias isotópicas conocidas o medidas de cada perfil isotópico según:

$$N_m \cdot A_m^i = N_{nat} \times A_{nat}^i + N_{enr} \times A_{enr}^i \quad \text{Ecuación 25}$$

donde A_m^i , A_{nat}^i y A_{enr}^i son las abundancias isotópicas conocidas o medidas del isótopo/masa i en cada uno de los perfiles isotópicos. Si dividimos la ecuación 25 por la ecuación 23 se obtiene la siguiente expresión matemática:

$$A_m^i = x_{nat} \times A_{nat}^i + x_{enr} \times A_{enr}^i \quad \text{Ecuación 26}$$

donde:

$$x_{nat} = \frac{N_{nat}}{N_{nat} + N_{enr}} \quad \text{y} \quad x_{enr} = \frac{N_{enr}}{N_{nat} + N_{enr}}$$

son las fracciones molares de cada uno de los perfiles isotópicos que contribuyen al perfil isotópico observado en la muestra alterada isotópicamente.

La ecuación final de la dilución isotópica se obtiene al dividir estas dos últimas expresiones:

$$\frac{N_{nat}}{N_{enr}} = \frac{x_{nat}}{x_{enr}} \quad \text{Ecuación 27}$$

Por tanto, dado que N_{enr} es conocido, para calcular la cantidad de materia en la muestra (*i.e.* N_{nat}) únicamente se tiene que determinar experimentalmente las fracciones molares de cada uno de los perfiles isotópicos presentes en la mezcla.

A.2.5.4.3. Resolución matemática

Si el elemento utilizado posee al menos 2 isótopos estables (o el compuesto utilizado posee al menos 2 masas en su perfil isotópico molecular) podemos definir una ecuación de abundancias isotópicas y fracciones molares (ecuación 26) para cada isótopo/masa. Supongamos que el elemento/compuesto posee n isótopos estables (o

masas en su distribución isotópica molecular) donde $n \geq 2$. Esa serie de ecuaciones se puede expresar, en notación matricial, como:

$$\begin{bmatrix} A_m^1 \\ A_m^2 \\ A_m^3 \\ \dots \\ A_m^{n-1} \\ A_m^n \end{bmatrix} = \begin{bmatrix} A_{nat}^1 & A_{enr}^1 \\ A_{nat}^2 & A_{enr}^2 \\ A_{nat}^3 & A_{enr}^3 \\ \dots & \dots \\ A_{nat}^{n-1} & A_{enr}^{n-1} \\ A_{nat}^n & A_{enr}^n \end{bmatrix} \begin{bmatrix} x_{nat} \\ x_{enr} \end{bmatrix} + \begin{bmatrix} e^1 \\ e^2 \\ e^3 \\ \dots \\ e^{n-1} \\ e^n \end{bmatrix}$$

Ecuación 28

En el caso de que $n > 2$ tenemos más ecuaciones que incógnitas (fracciones molares) y se ha de incluir un vector de error en la ecuación 28. Los valores de las incógnitas x_{nat} y x_{enr} y su incertidumbre se obtienen mediante ajuste por mínimos cuadrados del vector de error utilizando la técnica de mínimos cuadrados múltiples que se puede encontrar en cualquier libro básico de Quimiometría (o utilizando la función “Estimacion.Lineal” en EXCEL). El proceso de calcular las fracciones molares en sistemas como el que aparece en la ecuación 24 se viene denominando “Deconvolución de Perfiles Isotópicos” en la literatura moderna [117].

A.3. ESPECTROMETRÍA DE MASAS CON FUENTE DE PLASMA DE ACOPLAMIENTO INDUCTIVO (ICP-MS)

A.3.1. Introducción

Desde la primera publicación en 1980 del empleo de un plasma de acoplamiento inductivo (ICP) como fuente de ionización para espectrometría de masas (MS) [137], hasta el día de hoy, la técnica de ICP-MS ha experimentado un gran desarrollo y las prestaciones analíticas alcanzadas la han convertido en una de las técnicas más versátiles y poderosas para la determinación de elementos traza y ultratrazas [104,138], con aplicaciones en el análisis cuantitativo de péptidos y proteínas [139-141], metabolismo [86,142], análisis biomédico y farmacéutico [143,144] y estudios de trazabilidad [145], por citar algunas áreas. Este hecho se ve reflejado en el crecimiento exponencial observado durante los últimos 25 años en el número de trabajos publicados que utilizan un ICP-MS como detector (Figura 6).

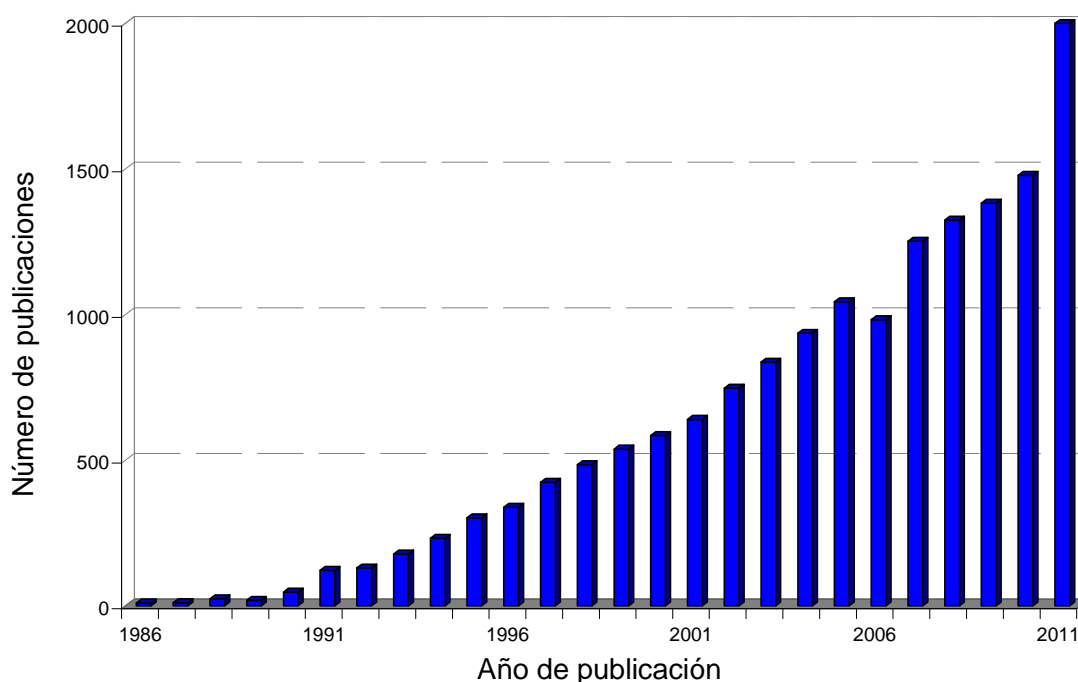


Figura 6. Crecimiento exponencial del número de publicaciones científicas utilizando ICP-MS en los últimos 25 años. Fuente Web of Science®.

En el ICP-MS, los iones del analito se generan en un plasma de acoplamiento inductivo (ICP) que se forma en una antorcha de cuarzo, consistente en tres tubos concéntricos de diámetro variable a través de los cuales fluyen corrientes de argón

A. INTRODUCCIÓN

(Figura 7). Por el tubo central de la antorcha penetra el aerosol de la muestra, generado previamente en un nebulizador. Este aerosol es arrastrado por un flujo de Ar ($0,9-1,5 \text{ L}\cdot\text{min}^{-1}$) denominado gas portador. Además, por el tubo intermedio entra un flujo de Ar auxiliar ($0-2 \text{ L}\cdot\text{min}^{-1}$) que centra el plasma, mientras que por el tubo exterior entra el flujo de Ar ($12-20 \text{ L}\cdot\text{min}^{-1}$) necesario para formar el plasma (gas plasmógeno) y refrigerar la antorcha. La antorcha está rodeada en su extremo superior por una bobina de inducción conectada a un generador de radiofrecuencias (RF). Al aplicar a la bobina una potencia de RF ($0,5-2 \text{ kW}$), se crea una corriente alterna que oscila a la frecuencia del generador (habitualmente 27 ó 40 MHz). Esta oscilación eléctrica origina en el interior de la antorcha un intenso campo electromagnético. Para iniciar el plasma, el Ar es sembrado con electrones mediante una chispa generada por un Tesla. Los electrones acelerados por el campo electromagnético (acoplamiento inductivo) chocan con otros átomos de Ar provocando nuevas ionizaciones y mayor número de electrones, produciéndose una reacción en cadena que origina el plasma. Éste se mantiene en estado estacionario por el continuo aporte de energía de RF desde el generador. El plasma resultante es una bola de gas brillante con forma anular y con una temperatura de operación entre 5.000 y 10.000 K.

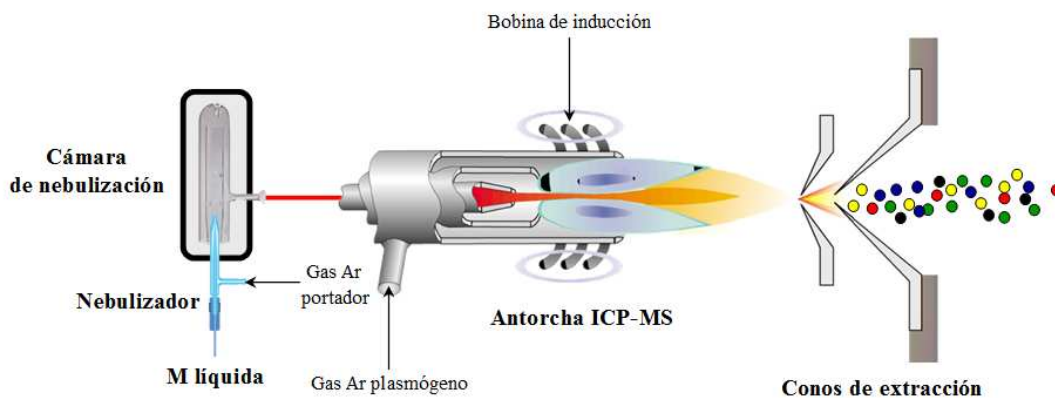


Figura 7. Esquema de una fuente de plasma de acoplamiento inductivo (ICP).

De esta manera, cuando la muestra se introduce en el centro del plasma, éste posee una energía suficiente para provocar la casi total destrucción de la matriz de la muestra y la desolvatación, vaporización, atomización e ionización de sus componentes.

Los analitos se ionizarán en mayor o menor grado en función de la densidad electrónica del plasma, la temperatura y sus diferentes potenciales de ionización, de acuerdo a la ecuación de Saha [146]. Por ello, y dado que el primer potencial de

A.3. ESPECTROMETRÍA DE MASAS CON FUENTE ICP (ICP-MS)

ionización del gas plasmógeno (argón) es de 15,8 eV y que la mayoría de los elementos de la tabla periódica tienen un primer potencial de ionización menor de 9 eV, el grado de ionización en el plasma para la mayoría de los elementos será superior al 80%. Sin embargo, los elementos con potenciales de ionización más altos y por tanto próximos al del argón, como Cl, Br, I, P, Hg y el propio azufre (10,36 eV), se ionizarán en mucha menor extensión [147].

Una vez generados los iones en el ICP, es necesario transferirlos desde el plasma, donde la temperatura es de 5.000-10.000 K y la presión de una atmósfera (760 Torr), al espectrómetro de masas que trabaja a temperatura ambiente y baja presión ($<10^{-5}$ Torr). Para ello, como se muestra en la Figura 7, se utiliza una interfase constituida por dos conos de níquel, el “*sampler*” y el “*skimmer*”, separados por una cámara de expansión en la que la presión es intermedia (1 Torr) entre la del ICP y la del alto vacío del analizador de masas. De ahí, los iones se dirigen al analizador de masas donde son separados en función de su relación masa/carga y finalmente alcanzan el sistema de detección, que típicamente es un multiplicador de electrones secundarios (SEM) o copas de Faraday en el caso del equipo ICP-MS multicolector.

El ICP como fuente de ionización produce mayoritariamente iones monopositivos de los elementos químicos presentes en la muestra. Por tanto, los espectros de masas con el ICP son sencillos y reflejan la abundancia isotópica de los elementos analizados. No obstante, dichos espectros de masas se encuentran sujetos a interferencias espectrales [148], esto es, todo ión monoatómico o poliatómico que coincide en relación masa/carga con el analito de interés, de modo que a la señal del analito se suma la señal del ión interferente. Estas interferencias espectrales pueden ser debidas a combinaciones de elementos de la matriz de la muestra o resultado de la combinación del gas plasmógeno (Ar), con los gases de la atmósfera (O_2 , N_2), con reactivos y disolventes usados para preparar las disoluciones de la muestra, y/o con la matriz de la misma (p.e. $^{40}Ar^{16}O^+$ sobre $^{56}Fe^+$, $^{16}O_2^+$ sobre ^{32}S , ^{204}Hg sobre ^{204}Pb , $^{136}Ba^{2+}$ sobre $^{68}Zn^+$, etc.). En la mayoría de los casos, la eliminación de este tipo de interferencias se puede llevar a cabo mediante equipos ICP-MS con analizadores de masas de alta resolución [124-126] o bien mediante el empleo de ICP-MS con analizadores de masas de cuadrupolo equipados con celda de reacción y/o colisión, que son más baratos que los anteriores [119-123].

A.3.2. Monitorización de azufre por ICP-MS

La determinación de azufre por ICP-MS está dificultada por la baja eficiencia de ionización del azufre en el plasma ICP y por las interferencias espectrales que afectan a todos sus isótopos estables. En primer lugar, la eficiencia de ionización del azufre en un plasma de argón se estima próxima al 10% [149], debido al alto valor de su primer potencial de ionización (10,36 eV). Además, el azufre es relativamente ligero y por tanto no se transmite de una manera tan efectiva como otros iones más pesados, lo que se traduce en una baja sensibilidad en comparación con otros elementos. Por ejemplo, los límites de detección de azufre por ICP-MS se encuentran en el orden de las partes por billón (ppb), mientras que para el Fe, Ni, y Cu (8 eV aprox.) se encuentran próximos a las partes por trillón (ppt) e incluso se puede hablar de partes por cuatrillón (ppq) para elementos más pesados como U, Th y Nb (6 eV aprox.).

En segundo lugar, como se comentó anteriormente, las interferencias espectrales afectan a todos los isótopos estables de azufre. Así, con la tecnología actual, no es posible resolver la interferencia isobárica del $^{36}\text{Ar}^+$ sobre el ^{36}S , ya que el poder de resolución necesario para separar ambos isótopos es tremendamente elevado. Consecuentemente, este isótopo no puede ser monitorizado mediante medidas de ICP-MS utilizando plasmas de argón. Hasta el comienzo de la presente Tesis Doctoral existían 3 tipos de equipos ICP-MS comerciales que permiten monitorizar el azufre y serán comentados a continuación.

A.3.2.1. ICP-MS de tipo cuadrupolo

En general, los equipos ICP-MS con analizador de masas de tipo cuadrupolo son los más empleados debido a su menor coste en comparación con otros instrumentos ICP-MS. El analizador de masas de tipo cuadrupolo está formado por cuatro barras conductoras de sección hiperbólica, alineadas paralelamente entre sí y equidistantes de un eje central imaginario, tal como se ilustra en la Figura 8. Cada pareja de barras opuestas está conectada eléctricamente y se les aplica una combinación de corriente continua (DC) y voltajes de radiofrecuencia (RF), mientras que cada pareja adyacente está eléctricamente aislada. La magnitud de cada par de voltajes de DC y RF determina la relación m/z que es capaz de describir una trayectoria estable, evitando colisionar con las barras y por tanto capaces de pasar el filtro de masas cuadrupolar hasta alcanzar el detector. Todos los demás iones chocarán con las superficies del cuadrupolo a estos valores de DC y RF y por tanto no serán detectados.

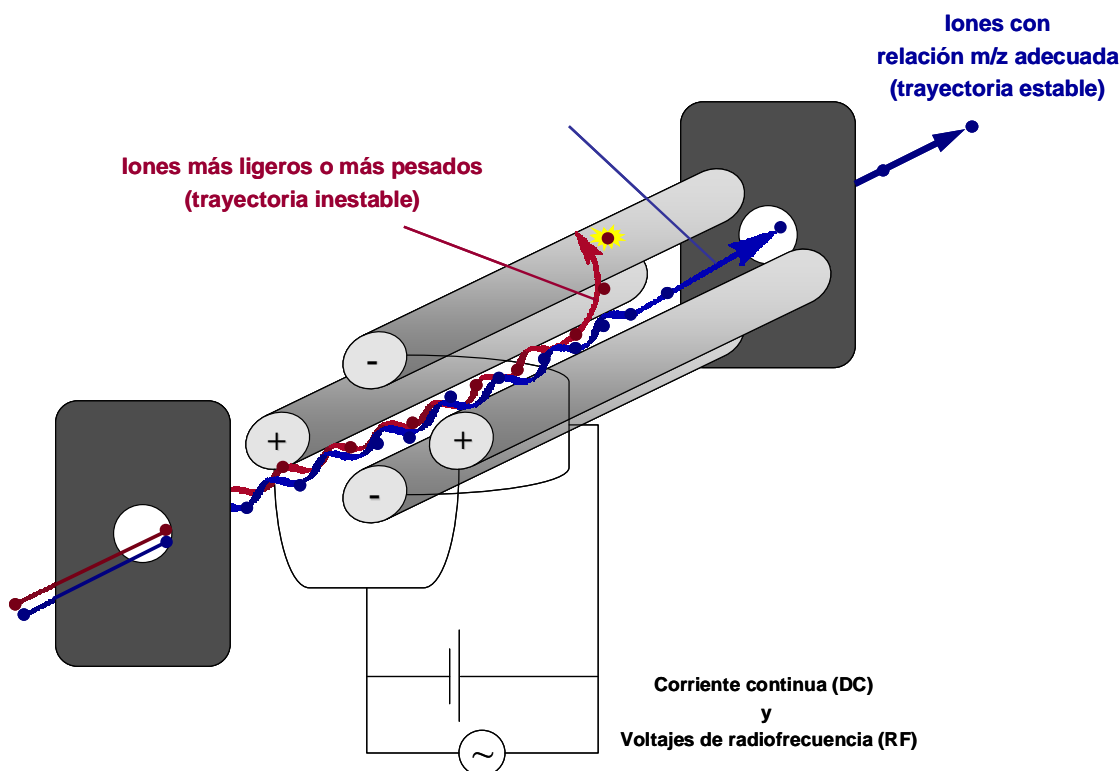


Figura 8. Esquema de un analizador de masas de tipo cuadrupolo.

Los equipos ICP-MS de tipo cuadrupolo trabajan a baja resolución. Consecuentemente, con estos analizadores de masas no es posible separar ninguno de los isótopos de azufre de sus principales interferencias poliatómicas (ver Tabla 2). Por ejemplo, el isótopo ^{32}S está interferido por la especie poliatómica $^{16}\text{O}_2^+$ altamente abundante y la resolución necesaria para separar ambos iones es de 1.801 (frente a la resolución de aproximadamente 300 que se consigue con un cuadrupolo). Para evitar este problema, algunos autores ensayaron la técnica de vaporización electrotérmica [150-152] o más recientemente sistemas de desolvatación [153,154] generando así un aerosol seco de la muestra. Alternativamente, dado que el azufre forma fácilmente óxidos estables, se puede detectar como ión molecular (SO^+) monitorizando los isótopos de azufre a masas 48, 49 y 50 que están menos interferidas [155-157]. De esta manera, se han conseguido precisiones en la medida de relaciones isotópicas de azufre ($^{34}\text{S}/^{32}\text{S}$) del orden del 1% y con límites de detección entre 34 y 270 ppb [156].

A.3.2.2. ICP-MS con celda de colisión/reacción

Los equipos ICP-MS con analizadores de masas de tipo cuadrupolo equipados con celda de colisión/reacción mejoran las prestaciones anteriores. En estos equipos

se sitúa una celda presurizada con un gas, entre las lentes iónicas y el filtro de masas cuadrupolo, lo que permite la discriminación física o química de la interferencia.

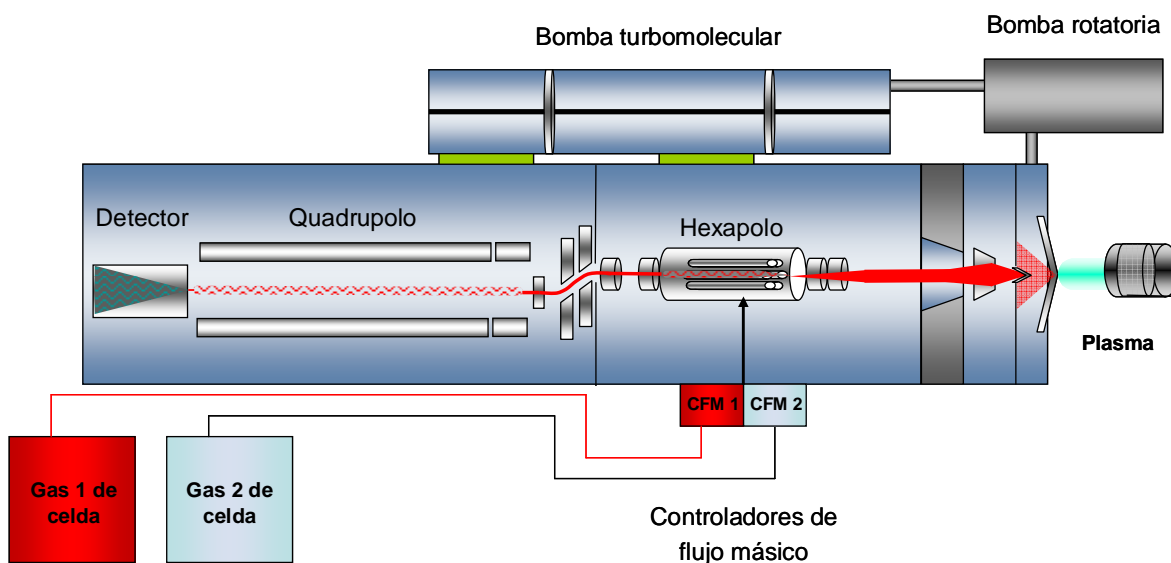


Figura 9. Esquema del equipo ICP-MS de tipo cuadrupolo equipado con celda de colisión/reacción modelo X Series 2.

Para el caso que nos ocupa, utilizando xenón (Xe) como gas de colisión [66] se pueden eliminar las especies poliatómicas de O_2^+ interferentes, lo que permite determinar los isótopos de azufre a sus masas naturales 32, 33 y 34. Asimismo, se puede utilizar oxígeno (O_2) como gas de reacción [158], lo que permite monitorizar los óxidos estables de azufre generados en la celda. Con esta instrumentación se mejoran los límites de detección (1-5 ppb aprox.) y la precisión en las relaciones isotópicas medidas (RSD 0,1-0,5%).

A.3.2.3. ICP-MS de doble enfoque (DF)

Los equipos ICP-MS de doble enfoque (DF) tanto con detección simple como los multicolectores, permiten trabajar en alta resolución (hasta $m/\Delta m$ 10.000) y por ello es posible monitorizar los isótopos 32, 33 y 34 de azufre libres de interferencias espectrales.

A.3.2.3.1. DF-ICP-MS con detección simple

Los equipos DF-ICP-MS con detección simple se introdujeron muy a finales de los años ochenta [159]. Están provistos de un sistema analizador de masas de doble enfoque, constituido por un sector magnético y un sector electrostático, los cuales dispersan a los iones de acuerdo a su momento y energía cinética, respectivamente. Como el enfoque magnético se realiza previo al electrostático, se conoce como doble enfoque con geometría Nier-Johnson inversa.

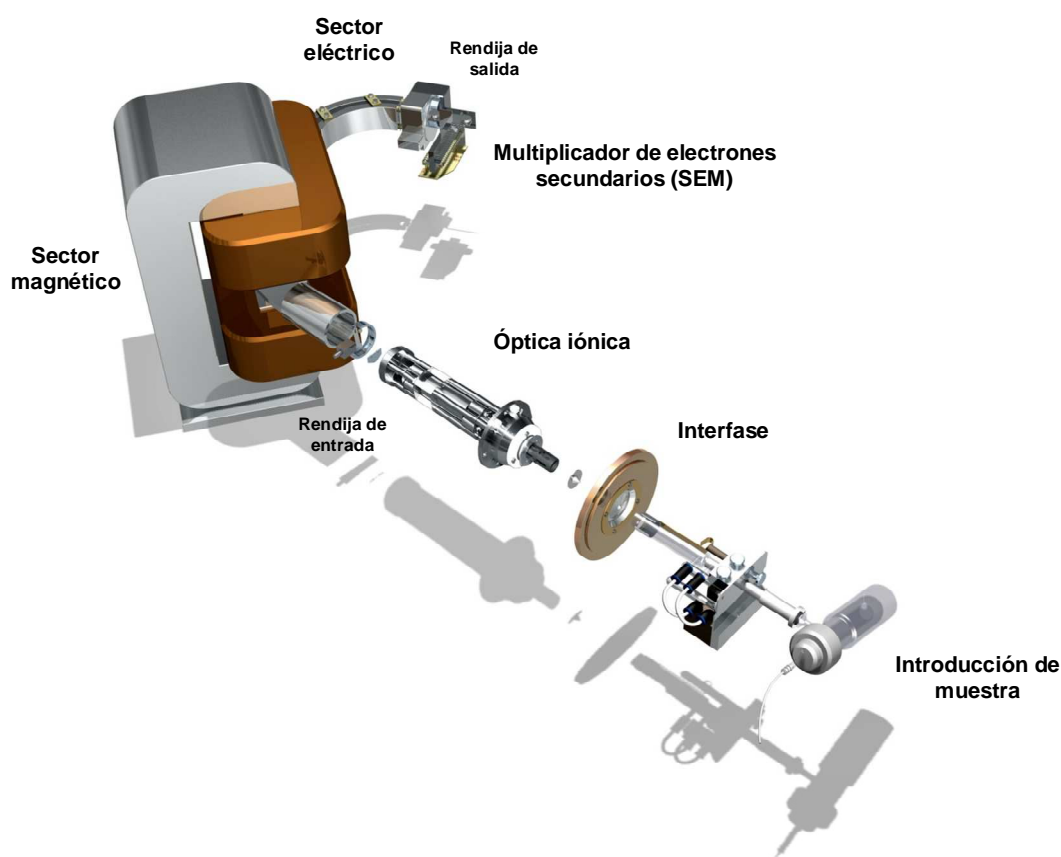


Figura 10. Esquema del equipo DF-ICP-MS modelo Element 2.

En este tipo de analizadores de masas los iones son acelerados a la salida de la fuente sometiéndolos a altísimos potenciales (de hasta -8.000 voltios) mediante una serie de placas electrostáticas que aceleran y enfocan los iones. En el sector magnético, si el campo magnético aplicado es perpendicular al vector de velocidad de los iones, estos serán obligados a describir trayectorias circulares, resultantes de la compensación de las fuerzas centrípeta y centrífuga. Por tanto, el campo magnético separa a los iones en función de su momento (masa \cdot velocidad), lo que provoca que el haz se disperse en el espacio y que cada ión tenga un radio de curvatura

determinado de acuerdo a su relación m/z . Esto conduce a que iones de una determinada relación m/z (para un valor dado de campo magnético y de potencial de aceleración) sean enfocados en la rendija de entrada del detector y los demás colisionen con el analizador y se pierdan al describir trayectorias no estables.

En el sector electrostático, cuando el ión entra en el campo describe una trayectoria circular de tal manera que la fuerza electrostática se compensa con la centrífuga, con lo que el radio de curvatura va a depender ahora no de la masa del ión, sino de su energía cinética.

Los analizadores de doble enfoque necesitan una alta energía del haz iónico para una efectiva transmisión y enfoque. Si comunicáramos esa energía tan alta al haz iónico en un cuadrupolo, los iones tendrían demasiada energía para verse afectados por los campos y no se llevaría a cabo su separación efectiva. Por otro lado, cuanto mayor es la energía del haz, menos se ve afectado por las interferencias espacio-carga que provocan la dispersión de los iones y, por tanto, la transmisión iónica es mucho mayor en este tipo de ICP-MS, lo que conduce a una mayor sensibilidad.

El equipo de doble enfoque con detección simple permite trabajar en tres tipos de resolución diferente: baja (300), media (4.000, la escogida en nuestro caso) y alta (10.000). Mediante la selección del poder de resolución adecuado, se consigue la separación de las interferencias poliatómicas a lo largo del plano focal del espectrómetro de masas.

En la Figura 11 se muestran los espectros de masas obtenidos a media resolución para m/z 32, 33 y 34 en el Element 2 utilizando una disolución de azufre de abundancia natural. Como se puede ver, los tres isótopos de azufre están afectados por la presencia de iones poliatómicos interferentes que aparecen a masas superiores que las del isótopo de interés. Sin embargo, es posible seleccionar un rango de masas donde poder medir la señal del azufre exenta de la señal de los iones interferentes. Así, tenemos equipos DF-ICP-MS con detección simple [69,129,160] con los que han sido documentados excelentes límites de detección (10 ppt), así como muy buenas precisiones en la medida de relaciones isotópicas de azufre (RSD 0,04-0,09%).

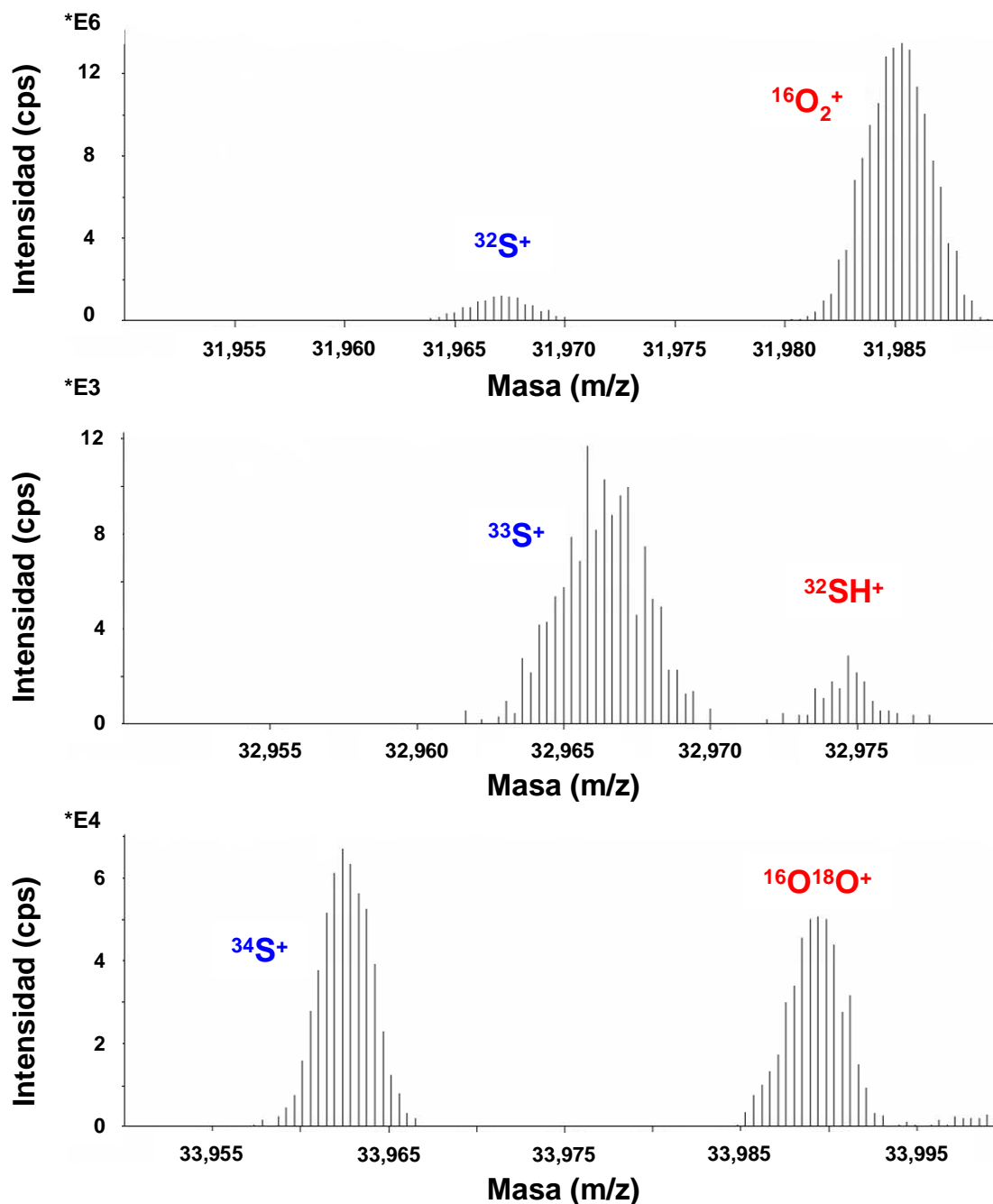


Figura 11. Espectro de masas de los isótopos de azufre ^{32}S , ^{33}S y ^{34}S obtenidos en el Element 2, donde se puede apreciar la resolución de las principales interferencias poliatómicas.

A.3.2.3.2. DF-ICP-MS multicolector

Entre las diferentes posibilidades de instrumentación de espectrometría de masas elemental disponibles comercialmente, los equipos DF-ICP-MS multicolectores son la técnica de elección para la medida de relaciones isotópicas de elevada precisión. En el año 2006 se documentaron los primeros estudios utilizando esta

instrumentación para la determinación de relaciones isotópicas de azufre donde se recogen excelentes precisiones instrumentales (desde 0,1% a <0,005%) dependiendo de la concentración de este elemento [76,161,162].

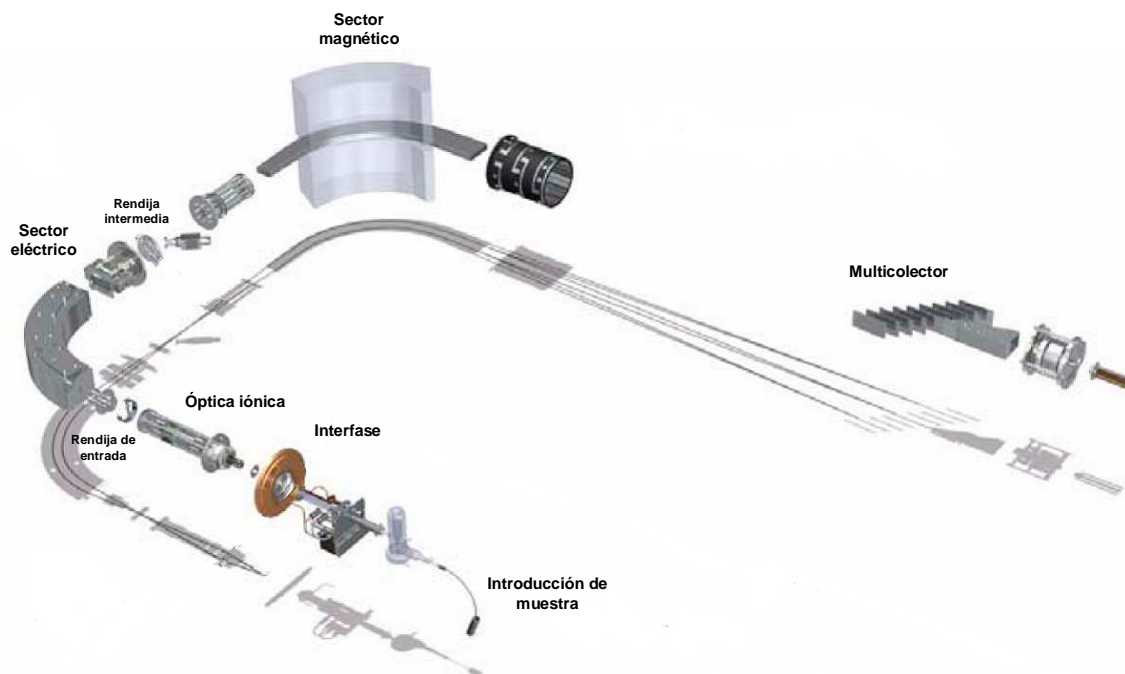


Figura 12. Esquema del equipo ICP-MS multicolector modelo Neptune.

El equipo ICP-MS multicolector se muestra esquematizado en la Figura 12. El Neptune presenta un analizador de masas de doble enfoque, formado por un sector electrostático y un sector magnético (configuración Nier-Johnson directa). Este equipo presenta la capacidad de hacer medidas en baja, media o pseudo-alta resolución; para ello tiene 3 tamaños de rendija de entrada antes del analizador electrostático.

Para conseguir la eliminación de las interferencias espectrales poliatómicas en el equipo ICP-MS multicolector, además de la selección del tamaño de rendija de entrada al analizador de masas (en nuestro caso, media resolución), es necesaria una buena colocación en la trayectoria de los iones de interés de cada uno de los colectores utilizados para la detección de dichos iones. En este equipo se consigue la discriminación de las interferencias poliatómicas debido a que se encuentran desplazadas a unas pocas centésimas de relación m/z respecto a nuestro analito. Este sistema de eliminación de interferencias poliatómicas es válido siempre y cuando éstas se encuentren desplazadas únicamente a un lado de la relación m/z del analito, lo que se cumple para aquellos elementos con m/z inferior a 80. La pseudo-resolución

de las interferencias poliatómicas que afectan a los isótopos estables de azufre utilizando un equipo MC-ICP-MS se ilustra en la Figura 13. La forma clásica de llevar a cabo medidas en alta resolución para eliminar interferencias espectrales es utilizar una rendija de entrada estrecha y una rendija de salida al detector también estrecha. El resultado son picos triangulares sin ningún tipo de zonas planas (ver Figura 11). Los perfiles de pico planos son un prerrequisito indispensable para la medida de relaciones isotópicas de elevada precisión, ya que con picos triangulares las variaciones residuales en el sector magnético o electroestático que siempre están presentes, e incluso el propio ruido instrumental, reducen la estabilidad de la señal y por tanto la precisión de la medida. Para conseguir perfiles de pico planos se necesita una rendija de entrada lo suficientemente estrecha para separar la señal del analito de la del ión interferente (30 μm), pero rendijas de salida al detector más anchas (250 μm o de baja resolución).

Lo que va a ocurrir es que primero la especie interferente más pesada llega al detector mientras nuestro analito está atrapado en la zona de masas bajas de la rendija de salida (región de la derecha en la Figura 13-i). Cuando ambas especies llegan al detector se nos forma otra zona plana cuya señal es la suma de la contribución del analito y del interferente (región media en la Figura 13-ii) y finalmente en el último plano solo contribuye nuestro analito mientras la especie interferente queda atrapada en la zona de masas altas de la rendija de salida (región de la izquierda en la Figura 13-iii).

Esto es lo que se conoce como pseudo-resolución, las señales no están perfectamente separadas, pero la gran estabilidad del imán nos permite seleccionar una zona donde medir nuestro analito libre de interferencias. Esta zona de medida se destaca en color verde en la Figura 14. Como se ha descrito anteriormente, el radio de la trayectoria descrita por un ión en el seno de un campo magnético, manteniendo fijo el valor del campo y el potencial de aceleración, es función de la relación m/z que posea. Por tanto, si se coloca un conjunto de detectores a la salida del imán, en vez de un sector eléctrico, se podría llevar a cabo la detección simultánea de un cierto número de iones generados en el plasma dentro de un rango de masas definido por la geometría del sistema. Es decir, en el equipo ICP-MS multicolector, dado un valor de campo magnético y un potencial de aceleración, sólo un rango de masas definido llevará una trayectoria estable y alcanzará simultáneamente el detector constituido por 9 copas de Faraday, de las cuales 8 son móviles y otra está fija en el canal central, posibilitando una detección multiisotópica simultánea.

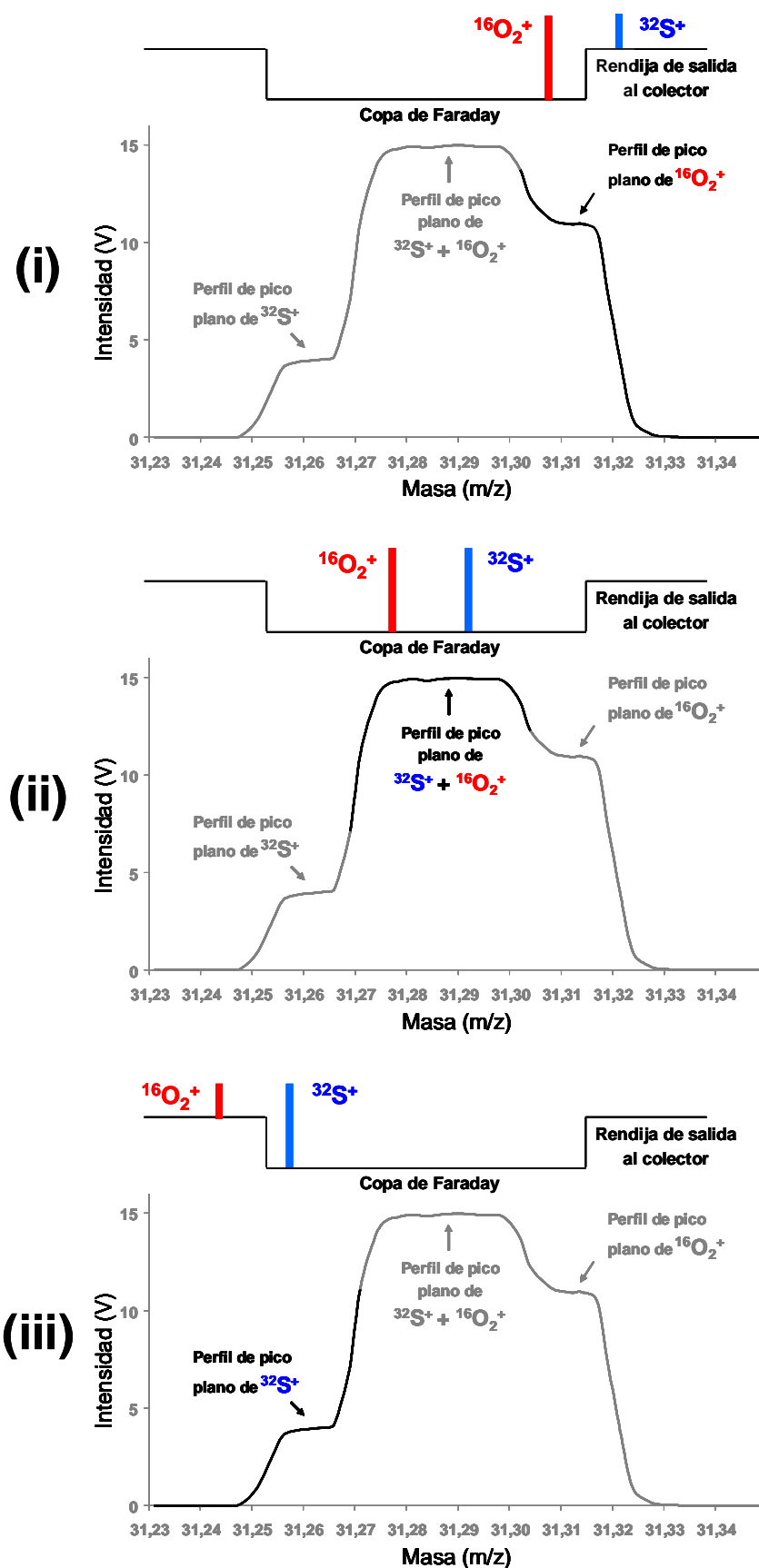


Figura 13. Pseudo-resolución de interferencias poliatómicas en el ICP-MS multicollector.

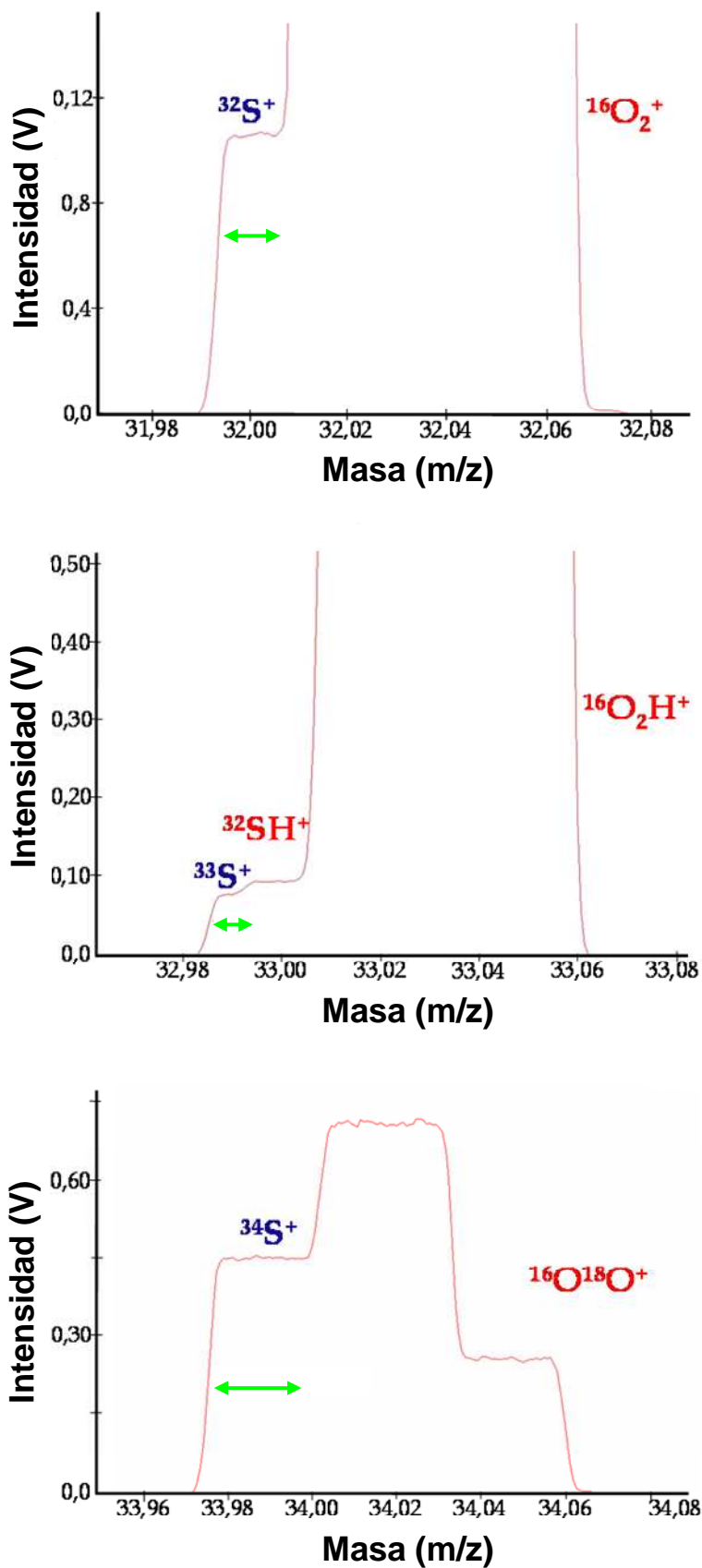


Figura 14. Espectro de masas obtenido en el ICP-MS multicolector para los isótopos de azufre ^{32}S , ^{33}S y ^{34}S .

A.3.3. El ICP-MS en metodologías híbridas

Por definición, una metodología híbrida surge de la combinación de dos o más técnicas analíticas a través de una interfase adecuada, de modo que se genera una información única e integral de la composición de la muestra y más completa que la alcanzada independientemente por cada técnica. En la actualidad, el empleo del ICP-MS como sistema de detección en multitud de metodologías híbridas se explica atendiendo a sus excelentes características como detector específico elemental, tales como: extremada sensibilidad, amplios intervalos lineales, capacidad multi-elemental y multi-isotópica y capacidad para introducir de forma continua o directa muestras gaseosas o líquidas [138,163]. Es necesario recordar que el ICP-MS no proporciona información estructural de la (bio)molécula de estudio. Siempre que se quiera identificar una biomolécula será necesario un análisis adicional, normalmente llevado a cabo con técnicas de espectrometría de masas molecular.

El ICP-MS es la técnica más utilizada como sistema de detección en las metodologías híbridas utilizadas para el análisis de especiación elemental [164,165] y están basadas en el acoplamiento de una técnica de separación poderosa con la detección por ICP-MS, lo que permite la determinación de compuestos que contengan o tengan asociado uno o varios heteroátomos medibles por ICP-MS (entendiendo por heteroátomo en un compuesto orgánico cualquier elemento distinto de C, O, H y N) [166-171]. Este heteroátomo puede estar presente en la biomolécula de forma natural o puede haber sido introducido intencionadamente. Por tanto, las principales características analíticas del ICP-MS para la caracterización de biomoléculas en muestras complejas, la convierten en una técnica complementaria ideal a las de espectrometría de masas moleculares existentes, al proporcionar información cuantitativa de gran valor.

De esta manera, y dado que la cromatografía de gases (GC) es una técnica de separación adecuada principalmente para compuestos orgánicos volátiles, la metodología híbrida GC-ICP-MS [172] ha sido aplicada en estudios de especiación de azufre en muestras de origen petroquímico [133,173,174], en el análisis de pesticidas [175] y en muestras de interés biológico previa derivatización [176]. Recientemente, se determinaron variaciones naturales de azufre en diferentes compuestos orgánicos volátiles mediante esta metodología [177]. Dado que el mal aliento está causado por varias moléculas que contienen azufre, como el sulfuro de hidrógeno H_2S , el sulfuro de dimetilo $(CH_3)_2S$ y, en especial, el metilmercaptano CH_3SH , se ha propuesto el empleo de GC-ICP-MS con detección de azufre como una herramienta innovadora para el estudio de la halitosis [178].

Asimismo, la electroforesis capilar (CE) acoplada al ICP-MS origina la metodología híbrida CE-ICP-MS [179] que ha sido utilizada con éxito para la determinación de aminoácidos que contienen azufre [180] y en estudios de especiación de metalotioneínas [181-184], una proteína de bajo peso molecular con un alto contenido en cisteínas (20 residuos), que está relacionada con mecanismos de detoxificación de metales nocivos (p.e. cadmio, mercurio, etc.).

Las metodologías híbridas HPLC-ICP-MS y LA-ICP-MS dado que han sido utilizadas en la presente Tesis Doctoral serán presentadas con más detalle a continuación.

A.3.3.1. Determinación de azufre por HPLC-ICP-MS

La enorme versatilidad del HPLC permite la separación de mezclas complejas en cada uno de sus componentes, en función de su volumen hidrodinámico (exclusión por tamaños), carga (intercambio iónico), carácter hidrofílico/hidrofóbico (fase normal o reversa) o afinidad. Sin lugar a dudas, la metodología híbrida HPLC-ICP-MS [185,186] es la que ha despertado un mayor interés en el campo de la cuantificación de biomoléculas [113,140,167,187]. El fácil acoplamiento entre el cromatógrafo de líquidos y el ICP-MS representa uno de sus mayores atractivos. Se trata de un acoplamiento sencillo y directo, dado que las velocidades de flujo de las fases móviles empleadas en la mayoría de las separaciones por HPLC, como las utilizadas en la presente Tesis Doctoral (**artículos científicos IV, V, VI y VII**), son compatibles con la velocidad de aspiración de los nebulizadores concéntricos convencionales ($1.000 \mu\text{L}\cdot\text{min}^{-1}$) o microconcéntricos ($200 \mu\text{L}\cdot\text{min}^{-1}$).

El principal inconveniente está relacionado con la incompatibilidad del ICP-MS con ciertas fases móviles comúnmente empleadas en separaciones por HPLC. Tal es el caso de fases móviles con un alto contenido en sales o disolventes orgánicos. Por un lado, es conveniente que las fases móviles posean un contenido salino inferior a 50 mM para evitar el colapso del plasma y/o la obturación del nebulizador y de los conos de la interfase. Por otro lado, el empleo de fases orgánicas es bastante incompatible con la determinación mediante HPLC-ICP-MS de elementos con elevado potencial de ionización, como es el caso del azufre. Así, la separación de péptidos y/o proteínas mediante cromatografía líquida en fase reversa [188] requiere el empleo de fases móviles con altos porcentajes de modificador orgánico (acetonitrilo o metanol) que afectan negativamente a la estabilidad del plasma, produciendo un marcado descenso en su temperatura (enfriamiento), disminuyendo su capacidad de ionización y con ello

la intensidad de la señal analítica (sensibilidad) a lo largo del gradiente de separación cromatográfica, pudiendo llegar a provocar eventualmente la extinción del plasma. Además, se generan depósitos de carbono en los conos que pueden llegar a obturarlos. Por esta razón, el porcentaje de disolvente orgánico presente en las fases móviles se mantiene normalmente por debajo del 20%.

Una alternativa prometedora consiste en reducir el flujo de la fase móvil a niveles de cromatografía capilar ($5 \mu\text{L}\cdot\text{min}^{-1}$ y 0,3 mm de diámetro interno) [189] o de nanocromatografía ($0,3 \mu\text{L}\cdot\text{min}^{-1}$ y 0,075 mm de diámetro interno) [190]. Entre sus ventajas destacan la alta eficacia conseguida en la separación, combinada con el bajo consumo de fase móvil y de muestra. Así, el bajo flujo de fase móvil hace que el plasma tenga unas características especiales, muy próximas a las de un plasma seco como el obtenido en GC-ICP-MS. Esto se traduce en una reducción importante de las interferencias poliatómicas ($^{16}\text{O}_2^+$, $^{16}\text{O}^{18}\text{O}^+$, etc.) que afectan la medida de los isótopos de azufre por ICP-MS, conduciendo a fondos más bajos y por tanto, mejores límites de detección. En este tipo de estudios, es necesario el empleo de micronebulizadores de alta eficacia que trabajen de forma óptima con los microflujos empleados [191-193].

Otra posibilidad adicional consiste en el empleo de aparatos más modernos de HPLC (denominados generalmente como UPLC) que incorporan mejoras para poder trabajar a presiones más altas (1.000 atm) lo que permite poder utilizar partículas de tamaño más pequeño en las columnas de separación cromatográfica ($< 2 \mu\text{m}$), mejorando considerablemente el tiempo de análisis en estudios de especiación [194]. Muy recientemente, se ha demostrado el potencial de esta metodología UPLC-ICP-MS para discriminar de forma cuantitativa diferentes muestras biológicas basándose únicamente en el contenido de azufre y/o sus metabolitos [195].

Antes del comienzo de la presente Tesis Doctoral el número de publicaciones relacionadas con la detección y determinación selectiva de aminoácidos, péptidos y/o proteínas en muestras de interés biológico a través de su contenido en azufre mediante la metodología híbrida HPLC-ICP-MS era realmente escaso [157,196-198]. Asimismo, no se habían descrito estudios de metabolismo empleando isótopos estables de azufre que utilizarasen el ICP-MS para su monitorización, a excepción del estudio del metabolismo de fármacos [92]. La monitorización de azufre era y sigue siendo una práctica habitual en estudios de especiación multielemental en muestras complejas de origen biológico, ya que la elución simultánea del azufre con un metal es una evidencia de que dicho metal se encuentra enlazado a una proteína o péptido [199,200]. Posteriormente, durante el transcurso de esta Tesis Doctoral, se han publicado numerosos trabajos entre los que destacan el análisis cuantitativo de

péptidos y proteínas [68,201-204], estudios con trazadores isotópicos de azufre [205,206] y aplicaciones en análisis biomédico y farmacéutico [171,207]. Las referencias más significativas sobre la determinación de azufre por HPLC-ICP-MS se recogen en el **artículo de revisión bibliográfica** que se adjunta al final de esta introducción.

A.3.3.2. Determinación de azufre por LA-ICP-MS

Para el análisis directo de muestras sólidas, la ablación láser (LA) [208] se puede utilizar como técnica de introducción de muestra al ICP-MS, generando la metodología híbrida LA-ICP-MS [209]. Conceptualmente, es un proceso muy simple: un haz láser pulsado de alta energía se focaliza sobre la superficie de la muestra a analizar en una atmósfera de gas inerte a presión atmosférica; el haz láser convierte, instantáneamente un volumen finito de la muestra sólida en un aerosol de los constituyentes (electrones, iones, moléculas y aglomerados) [210]. El aerosol generado por el haz láser (*i.e.* muestra volatilizada) se arrastra mediante una corriente de gas inerte a la fuente de iones, ICP, donde se vaporiza, atomiza e ioniza. Finalmente, los iones cargados positivamente se analizan en el espectrómetro de masas [211].

La metodología híbrida LA-ICP-MS se presenta como una técnica idónea para el análisis con resolución espacial (10-100 μm lateral y 0,1-1 μm en profundidad), al poder acoplar el gran poder de detección de la espectrometría de masas con fuente ICP, con la resolución espacial de un haz láser focalizado combinado con un sistema de movilidad en las tres dimensiones con relación a la superficie de la muestra [212]. En el caso particular del azufre, la metodología híbrida LA-ICP-MS se ha utilizado principalmente en aplicaciones geológicas para la determinación de relaciones isotópicas de azufre en materiales ricos en este elemento [161,162], para determinar concentraciones de azufre en proteínas separadas por electroforesis bidimensional en gel [213] y para generar imágenes elementales de tejidos biológicos en aplicaciones biomédicas [214].

A continuación y como punto final de esta introducción se incluye un **artículo de revisión bibliográfica** que ha sido elaborado muy recientemente sobre la medida de azufre por ICP-MS y sus aplicaciones más significativas.

A.3.4. Revisión bibliográfica sobre la medida de azufre por ICP-MS y sus aplicaciones

1 **Sulfur analysis by ICP-MS: a review**

2

3 J. Giner Martínez-Sierra, J. M. Marchante Gayón and J. I. García Alonso

4

5 Department of Physical and Analytical Chemistry, University of Oviedo, Julian

6 Clavería 8, 33006, Oviedo, Spain. E-mail: jiga@uniovi.es; Fax: +34 985103125

7

8

9

10

11 **ABBREVIATIONS**

12

13 API, active pharmaceutical ingredient;

14 capLC, capillary liquid chromatography;

15 CC, collision cell;

16 CE, capillary electrophoresis;

17 Cys, cysteine;

18 DL, detection limit;

19 DRC, dynamic reaction cell;

20 ETV, electrothermal vaporization;

21 GC, gas chromatography;

22 HPLC, high performance liquid chromatography;

23 HR, high resolution;

24 ICP-MS, inductively coupled plasma mass spectrometry;

25 ID, isotope dilution;

26 IDA, isotope dilution analysis;

27 IR, isotope ratio;

28 LA, laser ablation;

29 LC, liquid chromatography;

30 LR, low resolution;

31 MC-ICP-MS, multicollector ICP-MS;

32 Met, methionine;

33 MR, medium resolution;

34 MT, metallothionein

35 ORS, octapole reaction system;

36 Q-ICP-MS, quadrupole ICP-MS;

37 RC, reaction cell;

38 SEC, size exclusion chromatography;

39 SF-ICP-MS, sector field ICP-MS;

40 UPLC, ultra performance liquid chromatography;

41

42

43 **ABSTRACT**

44

45 In recent years the number of applications of sulfur (S) analysis using inductively coupled
46 plasma mass spectrometry (ICP-MS) as detector has increased significantly. Herein, following
47 the remarkable work of N. Jakubowsky *et al.* in 2005 regarding the speciation of sulfur¹ we
48 describe in some depth the application of ICP-MS for S analysis with emphasis placed on the S-
49 specific detection in hyphenated techniques such as HPLC, GC, CE and LA coupled on-line to
50 ICP-MS.

51

52 The different approaches available for S isotope determinations by ICP-MS are detailed.
53 Particular attention has been paid to the quantification of peptides/proteins and the analysis of
54 metalloptides/metalloproteins *via* sulfur by HPLC-ICP-MS. Likewise, the speciation analysis
55 of metal-based pharmaceuticals and metallodrugs and non-metal selective detection of
56 pharmaceuticals *via* S are highlighted. Labelling procedures for metabolic applications are as
57 well included. Finally, the measurement of natural variations in S isotope composition with
58 multicollector ICP-MS instruments is also covered in this review.

59

60

61 **DETERMINATION OF SULFUR BY ICP-MS OPERATED IN BULK MODE**

62

63 Sulfur-containing compounds are almost ubiquitous and therefore the detection of sulfur can be
64 applied in many fields such as peptide/protein analysis, pharmaceutical research (drugs and
65 metabolites), industrial analysis (petroleum matrices and steels), environment analysis
66 (pesticides), *etc.* Sulfur (S) has four stable isotopes at nominal masses of 32, 33, 34 and 36,
67 with natural isotope abundances of 94.93, 0.76, 4.29 and 0.02%, respectively². In recent years,
68 the ICP-MS technique has matured from being known as only a “metal” detector to become
69 capable of detecting most of the elements present in the periodic table. For S isotope analysis,
70 this trend has been especially boosted by the availability of collision and reaction cells and more
71 robust HR-ICP-MS instrumentation, as well as the development of suitable interface
72 technologies for the coupling of separation techniques to ICP-MS. The significant expansion in
73 this topic is reported in Figure 1 where it is shown the number of peer-reviewed papers in the
74 Web of Science® database published between 1998 and 2011 that deal with S analysis by ICP-
75 MS (search terms: sulfur and ICP-MS).

76

77 The high first ionisation potential of sulfur (10.357 eV) leads to a relatively low ionisation
78 efficiency in an argon-based plasma. In addition, S is relatively light and thus is not transmitted
79 by typical instrumental ion optics as effectively as heavier masses. As a result, current ICP-MS
80 are expected to achieve DL for sulfur in the parts-per-billion range. Despite the fact that S
81 detection is hampered by spectral interferences which are formed inside the plasma (mainly
82 oxygen dimmers), different approaches can be found in the literature regarding S isotope
83 analysis as commented below for S determinations by ICP-MS operated in bulk mode.

84

85 **(i) Quadrupole based ICP-MS instruments.** Using current ICP-MS technology, ³⁶S cannot be
86 monitored due to the fact that ³⁶S⁺ is irresolvable from the elemental isobar of ³⁶Ar⁺. Therefore
87 S concentrations and IR can be determined by ICP-MS using the remaining three isotopes at
88 masses 32, 33 and 34. A mass resolution of at least $m/\Delta m$ 1800 is needed to differentiate
89 between ³²S⁺ and ¹⁶O₂⁺ ions, which cannot be achieved by Q-ICP-MS (300 aprox.). To avoid the
90 interference problem, Naka *et al.* applied an ETV technique to generate a water-free aerosol of
91 the sample for the determination of trace amounts of S in steel³. Similarly, Resano *et al.*
92 determined impurities of S in Bisphenol A at ultratrace levels by solid sampling ETV-ICP-MS⁴.
93 In both cases ³⁴S was the isotope selected for the determination of total S by Q-ICP-MS. Yu *et al.*
94 developed an ID method for the determination of S in fossil fuels by Q-ICP-MS using ETV
95 sample introduction and a 5% N₂-Ar plasma⁵. Recently, the determination of total S in high- and
96 low-boiling petroleum products by ID with Q-ICP-MS was carried out under dry plasma
97 conditions after thermal vaporization of an isotope-diluted sample, using a ³⁴S-labelled
98 dibenzothiophene spike⁶.

99

100 The oxidation of S can be approached for a shift in the mass range and hence promoting the
101 formation of the stable SO^+ molecular ion which is less interfered. In this way, the multi-element
102 determination with on-line removal of sulfate anions in plant digests was presented⁷. The S
103 retained by the column was eluted afterwards and the total S content in digested plant solutions
104 was determined at m/z 48. In a further work, the accurate determination of $^{34}\text{S}/^{32}\text{S}$ IR in
105 aqueous solutions and in plant digests enriched in ^{34}S was achieved using m/z 48 and 50 by Q-
106 ICP-MS⁸. Kwok *et al.* combined ultrasonic nebulization with membrane desolvation to determine
107 APIs by heteroatom ICP-MS detection⁹. This approach reduced interferences sufficiently so that
108 a standard argon Q-ICP-MS could be utilized. DL for S in amoxicillin was 3 ng/mL. Feldmann
109 and coworkers demonstrated the general suitability of a desolvation system for S analysis by
110 the improvement of the sulfur DL of the used Q-ICP-MS by a factor of 2000¹⁰. Ciavardelli *et al.*
111 showed that Q-ICP-MS was a suitable technology to investigate protein phosphorylation
112 stoichiometries with high confidence and sensitivity, by quantifying P and S as oxide ions¹¹.

113

114 An alternative for the detection of S by Q-ICP-MS is to use the so-called interference standard
115 signal method evaluated by Amais *et al.* to improve the accuracy of the determination of S in
116 food samples¹², whereas plasma naturally occurring species are used to correct for variations in
117 the interference signal rather than the analyte. Subsequently, the interference standard method
118 was applied to determine S in fuel samples by Q-ICP-MS and oxide ion detection¹³.

119

120 **(ii) Quadrupole based collision/reaction cell ICP-MS.** A cell pressurized with a
121 collision/reaction gas is placed between the ion lenses and the Q mass filter in the ICP-MS
122 instrument which allows the physical or chemical discrimination of the O_2 interference. Mason *et al.*
123 reported the determination of sulfur IR and concentrations in water samples using ICP-MS
124 incorporating hexapole ion optics¹⁴. The interfering O_2^+ background ions at $m/z=32$ and $m/z=34$
125 were dramatically reduced through ion-molecule reactions with Xe gas allowing S to be
126 measured directly as its natural isotope masses. Later, Woods *et al.* used an ICP-MS
127 instrument fitted with an octopole reaction system (ORS) to directly measure the inorganic
128 contents of several biofuel materials¹⁵. Sulfur was determined by removing the O_2 interference
129 by reaction with Xe cell gas.

130

131 Oxygen can be employed as reactive gas in the cell. Bandura *et al.* detected ultratrace S as
132 SO^+ using reaction with O_2 in a DRC to oxidize S^{+16} . Likewise Yang *et al.* developed a method
133 for the routinely determination of S and other elements in steels by ICP-MS equipped with a
134 DRC¹⁷. Sulfur was determined in standard and digested sample solutions as the oxide ion
135 $^{32}\text{S}^{16}\text{O}$ at m/z 48 using the reaction of S^+ ions with O_2 in the cell.

136

137 **(iii) High resolution ICP-MS instruments.** Double focusing sector field ICP-MS either single
138 collector or multicollector with high mass resolution up to $m/\Delta m$ 10.000 allowed all major
139 spectral interferences with S to be resolved by applying a MR of about 4000. The application of

140 SF-ICP-MS was proposed for determination of S and other elements in human serum¹⁸ and for
141 the fast and sensitive determination and IR measurement of non-metals in high-purity process
142 chemicals¹⁹. Later on, Prohaska *et al.* reported the precise stable sulfur IR measurements of
143 ³⁴S/³²S for very low concentrations of S in standard solutions by SF-ICP-MS operated in MR²⁰.
144 The use of a torch with a Pt guard electrode and a microconcentric nebulizer combined with a
145 membrane desolvation unit allowed DL in solution of 0.01 ng g⁻¹, limited only by blank levels.
146 Moreover, S IR could be determined at concentration levels down to 1 ng g⁻¹ with a precision of
147 better than 0.1% relative standard deviation (RSD) (n=10). A precision of 0.04% RSD could be
148 achieved at higher concentration levels. Makishima *et al.* developed a method for the
149 determination of total S at microgram per gram levels in geological materials, applying ID with
150 SF-ICP-MS²¹. After the addition of a ³⁴S-enriched spike to the sample, oxidation of S into
151 extremely stable sulfate was performed by bromine formed by *in situ* oxidation of HBr. Evans *et al.*
152 carried out the high accuracy analysis of low level S in diesel fuel by ID SF-ICP-MS²², using
153 silicon for mass bias correction of natural IR. In the same vein, Heilmann *et al.* used a high-
154 efficiency nebulizer for direct sample injection of gasoline and related fuel samples in a SF-ICP-
155 MS²³. The accurate determination of S was carried out by IDMS after the preparation of a
156 micro-emulsion consisting of the corresponding organic sample and an aqueous ³⁴S-enriched
157 spike solution with additions of tetrahydronaphthalene and Triton X-100. Later, an analytical
158 procedure for complete separation of sulfate in aqueous solutions and precise sulfur IR
159 determination using SF-ICP-MS was developed by You *et al.*²⁴. The use of a membrane
160 desolvation system allowed them to work at LR for rapid, sensitive and precise sulfur IR
161 determination in water samples. At the same time, Hearn *et al.* described a comparison of high
162 accuracy ID techniques for the measurement of low level S in gas oils by three metrology
163 institutes²⁵. ICP-MS in combination with microwave digestion was then exploited in the
164 certification of two new diesel fuel reference materials. Furthermore, a high ratio IDMS
165 calibration technique for chemical metrology was developed²⁶. It was applied for the analysis of
166 a diesel fuel sample with a very high analyte concentration (approximately 4000 mg g⁻¹ S).

167

168 Among the different elemental MS instrumentation available, multicollector ICP-MS is the
169 technique of choice whenever high precision sulfur IR measurements are required. Sulfur
170 isotopes can become locally enriched or depleted through a variety of kinetic and
171 thermodynamic factors, as reported by the IUPAC. Thus, measurable differences in S isotopic
172 composition, which often occur around the third or fourth significant figure, can be used as a
173 kind of natural "fingerprinting", providing information about the geographic, chemical, and
174 biological origin of substances. Sulfur isotopic composition of selected S-bearing materials is
175 reported in Figure 3. The use of MC-ICP-MS for sulfur IR measurements has proven to
176 overcome precision limitations of sequential mode measurements, enabling instrumental
177 precision between 0.1% and <0.005% depending on S concentration. For the measurement of
178 natural variations in S isotope composition Clough *et al.* developed an accurate and precise
179 method for the determination of δ³⁴S measurements of S in bottled mineral waters by pneumatic

180 nebulization sample introduction MC-ICP-MS²⁷. Later, a systematic comparison of $\delta^{34}\text{S}$
181 measurements by MC-ICP-MS and the evaluation the full uncertainty budget using two different
182 metrological approaches was reported²⁸. It was highlighted that typical expanded uncertainties
183 when measuring $\delta^{34}\text{S}$ values of $\sim 1\%$ would be fit for purpose for authenticity and/or counterfeit
184 detection studies. Likewise, a direct procedure for the measurement of S isotope variability in
185 samples containing high amounts of dissolved organic matter was developed²⁹, showing the
186 potential of the method to estimate the natural variability of S in foods and beverages.

187

188 Martínez-Sierra *et al.* applied a MC-ICP-MS instrument operating in bulk mode to perform
189 precise and accurate sulfur IR measurement focused on the characterisation in isotope
190 composition and concentration of enriched ^{33}S and ^{34}S spikes and ^{34}S -labelled yeast³⁰. In a very
191 recent paper, Mann *et al.* reported the determination of S concentrations by ID MC-ICP-MS in
192 synthetically prepared mixtures using a ^{33}S -enriched spike material³¹. Likewise, Makishima *et al.*
193 examined the analytical performance of MC-ICP-MS, employing amplifiers with a 10(12) ohm
194 resistor, for bulk S determination in biological and geological samples³².

195

196 **iv) Triple Quad ICP-MS.** In a very recent publication, a completely new way of polyatomic
197 interference removal for detection of S in ICP-MS based on the concept of tandem mass
198 spectrometry typically used in molecular MS was presented³³. In brief, the first Q can be
199 operated as 1 amu window band-pass mass filter to select target analyte ions (^{32}S and its on-
200 mass polyatomic interferences). Thus, only selected ions enter the cell and react with O_2 ,
201 reducing the interferences produced by matrix ions and background noise. The product ion
202 formed for the target, $^{48}\text{SO}^+$, could then be detected with enhanced sensitivity and selectivity.

203

204 **HYPHENATED TECHNIQUES: HPLC-ICP-MS**

205

206 Sulfur is an essential trace element present in multitude of biologically important compounds. In
207 particular, S is present in the proteinogenic aminoacids Cys and Met, and therefore most of the
208 proteins and their corresponding tryptic peptides can be detected and determined via their S
209 content using ICP-MS detection. Among the different hyphenated approaches, nowadays
210 HPLC-ICP-MS is the technique of choice for sulfur speciation particularly in biological material
211 due to the mainly aqueous and polar nature of biological fluids³⁴. In 1988 Jiang *et al.* reported
212 for the first time the separation of inorganic sulfates and S-containing aminoacids by LC and
213 detection on-line as $^{34}\text{S}^+$ by ICP-MS³⁵. More than a decade afterwards, Divjak *et al.* used ICP-
214 MS as element-specific detector for sulfide, sulfite, sulfate, and thiosulfate after their on-line LC
215 separation³⁶. The sulfur-containing anions were detected as SO^+ at m/z 48 with a Q-ICP-MS
216 tuned for the production of high oxide ratios.

217

218 **Analysis of metallopeptides/metalloproteins by HPLC-ICP-MS**

219

220 The most widely used approach to identify the metal bound to a protein is through HPLC-ICP-
221 MS³⁷. The analytical methodologies for metalloproteomics and heteroatom-tagged proteomic
222 studies were discussed in an excellent review with a focus on S sensitive detection by ICP-
223 MS³⁸.

224

225 Sulfur assimilation and production of sulfur-containing compounds play critical roles in many
226 biological processes, including the role of S containing compounds such as glutathione and
227 phytochelatin in trace element homeostasis in plants³⁹.

228

229 The speciation analysis of MT-like proteins of the mussel *Mytilus edulis* at basal levels by SEC-
230 ICP-MS was carried out⁴⁰. Sulfur was measured at MR in a SF-ICP-MS. Likewise, the molecular
231 weight fractions that contained particular elements of interest at trace levels in aqueous extracts
232 of proteins from liver were investigated⁴¹.

233

234 Koplík *et al.* investigated soluble species of S, P, Se and eight metals in soybean flour and
235 common white bean seeds by SEC-ICP-MS⁴². Sulfur specific chromatograms were obtained
236 measuring intensities of ⁴⁸SO⁺ oxide ions. Later, the simultaneous determination of S, Fe, Zn
237 and P in barley grain tissues by both SEC and ion pairing LC-ICP-MS was carried out⁴³.
238 Oxygen was added to the ORS of the ICP-MS, thus greatly improving the sensitivity of S,
239 measured as ⁴⁸SO⁺. Recently, a comparative study of 25 element concentrations (including S)
240 by SF-ICP-MS and binding by SEC-ICP-MS in transgenic and non-transgenic soybean seeds
241 has been conducted⁴⁴.

242

243 Hann *et al.* developed a methodology for the determination of metal-sulfur ratios in
244 metalloproteins⁴⁵. Separation of metalloproteins from inorganic impurities was carried out *via*
245 SEC and the simultaneous determination of Fe/S and Mn/S ratios on transient signals was
246 performed with both SF-ICP-MS and ICP-MS with DRC technology. Subsequently, they
247 investigated the metal integration in native and recombinant copper proteins⁴⁶. SEC and IC
248 separation protocols were implemented for hyphenated ICP-MS analysis. The determination of
249 stoichiometric S/Cu ratios by SEC-ICP-MS and IC-ICP-MS was performed measuring sulfur
250 (³²S¹⁶O⁺) using O₂ as reaction gas in the DRC. Similarly, El Balkhi *et al.* used S detection by
251 ICP-MS to calibrate SEC columns without UV detection. This simple SEC-ICP-MS method was
252 applied for plasma copper proteins in plasma healthy subjects and an untreated Wilson disease
253 patient⁴⁷.

254

255 Yoshida *et al.* detected an urinary sulfur-containing metabolite produced by intestinal bacteria
256 following oral administration of dimethylarsinic acid to rats⁴⁸. To examine whether the metabolite
257 contained S or not, the detection mass was set to m/z 75 (⁷⁵As⁺) and m/z 34 (³⁴S⁺), and
258 determined by HPLC coupled to CC ICP-MS. Later, Hansen *et al.* ascribed the S nature of the
259 metabolite due to the coelution of m/z 34 (³⁴S) and m/z 48 (³²S¹⁶O) and the arsenic peak (m/z

260 75) using Q-ICP-MS⁴⁹. Afterwards, the simultaneous detection of S and As in thioarsenicals
261 using xenon-based CC ICP-MS in combination with HPLC was applied to fortified sample of
262 NIST freeze dried urine⁵⁰. Feldmann and coworkers developed a method for the quantitative
263 determination of S and As in arseno-peptide complexes by HPLC-ICP-MS [10]. A critical
264 assessment of current analytical methodology regarding the quantification of phytochelatins and
265 their metal(loid) complexes has been very recently published⁵¹.

266

267 The simultaneous speciation of S and Se in *Allium* plants by HPLC coupled with an ICP-MS
268 equipped with an ORS in which S was monitored at m/z 34 was reported⁵². Wang *et al.*
269 established a method of SEC-ICP-MS combined with post-column IDA for the determination of
270 metalloproteins and S-containing proteins in the brain cytosol of maternal and infant rats after *in*
271 *utero* exposure to low-doses of MeHg⁵³. The enriched spikes included ³⁴S, ⁶⁵Cu, ⁶⁷Zn and ¹⁹⁸Hg
272 and O₂ was used as a reactive gas in order to determine S in the hexapole CC ICP-MS. Caruso
273 and coworkers developed a method for the screening of the main chemical warfare hydrolysis
274 degradation products of S mustards using reversed-phase HPLC-ICP-MS equipped with
275 collision/reaction cell technology for element-specific detection of S at m/z 32⁵⁴.

276

277 The cysteine-rich peptide hormone hepcidin was analysed *via* S detection using ICP-MS after
278 capLC for separation of the species⁵⁵. SF-ICP-MS was used for hepcidin determination in urine
279 samples by online ID using a ³⁴S post-column spike. The quality of water soluble quantum dots
280 (QD) and their bioconjugates was studied as well by HPLC-ICP-MS⁵⁶. The ³²S profile obtained
281 by SEC coupled to SF-ICP-MS was used to obtain an approximate bioconjugate stoichiometry
282 (biomolecule/QD), information highly demanded today for reliable quantitative immunoassays.
283 Recently, a method for the direct and quantitative determination of dissolved organic S in
284 natural organic matter by HPLC-ICP-MS has been presented⁵⁷.

285

286 **Quantification of peptides/proteins *via* sulfur by HPLC-ICP-MS**

287

288 The potential of ICP-MS strategies for absolute protein quantification is a topic of fast growing
289 interest⁵⁸⁻⁶⁰. The role of S and sulfur IDA in quantitative protein analysis was detailed in 2008 in
290 a high quality review⁶¹. At the same time, Prange and coworkers presented S as natural
291 element tag for the quantitative analysis of biomolecules⁶². In fact, the quantification of S-
292 containing peptides and proteins by HPLC coupled to ICP-MS offers an alternative method for
293 quantitative proteomics. Provided that the protein sequence is known (number of S-containing
294 amino acids, *i.e.* Cys and Met) the protein amount can then be directly calculated from the
295 determined S content in a certain protein fraction.

296

297 In the pioneering work of Wind *et al.* the determination of the phosphorylation degree in
298 phosphoproteins and phosphopeptides containing Cys and/or Met residues by the simultaneous
299 measurement of S and P in proteins by ICP-MS was introduced⁶³. SF-ICP-MS was used at a

300 MR of 4000, with low solvent load on the plasma by use of capLC at 4 $\mu\text{L}/\text{min}$ ensuring good DL
301 for $^{32}\text{S}^+$ and $^{31}\text{P}^+$. The stoichiometric P to S ratio was experimentally determined by capLC-ICP-
302 MS and converted into the degree of phosphorylation using protein/peptide sequence
303 information. Subsequently, they demonstrated the concept of protein quantification by capLC-
304 ICP-MS and S detection by using insulin as a model analyte⁶⁴.

305

306 A method for absolute quantification of proteins via S by SEC coupled to ICP-MS with a
307 hexapole CC was developed⁶⁵. The absolute quantity of the model proteins bovine serum
308 albumin (BSA), superoxide dismutase (SOD), and MT-II was calculated by the ID equation
309 using a ^{34}S enriched post-column spike and the content of S in the proteins. The DL for BSA,
310 SOD, and MT-II were 8, 31, and 15 pmol, respectively. The ratios of S/Cu and S/Zn in the
311 proteins were also determined. In parallel, Lobinski and co-workers presented species
312 unspecific IDA by nanoHPLC-ICP-MS for absolute quantification of S-containing peptides in
313 protein tryptic digests⁶⁶. Their approach made use of pre-column addition of the $^{34}\text{SO}_4^{2-}$ spike,
314 while the interferences with the monitored $^{32}\text{S}^+$ and $^{34}\text{S}^+$ were reduced using a Q-ICP-MS fitted
315 with a xenon filled CC. Additionally, the potential of sulfur IDA in nanoHPLC-ICP-MS was
316 presented as generic tool for absolute protein quantification⁶⁷. Later, the coupling of capLC and
317 SF-ICP-MS to the separation and determination of standard proteins via S detection was
318 applied⁶⁸. Post-column IDA using a $^{34}\text{SO}_4^{2-}$ spike was demonstrated as a promising label-free
319 approach for absolute protein quantifications by the analysis of two certified reference materials.

320

321 In a very recent publication, a dedicated sample preparation protocol for the quantitative
322 analysis of the proteinogenic S containing amino acids Met and Cys by LC-ICP-MS was
323 reported⁶⁹. Met and Cys were derivatised to methionine sulfone and cysteic acid by oxidation
324 with performic acid prior protein hydrolysis. Anion exchange LC enabled the separation of all
325 relevant S species detected on m/z $^{32}\text{S}^{16}\text{O}$ by ICP-MS using O_2 as the reaction gas. More
326 recently, the use of a new triple quadrupole ICP-MS has provided the lowest DL ever reported
327 for the analysis of S-containing species previously separated by capHPLC.

328

329 **Speciation analysis of metal-based pharmaceuticals and metallodrugs by HPLC-ICP-MS**

330

331 The application of hyphenated techniques as tools for speciation analysis of metal-based
332 pharmaceuticals and metallodrugs has been very recently reviewed⁷⁰. Due to the multielement
333 capabilities of ICP-MS, data on both the metal(lloid) from the drug and other intrinsic elements
334 (*i.e.* S) can be recorded simultaneously, providing initial information about the stoichiometry of
335 possible drug-biomolecule interactions.

336

337 In order to gain a deeper insight into the interactions of reactive metabolites with S-containing
338 molecules Corcoran *et al.* investigated the metabolic fate of the chlorinated xenobiotic
339 diclofenac *via* the specific detection of S and Cl by HPLC-ICP-MS⁷¹. Later, the determination of

340 S-containing impurities in cimetidine drug substance at mass fractions below 0.1% relative to
341 cimetidine by reversed-phase HPLC with SF-ICP-MS was carried out⁷². The use of element-
342 specific detection via HPLC-ICP-MS for Br-, Cl-, and S-containing compounds was approached
343 as an alternative to metabolite detection and profiling after the administration of 4-bromoaniline
344 in rat urine⁷³. Likewise a HPLC-ICP-MS methodology with S-specific detection for obtaining
345 metabolite profiles in rat urine for the drug omeprazole administered as a 1:1 mixture of ³²S and
346 ³⁴S-labelled material was developed⁷⁴. Analysis based on the monitoring of the
347 chromatographic eluent at either m/z 48 (for ³²S) or m/z 50 (for ³⁴S) by reaction of S with O₂ in
348 the hexapole CC of the ICP-MS provided a facile method for metabolite profiling. In this vein it
349 was investigated the metabolic fate of 3-chloro-4-fluoroaniline in rat following intraperitoneal
350 administration of the drug⁷⁵. Metabolite profiling in urine samples was carried out using HPLC-
351 ICP-MS with Cl-35 and S-34 specific detection.

352

353 Pt-containing drugs are used as anticancer pharmaceuticals and show a strong affinity for thiol-
354 containing substances (e.g. S aminoacids). Therefore, researchers have investigated the
355 interactions of Pt-containing drugs with proteins and other possible binding sites within the
356 organism. Stefánka *et al.* developed an HPLC-CP-MS method that utilized a DRC-ICP-MS
357 instrument for the simultaneous detection of S (³²S¹⁶O⁺) and Pt. They investigated the reaction
358 of cisplatin with the S-containing Met⁷⁶. The determined Pt/S stoichiometry was employed for
359 characterization of the formed adducts.

360

361 Gammelgaard and coworkers described a LC-ICP-MS method for the simultaneous detection of
362 S and Se in selenotrisulfides⁷⁷. Both S and Se were reacted with O₂ in the DRC and detected
363 as oxides. S/Se elemental ratios and S and Se IR were determined, showing the potential of the
364 developed method for the characterisation and quantification of biomolecules and drug
365 metabolites. Subsequently, they separated and identified the S-Se compound S-
366 (methylseleno)cysteine in intestinal epithelial cells incubated with methylseleninic acid⁷⁸. The
367 Se-S ratio was confirmed to be 1:1 by simultaneous monitoring of Se and S as the oxides by
368 LC-ICP-MS.

369

370 An on-line 2-dimensional SEC/anion exchange LC-ICP-MS methodology was developed to
371 characterize the interaction of a ruthenium-based anticancer drug with human plasma proteins
372 *in vitro* and *in vivo*⁷⁹. The stoichiometry of the drug-protein binding was determined through the
373 molar Ru/S ratio. To monitor the signal of S, ³²S was converted to ⁴⁸SO in the DRC using O₂ as
374 reaction gas. Later, a fast column switching LC x LC setting in combination with elemental
375 detection for screening the interaction of metallodrugs with proteins in biological samples was
376 reported⁸⁰. Absolute DL in the pmol-range were obtained for proteins considering the hetero-
377 elemental tag S, which was detected as SO⁺ employing DRC technique. Recently, an
378 anticancer drug candidate of Ru was analyzed by CE and SEC/anion exchange LC-ICP-MS in
379 mouse plasma after intravenously administration⁸¹. The performance of the analytical

380 methodology was compared and the interaction of drug with mouse plasma proteins
381 characterized *in vivo*. The majority of Ru was bound to albumin and the stoichiometry of the
382 drug-protein binding was determined through the molar Ru/S ratio.

383

384 **Non-metal selective detection of pharmaceuticals by HPLC-ICP-MS**

385

386 ICP-MS can be advantageously applied in pharmaceutical and biomedical analysis especially
387 during the drug development and quantitative analysis of metabolites⁸². The state-of-the-art of
388 ICP-MS for the determination of inorganic impurities in drugs and pharmaceuticals was
389 reported⁸³. At the same time, the application of ICP-MS in drug metabolism studies was
390 reviewed⁸⁴. HPLC-ICP-MS is making significant inroads for non-metal selective detection of
391 pharmaceuticals⁸⁵. The analysis of several pharmaceutical compounds by reversed phase LC-
392 ICP-MS was carried out⁸⁶. The S-containing drugs of formula $C_{19}H_{16}N_2O_2S$ and $C_{20}H_{26}N_2O_3S$
393 and an impurity (C_8H_6BrNS) were detected at m/z 34 in a Q-ICP-MS. The group of Vanhaecke
394 *et al.* investigated glutathione-trapped reactive drug metabolites of clozapine recording S and Cl
395 traces by reversed phase HPLC-ICP-MS⁸⁷. DRC-ICP-MS was found to be unsuitable for the
396 monitoring of two S isotopes in an organic matrix with HPLC-ICP-MS due to ArC^+ interferences.
397 Thus they used HPLC-SF-ICP-MS to clearly differentiate between the non-reactive metabolites
398 of the drug and the reactive metabolites, bound to glutathione. In a very recent paper the
399 determination of S-containing drug metabolites from *in vitro* and *in vivo* metabolism studies by
400 LC-ICP-MS has been reported⁸⁸.

401

402 HPLC coupled to MC-ICP-MS was approached in two different publications for the analysis of
403 genuine and counterfeit pharmaceuticals for the extracted active ingredients of both ViagraTM
404 (sildenafil citrate) and the antiviral drug HeptodinTM (lamivudine)^{89,90}.

405

406 The potential of UPLC-ICP-MS as a fast technique for speciation analysis was introduced by
407 Bendahl *et al.* in 2005 using Se as an example⁹¹. A methodology for quantitative drug
408 bioanalysis for the determination of two S-containing drugs in the serum and synovial fluid of
409 inflammatory arthritis patients was approached⁹². The DL by UPLC-ICP-MS was 0.45 ng/mL of
410 S detected as oxide in the DRC. Recently, Thompson *et al.* utilized UPLC-ICP-MS to profile a
411 range of different bio-fluids and tissue extracts for S and P-containing metabolites⁹³.
412 Additionally, MacDonald *et al.* developed a methodology by UPLC-ICP-MS with S-specific
413 detection to detect and quantify the glutathione-clozapine adducts produced *via* the *in vitro*
414 formation of reactive metabolites⁹⁴.

415

416 **³⁴S-enriched labelling procedures and further detection by HPLC-ICP-MS**

417

418 Tracer studies on the metabolism of S have been carried out traditionally using radioactive ³⁵S
419 with a half-life of 87.5 days. The application of enriched stable isotopes as tracers in biological

420 systems has been recently discussed⁹⁵. In metabolism and in metabolism-mediated toxicity
421 studies (e.g., by formation of GSH conjugates) both ³³S and ³⁴S could be used as tracers due to
422 their low isotope abundance in natural sulfur. Heteroisotope and heteroatom tagging with ³⁴S-
423 enriched Met in cell-free protein synthesis was evaluated by Ogra *et al.*⁹⁶. ³⁴S-Met was
424 synthesised and the chemical and isotopic purities were confirmed by HPLC-ICP-MS. Recently,
425 the analysis of S-containing small molecular weight biomolecules in ³⁴S-labelled yeast was
426 introduced by Martinez-Sierra *et al.*⁹⁷. Different mass spectrometric platforms were compared in
427 terms of analytical figures of merit, proving the validity of the HPLC-ICP-MS approach for
428 isotopic tracer studies. Subsequently, they reported for the first time the use of ³⁴S-labelled
429 yeast for S metabolic tracer experiments in laboratory animals⁹⁸. Quantitative determination of
430 tracer/tracee ratios using HPLC-ICP-MS were performed by a dual isotope procedure in which
431 enriched ³³S was employed as quantification spike. A general scheme of the dual isotope
432 procedure using S enriched stable isotopes and isotope pattern deconvolution (IPD) with ICP-
433 MS detection is reported in Figure 2. The developed procedure opened the way for future
434 metabolic studies in which healthy and diseased animals are compared for the discovery of
435 novel biomarkers. Pfeffer *et al.* described a novel ³⁴S labelling procedure that enabled *in vivo*
436 quantification of intracellular fluxes of recombinant protein under “production like” conditions⁹⁹.
437 The stable S isotope ³⁴S was administered as sodium sulfate during chemostat cultivations of
438 the yeast *Pichia pastoris* and the intra- and extracellular sulfur 32 to 34 ratios of purified
439 recombinant protein were measured by HPLC coupled to SF-ICP-MS.

440

441 **HYPHENATED TECHNIQUES: GC-ICP-MS**

442

443 ICP-MS coupled on line with GC can be advantageously exploited in studies of S volatile
444 (bio)species and hence there are already some applications of S-containing species determined
445 by GC-ICP-MS. For example, the determination of volatile S compounds (VSCs) in human
446 breath by GC-ICP-MS was proposed by Sanz-Medel and coworkers¹⁰⁰. The same authors
447 developed a selective and sensitive method with S-specific detection for the determination of
448 total homocysteine (after derivatisation) in human serum by GC-ICP-MS¹⁰¹. Likewise, as a
449 promising tool to perform phytoremediation studies, the simultaneous monitoring of volatile S
450 and Se species from Se accumulating plants using solid-phase microextraction for sample
451 introduction was approached¹⁰². A sensitive and highly selective methodology for the
452 determination of a wide range of pesticides, based on the simultaneous element-specific
453 determination of S, P, Cl, Br and I by GC-ICP-MS was developed by Profröck *et al.*¹⁰³. The
454 method was applied to the analysis of five different real samples extracted from fruits and
455 vegetables offering the possibility of using GC-ICP-MS for rapid screening of hetero-element
456 containing compounds in an environmentally relevant sample matrix.

457

458 Sulfur is one of the most abundant heteroelements in crude oils and petroleum matrices¹⁰⁴. The
459 volatility and the relatively low molecular mass of S compounds in petroleum, favoured GC with

460 ICP MS detection for speciation analysis¹⁰⁵. In this vein, the speciation of S in hydrocarbon
461 products by GC-ICP-MS was proposed¹⁰⁶, providing specific information on S-containing
462 compounds present in petroleum products at the ng g⁻¹ range. Later, Geiger *et al.* applied a GC-
463 ICP-MS methodology for the sensitive analysis of total S as well as S speciation in various
464 hydrocarbon matrices¹⁰⁷.

465

466 Heumann and coworkers developed a species-specific ID GC-ICP-MS method for accurate
467 determination of thiophene and dibenzothiophene derivatives in low- and high-boiling petroleum
468 products¹⁰⁸. For the ID step ³⁴S-labelled thiophene, dibenzothiophene, and mixed
469 dibenzothiophene/4-methyldibenzothiophene spike compounds were synthesized on the
470 milligram scale from elemental ³⁴S-enriched sulfur. The authors pointed out the especially
471 usefulness of the method for highly accurate determinations of corresponding S species in
472 standards and reference materials or for validation of other analytical techniques. Subsequently,
473 they developed a species-unspecific ID GC-ICP-MS method for S multispecies quantification in
474 petroleum products¹⁰⁹, using a single ³⁴S-labelled dimethyldisulfide spike compound. This
475 methodology was proposed for S multispecies determinations on a routine basis.

476

477 The analysis of natural variations in the isotopic compositions of S (as $\delta^{34}\text{S}$ measurements) of
478 gaseous SF₆ standards using GC hyphenated to MC-ICP-MS was performed¹¹⁰. Later, it was
479 demonstrated the coupling of GC and MC-ICP-MS as a simple and robust method for
480 measuring the $\delta^{34}\text{S}$ values of individual organosulfur compounds within complex environmental
481 samples (crude oil)¹¹¹.

482

483 **HYPHENATED TECHNIQUES: CE-ICP-MS**

484

485 The determination of S-to-metal(loid) ratios using the multi-element capacity of ICP-MS can be
486 used to universally characterize the stoichiometric composition of metalloprotein complexes,
487 since the number of S atoms in the target protein is known from the amino acid sequence. CE-
488 ICP-MS is considered as a powerful tool for the analysis of intact metal-containing and
489 metalbinding proteins¹¹². The role of this hyphenated technique for studying interactions
490 between metals and biomolecules has been reviewed elsewhere¹¹³. Metallothioneins (MTs)
491 have been the most frequently analyzed proteins with CE-ICP-MS¹¹⁴. MTs are small cysteine-
492 rich proteins (20 Cys residues) of about 6 kDa size optimized for binding of divalent cations
493 such as Zn²⁺, Cd²⁺ or Cu²⁺, which have widespread functions in homeostasis of both essential
494 and toxic metals. Due to the element-specific detection, matrix components do not interfere with
495 ICP-MS, which makes the analyses rather straightforward. Prange *et al.*¹¹⁵ published the first
496 work in which CE-ICP-MS was applied in comparative studies of the distributions of the MT
497 isoforms MT-1, MT-2, and MT-3 at a non-induced level in human real samples taken from
498 patients with Alzheimer's disease and from a control group. The same authors applied on-line
499 ID in combination with CE-ICP-MS for the quantification of MTs *via* S measurements¹¹⁶.

500

501 Schaumlöffel *et al.* reported the characterization and quantification of MT isoforms based on the
502 combination of an on-line species unspecific ID method with CE-ICP-MS¹¹⁷. MT isoforms were
503 separated by CE and the elements S, Cu, Zn, and Cd were detected simultaneously by ICP-
504 MS. MT from rabbit liver and a further purified MT-1 isoform were quantified by determination of
505 S, and the stoichiometric compositions of the metalloprotein complexes were characterized by
506 determination of their S-to-metal ratios. The separation of MTs isoforms was improved by Wang
507 *et al.* by applying surface-modified capillaries¹¹⁸. On-line IDA using a multi-isotope spike (³³S,
508 ¹⁰⁶Cd, ⁶⁵Cu, ⁷⁰Zn) combined with CE-ICP-MS indicated the stoichiometric molar metal contents
509 in the MT complexes. Similarly, the determination of metal complexes with MT induced in the
510 liver of a rat exposed to intravenously administered Cd²⁺ was applied¹¹⁹. CE-ICP MS allowed
511 the separation of four mixed-metal complexes with one or more MT isoforms. IDA using a multi-
512 isotope spike (³³S, ¹⁰⁶Cd, ⁶⁵Cu, ⁷⁰Zn) was developed for the accurate quantification of the MT
513 content in each of the species and the determination of the stoichiometry of the metal complex.
514 The separation and simultaneous element-specific detection of S, Cd, Cu and Zn by CE-ICP-
515 MS in commercially available MT preparations and MT-like proteins extracted from liver
516 samples of bream (*Abramis brama*) was carried out¹²⁰.

517

518 Yeh *et al.* developed a method for the determination of S-containing amino acids in urine and
519 nutritive complement samples by CE-ICP-MS¹²¹. Additionally, the determination of the
520 stoichiometric Zn/protein ratio for the *Aeromonas hydrophila* metallo beta-lactamase AE036 was
521 performed¹²². CE was used to separate free Zn ions from the Zn bound to the metalloprotein
522 and ICP-MS was used as S and Zn specific detector.

523

524 **HYPHENATED TECHNIQUES: LA-ICP-MS**

525

526 The application of LA-ICP-MS allows precise, relatively fast and spatially resolved
527 measurements of major, minor and trace elements as well as IR measurements with minimal
528 sample preparation and hence, it offers superior technology for direct solid sampling in
529 analytical chemistry¹²³. The spatial resolution of S isotope analysis in solid samples provides a
530 powerful insight into geological and biological processes that cannot be obtained using
531 traditional bulk analytical techniques. The group of Becker *et al.* developed a method for the
532 direct determination by LA-ICP-MS of S and P concentrations in small protein spots separated
533 by two-dimensional (2D) gel electrophoresis¹²⁴. Subsequently the method was applied to the
534 multielement determination in separated protein spots using S as the internal standard element
535 for quantification purposes¹²⁵. LA-ICP-MS has been successfully applied as a powerful imaging
536 technique to produce quantitative images of detailed regionally specific element distributions in
537 thin tissue sections of rodent or human¹²⁶. Specifically, a method for 2D screening of S in a
538 cryo-section of rat brain tissue for the detection of a small size tumor was developed¹²⁷. Later
539 on, it was applied for 2D screening of S and other elements in the cross section of the

540 hippocampus of human brain samples¹²⁸. It was pointed out the potential of the method to help
541 physicians to better understand the chemical basis of many brain diseases. The same authors
542 developed an imaging mass spectrometric method using LA-ICP-MS to determine heavy metal
543 distribution in longitudinal tissue sections of a marine snail¹²⁹. Together with the imaging of
544 metals the distribution of S was analysed, showing an inhomogeneous distribution for all
545 elements investigated.

546

547 Boulyga *et al.* developed an accurate, sensitive and fast method for the determination of S
548 traces in different petroleum products such as “sulfur free” premium gasoline, diesel fuel and
549 heating oil by ID LA-ICP-MS using ³⁴S-labelled dibenzothiophene as a spike compound¹³⁰.
550 Subsequently, an ID methodology by LA-ICP-MS for the direct multi-element determination of S,
551 Cl and heavy metals in powdered coal samples was approached¹³¹ using ³⁴S-enriched sulfate in
552 an aqueous multi-element spike solution.

553

554 The determination of S concentrations in single quartz-hosted fluid inclusions by LA-ICP-MS
555 was accomplished¹³². Subsequently, the precisions and accuracies of *in situ* LA-ICP-MS
556 microanalysis of S, Cl and Br in single fluid inclusions were determined¹³³. Recently, the
557 detection of trace amounts of S, P and Cl by LA-ICP-MS to identify local defects in coated
558 glasses was carried out¹³⁴.

559

560 Sulfur is a major matrix element and relatively homogeneously distributed in hair. Thus, S as
561 ³²S¹⁶O⁺ was successfully used as internal standard under suitable reaction gas conditions to
562 simultaneously monitor heavy-metal intoxication (Hg and Pt) in single hair by LA-ICP-MS¹³⁵.
563 Additionally, S was used to normalize Pb intensity and to correct for variations in ablation
564 efficiency and plasma condition to quantitatively determine Pb distribution along a single human
565 hair strand by LA coupled to a Q-ICP-MS¹³⁶. Santamaria-Fernandez *et al.* reported the
566 measurement of longitudinal variations of sulfur IR in single hair strands using LA-MC-ICP-
567 MS¹³⁷. It was proved the ability of the method to resolve longitudinal differences in S isotopic
568 composition and hence showing potential as a tool for tracking recent geographical movements
569 or applied to human identification.

570

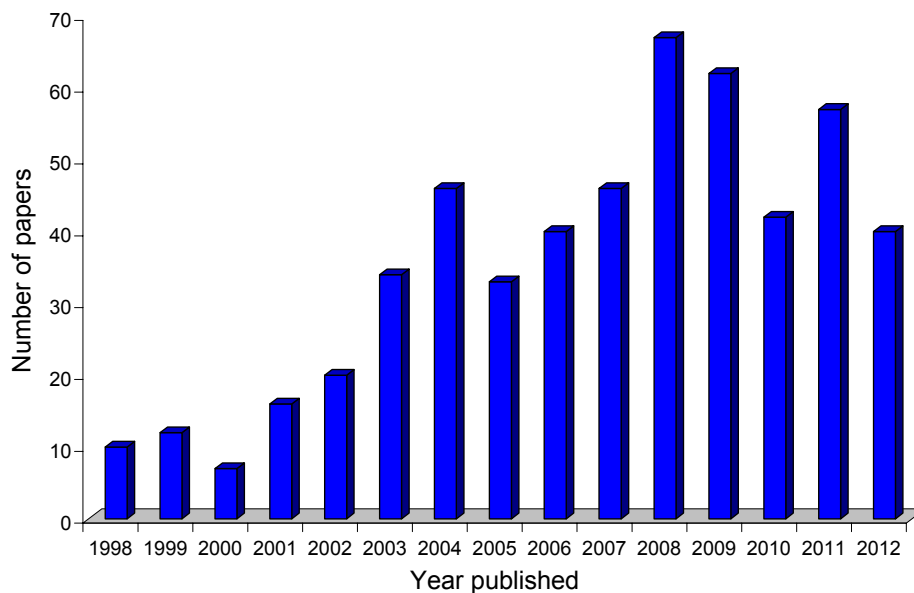
571 LA sample introduction in combination with the determination of $\delta^{34}\text{S}$ measurements of S by
572 MC-ICP-MS has been applied for the analysis of the bulk tablet of genuine and counterfeit
573 pharmaceuticals Viagra^{TM27} and the antiviral drug Heptodin^{TM89,90}.

574

575 The presence of S in nearly all natural environments makes the S isotopic composition
576 (expressed in terms of $\delta^{34}\text{S}$) a very important geochemical tracer for the interpretation of
577 geological and environmental processes. In this way, Mason *et al.* developed a method for the
578 accurate and precise measurement of S isotopes (³²S, ³³S, ³⁴S) in S-rich solid materials by LA-
579 MC-ICP-MS¹³⁸. Five pyrite (FeS₂) mineral samples were analysed, showing the validity of the

580 technique for the accurate analysis of sulfide minerals and the potential importance of *in situ*
581 *versus* bulk methods for targeting the desired part of a sample for S stable isotope analysis. In a
582 similar vein, the *in situ* S isotope analysis by LA-MC-ICP-MS was applied to hydrothermal
583 sulfides to resolve minor variations in $\delta^{34}\text{S}$ across growth zoning in pyrite¹³⁹. Afterwards,
584 Craddock *et al.* applied the LA-MC-ICP-MS technique for the determination of $^{34}\text{S}/^{32}\text{S}$ IR in a
585 wide range of S-bearing minerals¹⁴⁰, highlighting its usefulness for geologic samples with
586 complex matrix and for which HR *in situ* analysis is critical.
587
588

589



590

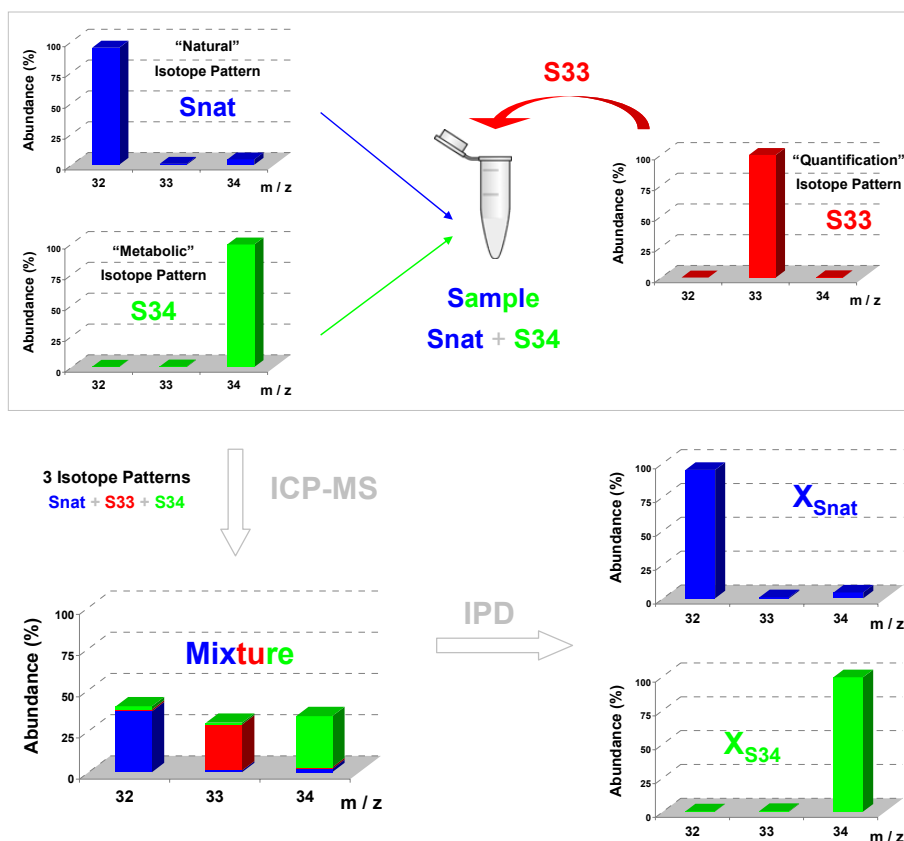
591 **Figure 1.** Number of peer-reviewed papers listed in the Web of Science® database over the
592 last 15 years on sulfur analysis by ICP-MS (search terms in topic: sulfur and ICP-MS).

593

594

595

596



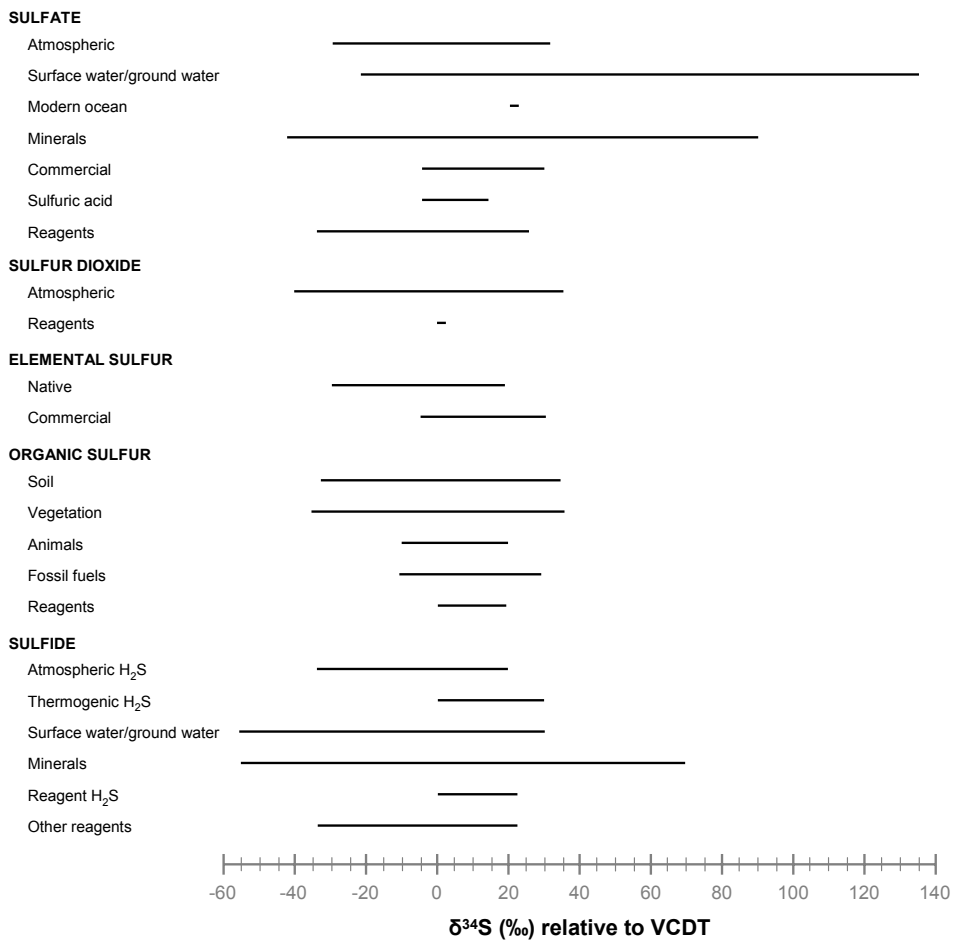
597

598

599 **Figure 2.** General workflow in ICP-MS analysis using sulfur enriched stable isotopes and
 600 isotope pattern deconvolution (IPD) for metabolic studies. For more details see references
 601 [30,97,98].

602

603



604

605

606 **Figure 3.** Sulfur isotopic composition of selected sulfur-bearing materials adapted from
 607 reference [2].

608

- 1 N. Jakubowski, N. Mihalopoulos, S. Mann and W. D. Lehmann. **Speciation of sulfur** pp 378-407 in *Handbook of elemental speciation II: species in the environment, food, medicine & occupational health*. R. Cornelis, H. Crews, J. Caruso and K. G. Heumann. © 2005, John Wiley & Sons, Ltd.
- 2 J. R. De Laeter, J. K. Bohlke, P. De Bièvre, H. Hidaka, H. S. Peiser, K. J. R. Rosman and P. D. P. Taylor. **Atomic weight of the elements: Review 2000**. *Pure Appl. Chem.* 2003, 75, 683-800.
- 3 H. Naka and D. C. Grégoire. **Determination of trace amounts of sulfur in steel by electrothermal vaporization - inductively coupled plasma mass spectrometry**. *J. Anal. At. Spectrom.*, 1996, 11, 359-363.
- 4 M. Resano, M. Verstraete, F. Vanhaecke, L. Moens and J. Claessens. **Direct determination of sulfur in Bisphenol A at ultratrace levels by means of solid sampling-electrothermal vaporization-ICP-MS**. *J. Anal. At. Spectrom.*, 2001, 16, 793-800.
- 5 L. L. Yu, W. R. Kelly, J. D. Fassett and R. D. Vocke. **Determination of sulphur in fossil fuels by isotope dilution electrothermal vaporization inductively coupled plasma mass spectrometry**. *J. Anal. At. Spectrom.*, 2001, 16, 140-145.
- 6 J. Heilmann and K. Heumann. **Sulfur trace determination in petroleum products by isotope dilution ICP-MS using direct injection by thermal vaporization (TV-ICP-IDMS)**. *Anal. Bioanal. Chem.*, 2009, 393, 393-397.
- 7 A. A. Menegario and M. F. Gine. **On-line removal of anions for plant analysis by inductively coupled plasma mass spectrometry**. *J. Anal. At. Spectrom.*, 1997, 12, 671-674.
- 8 A. A. Menegario, M. F. Gine, J. A. Bendassolli, A. C. S. Bellato and P. C. O. Trivelin. **Sulfur isotope ratio ($^{34}\text{S}:$ ^{32}S) measurements in plant material by inductively coupled plasma mass spectrometry**. *J. Anal. At. Spectrom.*, 1998, 13, 1065-1067.
- 9 K. Kwok, J. E. Carr, G. K. Webster and J. W. Carnahan. **Determination of active pharmaceutical ingredients by heteroatom selective detection using inductively coupled plasma mass spectrometry with ultrasonic nebulization and membrane desolvation sample introduction**. *Appl. Spectrosc.*, 2006, 60, 80-85.
- 10 K. Bluemlein, E. M. Krupp and J. Feldmann. **Advantages and limitations of a desolvation system coupled online to HPLC-ICP-QMS/ES-MS for the quantitative determination of sulfur and arsenic in arseno-peptide complexes**. *J. Anal. At. Spectrom.*, 2009, 24, 108-113.
- 11 D. Ciavardelli, P. Sacchetta, G. Federici, C. Di Illio and A. Urbani. **Protein phosphorylation stoichiometry by simultaneous ICP-QMS determination of phosphorus and sulfur oxide ions: A multivariate optimization of plasma operating conditions**. *Talanta*, 2010, 80, 1513-1525.
- 12 R. S. Amais, G. L. Donati and J. A. Nobrega. **Application of the interference standard method for the determination of sulfur, manganese and iron in foods by inductively coupled plasma mass spectrometry**. *Anal. Chim. Acta*, 2011, 706, 223-228.

- 13 G. L. Donati, R. S. Amais and J. A. Nóbrega. **Interference standard and oxide ion detection as strategies to determine phosphorus and sulfur in fuel samples by inductively coupled plasma quadrupole mass spectrometry.** *J. Anal. At. Spectrom.*, 2012, 27, 1274-1279.
- 14 P. R. D. Mason, K. Kaspers and M. J. van Bergen. **Determination of sulfur isotope ratios and concentrations in water samples using ICP-MS incorporating hexapole ion optics.** *J. Anal. At. Spectrom.*, 1999, 14, 1067-1074.
- 15 G. D. Woods and F. I. Fryer. **Direct elemental analysis of biodiesel by inductively coupled plasma-mass spectrometry.** *Anal. Bioanal. Chem.*, 2007, 389, 753-761.
- 16 D. R. Bandura, V. I. Baranov and S. D. Tanner. **Detection of ultratrace phosphorus and sulfur by quadrupole ICPMS with dynamic reaction cell.** *Anal. Chem.*, 2002, 74, 1497-1502.
- 17 C. H. Yang and S. J. Jiang. **Determination of B, Si, P and S in steels by inductively coupled plasma quadrupole mass spectrometry with dynamic reaction cell.** *Spectrochim. Acta Part B*, 2004, 59, 1389-1394.
- 18 J. Riondato, F. Vanhaecke, L. Moens and R. Dams. **Determination of trace and ultratrace elements in human serum with a double focusing magnetic sector inductively coupled plasma mass spectrometer.** *J. Anal. At. Spectrom.*, 1997, 12, 933-937.
- 19 Wildner H. **Application of inductively coupled plasma sector field mass spectrometry for the fast and sensitive determination and isotope ratio measurement of non-metals in high-purity process chemicals.** *J. Anal. At. Spectrom.*, 1998, 13, 573-578.
- 20 T. Prohaska, C. Latkoczy and G. Stingeder. **Precise sulfur isotope ratio measurements in trace concentration of sulfur by inductively coupled plasma double focusing sector field mass spectrometry.** *J. Anal. At. Spectrom.*, 1999, 14, 1501-1504.
- 21 A. Makishima and E. Nakamura. **Determination of total sulfur at microgram per gram levels in geological materials by oxidation of sulfur into sulfate with in situ generation of bromine using isotope dilution high-resolution ICPMS.** *Anal. Chem.*, 2001, 73, 2547-2553.
- 22 P. Evans, C. Wolff-Briche and B. Fairman. **High accuracy analysis of low level sulfur in diesel fuel by isotope dilution high resolution ICP-MS, using silicon for mass bias correction of natural isotope ratios.** *J. Anal. At. Spectrom.*, 2001, 16, 964-969.
- 23 J. Heilmann, S. F. Boulyga and K. G. Heumann. **Accurate determination of sulfur in gasoline and related fuel samples using isotope dilution ICP-MS with direct sample injection and microwave-assisted digestion.** *Anal. Bioanal. Chem.*, 2004, 380, 190-197.
- 24 You CF and M. D. Li. **Precise determination of sulfur isotopic ratio in aqueous solutions by inductively coupled plasma mass spectrometry.** *J. Anal. At. Spectrom.*, 2005, 20, 1392-1394.
- 25 R. Hearn, M. Berglund, M. Ostermann, N. Pusticek and Taylor P. **A comparison of high accuracy isotope dilution techniques for the measurement of low level sulfur in gas oils.** *Anal. Chim. Acta*, 2005, 532, 55-60.

- 26 R. Hearn, P. Evans and M. Sargent. **Development of a high ratio isotope dilution mass spectrometry calibration technique for chemical metrology.** *J. Anal. At. Spectrom.*, 2005, 20, 1019-1023.
- 27 R. Clough, P. Evans, T. Catterick and E. H. Evans. **$\delta^{34}\text{S}$ measurements of sulfur by multicollector inductively coupled plasma mass spectrometry.** *Anal. Chem.*, 2006, 78, 6126-6132.
- 28 R. Santamaria-Fernandez and R. Hearn. **Systematic comparison of delta(34)S measurements by multicollector inductively coupled plasma mass spectrometry and evaluation of full uncertainty budget using two different metrological approaches.** *Rapid Commun. Mass Spectrom.*, 2008, 22, 401-408.
- 29 J. Giner Martínez-Sierra, R. Santamaria-Fernandez, R. Hearn, J. M. Marchante Gayón and J. I. García Alonso. **Development of a direct procedure for the measurement of sulfur isotope variability in beers by MC-ICP-MS.** *J. Agric. Food Chem.*, 2010, 58, 4043-4050.
- 30 J. Giner Martínez-Sierra, F. Moreno Sanz, P. Herrero Espílez, J. M. Marchante Gayón and J. I. García Alonso. **Biosynthesis of sulfur-34 labelled yeast and its characterisation by multicollector-ICP-MS.** *J. Anal. At. Spectrom.*, 2007, 22, 1105-1112.
- 31 J. L. Mann, R. D. Vocke and W. R. Kelly. **Determination of low-level (sub-microgram) sulfur concentrations by isotope dilution multi-collector inductively couple plasma mass spectrometry using a ^{33}S spike and internal normalization for mass bias correction.** *Rapid Commun. Mass Spectrom.*, 2012, 26, 1175-1180.
- 32 A. Makishima and E. Nakamura. **High-resolution MC-ICPMS employing amplifiers with a 10(12) ohm resistor for bulk sulfur determination in biological and geological samples.** *J. Anal. At. Spectrom.*, 2012, 27, 891-895.
- 33 S. Diez Fernández, N. Sugishama, J. Ruiz Encinar and A. Sanz-Medel. **Triple quad ICP-MS (ICPQQQ) as a new tool for absolute quantitative proteomics and phosphoproteomics.** *Anal. Chem.*, 2012, 84, 5851-5857.
- 34 T. Wang. **Liquid Chromatography - Inductively Coupled Plasma Mass Spectrometry (LC-ICP-MS).** *J. Liq. Chromatogr. Relat. Technol.*, 2007, 30, 807-831.
- 35 S. J. Jiang and R. S. Houk. **Inductively coupled plasma mass spectrometric detection for phosphorus and sulfur compounds separated by liquid chromatography.** *Spectrochim. Acta Part B: Atomic Spectroscopy*, 1988, 43, 405-411.
- 36 B. Divjak and W. Goessler. **Ion chromatographic separation of sulfur containing inorganic anions with an ICP-MS as element-specific detector.** *J. Chromatogr. A*, 1999, 844, 161-169.
- 37 W. Shi and M. R. Chance. **Metallomics and metalloproteomics.** *Cell. Mol. Life Sci.*, 2008, 65, 3040-3048.
- 38 J. Szpunar. **Advances in analytical methodology for bioinorganic speciation analysis: metallomics, metalloproteomics and heteroatom-tagged proteomics and metabolomics.** *Analyst*, 2005, 130, 442-465.

- 39 G. Na, D. E. Salt. **The role of sulfur assimilation and sulfur-containing compounds in trace element homeostasis in plants.** *Environ. Exp. Bot.*, 2011, 72, 18-25.
- 40 C. N. Ferrarello, M. R. Fernández de la Campa, J. F. Carrasco and A. Sanz-Medel. **Speciation of metallothionein-like proteins of the mussel *Mytilus edulis* at basal levels by chromatographic separations coupled to quadrupole and double-focusing magnetic sector ICPMS.** *Anal. Chem.*, 2000, 72, 5874-5880.
- 41 J. Wang, D. Dreessen, D. R. Wiederin and R. S. Houk. **Measurement of trace elements in proteins extracted from liver by size exclusion chromatography-inductively coupled plasma-mass spectrometry with a magnetic sector mass spectrometer.** *Anal. Biochem.*, 2001, 288, 89-96.
- 42 R. Koplík, H. Pavelková, J. Cincibuchová, O. Mestek, F. Kvasnicka and M. Suchánek. **Fractionation of phosphorus and trace elements species in soybean flour and common white bean seeds by size exclusion chromatography-inductively coupled plasma mass spectrometry.** *J. Chromatogr. B*, 2002, 770, 261-273.
- 43 D. P. Persson, T. H. Hansen, K. H. Laursen, J. K. Schjoerring and S. Husted. **Simultaneous iron, zinc, sulfur and phosphorus speciation analysis of barley grain tissues using SEC-ICP-MS and IP-ICP-MS.** *Metallomics*, 2009, 1, 418-426.
- 44 L. R. V. Mataveli, P. Pohl, S. Mounicou, M. A. Z. Arruda and J. Szpunar. **A comparative study of element concentrations and binding in transgenic and non-transgenic soybean seeds.** *Metallomics*, 2010, 2, 800-805.
- 45 S. Hann, G. Koellensperger, C. Obinger, P. G. Furtmüller and G. Stingeder. **SEC-ICP-DRC and SEC-ICP-SFMS for determination of metal-sulfur ratios in metalloproteins.** *J. Anal. At. Spectrom.*, 2004, 19, 74-79.
- 46 S. Hann, C. Obinger, G. Stingeder, M. Paumann, P. G. Furtmüller and G. Koellensperger. **Studying metal integration in native and recombinant copper proteins by hyphenated ICP-DRC-MS and ESI-TOF-MS capabilities and limitations of the complementary techniques.** *J. Anal. At. Spectrom.*, 2006, 21, 1224-1231.
- 47 S. El Balkhi, J. Poupon, J. M. Trocello, F. Massicot, F. Woimant and O. Laprevote. **Human plasma copper proteins speciation by size exclusion chromatography coupled to inductively coupled plasma mass spectrometry. Solutions for columns calibration by sulfur detection.** *Anal. Chem.*, 2010, 82, 6904-6910.
- 48 K. Yoshida, K. Kuroda, X. Zhou, Y. Inoue, Y. Date, Wanibuchi H, Fukushima S, Endo G. **Urinary sulfur-containing metabolite produced by intestinal bacteria following oral administration of dimethylarsinic acid to rats.** *Chem. Res. Toxicol.*, 2003, 16, 1124-1129.
- 49 H. R. Hansen, A. Raab, M. Jaspars, B. F. Milne and J. Feldmann. **Sulfur-containing arsenical mistaken for dimethylarsinous acid [DMA(III)] and identified as a natural metabolite in urine: Major implications for studies on arsenic metabolism and toxicity.** *Chem. Res. Toxicol.*, 2004, 17, 1086-1091.
- 50 J. L. Ellis, S. D. Conklin, C. M. Gallawa, K. M. Kubachka, A. R. Young, P. A. Creed, J. A. Caruso and J. T. Creed. **Complementary molecular and elemental detection of speciated**

thioarsenicals using ESI-MS in combination with a xenon-based collision-cell ICP-MS with application to fortified NIST freeze-dried urine. *Anal. Bioanal. Chem.*, 2008, 390, 1731-1737.

51 B. A. Wood and J. Feldmann. **Quantification of phytochelatin and their metal(loid) complexes: critical assessment of current analytical methodology.** *Anal. Bioanal. Chem.*, 2012, 402, 3299-3309.

52 Y. Ogra, K. Ishiwata, Y. Iwashita and K. T. Suzuki. **Simultaneous speciation of selenium and sulfur species in selenized odorless garlic (*Allium sativum* L. Shiro) and shallot (*Allium ascalonicum*) by HPLC-inductively coupled plasma-(octopole reaction system)-mass spectrometry and electrospray ionization-tandem mass spectrometry.** *J. Chromatogr. A*, 2005, 1093, 118-125.

53 M. Wang, W. Y. Feng, H. J. Wang, Y. Zhang, J. Li, B. Li, Y. L. Zhao and Z. F. Chai. **Analysis of mercury-containing protein fractions in brain cytosol of the maternal and infant rats after exposure to a low-dose of methylmercury by SEC coupled to isotope dilution ICP-MS.** *J. Anal. At. Spectrom.*, 2008, 23, 1112-1116.

54 K. K. Kroening, D. D. Richardson, S. Afton and J. A. Caruso. **Screening hydrolysis products of sulfur mustard agents by high-performance liquid chromatography with inductively coupled plasma mass spectrometry detection.** *Anal. Bioanal. Chem.*, 2009, 393, 1949-1956.

55 T. Konz, M. Montes-Bayón, J. Bettmer and A. Sanz-Medel. **Analysis of hepcidin, a key peptide for Fe homeostasis, via sulfur detection by capillary liquid chromatography-inductively coupled plasma mass spectrometry.** *J. Anal. At. Spectrom.*, 2011, 26, 334-340.

56 L. Trapiella-Alfonso, A. R. M. Bustos, J. R. Encinar, J. M. Costa-Fernández, R. Pereiro and A. Sanz-Medel. **New integrated elemental and molecular strategies as a diagnostic tool for the quality of water soluble quantum dots and their bioconjugates.** *Nanoscale*, 2011, 3, 954-957.

57 O. J. Lechtenfeld, B. P. Koch, W. Geibert, K. U. Ludwichowski and G. Kattner. **Inorganics in organics: quantification of organic phosphorus and sulfur and trace element speciation in natural organic matter using HPLC-ICP-MS.** *Anal. Chem.*, 2011, 83, 8968-8974.

58 A. Sanz-Medel, M. Montes-Bayon, M. R. F. de la Campa, J. R. Encinar and J. Bettmer. **Elemental mass spectrometry for quantitative proteomics.** *Anal. Bioanal. Chem.*, 2008, 390, 3-16.

59 J. Bettmer, M. Montes-Bayón and J. R. Encinar. **The emerging role of ICP-MS in proteomic analysis.** *J. Proteomics*, 2009, 72, 989-1005.

60 M. Wang, W. Y. Feng, Y. L. Zhao and Z. F. Chai. **ICP-MS-based strategies for protein quantification.** *Mass Spectrom. Rev.*, 2010, 29, 326-348.

61 C. Rappel and D. Schaumlöffel. **The role of sulfur and sulfur isotope dilution analysis in quantitative protein analysis.** *Anal. Bioanal. Chem.*, 2008, 390, 605-615.

62 A. Prange and D. Pröfrock. **Chemical labels and natural element tags for the quantitative analysis of bio-molecules.** *J. Anal. At. Spectrom.*, 2008, 23, 432-459.

- 63 M. Wind, H. Wesch and W. D. Lehmann. **Protein phosphorylation degree: determination by capillary liquid chromatography and inductively coupled plasma mass spectrometry.** *Anal. Chem.*, 2001, 73, 3006-3010.
- 64 M. Wind, A. Wegener, A. Eisenmenger, R. Kellner and W. D. Lehmann. **Sulfur as the key element for quantitative protein analysis by capillary liquid chromatography coupled to element mass spectrometry.** *Angew. Chem.-Int. Edit.*, 2003, 42, 3425-3427.
- 65 M. Wang, W. Feng, W. Lu, B. Li, B. Wang, M. Zhu, Y. Wang, H. Yuan, Y. Zhao and Z. Chai. **Quantitative analysis of proteins via sulfur determination by HPLC coupled to isotope dilution ICP-MS with hexapole collision cell.** *Anal. Chem.*, 2007, 79, 9128-9134.
- 66 D. Schaumlöffel, P. Giusti, H. Preud'Homme, J. Szpunar and R. Lobinski. **Precolumn isotope dilution analysis in nano HPLC-ICP-MS for absolute quantification of sulfur-containing peptides.** *Anal. Chem.*, 2007, 79, 2859-2868.
- 67 D. Schaumlöffel. **New ways in qualitative and quantitative protein analysis: Nano chromatography coupled to element mass spectrometry.** *J. Trace Elem. Med. Biol.*, 2007, 21, 18-22.
- 68 N. Zinn, R. Krüger, P. Leonhard and J. Bettmer. **µLC coupled to ICP-SFMS with post-column isotope dilution analysis of sulfur for absolute protein quantification.** *Anal. Bioanal. Chem.*, 2008, 391, 537-543.
- 69 E. Rampler, T. Dalik, G. Stingeder, S. Hann and G. Koellensperger. **Sulfur containing amino acids - challenge of accurate quantification.** *J. Anal. At. Spectrom.*, 2012, 27, 1018-1023.
- 70 B. Meermann and M. Sperling. **Hyphenated techniques as tools for speciation analysis of metal-based pharmaceuticals: developments and applications.** *Anal. Bioanal. Chem.*, 2012, 403, 1501-1522.
- 71 O. Corcoran, J. K. Nicholson, E. M. Lenz, F. Abou-Shakra, J. Castro-Perez, A. B. Sage and I. D. Wilson. **Directly coupled liquid chromatography with inductively coupled plasma mass spectrometry and orthogonal acceleration time-of-flight mass spectrometry for the identification of drug metabolites in urine: application to diclofenac using chlorine and sulfur detection.** *Rapid Commun. Mass Spectrom.*, 2000, 14, 2377-2384.
- 72 E. H. Evans, J. C. Wolff and C. Eckers. **Sulfur-specific detection of impurities in Cimetidine drug substance using liquid chromatography coupled to high resolution inductively coupled plasma mass spectrometry and electrospray mass spectrometry.** *Anal. Chem.*, 2001, 73, 4722-4728.
- 73 F. R. Abou-Shakra, A. B. Sag, J. Castro-Perez, J. K. Nicholson, J. C. Lindon, G. B. Scarfe and I. D. Wilson. **High-performance liquid chromatography-UV diode array, inductively coupled plasma mass spectrometry (ICPMS) and orthogonal acceleration time-of-flight mass spectrometry (oa-TOFMS) applied to the simultaneous detection and identification of metabolites of 4-bromoaniline in rat urine.** *Chromatographia*, 2002, 55, S9-S13.
- 74 B. P. Jensen, C. Smith, I. D. Wilson and L. Weidolf. **Sensitive sulphur-specific detection of omeprazole metabolites in rat urine by high-performance liquid**

chromatography/inductively coupled plasma mass spectrometry. *Rapid Commun. Mass Spectrom.*, 2004, 18, 181-183.

75 C. J. Duckett, J. C. Lindon, H. Walker, F. Abou-Shakra, I. D. Wilson and J. K. Nicholson. **Metabolism of 3-chloro-4-fluoroaniline in rat using [14C]-radiolabelling, 19F-NMR spectroscopy, HPLC-MS/MS, HPLC-ICPMS and HPLC-NMR.** *Xenobiotica*, 2006, 36, 59-77.

76 Z. Stefánka, S. Hann, G. Koellensperger and G. Stingeder. **Investigation of the reaction of cisplatin with methionine in aqueous media using HPLC-ICP-DRCMS.** *J. Anal. At. Spectrom.*, 2004, 19, 894-898.

77 S. Stürup, L. Bendahl and B. Gammelgaard. **Optimization of LC-DR-ICP-MS for speciation of selenotrisulfides with simultaneous detection of sulphur and selenium as oxides combined with determination of elemental and isotope ratios.** *J. Anal. At. Spectrom.*, 2006, 21, 201-203.

78 C. Gabel-Jensen, K. Lunoe, K. G. Madsen, J. Bendix, C. Cornett, S. Sturup, H. R. Hansen and B. Gammelgaard. **Separation and identification of the selenium-sulfur amino acid S-(methylseleno) cysteine in intestinal epithelial cell homogenates by LC-ICP-MS and LC-ESI-MS after incubation with methylseleninic acid.** *J. Anal. At. Spectrom.*, 2008, 23, 727-732.

79 M. Sulyok, S. Hann, C. G. Hartinger, B. K. Keppler, G. Stingeder and G. Koellensperger. **Two dimensional separation schemes for investigation of the interaction of an anticancer ruthenium(III) compound with plasma proteins.** *J. Anal. At. Spectrom.*, 2005, 20, 856-863.

80 S. Hann, T. Falta, K. Boeck, M. Sulyok and G. Koellensperger. **On-line fast column switching SEC x IC separation combined with ICP-MS detection for mapping metallodrug-biomolecule interaction.** *J. Anal. At. Spectrom.*, 2010, 25, 861-866.

81 A. K. Bytzek, K. Boeck, G. Hermann, S. Hann, B. K. Keppler, C. G. Hartinger and G. Koellensperger. **LC- and CZE-ICP-MS approaches for the in vivo analysis of the anticancer drug candidate sodium trans-[tetrachloridobis(1H-indazole)ruthenate(III)] (KP1339) in mouse plasma.** *Metallomics*, 2011, 3, 1049-1055.

82 J. Q. Huang, X. Hu and J. R. Zhang. **The application of inductively coupled plasma mass spectrometry in pharmaceutical and biomedical analysis.** *J. Pharm. Biomed. Anal.*, 2006, 40, 227-234.

83 R. N. Rao and M. V. N. K. Talluri. **An overview of recent applications of inductively coupled plasma-mass spectrometry (ICP-MS) in determination of inorganic impurities in drugs and pharmaceuticals.** *J. Pharm. Biomed. Anal.*, 2007, 43, 1-13.

84 B. Gammelgaard and B. P. Jensen. **Application of inductively coupled plasma mass spectrometry in drug metabolism studies.** *J. Anal. At. Spectrom.*, 2007, 22, 235-249.

85 J. E. Carr, A. E. Dill, K. Kwok, J. W. Carnahan and G. K. Webster. **LC-ICP-MS for nonmetal selective detection of pharmaceuticals.** *Curr. Pharm. Anal.*, 2008, 4, 206-214.

86 A. S. Pereira, M. Schelfaut, F. Lynen and P. Sandra. **Design and evaluation of a multi-detection system composed of ultraviolet, evaporative light scattering and inductively**

coupled plasma mass spectrometry detection for the analysis of pharmaceuticals by liquid chromatography. *J. Chromatogr. A*, 2008, 1185, 78-84.

87 K. De Wolf, L. Balcaen, E. Van De Walle, F. Cuyckens and F. Vanhaecke. **A comparison between HPLC-dynamic reaction cell-ICP-MS and HPLC-sector field-ICP-MS for the detection of glutathione-trapped reactive drug metabolites using clozapine as a model compound.** *J. Anal. At. Spectrom.*, 2010, 25, 419-425.

88 C. Losada, J. J. Alberti, J. Saurina and S. Sentellas. **Determination of S-containing drug metabolites from in vitro and in vivo metabolism studies by using LC-ICP/MS.** *Anal. Bioanal. Chem.*, 2012, 404, 539-551.

89 R. Santamaria-Fernandez, R. Hearn and J. C. Wolff. **Detection of counterfeit tablets of an antiviral drug using $\delta^{34}\text{S}$ measurements by MC-ICP-MS and confirmation by LA-MC-ICP-MS and HPLC-MC-ICP-MS.** *J. Anal. At. Spectrom.*, 2008, 23, 1294-1299.

90 R. Santamaria-Fernandez, R. Hearn and J. C. Wolff. **Detection of counterfeit antiviral drug Heptodin (TM) and classification of counterfeits using isotope amount ratio measurements by multicollector inductively coupled plasma mass spectrometry (MC-ICPMS) and isotope ratio mass spectrometry (IRMS).** *Sci. Justice*, 2009, 49, 102-106.

91 L. Bendahl, S. Stürup, B. Gammelgaard, S. H. Hansen. **UPLC-ICP-MS – A fast technique for speciation analysis.** *J. Anal. At. Spectrom.*, 2005, 20, 1287-1289.

92 H. G. Gika, A. Theodoridou, F. Michopoulos, G. Theodoridis, E. Diza, L. Settas, P. Nikolaidis, C. Smith and I. D. Wilson. **Determination of two COX-2 inhibitors in serum and synovial fluid of patients with inflammatory arthritis by ultra performance liquid chromatography-inductively coupled plasma mass spectroscopy and quadrupole time-of-flight mass spectrometry.** *J. Pharm. Biomed. Anal.*, 2009, 49, 579-586.

93 D. F. Thompson, F. Michopoulos, C. J. Smith, C. J. Duckett, R. W. Wilkinson, P. Jarvis and I. D. Wilson. **Profiling biological samples using ultra performance liquid chromatography-inductively coupled plasma-mass spectrometry (UPLC-ICP-MS) for the determination of phosphorus and sulfur-containing metabolites.** *Mol. Biosyst.*, 2011, 7, 1149-1157.

94 C. MacDonald, C. Smith, F. Michopoulos, R. Weaver and I. D. Wilson. **Identification and quantification of glutathione adducts of clozapine using ultra-high-performance liquid chromatography with orthogonal acceleration time-of-flight mass spectrometry and inductively coupled plasma mass spectrometry.** *Rapid Commun. Mass Spectrom.*, 2011, 25, 1787-1793.

95 S. Stürup, H. R. Hansen and B. Gammelgaard. **Application of enriched stable isotopes as tracers in biological systems: a critical review.** *Anal. Bioanal. Chem.*, 2008, 390, 541-554.

96 Y. Ogra, T. Kitaguchi, N. Suzuki and K. T. Suzuki. **In vitro translation with [S-34]-labeled methionine, selenomethionine, and telluromethionine.** *Anal. Bioanal. Chem.*, 2008, 390, 45-51.

97 J. Giner Martínez-Sierra, F. Moreno Sanz, P. Herrero Espílez, R. Santamaria-Fernandez, J. M. Marchante Gayón and J. I. García Alonso. **Evaluation of different analytical strategies for**

the quantification of sulfur-containing biomolecules by HPLC-ICP-MS: application to the characterisation of ^{34}S -labelled yeast. *J. Anal. At. Spectrom.*, 2010, 25, 989-997.

98 J. G. Martínez-Sierra, F. M. Sanz, P. H. Espílez, J. M. M. Gayón, J. R. Fernández, J. I. G. Alonso. **Sulfur tracer experiments in laboratory animals using ^{34}S -labelled yeast.** *Anal. Bioanal. Chem.*, DOI 10.1007/s00216-012-6420-x.

99 M. Pfeffer, M. Maurer, G. Köllensperger, S. Hann, A. B. Graf and D. Mattanovich. **Modeling and measuring intracellular fluxes of secreted recombinant protein in *Pichia pastoris* with a novel ^{34}S labeling procedure.** *Microb. Cell Fact.*, 2011, 10:47.

100 J. Rodríguez-Fernández, M. Montes-Bayón, R. Pereiro and A. Sanz-Medel. **Gas chromatography double focusing sector-field ICP-MS as an innovative tool for bad breath research.** *J. Anal. At. Spectrom.*, 2001, 16, 1051-1056.

101 R. R. St. Remy, M. Montes-Bayón and A. Sanz-Medel. **Determination of total homocysteine in human serum by capillary gas chromatography with sulfur-specific detection by double focusing ICP-MS.** *Anal. Bioanal. Chem.*, 2003, 377, 299-305.

102 J. Meija, M. Montes-Bayón, D. L. Le Duc, N. Terry and J. A. Caruso. **Simultaneous monitoring of volatile selenium and sulfur species from Se accumulating plants (wild type and genetically modified) by GC/MS and GC/ICPMS using solid-phase microextraction for sample introduction.** *Anal. Chem.*, 2002, 74, 5837-5844.

103 D. Pröfrock, P. Leonhard, S. Wilbur and A. Prange. **Sensitive, simultaneous determination of P, S, Cl, Br and I containing pesticides in environmental samples by GC hyphenated with collision-cell ICP-MS.** *J. Anal. At. Spectrom.*, 2004, 19, 623-631.

104 G. Caumette, C. P. Lienemann, I. Merdrignac, B. Bouyssiére and R. Lobinski. **Element speciation analysis of petroleum and related materials.** *J. Anal. At. Spectrom.*, 2009, 24, 263-276.

105 B. Bouyssiére, J. Szpunar and R. Lobinski. **Gas chromatography with inductively coupled plasma mass spectrometric detection in speciation analysis.** *Spectrochim. Acta Part B*, 2002, 57, 805-828.

106 B. Bouyssiére, P. Leonhard, D. Pröfrock, F. Baco, C. L. Garcia, S. Wilbur and A. Prange. **Investigation of the sulfur speciation in petroleum products by capillary gas chromatography with ICP-collision cell-MS detection.** *J. Anal. At. Spectrom.*, 2004, 19, 700-702.

107 W. M. Geiger, S. McSheehy and M. J. Nash. **Application of ICP-MS as a multi-element detector for sulfur and metal hydride impurities in hydrocarbon matrices.** *J. Chromatogr. Sci.*, 2007, 45, 677-682.

108 J. Heilmann and K. G. Heumann. **Development of a species-specific isotope dilution GC-ICP-MS method for the determination of thiophene derivatives in petroleum products.** *Anal. Bioanal. Chem.*, 2008, 390, 643-653.

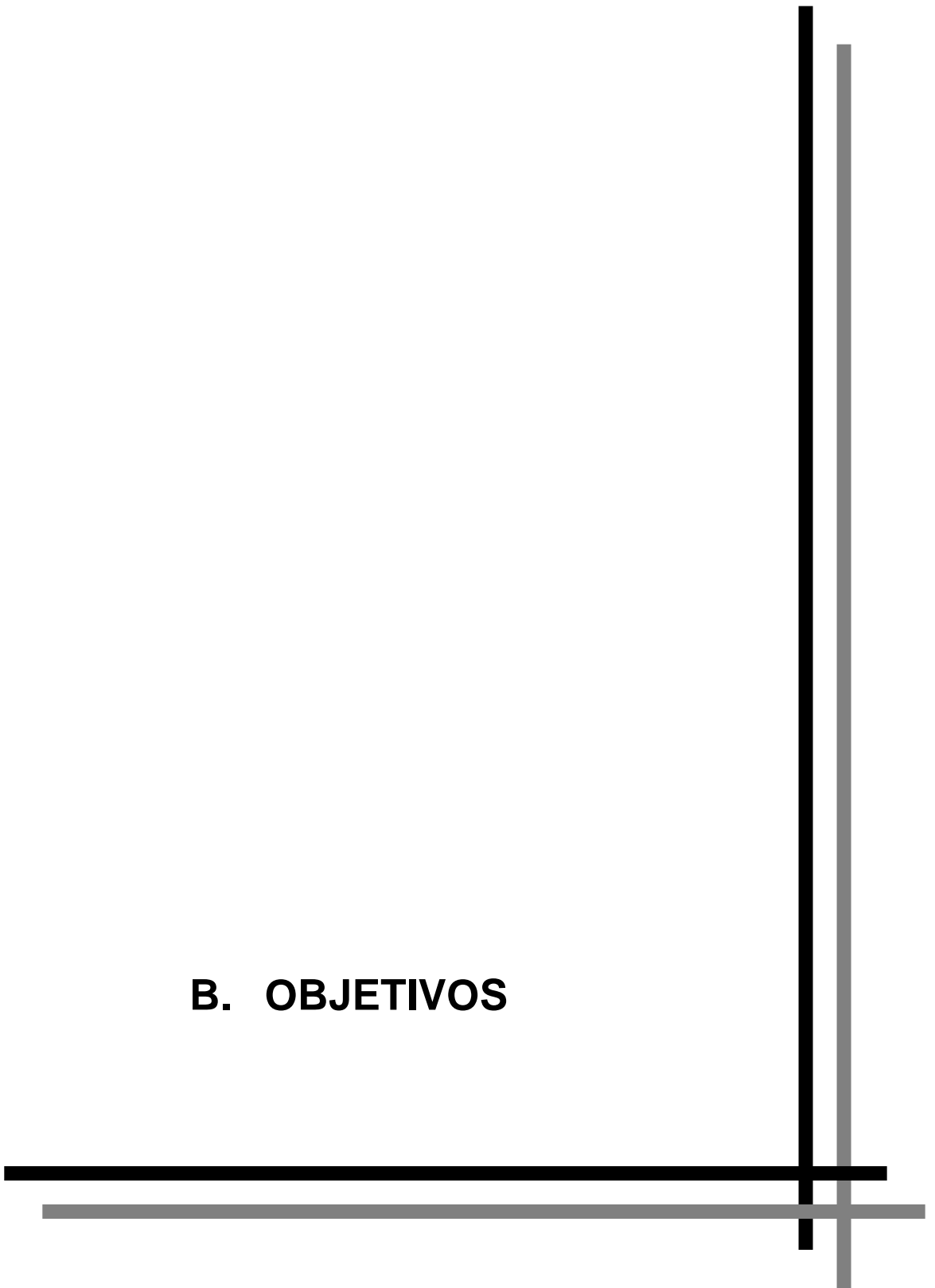
109 J. Heilmann and K. G. Heumann. **Development of a species-unspecific isotope dilution GC-ICP-MS method for possible routine quantification of sulfur species in petroleum products.** *Anal. Chem.*, 2008, 80, 1952-1961.

- 110 E. M. Krupp, C. Pécheyran, S. Meffan-Main and O. F. Donard. **Precise isotope-ratio determination by CGC hyphenated to ICP-MCMS for speciation of trace amounts of gaseous sulfur, with SF₆ as example compound.** *Anal. Bioanal. Chem.*, 2004, 378, 250-255.
- 111 A. Amrani, A. L. Sessions and J. F. Adkins. **Compound-specific δ³⁴S analysis of volatile organics by coupled GC-multicollector-ICP-MS.** *Anal. Chem.*, 2009, 81, 9027-9034.
- 112 R. Haselberg, G. J. de Jong and G. W. Somsen. **Capillary electrophoresis-mass spectrometry for the analysis of intact proteins.** *J. Chromatogr. A*, 2007, 1159, 81-109.
- 113 X. B. Yin, Y. Li and X. P. Yan. **CE-ICP-MS for studying interactions between metals and biomolecules.** *Trac-Trends Anal. Chem.*, 2008, 27, 554-565.
- 114 A. Prange and D. Pröfrock. **Application of CE-ICP-MS and CE-ESI-MS in metalloproteomics: challenges, developments and limitations.** *Anal. Bioanal. Chem.*, 2005, 383, 372-389.
- 115 A. Prange, D. Schaumlöffel, P. Brätter, A. N. Richarz and C. Wolf. **Species analysis of metallothionein isoforms in human brain cytosols using capillary electrophoresis hyphenated to inductively coupled plasma – sector field mass spectrometry.** *Fresenius J. Anal. Chem.*, 2001, 371, 764-774.
- 116 A. Prange and D. Schaumlöffel. **Hyphenated techniques for the characterization and quantification of metallothionein isoforms.** *Anal. Bioanal. Chem.*, 2002, 373, 441-453.
- 117 D. Schaumlöffel, A. Prange, G. Marx, K. G. Heumann and P. Brätter. **Characterization and quantification of metallothionein isoforms by capillary electrophoresis - inductively coupled plasma - isotope dilution mass spectrometry.** *Anal. Bioanal. Chem.*, 2002, 372, 155-163.
- 118 Z. Wang and A. Prange. **The use of surface modified capillaries in the separation and characterisation of metallothionein isoforms by capillary electrophoresis inductively coupled plasma mass spectrometry.** *Anal. Chem.*, 2002, 74, 626-631.
- 119 K. Polec-Pawlak, D. Schaumlöffel, J. Szpunar, A. Prange and R. Lobinski. **Analysis for metal complexes with metallothionein in rat liver by capillary zone electrophoresis using ICP double-focussing sector-field isotope dilution MS and electrospray MS detection.** *J. Anal. At. Spectrom.*, 2002, 17, 908-912.
- 120 D. Pröfrock, P. Leonhard and A. Prange. **Determination of sulfur and selected trace elements in metallothionein-like proteins using capillary electrophoresis hyphenated to inductively coupled plasma mass spectrometry with an octopole reaction cell.** *Anal. Bioanal. Chem.*, 2003, 377, 132-139.
- 121 C. F. Yeh, S. J. Jiang and T. S. His. **Determination of sulfur-containing amino acids by capillary electrophoresis dynamic reaction cell inductively coupled plasma mass spectrometry.** *Anal. Chim. Acta*, 2004, 502, 57-63.
- 122 V. Van Lierde, C. C. Chéry, K. Strijckmans, M. Galleni, B. Devreese, J. Van Beeumen, L. Moens and F. Vanhaecke. **Capillary electrophoresis hyphenated to inductively coupled plasma-sector field-mass spectrometry for the stoichiometric determination of Zn bound to *Aeromonas hydrophila* Zn beta-lactamase.** *J. Anal. At. Spectrom.*, 2004, 19, 888-893.

- 123 N. S. Mokgalaka and J. L. Gardea-Torresdey. **Laser ablation inductively coupled plasma mass spectrometry: Principles and applications.** *Appl. Spectrosc. Rev.*, 2006, 41, 131-150.
- 124 J. S. Becker, S. F. Boulyga, J. S. Becker, C. Pickhardt, E. Damoc and M. Przybylski. **Structural identification and quantification of protein phosphorylations after gel electrophoretic separation using Fourier transform ion cyclotron resonance mass spectrometry and laser ablation inductively coupled plasma mass spectrometry.** *Int. J. Mass Spectrom.*, 2003, 228, 985-997.
- 125 J. S. Becker, M. Zoriy, U. Krause-Buchholz, J. S. Becker, C. Pickhardt, M. Przybylski, W. Pompel and Gerhard Rödel. **In-gel screening of phosphorus and copper, zinc and iron in proteins of yeast mitochondria by LA-ICP-MS and identification of phosphorylated protein structures by MALDI-FT-ICR-MS after separation with two-dimensional gel electrophoresis.** *J. Anal. At. Spectrom.*, 2004, 19, 1236-1243.
- 126 J. S. Becker, M. Zoriy, A. Matusch, B. Wu, D. Salber, C. Palm and J. S. Becker. **Bioimaging of metals by laser ablation inductively coupled plasma mass spectrometry (LA-ICP-MS).** *Mass Spectrom. Rev.*, 2010, 29, 156-175.
- 127 J. S. Becker, M. V. Zoriy, M. Dehnhardt, C. Pickhardt and K. Zilles. **Copper, zinc, phosphorus and sulfur distribution in thin section of rat brain tissues measured by laser ablation inductively coupled plasma mass spectrometry: possibility for small-size tumor analysis.** *J. Anal. At. Spectrom.*, 2005, 20, 912-917.
- 128 J. S. Becker, M. V. Zoriy, C. Pickhardt, N. Palomero-Gallagher and K. Zilles. **Imaging of copper, zinc, and other elements in thin section of human brain samples (hippocampus) by laser ablation inductively coupled plasma mass spectrometry.** *Anal. Chem.*, 2005, 77, 3208-3216.
- 129 M. C. Santos, M. Wagner, B. Wu, J. Scheider, J. Oehlmann, S. Cadore, J. S. Becker. **Biomonitoring of metal contamination in a marine prosobranch snail (*Nassarius reticulatus*) by imaging laser ablation inductively coupled plasma mass spectrometry (LA-ICP-MS).** *Talanta*, 2009, 80, 428-433.
- 130 S. F. Boulyga, J. Heilmann and K. G. Heumann. **Isotope dilution ICP-MS with laser assisted sample introduction for direct determination of sulfur in petroleum products.** *Anal. Bioanal. Chem.*, 2005, 382, 1808-1814.
- 131 S. F. Boulyga, J. Heilmann, T. Prohaska and K. G. Heumann. **Development of an accurate, sensitive, and robust isotope dilution laser ablation ICP-MS method for simultaneous multi-element analysis (chlorine, sulfur, and heavy metals) in coal samples.** *Anal. Bioanal. Chem.*, 2007, 389, 697-706.
- 132 M. Guillong, C. Latkoczy, J. H. Seo, D. Günther and C. A. Heinrich. **Determination of sulfur in fluid inclusions by laser ablation ICP-MS.** *J. Anal. At. Spectrom.*, 2008, 23, 1581-1589.
- 133 J. H. Seo, M. Guillong, M. Aerts, Z. Zajacz and C. A. Heinrich. **Microanalysis of S, Cl, and Br in fluid inclusions by LA-ICP-MS.** *Chem. Geol.*, 2011, 284, 35-44.

- 134 I. Konz, B. Fernandez, R. Pereiro, M. L. Fernandez and A. Sanz-Medel. **P, S and Cl trace detection by laser ablation double-focusing sector field ICP-MS to identify local defects in coated glasses.** *J. Anal. At. Spectrom.*, 2011, 26, 1526-1530.
- 135 C. Stadlbauer, T. Prohaska, C. Reiter, A. Knaus and G. Stingeder. **Time-resolved monitoring of heavy-metal intoxication in single hair by laser ablation ICP-DRCMS.** *Anal. Bioanal. Chem.*, 2005, 383, 500-508.
- 136 P. Cheajesadagul, W. Wananukul, A. Siripinyanond and J. Shiowatana. **Metal doped keratin film standard for LA-ICP-MS determination of lead in hair samples.** *J. Anal. At. Spectrom.*, 2011, 26, 493-498.
- 137 R. Santamaria-Fernandez, J. Giner Martínez-Sierra, J. M. Marchante Gayón, J. I. García Alonso and R. Hearn. **Measurement of longitudinal sulfur isotopic variations by laser ablation MC-ICP-MS in single human hair strands.** *Anal. Bioanal. Chem.*, 2009, 394, 225-233.
- 138 P. R. D. Mason, J. Kosler, J. C. M. de Hoog, P. J. Sylvester and S. Meffan-Main. **In situ determination of sulfur isotopes in sulfur-rich materials by laser ablation multiple-collector inductively coupled plasma mass spectrometry (LA-MC-ICP-MS).** *J. Anal. At. Spectrom.*, 2006, 21, 177-186.
- 139 C. Bendall, Y. Lahaye, J. Fiebig, S. Weyer and G. P. Brey. **In situ sulfur isotope analysis by laser ablation MC-ICP-MS.** *Appl. Geochem.*, 2006, 21, 782-787.
- 140 P. R. Craddock, O. J. Rouxel, L. A. Ball and W. Bach. **Sulfur isotope measurement of sulfate and sulphide by high-resolution MC-ICP-MS.** *Chem. Geol.*, 2008, 253, 102-113.

B. OBJETIVOS



Como se ha puesto de manifiesto a lo largo de la introducción de la presente Tesis Doctoral, la alteración intencionada de la composición isotópica de un elemento en un ser vivo mediante el uso de isótopos estables permite obtener información sobre el metabolismo de ese elemento. Dado que la composición isotópica del azufre varía en la naturaleza, si se quiere seguir la pista del azufre en un ser vivo utilizando un trazador marcado isotópicamente, la cantidad de trazador metabólico utilizada debe ser lo suficientemente elevada como para alterar la composición isotópica del azufre por encima de los límites de variabilidad natural, lo que permitiría detectar *a posteriori* la variación inducida. La determinación de los pequeños cambios observados en la naturaleza en la composición isotópica del azufre exige medidas de relaciones isotópicas de elevada precisión como las que se pueden conseguir con los equipos ICP-MS multicolectores.

Tradicionalmente, los estudios fundamentales sobre el metabolismo del azufre se han llevado a cabo utilizando el isótopo radioactivo azufre-35 como trazador. En los últimos años, la creciente popularidad del ICP-MS ha acelerado el uso de isótopos estables para estudios de metabolismo. En este sentido, la baja abundancia isotópica que presentan los isótopos estables azufre-33 y azufre-34 en la naturaleza los hace muy adecuados para su uso como trazadores. Sin embargo, antes del comienzo de la presente Tesis Doctoral, en la literatura apenas se habían descrito estudios metabólicos empleando isótopos estables de azufre y detección por ICP-MS. Además, en ningún caso se había propuesto el empleo de trazadores múltiples de azufre para realizar este tipo de estudios.

La determinación de azufre puede ser usada como herramienta genérica para la detección y cuantificación de péptidos y proteínas. Los estudios de metabolismo de proteínas en mamíferos utilizando isótopos estables enriquecidos de azufre requieren la síntesis previa de los aminoácidos proteinogénicos cisteína y/o metionina (o péptidos o proteínas que los contengan) marcados con el isótopo enriquecido, dado que los mamíferos no son capaces de sintetizar estos aminoácidos y necesitan obtenerlos a través de la alimentación. Los compuestos de azufre marcados con isótopos estables se podrían administrar por vía oral para obtener información sobre el metabolismo del azufre en los seres vivos sin la necesidad de utilizar isótopos radiactivos.

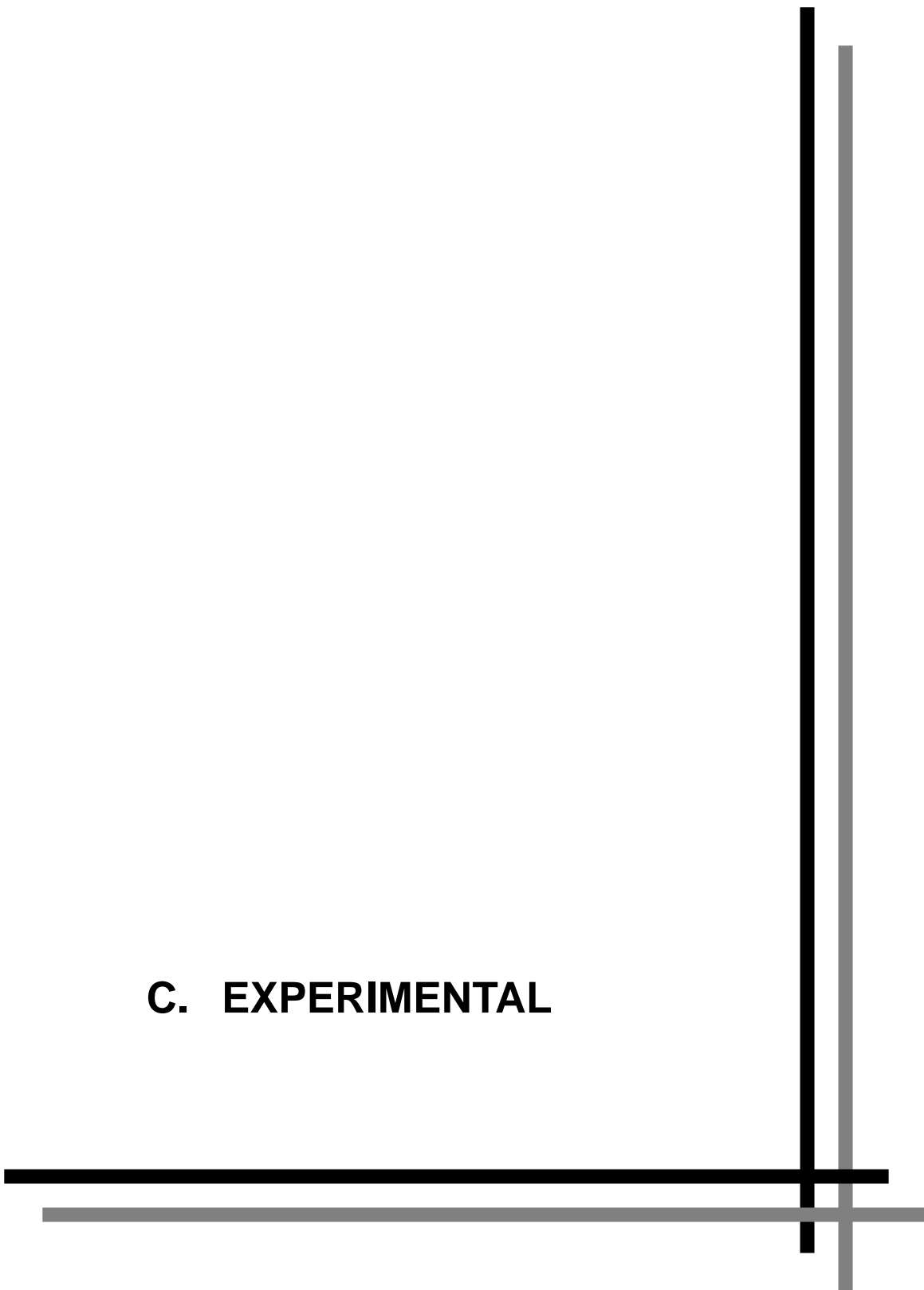
Por todo ello, el objetivo general de esta Tesis Doctoral consiste en el **desarrollo de metodologías analíticas para el estudio del metabolismo del azufre utilizando isótopos estables enriquecidos.**

B. OBJETIVOS

Metodológicamente este objetivo general ha sido abordado a través de los siguientes objetivos específicos:

1. Desarrollo de un procedimiento directo para la medida de la variabilidad natural de la composición isotópica de azufre en muestras de cerveza mediante ICP-MS multicolector.
2. Medida de variaciones naturales en la composición isotópica de azufre en muestras de cabello humano mediante ablación láser acoplada a un ICP-MS multicolector.
3. Preparación de levadura marcada isotópicamente con azufre-34 y su caracterización en composición isotópica y concentración total de azufre mediante ICP-MS multicolector.
4. Evaluación de diferentes estrategias analíticas para la cuantificación de biomoléculas que contienen azufre mediante HPLC-ICP-MS y su posterior aplicación a la caracterización de levadura marcada con azufre-34.
5. Estudios con trazadores estables de azufre en animales de laboratorio utilizando levadura marcada con azufre-34.

C. EXPERIMENTAL



C.1. INSTRUMENTACIÓN

C.1.1. Espectrómetros de masas con fuente de plasma de acoplamiento inductivo (ICP-MS)

A lo largo de esta Tesis Doctoral se han empleado cinco equipos ICP-MS con distintas configuraciones para la detección específica de azufre. Los modelos de ICP-MS utilizados se recogen en la Figura 15 y son: (i) un equipo ICP-MS con analizador de masas de tipo cuadrupolo (HP-4500); (ii) un instrumento ICP-MS con analizador de masas de tipo cuadrupolo equipado con celda de colisión/reacción (X Series 2); (iii) dos equipos ICP-MS con analizador de masas de doble enfoque y con detección simple (Element 1 y Element 2); y (iv) un equipo ICP-MS con analizador de masas de doble enfoque y con detección múltiple (Neptune).

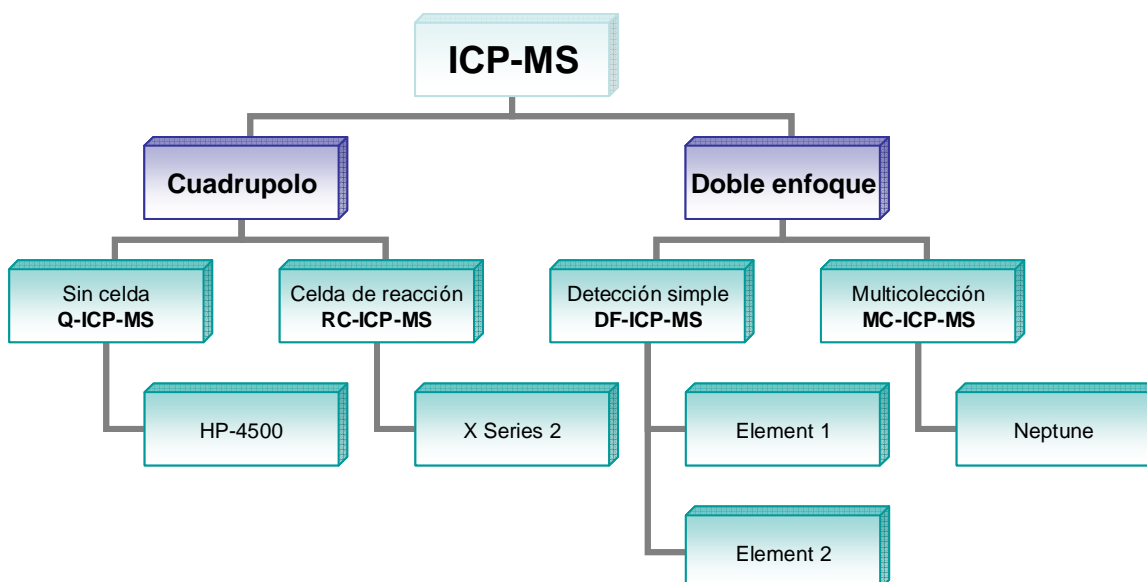


Figura 15. Modelos de ICP-MS empleados en la presente Tesis Doctoral.

C.1.1.1. ICP-MS de cuadrupolo

El equipo ICP-MS de cuadrupolo utilizado fue un Hewlett Packard modelo HP 4500 (Yokogawa Analytical Systems Inc., Tokio, Japón) cuyo esquema se recoge en la Figura 16. Está equipado con un nebulizador concéntrico tipo Meinhard, una cámara de nebulización de doble paso tipo Scott refrigerada a 2 °C y una antorcha de cuarzo tipo Fassel con un tubo inyector de 1,5 mm de diámetro interno. Los conos de níquel

C. EXPERIMENTAL

de la interfase de extracción (muestreo "sampler", separador "skimmer") poseen unos diámetros internos de 1 y 0,4 mm, respectivamente.

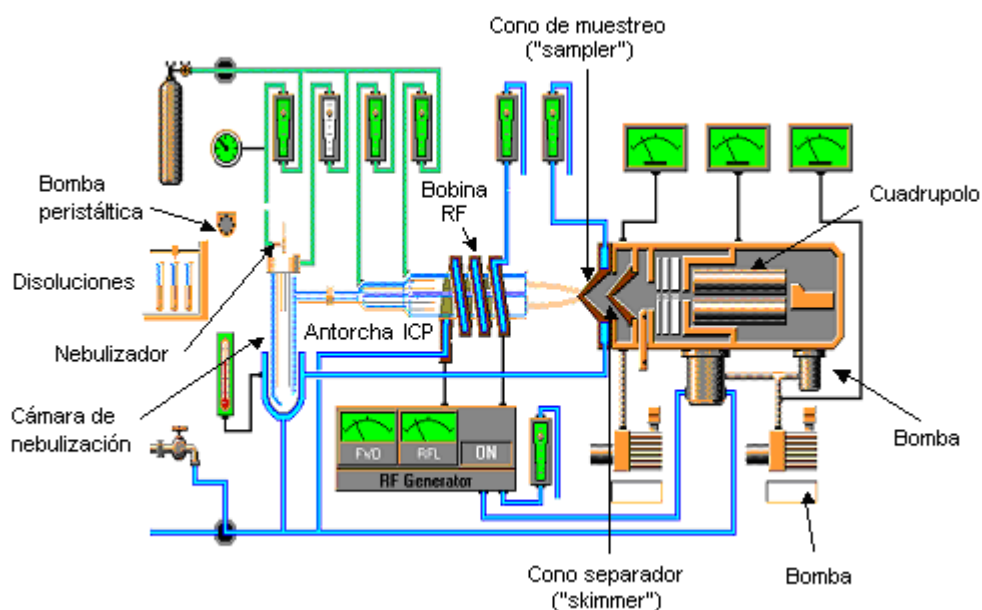


Figura 16. Esquema del equipo ICP-MS de tipo cuadrupolo modelo HP 4500.

El detector, tipo SEM (multiplicador de electrones secundarios), trabaja automáticamente en modo digital o analógico dependiendo del número de iones que alcancen el detector. Dado que el azufre forma fácilmente óxidos, se utilizó el ICP-MS HP-4500 en condiciones de plasma frío, las cuales favorecen la formación de óxidos estables, con objeto de detectar el azufre como ión molecular $^{32}\text{S}^{16}\text{O}^+$ a m/z 48. Las condiciones óptimas para la determinación de azufre nebulizando una disolución de $500 \text{ ng}\cdot\text{g}^{-1}$ de ácido sulfúrico en agua fueron: una potencia de radiofrecuencia de 950 W, ajustando la posición de la antorcha en 5,8 mm y aumentado el flujo de gas portador hasta $1,4 \text{ L}\cdot\text{min}^{-1}$ de argón. La señal del equipo fue optimizada cada día de medida con una solución de $10 \text{ ng}\cdot\text{g}^{-1}$ de Li, Y, y Tl en ácido nítrico al 1%, midiendo las m/z 7, 89 y 205 respectivamente (cubriendo así todo el intervalo de masas), con objeto de preparar al equipo para el análisis y llevar a cabo un control de calidad del instrumento.

C.1. INSTRUMENTACIÓN

C.1.1.2. ICP-MS de cuadrupolo equipado con celda de colisión/reacción

Se utilizó un equipo ICP-MS con analizador de masas de tipo cuadrupolo, equipado con celda de colisión/reacción de Thermo Instruments (Bremen, Alemania) modelo X Series 2, cuyo esquema se recoge en la Figura 9. El equipo está provisto de un nebulizador neumático concéntrico y una cámara de nebulización de paso sencillo de Pyrex, refrigerada mediante una célula con efecto Peltier. La antorcha utilizada es de cuarzo, con un canal central de un diámetro aproximado de 1,5 mm. Los conos de la interfase de extracción, “sampler” y “skimmer” son de níquel y tienen unos orificios centrales de 1 y 0,7 mm. El equipo tiene como analizador de masas un cuadrupolo y posee además un hexapolo como celda de colisión/reacción para la reducción de las interferencias poliatómicas. Ambos trabajan bajo un potencial de -7 V. El ICP-MS X Series 2 se optimizó utilizando oxígeno (O₂) como gas reactivo en la celda, por lo que la detección de azufre se realizó a través de su óxido a m/z 48. El flujo óptimo de gas reactivo fue de 0,45 mL·min⁻¹ de O₂.

Para cada día de medida se optimizaron diversos parámetros como la posición de la antorcha y el voltaje de las lentes, con el fin de trabajar siempre bajo condiciones de máxima sensibilidad. Para estas optimizaciones se utilizó una disolución multielemental de 10 ng·g⁻¹ de As, Be, Bi, Ca, Co, In, Li, Ni, y U en HCl 2% y una disolución de SO₄²⁻ de 200 ng·g⁻¹ en HNO₃ 2%.

C.1.1.3. ICP-MS de doble enfoque con detección simple

Se han utilizado dos equipos ICP-MS de doble enfoque con detección simple de Thermo Instruments, modelos Element 1 y Element 2, siendo el segundo instrumento una versión mejorada del primero. La Figura 10 recoge un esquema con las características más significativas del Element 2.

Este instrumento está equipado con un nebulizador concéntrico tipo Meinhard, una cámara de nebulización de doble paso tipo Scott sin refrigeración y una antorcha de cuarzo tipo Fassel, con un canal central (tubo inyector) de 1 mm de diámetro interno. Los conos de la interfase, el de extracción “sampler” y el de muestreo “skimmer”, son de níquel, con un diámetro de 1 mm y 0,7 mm, respectivamente. El detector empleado fue un multiplicador de electrones secundarios (SEM) que opera de forma dual (analógico y pulsos).

C.1.1.4. ICP-MS de doble enfoque multicolector

Para la medida de relaciones isotópicas de azufre de elevada precisión se emplearon los equipos MC-ICP-MS modelo Neptune (Thermo Instruments, Bremen, Alemania) instalados en el Centro de Apoyo Científico y Tecnológico a la Investigación (CACTI) de la Universidad de Vigo y en LGC Ltd. (Queens Road, Teddington, TW11 0LY, Reino Unido). Un esquema de este instrumento se muestra en la Figura 12. El sistema de introducción de muestra está formado por un nebulizador microconcéntrico PFA-100 y una cámara de nebulización ciclónica. Los conos de la interfase de extracción empleados fueron de Ni. Los parámetros de operación se optimizaron diariamente.

En la Figura 17 se recogen las tres configuraciones de copas de Faraday empleadas a lo largo de presente Tesis Doctoral. En primer lugar, para la caracterización, tanto en composición isotópica como en concentración total de azufre, de los trazadores enriquecidos en azufre-33 y azufre-34 así como de la levadura enriquecida en azufre-34, se empleó una configuración de copas de Faraday que incluye los tres isótopos estables de azufre medibles por ICP-MS (**artículo científico III**). Esta misma configuración de copas se utilizó para evaluar la respuesta analítica del equipo multicolector cuando se trabaja acoplado en línea una separación cromatográfica en modo isocrático (**artículo científico IV**).

Para la medida de las variaciones isotópicas longitudinales de azufre en cabello humano mediante ablación láser (LA) acoplada a un equipo ICP-MS multicolector (**artículo científico II**), dado que estas variaciones isotópicas se expresaron en notación delta ($\delta^{34}\text{S}$), se empleó una configuración de copas de Faraday más sencilla que incluye únicamente los isótopos estables de azufre-34 y 32.

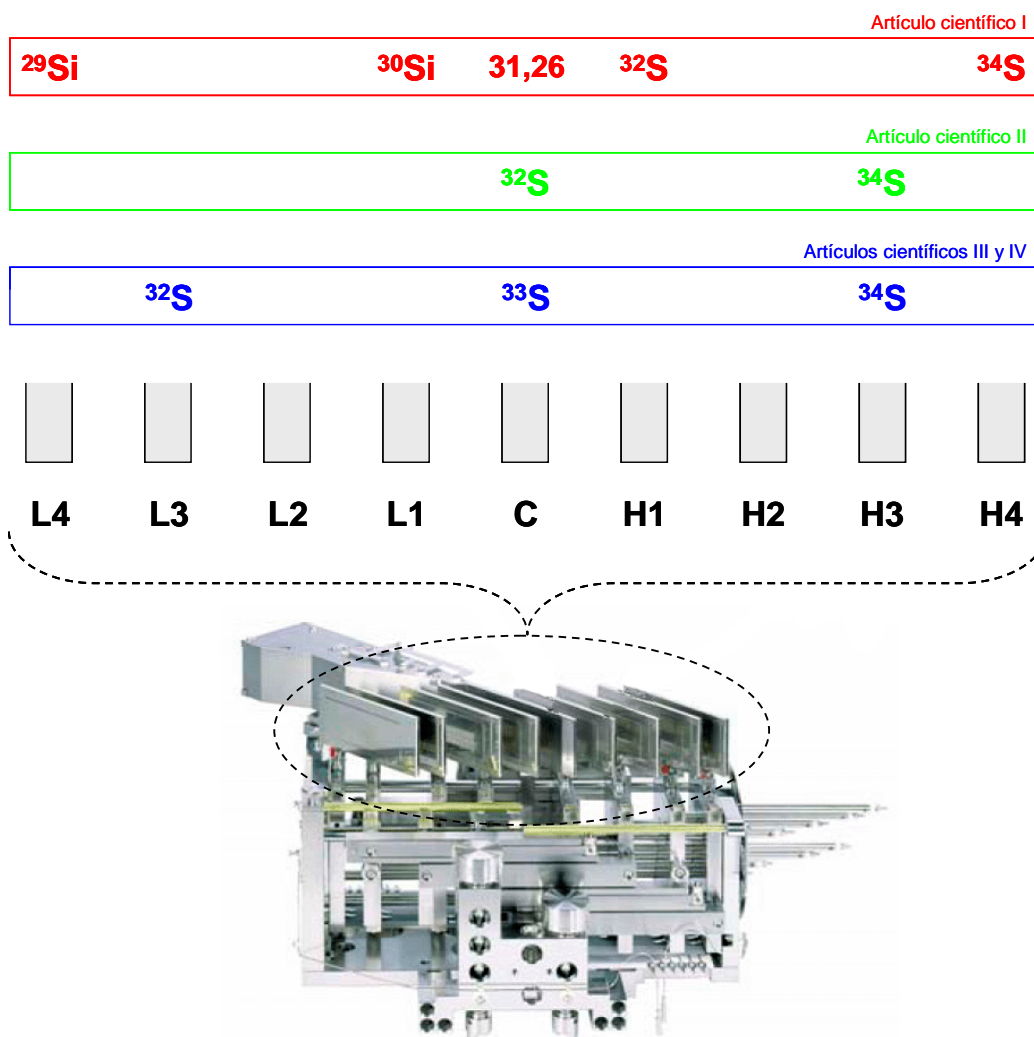


Figura 17. Configuraciones de copas de Faraday empleadas a lo largo de la Tesis Doctoral para la medida de relaciones isotópicas de azufre en el ICP-MS multicolelector.

Finalmente, para la medida de la variabilidad natural de las relaciones isotópicas de azufre en cervezas mediante MC-ICP-MS (**artículo científico I**), se utilizó una configuración de copas de Faraday en la que se incluyen los isótopos de silicio-29 y 30 para corregir los efectos de matriz que afectan a la transmisión iónica de los isótopos de azufre-32 y 34 en el espectrómetro de masas. La Figura 18 recoge el espectro de masas típico que se obtiene en el equipo ICP-MS multicolelector utilizado para la medida de relaciones isotópicas de azufre y silicio trabajando a media resolución. Para ello, la copa de Faraday central se fija en un valor m/z 31,26. Esto permite la medida simultánea y libre de interferencias de los isótopos de azufre y silicio seleccionados.

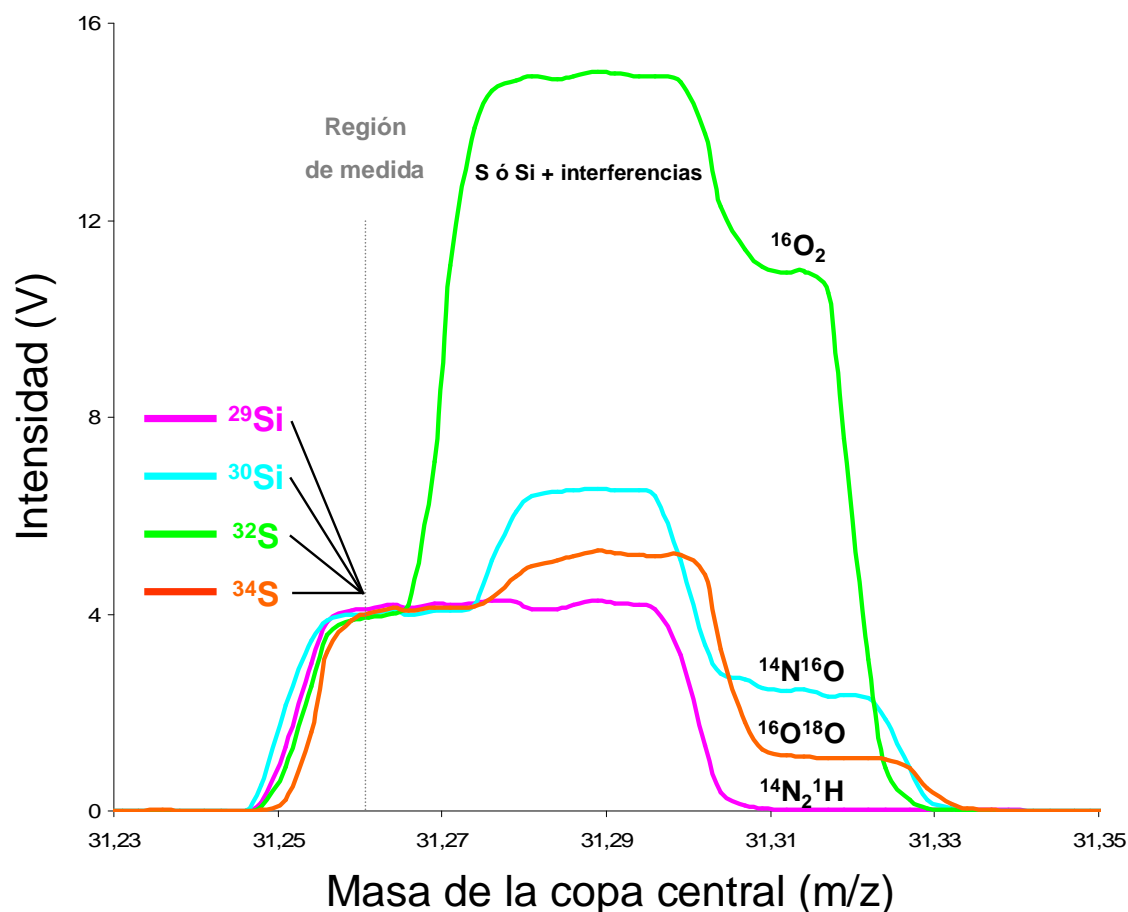


Figura 18. Espectro de masas obtenido para la medida simultánea de relaciones isotópicas de azufre y silicio en el equipo ICP-MS multicolector.

En esta representación, las intensidades de los isótopos de silicio y azufre-34 se han normalizado frente a la señal del azufre-32.

C.1.2. Instrumentación utilizada para las separaciones por cromatografía líquida de alta resolución (HPLC)

En las separaciones por HPLC se empleó la siguiente instrumentación:

■ Equipo de HPLC compuesto por una bomba de alta presión de doble pistón LC-20 AD VP (Shimadzu, Kyoto, Japón) y una válvula de inyección de seis vías, modelo 7125 (Rheodyne, Cotati, CA, USA) con bucles de inyección intercambiables de PEEK (polyether ether ketone) de 20, 50 y 100 μL de capacidad.

■ Equipo de HPLC Agilent modelo 1100 (Agilent Technologies, Waldbronn, Alemania), que consta de cuatro canales para fases móviles, desgasificador en línea mediante ultrasonidos, bomba cuaternaria, sistema de termostatación de las

columnas y un detector de diodos en línea (DAD) UV-Vis con lámparas de deuterio y wolframio con un rango de longitudes de onda de 190 a 950 nm.

A lo largo de esta Tesis Doctoral se han utilizado las siguientes columnas de cromatografía líquida:

- Columna de HPLC de fase inversa, C18 Supelco Discovery® BIO Wide Pore (Supelco, Sigma-Aldrich, Dorset, UK) de dimensiones 15 cm x 2,1 mm (longitud x d.i.); 5 µm de tamaño de partícula.
- Columna de HPLC de fase inversa, Mediterranea Sea₁₈ (Teknokroma, Barcelona, España) de dimensiones 15 cm x 4,6 mm (longitud x d.i.); 5 µm de tamaño de partícula.
- Columna cromatográfica de exclusión por tamaños (SEC) Superdex™ 200 10/300 GL (GE Healthcare, Piscataway, NJ) con un rango de exclusión molecular de 10-600 kDa y dimensiones 30 cm x 10 mm (longitud x d.i.); 13 µm de tamaño promedio de partícula.
- Columna cromatográfica de exclusión por tamaños (SEC) Superdex™ Peptide HR 10/300 GL (GE Healthcare, Piscataway, NJ) con un rango de exclusión molecular de 100-7000 Da y dimensiones 30 cm x 10 mm (longitud x d.i.); 13 µm de tamaño promedio de partícula.

C.1.3. Sistema de ablación láser

- Se utilizó un sistema de ablación láser UP-213 disponible comercialmente (New Wave Research Inc., Huntingdon, Cambridgeshire, Reino Unido) equipado con láser de Nd:YAG operando en el ultravioleta lejano (213 nm).
- Desde el sistema de ablación láser, se utilizó helio como gas portador debido a sus mejoradas características de arrancado y posterior transporte de los analitos al ICP-MS [215].
- Para introducir al plasma muestras líquidas se utilizó una pieza de vidrio en forma de “Y”. Por uno de los canales circulaba la corriente de He utilizada para transportar el material al ICP-MS y por el segundo de los canales circulaba la solución líquida tras haber sido sometida a un proceso de nebulización ultrasónica y desolvatación (USN CETAC U-6000AT+, CETAC Technologies, Omaha, NE, USA).

C.1.4. Otra instrumentación

- Las pesadas se realizaron en una balanza analítica con una resolución de 0,1 mg, modelo Classic de Mettler Toledo (España).
- En los análisis por dilución isotópica post-columna, se empleó una bomba peristáltica Minipuls 2 (Scharlab, Barcelona, España) para la adición continua del isótopo enriquecido a la salida del sistema cromatográfico.
- Horno de microondas modelo Ethos I de Milestone (Socisole, Italia) equipado con un rotor para diez bombas de teflón de media presión y sensor de temperatura.
- Microondas focalizado modelo Discovery (CEM, Matthews, NC, USA) con automuestreador modelo Explorer (CEM).
- Para el ajuste del pH se empleó un pH-metro modelo Basic 20 de Crison (España).
- Se empleó una microcentrífuga MiniSpin Plus de Eppendorf AG (Hamburgo, Alemania) y una centrifuga Biofuge Stratos modelo Heraeus (Hanau, Alemania).
- Se utilizó un agitador mecánico a vibración Vortex modelo classic (VELP Scientifica, Usmate, Italia).
- Concentrador centrífugo de Eppendorf (SpeedVac Vacufuge concentrator, San Diego, USA).
- Liofilizador modelo LyoLab 3000 de Heto-Holten (Allerød, Dinamarca)
- Baño de agua termostatzado de control digital modelo Digiterm 100 (JP Selecta, Barcelona, España).

C.2. MATERIALES Y REACTIVOS

- Todos los reactivos utilizados fueron de grado analítico. Se empleó agua ultrapura con un valor de carbono orgánico total TOC < 5ppb, filtrada (0,22 µm) y desionizada (18 MΩ·cm) obtenida mediante un sistema Milli-Q (Millipore Co, Bedford, MA, USA).
- Las disoluciones patrón de azufre de abundancia natural, se obtuvieron por dilución de una disolución patrón certificada de 1000 mg·L⁻¹ de azufre, como ácido sulfúrico en agua, suministrada por Merck (Darmstadt, Alemania).
- Los isótopos estables enriquecidos empleados, azufre-33 (99,92%) y azufre-34 (99,50%), fueron proporcionados por Cambridge Isotope Laboratories (Andover, MA, USA).
- Se emplearon los siguientes materiales de referencia de azufre certificados en composición isotópica, proporcionados por el *National Institute of Standards and Technology* (NIST, USA):
 - NIST RM8553: Azufre elemental ($\delta^{34}\text{S}_{\text{V-CDT}} = 16 \pm 0,3\text{‰}$).
 - NIST RM8554: Sulfuro de plata ($\delta^{34}\text{S}_{\text{V-CDT}} = -0,3 \pm 0,3\text{‰}$).
 - NIST RM8556: Sulfuro de cinc ($\delta^{34}\text{S}_{\text{V-CDT}} = 17,44 \pm 0,3\text{‰}$).
- Ácido nítrico y ácido clorhídrico ultrapuros obtenidos mediante destilación lenta “sub-boiling” de ácido nítrico concentrado al 65% (p/v) y ácido clorhídrico concentrado al 37% (p/v) respectivamente, de calidad pro-análisis (Merck).
- Peróxido de hidrógeno al 30% (p/v) de alta pureza (Suprapur®, Merck).
- Los patrones de DL-Metionina (>99% de pureza), DL-cisteína (>95% de pureza) y L-glutatió reducido (>97% de pureza) se obtuvieron de Fluka (Buchs, Suiza).
- Metanol de calidad HPLC suministrado por Merck.
- Ácido heptafluorobutírico (HFBA) suministrado por Sigma-Aldrich Co. (St. Louis, MO, USA).
- Material de referencia certificado: control sérico de origen humano, liofilizado, suministrado por Seronorm Trace Element Serum (Level 2, NO0371).
- Gas argón de 99,999% de pureza suministrado por Air Liquide (Madrid, España).

C. EXPERIMENTAL

- Se han utilizado filtros de jeringa de 0,22 μm de tamaño de poro (Millipore, Bedford, MA, USA) de un solo uso, y jeringas de 1 y 5 mL BD Plastipak™ (Becton, Dickinson and Company, España).
- Membranas de ultrafiltración con un corte de masa molecular de 10 kDa, para volúmenes de muestra hasta 4 mL (Microcón YM-10) y 0,5 mL (Centricón YM-10) suministrados por Millipore.

C.3. PROCEDIMIENTOS EXPERIMENTALES

C.3.1. Corrección del efecto de discriminación de masas

En la mayoría de los estudios realizados en la presente Tesis Doctoral, la corrección del efecto de discriminación de masas se llevó a cabo midiendo diariamente una disolución patrón de azufre con composición isotópica natural, en las mismas condiciones que las utilizadas para medir relaciones isotópicas en las muestras. El factor de discriminación de masas se calculó utilizando un modelo exponencial [216].

Para ello, el $\ln\left(\frac{R_{\text{experimental}}}{R_{\text{teórica}}}\right)$ se representó frente a la diferencia de masa de los isótopos medidos (-1 para la relación $^{33}\text{S}/^{32}\text{S}$ y -2 para la relación $^{34}\text{S}/^{32}\text{S}$). La pendiente de la recta obtenida es el factor de discriminación de masas. Así, todas las relaciones obtenidas experimentalmente se corrigen utilizando este factor de acuerdo a la ecuación:

$$R_{\text{corregida}} = \frac{R_{\text{experimental}}}{e^{K \cdot \Delta M}} \quad \text{Ecuación 29}$$

donde R simboliza una relación isotópica, ΔM es la diferencia de masa de los isótopos medidos y K el denominado factor de discriminación de masas.

Para la medida de variaciones naturales en la composición isotópica de azufre en muestras de cerveza (**artículo científico I**), dado que se utilizó silicio para realizar una corrección interna del factor de discriminación de masas, se empleó la siguiente ecuación:

$$\left(\frac{^{34}\text{S}}{^{32}\text{S}}\right)_{\text{cor}} = \frac{\left(\frac{^{34}\text{S}}{^{32}\text{S}}\right)_{\text{med}}}{\left(\frac{\left(\frac{^{30}\text{Si}}{^{29}\text{Si}}\right)_{\text{med}}}{\left(\frac{^{30}\text{Si}}{^{29}\text{Si}}\right)_{\text{ref}}}\right)^{\frac{\ln\left(\frac{\text{Masa}^{34}\text{S}}{\text{Masa}^{32}\text{S}}\right)}{\ln\left(\frac{\text{Masa}^{30}\text{Si}}{\text{Masa}^{29}\text{Si}}\right)}}} \quad \text{Ecuación 30}$$

donde las abreviaturas *cor*, *med* y *ref* indican una relación isotópica corregida, medida experimentalmente y de referencia, respectivamente.

C.3.2. Cálculo del tiempo muerto del detector

La ecuación que se ha empleado para corregir las intensidades medidas por ICP-MS es la siguiente:

$$I_{\text{corregida}} = \frac{I_{\text{medida}} \text{ (cps)}}{1 - I_{\text{medida}} \text{ (cps)} \cdot T \text{ (s)}} \quad \text{Ecuación 31}$$

donde I_{medida} son las cuentas por segundo medidas experimentalmente e $I_{\text{corregida}}$ son las cuentas por segundo que se medirían si no existiera error debido al tiempo muerto T .

El tiempo muerto se puede calcular de diversas formas, normalmente utilizando métodos gráficos [217]. En nuestro caso fue determinado de acuerdo al método propuesto por Vanhaecke y col. [218]. Para ello, se midió la relación isotópica $^{34}\text{S}/^{32}\text{S}$ a diferentes concentraciones crecientes de azufre, empleando un tiempo muerto de cero segundos en el software del instrumento. A continuación se representó la relación $^{34}\text{S}/^{32}\text{S}$ normalizada (relación isotópica corregida por el tiempo muerto dividida por la relación isotópica teórica) para diferentes tiempos muertos asignados entre 0 y 100 ns a las diferentes concentraciones de azufre estudiadas. Como se puede observar en la Figura 19, en el equipo DF-ICP-MS, para cada concentración se obtiene una recta y todas ellas se cruzan para un valor dado del tiempo muerto (45 ± 1 ns). Este valor es el tiempo muerto del detector ya que corrigiendo las intensidades medidas con este valor, la relación isotópica es independiente de la concentración de azufre. Este valor se introdujo en el “software” del equipo para realizar una corrección automática de todas las intensidades medidas y está de acuerdo con otros valores obtenidos en nuestro laboratorio para otros elementos [219-221] tal como se esperaba dado que su valor debería ser independiente de las m/z medidas.

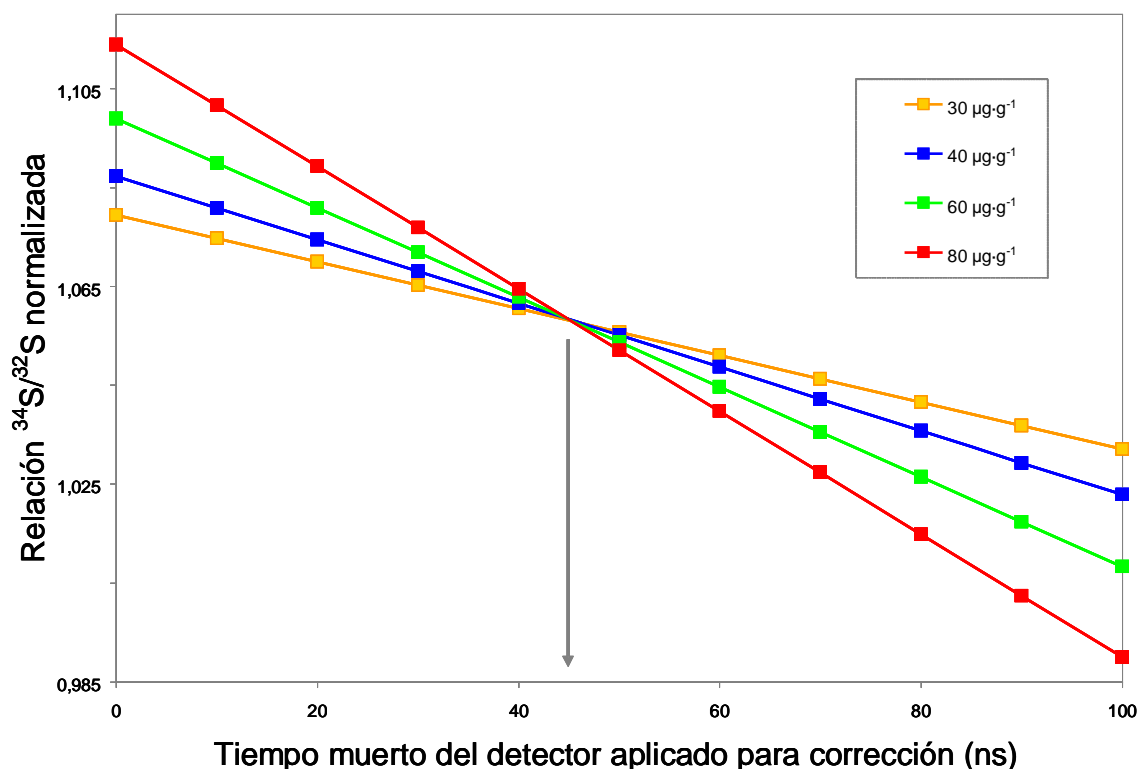


Figura 19. Relación isotópica normalizada $^{34}\text{S}/^{32}\text{S}$ a diferentes concentraciones de azufre para el cálculo del tiempo muerto del detector en el equipo DF-ICP-MS.

C.3.3. HPLC-ICP-MS con dilución isotópica inespecífica

El acoplamiento HPLC-ICP-MS resulta muy sencillo, ya que los flujos de trabajo utilizados habitualmente en HPLC ($1 \text{ mL}\cdot\text{min}^{-1}$ aproximadamente) son perfectamente compatibles con la mayoría de los nebulizadores convencionales empleados en el ICP-MS. Desde el punto de vista técnico, el acoplamiento consiste en unir la salida de la columna analítica al nebulizador a través de un tubo inerte de PEEK y de reducida longitud (lo más corto posible) para evitar volúmenes muertos y ensanchamiento de los picos cromatográficos. El esquema del acoplamiento HPLC-ICP-MS utilizado a lo largo de la presente Tesis Doctoral para el análisis de especiación de azufre se recoge en la Figura 20.

Para llevar a cabo la cuantificación de azufre en los diferentes picos cromatográficos por dilución isotópica inespecífica, el eluyente se mezcló a la salida de la columna cromatográfica con un flujo continuo ($0,1 \text{ mL}\cdot\text{min}^{-1}$) de una disolución del patrón enriquecido (trazador S33) que se impulsa utilizando una bomba peristáltica. La mezcla de ambos flujos se consiguió mediante una pieza en "T" a la salida de la columna analítica, siendo la mezcla nebulizada directamente en el plasma. Para

conocer con exactitud el flujo de la disolución de trazador (f_{Sp}) se llevó a cabo una calibración diaria (al principio y al final del análisis) del flujo de bombeo de la bomba peristáltica.

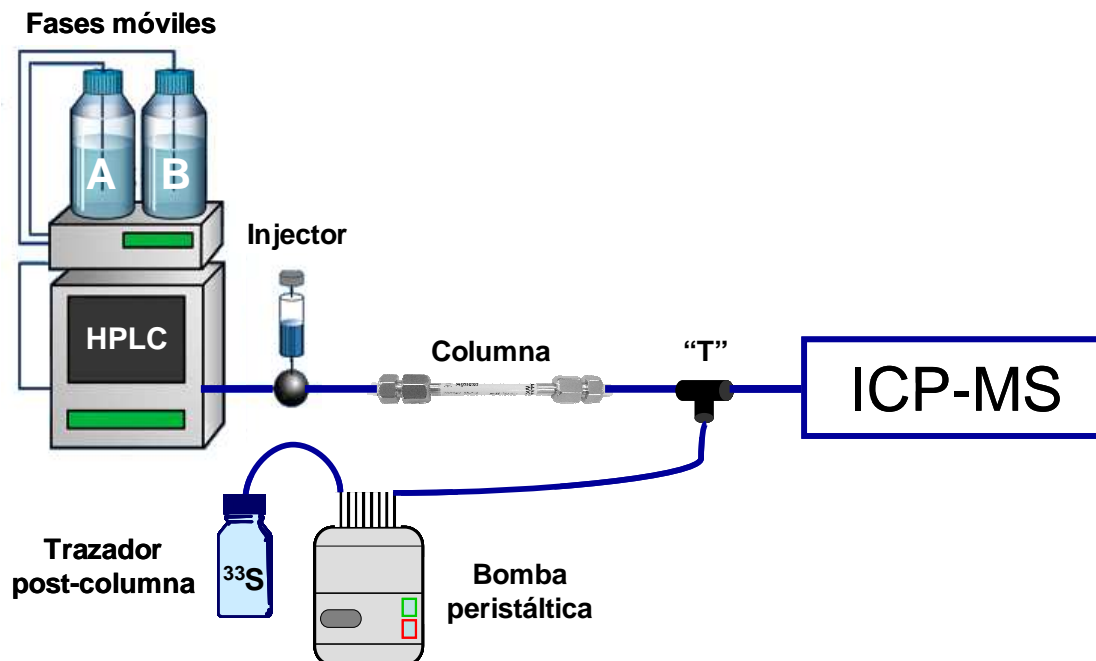


Figura 20. Esquema del acoplamiento HPLC-ICP-MS utilizado en el análisis por dilución isotópica inespecífica.

C.3.4. Estudios con muestras de cerveza

Con objeto de estudiar los efectos de matriz observados en la medida de relaciones isotópicas de azufre y silicio por ICP-MS multicolector en muestras de cerveza, se evaluaron cinco factores de dilución. Para ello, se prepararon diluciones 1:1, 1:3, 1:5, 1:10 y 1:20 de una muestra de cerveza con una disolución de ácido nítrico ultrapuro al 1% (v/v). Se realizaron dos estudios independientes. En el primero de ellos se adicionó a cada una de las diluciones anteriores un estándar de silicio hasta una concentración final de $15 \mu\text{g}\cdot\text{g}^{-1}$. En el segundo experimento no se añadió silicio exógeno. A lo largo de todo el estudio, se utilizaron tres materiales de referencia certificados en el valor delta para el azufre. El primero de ellos, NIST RM8553 se utilizó como estándar secundario para poder expresar los resultados de acuerdo a la notación $\delta_{\text{V-CDT}}$ y los otros dos, NIST RM8554 y RM8556 se utilizaron como controles de calidad de la metodología utilizada. Un estándar de silicio, previamente caracterizado en composición isotópica utilizando el material de referencia certificado

IRMM 017, se añadió a los tres materiales de referencia certificados en composición isotópica de azufre con objeto de corregir el efecto de discriminación de masas observado. A la vista de los resultados obtenidos, se seleccionó una dilución 1:3 y la no adición de silicio para la medida de un total de 26 muestras de cerveza por ICP-MS multicolector.

C.3.5. Estudios con muestras de pelo

Las muestras de pelo (hebras) se fijaron de manera individual sobre placas de cristal de microscopio utilizando pegamento en barra Scotch (ver Figura 21A). De esta manera se pudieron fijar varias hebras de pelo en la misma placa de vidrio lo que permitió realizar diferentes estudios sin necesidad de cambiar de muestra. Dado que no existe un protocolo estándar para eliminar la contaminación superficial de las muestras de pelo, se evaluaron tres procedimientos de limpieza diferentes. El primer procedimiento se basó en el lavado sucesivo de las hebras de pelo con tres alícuotas de 5 mL de agua Milli-Q. El segundo procedimiento de limpieza incluyó un lavado con agua Milli-Q (1 x 5 mL), acetona (3 x 5 mL) y finalmente agua Milli-Q (1 x 5 mL). El tercer procedimiento evaluado consistió en una etapa de pre-ablación realizada con el equipo de ablación láser inmediatamente antes de la medida con el sistema LA-ICP-MS.

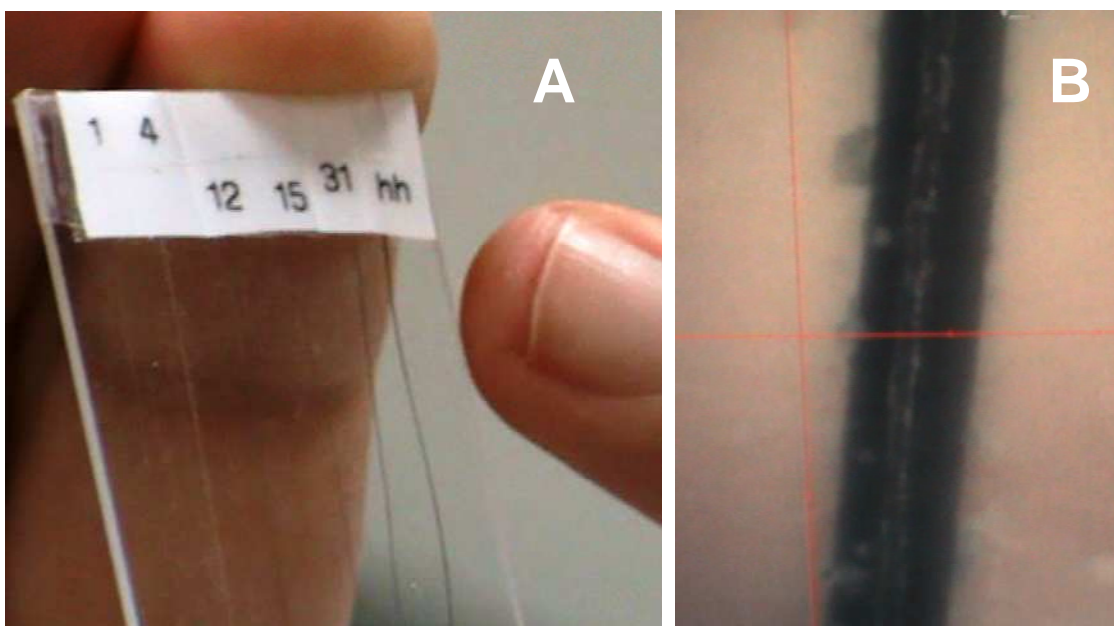


Figura 21. Detalle del soporte utilizado para fijar las muestras de pelo (A) e imagen de una hebra de pelo tras la ablación (B).

La optimización de los parámetros de ablación para la medida de variaciones longitudinales de la relación isotópica $^{34}\text{S}/^{32}\text{S}$ a lo largo de una hebra de pelo mediante la metodología híbrida LA-ICP-MS se realizó utilizando muestras de pelo de caballo, con una composición isotópica homogénea, proporcionadas por la Universidad de Queen (Belfast, Reino Unido). La Figura 21B muestra una imagen de una hebra de pelo tras la ablación. Asimismo, dada la similitud de las matrices, se utilizó este material para realizar la corrección externa del efecto de discriminación de masas en las muestras de cabello humano. Tras la puesta a punto del método, se recogieron muestras de cabello de al menos 4 cm de longitud donadas por tres voluntarios, dos de ellos residentes de forma permanente en el Reino Unido y un tercero, que llamamos “viajero”, el cual pasó los últimos seis meses entre diferentes países europeos (incluyendo Reino Unido) y Australia.

C.3.6. Caracterización de los trazadores isotópicos mediante ICP-MS multicolector

La composición isotópica y la concentración de las disoluciones enriquecidas isotópicamente en azufre-33 y 34 utilizadas como trazadores (S33 y S34) se determinaron en el ICP-MS multicolector. Para ello, en primer lugar se midieron las relaciones isotópicas $^{33}\text{S}/^{32}\text{S}$ y $^{34}\text{S}/^{32}\text{S}$ en una disolución patrón de azufre natural de $20 \mu\text{g}\cdot\text{g}^{-1}$, con objeto de determinar el factor de discriminación de masas a aplicar a las relaciones isotópicas medidas posteriormente.

A continuación se midieron las mismas relaciones isotópicas en cada una de las disoluciones de trazador, previamente diluidas 50 veces. A partir de estos datos se calculó la composición isotópica de los trazadores utilizando la ecuación:

$$A_i = \frac{R_i}{\sum_{i=1}^n R_i} \quad \text{Ecuación 32}$$

donde A_i es la abundancia del isótopo i ; R_i es la relación isotópica del isótopo i frente al isótopo de referencia una vez corregido el factor de discriminación de masas y $\sum_{i=1}^n R_i$ es la suma de todas las relaciones isotópicas existentes entre los distintos isótopos del elemento y el isótopo de referencia (^{33}S y ^{34}S en los trazadores enriquecidos en el isótopo de azufre-33 y 34 respectivamente).

C. EXPERIMENTAL

Las abundancias isotópicas en cada uno de los trazadores (S33 y S34) aparecen en la Tabla 3. A partir de estas abundancias es posible calcular el peso atómico del azufre en cada una de las disoluciones enriquecidas isotópicamente utilizando la siguiente expresión:

$$Aw_{sp} = \frac{\sum(Aw^i \cdot A^i)}{100} \quad \text{Ecuación 33}$$

donde Aw^i es el peso isotópico del isótopo i , A^i es la abundancia isotópica del isótopo i y Aw_{sp} es el peso atómico del trazador. Los pesos isotópicos del ^{32}S , ^{33}S y ^{34}S son 31,972071; 32,971458 y 33,967867 respectivamente.

Finalmente, las concentraciones de azufre en los trazadores S33 y S34 se calcularon por dilución isotópica inversa. Para ello, se prepararon tres mezclas de disolución de trazador diluido 50 veces con disolución patrón de azufre natural de $20 \mu\text{g}\cdot\text{g}^{-1}$ en relaciones de peso 3:1, 1:1 y 1:3 respectivamente. Las nuevas relaciones $^{33}\text{S}/^{32}\text{S}$ y $^{34}\text{S}/^{32}\text{S}$ se midieron en las mezclas. La concentración de azufre en las disoluciones enriquecidas isotópicamente se calculó a partir de las R_m medidas utilizando la ecuación 13, si bien en este caso C_s es conocida y la incógnita a calcular es C_{sp} (el resto de parámetros son conocidos o se habrán calculado previamente tal como se ha descrito). Los resultados se muestran en la Tabla 3.

Tabla 3. Concentración, composición isotópica y peso atómico de las disoluciones enriquecidas isotópicamente en azufre-33 y azufre-34 utilizadas como trazadores.

Trazador	Concentración ($\mu\text{g}\cdot\text{g}^{-1}$) (n=3)	Composición isotópica (%)			Peso atómico
		^{32}S	^{33}S	^{34}S	
S33	1095 ± 3	0,01	99,70	0,29	32,975
S34	1231 ± 3	0,21	0,42	99,37	33,959

Cabe destacar que el enriquecimiento isotópico es mayor del 99% para los dos trazadores utilizados y que la incertidumbre en la concentración expresada como la desviación estándar de las medidas es menor del 0,3%, a pesar de que este dato es el resultado de tres mezclas en donde las proporciones de disolución de patrón de azufre natural y trazador isotópico son muy dispares.

C.3. PROCEDIMIENTOS EXPERIMENTALES

C.3.7. Preparación de levadura marcada con azufre-34

Para la preparación de levadura marcada con azufre-34 se utilizó en todos los casos células de *Saccharomyces cerevisiae* de la cepa AMW-13C. Este tipo de levadura presenta auxotrofia con respecto a los aminoácidos histidina, leucina y triptófano y la base nitrogenada uracilo. Esto quiere decir que este microorganismo carece de las rutas metabólicas funcionales que generan estos nutrientes y por tanto sólo es capaz de proliferar en un medio de cultivo que contenga dichas sustancias.

Con objeto de determinar las mejores condiciones de crecimiento de la levadura para su enriquecimiento en azufre-34, se llevó a cabo una serie de experimentos que se describe a continuación. En primer lugar, para analizar la cantidad mínima de azufre que aporta un crecimiento máximo, se utilizó un medio de cultivo comercial (YNB). Este medio fue seleccionado al carecer de los aminoácidos cisteína y metionina (típicamente en una concentración de $20 \text{ mg}\cdot\text{L}^{-1}$), así como de la fuente de nitrógeno utilizada para el crecimiento de levaduras (sulfato amónico, normalmente en una concentración de $5,0 \text{ g}\cdot\text{L}^{-1}$). De esta manera, se eliminan las fuentes principales de azufre presentes en los medios de cultivo convencionales.

A este medio comercial se le adicionó como fuente de nitrógeno cloruro amónico al 0,5% y como fuente de carbono glucosa al 3%, ambos elementos (N y C) indispensables para el crecimiento de las levaduras. Una vez preparado el medio de crecimiento, se ensayaron diferentes concentraciones finales de azufre en forma de sulfato amónico (0, 30, 300 y $10000 \mu\text{M}$) para analizar la cantidad mínima de azufre que aporta un crecimiento máximo. Como se puede ver en la Figura 22, se observó un ritmo de crecimiento similar en los diferentes medios tanto en condiciones de crecimiento fermentativas como oxidativas.

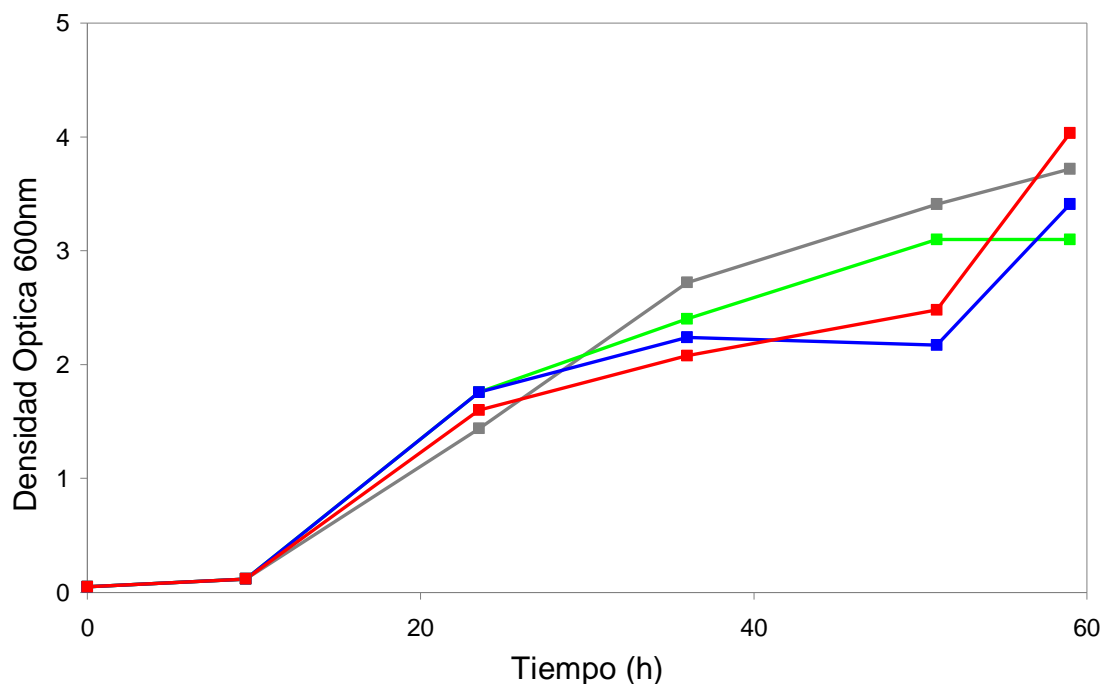


Figura 22. Crecimiento típico de la levadura en medio de cultivo YNB tras la adición de cantidades crecientes de azufre (como sulfato) (0 [■], 30 µM [■], 300 µM [■] y 10mM [■]).

Asimismo, el ritmo de crecimiento de la levadura (medido como el aumento de la densidad óptica del medio a 600 nm) era independiente de la concentración de azufre adicionada al medio, lo que indicaba claramente que el azufre no es un factor limitante para el crecimiento de la levadura cuando se usa un medio sintético basado en YNB. Teniendo en cuenta la información detallada sobre la composición química de todos los nutrientes, se comprobó *a posteriori* que el propio medio YNB comercial contiene suficiente azufre endógeno, principalmente como sulfato de magnesio ($0,5 \text{ g}\cdot\text{L}^{-1}$) y en menores concentraciones en compuestos suministradores de elementos esenciales de Cu, Mn y Zn ($1 \text{ mg}\cdot\text{L}^{-1}$ aprox.) para asegurar el crecimiento de las levaduras.

En un segundo experimento se utilizó cloruro de bario para eliminar el azufre presente en el medio YNB comercial, mediante precipitación como sulfato de bario. Sin embargo, tras la filtración del precipitado blanco formado, los resultados obtenidos fueron idénticos a aquellos mostrados en la Figura 22, indicando que todavía estaba presente en el medio una cantidad de azufre suficientemente alta como para soportar el crecimiento de la levadura.

Finalmente, se decidió preparar un medio de cultivo sintético completo, a partir de reactivos de alta pureza. Para ello, se sustituyeron los compuestos que presentan azufre en su composición, típicamente sulfatos inorgánicos, por otras sales

C. EXPERIMENTAL

inorgánicas como cloruros o nitratos de elevada pureza. El contenido de este medio de cultivo se indica en la Tabla 4, donde se han clasificado los nutrientes en grupos afines tales como aminoácidos, vitaminas, compuestos suministradores de elementos esenciales, sales inorgánicas y fuentes de carbono y nitrógeno.

Como fuente de carbono se utilizó glucosa al 3%. Para ello se preparó un lote de glucosa al 30% que se distribuyó en tubos de 50 mL. La disolución se esterilizó por filtración y se conservó en nevera a 4 °C hasta su uso. La fuente de nitrógeno comúnmente empleada es el sulfato amónico al 0,5%. Por tanto, se sustituyó esta sal inorgánica por cloruro amónico. Análogamente a la fuente de carbono, se preparó un lote de fuente de nitrógeno al 10%, se esterilizó por filtración, se distribuyó en tubos de 50 mL y se conservó a temperatura ambiente hasta su uso.

Se preparó un lote de aminoácidos veinte veces más concentrado que en el medio de cultivo, se esterilizó por filtración, se distribuyó en tubos de 50 mL y se conservó en nevera a 4 °C hasta su uso. En este punto se debe destacar la obligada ausencia de los aminoácidos organo-azufrados cisteína y metionina. Se preparó un lote de vitaminas de tal manera que tras esterilizar por filtración, se dividió en fracciones de 1 mL en tubos eppendorf y se conservó en congelador a -20 °C. Esta disolución se obtuvo cien veces más concentrada para utilizar únicamente una fracción por cada litro de medio de cultivo. Por otra parte, las vitaminas biotina (B7) y tiamina (B1) presentan azufre en su estructura. Sin embargo, dado el carácter esencial de estas vitaminas, así como la pequeña cantidad añadida de las mismas, se decidió incluirlas en la preparación del medio.

El lote de los compuestos suministradores de elementos esenciales se preparó de una manera similar al de vitaminas, obteniendo una disolución cien veces más concentrada que en el medio de cultivo y fraccionándola en alícuotas de 1 mL en tubos eppendorf que se conservaron hasta su uso en congelador a -20 °C. Para ello, los compuestos suministradores de cobre, manganeso y zinc, presentes en forma de sulfato en la fórmula comercial, se reemplazaron por nitratos y cloruros de elevada pureza. Finalmente, se preparó un lote de sales inorgánicas veinte veces más concentrado, donde se sustituyó el sulfato de magnesio por su cloruro homólogo y tras la esterilización de la disolución resultante por filtración, se distribuyó en tubos de 50 mL y se conservó a temperatura ambiente hasta su uso.

C.3. PROCEDIMIENTOS EXPERIMENTALES

C. EXPERIMENTAL

Tabla 4. Composición del medio de cultivo para el crecimiento de la levadura (por litro)


Fuente de carbono	
Glucosa	30 g
Fuente de nitrógeno	
NH ₄ Cl	5 g
Aminoácidos	
Histidina (His)	20 mg
Triptófano (Trp)	20 mg
Leucina (Leu)	20 mg
Arginina (Arg)	20 mg
Lisina (Lys)	20 mg
Treonina (Thr)	20 mg
Valina (Val)	20 mg
Tirosina (Tyr)	20 mg
Isoleucina (Ile)	20 mg
Vitaminas	
Biotina (vit. B7)	2 µg
Pantotenato cálcico (vit. B5)	400 µg
Ácido fólico (vit. B9)	2 µg
Inositol (vit. B8)	2 mg
Niacina (vit. B3)	400 µg
Ácido <i>p</i> -aminobenzoico (vit. BX)	200 µg
Hidrocloruro de piridoxina (vit. B6)	400 µg
Riboflavina (vit. B2)	200 µg
Hidrocloruro de tiamina (vit. B1)	400 µg
Compuestos suministradores de elementos esenciales	
Ácido bórico	500 µg
Nitrato de cobre	40 µg
Yoduro de potasio	100 µg
Cloruro férrico	200 µg
Cloruro de manganeso	400 µg
Molibdato de sodio	200 µg
Cloruro de zinc	400 µg
Sales inorgánicas	
Fosfato de monopotasio	1 g
Cloruro de magnesio	0,5 g
Cloruro de sodio	0,1 g
Cloruro de calcio	0,1 g

C.3. PROCEDIMIENTOS EXPERIMENTALES

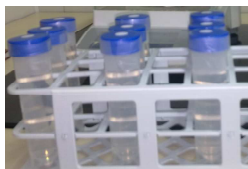
C. EXPERIMENTAL

Una vez preparados cada uno de los lotes de nutrientes necesarios, para la elaboración de un litro de medio de cultivo exento de azufre de abundancia natural únicamente se tienen que mezclar el contenido de dos tubos de 50 mL de disolución de glucosa y uno de cloruro amónico, aminoácidos y sales inorgánicas. Además, se debe adicionar un tubo eppendorf de vitaminas y otro con la disolución de compuestos suministradores de elementos esenciales. La Figura 23 recoge el procedimiento de preparación del medio de cultivo “exento” de azufre de abundancia natural para el crecimiento de la levadura.

Glucosa

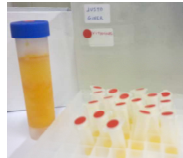


Fuente de nitrógeno

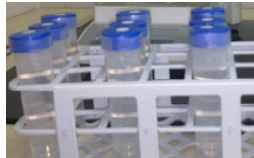


$(\text{NH}_4)_2\text{SO}_4 \rightarrow (\text{NH}_4)\text{Cl}$

Vitaminas

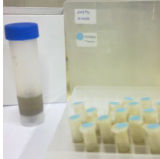


Aminoácidos




Elementos esenciales

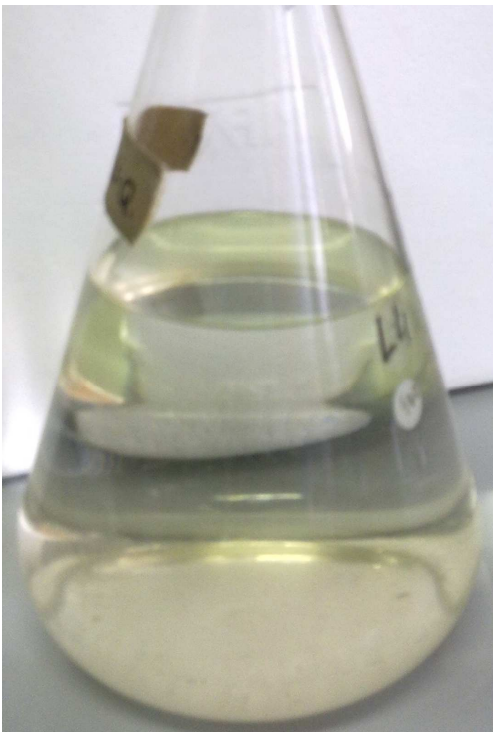
$\text{CuSO}_4 \rightarrow \text{Cu}(\text{NO}_3)_2$
 $\text{MnSO}_4 \rightarrow \text{MnCl}_2$
 $\text{ZnSO}_4 \rightarrow \text{ZnCl}_2$



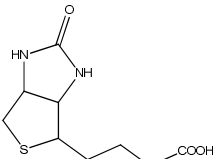
Sales inorgánicas

$\text{MgSO}_4 \rightarrow \text{MgCl}_2$

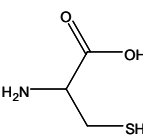




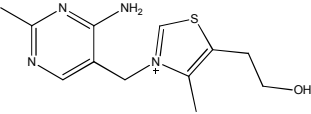
Biotina



~~Cistina~~



Tiamina



~~Metionina~~

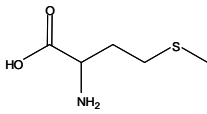


Figura 23. Resumen del procedimiento de preparación del medio de cultivo para el crecimiento de levaduras “exento” de azufre de abundancia natural.

C.3. PROCEDIMIENTOS EXPERIMENTALES

C. EXPERIMENTAL

Tras añadir las cantidades necesarias de cada uno de los nutrientes, el pH del medio resultante era $4,3 \pm 0,1$ ($n=5$). Dado que el pH óptimo para el crecimiento de las levaduras es 5,5 se debe añadir una disolución reguladora. Típicamente se utiliza el tampón MES para este fin, pero de nuevo, dado que contiene azufre en su composición (ácido 2-morfolinoetanosulfónico, $C_6H_{13}NO_4S$) se empleó un tampón acético/acetato 0,2 M de pH 5,6. Finalmente se añade agua ultrapura hasta completar el volumen deseado del medio de cultivo.

Este medio de cultivo sintético resultó ser efectivo para un crecimiento de levadura dependiente de la cantidad de azufre, ya que tal como se muestra en la Figura 24, se detectaron condiciones limitantes de azufre en el crecimiento de *Saccharomyces cerevisiae*.

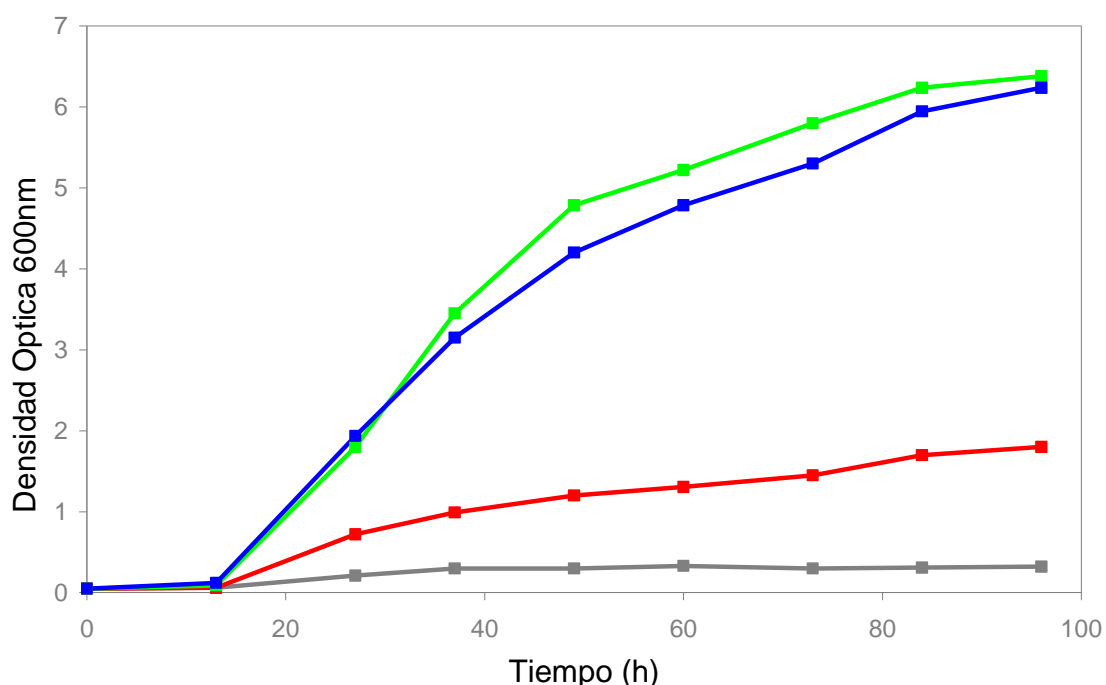


Figura 24. Efecto de la concentración adicionada de sulfato al nuevo medio de cultivo, sobre el crecimiento de la levadura (0 μ M [■], 10 μ M [■], 50 μ M [■] y 100 μ M [■]).

Nuestros resultados indican que cuando la concentración de sulfato amónico en el medio de cultivo sintético está por debajo de 50 μ M, el azufre actúa como un nutriente limitante en el crecimiento de la levadura. Por encima de esta concentración la tasa de crecimiento es máxima. Esto se confirmó en experimentos posteriores en los cuales se observó que el crecimiento de la levadura y por tanto la biomasa generada en condiciones de exceso de sulfato amónico (10.000 μ M) era similar al mostrado en la Figura 24 para una concentración 50 ó 100 μ M. Para los estudios siguientes de marcaje isotópico con azufre-34, se seleccionó una concentración de

C.3. PROCEDIMIENTOS EXPERIMENTALES

C. EXPERIMENTAL

100 μM de sulfato amónico $(\text{NH}_4)_2^{34}\text{SO}_4$ como fuente de azufre enriquecido. Además, se seleccionó un tiempo de crecimiento de 48 h como compromiso entre el tiempo de incubación y la biomasa alcanzada.

Como se comentó anteriormente, se usó a lo largo de todos los experimentos la cepa AMW-13C de la levadura *Saccharomyces cerevisiae*, de la cual se conserva un stock en glicerol a $-80\text{ }^\circ\text{C}$. A partir de una alícuota de esta cepa, se preparó una cantidad mucho mayor para la realización de los experimentos, mediante el crecimiento de las células en medio sólido. Los recursos utilizados para el crecimiento de las células de levadura en medio sólido se recogen en la Figura 25.



Figura 25. Recursos utilizados para el crecimiento de las células de levadura en medio sólido.

Se sembraron en condiciones estériles 100-200 μL de levadura en una placa de Petri con medio YPD y agar al 2%. Para sembrar (o inocular) la levadura, en primer lugar se calienta al rojo el asa de siembra, enfriándose a continuación sobre el propio gel de la placa y finalmente se procede a extender la levadura por la placa con ayuda de este asa. El gel de la placa de Petri consiste en un 2% de agar, que es un agente solidificante utilizado para la preparación de medios de cultivo microbiológicos sólidos y medio de cultivo YPD. La composición de este medio YPD es de glucosa 2-4%, pectona 2% y extracto de levadura 1%. Las células en medio sólido se dejaron crecer

C.3. PROCEDIMIENTOS EXPERIMENTALES

C. EXPERIMENTAL

en una estufa de incubación a 28 °C de temperatura durante 48 horas aproximadamente. Una vez conseguido el crecimiento de las células en medio sólido, la placa de Petry con la levadura se conserva en nevera a 4 °C hasta su uso.

El siguiente paso antes de sembrar la levadura en el medio de cultivo sintético exento de azufre de abundancia natural, es conocer exactamente la cantidad de células que se van a añadir a este medio de cultivo. Para ello se realiza un preinóculo en un medio líquido YPD, recogiendo con ayuda del asa de siembra un poco de levadura de la placa de Petry y añadiéndolo sobre este medio líquido rico en nutrientes. El cultivo resultante se coloca en un recipiente adecuado en un volumen inferior al 20% del volumen total con el fin de conseguir una buena aireación y se hace crecer en unas condiciones de 28 °C de temperatura y a 200 revoluciones por minuto (rpm) en un agitador circular (ver Figura 26). Típicamente se alcanza un valor de densidad óptica de 4 o superior en 12-15 horas.



Figura 26. Cámara termostatzada y agitador circular utilizado para el crecimiento de los medios líquidos.

El crecimiento celular se determinó midiendo la turbidez del cultivo a 600 nm. Para ello se coge 1 mL del cultivo y se centrifuga a 14000 rpm durante 2 minutos. Se desecha el sobrenadante ya que puede interferir en la medida espectrofotométrica posterior y el material celular sedimentado (pellet) se resuspende en 1 mL de agua estéril. Para determinar la densidad óptica del cultivo a 600 nm ($D.O_{600}$) se añade un volumen conocido de la suspensión de células al tubo de medida y se completa el volumen hasta 3 mL. Se determina el valor de absorbancia del cultivo que será igual al valor medido multiplicado por el factor de dilución correspondiente. Una vez conocido el valor $D.O_{600}$ del cultivo utilizado para el preinóculo, se calcula el volumen adecuado de cultivo que se quiere inocular en el medio enriquecido en azufre-34 para tener una

C.3. PROCEDIMIENTOS EXPERIMENTALES

C. EXPERIMENTAL

determinada y conocida cantidad de células inicial (típicamente un valor $D.O._{600}$ de 0,05 ó 0,1). A continuación se recoge del cultivo el volumen calculado de preinóculo, las células se lavan 2 veces con agua estéril a 14.000 rpm durante 2 minutos para eliminar el azufre inorgánico de abundancia natural presente en el medio YPD original y finalmente se inocula este preinóculo lavado en el medio enriquecido. Las condiciones de cultivo para el crecimiento de las levaduras marcadas isotópicamente con azufre-34 fueron las mismas que las detalladas para el preinóculo, esto es, 28 °C de temperatura y a 200 rpm en un agitador circular (ver Figura 26).

Se realizó el seguimiento del ritmo de crecimiento celular de la levadura midiendo la densidad óptica del medio de cultivo espectrofotométricamente a 600 nm. La Figura 27 muestra las imágenes tomadas cada 6 horas del cultivo celular así como el valor de $D.O._{600}$ obtenido al correspondiente tiempo de incubación.

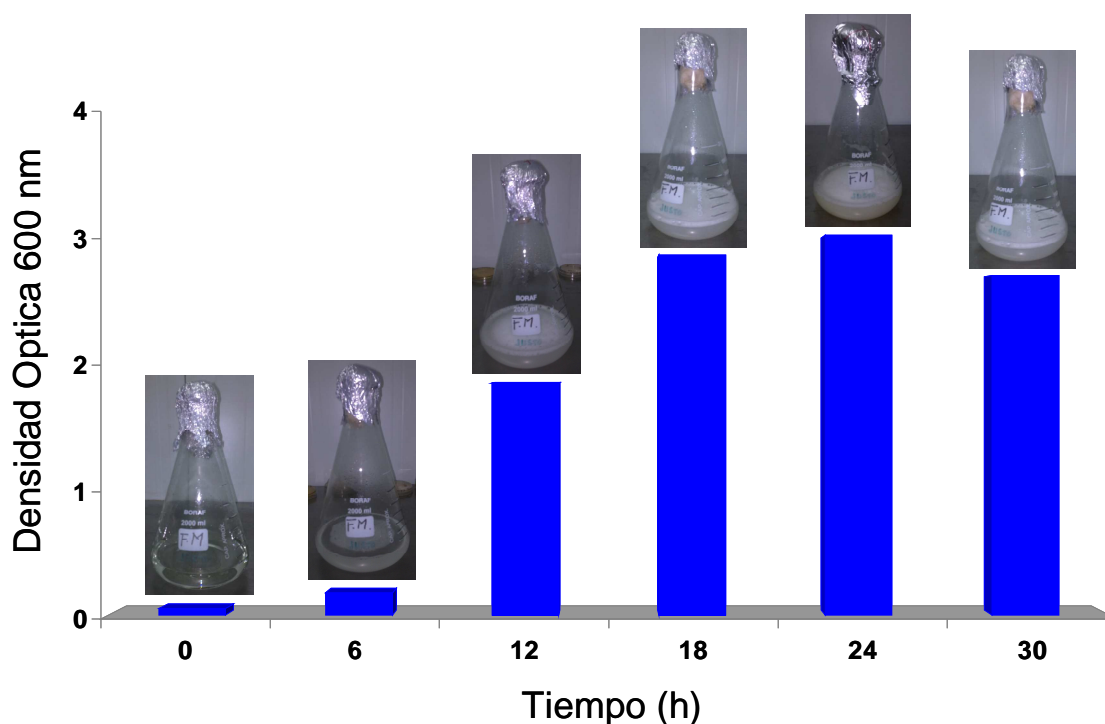


Figura 27. Seguimiento del crecimiento celular y evolución del medio de cultivo enriquecido con azufre-34 mediante medidas de turbidez a 600 nm.

Una vez terminado el tiempo de incubación, se recogen las células de levadura y se centrifugan a 6.000 revoluciones durante 10 minutos. Se desecha el sobrenadante y se hacen dos lavados sucesivos con agua estéril para eliminar el exceso de azufre-34 inorgánico que no se ha incorporado a las células. Finalmente las células enteras

C.3. PROCEDIMIENTOS EXPERIMENTALES

de levadura marcada con azufre-34 (pellet) se almacenan a -20 °C hasta su uso. En la Figura 28 se muestran diferentes etapas del proceso de preparación de levadura marcada con azufre-34.

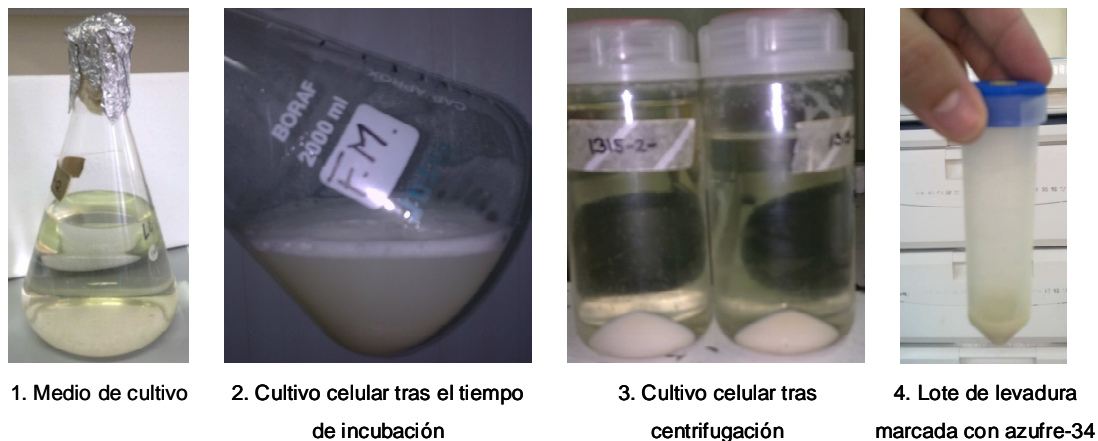


Figura 28. Etapas del proceso de preparación de levadura marcada con azufre-34.

Para la caracterización de los lotes preparados de levadura marcada con azufre-34, se utilizó la ecuación 34, que relaciona el peso seco de la levadura con el valor obtenido mediante medidas de turbidez a 600 nm de una alícuota del lote.

$$1 D.O._{600\text{ nm}} = 3,55 \cdot 10^7 \frac{\text{células}}{\text{mL}} = 0,86 \frac{\text{mg peso seco}}{\text{mL}} \quad \text{Ecuación 34}$$

C.3.8. Digestión de las muestras sólidas

Previamente al análisis por ICP-MS, las muestras sólidas se pusieron en disolución mediante digestión ácida en horno de microondas. Para ello, una cantidad de muestra de alrededor de 0,1 g se deposita en la bomba de digestión de microondas. A continuación, se adicionan 1,5 mL de ácido nítrico y 0,5 mL de peróxido de hidrógeno. En aquellos casos en los que se cuantifica por dilución isotópica, se adiciona además la cantidad apropiada de trazador enriquecido. La mezcla se somete al programa de microondas siguiente: 250 W de potencia durante 5 minutos hasta alcanzar una temperatura de 170 °C. Una vez finalizada la digestión ácida asistida por microondas, y dado que para el análisis por ICP-MS es conveniente nebulizar disoluciones con un contenido inferior al 5% de ácido nítrico, las muestras se diluyeron apropiadamente con agua Milli-Q.

C.3.9. Deconvolución de perfiles isotópicos (IPD)

Se denomina perfil isotópico de un elemento al conjunto de las abundancias isotópicas relativas de todos sus isótopos estables. El perfil isotópico natural de un elemento es el perfil isotópico que se encuentra en la naturaleza y que se puede considerar constante e invariable. Las abundancias isotópicas naturales de los elementos están tabuladas incluyendo sus incertidumbres [44], por lo que el cálculo del perfil isotópico natural de cualquier elemento químico se puede realizar fácilmente. Sin embargo, cuando utilizamos un elemento enriquecido isotópicamente, hablamos de un perfil isotópico alterado. En este perfil, la abundancia relativa de uno o varios isótopos estables de dicho elemento es claramente distinta de la natural. Se denomina Deconvolución de Perfiles Isotópicos (IPD) al proceso matemático que permite el cálculo de la contribución de cada perfil isotópico de un mismo elemento sobre el perfil isotópico medido experimentalmente en la muestra por espectrometría de masas [222]

En estudios de metabolismo utilizando isótopos estables enriquecidos de azufre, la muestra a analizar contiene una cantidad desconocida tanto del perfil isotópico natural (S_{nat}) como del perfil isotópico alterado utilizado como trazador metabólico (S₃₄) incorporado al organismo en estudio. Un segundo perfil isotópico alterado (S₃₃) se añade a la muestra para cuantificar el azufre mediante el análisis por dilución isotópica y su contribución es, por tanto, conocida. Esto supone, por tanto, el uso de un perfil isotópico natural (S_{nat}) y dos perfiles isotópicos alterados de azufre (S₃₃ y S₃₄). El procedimiento general del análisis por ICP-MS utilizando isótopos estables enriquecidos de azufre y la herramienta matemática de deconvolución de perfiles isotópicos (IPD) se esquematiza en la Figura 29.

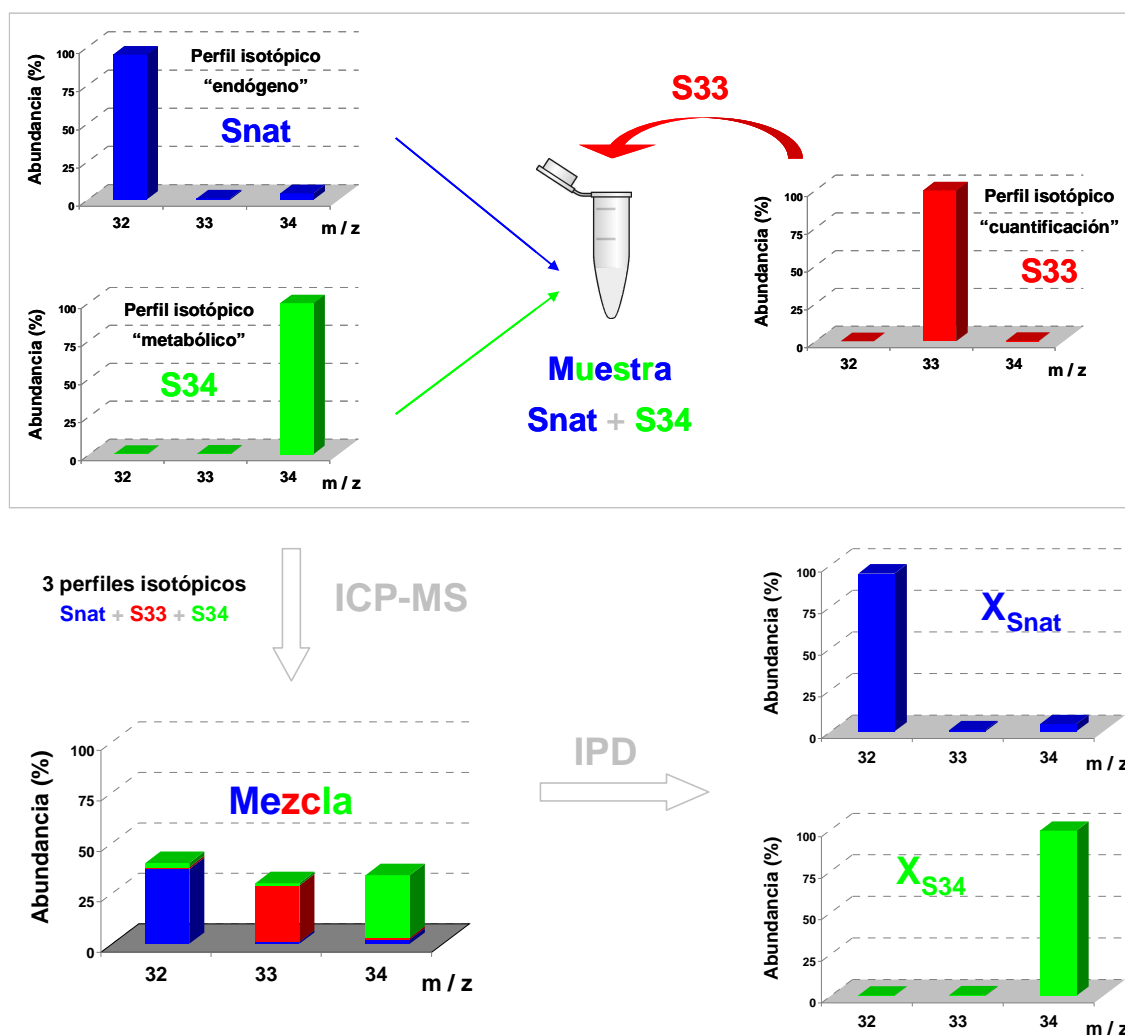


Figura 29. Esquema general del análisis por ICP-MS utilizando isótopos estables enriquecidos de azufre y Deconvolución de Perfiles Isotópicos (IPD).

El balance de masas para el número de moles totales del elemento en la mezcla, N_m , vendrá dado por:

$$N_m = N_{nat} + N_{34} + N_{33} \quad \text{Ecuación 35}$$

donde N_{nat} es el número de moles de azufre natural (Snat), N_{34} son los moles de azufre procedentes del trazador metabólico S34 y N_{33} son los moles de azufre procedentes del trazador S33 utilizado para la cuantificación por dilución isotópica.

El balance de masas de la Ecuación 35 puede calcularse también para todos y cada uno de los isótopos de azufre que configuran su perfil isotópico en la mezcla. Por ejemplo, para el isótopo 32 de azufre, el balance de masas sería:

$$N_m^{32} = N_{nat}^{32} + N_{34}^{32} + N_{33}^{32} \quad \text{Ecuación 36}$$

La Ecuación 36 se puede expresar como una combinación lineal de la cantidad total del elemento en cada uno de los perfiles isotópicos y de las abundancias isotópicas conocidas o medidas de cada perfil, según:

$$N_m \cdot A_m^{32} = N_{nat} \cdot A_{nat}^{32} + N_{34} \cdot A_{34}^{32} + N_{33} \cdot A_{33}^{32} \quad \text{Ecuación 37}$$

donde A_m^{32} , A_{nat}^{32} , A_{34}^{32} y A_{33}^{32} son las abundancias isotópicas del isótopo 32 en cada uno de los perfiles isotópicos medidos experimentalmente (A_m^{32}) o conocidos (A_{nat}^{32} , A_{34}^{32} y A_{33}^{32}). Si dividimos la Ecuación 37 entre la Ecuación 35 se obtiene la siguiente expresión matemática:

$$A_m^{32} = x_{nat} \cdot A_{nat}^{32} + x_{34} \cdot A_{34}^{32} + x_{33} \cdot A_{33}^{32} \quad \text{Ecuación 38}$$

donde $x_{nat} = \frac{N_{nat}}{N_m}$, $x_{34} = \frac{N_{34}}{N_m}$ y $x_{33} = \frac{N_{33}}{N_m}$ son las fracciones molares de cada uno de los perfiles isotópicos que contribuyen al perfil isotópico observado en la muestra.

Como el azufre presenta 3 isótopos estables que pueden ser medidos por ICP-MS (^{32}S , ^{33}S y ^{34}S), se pueden definir 3 ecuaciones diferentes (una para cada isótopo) que expresan la combinación lineal de abundancias isotópicas y fracciones molares (Ecuación 38). Esta serie de ecuaciones se puede expresar, en notación matricial, como:

$$\begin{bmatrix} A_m^{32} \\ A_m^{33} \\ A_m^{34} \end{bmatrix} = \begin{bmatrix} A_{nat}^{32} & A_{34}^{32} & A_{33}^{32} \\ A_{nat}^{33} & A_{34}^{33} & A_{33}^{33} \\ A_{nat}^{34} & A_{34}^{34} & A_{33}^{34} \end{bmatrix} \begin{bmatrix} x_{nat} \\ x_{34} \\ x_{33} \end{bmatrix} \quad \text{Ecuación 39}$$

La solución exacta de la Ecuación 39 proporciona los valores de las incógnitas x_{nat} , x_{34} y x_{33} . El proceso de calcular las fracciones molares en sistemas como el que aparece en la Ecuación 39 se viene denominando Deconvolución de Perfiles Isotópicos (IPD) en la literatura moderna [117].

Una vez que se han determinado los valores de las fracciones molares en la muestra, se calculan las relaciones $\frac{x_{nat}}{x_{33}}$ y $\frac{x_{34}}{x_{33}}$ que coinciden con las relaciones de moles $\frac{N_{nat}}{N_{33}}$ y $\frac{N_{34}}{N_{33}}$ respectivamente. Es decir:

$$\frac{x_{nat}}{x_{33}} = \frac{N_{nat}}{N_{33}} \quad \text{Ecuación 40} \quad \text{y} \quad \frac{x_{34}}{x_{33}} = \frac{N_{34}}{N_{33}} \quad \text{Ecuación 41}$$

Como la cantidad añadida del trazador de azufre-33 (N_{33}) es conocida, es posible determinar directamente la cantidad de elemento natural y trazador de azufre-34 en la mezcla.

C.3.10. Estudios con ratas Wistar

Los experimentos *in vivo* se realizaron en la Unidad de Laboratorio Animal de la Universidad de Oviedo, siguiendo las directrices respecto a la protección de animales utilizados para experimentación y otros fines científicos, recogidas en la Directiva Europea de Experimentación Animal (86/609/EEC).

En concreto, a un grupo de cinco ratas Wistar macho, de pesos 95-105 g se les administró levadura marcada con azufre-34 (1,0 g aprox.) en una dosis única. A continuación, se mantuvieron en jaulas metabólicas a una temperatura estable de 22 °C con ciclos de luz/oscuridad de 12/12 horas. Las ratas fueron sacrificadas por exanguinación mediante una punción en el corazón, a las 6, 12, 24, 48 y 96 horas después de la administración de la levadura marcada, empleando como anestésico isoflurano al 5% vaporizado en oxígeno. Las muestras de sangre se dejaron coagular a temperatura ambiente durante 1 hora y a continuación se llevó a cabo una centrifugación (3.000 rpm, 15 min, 4 °C) para separar los eritrocitos de la fracción de suero sanguíneo de cada muestra.

Inmediatamente después de la exanguinación, se extrajeron los órganos de cada una de las ratas Wistar objeto de estudio: bazo, cerebro, corazón, hígado, intestino delgado, páncreas, pulmón, riñón y testículo. Cada órgano se depositó individualmente en tubos tipo Falcón cónicos estériles de polipropileno (50 mL) y se congelaron mediante inmersión en nitrógeno líquido (-195,8 °C). A continuación, se sometieron a una etapa de liofilización durante 48 horas y tras eliminar el agua de los tejidos por

C. EXPERIMENTAL

sublimación, éstos se machacaron y homogeneizaron en un mortero de ágata. El polvo resultante de cada uno de los tejidos se guardó a -80 °C hasta su análisis.

La orina y las heces de las ratas se recogieron de sus respectivos colectores a los tiempos de muestreo anteriormente indicados. La orina se centrifugó (3.000 rpm x 5 min y 4 °C) y se congeló a -20 °C hasta su posterior análisis. Las muestras de heces se trataron exactamente igual que los tejidos.

En la Figura 30 se recoge un esquema representativo del procedimiento experimental *in vivo* realizado con ratas Wistar sanas alimentadas con levadura marcada con azufre-34.

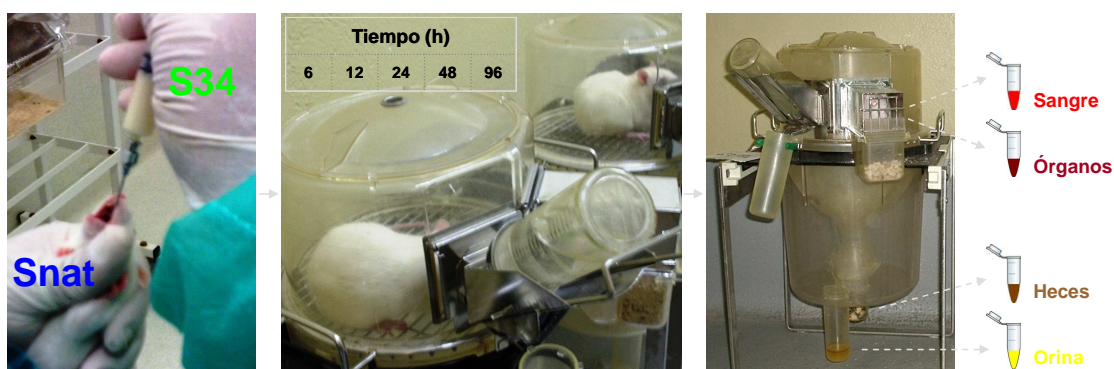
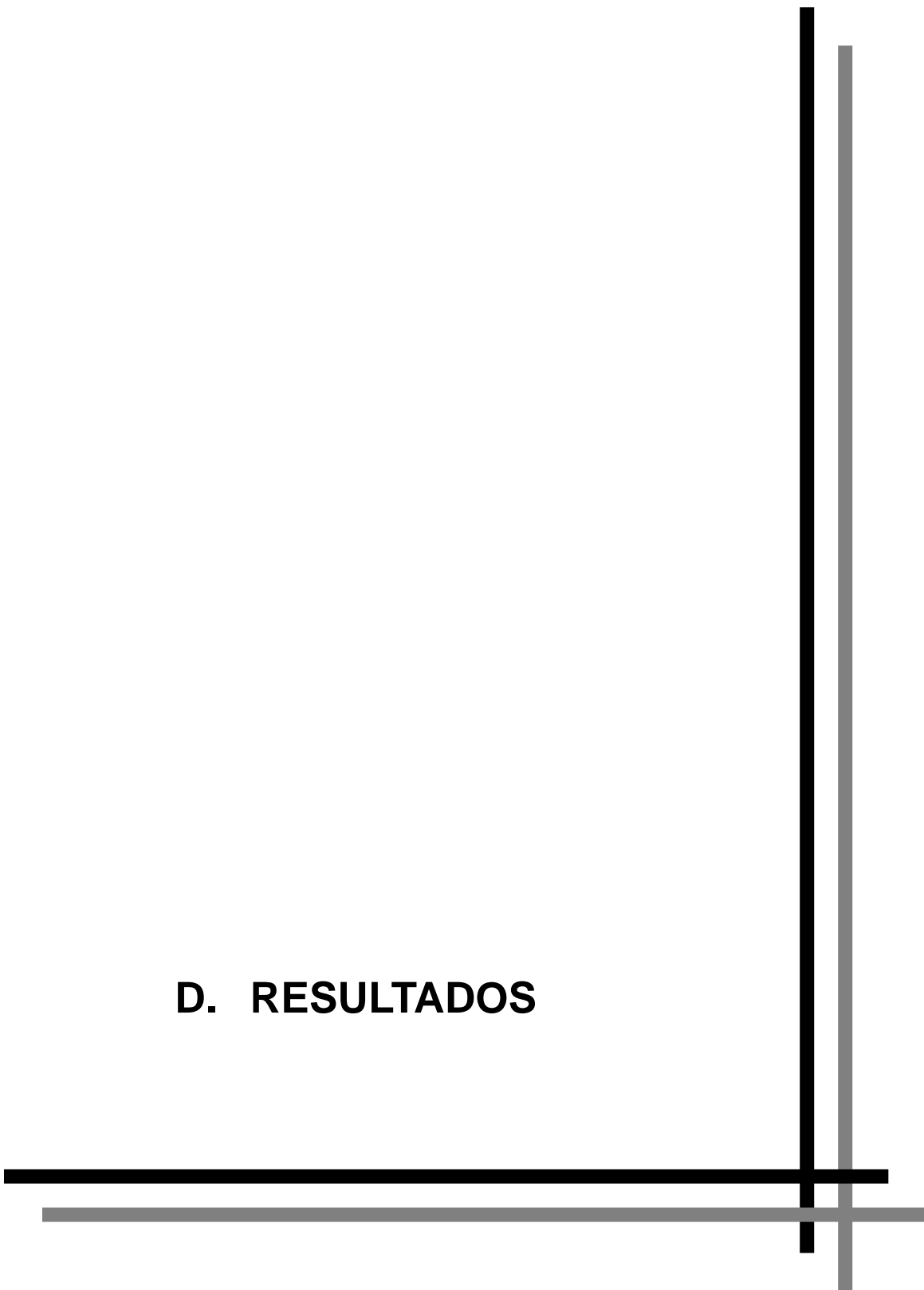


Figura 30. Esquema representativo del procedimiento experimental *in vivo* realizado con ratas Wistar.

C.3. PROCEDIMIENTOS EXPERIMENTALES

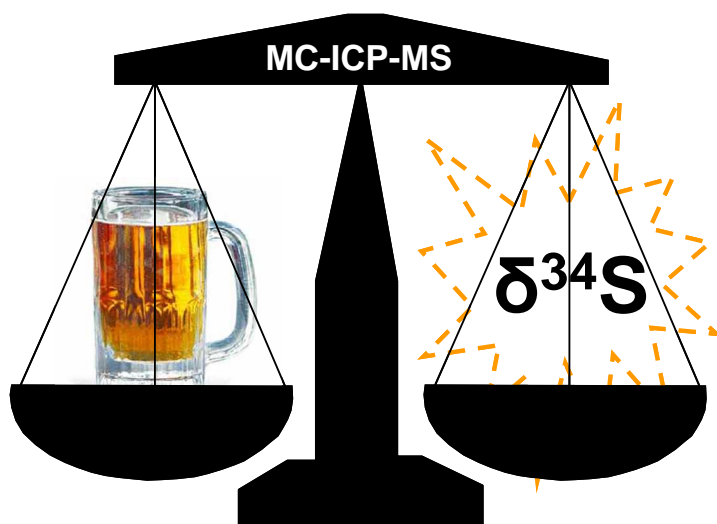
D. RESULTADOS



D.1. ESTUDIOS DE VARIABILIDAD NATURAL DE LA COMPOSICIÓN ISOTÓPICA DE AZUFRE MEDIANTE ICP-MS MULTICOLECTOR

D.1.1. Desarrollo de un procedimiento directo para la medida de la variabilidad isotópica de azufre en muestras de cerveza mediante ICP-MS multicolector

D.1.1.1. Artículo científico I: J. Agr. Food Chem., 2010, 58, 4043-4050



Development of a Direct Procedure for the Measurement of Sulfur Isotope Variability in Beers by MC-ICP-MS

J. GINER MARTÍNEZ-SIERRA,[†] R. SANTAMARIA-FERNANDEZ,[‡] R. HEARN,[‡]
J. M. MARCHANTE GAYÓN,[†] AND J. I. GARCÍA ALONSO^{*,†}

[†]Department of Physical and Analytical Chemistry, University of Oviedo, Julian Clavería 8, 33006 Oviedo, Spain, and [‡]LGC Ltd., Queens Road, Teddington, Middlesex TW11 0LY, U.K.

In this work, a multi-collector inductively coupled plasma mass spectrometer (MC-ICP-MS) was evaluated for the direct measurement of sulfur stable isotope ratios in beers as a first step toward a general study of the natural isotope variability of sulfur in foods and beverages. Sample preparation consisted of a simple dilution of the beers with 1% (v/v) HNO₃. It was observed that different sulfur isotope ratios were obtained for different dilutions of the same sample indicating that matrix effects affected differently the transmission of the sulfur ions at masses 32, 33, and 34 in the mass spectrometer. Correction for mass bias related matrix effects was evaluated using silicon internal standardization. For that purpose, silicon isotopes at masses 29 and 30 were included in the sulfur cup configuration and the natural silicon content in beers used for internal mass bias correction. It was observed that matrix effects on differential ion transmission could be corrected adequately using silicon internal standardization. The natural isotope variability of sulfur has been evaluated by measuring 26 different beer brands. Measured $\delta^{34}\text{S}$ values ranged from -0.2 to 13.8 ‰. Typical combined standard uncertainties of the measured $\delta^{34}\text{S}$ values were ≤ 2 ‰. The method has therefore great potential to study sulfur isotope variability in foods and beverages.

KEYWORDS: Sulfur isotope ratios; natural variability; beer; MC-ICP-MS; matrix effects

INTRODUCTION

The natural variability of the isotopic composition of an element needs to be evaluated for different purposes. First, the isotopic composition of a given element in a certain product is acquired during its manufacture, and it is unique to its history and origin. When two separate samples of the same product are chemically the same and have identical isotopic profiles, then there is a high degree of certainty that both samples originate from the same source. Manufacturing and/or biological processes can result in the formation of products whose stable isotope composition is characteristic of that process. Therefore, the isotopic composition of different elements (C, S, Sr, Pb, etc.) can be used for traceability purposes.

A second purpose of these natural variability studies is to evaluate the minimum amount of an enriched isotope which would be needed for tracer work. For example, if we want to follow the metabolic pathway of a certain element in the human body by using an isotopically enriched tracer, the amount of tracer to be used should be enough to change the isotopic composition of the element above the natural variability limits. The isotopic composition of most elements in the human body depends mainly on food and drink intake. Therefore, the natural isotope variability of the elements in foods and beverages could be used to estimate the natural variability in the human body.

Differences in sulfur isotopic composition, observed in sulfur-containing compounds from different sources (1), have been

widely reported (2–14). The relative difference between measured isotope ratios of an element is usually expressed using the per mil notation (‰). Sulfur ³⁴S/³²S isotope ratios, expressed as $\delta^{34}\text{S}$ ‰ values, have been reported to discriminate geographical origin in meat (15), butter produced from cow's milk (16), and cheese (17). Natural variations of ³⁴S/³²S isotope amount ratios often occur around the third or fourth significant figure and are commonly measured by gas source isotope ratio mass spectrometry (GS-IRMS) after a tedious and laborious sample preparation procedure. Quadrupole collision/reaction cell and sector field ICP-MS instruments have been used for the measurement of sulfur isotope ratios (18–22). Because of plasma instabilities and because data acquisition is performed in a sequential mode, the precision obtained in these studies allow only relatively large variations in sulfur isotopic composition to be detected. Continuous flow methods involving the use of MC-ICP-MS have recently been reported (23–27). The use of MC-ICP-MS offers the capability of detecting and measuring multiple isotopes simultaneously with minimal sample preparation (e.g., in comparison with GS-IRMS) and typical instrumental precision from 0.1% to <0.005% (12, 13, 28) depending on sulfur concentration.

The main problem affecting isotope ratio measurements by MC-ICP-MS is the existence of matrix effects on the mass bias correction factor. The transmission of the ions in the mass spectrometer will change slightly in the presence of high concentrations of the matrix, and this change will not be the same for different isotopes of the same element. Therefore, apparent changes in isotope ratios could be due to matrix effects and not

*Corresponding author. E-mail: jiga@uniovi.es.

to real changes in the sample. There are different alternatives to eliminate or correct for these matrix effects. The traditional solution is the separation of the element from the matrix and the use of a certified isotopic standard of the element for external mass bias correction. As an alternative, internal mass bias correction, using another element close in mass, can be applied. For sulfur measurements, silicon internal standardization has been used to correct for mass bias effects (25). It was observed that silicon could correct for matrix effects from sodium, chlorine and calcium in waters (25). In this article, we explore the capabilities of silicon for the correction of mass bias related matrix effects in the determination of sulfur natural isotope variations by MC-ICP-MS in samples containing large amounts of dissolved organic matter. Then, a simple dilution of the sample would be enough, opening the way for large studies on sulfur isotope variations in foods and beverages with a very simple sample preparation. To demonstrate the potential of the method, 26 beer samples representative of those currently on sale in the U.K. were analyzed. $\delta^{34}\text{S}$ values, reported relative to the Vienna Canyon Diablo Troilite (VCDT) scale (29), were obtained. NIST RM8553 was used as the working standard to anchor our results to the VCDT scale.

EXPERIMENTAL SECTION

Reagents and Standards. High purity reagents were used throughout. Water was taken directly from an 18.2 M Ω cm supply (Elga Ltd., High Wycombe, U.K.). Three sulfur reference materials (RM) were employed in this study: (a) National Institute of Science and Technology (NIST) RM8553, Soufre de Lacq-Elemental sulfur, $\delta^{34}\text{S} = 16 \pm 0.3$ (‰); (b) NIST RM8554, IAEA-SI Silver sulfide (AgS), $\delta^{34}\text{S} = -0.3 \pm 0.3$ (‰); and (c) NIST RM8556, NBS 123 Sphalerite, $\delta^{34}\text{S} = 17.44 \pm 0.3$ (‰).

Each reference material was separately prepared by digesting an aliquot in a closed vessel microwave digester (Multiwave 3000, Perkin-Elmer, Beaconsfield, U.K.) with high purity HNO₃ acid (ROMIL, Cambridge, U.K.) and subsequent dilution with high purity water. Two reference values are given for RM8553. This work adopts the $\delta^{34}\text{S}$ value of $+16 \pm 0.3$ ‰, and RM8553 was selected as the main working standard because it required the least sample preparation. Both RM8554 and RM8556 were used to evaluate instrumental performance. The Si internal standard source was an Assurance Spex CertiPrep ICP (1,000 $\mu\text{g g}^{-1}$) standard solution (Spex Certiprep Ltd., Stanmore, Middlesex, U.K.). The isotopic composition of the Spex Si standard was measured in-house using the certified IRMM017 Si material for bracketing during the MC-ICP-MS measurements. The Spex silicon standard was added to RM8553, RM8554, and RM8556 to correct for mass bias in the sulfur measurements. The direct addition of IRMM017 to the sulfur isotopic standards RM8553, RM8554, and RM8556 was not performed in order to save the expensive IRMM017 standard.

Instrumentation. The MC-ICP-MS instrument used in this study was Neptune (ThermoFisherScientific, Bremen, Germany). Neptune has an argon plasma ion source, forward Nier-Johnson geometry, and nine Faraday cup detectors. Typical operating conditions have been published elsewhere (30). The instrument, located at LGC, can be used to measure simultaneous ion signals in three resolution modes, low, medium, and high. The spectral interferences affecting the accuracy of the sulfur and silicon isotope ratio measurements (mainly $^{16}\text{O}_2^+$, $^{16}\text{O}^{18}\text{O}^+$, $^{14}\text{N}^{14}\text{N}^+\text{H}^+$, and $^{14}\text{N}^{16}\text{O}^+$, respectively) were resolved using the Neptune instrument working at medium resolution. The potential hydride interference of $^{28}\text{Si}^+\text{H}^+$ previously reported (31) was not detected. A typical mass scan obtained for sulfur and silicon isotope ratio measurements working at medium resolution in the Neptune MC-ICP-MS is shown in Figure 1. The axial Faraday cup (C) was fixed at mass 31.26 (amu) for multiple interference-free simultaneous measurements of ^{29}Si (L4), ^{30}Si (L1), ^{32}S (H1), and ^{34}S (H4) isotopes. In this scan, the signal intensities of Si isotopes 29 and 30 and ^{34}S have been normalized to that of ^{32}S .

The instrumental mass discrimination of the measured $^{34}\text{S}/^{32}\text{S}$ isotope amount ratio was corrected by interpolation of the mass discrimination observed for $^{30}\text{Si}/^{29}\text{Si}$ isotope amount ratio using Russell's equation (32).

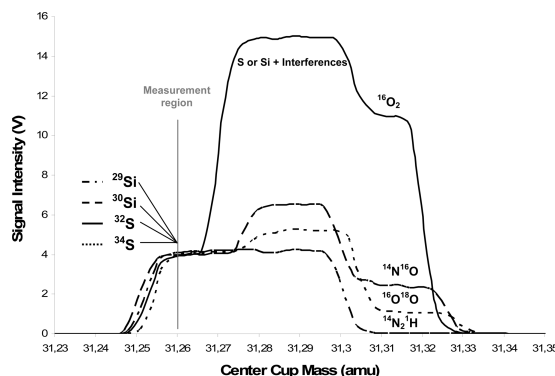


Figure 1. Typical mass scan obtained for sulfur and silicon isotope ratio measurements working at medium resolution in the Neptune MC-ICP-MS instrument. The center Faraday cup has been fixed at mass 31.26 (amu) for multiple interference free simultaneous measurements of S and Si isotopes. In this scan, the signal intensities of Si isotopes and ^{34}S have been normalized to that of ^{32}S .

The corrected ratio is a function of the two measured isotope ratios and the relative atomic mass difference between the isotope pairs. For the beer samples, the $^{30}\text{Si}/^{29}\text{Si}$ reference isotope amount ratio used was taken from the last compilation of the IUPAC values (1) including the natural variability in the silicon isotope abundances as uncertainty. For the sulfur isotopic reference materials, the $^{30}\text{Si}/^{29}\text{Si}$ reference isotope amount ratio used was that measured for the Spex silicon standard. Mass bias was typically 3.3% per atomic mass unit.

It is important to highlight that the mass difference between ^{29}Si and ^{34}S is close to the limit of the mass range of the Neptune's Faraday detector array ($\pm 8.5\%$ relative to the mass focused into the fixed center channel). However, by adjusting the dispersion and focus lenses to -5 V and 15 V, respectively, and fixing the center cup at mass 31.26 amu, all of the isotopes of interest can be measured within the same cup configuration, as previously reported by Mason et al (18). As a result, this cup configuration drastically reduces the time needed for the analysis of liquid solutions when compared to a similar analysis reported before where S and Si isotope ratios ($^{30}\text{Si}/^{28}\text{Si}$) had to be monitored using two separate cup configurations (25). In addition, the new method can be applied to the measurement of transient signals where a mass bias correction can be performed simultaneously. For the method used in this study, each complete acquisition comprised 5 cycles divided into 5 blocks, and the total acquisition time for each sample measurement was less than 4 min. A microconcentric glass nebulizer (Micromist) and a quartz sample introduction system (SIS) spray chamber were used in this study. Operating conditions and data acquisition parameters are summarized in Table 1.

Measurement of $\delta^{34}\text{S}$ in Beers by MC-ICP-MS. A suite of 26 beers representative of those currently on sale at specialized stores and supermarkets in England were measured. Sample preparation was kept to a minimum, and beer samples were simply diluted with 1% (v/v) HNO₃ to approximately 1:3 for direct measurement in the MC-ICP-MS. No problems with signal losses, blocked cones, or nebulizers were observed. NIST reference materials were doped with the Spex silicon standard at approximately $5 \mu\text{g g}^{-1}$ to correct for mass bias effects using the equation:

$$\left(\frac{^{34}\text{S}}{^{32}\text{S}}\right)_{\text{cor}} = \frac{\left(\frac{^{34}\text{S}}{^{32}\text{S}}\right)_{\text{meas}}}{\left(\frac{\ln\left(\frac{\text{Mass}^{34}\text{S}}{\text{Mass}^{32}\text{S}}\right)}{\ln\left(\frac{\text{Mass}^{30}\text{Si}}{\text{Mass}^{29}\text{Si}}\right)}\right)} \quad (1)$$

Article

Table 1. Operating Conditions and Data Acquisition Parameters for the Measurement of Sulfur and Silicon Isotope Ratios in Beer Samples

MC-ICP-MS Settings		
Rf power		1350 W
cool gas flow		14.0 L min ⁻¹ Ar
auxiliary gas flow		0.7 L min ⁻¹ Ar
sample gas flow		1.0 L min ⁻¹ Ar
sampler and skimmer cones		Ni
extraction voltage		-2000 V
focus lens		15 V
dispersion Lens		-5 V
Data Acquisition Parameters		
resolution mode	medium	
	L4	²⁹ Si
	L1	³⁰ Si
cup configuration	C	31.26
	H1	³² S
	H4	³⁴ S
acquisition method	5 blocks, 5 cycles, 4.194 s integration	

where the abbreviations cor, meas, and ref indicate corrected, measured, and reference, respectively. Silicon was present in beer samples at relatively high levels; thus, the external addition of silicon to beer samples was not required. For the beer samples, the reference isotope ratio for silicon was taken from the IUPAC tables (1), and then eq 1 was applied. NIST RM8553 was used as the working standard for $\delta^{34}\text{S}$ measurements. A solution containing NIST RM8553 and silicon was analyzed every 5 samples and corrected for mass bias also using eq 1. In this case, the reference silicon isotope ratio was that measured for the Spex silicon standard. Then, the $\delta^{34}\text{S}$ value relative to the VCDT was calculated using:

$$\delta^{34}\text{S}_{\text{VCDT}} = \left(\left(\frac{\left(\frac{^{34}\text{S}}{^{32}\text{S}} \right)_{\text{beer, cor}}}{\left(\frac{^{34}\text{S}}{^{32}\text{S}} \right)_{\text{RM8553, cor}}} \right) \times \left(\frac{\delta^{34}\text{S}_{\text{RM8553}}}{1000} + 1 \right) - 1 \right) \times 1000 \quad (2)$$

Finally, NIST RM8554 and NIST RM8556 were also analyzed to monitor the performance of the instrument at both ends of the range of variation in $\delta^{34}\text{S}$. In total, 26 beers and 3 sulfur reference materials, as summarized in Table 2, were analyzed.

Evaluation of Uncertainty Sources. Combined standard uncertainties were calculated following the Kragten spreadsheet method (33) taking into account instrumental variability, the uncertainties associated with the reference materials used in the calculation, and the mass bias correction applied to the observed isotope ratios. In total, seven uncertainty sources were identified, and they are shown in Table 3. The first six uncertainty sources arise from the application of eq 1 both to the beer sample and to the RM8553. The final uncertainty source is the uncertainty in the $\delta^{34}\text{S}$ value of RM8553 relative to the VCDT. Typical values for one of the samples are shown in Table 3. For the four measured isotope ratios, their uncertainties were taken as the standard error of the mean. For the reference silicon isotope ratio values, the uncertainties were calculated as described in the Results and Discussion section.

Finally, the uncertainty of each $\delta^{34}\text{S}$ value was calculated in accordance with error propagation laws as described in EURACHEM Guide (34) using the Kragten procedure. Combined standard uncertainties for the measured samples are given in Table 2.

RESULTS AND DISCUSSION

Uncertainties of the Reference Silicon Isotope Values.

(a). *Uncertainty of the Reference IUPAC Isotope Ratio.* The last representative isotope composition of silicon as tabulated by the IUPAC (1) indicates that the isotope abundances of ²⁸Si, ²⁹Si, and ³⁰Si were 0.92223(19), 0.04685(8), and 0.03092(11), respectively, where the values in parentheses indicate expanded uncertainties

due to natural variability. From these data, the reference isotope ratio ³⁰Si/²⁹Si would be 0.65998. For the calculation of the uncertainty of this value, we have taken into account the recent paper by Meija and Mester (35) in which they demonstrate that isotope abundances are correlated variables of constant sum and that the correlation coefficients between the variables will need to be taken into account for the calculation of the uncertainties in derived variables, such as atomic weights (35) or, in this case, isotope ratios.

For this purpose, we have taken the general equation for error propagation (eq 3 where $u(x_i)$ are the standard uncertainties for each parameter and $u(x_i, x_k)$ the covariances):

$$u(y(x_1, x_2, \dots, x_n)) = \sqrt{\sum_{i=1, n} \left(\frac{\partial y}{\partial x_i} \cdot u(x_i) \right)^2 + \sum_{i, k=1, n} \left(\frac{\partial y}{\partial x_i} \cdot \frac{\partial y}{\partial x_k} \cdot u(x_i, x_k) \right)} \quad (3)$$

Then, we can calculate the covariances $u(x_i, x_k)$ if we know the correlation coefficients between the variables using:

$$u(x_i, x_k) = r_{ik} \cdot u(x_i) \cdot u(x_k) \quad (4)$$

For the particular case of the uncertainty of a ratio R , u_R , of two correlated variables, x and y , the application of eqs 3 and 4 was derived in eq 5 as follows:

$$u_R = R \times \sqrt{\left(\frac{u_x}{x} \right)^2 + \left(\frac{u_y}{y} \right)^2 - 2 \times r_{xy} \times \left(\frac{u_x}{x} \right) \times \left(\frac{u_y}{y} \right)} \quad (5)$$

where r_{xy} is the correlation coefficient between the variables x and y , and u_x and u_y their standard uncertainties. For bi-isotopic elements, the correlation coefficients are always -1 (35); therefore, the uncertainty in the isotope ratio would be larger than that calculated assuming no correlation between the variables (the correlation always adds uncertainty to the isotope ratio of bi-isotopic elements as shown in eq 5). For tri-isotopic elements, such as silicon, the correlation coefficients will need to be evaluated. In a previous paper, we have calculated the correlation coefficients between the isotopes of silicon by applying the mass dependent fractionation law (36). We observed a perfectly negative correlation ($r = -1$) for the ²⁹Si/²⁸Si and ³⁰Si/²⁸Si ratios and a positive correlation ($r = 1$) for the ratio ³⁰Si/²⁹Si. Therefore, using eq 5, we have calculated the standard uncertainty for the ³⁰Si/²⁹Si ratio to be 0.00061, which is about half of that calculated assuming no correlation between the isotope abundances (0.00130). However, the uncertainty of the natural ³⁰Si/²⁸Si ratio increased only from 0.000060 to 0.000063 when the correlation was taken into account.

(b). *Isotope Ratios and Uncertainties of the Spex Silicon Standard.* A series of 30 measurements of the Spex silicon standard together with 11 measurements of the IRMM 017 silicon isotopic reference material were performed by bracketing the reference material between every three samples of the Spex standard. The final value found for the ratio ³⁰Si/²⁹Si in the Spex standard was 0.659477 with a standard error of the mean ($n = 30$) of 0.000027. This is only slightly larger than the standard uncertainty of the ratio ³⁰Si/²⁹Si in the IRMM 017 reference material, which was 0.000018 for a certified ratio of 0.659600.

Matrix Effects on Mass Bias. Matrix effects can have a major impact on the precision and accuracy of isotope ratio measurements by MC-ICP-MS (37); therefore, understanding their impact for any given isotopic system is an important aspect of method development. Beer constituents comprise more than 800 compounds (38), and therefore, matrix effects could affect isotope

Table 2. $\delta^{34}\text{S}_{\text{VCDT}}$ Values, Measurement Standard Deviations, and Combined Standard Uncertainties for Beer Samples, Using NIST RM8553 As the Working Standard^a

beer	$\delta^{34}\text{S}_{\text{VCDT}}$ (‰) average ($n = 3$)	standard deviation (‰) ($n = 3$)	combined standard Uc (‰)	% Uc (1)	% Uc (2)	% Uc (3)	% Uc (4)	% Uc (5)	% Uc (6)	% Uc (7)
Asahi	7.9	0.1	1.8	1.0	8.5	87.9	1.3	0.5	0.2	0.7
Baltika	4.7	0.2	2.0	2.2	21.2	74.7	0.8	0.3	0.1	0.6
Becks	3.4	0.8	1.9	1.6	3.6	91.9	1.6	0.4	0.2	0.7
Bock	1.9	0.4	1.8	0.9	2.1	94.6	0.9	0.5	0.2	0.8
Brahma	4.2	0.5	1.8	3.4	2.1	92.5	0.6	0.5	0.2	0.7
Brooklyn	-0.2	0.3	1.8	0.9	1.0	95.1	1.7	0.4	0.2	0.8
Budweiser	4.8	0.2	1.8	4.6	0.5	92.2	1.1	0.7	0.2	0.7
Carling	10.3	0.4	1.9	0.6	14.6	82.8	0.8	0.5	0.2	0.7
Cobra	7.9	0.5	1.9	3.3	8.5	85.8	1.3	0.4	0.2	0.7
Corona	10.7	0.2	1.7	0.4	1.4	95.8	0.9	0.5	0.2	0.8
Cusqueña	6.8	0.8	1.9	0.7	0.8	95.8	1.5	0.3	0.2	0.8
Desperado	9.1	0.3	1.8	4.4	4.7	88.7	0.8	0.5	0.2	0.7
Duvel	10.0	0.5	1.8	3.1	3.4	91.2	0.9	0.5	0.2	0.7
Erdinger	5.9	0.2	1.8	2.4	10.6	84.8	0.8	0.5	0.2	0.7
Estrella Damm	4.6	0.3	1.8	3.0	2.4	93.0	0.6	0.1	0.2	0.7
Guinness	9.8	0.6	1.8	1.3	4.1	92.0	1.5	0.3	0.2	0.7
Heineken	5.6	0.6	1.6	1.5	6.1	89.7	1.2	0.6	0.2	0.7
Kronenbourg	6.8	0.9	2.0	0.7	12.3	84.5	1.1	0.6	0.2	0.7
Lefte	2.0	0.8	1.9	1.1	3.1	93.2	1.5	0.3	0.2	0.7
Peeterman	7.5	0.4	1.9	0.9	13.9	83.1	0.8	0.5	0.2	0.7
Peroni	7.0	0.7	1.9	1.9	2.2	93.2	1.4	0.4	0.2	0.7
Pilsner	4.4	0.5	1.8	0.3	0.7	96.8	0.7	0.5	0.2	0.8
San Miguel	13.8	0.4	1.8	0.5	2.3	95.0	0.6	0.5	0.2	0.8
Shinga	9.6	0.4	1.8	1.4	6.9	89.0	1.5	0.3	0.2	0.7
Stella	7.8	0.8	1.9	1.4	0.5	95.1	1.7	0.4	0.2	0.8
Tiger	7.5	0.6	1.9	1.9	6.9	88.8	1.4	0.2	0.2	0.7
NIST RM 8554	-1.4	0.2	0.5	41.4	6.4	0.0	30.7	7.5	0.0	14.0
NIST RM 8556	17.3	0.3	0.4	15.0	4.4	0.0	43.4	13.0	0.0	24.2
average of beer samples				1.7	5.6	90.3	1.1	0.4	0.2	0.7

^a Full uncertainty budgets have been calculated for each sample and are summarized below. Seven uncertainty sources have been identified: % Uc (1) is the uncertainty of the measured $^{34}\text{S}/^{32}\text{S}$ isotope ratio in the beer sample, % Uc (2) is the uncertainty of the measured $^{30}\text{Si}/^{29}\text{Si}$ isotope ratio in the beer sample, % Uc (3) is the uncertainty of the IUPAC $^{30}\text{Si}/^{29}\text{Si}$ natural abundance isotope ratio, % Uc (4) is the uncertainty of the measured $^{34}\text{S}/^{32}\text{S}$ isotope ratio for the working standard, % Uc (5) is the uncertainty of the measured $^{30}\text{Si}/^{29}\text{Si}$ isotope ratio for the working standard, % Uc (6) is the uncertainty of the SPEX certified in house $^{30}\text{Si}/^{29}\text{Si}$ isotope ratio, and % Uc (7) is the uncertainty of the $\delta^{34}\text{S}_{\text{VCDT}}$ value of the working standard.

Table 3. Uncertainty Sources for the Measurement of $\delta^{34}\text{S}$ in Beer Samples

uncertainty source	typical value	standard uncertainty	comment
$^{34}\text{S}/^{32}\text{S}$ measured isotope ratio in beers	0.049530	0.000007	standard deviation of the mean ($n = 5$)
$^{30}\text{Si}/^{29}\text{Si}$ measured isotope ratio in beers	0.70397	0.00016	standard deviation of the mean ($n = 5$)
$^{30}\text{Si}/^{29}\text{Si}$ reference value IUPAC for beer samples	0.65998	0.00061	propagated uncertainty taking into account the correlation coefficients
$^{34}\text{S}/^{32}\text{S}$ measured isotope ratio in RM8553	0.049994	0.000008	standard deviation of the mean ($n = 5$)
$^{30}\text{Si}/^{29}\text{Si}$ measured isotope ratio in RM8553	0.703976	0.000050	standard deviation of the mean ($n = 5$)
$^{30}\text{Si}/^{29}\text{Si}$ corrected value Spex standard for RM8553	0.659477	0.000027	propagated uncertainty using IRMM 017 silicon as reference
$\delta^{34}\text{S}$ value for RM8553	16	0.15	certified value and uncertainty ($k = 2$)

ratio measurements. Although beer is usually made up of four main ingredients, water, hops, malted barley, and yeast (39), it is the precise recipe and timing of the brewing process that gives one beer a different taste from another. In general, the composition of beer varies from one brewery to another, but the following ingredients are present in all recipes: carbohydrates, ethanol (being the most important alcohol present), protein derived material, amines, nucleic acid derivatives, hop bitter acids, small amounts of vitamins of the B-group, phenolic compounds, and a range of inorganic compounds, which include major cations, trace metals, and anions. A wide variety of volatile sulfur compounds have also been reported in beer formulations (40). Given the complexity of beer matrices, it is expected that many of these components (41) may contribute as a potential source of matrix depending mass bias. Typical concentration of S in beer varies from 10 to 50 $\mu\text{g g}^{-1}$. Silicon content in beer also varies from 10 to 50 $\mu\text{g g}^{-1}$ and would show small isotopic variations typical of those tabulated by the IUPAC (1). **Figure 2** shows the

measured $^{30}\text{Si}/^{29}\text{Si}$ isotope ratios in a group of beer samples and in the NIST RM8553, 8554, and 8556 sulfur isotopic standards as a function of the order in which the samples were measured. Beer samples were simply diluted 1:3 with 1% (v/v) HNO_3 . As can be observed, the measured silicon isotope ratios in the NIST reference materials, corresponding to the Spex silicon standard added, are fairly stable with time with a small decrease at the end of the measurement series. The deviations from the expected ratio in the silicon standard ($^{30}\text{Si}/^{29}\text{Si} = 0.659477 \pm 0.000027$) are due to mass bias effects. However, the measured silicon isotope ratios in the beer samples are clearly different from those measured for the reference materials and changed depending on the nature of the measured sample. The maximum variation expected in the $^{30}\text{Si}/^{29}\text{Si}$ isotope ratios from natural variations would be in the range of 0.65998 ± 0.00061 , as calculated before. Therefore, the observed variations in the measured silicon isotope ratios cannot be explained only by natural variability and should indicate the presence of matrix effects on the instrumental mass bias.

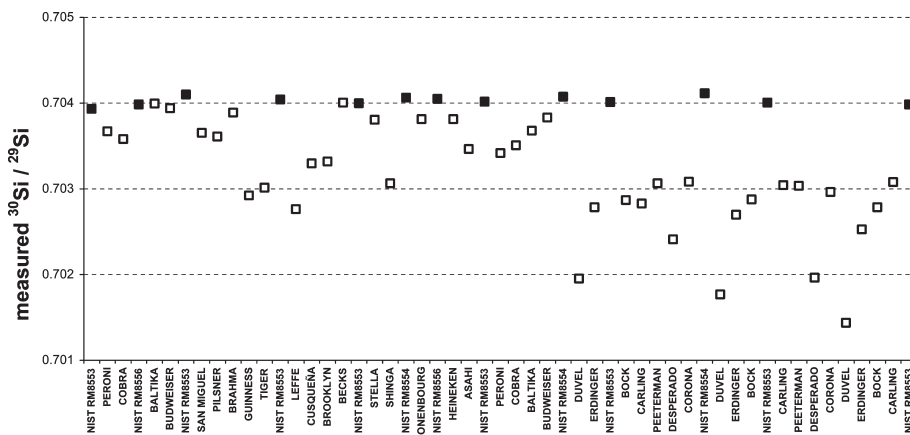


Figure 2. Measured $^{30}\text{Si}/^{29}\text{Si}$ isotope ratio plotted as a function of the order in which the NIST reference materials (■) and beer samples (□) were analyzed.

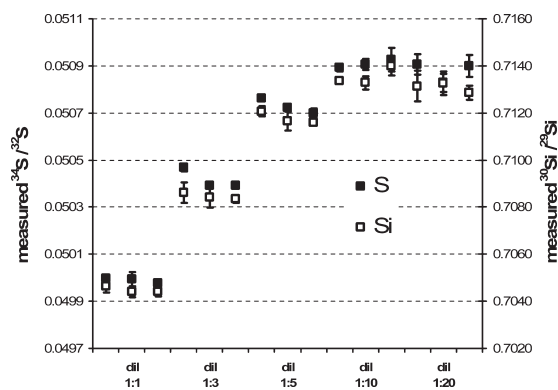


Figure 3. Measured $^{34}\text{S}/^{32}\text{S}$ and $^{30}\text{Si}/^{29}\text{Si}$ isotope amount ratios in a beer sample with increasing dilution factor. Error bars represent the instrumental uncertainty ($n = 3$).

The question is if similar changes are obtained for sulfur and if mass bias correction can be applied safely using silicon. For a complex system like beer, it is not feasible to study the matrix effects of each component by its addition to a certified sulfur standard as performed by Clough et al. for water (25). Therefore, in order to demonstrate the presence of matrix effects on the measured silicon isotope ratios, the effect of sample dilution was evaluated. If matrix effects were not present, the dilution of the sample would not change its isotopic composition.

Five dilution factors were tested, namely, 1:1, 1:3, 1:5, 1:10, and 1:20. In a first experiment, the Spex silicon standard was added to all dilutions of the same sample to a final concentration of $15 \mu\text{g g}^{-1}$ to ensure good counting statistics for silicon. In a separate experiment, the same solutions were prepared without the addition of exogenous silicon. Similar results were obtained in both experiments. Figure 3 shows the measured $^{34}\text{S}/^{32}\text{S}$ and $^{30}\text{Si}/^{29}\text{Si}$ isotope ratios (in triplicate dilutions) for the different dilutions of the same beer sample without silicon addition. As can be observed, isotope ratios increased with sample dilution up to a dilution factor of 10. After that, no further changes in the isotope ratios were observed. The increase in the isotope ratios with sample dilution indicates that matrix effects decrease the mass bias factor as the relative transmission of the heavier isotope is decreased against the

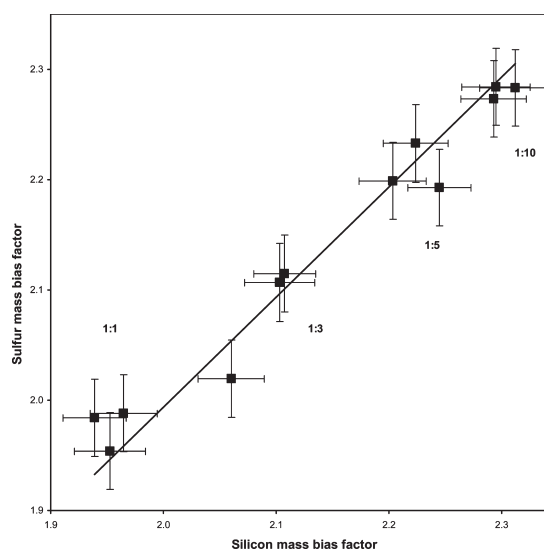


Figure 4. Correlation between the mass bias factors for sulfur and silicon for the different dilutions of the beer shown in Figure 3. Error bars indicate combined standard uncertainties.

lighter isotope. Similar observations, opposite to the expected behavior, have been reported previously (32).

In order to verify if silicon can be used for internal mass bias correction and to correct for matrix effects simultaneously the experimental mass bias factors (β in the Russell equation) were calculated for both elements in the following manner: for silicon, the natural IUPAC $^{30}\text{Si}/^{29}\text{Si}$ isotope ratio (0.65998 ± 0.00061) was used to calculate the mass bias factors and their uncertainties for all dilution factors of the same beer sample using the Russell equation and applying the Kragten procedure for the uncertainty propagation. Then, for sulfur, the isotope ratios measured at the dilution factor of 1:20 (where no matrix effects seemed to be present) were corrected with the β value calculated for silicon at this dilution factor ($\beta = 2.25 \pm 0.03$). Then, the β values for sulfur at the other dilution factors were calculated using the corrected isotope ratio value at the dilution of 1:20 as the reference. The Kragten procedure of uncertainty propagation was also applied

here. All β values calculated for silicon and sulfur at the dilution factors of 1:1, 1:3, 1:5, and 1:10 measured in triplicate are plotted in **Figure 4** including the uncertainty estimates. The data was adjusted by least-squares to a function of $y = ax$ with a given intercept of 0. The observed slope was $a = 0.997 \pm 0.004$ indicating that the mass bias factors measured for silicon could be applied to sulfur regardless of the dilution factor of the beer sample.

Finally, the different dilution factors of the same beer, both with and without the addition of silicon, were compared to the NIST RM8553 for the calculation of the $\delta^{34}\text{S}_{\text{VCDT}}$ values. The corrected $^{34}\text{S}/^{32}\text{S}$ isotope ratios for both sets of dilutions using silicon $^{30}\text{Si}/^{29}\text{Si}$ internal standardization are shown in **Figure 5**, expressed as $\delta^{34}\text{S}_{\text{VCDT}}$ (‰) using NIST RM8553 as the working standard. As can be observed, no significant differences were obtained with and without the addition of silicon to the samples. Also, no significant changes in the $\delta^{34}\text{S}$ values were detected for different dilution factors of the same sample except, perhaps, for the 1:1 dilution. A dilution factor of 1:3 was selected for further analyses in order to keep the maximum sensitivity possible, and no addition of exogenous Si was finally performed.

Analysis of Beers. The natural variability of sulfur isotope ratios in beers was measured by obtaining $\delta^{34}\text{S}_{\text{VCDT}}$ values for a suite of bottled beers representative of those currently sold in the U.K. NIST RM8553 was used as the working standard to anchor the results to the VCDT scale. NIST RM8554 and RM8556 were used to test instrumental performance. **Figure 6** illustrates the

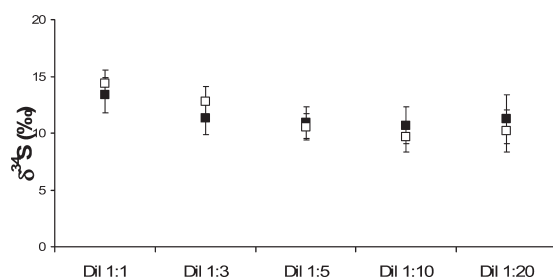


Figure 5. Corrected $^{34}\text{S}/^{32}\text{S}$ isotope ratios using $^{30}\text{Si}/^{29}\text{Si}$ internal standardization of (a) diluted samples with no added Silicon (■) and (b) diluted samples with added silicon (□). The results are expressed as $\delta^{34}\text{S}_{\text{VCDT}}$ (‰) using NIST RM8553 as the working standard. Error bars represent the combined standard uncertainty for each value.

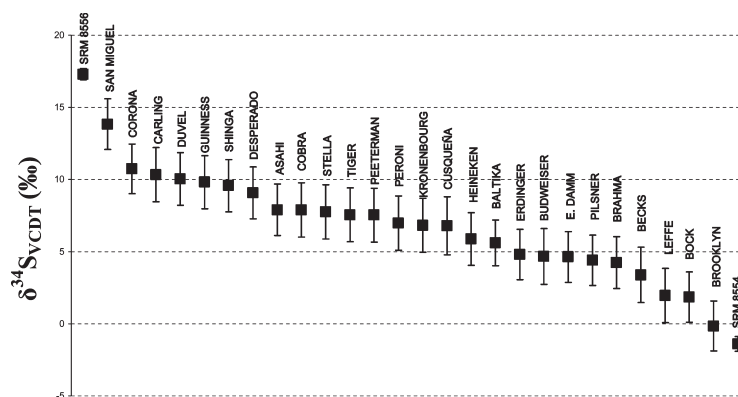


Figure 6. Neptune MC-ICP-MS $\delta^{34}\text{S}_{\text{VCDT}}$ values for the suite of beer samples. Values obtained for NIST RM8556 and NIST RM8554 are also included. Error bars represent the combined standard uncertainty for each value.

range of $\delta^{34}\text{S}_{\text{VCDT}}$ values in the beer samples investigated in this study, while the mean $\delta^{34}\text{S}_{\text{VCDT}}$ values ($n = 3$), measurement standard deviations, combined standard uncertainties, and each individual contribution (in %) are summarized in **Table 2**. Typical combined standard uncertainties of measured $\delta^{34}\text{S}_{\text{VCDT}}$ values ranged from 1.5 to 2.0 ‰. The major contributor to the standard uncertainty of the $\delta^{34}\text{S}_{\text{VCDT}}$ values in the beer samples was the uncertainty of the natural isotope composition of silicon used for mass bias assessment (ca. 90%). The experimental uncertainty in the measured silicon isotope ratio in the beer samples (ca. 5%) was the second important source of uncertainty. For the NIST RM8554 and RM8556 standards, the main sources of uncertainty were the uncertainty of the $^{34}\text{S}/^{32}\text{S}$ measured isotope ratio both in the sample and in the working standard RM8553 and the uncertainty of the $\delta^{34}\text{S}_{\text{VCDT}}$ value for NIST RM8553, typically contributing 20% relative to the combined standard uncertainty. In this case, the Spex silicon standard was used for mass bias assessment, and its uncertainty was much lower than the natural silicon variation used for the beer samples. **Table 2** shows also how important it is to calculate a full uncertainty budget because, if the measurement precision is reported as the standard deviation of replicate measurements, the actual measurement uncertainty will be underestimated.

Sulfur Isotope Ratios in Beers: Applications to Authenticity Testing and/or Tracer Studies. One of the objectives of this work was the determination of $\delta^{34}\text{S}$ values in beer samples with a view to the discrimination of beers of different brands. Manufacturing and/or biological processes can result in the formation of products whose stable isotope composition is characteristic of that process. Variations in isotopic ratios result from a complex interplay of historic, biological, and geological processes (1); so in this case, it is difficult to unambiguously identify a single source. However, the isotope ratio measurements can still be used to profile sources, and the combination with other analysis could be used to fingerprint beer brands. Brooklyn (North American beer) presented the lowest $\delta^{34}\text{S}$, whereas San Miguel (Spanish beer) showed the highest $\delta^{34}\text{S}$ value. We do not know yet if the isotopic composition of beer from the same manufacturer will be constant or whether it will vary depending on the manufacturing time of the year or other sources of variation. We must say that the analytical method presented in this work will not be able to distinguish between different beers of similar origin. In that case, the technique will need to be used in combination with other existing techniques (complementary information such as multi-element and multi-isotope analysis (42)).

For tracer studies, which are going to be performed in our laboratory using ^{34}S labeled yeast (30), the results obtained were very informative. The natural variability of sulfur isotope composition was previously measured for bottled water samples to be between -12 and $+22$ ‰ (25). Our results showed a narrower range of variation, ca. between -0.2 and $+13.8$ ‰. On the basis of these data, we could calculate the minimum amount of enriched ^{34}S which would be needed for a tracer experiment assuming that measurement uncertainty will be around 2 ‰. For example, a small laboratory animal (e.g., a Wistar rat weighting ca. 100 g) will contain ca. 0.175 g of protein sulfur. The administration of a single dose of 1 mg of enriched ^{34}S as isotopically labeled yeast will change the $^{34}\text{S}/^{32}\text{S}$ isotope ratio of sulfur in proteins, if completely equilibrated, from 0.045 to 0.051 which corresponds to a $\delta^{34}\text{S}_{\text{VCDT}}$ value of about $+100$. This change is now much larger than the expected natural variation of sulfur isotope ratios, and it is calculated assuming total isotope equilibration between sulfur isotopes in the body. As this is very unlikely to occur, sulfur isotope enrichment in certain serum proteins should be easily detected using this tracer amount.

To conclude, silicon internal standardization has been shown to be an effective method to correct for mass bias matrix effects in samples containing high amounts of dissolved organic matter. Our results are in agreement with those reported by Clough et al. (25) for the study of sulfur isotope variations in bottled mineral waters. The potential of the method has been tested with 26 beer samples from different brands. The $\delta^{34}\text{S}$ values have been calculated, and typical combined standard uncertainties of measured $\delta^{34}\text{S}$ values were ≤ 2 ‰. Although the discrimination power of sulfur isotope ratios could not be used to distinguish every single beer, results show the potential of the method to distinguish brands and to estimate the natural variability of sulfur in foods and beverages for future tracer experiments.

LITERATURE CITED

- De Laeter, J. R.; Bohlke, J. K.; De Bièvre, P.; Hidaka, H.; Peiser, H. S.; Rosman, K. J. R.; Taylor, P. D. P. Atomic weight of the elements: Review 2000. *Pure Appl. Chem.* **2003**, *75*, 683–800.
- Gao, X.; Thiemens, M. H. Variations on the isotopic composition of sulfur in enstatite and ordinary chondrites. *Geochim. Cosmochim. Acta* **1993**, *13*, 3171–3176.
- Strauss, H. The isotopic composition of sedimentary sulfur through time. *Palaeogeogr. Palaeoclimatol.* **1997**, *132*, 97–118.
- Wadleigh, M. A.; Blake, D. M. Tracing sources of atmospheric sulphur using epiphytic lichens. *Environ. Pollut.* **1999**, *106*, 265–271.
- Greenwood, J. P.; Mojzsis, S. J.; Coath, C. D. Sulfur isotopic compositions on individual sulfides in ALH84001 and Nakhla: implications for crust-regolith exchange on Mars. *Earth Planet. Sci. Lett.* **2000**, *184*, 23–25.
- Farquhar, J.; Savarino, J.; Jackson, T. L.; Thiemens, M. H. Evidence of atmospheric sulphur in the Martian regolith from sulphur isotopes in meteorites. *Nature* **2000**, *404*, 50–52.
- Mayer, B.; Prietzel, C.; Krouse, H. R. The influence of sulfur deposition rates on sulphate retention patterns and mechanisms in aerated forest soils. *Appl. Geochem.* **2001**, *16*, 1003–1019.
- Farquhar, J.; Wing, B. A.; McKeegan, K. D.; Harris, J. W.; Cartigny, P.; Thiemens, M. H. Mass-independent sulfur of inclusions in diamond and sulfur recycling on early earth. *Science* **2002**, *298*, 2369–2372.
- Tachibana, S.; Huss, G. R. Sulfur isotope composition of putative primary troilite in chondrules from Bishunpur and Semarkona. *Geochim. Cosmochim. Acta* **2005**, *69*, 3075–3097.
- Rai, V. K.; Jackson, T. L.; Thiemens, M. H. Photochemical mass-independent sulfur isotopes in achondritic meteorites. *Science* **2005**, *309*, 1062–1065.
- Ohmoto, H.; Watanabe, Y.; Ikemi, H.; Poulson, S. R.; Taylor, B. E. Sulphur isotope evidence for an oxic archaean atmosphere. *Nature* **2006**, *442*, 908–911.
- Ono, S.; Wing, B.; Johnston, D.; Farquhar, J.; Rumble, D. Mass-dependent fractionation of quadruple stable sulfur isotope system as a new tracer of sulfur biogeochemical cycles. *Geochim. Cosmochim. Acta* **2006**, *70*, 2238–2252.
- Rai, V. K.; Thiemens, M. H. Mass independently fractionated sulfur components in chondrites. *Geochim. Cosmochim. Acta* **2007**, *71*, 1341–1354.
- Ono, S.; Shanks, W. C.; Rouxel, O. J.; et al. S-33 constraints on the seawater sulphate contribution in modern seafloor hydrothermal vent sulfides. *Geochim. Cosmochim. Acta* **2007**, *71*, 1170–1182.
- Boner, M.; Forstel, H. Stable isotope variation as a tool to trace the authenticity of beef. *Anal. Bioanal. Chem.* **2004**, *378*, 301–310.
- Rossmann, A.; Haberhauer, G.; Holz, S.; Horn, P.; Pichlmayer, F.; Voerkelius, S. The potential of multielement stable isotope analysis for regional origin assignment of butter. *Eur. Food Res. Technol.* **2000**, *211*, 32–40.
- Pillonel, L.; Badertscher, R.; Froidevaux, P.; Haberhauer, G.; Holz, S.; Horn, P.; et al. Stable isotope ratios, major, trace and radioactive elements in emmental cheeses of different origins. *Food Sci. Technol.* **2003**, *36*, 615–623.
- Mason, P. R. D.; Kaspers, K.; van Bergen, M. J. Determination of sulfur isotope ratios and concentrations in water samples using ICP-MS incorporating hexapole ion optics. *J. Anal. At. Spectrom.* **1999**, *14*, 1067–1074.
- Prohaska, T.; Latkoczy, C.; Stingeder, G. Precise sulfur isotope ratio measurements in trace concentration of sulfur by high resolution inductively coupled plasma sector field mass spectrometry (HR-ICP-SFMS). *J. Anal. At. Spectrom.* **1999**, *14*, 1501–1504.
- Boulyga, S. F.; Heilmann, J.; Heumann, K. G. Isotope dilution ICP-MS with laser assisted sample introduction for direct determination of sulfur in petroleum products. *Anal. Bioanal. Chem.* **2005**, *382*, 1808–1814.
- Stürup, S.; Bendahl, L.; Gammelgaard, B. Optimization of LC-DRC-ICP-MS for speciation of selenotrisulfides with simultaneous detection of sulphur and selenium as oxides combined with determination of elemental and isotope ratios. *J. Anal. At. Spectrom.* **2006**, *21*, 201–203.
- Wang, M.; Feng, W.; Lu, W.; Li, B.; Wang, B.; Zhu, M.; et al. Quantitative analysis of proteins via sulfur determination by HPLC coupled to isotope dilution ICP-MS with hexapole collision cell. *Anal. Chem.* **2007**, *79*, 9128–9134.
- Santamaria-Fernandez, R.; Hearn, R. Systematic comparison of delta(34S) measurements by multicollector inductively coupled plasma mass spectrometry and evaluation of full uncertainty budget using two different metrological approaches. *Rapid Commun. Mass Spectrom.* **2008**, *22*, 401–408.
- Santamaria-Fernandez, R.; Hearn, R.; Wolff, J. C. Detection of counterfeit tablets of an antiviral drug using $\delta^{34}\text{S}$ measurements by MC-ICP-MS and confirmation by LA-MC-ICP-MS and HPLC-MC-ICP-MS. *J. Anal. At. Spectrom.* **2008**, *23*, 1294–1299.
- Clough, R.; Evans, P.; Catterick, T.; Evans, E. H. $\delta^{34}\text{S}$ measurements of sulfur by multicollector inductively coupled plasma mass spectrometry. *Anal. Chem.* **2006**, *78*, 6126–6132.
- Craddock, P. R.; Rouxel, O. J.; Ball, L. A.; Bach, W. Sulfur isotope measurement of sulfate and sulfide by high-resolution MC-ICP-MS. *Chem. Geol.* **2008**, *253*, 102–113.
- Santamaria-Fernandez, R.; Giner Martínez-Sierra, J.; Marchante-Gayón, J. M.; García-Alonso, J. I.; Hearn, R. Measurement of longitudinal sulfur isotopic variations by laser ablation MC-ICP-MS in single human hair strands. *Anal. Bioanal. Chem.* **2009**, *394*, 225–233.
- Moldovan, M.; Krupp, E. M.; Holliday, A. E.; Donard, O. F. X. High resolution sector field ICP-MS and multicollector ICP-MS as tools for trace metal speciation in environmental studies: a review. *J. Anal. At. Spectrom.* **2004**, *19*, 815–822.
- Krouse, H. R.; Coplen, T. B. Reporting of relative sulfur isotope ratio data. *Pure Appl. Chem.* **1997**, *69*, 293–295.
- Giner Martínez-Sierra, J.; Sanz, F. M.; Espílez, P. H.; Gayón, J. M. M.; Alonso, J. I. G. Biosynthesis of sulfur-34 labelled yeast and its characterisation by multicollector-ICP-MS. *J. Anal. At. Spectrom.* **2007**, *22*, 1105–1112.
- Enström, E.; Rodushkin, I.; Baxter, D. C.; Öhlander, B. Chromatographic purification for the determination of dissolved silicon

4050 *J. Agric. Food Chem.*, Vol. 58, No. 7, 2010

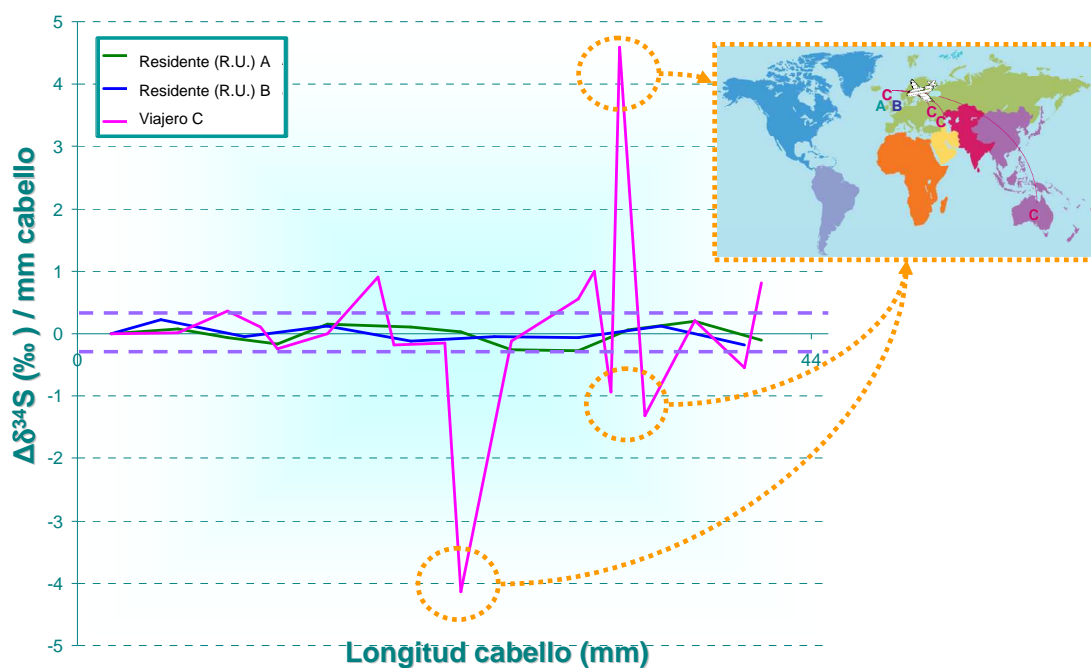
Giner Martínez-Sierra et al.

- isotopic compositions in natural waters by high-resolution multi-collector inductively coupled plasma mass spectrometry. *Anal. Chem.* **2006**, *78*, 250–257.
- (32) Ingle, C. P.; Sharp, B. L.; Horstwood, M. S. A.; Parrish, R. R.; Lewis, D. J. Instrument response functions, mass bias and matrix effects in isotope ratio measurements and semi-quantitative analysis by single and multi-collector ICP-MS. *J. Anal. At. Spectrom.* **2003**, *18*, 219–229.
- (33) Kragten, J. Calculating standard deviations and confidence intervals with a universally applicable spreadsheet technique. *Analyst* **1994**, *119*, 2161–2165.
- (34) Ellison S. L. R.; Rosslein M.; Williams A., Eds. *Quantifying Uncertainty in Analytical Measurement*, 2nd Edition, Eurachem/Citac Guide; 2000. <http://www.eurachem.org>.
- (35) Meija, J.; Mester, Z. Atomic weight uncertainty calculation from isotopic composition of the elements. *Metrologia* **2008**, *45*, 459–463.
- (36) García Alonso, J. I.; Rodríguez-González, P.; González-Gago, A.; González-Antuña, A. The determination of the uncertainties in the theoretical mass isotopomer distribution of molecules. *Anal. Chim. Acta* **2010**, *664*, 68–76.
- (37) Pietruszka, A. J.; Walker, R. J.; Candela, P. A. Determination of mass dependent molybdenum isotopic variations by MC-ICP-MS: an evaluation of matrix effects. *Chem. Geol.* **2006**, *225*, 121–136.
- (38) Hughes P. S.; Baxter E. D. *Beer: Quality, Safety and Nutritional Aspects*; The Royal Society of Chemistry: Cambridge, U.K., 2001; Chapters 1, 3, and 5.
- (39) Renée Brooks, J. R.; Buchmann, N.; Phillips, S.; Ehleringer, B.; et al. Heavy and light beer: a carbon isotope approach to detecting C4 carbon in beers from different origins, styles and prices. *J. Agric. Food Chem.* **2002**, *50*, 6413–6418.
- (40) Hill, P. G.; Smith, R. M. Determination of sulphur compounds in beer using headspace solid-phase microextraction and gas chromatographic analysis with pulsed flame photometric detection. *J. Chromatogr.* **2000**, *872*, 203–213.
- (41) Cortacero-Ramírez, S.; Hernáinz-Bermúdez de Castro, M.; Segura-Carretero, A.; Cruces-Blanco, C.; Fernández-Gutiérrez, A. Analysis of beer components by capillary electrophoretic methods. *Trends Anal. Chem.* **2003**, *22*, 440–455.
- (42) Kelly, S.; Heaton, K.; Hoogewerff, J. Tracing the geographical origin of food: the application of multi-element and multi-isotope analysis. *Trends Food Sci. Technol.* **2005**, *16*, 555–567.

Received for review June 9, 2009. Revised manuscript received March 8, 2010. Accepted March 9, 2010. The work described in this article was supported by the U.K. Department for Innovation, Universities & Skills as part of the National Measurement System Chemical & Biological Metrology Knowledge Base Programme. We thank the Ministry of Science and Technology, Madrid, Spain (project CTQ2006-05722) and the Education and Science Council of the Principado de Asturias (grant BP07-059).

D.1.2. Medida de variaciones isotópicas de azufre en cabello humano mediante ablación láser acoplada a ICP-MS multicolector

D.1.2.1. Artículo científico II: *Anal. Bioanal. Chem.*, 2009, 394, 225-233



Measurement of longitudinal sulfur isotopic variations by laser ablation MC-ICP-MS in single human hair strands

Rebeca Santamaria-Fernandez ·
Justo Giner Martínez-Sierra ·
J. M. Marchante-Gayón · J. Ignacio García-Alonso ·
Ruth Hearn

Received: 30 October 2008 / Revised: 7 January 2009 / Accepted: 9 January 2009 / Published online: 6 February 2009
© LGC Limited 2009

Abstract A new method for the measurement of longitudinal variations of sulfur isotope amount ratios in single hair strands using a laser ablation system coupled to a multicollector inductively coupled plasma mass spectrometer (LA-MC-ICP-MS) is reported here for the first time. Ablation parameters have been optimized for the measurement of sulfur isotope ratios in scalp human hair strands of 80–120- μm thickness and different washing procedures have been evaluated. The repeatability of the method has been tested and the ability to measure sulfur isotopic variations in 1,000- μm -long hair segments has been evaluated. A horse hair sample previously characterized for carbon and nitrogen isotope ratios in an interlaboratory study has been characterized by LA-MC-ICP-MS to be used as an in-house standard for the bracketing of human hair strands. $^{34}\text{S}/^{32}\text{S}$ isotope amount ratios have been measured and corrected for instrumental mass bias adopting the external standardization approach using National Institute of Standards and Technology (NIST) RM8553 and full uncertainty budgets have been calculated using the Kratzen approach. Results are reported as both $^{34}\text{S}/^{32}\text{S}$ isotope amount ratios and $\delta^{34}\text{S}_{\text{V-CDT}}$ values (sulfur isotopic differences relative to a reference sample expressed in the Vienna Canyon Diablo Troilite (V-CDT)



Rebeca Santamaria-Fernandez joined LGC in 2005 and is now a Senior Researcher in Isotope Ratio Mass Spectrometry at LGC in Teddington, UK. In 2007, she won the Allan Ure Award for her contribution to the application of atomic spectrometry to environmental science. Her current research interests focus on the development of new methodologies involving traceable high-precision isotope ratio measurements using IRMS

and multicollector ICP-MS technologies.

scale) calculated using NIST RM8553, NIST RM8554, and NIST RM8556 to anchor results to the V-CDT scale. The main advantage of the new method versus conventional gas source isotope ratio mass spectrometry measurements is that longitudinal variations in sulfur isotope amount ratios can be resolved. Proof of concept is shown with human scalp hair strands from three individuals, two UK residents and one traveler (long periods of time abroad). The method enables monitoring of longitudinal isotope ratio variations in single hair strands. Absolute ratios are reported and $\delta^{34}\text{S}_{\text{V-CDT}}$ values are plotted for comparison. Slight variations of <1.2% were detected in the hair strands from UK residents whereas the traveler presented a variation of >5%. Thus, the measurement of sulfur isotopic variations in hair samples has potential to be an indicator of geographical origin and recent movements and could be used in combination with isotope ratio measurements in water/foodstuffs from different geographical locations to provide important information in nutritional and geographical studies.

R. Santamaria-Fernandez (✉) · R. Hearn
LGC,
Queens Road, Teddington,
Middlesex TW11 0LY, UK
e-mail: rsf@lgc.co.uk

J. Giner Martínez-Sierra · J. M. Marchante-Gayón ·
J. I. García-Alonso
Department of Physical and Analytical Chemistry,
University of Oviedo,
Julian Clavería 8,
33006 Oviedo, Spain

Keywords Mass spectrometry/ICP-MS · Laser ablation · Forensics · Sulfur · Isotope ratio · MC-ICP-MS

Introduction

Hair and nails are becoming increasingly popular as biopsy tissues or exposure biomarkers [1]. The main reason is the ease of sample collection, transport, and handling. In particular, hair samples can be left behind and therefore can be collected covertly and non-invasively. Hair analysis has been widely used for assessment of environmental and occupational exposure [2–5], evaluation of migration patterns and diet changes [6–8], human identification and aging studies [9–11], and disease diagnosis [12].

The role of stable isotopes in human identification has been previously discussed by Fraser et al. [11] and the need for novel techniques to obtain information regarding the geographical origin, recent movements, and lifestyle of an individual has been highlighted [10]. The link between the stable isotopic composition of human tissues and the diet and lifestyle of an individual has been previously investigated [13, 14]. There seems to be a correlation between isotopic values of collagen found in bone samples and keratin hair protein and diet. Carbon and nitrogen isotope ratios in hair have been found to reflect the intake of animal protein [15] whereas hydrogen and oxygen isotope ratios have shown correlation with drinking and precipitation water [10, 16]. The potential use of carbon, nitrogen, and sulfur isotope ratios of human hair to provide information about human origin and migration has been studied [8]. This study reported a large variability for carbon and nitrogen isotope ratios within North American and European hair samples based at least partially on the levels of seafood, corn-fed beef, and grains in the diets. Moreover, in certain cases, it appeared that sulfur isotope ratio values helped to further constrain dietary interpretations, owing to the good preservation of sulfur content in hair [8].

A more recent study has shown the relationship between diet and recent migration through the measurement of hair carbon, nitrogen, and sulfur isotope ratio values in modern humans living in a rural community of England [6]. Generally, data from the three isotopic systems provided enough information to confirm dietary status and origin of the individual subjects.

Stable isotope ratio measurements in previous studies mentioned above have been performed by isotope ratio mass spectrometry (IRMS). Sulfur measurements are commonly performed by gas source isotope ratio mass spectrometry (GS-IRMS) in which S is measured as SO₂ or SF₆. However, the complex and tedious sample preparation methods used to convert the various S-containing species in geological, biological, and environmental matrices into SO₂ or SF₆ may

lead to additional S isotopic fractionation or contamination from the reagents employed. Moreover, different δ³⁴S values for the same material are obtained depending on which species, either SO₂ or SF₆ is introduced into the GS-IRMS [17]. An extra complication when using SO₂ is the isotopic composition of oxygen since ³⁴S¹⁶O₂⁺ is not resolved from ³²S¹⁶O¹⁸O⁺ during typical GS-IRMS analysis; therefore, the corrections for the oxygen isotopic contributions are necessary [18]. Differences in measured sulfur isotope amount ratios (³⁴S/³²S) are based on *n*(³⁴S)/*n*(³²S) measurements and are commonly expressed as δ³⁴S(‰) [19] (Eq. 1).

$$\delta^{34}\text{S}_{\text{V-CDT}}(\text{‰}) = \left[\frac{(^{34}\text{S}):(^{32}\text{S})_{\text{Sample}}}{(^{34}\text{S}):(^{32}\text{S})_{\text{V-CDT}}} - 1 \right] \times 1000 \quad (1)$$

The use of inductively coupled plasma mass spectrometry (ICP-MS) for the measurement of sulfur isotope amount ratios is becoming a relatively widespread analytical technique [20–22]. Recently, the use of multicollector inductively coupled plasma mass spectrometry (MC-ICP-MS) for S isotope ratio measurements has proven to overcome precision limitations of sequential mode measurements, enabling precise measurements of isotope amount ratios with instrumental precision between 0.1% and <0.005% [23]. Furthermore, the use of MC-ICP-MS as a high-throughput tool for δ³⁴S_{V-CDT} measurements for aqueous and solid samples using both internal and external standardization for correction of instrumental mass bias effects has been reported [24, 25].

Conventional analyses of hair samples by IRMS require previous grinding of the sample and therefore spatial resolution is limited to the sample size required for analyses.

The new methodology proposed here eliminates sample digestion or grinding steps since the single hair strands can be analyzed directly, thus providing the potential for a high-throughput forensic tool. The laser beam can be traversed along the length of the hair, with spatial resolution to produce ablation craters of 12 μm wide. The high spatial resolution allows analyses of individual hair strands, the thickness of which usually ranges from 40 to 120 μm for human scalp hair [26]. The collection of hair strands is obviously less invasive than that of hair bundles thus making the methodology more attractive to forensic scientist and police investigators. Only a small number of papers have been published to date using LA coupled to ICP-MS for the analyses of single hair strands [4, 7, 27–30]; most of them reported quantification of heavy metals in hair samples and only one publication focused on the measurement of uranium isotope amount ratios in hair strands. The main analytical challenges reside on the spatial resolution of the methodology and the precision of the sulfur isotope ratio measurements challenged by the coupling of the LA to the MC-ICP-MS.

In this work, a novel application using laser ablation coupled to a MC-ICP-MS for rapid and precise sulfur isotope amount ratio measurements in human scalp hair strands is presented. Laser ablation parameters have been carefully optimized to achieve highest resolution and relative instrumental precision for sulfur isotope ratio measurements below 0.05%. A horse hair sample previously characterized for carbon and nitrogen isotope ratios in an interlaboratory study [31] has been characterized for sulfur isotope ratios. Sulfur isotopic longitudinal differences in hair strands from three individual subjects have been studied and the potential of the method to resolve accurate longitudinal variations in hair strands versus the limited resolution of microwave digestion of hair samples is demonstrated.

Experimental

Instrumentation

MC-ICP-MS

All measurements were performed using a MC-ICP-MS (Neptune MC-ICP-MS, ThermoFinnigan, Bremen, Germany). The Neptune has an argon plasma ion source, forward Nier-Johnson geometry, and nine Faraday cups. The axial Faraday cup can be interchanged with a secondary electron multiplier enabling detection below the normal operating range of the Faraday cups. Further details of the instrument design may be found elsewhere [32].

The precision of the ratio measurements by MC-ICP-MS is considerably superior to those made by single collector ICP-MS [33]. Instrumental precision is a major contributor to the combined uncertainty of the isotope ratio; this explains the improvement on the uncertainties compared to those obtained by previous authors [34, 35] using single collector ICP-MS for the measurement of sulfur isotopic variations. There are also a number of polyatomic ions which interfere with $^{32}\text{S}^+$ and $^{34}\text{S}^+$ which can easily be resolved by operating the Neptune at medium resolution [24, 25, 36]. The MC-ICP-MS method used in this study and the correction of instrumental mass bias applied using external bracketing have been described in detail elsewhere [24, 25, 36]. Note that in this work mass bias is considered to be entirely due to instrumental effects and that mass discrimination is a different phenomenon, arising from biological, physical, or chemical processes [37].

Laser ablation system

A commercially available UP-213 laser ablation system (New Wave Research Inc., Huntingdon, Cambridgeshire,

UK) operating in the deep UV (213 nm) was employed using helium as a carrier gas due to its improved ablation and transport characteristics [38]. Where external standardization with liquid solutions was used, solutions were introduced to the plasma, after ultrasonic nebulization and desolvation (USN CETAC U-6000AT+, CETAC Technologies, Omaha, NE, USA) via a glass 'Y'-piece to the He carrier stream post-ablation. Ablation parameters were optimized and are shown in Table 1.

Reagents, standards, and samples

High-purity reagents were used unless otherwise stated. Water was taken directly from an $18.2 \text{ M}\Omega \text{ cm}^{-1}$ supply

Table 1 Operating conditions and data acquisition parameters for the LA-MC-ICP-MS for the measurement of S isotope ratios in single hair strands

MC-ICP-MS settings		
Rf power	1,350 W	
Cool gas flow	14.0 L min ⁻¹ Ar	
Auxiliary gas flow	0.9 L min ⁻¹ Ar	
Sample gas flow	0.8 L min ⁻¹ Ar	
Additional gas flow	0.6 L min ⁻¹ He	
Sampler and skimmer cones	Ni	
Extraction voltage	-2,000 V	
Focus lens	-1 V	
Dispersion lens	+8 V	
Laser ablation		
Wave length	213 nm	
Fluence	14 J cm ⁻²	
Scan speed	15 $\mu\text{m s}^{-1}$	
Repetition rate	20 Hz	
Output	90%	
Spot size	12 μm	
Pre-ablation		
Scan speed	70 $\mu\text{m s}^{-1}$	
Repetition rate	2 Hz	
Output	40%	
Spot size	12 μm	
USN/desolvator settings (bracketing with NIST RM solution)		
Ar sweep	1.70 L min ⁻¹	
Heater 1	140 °C	
Condenser	-3 °C	
Heater 2	160 °C	
Data acquisition parameters		
Collection mode	Dynamic	
Cup configuration	Main: S	
	C	31.982 (32 S)
	H4	34 S
Resolution mode	Medium	
Acquisition method	Three blocks, three cycles, 4.194-s integration, 2 s idle	

(Elga Ltd., High Wycombe, UK). The following sulfur reference materials were used in this study:

National Institute of Standards and Technology

NIST RM8553: Soufre De Lacq-Elemental Sulfur, $\delta^{34}\text{S}_{\text{V-CDT}} = 16 \pm 0.3$ (‰)

NIST RM8556: NBS 123 Sphalerite, $\delta^{34}\text{S}_{\text{V-CDT}} = 17.44 \pm 0.3$ (‰)

NIST RM8554: IAEA-S1 Silver Sulfide, $\delta^{34}\text{S}_{\text{V-CDT}} = -0.3 \pm 0.3$ (‰)

Each reference material was independently prepared by digesting an aliquot in a closed vessel microwave digester (Multiwave 3000, Perkin Elmer, Beaconsfield, UK) with high-purity HNO_3 (ROMIL, Cambridge, UK) and subsequent dilution with high-purity water.

Hair samples were collected from three individual subjects living in the UK. The first two were residents in the UK (A, B) and the third one a traveler (C) that had been in the UK for a just over a month before the analysis and had visited four different countries within the 6 months prior to sample collection. A pharmaceutical tablet with a S-containing active ingredient previously characterized by high-performance liquid chromatography MC-ICP-MS and LA-MC-ICP-MS [36] and a horse hair sample were also analyzed as in-house references. The horse hair sample was analyzed for carbon and nitrogen isotope amount ratios as part of an interlaboratory study organized in 2005 [31] and proved to be homogeneous for the isotopic compositions. The material was provided by Queen's University (Belfast, UK). The horse hair sample was then used for the bracketing of $^{34}\text{S}/^{32}\text{S}$ isotope amount ratio measurements in human hair. This way, the sample and the standard used for external standardization had similar matrices and could be mounted in the same glass slide, thus improving sample throughput. Measurements were performed by bracketing with a NIST RM8553 solution.

Sample preparation

To minimize sample preparation, hair strands were fixed on microscope glass slides using scotch adhesive tape. Several strands of hair could be fixed on the same glass slide, thus allowing repeatability and repeatability tests without having to change sample.

Although different washing procedures for the removal of surface contamination from hair samples have been proposed by previous authors [1, 28], no standard procedure has been prescribed. For the purpose of this work, two cleaning procedures and pre-ablation of hair strands were evaluated. The first cleaning procedure involved using three aliquots of 5 mL of Milli-Q water; the second cleaning procedure involved rinsing with Milli-Q water (1×5 mL) and acetone (3×5 mL) and a final rinse with water (1×5 mL).

Microwave digestion of hair samples

Microwave-assisted digestion of human and horse hair samples was carried out in a CEM Discover unit focused microwave reactor module (CEM Microwave Technology Ltd., Buckingham, UK). This new microwave reactor enabled sample sizes of <0.1 g to be digested within 2 min. Approximately 10 mg of hair (10 to 25 hair strands depending on length and thickness) were placed in a digestion vessel; 1.5 mL of concentrated HNO_3 and 0.5 mL of H_2O_2 were added and vials were subjected to 100 W during 2 min. Once cooled, the digests were diluted to 10 mL with Milli-Q water and sulfur isotope amount ratios were measured by MC-ICP-MS.

Mass bias correction

Isotope ratio measurements are affected by instrumental mass bias so a correction is required. The mass bias of MC-ICP-MS is characterized by the favored transmission of heavier ions, which is reflected in the measured isotope ratios. It is generally assumed that most of the mass bias that occurs in plasma source mass spectrometry results from space charge effects at the interface and the focusing lens region, but other processes may be equally or more important [39, 40]. In order to account for mass bias effects, the external standardization approach by sample-standard bracketing was performed. The $^{34}\text{S}/^{32}\text{S}$ isotope amount ratio was measured in a standard solution, and the measured bias was then used to correct the same ratio in the sample. In this case, a solution of NIST RM8553 of a typical concentration of sulfur of $5 \mu\text{g g}^{-1}$ was used. The standard solution was measured before and after each sample and raw $^{34}\text{S}/^{32}\text{S}$ isotope amount ratios were corrected using the "true" value (based upon a $\delta^{34}\text{S}_{\text{V-CDT}}$ of 16‰) of 0.04486919 [25].

Measurement of uncertainty

The uncertainties of the corrected $^{34}\text{S}/^{32}\text{S}$ isotope amount ratios and subsequent $\delta^{34}\text{S}_{\text{V-CDT}}$ values were calculated in accordance with the International Organization for Standardization Guide to the Expression of Uncertainty in

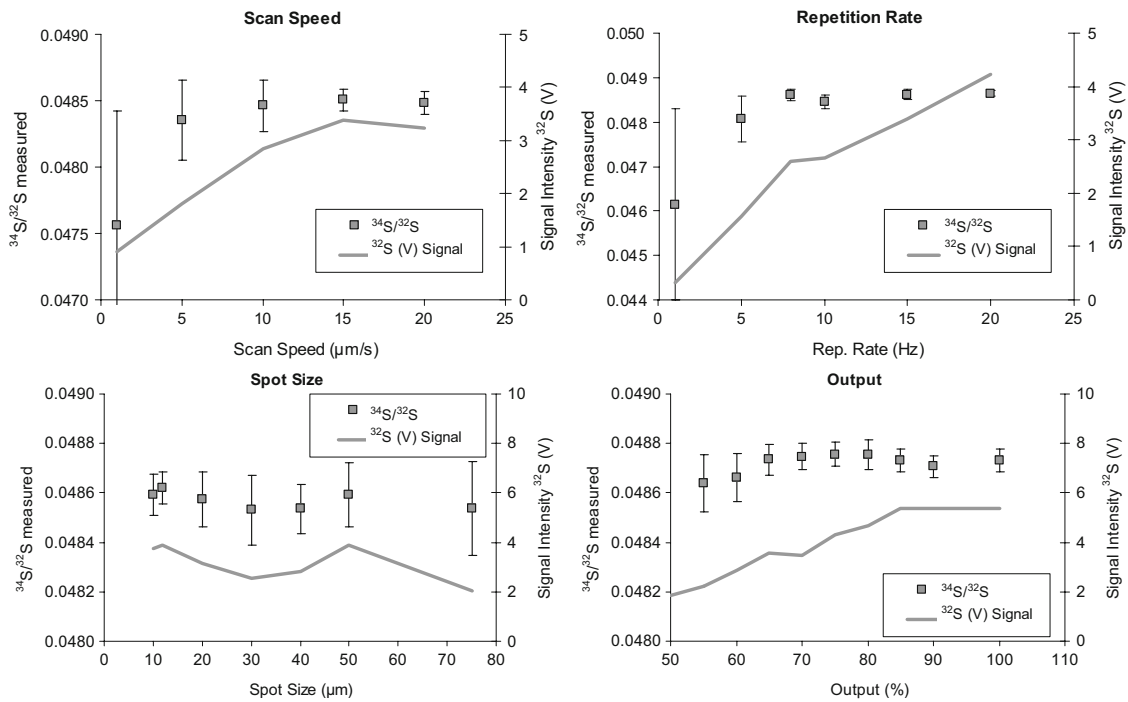


Fig. 1 Optimization of LA parameters for the measurement of S isotope ratios in single hair strands by MC-ICP-MS. In all cases, average values are shown for three replicate measurements of $^{34}\text{S}/^{32}\text{S}$ ratios and error bars represent combined expanded uncertainties ($k=2$)

Measurement (GUM) guidelines [41]. Combined uncertainties were calculated following the Kragten spreadsheet method [42] taking into account instrumental performance, correction for mass bias effects, and conversion to the Vienna Canyon Diablo Troilite (V-CDT) scale. A four-figure balance was used for sample preparation and the uncertainty of each mass was determined by the repeatability of calibrated weight measurements and the balance certificate.

Results and discussion

Optimization of LA parameters for longitudinal $^{34}\text{S}/^{32}\text{S}$ measurements in single hair strands

Laser parameters were optimized with a single hair strand to achieve greater sensitivity and good precision of isotope ratio measurements. The following parameters: repetition rates, spot size, scan speed, and laser energy output were evaluated independently and results are shown in Fig. 1. Compromise conditions were chosen for maximum signal and best internal precision. For repetition rates higher than 20 Hz, the hair strands became weak and fragmented in some cases; therefore, repetition rate was fixed at 20 Hz; the

output energy was fixed to 90% and the laser system has a fluence of 14 J cm^{-2} . Optimum scan speed was found to be $15 \mu\text{m s}^{-1}$ and the optimum spot size was fixed to $12 \mu\text{m}$. Those conditions led to typical signal intensities of 4 V for the major isotope ^{32}S and combined relative uncertainties of $<0.1\%$ for the measured $^{34}\text{S}/^{32}\text{S}$ isotope amount ratios. The ablated material was then transported to the plasma by a

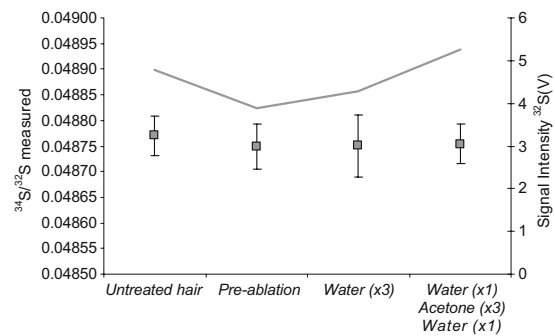
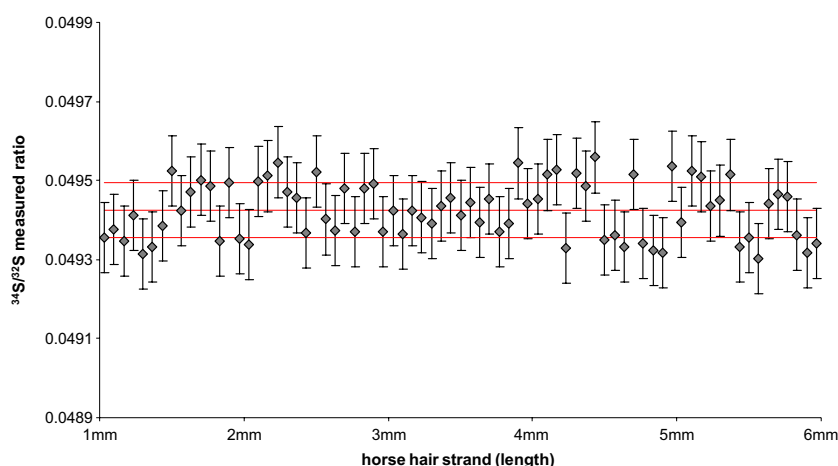


Fig. 2 Evaluation of washing procedure for single hair strands for the measurement of $^{34}\text{S}/^{32}\text{S}$ isotope ratios by LA-MC-ICP-MS. Average values are shown for three replicate measurements of $^{34}\text{S}/^{32}\text{S}$ ratios and error bars represent combined expanded uncertainties ($k=2$), $\leq 0.13\%$

Fig. 3 Internal variability of $^{34}\text{S}/^{32}\text{S}$ ratios in the horse hair strand of 0.14% was found. Sulfur isotope amount ratios were measured along 5 mm of hair. The overall average value and the expanded uncertainty ($k=2$) are plotted in red



0.6 L min⁻¹ helium carrier gas flow. An additional argon flow of 0.8 L min⁻¹ was added (glass Y-piece connecting gas flows). LA-MC-ICP-MS conditions are shown in Table 1.

Optimization of washing/pretreatment conditions

Two cleaning procedures and pre-ablation were evaluated. Results were compared with those of a non-treated hair strand and are shown in Fig. 2. Measurements were performed in triplicate in a random order and no significant differences were found for the three treatments. At this stage, pre-ablation was then chosen to minimize total time of analyses and the potential introduction of contamination during washing stages.

In-house characterization of horse hair strands for $^{34}\text{S}/^{32}\text{S}$ isotope amount ratios by LA-MC-ICP-MS

Prior to being used as a reference standard, the internal variability (within strand) and between-strand variability of S isotope amount ratios have been evaluated. Figure 3 shows the internal variability within 5 mm of horse hair and measurements were performed every 67 μm . Variability of sulfur isotope ratios within 5 mm of the hair strand was found to be below 0.14%. A pharmaceutical drug that has been subject of a previous study [36] was used as an internal quality control.

$^{34}\text{S}/^{32}\text{S}$ measurements were performed for the three NIST reference materials in solution as well as the horse hair strand ($n=9$) and pharmaceutical tablet ($n=9$). Linearity of the method within the V-CDT scale is proved by plotting measured $^{34}\text{S}/^{32}\text{S}$ isotope amount ratios measured for six replicates of each material versus the expected values assuming a $^{34}\text{S}/^{32}\text{S}$ ratio of 0.0441623 for V-CDT [43] (see Fig. 4). Average bracketing corrected S isotope

amount ratios for the pharmaceutical tablet and the horse hair sample was then calculated. The average $^{34}\text{S}/^{32}\text{S}$ isotope amount ratio for the horse hair strand was found to be 0.044526 ± 0.000067 ($n=9$) corresponding to a $\delta^{34}\text{S}_{\text{V-CDT}}$ value of $8.22 \pm 1\%$ (combined expanded uncertainty, $k=2$). The pharmaceutical tablets used as an instrumental check lead to an average $^{34}\text{S}/^{32}\text{S}$ isotope amount ratio of 0.044322 ± 0.000066 ($n=9$) corresponding to a $\delta^{34}\text{S}_{\text{V-CDT}}$ value of $3.61 \pm 1\%$ (combined expanded uncertainty, $k=2$). Results for the tablet agreed with $\delta^{34}\text{S}_{\text{V-CDT}}$ value of $3.6 \pm 1\%$ obtained previously [36]. Mass bias was found to be approximately 5% per mass unit.

Measurements in three horse hair strands were performed in six segments along 6 cm to detect any variability between hair strands. Between-strand variability was found

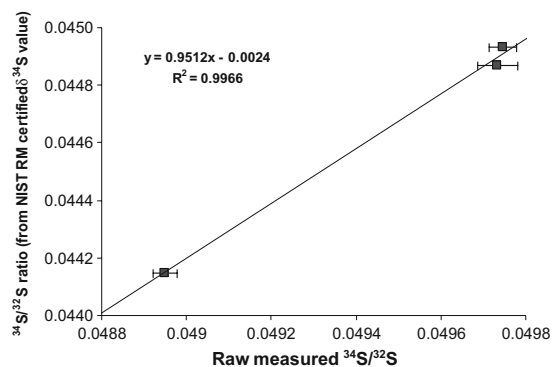
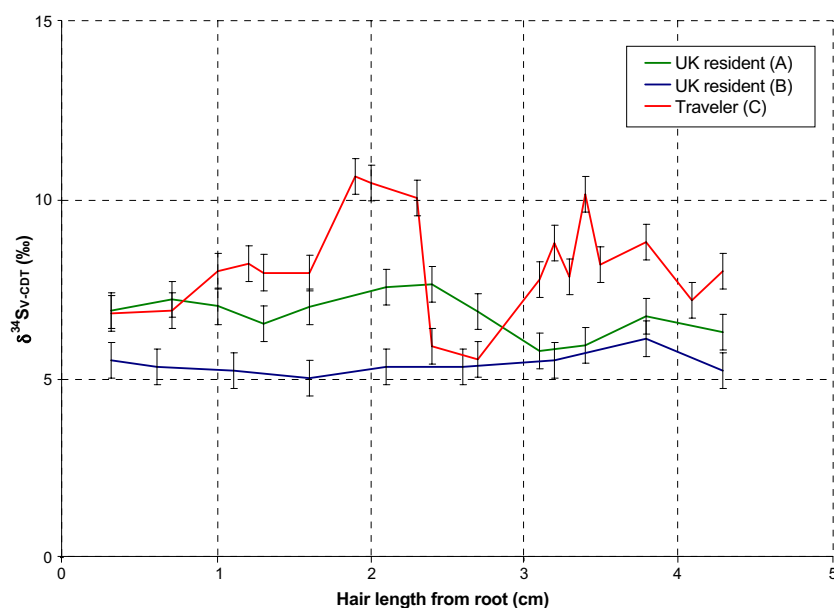


Fig. 4 Correlation between measured sulfur isotope amount ratios by MC-ICP-MS for the three chosen NIST RMs and the sulfur isotope amount ratios (obtained from Eq. 1, using the $\delta^{34}\text{S}_{\text{V-CDT}}$ (‰) reference values reported in the NIST certificates and a $^{34}\text{S}/^{32}\text{S}$ ratio of 0.0441623 for V-CDT [43])

Fig. 5 Longitudinal sulfur isotopic variations in scalp hair strands collected from three individuals. Measurements were performed in triplicate. *Error bars* represent combined uncertainties



to be below 0.15% and average sulfur $^{34}\text{S}/^{32}\text{S}$ isotope amount ratios found for strands 1, 2, and 3 were 0.044552 ± 0.000041 , 0.044527 ± 0.000043 , and 0.044527 ± 0.000035 , respectively. Combined uncertainties including the instrumental error and the variability within hair strands are quoted. The average $^{34}\text{S}/^{32}\text{S}$ isotope amount ratio was therefore 0.044525 ± 0.000080 corresponding to a $\delta^{34}\text{S}_{\text{V-CDT}}$ value of $8.44 \pm 1.2\%$ (combined expanded uncertainty, $k=2$). The sample was therefore chosen as a reference standard for external standardization of measurements in human hair samples.

Potential application: measurement of longitudinal sulfur isotopic variations in human hair strands

Human hair growth is estimated to be 0.5–1.5 cm per month [26], so measurements over a 4.3-cm segment of hair should contain information related to the past 3–9 months from the day of sample collection. Sulfur isotopic variations measured in human hair strands could then potentially aid prediction of geographical origin and recent movements of subjects or provide information on diet and lifestyle. Additionally, natural variations in sulfur isotope ratios need to be established for possible clinical tests using enriched sulfur isotopes [44].

As a preliminary study and to evaluate the potential of the method, scalp hair was collected from three individual subjects. Two UK residents A and B and a third subject (C) that had been to three different countries (including two European countries and Australia) within the past 6 months

(stay of >1 month in each country) and had been living in the UK for 1 month when samples were collected.

Measurements were performed along 4.3 cm of hair strand using the horse hair sample as an external standard to correct for instrumental mass bias effects. The pharmaceutical tablet was used as an instrumental check. Results for the three hair strands are shown in Fig. 5; measurements were performed in triplicate. Sulfur isotope amount ratios appeared to be stable over the 4.3 cm for subjects A and B with slight variations of <1.2%. Subject C showed strong

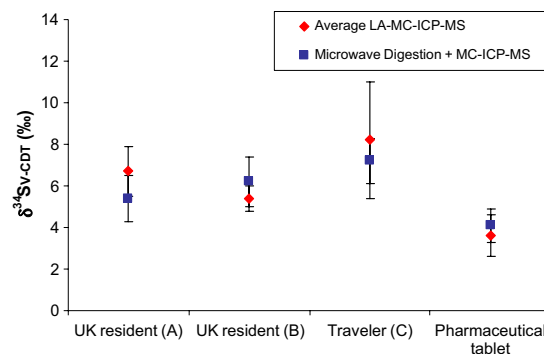


Fig. 6 Comparison between microwave digestion of hair samples and average value of the ablated hair strands (4 cm). Results are expressed in $\delta^{34}\text{S}$ and *error bars* represent combined expanded uncertainties ($k=2$). From this plot, samples cannot be distinguished; hence, the microwave digestion has no longitudinal resolution and cannot detect isotopic variations within the hair strand

variations of >5% that could be related to the recent movements. There are four different segments in the hair strand from subject C that could correspond to the four countries visited in this period. Although a more extensive study where hair samples are collected from a significant number of volunteers should be performed, the results shown in this work illustrate the ability of the method to measure longitudinal variations in human hair strands from different individuals and the potential correlation between geographical movements and variations in sulfur isotopic composition. Hence, the method has potential as both a tool for providing information that could be correlated with geographical origin/locations and a source of information in diet- and lifestyle-related studies.

Comparison of average results with microwave digestion

Digested hair samples were analyzed for sulfur isotope amount ratios by MC-ICP-MS. Instrumental mass bias was corrected using NIST RMs. Results for the hair samples and the pharmaceutical tablet are plotted in Fig. 6 for comparison. It is obvious that microwave digestion does not enable measurement of longitudinal variations but an average value has been calculated for each of the three samples and compared to the average value obtained from the longitudinal measurements performed by LA-MC-ICP-MS. From those results, the microwave digestion does not enable distinction of the three samples since longitudinal variations cannot be observed. Measurements performed after microwave digestion only reflect the average isotope ratio value and several strands of hair are required for each sample.

As a result, spatially resolved isotopic information after digestion of the hair sample is unavailable and therefore temporal changes will not be reflected in the measurement. The approach presented in this paper using LA-MC-ICP-MS requires only one single hair strand and provides spatially resolved isotopic information.

Conclusions

The new application of the LA-MC-ICP-MS method enables the measurement of longitudinally resolved variations of sulfur isotope amount ratios in single hair strands. The repeatability and precision of the method have been assessed with human and horse hair strands and typical combined expanded uncertainties of 0.12–0.15% have been obtained. The horse hair sample now characterized for sulfur isotope ratios can be used as an in-house reference standard for the measurement of isotopic variations in scalp human hair strands. The ability of the method to resolve longitudinal differences in sulfur isotopic composition has been shown. It appears that longitudinal stable sulfur

isotopic variations in hair have potential as an indicator of recent geographical movements and could be used as a tool for tracking recent geographical movements or applied to human identification. However, isotopic composition of human hair strands could be affected by several factors such as geographical movements, biological processes, or individual diets. The role of stable isotope profiling in human identification shows clear potential. In order to demonstrate such a role, stable isotopic variations across the globe should be studied and the method described in this work could be an effective tool to provide such information.

Further work will involve the collection of samples from individuals of both different geographical origin and different diet to evaluate a potential correlation between provenance/diet. If a significant correlation between samples from different geographical locations/diets and samples from individuals is observed, the method will be used to map geographical variations for a significant number of individuals. The combination of sulfur information with other isotopic systems to increase discrimination power will also be evaluated.

Acknowledgements The work described in this paper was supported by the UK Department for Innovation, Universities, and Skills as part of the National Measurement System Chemical and Biological Metrology Knowledge Base Program. The authors would like to thank the FIRMS network (<http://www.forensic-isotopes.rdg.ac.uk/>) for providing horse hair sample and particularly Wolfram Meier-Augenstein for helpful discussions. The authors are grateful for support from the Education and Science Council of the Principado de Asturias (grant BP07-059) towards Justo Giner Martinez-Sierra's secondment at LGC.

References

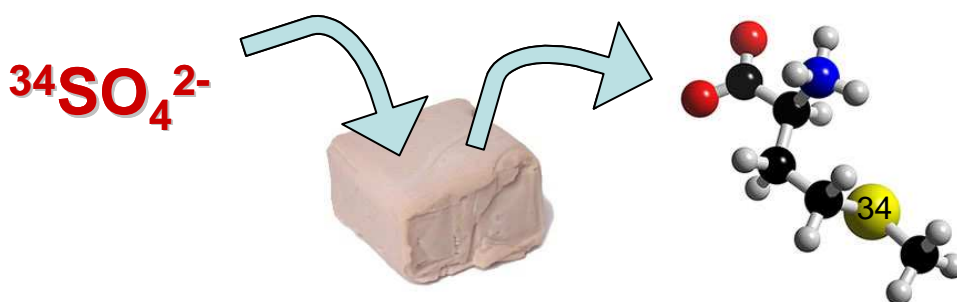
1. Rodushkin I, Axelsson MD (2000) *Sci Total Environ* 250:83–100
2. Bermejo-Barrera P, Moreda-Pineiro A, Romero-Barbeito T, Moreda-Pineiro J, Bermejo-Barrera A (1996) *Clin Chem* 42:1287–1288
3. Rodushkin I, Axelsson MD (2000) *Sci Total Environ* 262:21–36
4. Legrand M, Lam R, Jensen-Fontaine M, Salin ED, Man Chan H (2004) *J Anal At Spectrom* 19:1287–1288
5. Karpas Z, Lorber A, Sela H, Paz-Tal O, Hagag Y, Kurttio P, Salonen L (2005) *Health Phys* 89:315–321
6. Bol R, Marsh J, Heaton THE (2007) *Rapid Commun Mass Spectrom* 21:2951–2954
7. Legrand M, Lam R, Passos CJ, Mergler D, Salin ED, Chan HM (2007) *Environ Sci Technol* 41:593–598
8. Macko SA, Engel MH, Andrusevich V, Lubec G, O'Connell TC, Hedges RE (1999) *Philos Trans R Soc Lond B Biol Sci* 354:65–75
9. Khaliq A, Ahmad S, Anjum T, Jaffar M, Shah MH, Shaheen N, Tariq SR, Manzoor S (2005) *Environ Monit Assess* 104:45–57
10. Fraser I, Meier-Augenstein W (2007) *Rapid Commun Mass Spectrom* 21:3279–3285
11. Fraser I, Meier-Augenstein W, Kalin RM (2006) *Rapid Commun Mass Spectrom* 20:1109–1116
12. Klaus JP (2006) *Rapid Commun Mass Spectrom* 20:2973–2978

13. O'Connell TC, Hedges REM (2008) *Am J Phys Anthropol* 108:409–425
14. Petzke KJ, Boeing H, Metges CC (2005) *Rapid Commun Mass Spectrom* 19:1392–1400
15. Bol R, Pflieger C (2002) *Rapid Commun Mass Spectrom* 16:2195–2200
16. Ehleringer JR, Bowen GJ, Chesson LA, West AG, Podlesak DW, Cerling TE (2008) *Proc Natl Acad Sci USA* 105:2788–2793
17. Qi HP, Coplen TB (2003) *Chem Geol* 199:183–187
18. Coleman M (2004) *Handbook of stable isotope analytical techniques*, vol. I. Elsevier, Amsterdam
19. Krouse HR, Coplen TB (1997) *Pure Appl Chem* 69:293–295
20. Mason PRD, Kaspers K, van Bergen MJ (1999) *J Anal At Spectrom* 14:1067–1074
21. Evans P, Wolff-Briche C, Fairman B (2001) *J Anal At Spectrom* 16:964–969
22. Prohaska T, Latkoczy C, Stingeder G (1999) *J Anal At Spectrom* 14:1501–1504
23. Nowell G, Pearson D, Ottley C, Schwieters J, Dowall D (2003) In: Holland G, Tanner S (eds) *Plasma source mass spectrometry, applications and emerging technologies*. Royal Society of Chemistry, London, ISBN:0-85404-603-8
24. Clough R, Evans P, Catterick T, Evans EH (2006) *Anal Chem* 78:6126–6132
25. Santamaria-Fernandez R, Hearn R (2008) *Rapid Commun Mass Spectrom* 22:401–408
26. Robbins CR (2002) *Chemical and physical behavior of human hair*. Springer, New York
27. Elish E, Karpas Z, Lorber A (2007) *J Anal At Spectrom* 22:540–546
28. Stadlbauer C, Reiter C, Patzak B, Stingeder G, Prohaska T (2007) *Anal Bioanal Chem* 388:593–602
29. Stadlbauer C, Prohaska T, Reiter C, Knaus A, Stingeder G (2005) *Anal Bioanal Chem* 383:500–508
30. Sela H, Karpas Z, Zoiry M, Pickhardt C, Becker SJ (2007) *Int J Mass Spectrom* 261:199–207
31. FIRMS newsletter (2006) volume 4 issue 1. <http://www.forensic-isotopes.rdg.ac.uk/>
32. Weyer S, Schwieters J (2003) *Int J Mass Spectrom* 226:355–368
33. Prohaska T, Latkoczy C, Stingeder G (1999) *J Anal At Spectrom* 14:1501–1504
34. Mason PRD, Kaspers K, van Bergen MJ (1999) *J Anal At Spectrom* 14:1067–1074
35. Evans P, Wolff-Briche C, Fairman B (2001) *J Anal At Spectrom* 16:964–969
36. Santamaria-Fernandez R, Hearn R, Wolff JC (2008) *J Anal At Spectrom* 23:1294–1299
37. Ingle CP, Sharp BL, Horstwood MSA, Parrish RR, Lewis DJ (2003) *J Anal At Spectrom* 18:219–229
38. Günther D, Heinrich CA (1999) *J Anal At Spectrom* 14:1363–1368
39. Allen LA, Leach JJ, Houk RS (1997) *Anal Chem* 69:2384–2391
40. Heumann KG, Gallus SM, Rädlinger G, Vogl J (1998) *J Anal At Spectrom* 13:1001–1008
41. ISO (1995) *Guide to the expression of uncertainty in measurement*. International Organisation For Standardisation (ISO), Geneva
42. Kragten J (1994) *Analyst* 119:2161–2165
43. Ding T, Valkiers S, Kipphardt H, De Bievre P, Taylor PDP, Gonfiantini R, Krouse R (2001) *Geochim Cosmochim Acta* 65:2433–2437
44. Giner Martinez-Sierra J, Moreno Sanz F, Herrero Espilez P, Marchante Gayon JM, Garcia Alonso JI (2007) *J Anal At Spectrom* 22:1105–1112

D.2. PREPARACIÓN Y CARACTERIZACIÓN DE LEVADURA MARCADA CON AZUFRE-34

D.2.1. Preparación de levadura marcada con azufre-34 y su caracterización mediante ICP-MS multicolector

D.2.1.1. Artículo científico III: J. Anal. At. Spectrom., 2007, 22, 1105-1112



Biosynthesis of sulfur-34 labelled yeast and its characterisation by multicollector-ICP-MS†

J. Giner Martínez-Sierra,^a F. Moreno Sanz,^b P. Herrero Espílez,^b
J. M. Marchante Gayón^a and J. I. García Alonso^a

Received 24th April 2007, Accepted 9th July 2007

First published as an Advance Article on the web 24th July 2007

DOI: 10.1039/b706217f

Yeast labelled with ³⁴S (92.82% enriched) has been prepared by yeast growth on a ³⁴S-enriched, specially prepared, culture medium in the absence of natural abundance sulfur. The final product has been characterised both with reference to isotope enrichment and total sulfur concentration by isotope dilution analysis and isotope pattern deconvolution using a MC-ICP-MS instrument. Additionally, two different sulfur spike solutions of ³³S (99.70% enrichment) and ³⁴S (99.37% enrichment) were characterised by MC-ICP-MS with reference to a natural abundance sulfur standard solution. Spectral interferences on the determination of the isotopic composition of all sulfur solutions were also evaluated using a double focusing, single collector ICP-MS instrument. The more serious interferences observed were the presence of ³²SH⁺ and ³³SH⁺, which could be important for the natural abundance sulfur (interference on ³³S) and the ³³S-enriched sulfur (interference on ³⁴S), respectively. Fortunately, those interferences could be eliminated using the pseudo-high resolution mode of the multicollector instrument. The analytical procedure used was validated by the analysis of a blood serum reference material, which contained a certified concentration of sulfur, both using the ³⁴S and the ³³S spikes either separated or in combination using isotope pattern deconvolution. The results found were in agreement with the certified values.

Introduction

Sulfur is an essential trace element present in multitude of biologically important compounds. In particular, sulfur is present in two essential amino acids, methionine and cysteine, which cannot be synthesised by animals and have to be incorporated through the diet. These aminoacids are present in *ca.* 80% of proteins with an estimated amino acid abundance of 3–4% in eukaryotic proteomes.¹ The detection and determination of proteins *via* their sulfur content has been investigated by several authors using ICP-MS detection^{2–6} showing compound independent sensitivity. For example, studies carried out on different inorganic sulfur standards showed that sulfate is an adequate internal standard for protein quantitation purposes.⁷

Tracer studies on the metabolism of sulfur have been carried out traditionally using radioactive ³⁵S with a half-life of 87.5 d,^{8–12} with only a few papers using stable sulfur isotopes.^{13,14} The increasing popularity of ICP-MS has boosted the use of stable isotopes for metabolism studies in recent years.^{15–17} However, no ICP-MS metabolism studies using stable sulfur isotopes have been described apart from the study of natural

variations in sulfur isotope ratios¹⁸ or drug metabolism studies.¹⁴ Sulfur has four stable isotopes at nominal masses of 32, 33, 34 and 36, with natural isotope abundances of 94.93, 0.76, 4.29 and 0.02%, respectively.¹⁹ Each of the four sulfur isotopes suffers from spectral interferences from background species in the plasma when measuring by ICP-MS.²⁰ Using current ICP-MS instruments, ³⁶S is irresolvable from the elemental isobar of ³⁶Ar⁺, so ³⁶S cannot be used as tracer in metabolism studies using ICP-MS. Therefore, sulfur concentrations and isotope ratios in the sample need to be estimated by ICP-MS using the remaining three isotopes at masses 32, 33 and 34, either with reaction–collision cell^{4,21,22} or double focusing instruments.²³ Electrothermal vaporisation²⁴ and laser ablation^{20,25} have also been used for sulfur isotope ratio measurements. For tracer studies, both ³³S and ³⁴S could be used due to their low isotope abundance in natural sulfur.

In many diseases, particularly in cancer, survival rates can be greatly increased with early diagnosis and intervention. Hence, there is a great need for the development of novel methods capable of discovering protein biomarkers which possess high predictive and prognostic characteristics that can be translated into clinical practice.²⁶ Proteomic patterns, as an approach for disease diagnosis, are based on the study of the distribution of proteins from a clinical sample such as serum, which can be used as a diagnostic fingerprint, with the hope of discovering proteins that can be used as biomarkers to diagnose diseases at an early stage.²⁷ Nowadays, protein patterns are measured in blood serum using MALDI after an affinity separation from large proteins.²⁸ The measurement

^a Department of Physical and Analytical Chemistry, University of Oviedo, Julian Clavería 8, 33006 Oviedo, Spain. E-mail: jiga@uniovi.es; Fax: +34 985103125

^b Department of Biochemistry and Molecular Biology, University of Oviedo, Oviedo, Spain

† Presented at the 2007 European Winter Conference on Plasma Spectrochemistry, Taormina, Italy, February 18–23, 2007.

of sulfur by ICP-MS after two-dimensional protein separation could be an additional source of information in quantitative oncoproteomics.

The work presented here is the first step on a long-term project focused on the evaluation of the use of two sulfur stable isotopes (^{33}S and ^{34}S) to study differential protein expression in cancer research. For this purpose, yeast labelled with ^{34}S has been synthesised and characterised to be applied later as tracer in laboratory animals. Additionally, the two sulfur enriched spikes (^{33}S and ^{34}S) were characterised and the method of isotope pattern deconvolution^{29,30} was tested for the simultaneous measurement of sulfur concentration and isotopic composition in serum samples. In this work, both multi-collector and double focusing ICP-MS instruments were used for the precise and accurate measurement of sulfur isotope ratios both for the characterisation of the tracers used and the labelled yeast prepared. The use of high resolution was necessary to eliminate polyatomic interferences occurring at ^{32}S , ^{33}S and ^{34}S .

Experimental

Instrumentation

The double focusing inductively coupled plasma mass spectrometer (DF-ICP-MS) used was an Element from Finnigan-MAT (Bremen, Germany), operating at the medium resolution mode ($m/\Delta m = 3000$). All measurements were made with the standard configuration of the Element, that is, a Scott-type spray chamber working at room temperature, a Meinhard concentric nebulizer and a Fassel torch. The instrument is located in a clean room. The optimum instrumental settings for the measurement of sulfur isotope ratios by DF-ICP-MS are summarised in Table 1. The nebulizer gas flow rate, torch position and ions lens settings were optimised for higher sensitivity, aspirating a $10 \mu\text{g L}^{-1}$ Be, In and U in 1% w/w HNO_3 solution, and the acquisition parameters were optimised for better precision of the measurements of the sulfur isotope ratios.

Precise isotope ratio determinations were carried out on a Neptune double focusing multiple collector inductively coupled plasma mass spectrometer (MC-ICP-MS) from ThermoFinnigan (Bremen, Germany) equipped with 9 Faraday collectors, eight

movable and one fixed Faraday cup. The sample introduction system was a PFA-100 microconcentric nebulizer and a cyclonic spray chamber. The skimmer cone employed was the standard one for the Neptune, designated as H-cone. This instrument provides high mass resolution capabilities and can be operated at three different resolving power settings by changing the entrance slit width while keeping constant the detector slit, although medium resolution was suitable for all measurements performed in this work. Lens settings were optimised for maximum analyte sensitivity. Instrumental operating conditions and data acquisition parameters are shown in Table 1. An electronic baseline was measured before each block of measurements.

A Milestone (Microwave Laboratory Systems, Sociso, Italy) Model ETHOS 1 with medium pressure PTFE vessels was employed for the digestion of elemental sulfur for both enriched ^{33}S and ^{34}S sulfur tracers. The microwave oven programme used applied a power of 700 W for 15 min, reaching a final temperature of 185°C .

Reagents and materials

A certified, NIST-traceable, standard solution of 1000 mg L^{-1} of natural abundance S (as sulfuric acid in water) was purchased from Merck (Darmstadt, Germany). Further dilutions of this stock standard solution were made using ultra-pure water obtained from a Milli-Q system (Millipore Co., Bedford, MA, USA) to prepare the different working aqueous standard solutions as required. Enriched ^{33}S and ^{34}S were supplied from Cambridge Isotope Laboratories (Andover, MA, USA) as elemental powder. After digestion the spike solutions were kept refrigerated at 4°C . Hydrogen peroxide and nitric acid (additionally purified by sub-boiling distillation) from Merck were used for sample and spike digestions. The standard reference material used for validation of the isotope dilution procedure was Seronorm Trace Elements Serum, Level 2, NO0371, which was stored refrigerated at 4°C . For the preparation of ^{34}S -enriched yeast, the $\text{H}_2^{34}\text{SO}_4$ spike solution was first converted to ammonium sulfate by the addition of ammonia.

Yeast cells were grown using high purity nutrients obtained from Sigma-Aldrich Co. (St. Louis, MO, USA): myo-inositol, nicotinic acid, thiamine hydrochloride, potassium phosphate monobasic, boric acid, pyridoxine hydrochloride,

Table 1 Instrumental operating conditions and acquisition parameters used in the Element DF-ICP-MS and in the Neptune MC-ICP-MS

	Element	Neptune
Instrument operating conditions		
Rf power	1350 W	1200 W
Cool gas flow	14 L min^{-1} Ar	14 L min^{-1} Ar
Auxiliary gas flow	1.20 L min^{-1} Ar	0.9 L min^{-1} Ar
Sample gas flow	0.870 L min^{-1} Ar	0.935 L min^{-1} Ar
Acquisition parameters		
Resolution mode	3000	Medium (~ 3000)
Acquisition method	5 runs, 300 passes, 0.01 s sample time, 10 samples per peak 0.3 s settling time	5 blocks, 10 cycles, 4.194 s integration, 3 s idle time
Detection mode	Counting	Static
Isotopes measured	^{32}S , ^{33}S , ^{34}S	
Cup configuration		L3 ^{32}S C ^{33}S H3 ^{34}S

D-pantothenic acid calcium salt, 4-aminobenzoic acid, magnesium chloride hexahydrate, manganese(II) chloride tetrahydrate, riboflavin 5'-monophosphate sodium salt, calcium chloride dihydrate, potassium iodide, sodium molybdate dihydrate, (+)-biotin *N*-hydroxysuccinimide ester, folic acid, sodium chloride, copper(II) nitrate 2.5-hydrate, ammonium chloride, zinc chloride, iron(III) chloride anhydrous, histidine, tryptophan, leucine, arginine, lysine, threonine, valine, tyrosine and isoleucine.

Procedures

Biosynthesis of ^{34}S -labelled yeast. *Saccharomyces cerevisiae* (common baker's yeast), AMW13C strain, was used for all experiments. A synthetic complete culture medium had to be prepared with high purity nutrients in order to achieve a culture medium low in natural abundance sulfur. The content of this culture medium is indicated in Table 2. The yeast cells were grown on this medium using glucose as carbon source and ammonium chloride as nitrogen source. Yeast was grown in the presence of 100 μM of ^{34}S as $(\text{NH}_4)_2\text{SO}_4$ at 28 $^\circ\text{C}$ and 230 rpm during 48 h at pH 5.2. The yeast growth was followed by measuring the optical density spectrophotometrically at

Table 2 Composition of the culture medium for yeast growth (per litre)

<i>Carbon source</i>	30 g
Glucose	
<i>Nitrogen source</i>	5 g
NH_4Cl	
<i>Amino acids</i>	
Histidine	20 mg
Tryptophan	20 mg
Leucine	20 mg
Arginine	20 mg
Lysine	20 mg
Threonine	20 mg
Valine	20 mg
Tyrosine	20 mg
Isoleucine	20 mg
<i>Vitamins</i>	
Biotin	2 μg
Calcium pantothenate	400 μg
Folic acid	2 μg
Inositol	2 mg
Niacin	400 μg
<i>p</i> -Aminobenzoic acid	200 μg
Pyridoxine hydrochloride	400 μg
Riboflavin	200 μg
Thiamide hydrochloride	400 μg
<i>Compounds supplying trace elements</i>	
Boric acid	500 μg
Copper nitrate	40 μg
Potassium iodide	100 μg
Ferric chloride	200 μg
Manganese chloride	400 μg
Sodium molybdate	200 μg
Zinc chloride	400 μg
<i>Inorganic salts</i>	
Monopotassium phosphate	1 g
Magnesium chloride	0.5 g
Sodium chloride	0.1 g
Calcium chloride	0.1 g

600 nm. Finally, cells were collected by centrifugation and rinsed twice with ultra-pure water to remove excess inorganic sulfur. The cells were stored at $-18\text{ }^\circ\text{C}$ until their characterisation by MC-ICP-MS.

Isotope dilution analysis. The enriched spikes after dissolution were mixed with the natural abundance sulfur certified standard and its concentration calculated by reverse isotope dilution analysis. Additionally, the reference serum samples were diluted 1 + 200 with ultra-pure water after the addition of a known amount of the ^{34}S and/or ^{33}S spike solution(s). All serum samples and aqueous standards for mass bias correction were prepared by weight in thoroughly washed polypropylene containers in order to avoid contamination from trace elements. The optimum spike to sample ratio was calculated as described previously,³¹ using the random error propagation theory. Taking into account the natural abundances published by Rosman and Taylor¹⁹ and the isotope composition of the spike, the optimum isotope ratio was 0.21 for ^{34}S (32/34) and 0.35 for ^{33}S (32/33).

The total sulfur content in yeast labelled with ^{34}S was also measured by isotope dilution analysis using natural abundance S and/or ^{33}S -enriched sulfur as spikes. All measurements were performed by multi-collector ICP-MS using the conditions indicated in Table 1. A natural abundance sulfur standard was measured prior to the samples for mass bias correction. Finally, the concentration of the analyte was calculated using the isotope dilution equation described previously.³²

Isotope pattern deconvolution. Mixtures of samples with natural abundance sulfur, ^{34}S -enriched and ^{33}S -enriched were prepared and the concentrations of both natural abundance sulfur and ^{34}S enriched sulfur were calculated using isotope pattern deconvolution³⁰ with reference to the ^{33}S spike. This procedure takes into account that the isotope composition of the final mixture will be a linear function of the isotope patterns of the three components used here: natural sulfur (nat), ^{34}S -enriched (34) and ^{33}S -enriched (33) according to the following equation:

$$\begin{bmatrix} A_m^{32} \\ A_m^{33} \\ A_m^{34} \end{bmatrix} = x_{\text{nat}} \begin{bmatrix} A_{\text{nat}}^{32} \\ A_{\text{nat}}^{33} \\ A_{\text{nat}}^{34} \end{bmatrix} + x_{34} \begin{bmatrix} A_{34}^{32} \\ A_{34}^{33} \\ A_{34}^{34} \end{bmatrix} + x_{33} \begin{bmatrix} A_{33}^{32} \\ A_{33}^{33} \\ A_{33}^{34} \end{bmatrix}$$

where x_{nat} , x_{34} and x_{33} are the unknown molar fractions of each component in the mixture m and A_m , A_{nat} , A_{34} and A_{33} are the corresponding isotope abundances for the mixture and for each component, respectively. Once the molar fractions are calculated from the isotope composition in the mixture the amount of natural sulfur and ^{34}S -enriched can be calculated using the known amount of ^{33}S spike added. As we have the same number of isotopes as unknowns no uncertainty calculations can be performed from the multiple linear regression.

Results and discussion

Measurement of sulfur isotope ratios

Parameters affecting the accuracy of the isotope ratio measurements such as spectral interferences, detector dead time in

the double focusing ICP-MS and mass bias were evaluated both using the multi-collector and the double focusing ICP-MS instruments.

Spectral interferences. As is well known, all sulfur isotopes suffer interference from polyatomic species arising from gases in the plasma, water and sulfur itself (formation of SH^+). Mass spectra at medium resolution were recorded for the three measured isotopes using a natural sulfur solution on both instruments. The results obtained are shown in Fig. 1 for (a) ^{32}S , (b) ^{33}S and (c) ^{34}S . As can be seen, all three isotopes were affected by the presence of interfering polyatomic peaks occurring at a higher mass than that of the isotope of interest. The most difficult interference for the multi-collector instrument is the presence of the $^{32}\text{SH}^+$ peak over ^{33}S . As can be observed, the mass range which can be used for the measurement of isotope ratios is very narrow on this isotope. Similar problems were observed on ^{34}S when using the ^{33}S -enriched spike. However, in this case the peaks were better separated, as can be deduced from the resolution power required (3907 for $^{32}\text{SH}^+ - ^{33}\text{S}$ and 2977 for $^{32}\text{SH}^+ - ^{34}\text{S}$). As can also be observed for the measurements in the Element at medium

resolution, adequate separation for such spectral interferences is possible.

Detector dead time. For reliable isotope ratio determinations when using counting detectors, as in the double focusing ICP-MS, the detector dead time has to be appropriately corrected. For the multi-collector instrument, using Faraday cups, no detection dead time needs to be taken into account. The detector dead time in the Element was determined according to the method proposed by Vanhaecke *et al.*³³ For its evaluation, standard solutions containing increasing concentrations of S were prepared and the main isotopes of S (^{32}S , ^{33}S and ^{34}S) were measured at medium resolution by de-selecting the dead time correction option in the instrument software, under the instrumental settings shown in Table 1. A dead time value of 45 ± 1 ns was obtained and finally used to correct the measured intensities in further experiments. This dead time value is in agreement with other values obtained in our laboratory several years ago on the same instrument.³⁴⁻³⁶

Mass bias. Mass discrimination is another effect causing deviations of measured isotope ratios from the expected ratios and must be evaluated to produce accurate results. Previous

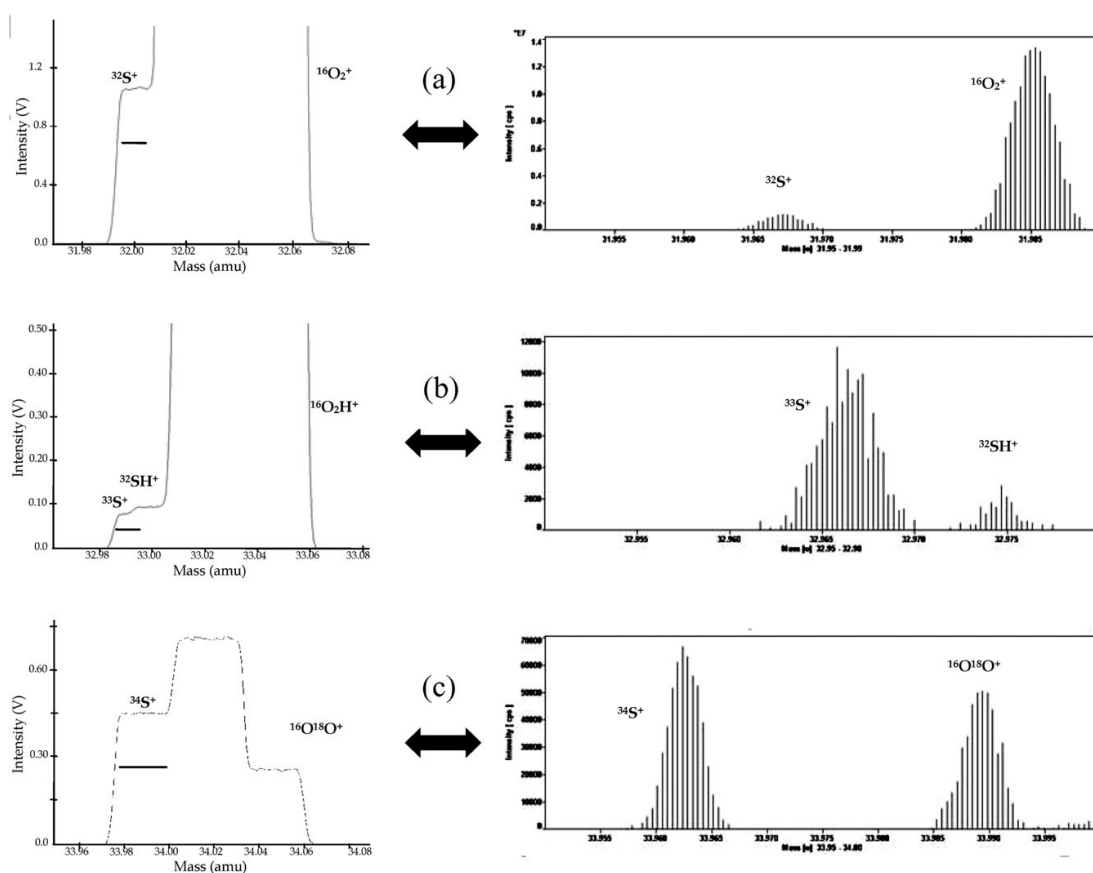


Fig. 1 Mass spectra of (a) ^{32}S , (b) ^{33}S and (c) ^{34}S obtained with the Neptune (left) and Element (right).

Table 3 Mass bias and isotope ratio precision

	Element				Mass bias (% per amu)	Neptune			
	Isotope ratios					Isotope ratios			
	33/32		34/32			33/32		34/32	
Ratio	Sd	Ratio	Sd	Ratio	Sd	Ratio	Sd	Ratio	Sd
2.92	0.008 253	0.000 032	0.047 912	0.000 086	4.03	0.008 327	0.000 009	0.048 995	0.000 071
2.98	0.008 284	0.000 025	0.047 969	0.000 099	4.57	0.008 687	0.000 032	0.049 514	0.000 024
3.04	0.008 214	0.000 069	0.048 021	0.000 087	4.41	0.008 653	0.000 035	0.049 357	0.000 034
					4.63	0.008 706	0.000 030	0.049 573	0.000 024
					4.49	0.008 655	0.000 029	0.049 434	0.000 025

work in our laboratory³⁷ showed that the observed molar response for the Element increased with increase in mass. In other words, heavier isotopes are preferentially transmitted and therefore a mass bias effect exists. Corrections for mass discrimination can be carried out by measuring a standard solution with natural isotopic composition under the same conditions of the sample with which the isotopic ratio has to be determined. Thus, a natural standard solution containing sulfur at similar concentrations to those present in the samples was measured in parallel with the ³³S and ³⁴S enriched spikes, serum and yeast samples in order to correct for mass bias. Results obtained on both instruments for the mass bias factor measured on different days using the exponential model of mass bias³⁸ are given in Table 3. As can be observed, the mass bias factor is quite constant for both ICP-MS instruments on different days but higher for the Neptune in comparison to the Element.

Typical isotope ratio precisions observed on both instruments are also given in Table 3 for the measured natural abundance sulfur standard at the same concentration level (20 ppm). As can be observed, isotope ratio precisions approach 0.2% in the Element for the natural 34/32 ratio and 0.05% in the Neptune for the same ratio. Worse precision was obtained for the very low natural 33/32 ratio.

Characterisation of the ³³S and ³⁴S enriched isotope solutions

The isotopic composition and the concentration of the enriched isotope solutions of ³³S and ³⁴S were determined by multi-collector ICP-MS using the Merck standard as reference. This Merck standard is certified in concentration but not in isotopic composition. For mass bias correction the average natural isotope abundances published by IUPAC were used,¹⁹ which include the natural variations in sulfur isotope abundances in the stated uncertainties. For the purpose of quantitation, three different blends for each enriched isotope were prepared containing different ratios of enriched isotope and natural sulfur ("3 to 1", "1 to 1" and "1 to 3"). Additionally, a mass bias correction solution (Merck sulfur standard), the pure enriched spike and a blank were also measured. Finally, the concentrations of the enriched isotope solutions were calculated by reverse isotope dilution analysis with reference to the certified Merck standard. No difference between the different blends prepared was observed. The calculated concentrations (average for the three different blends) are given in Table 4, together with their isotope composition and elemental atomic weight. As can be observed,

the isotope enrichment is higher than 99% for the two spikes used (close to the nominal enrichment of 99.92% for ³³S and 99.50% for ³⁴S as supplied by Cambridge Isotope Laboratories) and the concentration uncertainty, expressed as the combined uncertainty of the measurements, is lower than 0.5%. The uncertainty values for the isotopic composition of the spikes given in Table 4 were also calculated using Kratzen's method,³⁹ taking into account both the published uncertainties in the isotopic composition of natural sulfur¹⁹ and the experimental isotope ratio uncertainties both for the mass bias correction standard and the spiked samples. The major sources of uncertainty were the uncertainty in the natural abundance of ³⁴S and the blank correction for ³²S in the ³³S-enriched spike.

Evaluation of the isotope dilution method for the determination of total sulfur

The evaluation of the spikes for the determination of total sulfur by isotope dilution analysis was carried out by analysis of Seronorm Trace Elements Serum, Level 2, NO0371, which contained a certified concentration of sulfur. For this purpose, about 50 mg of reconstituted serum was weighed (in triplicate), mixed with the spike(s) solution and diluted by a factor of 200 with ultra-pure water. After equilibration, the isotope ratios in the different blends prepared were measured in the multi-collector instrument. The concentration found ($\mu\text{g g}^{-1}$) was 1336 ± 15 using the ³³S spike and 1346 ± 11 using the ³⁴S spike. The reference value was $1330 \pm 126 \mu\text{g g}^{-1}$. As can be observed, the results obtained are well within the ranges given for the certificate at the 95% confidence level using both spike isotopes.

Evaluation of isotope pattern deconvolution for the simultaneous determination of natural abundance sulfur and ³⁴S-enriched sulfur

Blends containing the reference serum and the two enriched spikes were prepared in order to evaluate the isotope pattern

Table 4 Concentration, isotopic composition and atomic weight of the ³³S and ³⁴S-enriched isotope solutions used as spikes

	Concentration (ppm)	Isotopic composition (%)			Atomic weight
		³² S	³³ S	³⁴ S	
³³ S spike	1095 ± 5	0.01 ± 0.06	99.70 ± 0.06	0.29 ± 0.01	32.975
³⁴ S spike	1232 ± 6	0.21 ± 0.01	0.42 ± 0.01	99.37 ± 0.01	33.959

Table 5 Evaluation of isotope pattern deconvolution for the simultaneous determination of natural sulfur and ^{34}S -enriched sulfur

Blend (concentrations in ppm for nat S, ^{33}S and ^{34}S)	Isotope ratios (corrected)				Recovery (nat S) (%)	Recovery (^{34}S) (%)
	32/33		34/33			
	Ratio	Sd	Ratio	Sd		
9.79, 5.13, 5.21	1.6913	0.0024	1.095 50	0.000 25	101	96
4.55, 10.18, 4.63	0.397 86	0.000 07	0.486 27	0.000 07	100	95
4.74, 4.91, 11.97	0.842 30	0.000 20	2.482 28	0.000 89	100	94
15.80, 1.64, 2.75	7.7277	0.0027	1.923 77	0.000 68	98	95
19.70, 1.30, 0.95	12.571	0.032	1.2674	0.0011	101	95
6.67, 7.01, 7.11	0.830 27	0.000 26	1.057 33	0.000 20	99	95
4.73, 6.08, 2.51	0.689 82	0.000 16	0.800 22	0.000 20	99	96
2.42, 2.69, 2.16	0.801 78	0.000 31	0.835 17	0.000 21	100	95
0.86, 0.38, 0.69	1.5721	0.0016	1.6422	0.0015	94	98
0.21, 0.92, 0.20	0.194 75	0.000 69	0.235 67	0.000 37	97	96
0.08, 0.04, 0.07	1.404	0.022	1.631	0.016	84	98
0.05, 0.02, 0.04	1.29	0.11	1.625	0.026	77	98
0.02, 0.01, 0.02	0.94	0.14	1.636	0.069	56	99

deconvolution (IPD) procedure for the simultaneous determination of natural abundance sulfur and ^{34}S -enriched sulfur using ^{33}S -enriched sulfur as quantitation isotope. The result obtained for the serum samples was 1298 ± 10 , also in agreement with the reference value. The average recovery for natural abundance sulfur in serum was $97.7 \pm 0.2\%$ and that from the added ^{34}S was $94.5 \pm 0.3\%$ for the triplicate experiment.

The IPD procedure was further tested by preparing blends containing the natural abundance Merck standard and the two enriched isotopes at different concentration levels and different blend ratios. The objective of this study was to test the future use of the ^{33}S tracer as post-column spike after the chromatographic separation of serum proteins in order to measure simultaneously the concentration of natural abundance sulfur and ^{34}S -enriched sulfur in the different proteins separated by chromatography. The results obtained for the different blends are summarised in Table 5. As can be observed, isotope ratio precision approached 0.02% for the high concentration levels, particularly for the 34/33 ratio. As the concentration level decreases below 0.1 ppm of each sulfur spike the precision worsened to more than 1% RSD for both measured ratios. The recovery approached 100% both for natural sulfur and ^{34}S for all prepared blends except for natural sulfur at low concentration levels. This could be due both to the high uncertainty in the measured 32/33 isotope ratio at these concentration levels and the blank correction applied (counts for the blank were subtracted from those of the samples). As a conclusion, it seems that the IPD procedure can be used for the simultaneous quantitation of both natural sulfur and isotopically enriched ^{34}S in tracer experiments. It is clear that, in the application of IPD for transient isotope ratio measurements, the expected precision of the measurements will worsen significantly.

Biosynthesis of the ^{34}S enriched yeast

Tracer experiments on protein synthesis using ^{34}S in animals require the previous synthesis of methionine and/or cysteine labelled with the enriched isotope as it is well known that animals cannot synthesise those amino acids and need to obtain them from their food. In contrast, other biota can

reduce sulfate and synthesise organo-sulfur compounds.⁴⁰ Also, we have evaluated the growing of common baker's yeast (*Saccharomyces cerevisiae*) in a medium enriched with ^{34}S (in the form of sulfate) for the labelling of methionine and/or cysteine with ^{34}S .

In order to determine the best growing conditions for *S. cerevisiae* enrichment with ^{34}S we have performed the following experiments. First, we used a standard yeast nitrogen base (YNB) medium with 0.5% ammonium chloride and 3% glucose as nitrogen and carbon sources, respectively, to analyse the minimal amount of sulfur that supports maximal growth. The final concentration of ammonium sulfate in each medium was 0, 30, 300 and 10000 μM . As can be seen in Fig. 2, a similar growth rate was observed in the different media both at fermentative and oxidative growing conditions. This result strongly suggests that sulfur was not a limiting factor for yeast growth when we used a synthetic complete medium based in YNB. Endogenous sulfur in YNB is found, mainly as magnesium sulfate, in salts (0.5 g L^{-1}) and as sulfate of Cu, Mn, and Zn in trace elements. In a second experiment we used barium chloride to try and precipitate the sulfur present in the YNB based medium as barium sulfate. However, after the filtration of barium sulfate, the results obtained were identical with those shown in Fig. 2, indicating that enough sulfate was still present in the medium to support yeast growth. It was decided to prepare a complete synthetic medium, prepared from high purity reagents, with the composition indicated in Table 2. This medium was the most effective for sulfur-dependent yeast growth. As is summarized in Fig. 3, we have detected limiting sulfur conditions for *S. cerevisiae* growth. Our results indicate that below 50 μM , ammonium sulfate is acting as a limiting nutrient in the growth of yeast. Above this concentration the yeast is growing at its maximum rate. This has been confirmed by further experiments in which the yeast growth was studied at higher concentrations of ammonium sulfate in the medium. With both 1 mM and 10 mM ammonium sulfate in the medium the yeast is growing at its maximal rate, as shown in Fig. 3. Therefore, 100 μM ammonium sulfate was selected as the concentration of the sulfur source in the ^{34}S labelling experiments.

Moreover, the biomass was identical for the consumption of the same amount of glucose in the case of the cells grown in

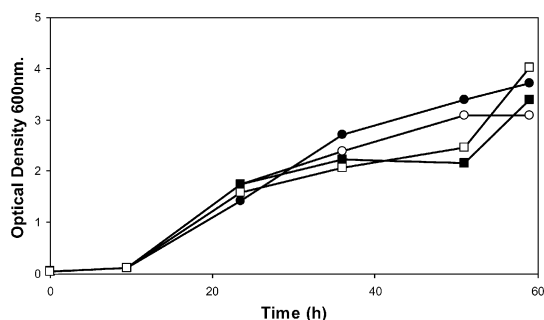


Fig. 2 Typical growth of the yeast in YNB culture media after the addition of increasing amounts of sulfur (as sulfate) (0 [●], 30 μM [○], 300 μM [■] and 10 mM [□]).

minimal sulfate (50 μM) with that of cells grown in excess of ammonium sulfate. Thus, a growth time of 48 h was selected to balance incubation time and the achieved biomass.

Therefore, the incorporation of ^{34}S , as ammonium sulfate, into yeast cells was determined by using the growing conditions established above. The corresponding ^{34}S -labelled yeast stock obtained was kept at $-20\text{ }^{\circ}\text{C}$ and characterized by MC-ICP-MS.

Characterisation of the ^{34}S -labelled yeast

As a first approach, the isotopic composition and the total sulfur concentration in the ^{34}S -labelled yeast were measured by multi-collector ICP-MS after microwave digestion of the samples. No matrix effects on mass bias were expected after nitric digestion of the yeast. The following isotopic abundances (expressed in %) for the ^{34}S -labelled yeast were found: 6.73 ± 0.21 , 0.45 ± 0.03 and 92.82 ± 0.21 for ^{32}S , ^{33}S and ^{34}S , respectively, which is consistent with 93.5% of enriched ^{34}S and 6.5% of natural abundance sulfur. The uncertainty values for the isotopic composition of the yeast were also calculated using Kratzen's method.³⁹ As can be observed, some residual natural abundance sulfur was still present during the growing of the yeast. However, 92.82% enrichment in ^{34}S should be enough to perform tracer experiments in animals.

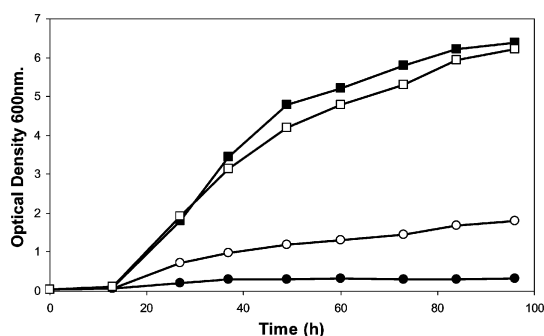


Fig. 3 Effect of the sulfate concentration added to the new culture medium on the growing of the yeast (0 [●], 10 μM [○], 50 μM [■] and 100 μM [□]).

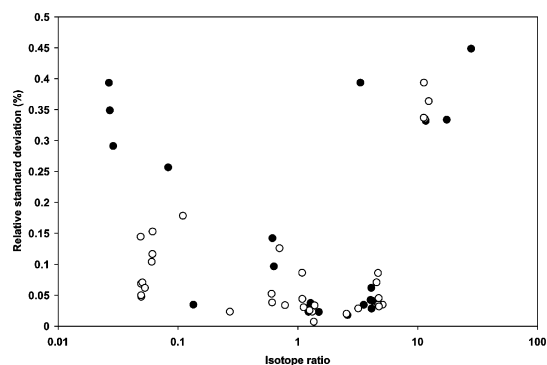


Fig. 4 Relative standard deviations (%) observed for the 33/32 (○) and the 34/32 (●) isotope ratios measured in the multi-collector ICP-MS instrument for all measured solutions at concentration levels above $1\text{ }\mu\text{g g}^{-1}$ total sulfur.

The total concentration of sulfur was determined both by isotope dilution analysis (using natural sulfur and ^{33}S as spikes) and by isotope pattern deconvolution. The results obtained, expressed as $\mu\text{g S per g}$ of dry weight, were 682 ± 10 using natural S, 677 ± 10 using ^{33}S and 677 ± 11 using ^{33}S and ^{34}S by the IPD approach. As can be observed, all procedures provide similar concentration values. Future work in the characterisation of the yeast will be to establish the concentration and isotope composition of methionine, cysteine and other possible ^{34}S -containing compounds.

Sulfur isotope ratio precision in the multi-collector ICP-MS instrument

All measurements in the multi-collector ICP-MS instrument were performed at ppm level concentrations of sulfur except for those indicated in Table 5 for isotope pattern deconvolution. When taking into account all measurements performed during this work (characterisation of the spikes, mass bias correction, isotope dilution analysis, *etc.*) it was observed that isotope ratio precision was dependent both on concentration level (see Table 5) and on the measured ratio itself. When the concentration of total sulfur was above 1 ppm the isotope ratio precision, expressed as relative standard deviation in %, was better than 0.05% for ratios between *ca.* 0.1 and 10 both for the 33/32 and the 34/32 ratios. For ratios lower than 0.1 or higher than 10 isotope ratio precision worsened considerably. All these data are summarised in Fig. 4. Please note that standard deviations correspond to the population and are not divided by the square root of n (in this case $n = 50$). Of course, these values are only indicative for future studies when isotope ratios are measured in transient signals.

Conclusions

In this work we have applied a multi-collector ICP-MS instrument in order to perform precise and accurate sulfur isotope ratios focused on: (i) the characterisation of enriched ^{33}S and ^{34}S spikes, both in isotope composition and concentration using a certified, natural abundance, sulfur solution as reference; (ii) the

determination of total sulfur in a serum reference material using the enriched isotopes characterised previously in order to validate the analytical procedure; (iii) the evaluation of an isotope pattern deconvolution approach for the simultaneous determination of natural abundance and ^{34}S -labelled sulfur using the ^{33}S spike as reference (this procedure will be applied later for post-column isotope dilution analysis in the speciation of sulfur in blood serum after the use of ^{34}S as tracer in metabolic studies); and (iv) synthesis of yeast labelled with ^{34}S by growing the yeast in a specially prepared sulfur-free medium. This yeast has been characterised both in isotope composition (92.82% enriched in ^{34}S) and total sulfur concentration.

Future studies in our laboratory will be devoted to the characterisation of the yeast in terms of its sulfur-containing amino acids and the possible use of this material as tracer in laboratory animals to study the kinetics of protein synthesis after oral administration. It is clear that the data obtained here in the bulk mode will be only indicative for future studies on isotope ratio measurements in transient signals.

Acknowledgements

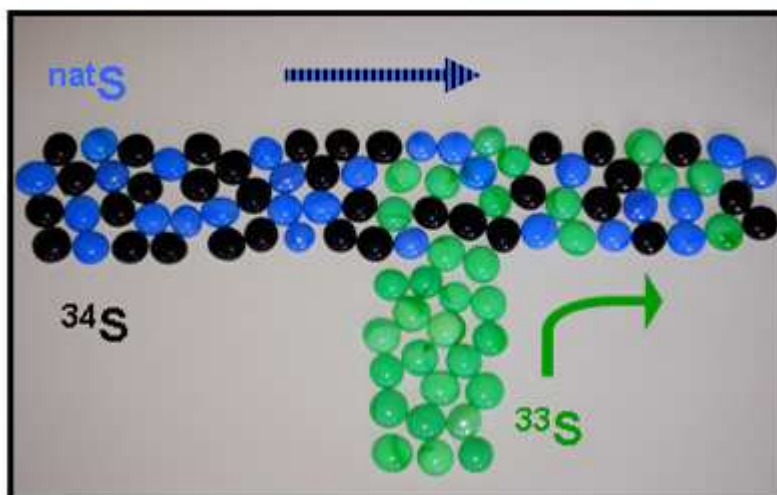
This work is supported by the Ministry of Science and Technology, Madrid, Spain (projects BQU2003-03438, BFU2004-02855-C02-02 and CTQ2006-05722). The authors would like to thank Mr. Jorge Millos (CACTI, University of Vigo, Spain) for his collaboration during the measurements on the Neptune MC-ICP-MS.

References

- 1 N. Jakubowski, N. Mihalopoulos, S. Mann and W. D. Lehmann, 'Speciation of Sulfur' in *Handbook of Elemental Speciation II: Species in the Environment, Food, Medicine and Occupational Health*, eds. R. Cornelis, J. Caruso, H. Crews and K. G. Heumann, John Wiley and Sons Ltd, England, 2005, pp. 378–407.
- 2 D. Schaumlöffel, A. Prange, G. Marx, K. G. Heumann and P. Brätter, *Anal. Bioanal. Chem.*, 2002, **372**, 155–163.
- 3 D. Pröfrock, P. Leonhard and A. Prange, *Anal. Bioanal. Chem.*, 2003, **377**, 132–139.
- 4 C. F. Yeh, S. H. Jiang and T. S. His, *Anal. Chim. Acta*, 2004, **502**, 57–63.
- 5 R. R. St. Remy, M. Montes-Bayón and A. Sanz-Medel, *Anal. Bioanal. Chem.*, 2003, **377**, 299–305.
- 6 M. Wind, A. Wegener, A. Eisenmenger, R. Kellner and W. D. Lehmann, *Angew. Chem., Int. Ed.*, 2003, **42**, 3425–3427.
- 7 E. Svantesson, J. Pettersson and K. E. Markides, *J. Anal. At. Spectrom.*, 2002, **17**, 491–496.
- 8 H. O. Singher and L. Marinelli, *Science*, 1945, **101**(2625), 414–415.
- 9 D. V. Davies and L. Young, *J. Anat.*, 1954, **88**, 174–83.
- 10 J. C. Sloper, D. J. Arnott and B. C. King, *J. Endocrinol.*, 1960, **20**, 9–23.
- 11 A. T. Lorincz, M. J. Miller, N. H. Xuong and E. P. Geiduschek, *Mol. Cell. Biol.*, 1982, **2**, 1532–1549.
- 12 K. E. Penttilä, *Biochem. J.*, 1990, **269**(3), 659–64.
- 13 F. J. Zhao, K. C. J. Verkampen, M. Birdsey, M. M. A. Blake-Kalff and S. P. McGrath, *J. Plant Nutr.*, 2001, **24**, 1551–1560.
- 14 B. P. Jensen, C. Smith, I. D. Wilson and L. Weidolf, *Rapid Commun. Mass Spectrom.*, 2004, **18**, 181–183.
- 15 I. J. Griffin, *J. Anal. At. Spectrom.*, 2002, **17**, 1186–1193.
- 16 A. Rodríguez-Cea, M. R. Fernández de la Campa, J. I. García Alonso and A. Sanz-Medel, *J. Anal. At. Spectrom.*, 2006, **21**, 270–278.
- 17 E. Sievers, K. Dorner, D. Garbe-Schonberg and J. Schaub, *J. Trace Elem. Med. Biol.*, 2001, **15**, 185–191.
- 18 R. Clough, P. Evans, T. Catterick and E. H. Evans, *Anal. Chem.*, 2006, **78**, 6126–6132.
- 19 K. J. R. Rosman and P. D. P. Taylor, *Pure Appl. Chem.*, 2003, **75**, 683–800.
- 20 C. Bendall, Y. Lahaye, J. Fiebig, S. Weyer and G. P. Brey, *Appl. Geochem.*, 2006, **21**, 782–787.
- 21 S. Stürup, L. Bendahl and B. Gammelgaard, *J. Anal. At. Spectrom.*, 2006, **21**, 201–203.
- 22 P. R. D. Mason, K. Kaspers and M. J. van Bergen, *J. Anal. At. Spectrom.*, 1999, **14**, 1067–1074.
- 23 T. Prohaska, C. Latkoczy and G. Stingeder, *J. Anal. At. Spectrom.*, 1999, **14**, 1501–1504.
- 24 L. L. Yu, W. R. Kelly, J. D. Fassett and R. D. Vocke, *J. Anal. At. Spectrom.*, 2001, **16**, 140–145.
- 25 P. R. D. Mason, J. Kosler, J. C. M. de Hoog, P. J. Sylvester and S. Meffan-Main, *J. Anal. At. Spectrom.*, 2006, **21**, 177–186.
- 26 J. Roboz, *Cancer Invest.*, 2005, **23**, 465–478.
- 27 Z. Xiao, D. Prieto, P. Conrads, T. D. Veenstra and H. J. Issaq, *Mol. Cell. Endocrinol.*, 2005, **230**, 95–106.
- 28 R. Aebersold and M. Mann, *Nature*, 2003, **422**, 198–207.
- 29 J. Mejía, G. Centineo, J. I. García Alonso, A. Sanz-Medel and J. A. Caruso, *J. Mass Spectrom.*, 2005, **40**, 807–814.
- 30 P. Rodríguez-González, A. Rodríguez Cea, R. Fernández de la Campa, J. I. García Alonso and A. Sanz-Medel, *Anal. Chem.*, 2005, **77**, 7724–7734.
- 31 J. I. García Alonso, *Anal. Chim. Acta*, 1995, **312**, 57–78.
- 32 P. Rodríguez-González, J. M. Marchante-Gayón, J. I. García Alonso and A. Sanz-Medel, *Spectrochim. Acta, Part B*, 2005, **60**, 151–207.
- 33 F. Vanhaecke, G. Wannemacker, L. Moens, R. Dams, C. Latkoczy and G. Stingeder, *J. Anal. At. Spectrom.*, 1998, **13**, 567–571.
- 34 C. Sariego Muñoz, J. M. Marchante Gayón, J. I. García Alonso and A. Sanz-Medel, *J. Anal. At. Spectrom.*, 1999, **14**, 1505–1510.
- 35 J. P. Valles Mota, J. Ruiz Encinar, M. R. Fernández de la Campa, J. I. García Alonso and A. Sanz-Medel, *J. Anal. At. Spectrom.*, 1999, **14**, 1467–1473.
- 36 J. Ruiz Encinar, J. I. García Alonso, A. Sanz-Medel, S. Main and P. J. Turner, *J. Anal. At. Spectrom.*, 2001, **16**, 315–321.
- 37 M. Montes Bayón, J. I. García Alonso and A. Sanz Medel, *J. Anal. At. Spectrom.*, 1998, **13**, 277–282.
- 38 P. D. P. Taylor, P. de Bièvre, A. J. Walder and A. Entwistle, *J. Anal. At. Spectrom.*, 1995, **10**, 395–398.
- 39 J. Kragten, *Analyst*, 1994, **119**, 2161–2165.
- 40 J. W. Anderson, 'Assimilation of inorganic sulfate into cysteine', in *The Biochemistry of Plants*, eds. P. K. Stumpf and E. E. Conn, Academic Press, New York, USA, 1980, vol. 5, p. 203.

D.2.2. Evaluación de diferentes estrategias analíticas para la cuantificación de biomoléculas que contienen azufre mediante HPLC-ICP-MS: aplicación a la caracterización de levadura marcada con azufre-34

D.2.2.1. Artículo científico IV: J. Anal. At. Spectrom., 2010, 25, 989-997



Evaluation of different analytical strategies for the quantification of sulfur-containing biomolecules by HPLC-ICP-MS: Application to the characterisation of ^{34}S -labelled yeast^{†‡}

J. Giner Martínez-Sierra,^a F. Moreno Sanz,^b P. Herrero Espílez,^b R. Santamaria-Fernandez,^c J. M. Marchante Gayón^a and J. I. García Alonso^{*a}

Received 1st December 2009, Accepted 3rd March 2010

First published as an Advance Article on the web 9th April 2010

DOI: 10.1039/b925366a

Different analytical strategies, such as Compound Independent Calibration (CIC), post-column Isotope Dilution Analysis (IDA) and post-column Isotope Pattern Deconvolution (IPD) were evaluated for the determination of sulfur-containing biomolecules. CIC graphs were obtained for the sulfur-containing compounds sulfate, cysteine, glutathione and methionine separated by isocratic HPLC using four different ICP-MS instruments. Instruments evaluated included two quadrupole based instruments (XSeries II and HP-4500), with and without a collision cell respectively, one single collector double focusing (Element 2) and one multicollector double focusing (Neptune). When isocratic HPLC separations were employed, CIC using sulfate standards could be applied for the determination of small peptides and amino acids in their native form. When gradient elution HPLC separations were performed, CIC was no longer suitable and enriched stable isotopes (^{33}S) were evaluated to compensate for gradient-derived changes in the sensitivity for sulfur in the ion source. It was observed that post-column IDA using ^{33}S was suitable for the absolute quantification of sulfate, cysteine, glutathione and methionine by HPLC-ICP-MS when gradient elution was performed. Unfortunately, traditional equations used for post-column IDA can no longer be applied when two different sulfur enriched isotopes are employed. In the characterisation of ^{34}S -labelled yeast we will have three different sulfur isotope patterns: natural abundance sulfur impurities, ^{34}S used as “labelling” tracer and ^{33}S used as post-column “quantification” tracer. So, for the characterisation of ^{34}S -labelled yeast we have developed a post-column IPD procedure that allowed us to obtain the “pattern specific molar flow chromatograms” and, hence, to discriminate between “natural abundance” and “ ^{34}S -enriched” sulfur species in the ^{34}S -labelled yeast.

1. Introduction

Inductively Coupled Plasma Mass Spectrometry (ICP-MS) is one of the most powerful analytical techniques for elemental detection in biological materials due to its low detection limits, the easy coupling with chromatographic techniques and the possibility of measuring highly precise isotope ratios.^{1,2} Heteroatom-labelled compounds can be easily followed by ICP-MS and find particular applications in metabolic studies as the isotopic composition of the labelled element can be simply measured during a chromatographic separation. In the field of proteomics the obvious choice for protein labelling is sulfur. The atomisation and ionisation capabilities of the ICP ion source allow direct and selective access to protein analysis *via* the determination of

sulfur, which is present in the proteinogenic amino acids cysteine (Cys) and methionine (Met). These two amino acids, either one or both, are present in *ca.* 98% of human proteins. For tracer studies, it is of paramount importance to take into consideration that Cys and Met cannot be synthesised by animals and have to be incorporated through the diet.³

The detection of sulfur by ICP-MS has become in recent years one of the most versatile and sensitive complementary tools in bio-inorganic analytical chemistry.⁴⁻⁶ This trend has been specially boosted by the availability of collision and reaction cells and more robust high resolution ICP-MS instrumentation, as well as the development of suitable interface technologies for the coupling of separation techniques to ICP-MS. Thus, different approaches can be found in the literature regarding the determination of sulfur by ICP-MS: i) quadrupole based ICP-MS instruments operating with cool plasma conditions⁷ to promote the formation of the stable SO^+ molecular ion, ii) quadrupole based collision/reaction cell ICP-MS instruments with xenon^{8,9} as cell gas to reduce the intensity of the polyatomic background species allowing sulfur to be measured directly as its natural isotope masses or iii) using oxygen¹⁰⁻¹⁴ as cell gas to generate SO^+ ions in the cell and iv) high resolution ICP-MS instruments either single collector¹⁵⁻¹⁸ or multicollector.¹⁹⁻²⁵

Compound Independent Calibration (CIC) is a quantitative technique based on the capability of certain spectrochemical

^aDepartment of Physical and Analytical Chemistry, University of Oviedo, Julian Clavería 8, 33006 Oviedo, Spain. E-mail: jiga@uniovi.es; Fax: +34 985103125

^bDepartment of Biochemistry and Molecular Biology, University of Oviedo, Oviedo, Spain

^cLGC Ltd., Queens Rd., Teddington, Middlesex, UK TW11 0LY

[†] This article is part of a themed issue highlighting some of the most recent and significant developments in the area of Sector Field ICP-Mass Spectrometry.

[‡] Electronic supplementary information (ESI) available: Compound independent calibrations. See DOI: 10.1039/b925366a

sources (such as plasmas) to provide an elemental response independent of the chemical structure of the molecules which might contain the element. The elemental response by ICP-MS, when operated under certain conditions, could be directly proportional to the absolute amount of the element introduced. Therefore, in contrast to molecular MS techniques, the signal is independent of the nature of the compound. In general, the influence of the nature of the species in ICP-MS is small or non-detectable, but this fact cannot always be assumed and must be demonstrated, particularly when using inorganic standards in the quantification of biomolecules.²⁶ In this sense CIC for the High Performance Liquid Chromatography HPLC-ICP-MS coupling in the field of phospho-peptide analysis²⁷ and for selenium speciation²⁸ was demonstrated to be a good strategy to obtain quantitative results.

Unfortunately, CIC will not work when matrix effects are present. For example, in reversed-phase gradient elution conditions the organic content of the mobile phase strongly influences the sensitivity in ICP-MS. Most reverse phase separations of proteins and peptides require gradient elution²⁹ and the response for the early eluting compounds will be completely different from that of the late eluting proteins or peptides because of matrix suppression effects. There are three general approaches to correct for matrix suppression effects in liquid chromatography coupled to ICP-MS: (i) pre-column standard addition (labelled or non-labelled); (ii) post-column standard addition (labelled or non-labelled) and (iii) the establishment of a correction function.

Previous work in our laboratory on the detection of elements associated with proteins in human serum^{30,31} by HPLC-ICP-MS demonstrated that post-column Isotope Dilution Analysis (IDA) can be used for the absolute quantification of those elements eluting from the separation column even when using gradient elution. This technique requires the simultaneous interference-free detection of two isotopes of the same element, so that possible changes in detection sensitivity affect both isotopes to the same extent, but not the isotope ratio. The isotopically enriched spike is added after the separation has taken place and allows for the compensation of sensitivity variations and drift. However, this procedure does not compensate for losses which occurred during sample preparation. To correct for those effects, a species-specific IDA might be recommended. Nevertheless, the inherent capability of quantifying species of unknown structure without the need of using species-specific standards for a methodological calibration has made post-column IDA a versatile and powerful tool to quantify proteins and metal species in complicated biological matrices. In fact, an increasing number of publications can be found in the literature regarding the use of post-column IDA with ICP-MS using sulfur as key element for elemental mass spectrometric analyses.^{9,32-34} A recent paper has outlined this application for protein standards.³⁵

However, when the sample to be analysed contains non-natural sulfur isotope compositions, such as those found in metabolic tracer experiments, traditional post-column IDA equations³⁶ can no longer be applied. The isotope composition of different sulfur-containing compounds detected in the sample could change depending on their metabolic pathway. Then, alternative equations will need to be developed. In the last few years we have applied a mathematical procedure called Isotope Pattern Deconvolution (IPD) which can extract molar fraction

information from measured isotope abundances for isolating distinct isotope signatures from mixtures of natural abundance and enriched tracers.³⁷ For sulfur we could measure up to three isotopes (³²S, ³³S, and ³⁴S) which would provide data for the deconvolution of three isotope patterns: natural abundance sulfur, ³⁴S used as "metabolic" tracer and ³³S used as post-column "quantification" tracer.³⁸

In a previous work,³⁹ we have prepared ³⁴S-labelled yeast by growing *Saccharomyces cerevisiae* in a specially prepared sulfur-free growing medium. The obtained ³⁴S-labelled yeast was characterised as total sulfur and contained about 93% of ³⁴S. The aim of this work is to develop analytical methodologies for the characterisation of this ³⁴S-labelled yeast, with regards to their sulfur-containing biomolecules, and to evaluate its suitability as the sulfur source for future tracer studies in laboratory animals. The most important parameter to be evaluated is the presence of ³⁴S in proteins as cysteine and methionine, since these amino acids are essential for mammals and therefore are effectively incorporated when supplied with the diet. For this purpose yeast seems to be an ideal substance for metabolic tracer experiments: it is harmless; it can be administered orally to the test subjects and sulfur-containing proteins, peptides and amino acids can be hydrolysed and adsorbed in the gastrointestinal tract.

2. Experimental

2.1. Reagents and materials

A certified standard solution of 1000 mg L⁻¹ of natural abundance S (as sulfuric acid in water) was purchased from Merck (Darmstadt, Germany). Enriched ³³S and ³⁴S were supplied from Cambridge Isotope Laboratories (Andover, MA, USA) as elemental powders. After digestion the spike solutions were characterised both in isotopic composition and in concentration by reverse IDA.³⁹ The standards of DL-Methionine (>99% purity), DL-Cysteine (>95% purity) and L-Glutathione reduced (>97% purity) were purchased from Fluka (Buchs, Switzerland). Bovine Serum Albumin (BSA) from Sigma-Aldrich Co. (St. Louis, MO, USA) was used to optimise the yeast hydrolysis conditions. For the chromatographic separations heptafluorobutyric acid (HFBA) from Sigma-Aldrich and HPLC-grade methanol from Merck were used. Ultrapure water was obtained from a Milli-Q system (Millipore Co., Bedford, MA, USA). Yeast labelled with ³⁴S (92.82% enriched) was previously prepared in our laboratory by yeast growth on a ³⁴S-enriched, specially prepared, culture medium in the absence of natural abundance sulfur and characterised both with reference to isotope enrichment and total sulfur concentration by IDA and IPD using a MC-ICP-MS instrument.³⁹ Hydrochloric acid (Merck) sub-boiling distilled was employed for hydrolysis purposes.

2.2. Instrumentation

2.2.1. HPLC system. Chromatographic separation was performed on an Agilent 1100 HPLC system (Agilent Technologies, Waldbronn, Germany). Samples (20 µL) were injected on a Discovery Bio Wide Pore C18 HPLC column equipped with a guard column. Reversed-phase chromatography was used with 0.3% HFBA as ion-pairing agent and 2% methanol in the mobile phase. Fig. 1 shows the chromatographic separation of

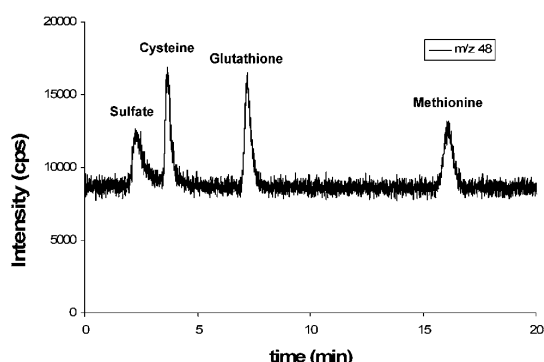


Fig. 1 Chromatographic separation of sulfate, cysteine, glutathione and methionine (100 ng g⁻¹ of each approx.) with the XSeries II ICP-MS as sulfur specific detector, using O₂ as reactive gas in the collision cell.

Table 1 Instrumental parameters of the different HPLC-ICP-MS instruments used

HPLC conditions			
Column	Discovery BIO Wide Pore C18 (15 cm × 2.1 mm; 5 μm)		
Injection loop	20 μL		
Flow rate	200 μL min ⁻¹		
Mobile phase (isocratic)	0.3% HFBA; 2% MeOH; pH 2.5		
Mobile phase (gradient)	0.3% HFBA; 2% MeOH; pH 2.5 for 5 min and then linear gradient to 14% MeOH at 2%·min ⁻¹ .		
ICP-MS conditions			
HP-4500		XSeries II	
RF power	950 W	Forward power	1300 W
Carrier gas	1.4 L min ⁻¹ Ar	Nebuliser gas	0.90 L min ⁻¹ Ar
Sample depth	5.8 mm	Reactive gas	0.45 mL min ⁻¹ O ₂
Element 2		Neptune	
RF power	1275 W	RF power	1350 W
Auxiliary gas flow	0.70 L min ⁻¹ Ar	Auxiliary gas flow	0.7 L min ⁻¹ Ar
Sample gas flow	0.97 L min ⁻¹ Ar	Sample gas flow	1.0 L min ⁻¹ Ar
Resolution mode	Medium	Resolution mode	Medium
		Cup configuration	³² S-L3, ³³ S-C, ³⁴ S-H3

a standard solution mixture containing the sulfur amino acids cysteine and methionine, the tripeptide glutathione and sulfate. As can be observed, the chromatographic conditions listed in Table 1 provided a good separation for the four sulfur compounds with an acquisition time of *ca.* 15 min.

2.2.2. ICP-MS systems. Four different ICP-MS instruments were used in this study. The most relevant operating conditions applied for the detection of sulfur-compounds after their reversed phase ion-pairing HPLC separation are reported in Table 1. The HP-4500 ICP-MS (Agilent Technologies) was optimised using Cool Plasma conditions.⁷ These conditions promote the formation of stable oxides (high oxide ratios) of

several elements. Due to the fact that sulfur readily forms oxides, sulfur can be detected as its oxide ³²S¹⁶O⁺ at *m/z* = 48. The XSeries II ICP-MS (Thermo Instruments) was optimised using O₂ as reactive gas in the collision cell. Sulfur was detected as its oxide at *m/z* 48. The Element 2 HR-ICP-MS (Thermo Instruments) was operated in medium resolution to resolve the polyatomic interferences affecting ³²S⁺, ³³S⁺ and ³⁴S⁺. The Neptune MC-ICP-MS (Thermo Instruments) was also operated in medium resolution to resolve the polyatomic interferences affecting the detection of sulfur by ICP-MS.

2.2.3. Microwave system. A focused microwave system Discovery (CEM, Matthews, NC, USA) with an autosampler Explorer (CEM) was used to perform the extraction of the sulfur-containing biomolecules from yeast or the BSA protein.

2.3. Procedures

2.3.1. Extraction and hydrolysis of yeast proteins. Cells of the ³⁴S-labelled yeast were collected by centrifugation and rinsed twice with ultra-pure water to remove inorganic sulfur. Then, the cells were suspended in ultrapure water and were broken by hard vortex (5 times × 1 min) in the presence of glass beads. After centrifugation at 14000 rpm for 10 min at 4 °C, the supernatant was transferred to a fresh tube. This fraction was considered to be the protein extract. The solid residue was also collected. The hydrolysis of yeast proteins and the solid residue was performed in an open focusing microwave oven with 3% v/v hydrochloric acid at 120 °C for 10 min. Both the protein extract and the solid residue were analysed directly after hydrolysis.

2.3.2. Post-column Isotope Dilution Analysis (IDA). The isotopically enriched spike, ³³S in the form of sulfate, was added after the separation has taken place. The continuous measurement of the isotope ratio ³²S/³³S in the ICP-MS allowed us to construct the so-called “mass flow chromatogram”.^{30,31} The integration of each peak in the mass flow chromatogram provided the absolute mass of sulfur present in each chromatographic peak.

2.3.3. Post-column Isotope Pattern Deconvolution (IPD). The object of IPD is to calculate the molar contribution of the different isotope patterns contained in a mixture when the isotope composition of the mixture is measured by Mass Spectrometry and the isotope patterns of the pure components are known.³⁷ For a sulfur tracer experiment at least three isotope patterns need to be considered: the natural abundance pattern (^{nat}S), present in the sample, and two isotopically enriched patterns. One of these isotopically enriched patterns has been added to the sample *in vivo* for metabolic purposes (³⁴S) while the second pattern (³³S) will be used for post-column quantification. For every point in the chromatogram the total molar flow will be given by:

$$N_m = N_{nat} + N_{34} + N_{33} \quad (1)$$

Where N_m is the total molar flow of the element entering the ion source and N_{nat} , N_{34} and N_{33} the molar flows of the same element

corresponding to the three different isotope patterns considered, either eluting from the column or added post-column.

The molar balance given in eqn (1) can be calculated also for all isotopes of the element. For example, for isotope 32 of sulfur we obtain:

$$N_m^{32} = N_{nat}^{32} + N_{34}^{32} + N_{33}^{32} \quad (2)$$

Eqn (2) can be also expressed as a linear combination of isotope abundances and molar flows for each isotope pattern as:

$$N_m \cdot A_m^{32} = N_{nat} \cdot A_{nat}^{32} + N_{34} \cdot A_{34}^{32} + N_{33} \cdot A_{33}^{32} \quad (3)$$

Where A_m^{32} , A_{nat}^{32} , A_{34}^{32} and A_{33}^{32} are the measured (A_m^{32}) or known (A_{nat}^{32} , A_{34}^{32} and A_{33}^{32}) isotope abundances for isotope 32 in each of the considered isotope patterns. By dividing eqn (3) by eqn (1) we obtain:

$$A_m^{32} = x_{nat} \cdot A_{nat}^{32} + x_{34} \cdot A_{34}^{32} + x_{33} \cdot A_{33}^{32} \quad (4)$$

Where $x_{nat} = \frac{N_{nat}}{N_m}$, $x_{34} = \frac{N_{34}}{N_m}$ and $x_{33} = \frac{N_{33}}{N_m}$ are the molar fractions (or molar flow fractions) from each of the isotope patterns contributing to the measured isotope profile observed in the mixture at each data point of the chromatogram.

As sulfur contains 3 ICP-MS-measurable stable isotopes (32, 33 and 34) we can establish 3 different equations expressing the linear combination of isotope abundances and molar fractions (eqn (4)). This series of equations can be expressed, in matrix form, as:

$$\begin{bmatrix} A_m^{32} \\ A_m^{33} \\ A_m^{34} \end{bmatrix} = \begin{bmatrix} A_{nat}^{32} & A_{34}^{32} & A_{33}^{32} \\ A_{nat}^{33} & A_{34}^{33} & A_{33}^{33} \\ A_{nat}^{34} & A_{34}^{34} & A_{33}^{34} \end{bmatrix} \cdot \begin{bmatrix} x_{nat} \\ x_{34} \\ x_{33} \end{bmatrix} \quad (5)$$

For sulfur, the exact solution of eqn (5) will provide the values of the molar fractions x_{nat} , x_{34} and x_{33} in each point of the chromatogram.

The post-column isotope dilution equation is now obtained by rationing the different molar fractions. For sulfur tracer studies, using ^{34}S as tracer and ^{33}S for post-column quantification, the post-column isotope dilution equations are:

$$\frac{x_{nat}}{x_{33}} = \frac{N_{nat}}{N_{33}}$$

and

$$\frac{x_{34}}{x_{33}} = \frac{N_{34}}{N_{33}}$$

The relative molar flows for each of the two isotope pattern (natural or ^{34}S -enriched) are calculated by the respective ratio of molar fractions. When we apply these equations to the whole chromatogram we can obtain two "pattern-specific molar flow chromatograms", one for natural abundance sulfur and the other for ^{34}S enriched sulfur.

3. Results and discussion

3.1. Compound Independent Calibration (CIC)

In order to evaluate the CIC capabilities of the four different ICP-MS used in this work, different concentration levels of

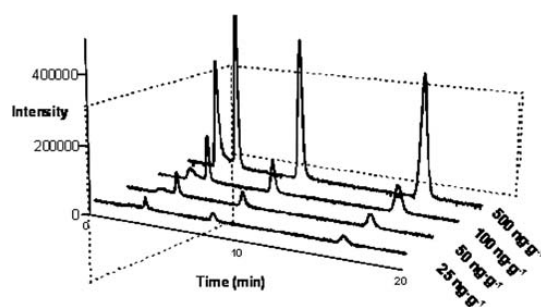


Fig. 2 Chromatograms showing different concentration levels (ranging from 25 ng g⁻¹ to 500 ng g⁻¹ for clarity) of sulfate, cysteine, methionine and glutathione injected in the HPLC-ICP-MS system using the Element 2 instrument.

a standard solution mixture of the sulfur-compounds sulfate, cysteine, methionine and glutathione ranging from 20 ng g⁻¹ to 20 μg g⁻¹ were prepared and injected in the HPLC-ICP-MS system. A typical plot of this experiment using the Element 2 ICP-MS instrument is shown in Fig. 2. We have observed that the plot of the peak areas of sulfate, cysteine, glutathione and methionine vs. sulfur concentration followed the same calibration line for the four different ICP-MS instruments. The obtained calibration graphs are shown in the Supplementary Information both for the quadrupole and double focusing instruments. For the quadrupole instruments sulfur detection was performed at mass 48 ($^{32}\text{S}^{16}\text{O}^+$) while for the double focusing instruments detection was performed at mass 32 using medium resolution. As it was observed, for all instruments and conditions the analytical response (peak area) was clearly compound independent and only depended on the total amount of sulfur present in the corresponding chromatographic peaks.

Under the experimental conditions used the detection limits for sulfur (based on three times the standard deviation of the intercept of the compound independent calibration graph) were determined to be 21 ng g⁻¹ for the Thermo X Series II, 42 ng g⁻¹ for the HP-4500, 25 ng g⁻¹ for the Neptune and 8 ng g⁻¹ for the Element 2. So, for low concentration measurements the Element 2 showed the best performance of the four instruments tested. Please note that using the CIC procedure only one detection limit is obtained for sulfur regardless of the compound retention time and peak shape.

The procedure of CIC was used to optimise the hydrolysis of yeast proteins after the microwave treatment of BSA as test protein. A calibration graph was prepared using sulfate standards and the concentrations of cysteine, methionine and glutathione found in the protein hydrolysates determined from this calibration graph. It was observed that protein hydrolysis using HCl as reagent was not quantitative and many sulfur containing peptides, which required gradient elution with methanol, were detected (chromatograms not shown). In order to avoid pressure build-up in the column and increased sulfur background from late eluting peaks gradient elution with methanol was evaluated. Obviously, gradient elution, particularly using organic modifiers, will show decreased response for high concentrations of methanol or acetonitrile. Most reverse phase separations of proteins require gradient elution²⁹ and the

response for the early eluting proteins will be completely different from that of the late eluting proteins. So, we decided to evaluate the use of post-column isotope dilution analysis to compensate for changes in ionisation efficiencies in the ion source.

3.2. Post-column isotope dilution analysis (IDA)

Sulfur contains four stable isotopes of masses 32, 33, 34 and 36. Isotope 32 of sulfur is the most abundant with *ca.* 94.93% natural isotope abundance. Minor isotopes 33 (0.76%) and 34 (4.29%) could then be used as post-column standards to compensate for sensitivity changes during elution. The minor sulfur isotope of mass 36 (0.02%) can not be used because of a direct overlap with the minor argon isotope ^{36}Ar present in large quantities in the ion source. In the case of the quantification of sulfur-containing biomolecules (amino acids, peptides and proteins) our selected spike isotope was ^{33}S in the form of sulfate and the continuous measurement of the isotope ratio $^{32}\text{S}/^{33}\text{S}$ in the ICP-MS allowed us to construct the so-called "mass flow chromatograms".^{30,31} The integration of each peak in the mass flow chromatogram provided the absolute mass of sulfur present in each chromatographic peak. The suitability of ^{33}S sulfate as post-column spike was demonstrated by the CIC curves shown in the ESI† as the sensitivity for sulfate was the same as for the other sulfur-containing standards.

In order to check the suitability of this procedure we have carried out the quantification of a mixture of standards of the sulfur amino acids cysteine and methionine, the tripeptide glutathione and sulfate, using a ^{33}S spike solution as post-column

spike under both the isocratic and gradient separation conditions given in Table 1. For comparison purposes, CIC using sulfate standards was also carried out. Typical chromatograms obtained both for isocratic and gradient conditions in two of the instruments tested are shown in Fig. 3. As can be observed, the response for ^{33}S is constant with time for the isocratic conditions but changes with time for the gradient conditions, as expected. For the XSeries II a reduction in sensitivity is observed at the end of the chromatogram while for the Element 2 an increase in sensitivity is observed for this particular chromatogram. Other runs in the Element 2 showed reduction in sensitivity similar to those observed for the quadrupole-based instrument. As the last peak in the chromatogram is methionine the effect of the

Table 2 Concentrations found for methionine calculated by CIC or using the ^{33}S post-column IDA approach both for isocratic and gradient elution conditions (single measurements)

	Prepared (ng g^{-1} expected)	Isocratic (ng g^{-1} found)		Gradient (ng g^{-1} found)	
		CIC	Post-column IDA	CIC	Post-column IDA
HP-4500	570	565	561	518	556
XSeries II	112	111	108	100	111
Element 2	238	236	239	96	110
				198	235
				208	241
				275	242

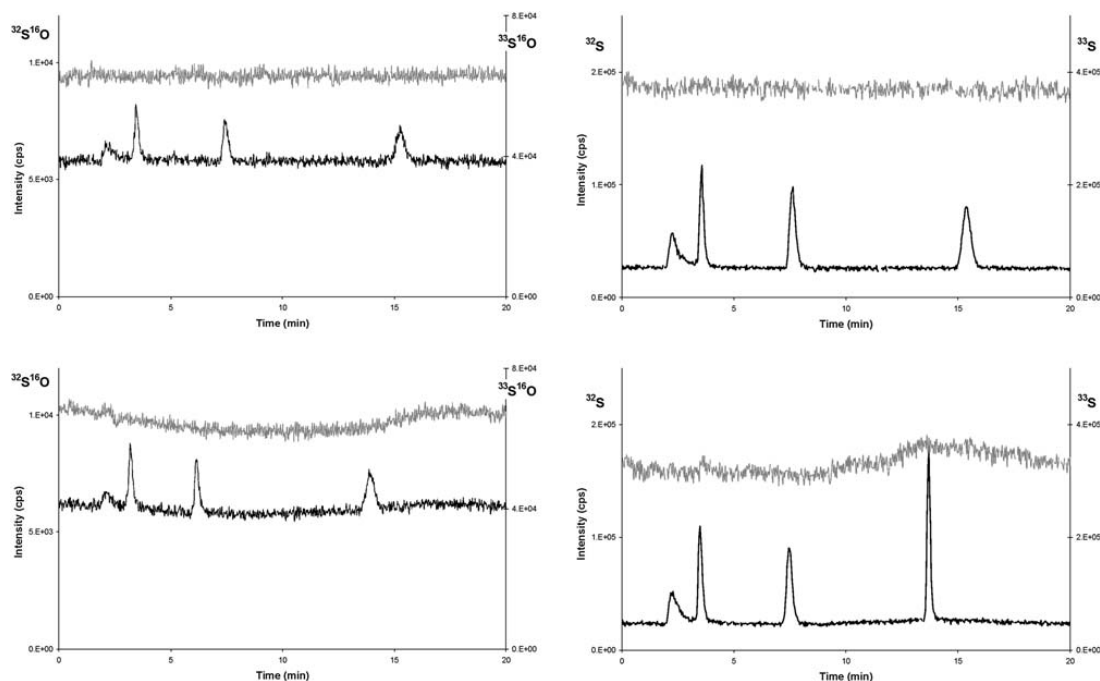


Fig. 3 Intensity chromatograms obtained by post-column Isotope Dilution Analysis (IDA) using both isocratic (top) and gradient elution (bottom) in the XSeries II (left) and the Element 2 (right) instruments.

different quantification procedures and elution conditions was evaluated for this compound. Table 2 reports the concentrations found for methionine in different chromatograms. For isocratic conditions CIC was found to provide accurate results similar to those found by post-column IDA. However, when gradient elution was performed only post-column IDA was able to provide accurate results regardless of the ICP-MS instrument used. For the Element 2 three different chromatograms were evaluated. In all cases, post-column IDA provided concentration results in agreement with the expected concentrations. So, the isotopically enriched ^{33}S spike added post-column allowed for the compensation of sensitivity variations and/or instrumental drift. So, post-column IDA in combination with Isotope Pattern Deconvolution was selected for the characterisation of the ^{34}S -labelled yeast.

3.3. Measurement of sulfur isotope abundances by HPLC-ICP-MS

The capabilities of all instruments for the measurement of sulfur isotope abundances by HPLC-ICP-MS were evaluated using the isotopically enriched spikes, ^{33}S and ^{34}S , previously characterised by conventional nebulisation on a multicollector ICP-MS instrument³⁹. For this purpose, the enriched isotope solutions were injected in the HPLC system coupled to the other three ICP-MS instruments tested. Sulfur elution appeared at the retention time of sulfate for both spikes confirming the nature of the sulfur compound obtained after digestion of the metallic sulfur. The peak areas of sulfate were used to characterise the spikes at masses 48, 49 and 50 for ^{32}S , ^{33}S and ^{34}S respectively in the HP-4500 and the XSeries II instruments. A natural abundance sulfate standard was used for mass bias correction. In addition, these two spike solutions were characterised in the Element 2 HR-ICP-MS by measuring ^{32}S , ^{33}S and ^{34}S at medium resolution. The results of three replicate samples are reported in Table 3. As can be observed, the best results, in comparison with the Neptune data, were obtained with the Element 2. However, both quadrupole instruments demonstrated that sulfur isotope abundances can be measured at the SO polyatomic ion but with lower precision and accuracy. Final characterisation of the ^{34}S -labelled yeast was performed only on the Element 2 instrument because of its better sensitivity and capabilities for isotope abundance measurements.

Table 3 Isotope composition of the ^{33}S and ^{34}S -enriched isotopes used as spikes

		Isotope composition (%)		
		^{32}S	^{33}S	^{34}S
^{33}S spike	Neptune ³⁹	0.01 ± 0.06	99.70 ± 0.06	0.29 ± 0.01
	Element 2	0.52 ± 0.44	99.15 ± 0.36	0.33 ± 0.12
	HP-4500	0.93 ± 0.83	97.94 ± 1.34	1.13 ± 1.01
	XSeries II	0.54 ± 0.51	99.11 ± 0.62	0.35 ± 0.21
^{34}S spike	Neptune ³⁹	0.21 ± 0.01	0.42 ± 0.01	99.37 ± 0.01
	Element 2	0.61 ± 0.44	0.36 ± 0.19	99.03 ± 0.43
	HP-4500	1.02 ± 0.85	0.85 ± 0.81	98.13 ± 1.05
	XSeries II	0.38 ± 0.51	0.77 ± 0.31	98.85 ± 0.71

3.4. Characterisation of the ^{34}S -labelled yeast

First, different hydrolysis procedures for the extraction of methionine and cysteine from the ^{34}S -labelled yeast previously prepared were evaluated. A complete hydrolysis of yeast protein into its constituent amino acids would be necessary for the quantitative analysis of methionine and cysteine. However, for the study of the isotope composition of these amino acids in the prepared yeast only a partial extraction would be required. When using enzymatic methods of hydrolysis high blank levels of methionine have been reported due to the hydrolysis of the protease itself as it contains methionine residues.⁴⁰ Therefore, this procedure was avoided as it would modify the original isotope composition of methionine in the labelled yeast. The hydrolysis of proteins with hydrochloric acid is the conventional protocol for the analysis of amino acids in proteins, typically with 6 mol L⁻¹ HCl at 110–120 °C for 24 h. Although it is a common biochemical procedure, it presents some disadvantages, such as possible oxidation of Met to Met-sulfoxide and Met-sulfone.⁴¹ In this way very low extraction efficiencies have been reported using HCl for methionine.⁴⁰ A 4M methanesulfonic acid reflux digestion for 16 h was found to be the most efficient for Met extraction in yeast.⁴⁰ Based on the literature search, two tentative procedures were evaluated for extraction of methionine and cysteine from the yeast sample by microwave-assisted hydrolysis either with hydrochloric acid or methanesulfonic acid. In preliminary experiments a standard of BSA (bovine serum albumin), which presents 35 residues of cysteine and 5 residues of methionine in its amino acid composition, was used to test the microwave hydrolysis conditions. For the extraction of Met by microwave-assisted hydrolysis with hydrochloric acid large variations in extraction efficiencies for Met were observed with different conditions of hydrolysis: the concentration of HCl, temperature, time and the effect of degassing the samples were tested. A method using 0.1 g of protein, 3% v/v HCl and 120 °C for 10 min. achieved the highest extraction efficiency (19% digestion using BSA as reference). For the extraction of Met by microwave-assisted hydrolysis with methanesulfonic acid (MSA) low concentrations of MSA were tested due to the large peak tail of this reagent (MSA eluted in the dead volume of the column under the chromatographic conditions summarized in Table 1). The main problem was that the MSA peak saturated the detector and, on the other hand, hid the early eluting analyte peaks. A method using 0.1 g of protein, 1.75% MSA, 150 °C for 2 h. achieved the highest extraction efficiency (39% using BSA as reference). For these experiments CIC was used for quantification. Finally, the HCl procedure was selected for the hydrolysis of the yeast sample as it produced no sulfur contamination in comparison with MSA in spite of its lower hydrolysis efficiency. Please note that the main objective of this work was to assess the isotope composition of sulfur containing compounds in the yeast and not its total concentration.

Cells of the ^{34}S -labelled yeast were collected by centrifugation and rinsed twice with ultra-pure water to remove the inorganic sulfur. Then, the cells were suspended in ultrapure water and were broken by hard vortex (5 times × 1 min.) in the presence of glass beads. Of paramount importance was the clean-up procedure of the glass beads used. The common biochemical procedure is to clean these glass beads with sulfuric acid and wash

Table 4 Total sulfur concentration and isotopic composition of the ^{34}S -enriched samples determined by HPLC-ICP-MS

$n = 3$	Concentration ($\mu\text{g S per g dry weight of yeast}$)	Isotope composition (%)		
		^{32}S	^{33}S	^{34}S
Total yeast ^{a,b}	670 \pm 15	9.5 \pm 0.6	0.43 \pm 0.02	90.0 \pm 0.7
Protein extract	151 \pm 4	9.1 \pm 0.2	0.43 \pm 0.03	90.5 \pm 0.5
Solid residue	430 \pm 9	7.9 \pm 0.3	0.42 \pm 0.01	91.7 \pm 0.6

^a Previously found concentration was 677 \pm 10 $\mu\text{g S per g dry weight of yeast}$.³⁹ ^b Previously measured isotope composition was 6.73%, 0.45% and 92.82% for ^{32}S , ^{33}S and ^{34}S respectively.³⁹

afterwards with milli-Q water until neutral pH. Using this procedure high amounts of sulfur in the blanks (up to 200 ng g^{-1} per sample) were found. It was necessary to include 3 consecutive washing steps with hydrochloric acid to completely remove the remaining sulfur attached to the glass beads. After cell rupture, centrifugation was performed at 14000 rpm for 10 min at 4 $^{\circ}\text{C}$. The supernatant, containing the protein extract, was transferred to a fresh tube. The solid residue was also collected for subsequent protein hydrolysis.

The isotope composition and total sulfur concentration of the original yeast and both the protein extract and the solid residue were determined after total microwave digestion of the sample using nitric acid. The results obtained are shown in Table 4 and were in good agreement with those previously reported using bulk mode.³⁹ We have to take into account that current measurements were performed by HPLC-ICP-MS and sulfur was detected as sulfate eluting close to the dead volume. When comparing the total concentrations of sulfur obtained in the protein extract and the solid residue we can observe that most of the sulfur remained in the residue and only *ca.* 25–30% was found in the protein extract with a total recovery of about 85% between protein extract and solid residue.

The isotope enrichment for ^{34}S measured now by HPLC-ICP-MS was a little lower than that reported previously and this fact could be due to natural abundance sulfate contamination of the samples. The sulfur isotope composition of both the protein extract and the solid residue was very similar to that obtained for total sulfur.

3.4.1. Application of post-column Isotope Pattern Deconvolution (IPD). The protein extract and the hydrolysis products for both the protein extract and the solid residue were subjected to post-column IPD for the identification and tentative quantification of sulfur-containing compounds. Gradient elution conditions were used in all cases to elute all possible sulfur containing compounds from the chromatographic column. Chromatograms of 60 min were obtained but only the first 15 min of each chromatogram are shown. The steps followed for the determination of sulfur-containing biomolecules in the protein extract are shown in Fig. 4. Please note that the signal at mass 33 (post-column spike) in Fig. 4A is unstable during the first minutes of the chromatogram even when the gradient has not started. We think that this behaviour is due to the elution in the dead volume of matrix components from the sample (such as inorganic salts). The intensity chromatogram (Fig. 4A) is

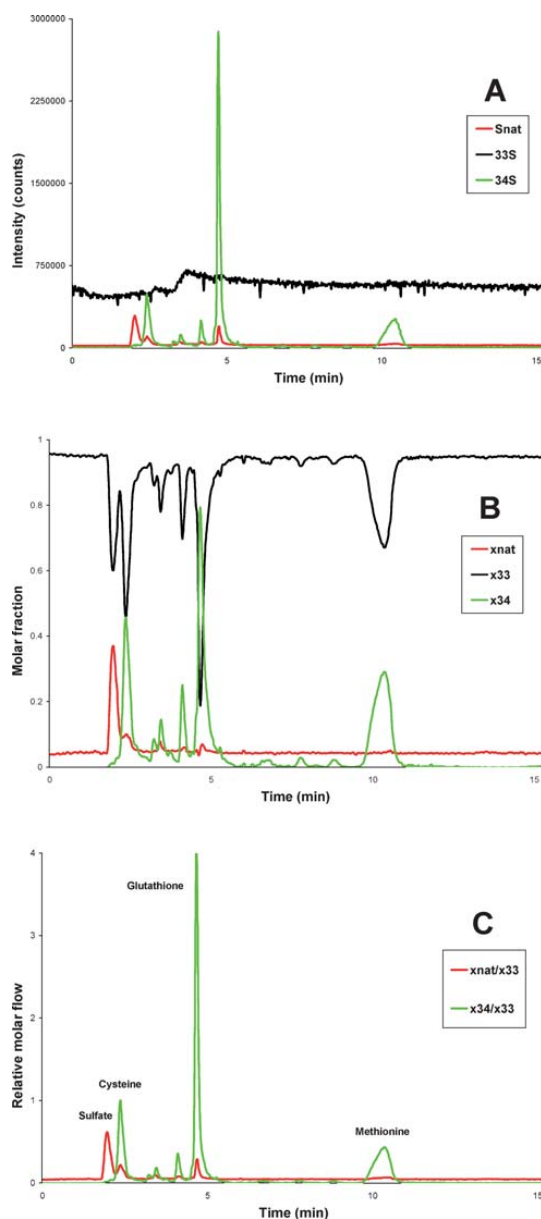


Fig. 4 Steps in the post-column IPD procedure for the direct injection of the protein extract. A) Intensities at the different masses detected, B) Molar fraction chromatogram and C) Pattern specific relative molar flow chromatograms for natural sulfur (red) and ^{34}S -sulfur (green). Only the first 15 min of a 60 min chromatogram are shown. Unknown late eluting peaks of low intensity were detected.

transformed into a molar fraction chromatogram (Fig. 4B) using eqn ([5]). The black, green and red lines correspond to the molar fractions of ^{33}S , ^{34}S and ^{nat}S respectively. The pattern specific relative molar flow chromatograms are shown in Fig. 4C where the identity of the known peaks is indicated. This chromatogram

Table 5 Natural sulfur and ^{34}S tracer concentration found by IPD in the different fractions of the ^{34}S -enriched yeast (as $\mu\text{g g}^{-1}\text{ S}$ per gram of ^{34}S -labelled yeast)

Sample	Sulfate		Cysteine		Glutathione		Methionine		Unidentified peaks	
	$^{\text{nat}}\text{S}$	^{34}S	$^{\text{nat}}\text{S}$	^{34}S	$^{\text{nat}}\text{S}$	^{34}S	$^{\text{nat}}\text{S}$	^{34}S	$^{\text{nat}}\text{S}$	^{34}S
Protein extract	0.25	0.04	0.02	0.5	0.04	0.9	— ^a	0.7	0.24	3.96
Protein extract hydrolysate	5.4	5.2	—	1.0	1.1	18.4	—	2.8	—	15.9
Solid residue hydrolysate	17.9	8.0	—	0.7	1.1	26.1	—	4.5	—	19.4

^a Not detected.

is obtained by dividing the molar fractions obtained for $^{\text{nat}}\text{S}$ and ^{34}S by those of ^{33}S . As the molar flow of ^{33}S is known, the absolute amount of sulfur in each chromatographic peak can be calculated by direct integration of the molar flow chromatographic peaks. For every compound detected, sulfate, cysteine, glutathione, methionine or unknown peaks, the amount of sulfur corresponding to each isotope pattern can be calculated.

The quantitative results obtained for the protein extract, the protein extract hydrolysate and the solid residue hydrolysate are presented in Table 5 both for the four studied sulfur species and for the unidentified peaks. The identification of the four sulfur species studied was performed by matching retention times with that of the corresponding natural abundance sulfur standard. The data were then referred to the original ^{34}S -labelled yeast and expressed as $\mu\text{g S}$ per gram of dry weight of yeast. As can be seen from the comparison of Tables 4 and 5, the total recovery of sulfur from the sample is low. On the one hand, the hydrolysis procedure is far from quantitative and, on the other hand, high molecular weight peptides and proteins present in the samples may not elute from the chromatographic column under the elution conditions used. However, the results shown demonstrate that most of the sulfur is present in yeast in organic form and with isotope enrichment for ^{34}S higher than 90%. This fact is relevant for the future use of this ^{34}S -labelled yeast material as tracer in laboratory animals for kinetic protein metabolism studies.

4. Conclusions

We have compared three different analytical strategies for the determination of sulfur-containing biomolecules by HPLC-ICP-MS. CIC was demonstrated for isocratic elution allowing the use of sulfate standards for the study and optimisation of protein hydrolysis conditions. When gradient elution was performed post-column IDA was required for accurate quantification of sulfur containing compounds as demonstrated for methionine. Finally, a procedure based on post-column IPD was developed for the separation of the isotope signatures of natural abundance and ^{34}S -enriched sulfur. This procedure allows the quantification of both isotope patterns using ^{33}S as post-column spike. These methodologies will be used in future tracer work for the *in vivo* synthesis of labelled proteins. The ^{34}S -enriched cysteine and methionine from the yeast diet will be *in vivo* incorporated into proteins thus leading to an altered ^{34}S abundance. The combination of this "metabolic labelling" procedure, using ^{34}S , with the

post-column IPD approach, using ^{33}S , will be the base of a quantitative platform for sulfur metabolism studies.

5. Acknowledgements

The work described in this paper was supported by the Ministry of Science and Innovation, Madrid, Spain (project CTQ2006-05722). Justo Giner Martínez-Sierra acknowledges his doctoral grant (BP07-059) from the Education and Science Council of the Principado de Asturias.

References

- 1 D. Beauchemin, Inductively Coupled Plasma Mass Spectrometry, *Anal. Chem.*, 2008, **80**, 4455–4486.
- 2 A. Sanz-Medel, Heteroatom(isotope)-tagged proteomics via ICP-MS: screening and quantification of proteins and their post-translational modifications, *Anal. Bioanal. Chem.*, 2008, **391**, 885–894.
- 3 N. Jakubowski, N. Mihalopoulos, S. Mann and W. D. Lehmann, "Speciation of Sulfur" in *Handbook of Elemental Speciation II: Species in the Environment, Food, Medicine and Occupational Health*, ed. R. Cornelis, J. Caruso, H. Crews and K. G. Heumann, John Wiley and Sons Ltd, England, 2005, pp. 378–407.
- 4 M. Wind, A. Wegener, A. Eisenmenger, R. Kellner and W. D. Lehmann, Sulfur as the key element for quantitative protein analysis by capillary liquid chromatography coupled to element mass spectrometry, *Angew. Chem., Int. Ed.*, 2003, **42**, 3425–3427.
- 5 A. Prange and D. Pröfrock, Chemical labels and natural element tags for the quantitative analysis of bio-molecules, *J. Anal. At. Spectrom.*, 2008, **23**, 432–459.
- 6 C. Rappel and D. Schaumlöffel, The role of sulfur and sulfur isotope dilution analysis in quantitative protein analysis, *Anal. Bioanal. Chem.*, 2008, **390**, 605–615.
- 7 B. Divjak and W. Goessler, Ion chromatographic separation of sulfur containing inorganic anions with an ICP-MS as element-specific detector, *J. Chromatogr., A*, 1999, **844**, 161–169.
- 8 D. Pröfrock, P. Leonhard and A. Prange, Determination of sulfur and selected trace elements in metallothionein-like proteins using capillary electrophoresis hyphenated to inductively coupled plasma mass spectrometry with an octopole reaction cell, *Anal. Bioanal. Chem.*, 2003, **377**, 132–139.
- 9 D. Schaumlöffel, P. Giusti, H. Preud'Homme, J. Szpunar and R. Lobinski, Precolumn isotope dilution analysis in nanoHPLC-ICP-MS for absolute quantification of sulfur-containing peptides, *Anal. Chem.*, 2007, **79**, 2859–2868.
- 10 D. R. Bandura, V. I. Baranov and S. D. Tanner, Detection of ultratrace phosphorus and sulfur by quadrupole ICPMS with dynamic reaction cell, *Anal. Chem.*, 2002, **74**, 1497–1502.
- 11 C.-F. Yeh, S.-J. Jiang and T.-S. Hsi, Determination of sulfur-containing amino acids by capillary electrophoresis dynamic reaction cell inductively coupled plasma mass spectrometry, *Anal. Chim. Acta*, 2004, **502**, 57–63.
- 12 S. Hann, G. Koellensperger, C. Obinger, P. G. Furtmüller and G. Stingeder, SEC-ICP-DRC and SEC-ICP-SFMS for determination of metal-sulfur ratios in metalloproteins, *J. Anal. At. Spectrom.*, 2004, **19**, 74–79.

- 13 S. Stürup, L. Bendahl and B. Gammelgaard, Optimization of LC-DRC-ICP-MS for the speciation of selenotrisulfides with simultaneous detection of sulfur and selenium as oxides combined with determination of elemental and isotope ratios, *J. Anal. At. Spectrom.*, 2006, **21**, 201–203.
- 14 S. Hann, C. Obinger, G. Stingeder, M. Paumann, P. G. Furtmüller and G. Koellensperger, Studying metal integration in native and recombinant copper proteins by hyphenated ICP-DRC-MS and ESI-TOF-MS capabilities and limitations of the complementary techniques, *J. Anal. At. Spectrom.*, 2006, **21**, 1224–1231.
- 15 T. Prohaska, C. Latkoczy and G. Stingeder, Precise sulfur isotope ratio measurements in trace concentration of sulfur by inductively coupled plasma double focusing sector field mass spectrometry, *J. Anal. At. Spectrom.*, 1999, **14**, 1501–1504.
- 16 A. Makishima and E. Nakamura, Determination of total sulfur at microgram per gram levels in geological materials by oxidation of sulfur into sulfate with in situ generation of bromine using isotope dilution high-resolution ICPMS, *Anal. Chem.*, 2001, **73**, 2547–2553.
- 17 P. Evans, C. Wolff-Briche and B. Fairman, High accuracy analysis of low level sulfur in diesel by isotope dilution high resolution ICP-MS, using silicon for mass bias correction of natural isotope ratios, *J. Anal. At. Spectrom.*, 2001, **16**, 964–969.
- 18 S. F. Boulyga, J. Heilmann and K. G. Heumann, Isotope dilution ICP-MS with laser-assisted sample introduction for direct determination of sulfur in petroleum products, *Anal. Bioanal. Chem.*, 2005, **382**, 1808–1814.
- 19 R. Clough, P. Evans, T. Catterick and E. H. Evans, $\delta^{34}\text{S}$ measurements of sulfur by multicollector inductively coupled plasma mass spectrometry, *Anal. Chem.*, 2006, **78**, 6126–6132.
- 20 C. Bendall, Y. Lahaye, J. Fiebig, S. Weyer and G. P. Brey, In situ sulfur isotope analysis by laser ablation MC-ICPMS, *Appl. Geochem.*, 2006, **21**, 782–787.
- 21 P. R. D. Mason, J. Kosler, J. C. M. de Hoog, P. J. Sylvester and S. Meffan-Main, In situ determination of sulfur isotopes in sulfur-rich materials by laser ablation multiple-collector inductively coupled plasma mass spectrometry (LA-MC-ICP-MS), *J. Anal. At. Spectrom.*, 2006, **21**, 177–186.
- 22 P. R. Craddock, O. J. Rouxel, L. A. Ball and W. Bach, Sulfur isotope measurement of sulfate and sulfide by high-resolution MC-ICP-MS, *Chem. Geol.*, 2008, **253**, 102–113.
- 23 R. Santamaria-Fernandez, R. Hearn and J.-C. Wolff, Detection of counterfeit tablets of an antiviral drug using $\delta^{34}\text{S}$ measurements by MC-ICP-MS and confirmation by LA-MC-ICP-MS and HPLC-MC-ICP-MS, *J. Anal. At. Spectrom.*, 2008, **23**, 1294–1299.
- 24 R. Santamaria-Fernandez and R. Hearn, Systematic comparison of $\delta^{34}\text{S}$ measurements by multicollector inductively coupled plasma mass spectrometry and evaluation of full uncertainty budget using two different metrological approaches, *Rapid Commun. Mass Spectrom.*, 2008, **22**, 401–408.
- 25 R. Santamaria-Fernandez, J. Giner Martínez-Sierra, J. M. Marchante Gayón, J. I. García Alonso and R. Hearn, Measurement of longitudinal sulfur isotopic variations by laser ablation MC-ICP-MS in single human hair strands, *Anal. Bioanal. Chem.*, 2009, **394**, 225–233.
- 26 E. Svantesson, J. Pettersson and K. E. Markides, The use of inorganic elemental standards in the quantification of proteins and biomolecular compounds by inductively coupled plasma spectrometry, *J. Anal. At. Spectrom.*, 2002, **17**, 491–496.
- 27 A. Pereira Navaza, J. Ruiz Encinar and A. Sanz-Medel, Absolute and accurate quantification of protein phosphorylation by using an elemental phosphorus standard and element mass spectrometry, *Angew. Chem., Int. Ed.*, 2007, **46**, 569–571.
- 28 L. Hinojosa Reyes, J. M. Marchante Gayón, J. I. García Alonso and A. Sanz Medel, Application of isotope dilution analysis for the evaluation of extraction conditions in the determination of total selenium and selenomethionine in yeast-based nutritional supplements, *J. Agric. Food Chem.*, 2006, **54**, 1557–1563.
- 29 W.-J. Quian, J. M. Jacobs, T. Liu, D. G. Camp II and R. D. Smith, Advances and Challenges in Liquid Chromatography-Mass Spectrometry-based Proteomics Profiling for Clinical Applications, *Mol. Cell. Proteomics*, 2006, **5**, 1727–1744.
- 30 C. S. Muñiz, J. M. M. Gayón, J. I. G. Alonso and A. Sanz-Medel, Speciation of essential elements in human serum using anion-exchange chromatography coupled to post-column isotope dilution analysis with double focusing ICP-MS, *J. Anal. At. Spectrom.*, 2001, **16**, 587.
- 31 L. H. Reyes, J. M. M. Gayón, J. I. G. Alonso and A. Sanz-Medel, Quantitative speciation of selenium in human serum by affinity chromatography coupled to post-column isotope dilution analysis ICP-MS, *J. Anal. At. Spectrom.*, 2003, **18**, 1210.
- 32 A. Prange, D. Schaumlöffel, P. Brätter, A.-N. Richarz and C. Wolf, Species analysis of metallothionein isoforms in human brain cytosols by use of capillary electrophoresis hyphenated to inductively coupled plasma-sector field mass spectrometry, *Fresenius J. Anal. Chem.*, 2001, **371**, 764–774.
- 33 N. Zinn, R. Krüger, P. Leonhard and J. Bettmer, μLC coupled to ICP-SFMS with post-column isotope dilution analysis of sulfur for absolute protein quantification, *Anal. Bioanal. Chem.*, 2008, **391**, 537–543.
- 34 J. Heilmann and K. G. Heumann, Development of a species-unspecific isotope dilution GC-ICPMS method for possible routine quantification of sulfur species in petroleum products, *Anal. Chem.*, 2008, **80**, 1952–1961.
- 35 M. Wang, W. Feng, W. Lu, B. Li, B. Wang, M. Zhu, Y. Wang, H. Yuan, Y. Zhao and Z. Chai, Quantitative analysis of proteins via sulfur determination by HPLC coupled to isotope dilution ICPMS with a hexapole collision cell, *Anal. Chem.*, 2007, **79**, 9128.
- 36 P. Rodríguez-González, J. M. Marchante-Gayón, J. I. García Alonso and A. Sanz-Medel, Isotope dilution analysis for elemental speciation: A tutorial review, *Spectrochim. Acta, Part B*, 2005, **60**, 151–207.
- 37 J. A. Rodríguez-Castrillón, M. Moldovan, J. I. García Alonso, J. J. Lucena, M. L. García-Tomé and L. Hernández-Apaolaza, Isotope pattern deconvolution as a tool to study iron metabolism in plants, *Anal. Bioanal. Chem.*, 2008, **390**, 579–590.
- 38 H. González Iglesias, M. L. Fernández Sanchez, J. A. Rodríguez-Castrillón, J. I. García Alonso, J. López Sastre and A. Sanz-Medel, Enriched stable isotopes and isotope pattern deconvolution for quantitative speciation of endogenous and exogenous selenium in rat urine by HPLC-ICP-MS, *J. Anal. At. Spectrom.*, 2009, **24**, 460–468.
- 39 J. Giner Martínez-Sierra, F. Moreno Sanz, P. Herrero Espílez, J. M. Marchante Gayón and J. I. García Alonso, Biosynthesis of sulfur-34 labelled yeast and its characterisation by multicollector-ICP-MS, *J. Anal. At. Spectrom.*, 2007, **22**, 1105–1112.
- 40 L. Yang, R. E. Sturgeon, S. McSheehy and Z. Mester, Comparison of extraction methods for quantitation of methionine and selenomethionine in yeast by species specific isotope dilution gas chromatography-mass spectrometry, *J. Chromatogr., A*, 2004, **1055**, 177–184.
- 41 K. Wrobel, S. S. Kannamkumarath, K. Wrobel and J. A. Caruso, Hydrolysis of proteins with methanesulfonic acid for improved HPLC-ICP-MS determination of seleno-methionine in yeast and nuts, *Anal Bioanal Chem*, 2003, **375**, 133–138.

D.2.2.2. Información suplementaria del artículo científico IV

Supplementary Material (ESI) for Journal of Analytical Atomic Spectrometry
This journal is © The Royal Society of Chemistry 2010

Demonstration of Compound Independent Calibration for four sulfur-containing compounds (sulfate, cysteine, glutathione and methionine) in isocratic HPLC-ICP-MS. Four different ICP-MS instruments were evaluated.

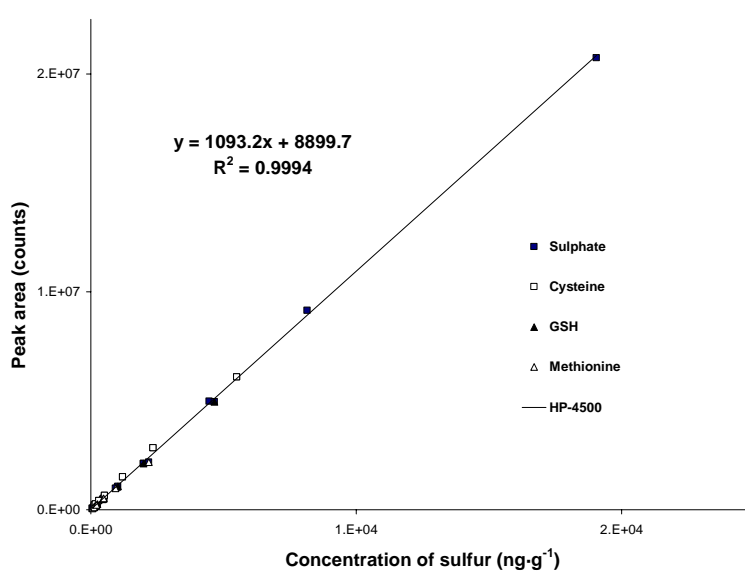


Figure 1. Demonstration of Compound Independent Calibration (CIC) for sulfur in HPLC-ICP-MS using the HP-4500 quadrupole instrument operated under Cool Plasma conditions at $m/z=48$ (SO^+).

Supplementary Material (ESI) for Journal of Analytical Atomic Spectrometry
This journal is © The Royal Society of Chemistry 2010

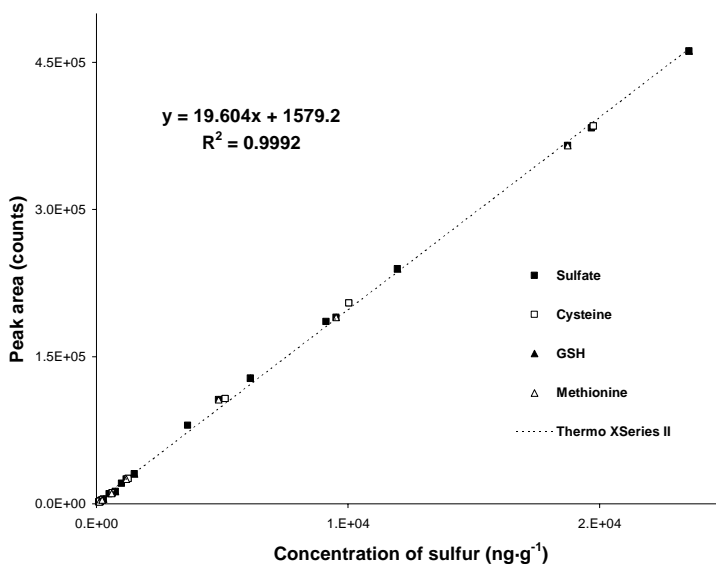


Figure 2. Demonstration of Compound Independent Calibration (CIC) for sulfur in HPLC-ICP-MS using the Thermo XSeries II quadrupole instrument with O₂ as reactive gas in the collision cell at m/z=48 (SO⁺).

Supplementary Material (ESI) for Journal of Analytical Atomic Spectrometry
This journal is © The Royal Society of Chemistry 2010

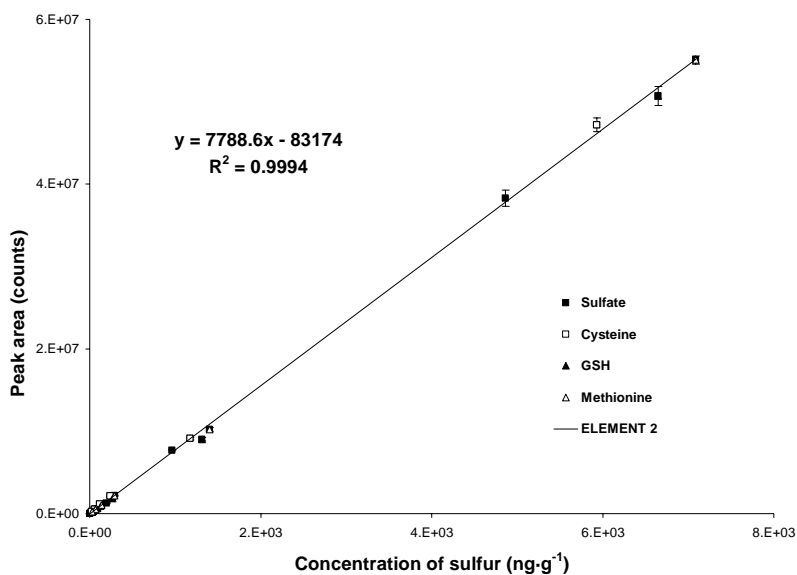


Figure 3. Demonstration of Compound Independent Calibration (CIC) for sulfur in HPLC-ICP-MS using the Element 2 double focusing instrument at $m/z=32$ and medium resolution mode ($R=4000$). Error bars represent the standard uncertainty of three replicates.

Supplementary Material (ESI) for Journal of Analytical Atomic Spectrometry
This journal is © The Royal Society of Chemistry 2010

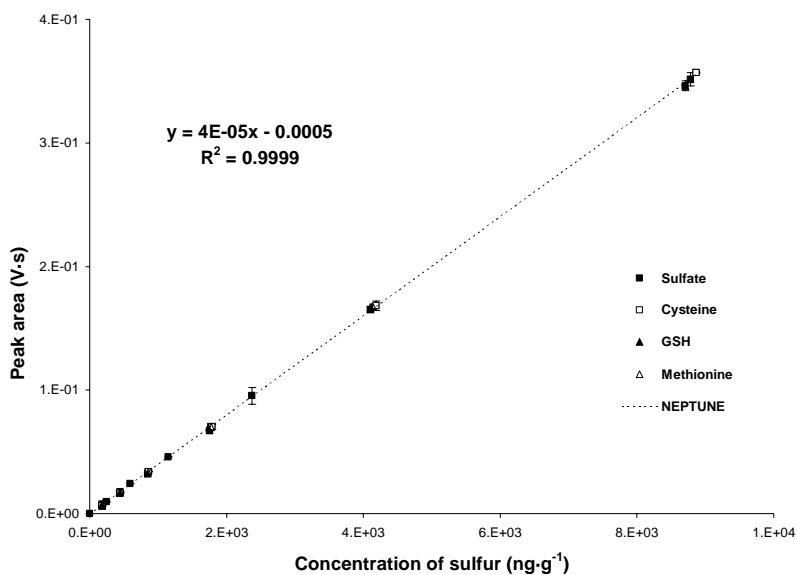
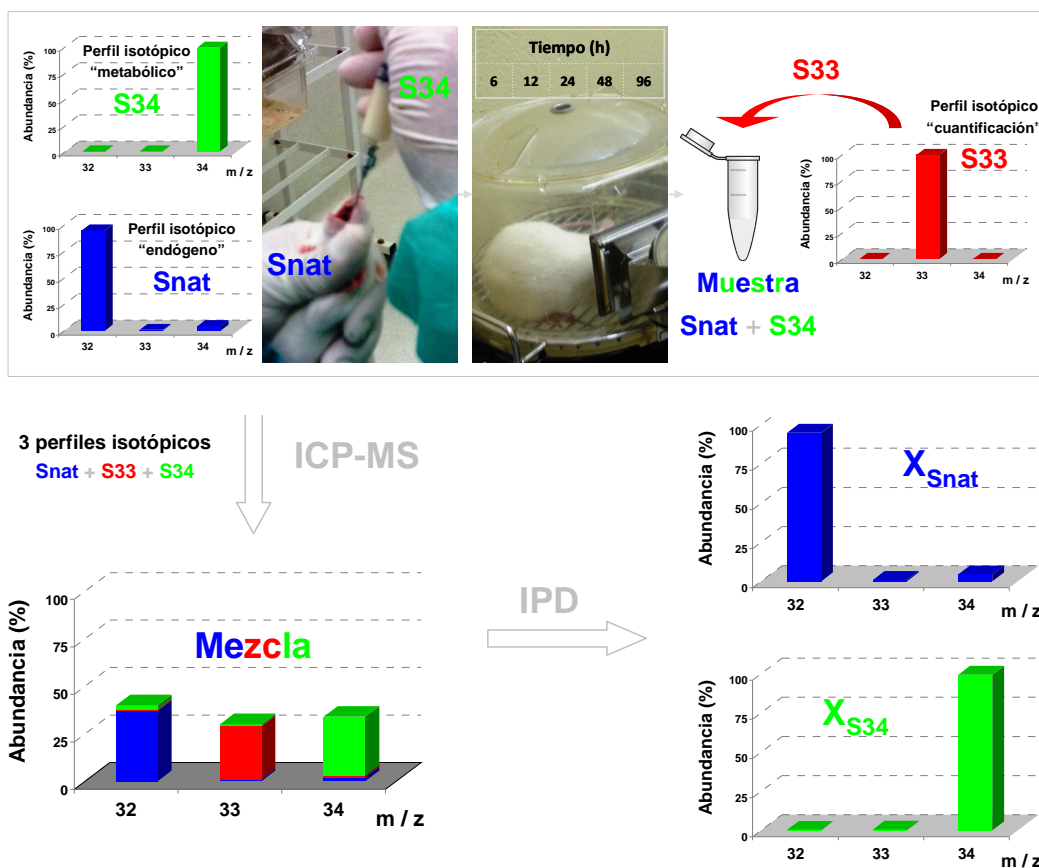


Figure 4. Demonstration of Compound Independent Calibration (CIC) for sulfur in HPLC-ICP-MS using the Neptune multicollector instrument at $m/z=32$ and pseudo high resolution mode. Error bars represent the standard uncertainty of three replicates.

D.3. ESTUDIOS *IN VITRO* E *IN VIVO* DEL METABOLISMO DEL AZUFRE UTILIZANDO ISÓTOPOS ESTABLES ENRIQUECIDOS

D.3.1. Estudios con trazadores estables de azufre en animales de laboratorio utilizando levadura marcada con azufre-34

D.3.1.1. *Artículo científico V. Anal. Bioanal. Chem., DOI 10.1007/s00216-012-6420-x*



Sulphur tracer experiments in laboratory animals using ^{34}S -labelled yeast

J. Giner Martínez-Sierra · F. Moreno Sanz ·
P. Herrero Espílez · J. M. Marchante Gayón ·
J. Rodríguez Fernández · J. I. García Alonso

Received: 10 July 2012 / Revised: 7 September 2012 / Accepted: 12 September 2012
© Springer-Verlag Berlin Heidelberg 2012

Abstract We have evaluated the use of ^{34}S -labelled yeast to perform sulphur metabolic tracer experiments in laboratory animals. The proof of principle work included the selection of the culture conditions for the preparation of sulphur labelled yeast, the study of the suitability of this labelled yeast as sulphur source for tracer studies using in vitro gastrointestinal digestion and the administration of the ^{34}S -labelled yeast to laboratory animals to follow the fate and distribution of ^{34}S in the organism. For in vitro gastrointestinal digestion, the combination of sodium dodecyl sulphate-polyacrylamide gel electrophoresis and high-performance liquid chromatography and inductively coupled plasma mass spectrometry (HPLC-ICP-MS) showed that labelled methionine, cysteine and other low molecular weight sulphur-containing biomolecules were the major

components in the digested extracts of the labelled yeast. Next, in vivo kinetic experiments were performed in healthy Wistar rats after the oral administration of ^{34}S -labelled yeast. The isotopic composition of total sulphur in tissues, urine and faeces was measured by double-focusing inductively coupled plasma mass spectrometry after microwave digestion. It was observed that measurable isotopic enrichments were detected in all samples. Finally, initial investigations on sulphur isotopic composition of serum and urine samples by HPLC-ICP-MS have been carried out. For serum samples, no conclusive data were obtained. Interestingly, chromatographic analysis of urine samples showed differential isotope enrichment for several sulphur-containing biomolecules.

Keywords Sulphur metabolism · Metabolic tracer · Sulphur-labelled yeast · HPLC-ICP-MS · Urine

Published in the topical collection *Isotope Ratio Measurements: New Developments and Applications* with guest editors Klaus G. Heumann and Torsten C. Schmidt.

Electronic supplementary material The online version of this article (doi:10.1007/s00216-012-6420-x) contains supplementary material, which is available to authorized users.

J. G. Martínez-Sierra · J. M. M. Gayón · J. I. G. Alonso (✉)
Department of Physical and Analytical Chemistry,
University of Oviedo,
Julian Clavería 8,
33006 Oviedo, Spain
e-mail: jiga@uniovi.es

F. M. Sanz · P. H. Espílez
Department of Biochemistry and Molecular Biology,
University of Oviedo,
Edificio Santiago Gascón, Campus de "El Cristo",
33006 Oviedo, Spain

J. R. Fernández
Innovative Solutions in Chemistry, Edificio
Científico-Tecnológico, Campus de "El Cristo",
33006 Oviedo, Spain

Introduction

The determination of proteins and peptides contained in blood serum and urine by mass spectrometry (MS) is of paramount interest as a diagnostic medium for the detection, identification and quantification of protein and peptide biomarkers associated with both health and disease [1–3]. On the one hand, serum is easily obtained and can be repetitively sampled [4]. Moreover, it has a high protein content (i.e. 60–80 mg mL⁻¹), with many of these proteins being secreted and shed from cells and tissues and hence potentially carrying an archive of important histological information whose determination could serve to improve early disease detection. For example, increased serum levels of prostate specific antigen and carbohydrate antigen 125 are routinely used for the detection of cancer in the prostate and ovary, respectively [5]. On the other hand, urine is a

promising biological fluid for the discovery of novel biomarkers [6, 7]. Urine samples are ideal bio-samples as urine is an easily accessible, non-invasive body fluid that carries proteins, peptides and amino acids related to renal systems that have not been found in plasma, and besides, being an ultrafiltrate of plasma, a remarkable amount of blood-derived proteins is also found in this biological fluid. For example, there are several reports on the use of urine analysis for the establishment of new diagnostic biomarkers for both kidney [8, 9] and non-renal diseases [10, 11].

The detection of sulphur by inductively coupled plasma mass spectrometry (ICP-MS) can be considered one of the most versatile and sensitive complementary tools in quantitative proteomics [12–14]. For the determination of proteins, sulphur is preferable to other elements bound to proteins because of its high abundance in proteins and stability in covalent form. Additionally, sulphur stable isotopes may find particular applications in protein turnover studies as the isotopic composition of this element can be simply measured during a chromatographic separation. However, tracer experiments on protein synthesis and breakdown using sulphur-enriched stable isotopes in mammals have not been described. These studies require the previous synthesis of methionine and/or cysteine labelled with the enriched isotope as it is well known that mammals cannot synthesise those amino acids and need to obtain them from their food. In contrast, other biota can reduce sulphate and synthesise organo-sulphur compounds [15]. In particular, prokaryotic microorganisms (e.g. *Escherichia coli*) as well as eukaryotic microorganisms (e.g. yeasts) are advantageous choices because of high growth rates [16]. The yeast *Saccharomyces cerevisiae* seems to be an ideal substance for using the biomass produced as a source of protein for animal or human food in metabolic tracer experiments [17]. This choice is undoubtedly influenced by its classification as generally regarded as safe by the US Food and Drug Administration. *S. cerevisiae* is a rich source of valuable protein, vitamin B complex, numerous minerals and enzymes, as well as immunomodulators; with a highly importance in traditional biotechnology such as baking, brewing and wine making [18]. Thus, it is harmless; it can be administered orally to the test subjects and sulphur-containing proteins, peptides and amino acids can be readily hydrolysed and absorbed in the gastrointestinal tract.

The work presented here with regards to the proof of principle study of the capabilities of ^{34}S -labelled yeast for sulphur tracer experiments reports on method development and is focused on: (1) the preparation of sulphur-labelled yeast; (2) the study of the suitability of the labelled yeast as sulphur source for tracer studies by an in vitro gastrointestinal digestion using the complementary information provided by sodium dodecyl sulphate-polyacrylamide gel electrophoresis (SDS-PAGE) and high-performance liquid

chromatography and inductively coupled plasma mass spectrometry (HPLC-ICP-MS) techniques; and (3) the determination of the kinetics of the induced sulphur isotopic variations by single collector ICP-MS in tissues, urine and faeces of healthy Wistar rats after ^{34}S -labelled yeast ingestion and initial investigations for the in vivo study on sulphur isotopic composition of serum and urine samples by HPLC-ICP-MS.

Experimental

Instrumentation

Sulphur-specific detection was performed using a Double-Focusing ICP-MS Element 2 (Thermo Fisher Scientific, Inc., Waltham, MA) working at medium resolution ($R=4,000$) in order to avoid the spectral interferences on sulphur determination. Isotopes measured and main operating parameters used for ICP-MS are summarised in Table S1 in the Electronic supplementary material (ESM).

Chromatographic separations were carried out using a dual-piston liquid chromatographic pump (Shimadzu LC-10AD, Shimadzu Corp., Kyoto, Japan) equipped with a Rheodyne PEEK manual sample injector, model 7125 (Cotati, CA), fitted with a PEEK injection loop. HPLC conditions for the different samples analysed (digested yeast, serum and urine) are reported in Tables S2, S3 and S4 respectively in the ESM. A peristaltic pump Minipuls 2 (Scharlab, Barcelona, Spain) and a T-piece were used to continuously mix the eluent from the chromatographic column with the ^{33}S isotope enriched solution.

A focused microwave system Discovery (CEM, Matthews, NC) with an autosampler Explorer (CEM) was used to perform the microwave acid digestion of the labelled samples. The microwave oven programme used applied a power of 250 W for 5 min, reaching a final temperature of 170 °C.

Reagents and materials

Ultrapure water was obtained from a Milli-Q system (Millipore Co., Bedford, MA) and was used throughout all the experiments. A certified standard solution of $1,000\text{ mgL}^{-1}$ of natural abundance sulphur (as sulphuric acid in water) was purchased from Merck (Darmstadt, Germany). Enriched ^{33}S and ^{34}S were supplied from Cambridge Isotope Laboratories (Andover, MA). Yeast cells were grown using high purity nutrients obtained from Sigma-Aldrich Co. (St. Louis, MO). Pepsin (from porcine stomach mucosa), pancreatine (from porcine pancreas), α -amylase (heat stable) and bile salts (approximately 50 % sodium cholate and 50 % sodium deoxycholate) were purchased from

Sigma-Aldrich and used for the preparation of the simulated gastric and intestinal juices in order to carry out the enzymatic digestion of the ^{34}S -labelled yeast. Hydrogen peroxide and nitric acid (additionally purified by sub-boiling distillation) from Merck were used for microwave acid digestion. The mobile phase for size exclusion chromatography (SEC) was prepared by dissolving Tris (hydroxymethane) aminomethane buffer (Merck) and sodium chloride ($\geq 99.5\%$) from Sigma-Aldrich. Hydrochloric acid (Merck) sub-boiling distilled was employed for pH adjustment. For reversed-phase chromatography, HPLC-grade methanol from Merck was used and mobile phases were degassed with He before use. Additionally for urine samples, ammonium acetate from Sigma-Aldrich was used. The standards of DL-methionine ($>99\%$ purity), DL-cysteine ($>95\%$ purity) and L-glutathione reduced ($>97\%$ purity) were purchased from Fluka (Buchs, Switzerland). Centricon (up to 0.5 mL of sample volume) centrifugal filter devices with nominal molecular weight limit (NMWL) of 10 kDa were purchased from Millipore.

Procedures

Preparation of ^{34}S -labelled yeast

High-purity nutrients were employed for the preparation of a synthetic complete culture medium low in natural abundance sulphur. The contents of this culture medium were indicated in reference [19] but supplemented with uracil (75 mg L^{-1}) and adenine (18 mg L^{-1}). The amino acid composition was also enhanced to a final concentration of 75 mg L^{-1} and supplemented with aspartic and glutamic acid, phenylalanine, proline and serine. The yeast growth was followed by measuring the optical density spectrophotometrically at 600 nm (OD_{600}). The culture was grown in the presence of $100\ \mu\text{M}$ of ^{34}S as $(\text{NH}_4)_2\text{SO}_4$ at $28\ ^\circ\text{C}$ in a rotary shaker at 200 rpm for about 24 h until the culture reached an $\text{OD}_{600}\approx 3$. Afterwards, cells were removed by centrifugation at 5,000 rpm, $4\ ^\circ\text{C}$ for 10 min. The pellet was rinsed twice with ultrapure water to remove excess inorganic sulphur and stored at $-80\ ^\circ\text{C}$ until their microwave acid digestion. The final product was characterised with reference to isotope enrichment by SF-ICP-MS.

In vitro gastrointestinal digestion

The simulated gastric fluid was prepared as described previously [20] by dissolving 0.15 g of pepsin in 15 mL of 150 mM sodium chloride and adjusting to pH 2 with 2 M hydrochloric acid. Next, 0.1 g of the labelled yeast was weighed into a 7-mL amber glass vial with screw cap (Supelco, Bellefonte, PA). Then 2 mL of the simulated gastric juice was added and the capped vial was placed in

a thermostatic bath at $37\ ^\circ\text{C}$ under mechanical shaking for 4 h. Finally, after the neutralisation of the resulting slurry with NaOH to pH 4–5, the hydrolysate was centrifuged at 5,000 rpm for 10 min and the supernatant stored at $-18\ ^\circ\text{C}$ until use. The simulated intestinal fluid was prepared by mixing equal amounts of a 1 % solution of bile salts in NaCl 150 mM and a solution of 3 % pancreatine plus 1 % α -amylase in NaCl 150 mM. A volume of 2 mL of the resulting simulated intestinal fluid was added to the resulting neutralised slurry obtained after the gastric digestion. Then the pH was adjusted to 7.4 by adding NaOH and the vial was placed in a thermostatic bath at $37\ ^\circ\text{C}$ under mechanical shaking for 4 h. Finally, the hydrolysate was centrifuged at 5,000 rpm for 10 min and the supernatant stored at $-18\ ^\circ\text{C}$ until use.

Sodium dodecyl sulphate-polyacrylamide gel electrophoresis

SDS-PAGE experiments were performed on a discontinuous buffered system according to the method of Laemmli [21] using 12 % separating gel and 4 % stacking gel. The samples were directly mixed with 4-fold volume of 0.0125 M Tris-HCl buffer containing 1 % (w/v) SDS, 2 % (v/v) 2-mercaptoethanol, 5 % (v/v) glycerol and 0.025 % (w/v) bromophenol blue and then heated for 5 min in boiling water before electrophoresis. Every sample (20 μL) was applied to each lane in a Mini-Protean[®] Tetra Cell vertical electrophoresis system from Bio-Rad Laboratories, Inc. during 90 min at 90 V. The gel was stained with 0.25 % Coomassie brilliant blue (R-250) in 50 % methanol and destained in 7 % acetic acid in methanolic solution (50 %, v/v).

Animal experiments

Animal experiments were carried out in the Biotery from the University of Oviedo following the guidelines regarding the protection of animals used for experimental and other scientific purposes (86/609/EEC). Six male Wistar rats weighting 95–105 g were used in this study. Five of them were fed ca. 1.0 g of ^{34}S -labelled yeast (containing 700 μg sulphur/g dry weight) by gavage in a single dose. Then, they were maintained in metabolic cages at $22\ ^\circ\text{C}$ with a light/dark cycle of 12/12 h. Rats were anaesthetised and full blood extracted at 6, 12, 24, 48 and 96 h after administration of the yeast and the tissues were obtained. Likewise, urine and faeces were collected at times 0, 6, 12, 24, 48, 72 and 96 h from the special receptacle under the metabolic cage. Organ tissue samples and faeces were lyophilised in a Heto Lyolab 3000 freeze-drier model from Heto-Holten (Allerød, Denmark). After lyophilisation, dried tissues and faeces were ground and homogenised in an agate mortar.

Finally, tissues, faeces and urine samples were stored at $-80\text{ }^{\circ}\text{C}$ until use.

Sample preparation for total sulphur isotope measurements by ICP-MS

Approximately 50 mg of sample powder was placed into a digestion vessel and 1.5 mL of sub-boiling nitric acid and 0.25 mL of suprapur hydrogen peroxide were added. The vessels were immediately closed after the addition of the reagents. The microwave program described above was applied. At the end of the acid digestion, the resulting solutions were made up to 25 mL with ultrapure water to be finally analysed by ICP-MS. For urine samples, sample preparation consisted on the removal of cell debris and particulates by centrifugation ($3,000\times g\times 5\text{ min}$ at $4\text{ }^{\circ}\text{C}$) and further dilution (1–100) with 1 % (v/v) nitric acid.

Sample preparation for serum chromatographic analysis

The blood sample was collected on polypropylene tubes with no additives and then stored at room temperature for 1-h clotting time. The clotted blood was then centrifuged for 15 min at $2,000\times g$ and $4\text{ }^{\circ}\text{C}$ to obtain serum samples. Rat serum was 5-fold diluted by the addition of ultrapure water containing 20 % acetonitrile to disrupt any potential protein-protein/peptide interactions and applied onto a centrifugal filter device (NMWL, 10 kDa). The sample was centrifuged for 20 min at $3,000\times g$ and $4\text{ }^{\circ}\text{C}$. Subsequently, two serum fractions were obtained. The first one is the concentrated sample (retained species) which is named HMW fraction and the second one is the ultrafiltrate, named LMW fraction. The filtrate was dried on a speed-vac concentrator (Eppendorf concentrator 5301). Finally, samples were stored at $-18\text{ }^{\circ}\text{C}$ until their analysis by HPLC-ICP-MS.

Preparation of urine for chromatographic analysis

Urine samples were centrifuged at $3,000\times g$ for 5 min at $4\text{ }^{\circ}\text{C}$ and cell debris (the sediment of broken cells or tissues) and other solid materials (particulates) in the pellet were discarded. Finally, the clarified urine samples (supernatants) were stored at $-20\text{ }^{\circ}\text{C}$ until their analysis by HPLC-ICP-MS.

Mathematical data treatment: isotope pattern deconvolution

We have applied the isotope pattern deconvolution procedure [22] to extract molar fraction information from the measured isotope composition. The measurement of the intensities for ^{32}S , ^{33}S and ^{34}S by ICP-MS would provide data for the deconvolution of the three isotope patterns of sulphur used: natural abundance sulphur, “Snat”, ^{34}S -enriched sulphur, “S34”, used as “metabolic” tracer and

^{33}S -enriched sulphur, “S33”, used as post-column “quantification” tracer [23]. For the tracer/tracee ratio evaluation in digested tissues the ratio of molar fractions $X_{\text{S}34}/X_{\text{Snat}}$ was calculated.

Results and discussion

Preparation of ^{34}S -labelled yeast

Labelling experiments with sulphur enriched stable isotopes need a culture medium with the lowest concentration of natural abundance sulphur. Thus, in a previous work [19], we have prepared ^{34}S -labelled yeast by growing *S. cerevisiae* in a specially prepared sulphur-free growing medium, using high purity nutrients. The obtained ^{34}S -labelled yeast contained about 93 % of ^{34}S , as total sulphur, and was accomplished in a small-scale experiment (i.e. 50 mL flask). However, the move from small- to large-scale production (i.e. 2,000 mL flask) typically requires further adjustment of culturing conditions during scale-up to large volumes. Under the new experimental conditions described in the procedures, an optimal yeast growth was achieved within 24 h and thus the incubation time for ^{34}S -labelled yeast preparation was substantially shortened [19]. The isotopic abundance (expressed in per cent) and determined by SF-ICP-MS for ^{34}S was found to be 64.5 ± 0.9 . A significant contamination of natural abundance sulphur from Adenine was detected after the growing of the yeast. However, the isotopic enrichment achieved should be enough to perform tracer experiments in mammals. A final total amount of 15.0 g of ^{34}S -labelled yeast (dry weight) was obtained.

In vitro gastrointestinal digestion and SDS-PAGE analysis

As a first approach, to check the protein profile of the labelled yeast before and after the in vitro gastrointestinal digestion, SDS-PAGE analysis of labelled proteins expressed in *S. cerevisiae* was carried out. To do that, 20 μL of supernatant of protein extract (lane 1), hydrolysates of simulated gastric digestion (lane 2) and hydrolysates of simulated intestinal digestion (lane 3), were applied to a 12 % SDS-PAGE and then stained with Coomassie brilliant blue. The results are shown in Fig. S1 in the ESM. As can be observed, the bands present in the protein extract of the yeast disappear for both the hydrolysates of simulated gastric and intestinal digestion, and only the bands corresponding to the enzymes added to simulate the digestion can be seen. These results strongly suggest an adequate digestibility of the proteins of the yeast (breaking down to small peptides and free amino acids) and allow us to postulate its further absorption and incorporation.

Characterisation of sulphur-containing biomolecules in yeast after in vitro gastrointestinal digestion by HPLC-ICP-MS

The suitability of the labelled yeast as sulphur source for metabolic tracer experiments was further evaluated using the analytical methodologies by HPLC-ICP-MS previously reported for the characterisation of the ^{34}S -labelled yeast with regards to their sulphur-containing biomolecules [23]. Taking into account the complementary information provided by SDS-PAGE about the size of the biomolecules present in both the simulated gastric and intestinal digestion hydrolysates, size exclusion and reversed-phase chromatography were selected for the separation of low molecular weight proteins, peptides, aminoacids and other biomolecules expected in those samples. In this way, samples were injected in the HPLC-ICP-MS system under the experimental conditions reported in Tables S1 and S2 in the ESM. Tentative identification of the species was performed by matching retention times with those of the corresponding natural abundance sulphur standards available.

As the sample to be analysed (i.e. digested ^{34}S -labelled yeast) contains non-natural sulphur isotope compositions, traditional post-column isotope dilution analysis equations [24] can no longer be applied. Taking into account that we are using an enzymatic method of hydrolysis, we can expect high levels of natural abundance sulphur contamination due to the hydrolysis of the reagents used for the gastrointestinal digestion, as they contain methionine and cysteine residues. Therefore, it is clear that the simulated gastrointestinal digestion procedure could modify the original isotope composition (i.e. 64.5 % of ^{34}S) of sulphur-containing biomolecules in the labelled yeast extracts. Figure 1 shows the pattern specific chromatograms for S34 and Snat acquired after the gastrointestinal digestion using both chromatographic separation modes. These chromatograms are obtained by dividing the molar fractions found for S34 and Snat by those of S33. As it can be observed, most of the isotopically labelled S34 appears now in the low molecular weight fraction (Fig. 1b). Methionine has apparently more S34 incorporated than cysteine (Fig. 1a) and the isotope enrichment for both compounds is much lower than in the original labelled yeast because of contamination with natural abundance sulphur-containing compounds coming from the reagents used during gastrointestinal digestion. Anyway, for both chromatographies, the results obtained were very informative. They support the idea that most of the sulphur is present in the yeast in organic form (low sulphate peak) and hence could be absorbed in the gastrointestinal tract, allowing us to perform in vivo metabolic tracer studies.

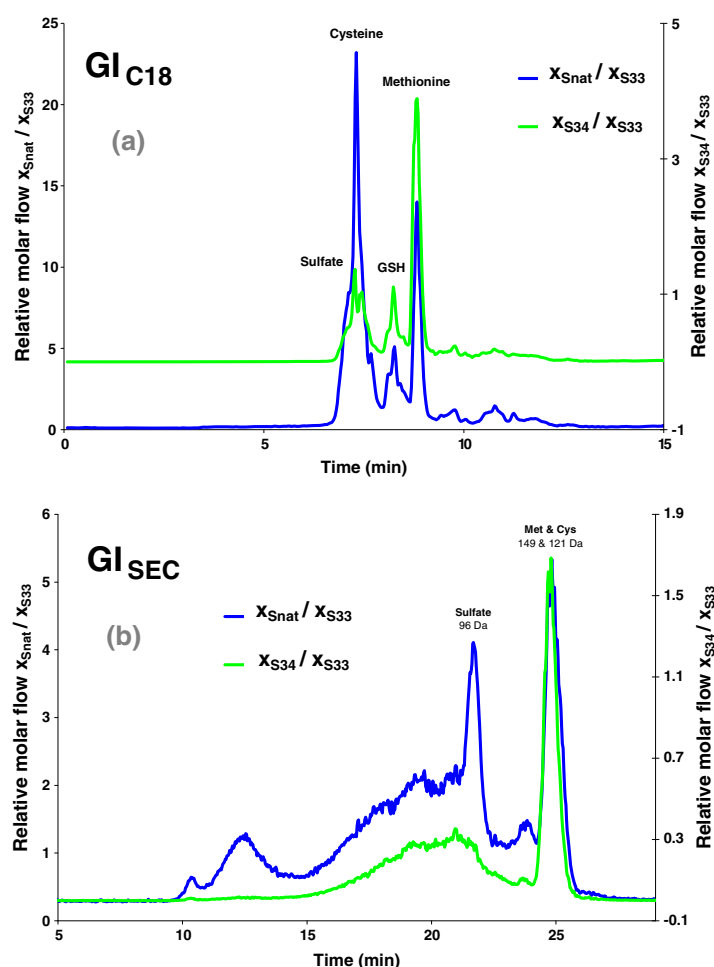
Total sulphur isotope ratio measurements by ICP-MS

In previous work, we have measured the natural variability of sulphur isotope composition in samples containing large amounts of dissolved organic matter [25] and in human scalp hair strands [26] by multicollector ICP-MS. Based on these data, we could calculate the minimum amount of enriched ^{34}S which would be needed for a tracer experiment, taking into account the range of variation shown was below 15‰ $\delta^{34}\text{S}$. For example, a small laboratory animal (e.g. a Wistar rat weighting ca. 100 g) will contain ca. 0.175 g of protein sulphur. The administration of a single dose of 1 mg of enriched ^{34}S as isotopically labelled yeast will change the $^{34}\text{S}/^{32}\text{S}$ isotope ratio of sulphur in proteins, if completely equilibrated, from 0.045 to 0.051 which corresponds to a $\delta^{34}\text{S}$ value of about +100‰. This change is now much larger than the expected natural variation of sulphur isotope ratios and hence sulphur isotope enrichment should be easily detected, even for single-collector ICP-MS, using this tracer amount.

To evaluate the suitability of the labelled yeast as sulphur source for metabolic tracer experiments, a kinetic in vivo study was carried out. The isotopic composition of total sulphur in tissues, urine and faeces of Wistar rats fed with ^{34}S -labelled yeast was measured by double focusing ICP-MS after microwave digestion, as described in the procedures. A certified natural abundance sulphur standard was measured prior to the samples for mass bias correction.

Tissues were taken as a function of time to evaluate the absorption efficiency, accumulation and the kinetics of sulphur metabolism. The results of the incorporation of S34 in tissues of Wistar rats after ^{34}S -labelled yeast ingestion are reported in Fig. 2. The values are reported as tracer/tracee ratios based on the molar fractions calculated for S34 (X_{S34}) and Snat (X_{Snat}) by Isotope Pattern Deconvolution as described in the procedures. The error bars indicate the standard deviation from three independent digestions of the same sample. The values of the $X_{\text{S34}}/X_{\text{Snat}}$ ratio obtained for intestine, pancreas and liver are shown in Fig. 2a. For intestine and pancreas a similar trend in the incorporation of enriched ^{34}S was found. It increased abruptly after 6 h of the single dose of ^{34}S -labelled yeast and then it decreased gradually. This behaviour is consistent with the role played by the small intestine as the organ where ^{34}S -labelled nutrients coming from the gastric digestion are absorbed and pancreas, which produces and secretes enzymes as exocrine gland. For liver, the profile for the incorporation of enriched ^{34}S has two maximums, the first at 6 h and the second at 48 h (Fig. 2a). Blood containing the absorbed sulphur labelled nutrients is carried away from the intestine *via* the hepatic portal vein and goes to the liver for filtering, removal of toxins and nutrient processing, and from there to the rest of the organs. This fact explains the first value at 6 h.

Fig. 1 Relative molar flow chromatograms using reverse phase (a) and SEC (b) for the simulated gastrointestinal digestion of the ^{34}S -labelled yeast



Moreover, the liver has a wide range of functions, including a major role in protein synthesis (mainly plasma proteins) and amino acid metabolism. This fact could explain the values found at 24 and 48 h.

Figure 2b shows the $X_{\text{S}^{34}}/X_{\text{S}^{33}}$ values obtained for brain, lung and spleen. An interesting maximum at 48 h was found in these tissues, which could reflect the specific protein turnover rate in these tissues. The spleen plays important roles in regard to red blood cells and the immune system. It removes old red blood cells and holds a reservoir of blood cells in case of a circulatory shock. This fact could support the behaviour found for this organ. A remarkable high accumulation at pulmonary and brain level was also found (Fig. 2b).

For heart, kidney and testicle time-related changes in the distribution of the enriched ^{34}S were fairly constant (Fig. 2c). This trend could be because these tissues synthesise proteins of longer half-lives or at lower turnover rates.

Kidneys act as a natural filter (cells and large proteins) for the blood, and remove wastes, making an ultrafiltrate that will eventually become urine. They are also responsible for the re-absorption of amino acids. Thus, it is not surprising the trend found for this organ.

The isotopic composition of total sulphur was also measured in urine and faeces of Wistar rats fed with ^{34}S -labelled yeast by single collector ICP-MS to study overall kinetics of excretion (Fig. 3). In faeces, it can be seen that enriched ^{34}S excretion has a maximum at 12 h which corresponds to the undigested labelled yeast. Then, for both faeces and urine, excretion of digested ^{34}S -labelled compounds followed a similar trend, with a maximum found in 24 h. The total elimination of enriched ^{34}S after a single dose of ^{34}S -labelled yeast was reached within 72 h.

It is not the objective of this work to discuss in detail sulphur metabolism but to show that relevant metabolic results can be obtained easily using this approach. As a

Sulphur tracer experiments in laboratory animals

Fig. 2 Values of the ratio X_{S34}/X_{Snat} in tissues of Wistar rats fed with ^{34}S -labelled yeast by single-collector ICP-MS. **a** Intestine, pancreas and liver; **b** brain, lung and spleen; and **c** heart, kidney and testicle

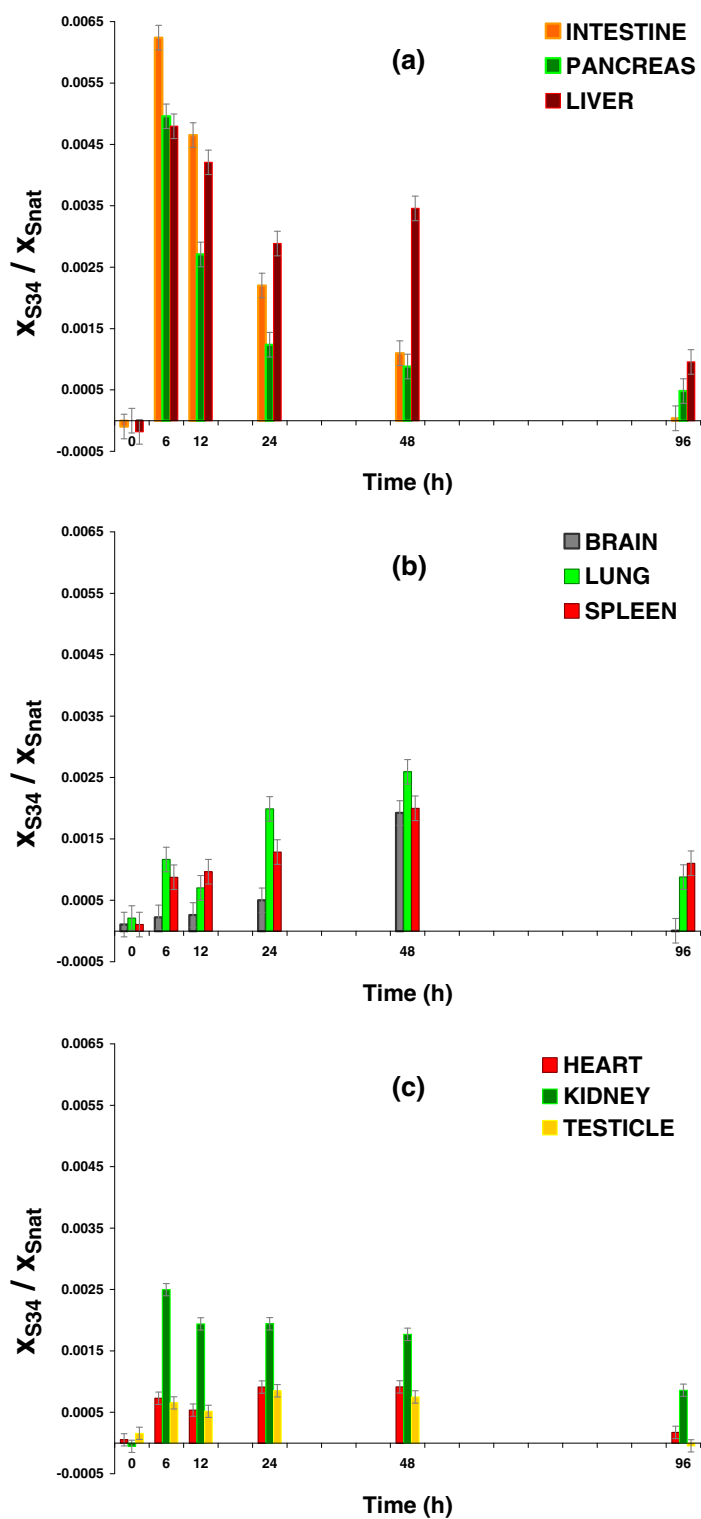
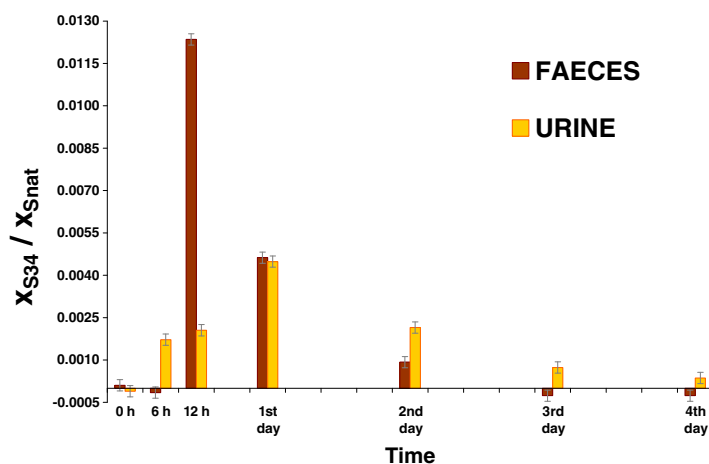


Fig. 3 Values of the ratio X_{S34}/X_{Snat} in excretion products (faeces and urine) of Wistar rats fed with ^{34}S -labelled yeast by single collector ICP-MS



conclusion to the total determination results we can say that a small S34 enrichment was detected in all tissues. The highest enrichment was detected in faeces which indicates that a large proportion of S34 was not absorbed. The isotope enrichment in urine was similar to that found in the tissues and decreased rapidly indicating that, after absorption, S34 was eliminated very fast from the organism. Now it is important to study the chemical form in which the S34 was present and for that we need to couple chromatographic separations to the ICP-MS. In all cases enriched ^{34}S was added post-column in order to quantify the amount of sulphur corresponding to each isotopic signature.

Sulphur isotopic composition of HMW and LMW biomolecules in serum samples by HPLC-ICP-MS

The analysis of serum is analytically challenging due to the high dynamic concentration range of constituent protein/peptide species (more than 10 orders of magnitude), ranging from albumin ($35\text{--}50\text{ mg mL}^{-1}$ in serum) to IL6 ($0\text{--}5\text{ pg mL}^{-1}$ in serum) [27]. Several high-abundance proteins such as albumin, immunoglobulins, haptoglobin, antitrypsin and transferrin typically constitute greater than 90 % of total protein mass and therefore these dominant proteins can prevent the detection of lower-abundance proteins or peptides that are of special interest for biomarker discovery [28]. Thus, prior to the injection in the HPLC-ICP-MS system, we have separated the serum in two different fractions: high molecular weight (HMW) proteins and low molecular weight (LMW) proteins by ultrafiltration. The LMW fraction is made up of several classes of physiologically important proteins such as cytokines, chemokines and peptide hormones, as well as proteolytic fragments of larger proteins and has been associated with pathological conditions such as cancer, diabetes and cardiovascular and infectious

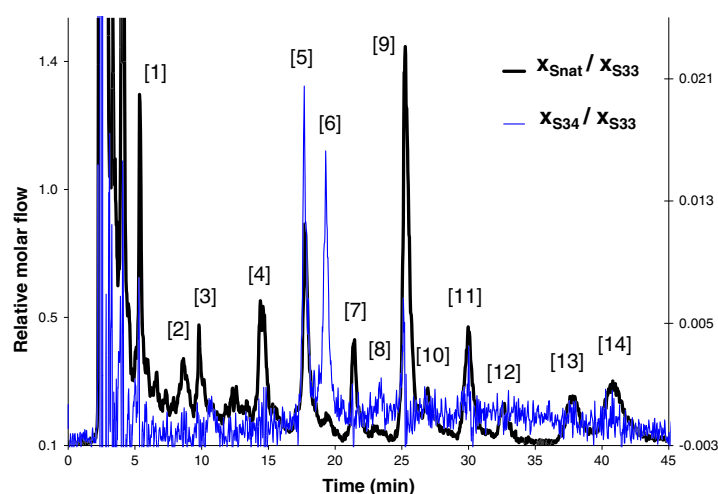
diseases [29, 30]. For removal of high-abundance proteins, centrifugal ultrafiltration has several advantages in comparison to other strategies and techniques such as solid phase extraction or organic solvent extraction because it is fast, easy to operate and inexpensive [29]. Thus, we have separated HMW and LMW proteins using a 10 kDa cut-off centrifugal filter device. Low speed centrifugation, use of diluted serum and use of denaturing conditions have been shown to be key variables for successfully performing serum centrifugal ultrafiltration for removal of highly abundant proteins together with the enrichment of LMW protein/peptides [31].

Then, SEC was evaluated for the separation of the HMW fraction of serum and SEC and reversed phase chromatography were evaluated for the separation of low molecular weight proteins, peptides, amino acids and other biomolecules expected in the LMW fraction of sera. The chromatographic conditions for the analysis of both HMW and LMW fraction of serum by HPLC-ICP-MS are summarised in Table S3 in the ESM.

For serum samples, no conclusive data were obtained. However, some information can be gained by SEC, as summarised in Fig. S2 in the ESM for the analysis of HMW serum and Fig. S3 in the ESM for LMW using two different chromatographic columns with separation ranges of 10–600 kDa and 100–7,000 Da, respectively. The tracer/tracee ratios expressed as X_{S34}/X_{Snat} , for both HMW and LMW fraction of serum varies with time with a maximum found in 6 h. Interestingly, the separation of the LMW fraction of serum results in two different chromatographic peaks with different isotopic composition. The second peak will probably be sulphate which was not isotopically enriched in the yeast sample. In general, the tracer/tracee ratios found in serum (0.009–0.008) were a bit higher than those found in tissues at 6 h but decreased rapidly to values below 0.004 in a similar way as the tissue samples. From the

Sulphur tracer experiments in laboratory animals

Fig. 4 Pattern specific relative molar flow chromatogram for S_{nat} (black) and S₃₄ (blue) obtained for a 6-h urine sample of a Wistar rat fed with ³⁴S-labelled yeast by reversed phase HPLC-ICP-MS with the Element 2 instrument as sulphur-specific detector



SEC data, no preferential enrichment of different fractions was obtained.

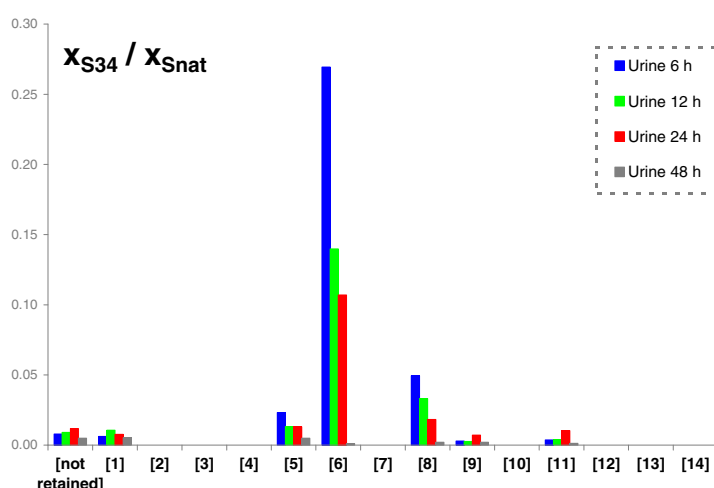
Sulphur isotopic composition of biomolecules in urine samples by HPLC-ICP-MS

In contrast to blood, which collection is invasive and requires meticulous preanalytical handling [29], urine sampling is really straightforward. However, urine, as a matrix, is one of the least desirable biological fluids. The range of protein/peptide concentrations in urine spans several orders of magnitude. The protein concentration of healthy urine is far less than in human plasma (approximately 60 mgmL⁻¹) with healthy adults excreting approximately 50–70 g of solids per day in the urine of which approximately 50–120 mg is protein [32]. Albumin is also a dominant protein in urine. In spite of its re-absorption from the glomerular

filtrate by the proximal renal tubules, this protein is physiologically excreted at rate not exceeding 30 mgday⁻¹ [33]. An additional problem consists on volume changes related to concentration changes and salt composition which vary widely. In order to make sample preparation as simple as possible, crude (undiluted) urine has been clarified as described in the procedures and then injected in the HPLC-ICP-MS system. Size exclusion and reversed-phase chromatography were evaluated for the separation of sulphur-containing biomolecules presented in urine. The chromatographic conditions employed are reported in Table S4 in the ESM.

The chromatographic profile of the sulphur-containing biomolecules by SEC-ICP-MS is similar to that found for the LMW fraction of serum, as can be seen in Fig. S4(A) in the ESM. Three main peaks are observed in the chromatogram with similar isotope enrichment. Again, no conclusive

Fig. 5 Bar chart of the X_{S34}/X_{Snat} ratio found in the chromatographic peaks selected for different sampling times in urine samples of healthy Wistar rats after the administration of the ³⁴S-labelled yeast. Preferential isotope enrichment, tracer/tracee ratios, in S₃₄ in certain species has been detected



data were obtained using this chromatography. Nevertheless, slight differences in the isotopic composition can be detected between the two major groups of biocompounds separated as shown in Fig. S4(B) in the ESM. The overall tracer/tracee ratios were always lower than 0.008 for the urine SEC data.

The chromatographic profile for the reversed phase separation of the sulphur compounds present in urine is shown in Fig. 4. As can be observed, the relative molar flow chromatograms show now a large number of well resolved sulphur-containing peaks. For the evaluation of the tracer/tracee ratios in urine, a number of 15 chromatographic peaks (the non-retained sulphur plus 14 other peaks) were selected to study their tracer/tracee ratios as a function of time in urine samples by HPLC-ICP-MS. The tracer/tracee ratios are indicated as a bar chart for the chromatographic peaks selected and are reported in Fig. 5. As can be seen, differential isotope enrichment for three sulphur-containing biomolecules in urine was detected (particularly important in peak 6). The tracer/tracee ratio for this particular compound was ca. 0.27 after 6 h which was a value much higher than that observed for tissue samples and even for faeces. Significant isotope enrichment was also detected for peaks 5, 8, 9 and 11. For these last two peaks, 9 and 11, the maximum enrichment was detected after 24 h while for the other peaks the maximum enrichment was for the first sample taken after 6 h.

So, we can speculate that peaks 5, 6 and 8 correspond to primary metabolites from the ingested yeast (perhaps methionine and cysteine) while peaks 9 and 11 correspond to secondary metabolites formed from the degradation of peptides or proteins where labelled methionine or cysteine were first incorporated. Unfortunately, no identification of the peaks was possible during this proof of principle study.

Conclusions

In this proof-of-principle work, the suitability of the ^{34}S -labelled yeast to perform tracer experiments in laboratory animals has been demonstrated for both in vitro and in vivo studies. Moreover, a procedure for the in vivo study of sulphur metabolism in serum and urine samples of healthy Wistar rats fed with ^{34}S -labelled yeast by HPLC-ICP-MS has been approached here for the first time. The combination of ^{34}S -isotopic enrichment (^{34}S as metabolic tracer) and absolute biomolecule quantification (using ^{33}S as quantification tracer) after HPLC-ICP-MS could be an alternative strategy for protein turnover or other sulphur-related metabolism studies.

Acknowledgments This work was supported by the Ministry of Science and Innovation, Madrid, Spain (project CTQ2009-12814) and the Education and Science Council of the Principado de Asturias

(grant BP07-059). Teresa Fernández and Agustín Brea from the Biotechnology of the University of Oviedo are gratefully acknowledged for their help and kind suggestions. The authors thank Rafael Peláez for his assistance in the experimental work regarding gels.

References

- Villar-Garea A, Griese M, Imhof A (2007) Biomarker discovery from body fluids using mass spectrometry. *J Chromatogr B* 849:105–114
- Apweiler R, Aslanidis C, Deufel T, Gerstner A, Hansen J, Hochstrasser D et al (2009) Approaching clinical proteomics: current state and future fields of application in fluid proteomics. *Clin Chem Lab Med* 47:724–744
- Silberring J, Ciborowski P (2010) Biomarker discovery and clinical proteomics. *TRAC Trends Anal Chem* 29:128–140
- Srinivas PR, Srivastava S, Hanash S, Wright GL (2001) Proteomics in early detection of cancer. *Clin Chem* 47:1901–1911
- Shau H, Chandler GS, Whitelegge JP, Gombain JA, Faull KF, Chang HR (2003) Proteomic profiling of cancer biomarkers. *Brief Funct Genom Proteomics* 2:147–158
- Fliser D, Novak J, Thongboonkerd V, Argilés A, Jankowski V, Girolami MA, Jankowski J, Mischak H (2007) Advances in urinary proteome analysis and biomarker discovery. *J Am Soc Nephrol* 18:1057–1071
- Ru QC, Katenhusen RA, Zhu LA, Silberman J, Yang S, Orchard TJ, Brzeski H, Liebman M, Ellsworth DL (2006) Proteomic profiling of human urine using multi-dimensional protein identification technology. *J Chromatogr A* 1111:166–174
- Wittke S, Fliser D, Haubitz M, Bartel S, Krebs R, Hausadel F, Hillmann M, Golovko I, Koester P, Haller H, Kaiser T, Mischak H, Weissinger EM (2003) Determination of peptides and proteins in human urine with capillary electrophoresis–mass spectrometry, a suitable tool for the establishment of new diagnostic markers. *J Chromatogr A* 1013:173–181
- Haubitz M, Wittke S, Weissinger EM, Walden M, Rupprecht HD, Floege J, Haller H, Mischak H (2005) Urine protein patterns can serve as diagnostic tools in patients with IgA nephropathy. *Kidney Int* 67:2313–2320
- Theodorescu D, Wittke S, Ross MM, Walden M, Conaway M, Just I, Mischak H, Frierson HF (2006) Discovery and validation of new protein biomarkers for urothelial cancer: a prospective analysis. *Lancet Oncol* 7:230–240
- Kaiser T, Kamal H, Rank A, Kolb HJ, Holler E, Ganser A, Hertenstein B, Mischak H, Weissinger EM (2004) Proteomics applied to the clinical follow-up of patients after allogeneic hematopoietic stem cell transplantation. *Blood* 104:340–349
- Wind M, Wegener A, Eisenmenger A, Kellner R, Lehmann WD (2003) Sulfur as the key element for quantitative protein analysis by capillary liquid chromatography coupled to element mass spectrometry. *Angew Chem Int Ed* 42:3425–3427
- Prange A, Proffrock D (2008) Chemical labels and natural element tags for the quantitative analysis of bio-molecules. *J Anal At Spectrom* 23:432–459
- Rappel C, Schaumlöffel D (2008) The role of sulfur and sulfur isotope dilution analysis in quantitative protein analysis. *Anal Bioanal Chem* 390:605–615
- Anderson JW (1980) Assimilation of inorganic sulfate into cysteine. In: Stumpf PK, Conn EE (eds) *The biochemistry of plants*, vol 5. Academic, New York, p 203
- Porro D, Sauer M, Branduardi P, Mattanovich D (2005) Recombinant protein production in yeasts. *Mol Biotechnol* 31:245–259

Sulphur tracer experiments in laboratory animals

17. Thomas D, Surdin-Kerjan Y (1997) Metabolism of sulfur amino acids in *Saccharomyces cerevisiae*. *Microbiol Mol Biol Rev* 61:503–532
18. Barnett JA (2003) Beginnings of microbiology and biochemistry: the contribution of yeast research. *Microbiology* 149:557–567
19. Giner Martínez-Sierra J, Moreno Sanz F, Herrero Espílez P, Marchante Gayón JM, García Alonso JI (2007) Biosynthesis of sulfur-34 labelled yeast and its characterisation by multicollector-ICP-MS. *J Anal At Spectrom* 22:1105–1112
20. Rodríguez-González P, Ruiz Encinar J, García Alonso JI, Sanz-Medel A (2005) Monitoring the degradation and solubilisation of butyltin compounds during in vitro gastrointestinal digestion using “triple spike” isotope dilution GC-ICP-MS. *Anal Bioanal Chem* 381:380–387
21. Laemmli UK (1970) Cleavage of structural proteins during the assembly of the head of bacteriophage T4. *Nature* 227:680–685
22. Rodríguez-González P, García Alonso JI (2010) Recent advances in isotope dilution analysis for elemental speciation. *J Anal At Spectrom* 25:239–259
23. Giner Martínez-Sierra J, Moreno Sanz F, Herrero Espílez P, Santamaria-Fernandez R, Marchante Gayón JM, García Alonso JI (2010) Evaluation of different analytical strategies for the quantification of sulfur-containing biomolecules by HPLC-ICP-MS: application to the characterisation of ³⁴S-labelled yeast. *J Anal At Spectrom* 25:989–997
24. Rodríguez-González P, Marchante-Gayón JM, García Alonso JI, Sanz-Medel A (2005) Isotope dilution analysis for elemental speciation: a tutorial review. *Spectrochim Acta B* 60:151–207
25. Giner Martínez-Sierra J, Santamaria-Fernandez R, Hearn R, Marchante Gayón JM, García Alonso JI (2010) Development of a direct procedure for the measurement of sulfur isotope variability in beers by MC-ICP-MS. *J Agric Food Chem* 58:4043–4050
26. Santamaria-Fernandez R, Giner Martínez-Sierra J, Marchante Gayón JM, García Alonso JI, Hearn R (2009) Measurement of longitudinal sulfur isotopic variations by laser ablation MC-ICP-MS in single human hair strands. *Anal Bioanal Chem* 394:225–233
27. Tirumalai RS, Chan KC, Prieto DA, Issaq HJ, Conrads TP, Veenstra TD (2003) Characterisation of the low molecular weight human serum proteome. *Mol Cell Proteomics* 2:1096–1103
28. Shou M, Conrads TP, Veenstra TD (2005) Proteomic approaches to biomarker detection. *Brief Funct Genom Proteomics* 4:69–75
29. Luque-Garcia JL, Neubert TA (2007) Sample preparation for serum/plasma profiling and biomarker identification by mass spectrometry. *J Chromatogr A* 1153:259–276
30. Martorella A, Robbins R (2007) Serum peptide profiling: identifying novel cancer biomarkers for early disease detection. *Acta Biomed* 78:123–128
31. Linke T, Doraiswamy S, Harrison EH (2007) Rat plasma proteomics: effects of abundant protein depletion on proteomic analysis. *J Chromatogr B* 849:273–281
32. Khan A, Packer NH (2006) Simple urinary sample preparation for proteomic analysis. *J Proteome Res* 5:2824–2838
33. Magagnotti C, Fermo I, Carletti RM, Ferrari M, Bachi A (2010) Comparison of different depletion strategies for improving resolution of the human urine proteome. *Clin Chem Lab Med* 48:531–535

D.3.1.2. Información suplementaria del artículo científico V

Analytical and Bioanalytical Chemistry

Electronic Supplementary Material

Sulfur tracer experiments in laboratory animals using ³⁴S-labelled yeast.

J. Giner Martínez-Sierra, F. Moreno Sanz, P. Herrero Espílez, J. M. Marchante Gayón,
J. Rodríguez Fernández and J. I. García Alonso

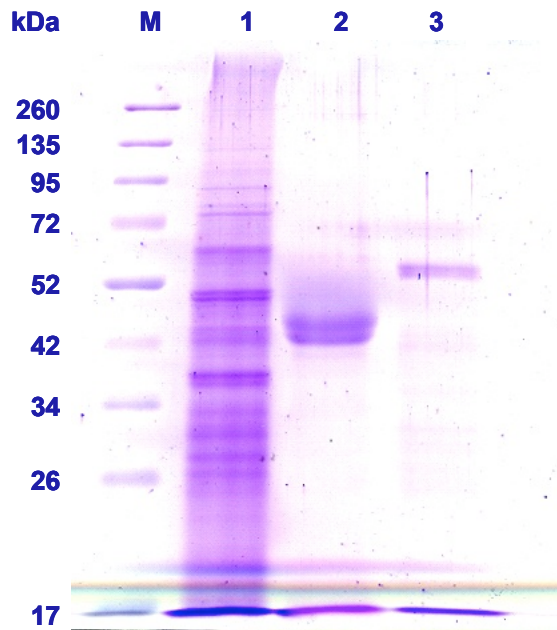


Fig. S1. SDS-PAGE analysis of labelled proteins expressed in *S. cerevisiae*. 20 μ L of supernatant of protein extract (lane 1), hydrolysates of simulated gastric digestion (lane 2) and hydrolysates of simulated intestinal digestion (lane 3), were applied to a 12% SDS-PAGE and then stained with Coomassie brilliant blue. M, sizes (kDa) of molecular weight markers

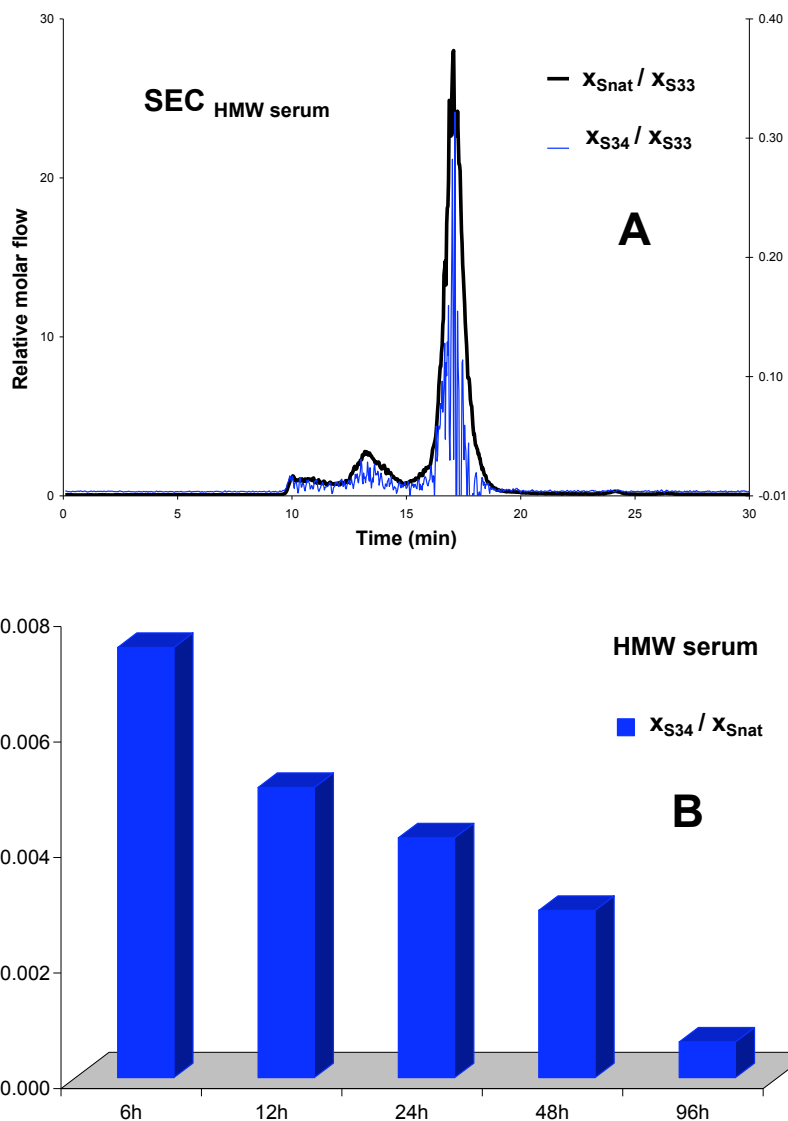


Fig. S2. Figures of merit obtained by SEC-ICP-MS with the Element 2 instrument as sulfur specific detector for the HMW fraction of serum of Wistar rats fed with ^{34}S -labelled yeast. (A) Pattern specific relative molar flow chromatogram for natural sulfur (black) and ^{34}S -sulfur (blue). (B) Tracer/tracee ratio calculated as $X_{S_{34}}/X_{S_{nat}}$ after integration of the whole chromatogram in A

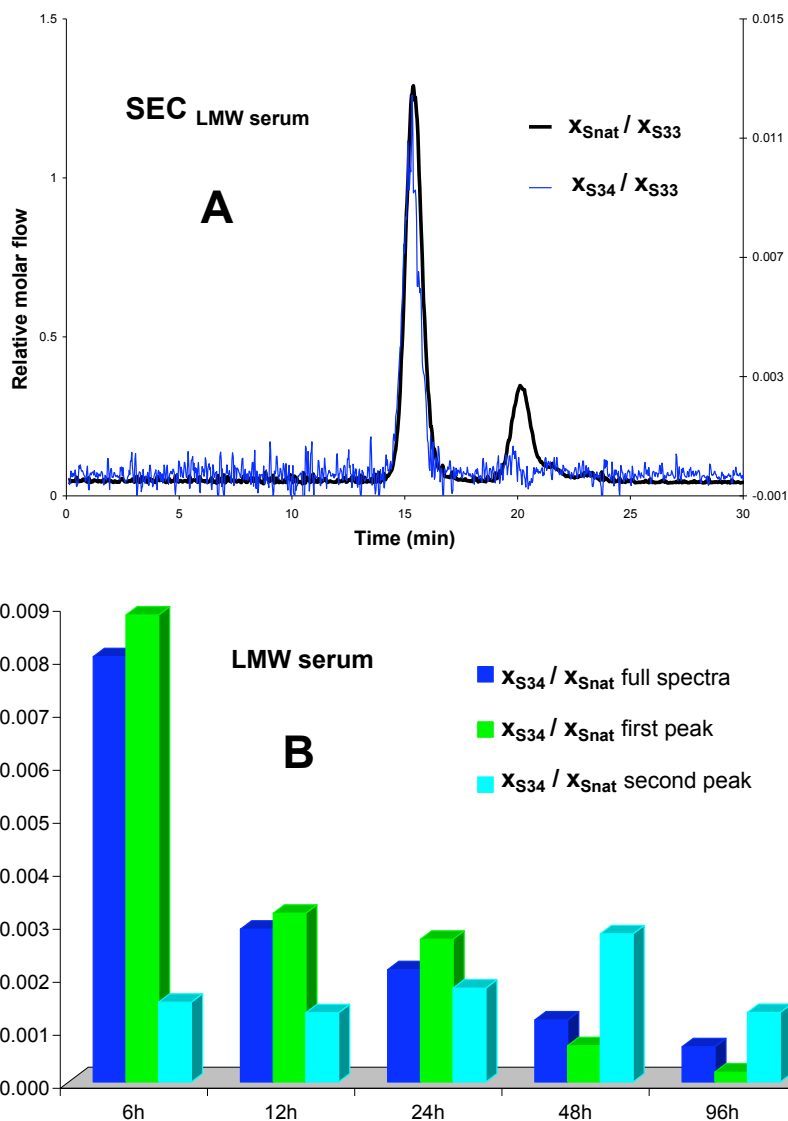


Fig. S3. Figures of merit obtained by SEC-ICP-MS with the Element 2 instrument as sulfur specific detector for the LMW fraction of serum of Wistar rats fed with ^{34}S -labelled yeast. (A) Pattern specific relative molar flow chromatogram for natural sulfur (black) and ^{34}S -sulfur (blue). (B) Tracer/tracee ratio calculated as $x_{S_{34}}/x_{S_{nat}}$ after integration in A

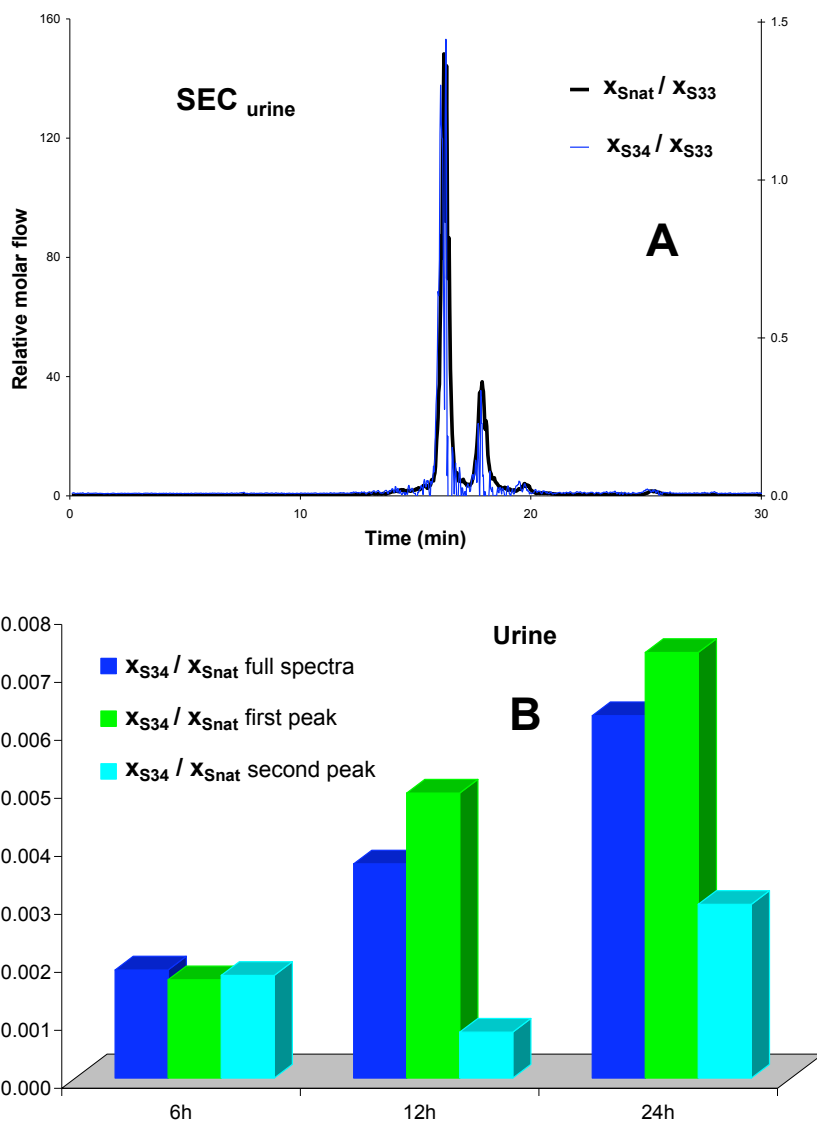


Fig. S4. Figures of merit obtained by SEC-ICP-MS with the Element 2 instrument as sulfur specific detector for urine of Wistar rats fed with ^{34}S -labelled yeast. (A) Pattern specific relative molar flow chromatogram for natural sulfur (black) and ^{34}S -sulfur (blue). (B) Tracer/tracee ratio calculated as $X_{\text{S34}}/X_{\text{Snat}}$ after integration in A

Table S1. Single collector ICP-MS operating conditions. Parameters were optimised for best sensitivity and precision of sulfur isotope ratio measurements

Element 2 ICP-MS conditions	
RF power	1325 W
Cool gas flow	15.50 L·min ⁻¹ Ar
Auxiliary gas flow	0.80 L·min ⁻¹ Ar
Sample gas flow	0.91 L·min ⁻¹ Ar
Isotopes measured	³² S - ³³ S - ³⁴ S
Resolution mode	Medium
Data acquisition parameters (<i>bulk mode – isotope ratio</i>)	
Runs / Passes	3 / 5
Data acquisition parameters (<i>chromatography</i>)	
Runs / Passes	1500 / 1

Table S2. Chromatographic conditions for the analysis of the simulated gastrointestinal digestion of the ^{34}S -labelled yeast by HPLC-ICP-MS

HPLC conditions	
<i>Size Exclusion Chromatography</i>	
Column	SEC Superdex Peptide HR 10/300 GL 30 cm x 10 mm (length x I.D.); 13-15 μm particle size
Injection loop	50 μL
Flow rate	750 $\mu\text{L}\cdot\text{min}^{-1}$
Mobile phase	30 mM Tris-HCl, pH 7.4 and 10 mM NaCl. Isocratic mode
<i>Reversed Phase Chromatography</i>	
Column	Supelco Discovery® BIO Wide Pore C18 15 cm x 2.1 mm (length x I.D.); 5 μm particle size
Injection loop	20 μL
Flow rate	200 $\mu\text{L}\cdot\text{min}^{-1}$
Mobile phase	(A) H_2O with 2% of MeOH and (B) MeOH with 2% of H_2O . Gradient mode (2 min, 0% B; 12 min, 50% B; 15 min, 50% B; 25 min, 0% B).

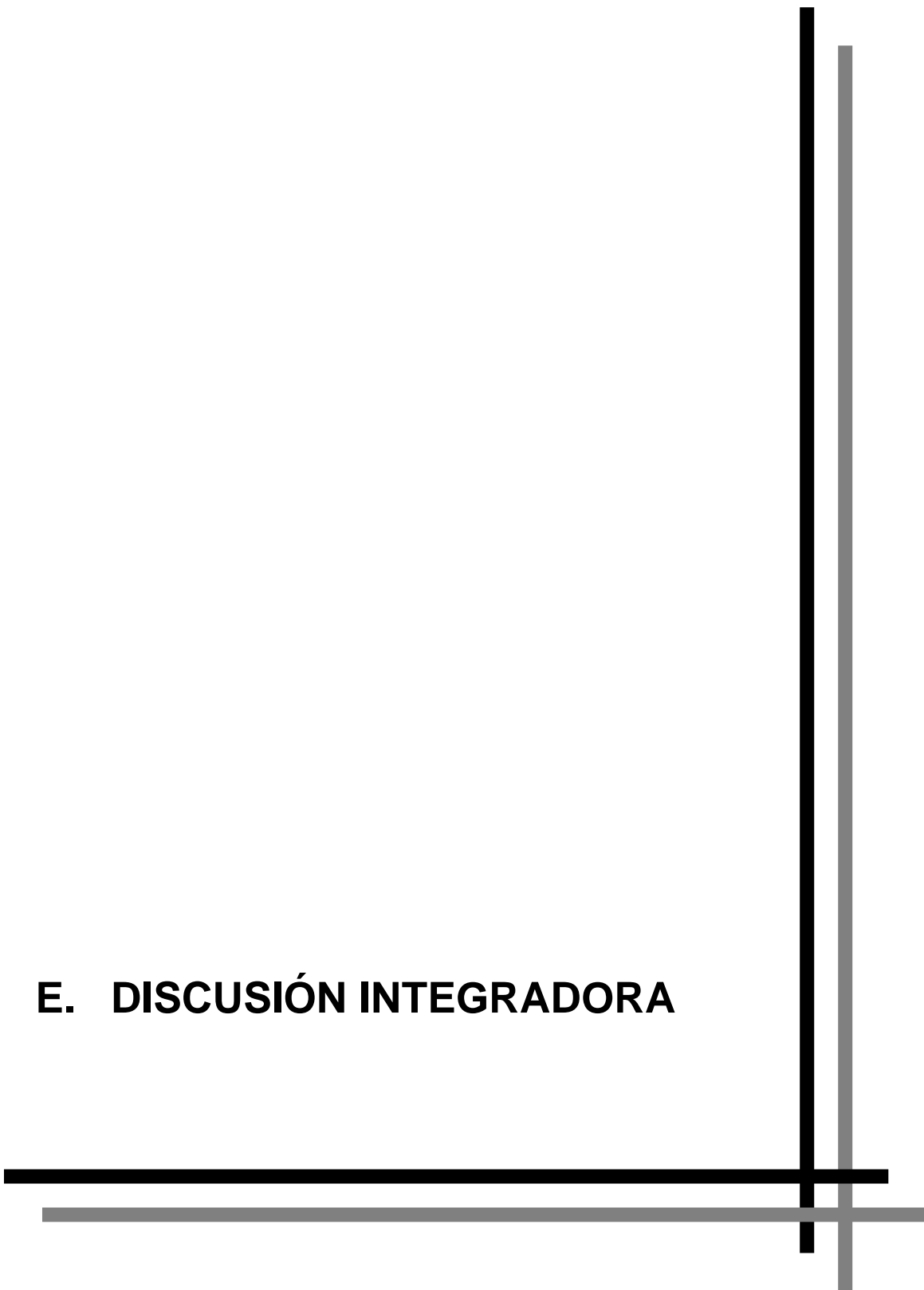
Table S3. Chromatographic conditions for the analysis of the HMW and LMW fraction of serum by HPLC-ICP-MS

HPLC conditions	
<i>Size Exclusion Chromatography</i> (for both HMW and LMW)	
Columns	SEC Superdex 200 and Peptide HR 10/300 GL 30 cm x 10 mm (length x I.D.) 13 µm average particle size
Injection loop	50 µL
Flow rate	750 µL·min ⁻¹
Mobile phase	30 mM Tris-HCl, pH 7.4 and 10 mM NaCl. Isocratic mode
<i>Reversed Phase Chromatography</i> (only for LMW)	
Column	Supelco Discovery® BIO Wide Pore C18 15 cm x 2.1 mm (length x I.D.) 5 µm particle size
Injection loop	20 µL
Flow rate	200 µL·min ⁻¹
Mobile phase	(A) 30 mM Tris-HCl, pH 7.4 and (B) MeOH. Gradient mode

Table S4. Chromatographic conditions for the analysis of sulfur-containing biomolecules in urine by HPLC-ICP-MS

HPLC conditions	
<i>Reversed Phase Chromatography</i>	
Column	Mediterranea Sea ₁₈ 15 cm x 4.6 mm (length x I.D.) 5 µm particle size
Injection loop	50 µL
Flow rate	1.0 mL·min ⁻¹
Mobile phase	(A) 75 mM ammonium acetate, pH 7.4, 2% MeOH; (B) 75 mM ammonium acetate, pH 7.4, 15% MeOH; Gradient mode (2 min, 0% B; 30 min, 100% B; 35 min, 100% B; 50 min, 0% B)
<i>Size Exclusion Chromatography</i>	
Column	SEC Superdex Peptide HR 10/300 GL 30 cm x 10 mm (length x I.D.) 13 µm average particle size
Injection loop	50 µL
Flow rate	0.75 mL·min ⁻¹
Mobile phase	30 mM Tris-HCl, pH 7.4 and 10 mM NaCl; Isocratic mode

E. DISCUSIÓN INTEGRADORA



El objetivo general de esta Tesis Doctoral consistió en el desarrollo de nuevas metodologías analíticas que permitan el estudio del metabolismo del azufre utilizando isótopos estables enriquecidos. Dado que la composición isotópica del azufre varía en la naturaleza, como punto de partida en nuestras investigaciones se tuvo en cuenta que si se quiere seguir la pista del azufre en un ser vivo utilizando un trazador marcado isotópicamente con azufre-34, obviamente la cantidad de trazador metabólico utilizada debe ser lo suficientemente elevada como para alterar la composición isotópica del azufre por encima de los límites de variabilidad natural, lo que permitiría detectar *a posteriori* la variación inducida. Asimismo, la estimación de los límites de variabilidad natural exige poder determinar cambios muy pequeños en la composición isotópica del azufre y por tanto son imprescindibles medidas de relaciones isotópicas de elevada precisión. En este sentido, el uso de equipos ICP-MS multicolectores permite la determinación en continuo, rápida y simultánea de varios isótopos, evitando el procedimiento largo y tedioso de preparación de muestra de la técnica más comúnmente utilizada para medir variaciones isotópicas naturales (IRMS) y con excelentes precisiones instrumentales. Por todo ello, el primer objetivo específico de la presente Tesis Doctoral consistió en estudiar la variabilidad natural de la composición isotópica de azufre mediante ICP-MS multicolector.

El principal problema que se puede encontrar en la medida de relaciones isotópicas mediante ICP-MS multicolector es la existencia de interferencias de matriz que afectan al factor de discriminación de masas. La transmisión de los iones en el espectrometro de masas puede cambiar ligeramente con la presencia de altas concentraciones de matriz y este cambio no tiene por qué ser idéntico para diferentes isótopos del mismo elemento. Por tanto, los cambios aparentes observados en las relaciones isotópicas (*i.e.* variabilidad natural) pueden ser debidos a efectos de matriz y no a cambios reales en la muestra. Existen diferentes alternativas para eliminar o corregir estos efectos de matriz. La solución tradicional consiste en la separación del elemento de la matriz y el uso de estándares certificados en composición isotópica del elemento para la corrección externa del factor de discriminación de masas. Como alternativa, se puede aplicar una corrección interna de la discriminación de masas, utilizando otro elemento próximo en masa al analito. Así, Clough y col. [76] utilizaron un estándar de silicio para corregir el efecto de discriminación de masas que afecta la medida de relaciones isotópicas de azufre. En dicho trabajo se observó que el silicio puede corregir los efectos de matriz derivados del sodio, cloro, y calcio en muestras de agua mineral embotellada.

La composición isotópica de la mayoría de los elementos en los seres vivos depende principalmente de la comida y bebida ingerida, por lo que la variabilidad natural en la composición isotópica de azufre tanto en alimentos como en bebidas se podría utilizar para estimar la variabilidad natural en los seres vivos. En el **artículo científico I** se exploró la capacidad del silicio para la corrección interna de los efectos de matriz en la determinación de variaciones isotópicas de azufre mediante MC-ICP-MS en muestras más complejas (*i.e.* con un elevado contenido de materia orgánica disuelta). La metodología explorada nos permitiría asimismo disponer de una herramienta útil para la medida de variaciones isotópicas inducidas en estudios de metabolismo del azufre. En este contexto, la cerveza es una muestra ideal, ya que su contenido presenta más de 800 compuestos [223]. Entre ellos, destacan los elevados niveles de los aminoácidos libres metionina y cisteína (más de 50 mg·L⁻¹ para la metionina [224]) con una concentración típica tanto de azufre como de silicio comprendida entre 10 y 50 µg·g⁻¹. A pesar de que la cerveza está generalmente compuesta de cuatro ingredientes principales (agua, lúpulos, cebada y levadura), es la receta exacta y el tiempo de elaboración lo que le confiere su sabor característico. En general los siguientes ingredientes se encuentran presentes en todas las recetas: hidratos de carbono, alcoholes (siendo el etanol el más importante), material derivado de proteínas, aminas, derivados de ácidos nucleicos, pequeñas cantidades de vitaminas del grupo B, compuestos fenólicos y una variedad de compuestos inorgánicos, que incluyen cationes, aniones y metales traza. Además, se han identificado un gran número de compuestos volátiles de azufre en muestras de cerveza [225]. Por tanto, dada la complejidad de la matriz de la cerveza, es de esperar que algunos de estos compuestos [226] contribuyan como potenciales interferencias.

En este trabajo de investigación se demostró que el procedimiento de corrección interna de los efectos de matriz utilizando silicio para la medida de relaciones isotópicas de azufre es efectivo en muestras complejas que contienen gran cantidad de materia orgánica disuelta. Para ello, se analizaron 26 muestras de cerveza de diferentes marcas representativas de las disponibles en los supermercados del Reino Unido. En la Figura 31 se recogen destacados en color rojo los países de elaboración (A) de las muestras de cerveza analizadas (B) mediante ICP-MS multicolector.



Figura 31. Países de elaboración (A) de las muestras de cerveza (B) analizadas mediante ICP-MS multicolector.

Los resultados se expresaron en notación delta relativos a la escala V-CDT. El rango de valores de delta observado en las 26 cervezas estudiadas varia entre -0,2 y +13,8‰ con una incertidumbre expandida asociada menor del 2‰. El método analítico presentado puede diferenciar grupos de cerveza. Sin embargo, dentro de un mismo grupo, la técnica debe ser usada en combinación con otras técnicas complementarias existentes que proporcionen información multicomponente (p.e. análisis multielemental y/o multiisotópico). A pesar de que el poder de discriminación de las relaciones isotópicas de azufre no se puede utilizar de manera aislada para distinguir diferentes cervezas de similar origen, los resultados muestran el potencial de la metodología desarrollada para ayudar a la protección de marcas en el campo de autenticidad de bebidas y alimentos utilizando la huella dactilar de azufre y su aplicación para estimar la variabilidad natural del azufre en bebidas y alimentos con una preparación de muestra muy sencilla.

Continuando con los trabajos encuadrados en el primer objetivo específico de esta Tesis Doctoral, en el **artículo científico II** se estudió la variabilidad natural de las relaciones isotópicas de azufre en pelo humano, que puede actuar a modo de archivo del azufre incorporado a la queratina del cabello. La queratina es una proteína muy rica en azufre, debido al alto contenido de los aminoácidos cisteína, metionina y ácido cisteico, lo que confiere al cabello un contenido total de azufre constante de aproximadamente el 5%, tanto entre diferentes muestras como a lo largo de un mismo pelo [227]. Con este fin se desarrolló un método novedoso que permite realizar la medida de relaciones isotópicas de azufre a lo largo de un pelo mediante un sistema de ablación láser acoplado a un ICP-MS multicolector. El empleo de un equipo MC-ICP-MS es fundamental en este tipo de estudios, ya que para poder estudiar la variabilidad natural y por tanto determinar cambios muy pequeños en la composición isotópica del azufre, se necesitan medidas de relaciones isotópicas de elevada

precisión. En la literatura existente hasta la fecha de realización de este trabajo, en muy pocos estudios se había utilizado ablación láser acoplada con un ICP-MS para el análisis de hebras de cabello [228-233]. Además, la mayoría recogían la cuantificación de metales pesados (p.e. Hg y U) y sólo una publicación estaba centrada en la medida de relaciones isotópicas en muestras de pelo [233].

Hoy en día existe una creciente popularidad en el empleo de muestras de pelo como tejido de biopsia o biomarcador de exposición [234], debido principalmente a su discreción, muestreo no invasivo, facilidad de transporte y manejo de este tipo de muestra. Así, el análisis del pelo se ha utilizado ampliamente para establecer la exposición ocupacional y ambiental [227,228,235,236], la evaluación de los perfiles migratorios y cambios en la dieta [229,237,238], la identificación humana y estudios de envejecimiento [239-241] y el diagnóstico de enfermedades [242]. Por otro lado, el papel de los isótopos estables en la identificación humana ha sido discutido previamente por Fraser y col. [241]. Asimismo, se ha investigado con anterioridad la conexión entre la composición isotópica estable de los tejidos humanos y la dieta y estilo de vida de un individuo [243,244], destacando la necesidad de desarrollar técnicas novedosas que proporcionen información relacionada con el origen geográfico y los movimientos recientes de una persona [240]. En este tipo de estudios se establece una relación entre la alimentación y los valores isotópicos de colágeno encontrados en muestras de hueso y proteína de pelo (*i.e.* queratina). Por ejemplo, se ha encontrado que las relaciones isotópicas de carbono y nitrógeno en pelo reflejan el consumo de proteína animal [245] mientras que las de hidrógeno y oxígeno están relacionadas con el agua potable y de lluvia [240,246]. Igualmente, se ha estudiado el uso potencial de las relaciones isotópicas de carbono, nitrógeno y azufre en pelo humano para proporcionar información sobre el origen humano y movimientos migratorios [238]. En este trabajo se documenta una amplia variabilidad en las relaciones isotópicas de carbono y nitrógeno de muestras de pelo de Norte América y Europa basadas al menos parcialmente en los niveles de marisco, carne de vaca alimentada con maíz y cereales de la dieta. Además en determinados casos, se comprobó que los valores de las relaciones isotópicas de azufre ayudaban a restringir más la interpretación de los datos, debido a la buena preservación del contenido de azufre en el pelo. De igual modo, un estudio más actual [237] ha mostrado la relación existente entre la dieta y los movimientos migratorios recientes de los habitantes de una comunidad rural de Inglaterra a través de la medida de relaciones isotópicas de carbono, nitrógeno y azufre en pelo humano. De una manera general, los datos

recogidos de los tres sistemas isotópicos proporcionaron suficiente información para confirmar la dieta y el origen de los individuos.

El análisis tradicional de muestras de pelo por IRMS requiere la molienda o digestión previa de la muestra y por tanto la resolución espacial está limitada por el tamaño de la muestra requerido para el análisis. En el mejor de los casos se requiere un mínimo de 10 mg de cabello (*i.e.* 10-25 hebras de pelo, dependiendo de su longitud y grosor).

El trabajo de investigación llevado a cabo en esta Tesis Doctoral describe una metodología analítica que posibilita la detección de variaciones isotópicas de azufre en la queratina del cabello humano utilizando un sistema de ablación láser acoplado a un ICP-MS multicolector (LA-MC-ICP-MS). La ventaja principal que ofrece este método frente al método más convencional (IRMS) es la resolución espacial que se logra al utilizar el láser para la ablación del cabello. Con esta novedosa metodología es posible detectar variaciones espaciales dentro de un solo cabello de una forma rápida y precisa a escala de micrómetros. El haz láser puede ir recorriendo el pelo a lo largo, produciendo cráteres de ablación (*i.e.* información) con una resolución espacial de 12 μm de ancho. La alta resolución espacial permite el análisis de muestras de cabello individual, con un grosor habitual comprendido entre 40 y 120 μm para pelo humano del cuero cabelludo [247].

El principal desafío analítico reside en la resolución espacial de la metodología y la precisión de las medidas de relaciones isotópicas de azufre en muestras de cabello humano a través del acoplamiento del sistema de ablación láser con un equipo ICP-MS multicolector. El método ha sido desarrollado y validado con materiales de referencia para medidas isotópicas. Asimismo, para la optimización de parámetros de ablación y de medida se han utilizado muestras de pelo de caballo certificadas en composición isotópica. Los parámetros del sistema de ablación láser (velocidad de barrido ($\mu\text{m}\cdot\text{s}^{-1}$), tasa de repetición (Hz), tamaño del punto (μm) y rendimiento energético (%)), se optimizaron cuidadosamente de manera independiente para conseguir la máxima resolución espacial y precisiones instrumentales para la medida de relaciones isotópicas de azufre por debajo del 0,05%.

Se recogieron muestras de cabello de al menos 4 cm de longitud donadas por tres voluntarios, dos de ellos residentes de forma permanente en el Reino Unido y un tercero, que llamamos "viajero", el cual ha pasado los últimos seis meses entre diferentes países europeos y Australia. Normalmente el cabello crece a una velocidad media de 1,25 cm/mes. Por tanto, la información obtenida midiendo las variaciones

isotópicas de azufre a lo largo de 4-6 cm de un pelo puede proporcionar información acerca de los 5-7 meses previos a la toma de la muestra. Los resultados obtenidos se recogen en la Figura 32. El cabello procedente del “viajero” revela variaciones isotópicas significativas de azufre que parecen estar relacionadas con sus movimientos geográficos. Por el contrario, las variaciones detectadas en el cabello de los dos individuos residentes en el Reino Unido fueron mínimas y similares para ambas muestras.

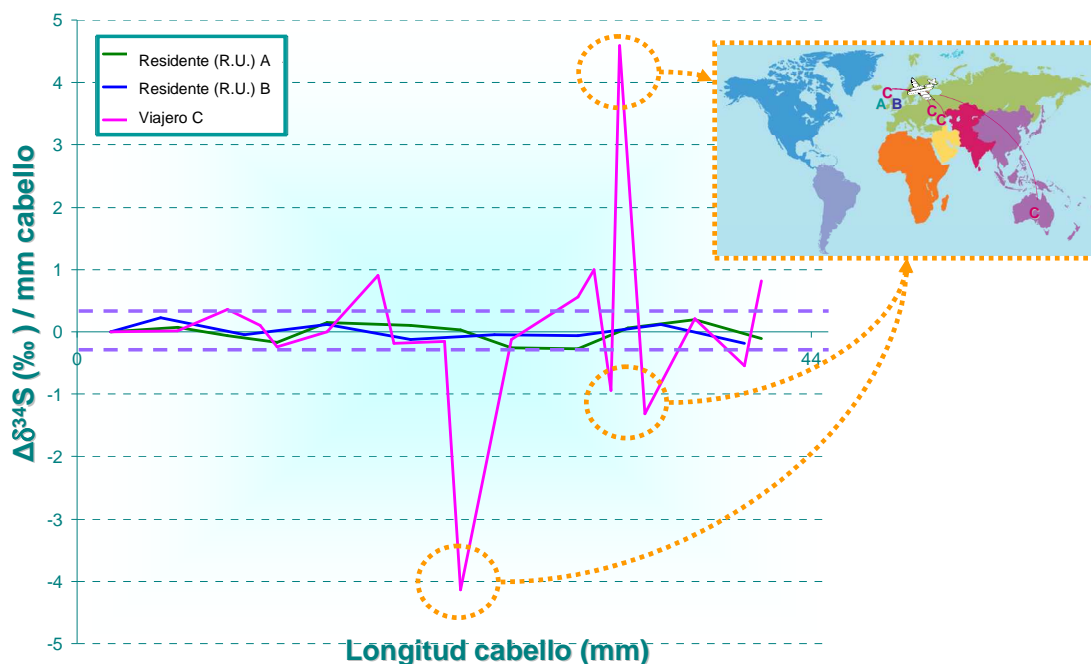


Figura 32. Variaciones isotópicas longitudinales de azufre en cabello humano determinadas mediante LA-MC-ICP-MS.

Los resultados obtenidos en este trabajo de investigación abren la posibilidad de utilizar la medida de variaciones isotópicas de azufre en una sola muestra de cabello mediante LA-MC-ICP-MS como un indicador de los movimientos geográficos de un individuo y/o cambios en la dieta. Asimismo, nos han permitido estimar la variabilidad natural de las relaciones isotópicas de azufre así como la cantidad mínima de trazador metabólico de azufre-34 que se necesita para poder realizar estudios de metabolismo del azufre utilizando trazadores estables en animales de laboratorio.

Una vez determinados los límites de variabilidad natural de la composición isotópica de azufre, el siguiente paso en nuestras investigaciones se centró en la preparación y caracterización de un trazador metabólico de azufre adecuado. Como se comentó en la introducción, la determinación de azufre puede ser usada como

herramienta genérica para la detección y cuantificación de péptidos y proteínas. En este punto es necesario tener en cuenta que los estudios de metabolismo de proteínas en mamíferos utilizando isótopos estables enriquecidos de azufre requieren la síntesis previa de los aminoácidos proteinogénicos cisteína y/o metionina marcada con el isótopo enriquecido, dado que los mamíferos no son capaces de sintetizar estos aminoácidos y necesitan obtenerlos a través de la alimentación. Por el contrario, otros seres vivos como las levaduras pueden reducir el sulfato inorgánico y sintetizar compuestos organo-azufrados [19]. Particularmente, la levadura *Saccharomyces cerevisiae* es una fuente rica de valiosas proteínas, vitaminas del grupo B, así como numerosos minerales y enzimas [248] y su empleo como trazador metabólico presenta varias ventajas en el contexto de este trabajo, dada su inocuidad al estar clasificada como organismo seguro para la salud por la FDA americana y la posibilidad de administrarla como alimento por vía oral. Por todo ello, el segundo objetivo específico de la presente Tesis Doctoral consistió en la preparación y caracterización de levadura marcada con azufre-34.

La baja abundancia de los isótopos ^{33}S , ^{34}S y ^{36}S en el azufre natural (0,76; 4,29 y 0,02% respectivamente) los hace muy adecuados para su uso como trazadores en estudios metabólicos, posibilidad que no había sido abordada hasta el comienzo de esta Tesis Doctoral. En el **artículo científico III** se documenta la preparación de dos trazadores isotópicos estables de azufre (S33 y S34) a partir de dos patrones de azufre elemental enriquecidos isotópicamente en los isótopos ^{33}S y ^{34}S respectivamente. Ambos trazadores se caracterizaron en composición isotópica y concentración empleando equipos ICP-MS de alta resolución para la medida exacta y precisa de relaciones isotópicas de azufre. Como se puede observar en la Tabla 5 el enriquecimiento isotópico para ambos trazadores fue mayor del 99%.

Tabla 5. Composición isotópica (%) del azufre de abundancia isotópica natural (S_{nat}) y de los trazadores de azufre utilizados (S33 y S34).

	Composición isotópica (%)		
	^{32}S	^{33}S	^{34}S
Perfil isotópico natural S_{nat}	94,93	0,76	4,29
Trazador de cuantificación S33	0,01	99,70	0,29
Trazador metabólico S34	0,21	0,42	99,37

Una vez preparados y caracterizados los trazadores isotópicos de azufre S34 y S33, se evaluó el método de la deconvolución de perfiles isotópicos (IPD) para la

determinación simultánea de concentración y composición isotópica de azufre total en muestras biológicas. La muestra a analizar contiene una cantidad desconocida tanto del elemento de abundancia isotópica natural (S_{nat}) como del trazador metabólico (S₃₄). El segundo perfil isotópico alterado (S₃₃) se añade a la muestra para cuantificar mediante el análisis por dilución isotópica y su contribución es, por tanto, conocida. Esta metodología permite la determinación simultánea tanto del azufre originalmente presente en la muestra como del azufre procedente del trazador y se validó aplicándola a la determinación del contenido total de azufre en un material de referencia certificado (suero humano).

A continuación, se preparó levadura marcada isotópicamente con azufre-34 siguiendo el procedimiento que ha sido detallado en la parte experimental de esta Tesis Doctoral y que se esquematiza a modo de resumen en la Figura 33.

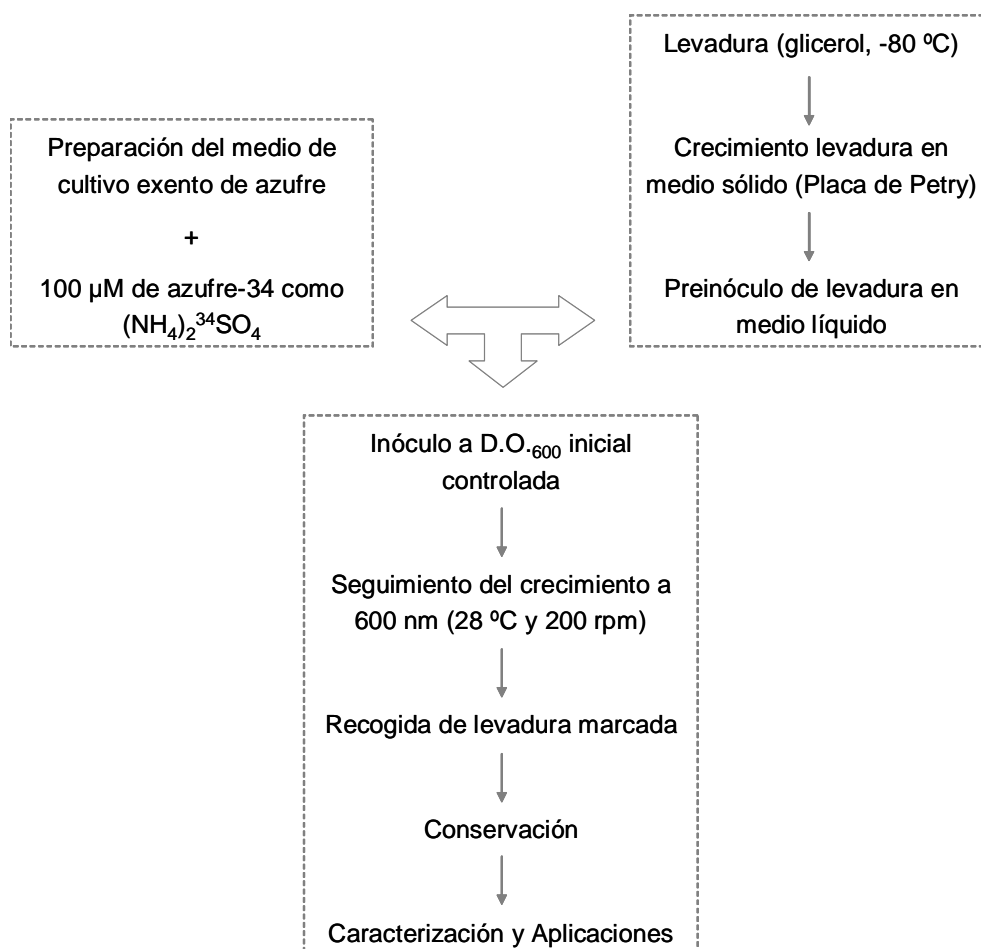


Figura 33. Resumen del procedimiento de preparación de levadura marcada con azufre-34.

Para ello, una cantidad conocida de S₃₄ en forma de sulfato de amonio se añadió a una disolución nutritiva de crecimiento de la levadura (*i.e.* medio de cultivo) preparado específicamente en nuestro laboratorio, exento de azufre de abundancia

natural con objeto de obtener un enriquecimiento máximo en azufre-34. La levadura marcada se caracterizó tanto en composición isotópica como en concentración total de azufre en el ICP-MS multicolector, tras una digestión ácida asistida por microondas. La composición isotópica final medida fue 6,73%; 0,45% y 92,82% para ^{32}S , ^{33}S y ^{34}S respectivamente. Como se puede deducir, algo de azufre natural estaba todavía presente durante el crecimiento de la levadura (algunas vitaminas contienen azufre y también las células originales). Sin embargo, un enriquecimiento de 92,82% en azufre-34 debería ser suficiente para llevar a cabo experimentos con trazadores en animales de laboratorio. La concentración total de azufre en la levadura marcada, expresada como μg de azufre por gramo de levadura seca, se determinó mediante IDA utilizando azufre natural (682 ± 10) o utilizando azufre-33 (677 ± 10) como trazadores para la cuantificación. También se determinó mediante IPD teniendo en cuenta ambos trazadores enriquecidos (677 ± 11). Los tres procedimientos utilizados para la cuantificación proporcionaron valores de concentración estadísticamente idénticos.

Un parámetro muy importante a evaluar en la levadura marcada es la presencia de azufre-34 en forma de cisteína y metionina libres o enlazados a proteínas que los contengan. En este sentido y con el objetivo de desarrollar metodologías de análisis para una caracterización más completa de la levadura marcada con azufre-34, en el **artículo científico IV** se evaluaron diferentes estrategias analíticas mediante HPLC-ICP-MS para la cuantificación de biomoléculas que contienen azufre. En primer lugar, se evaluó la capacidad de realizar una calibración independiente del compuesto (CIC) en cada uno de los cuatro equipos ICP-MS utilizados en este estudio (*i.e.* cuadrupolo sin celda trabajando en condiciones de plasma frío, con celda utilizando O_2 como gas de reacción, doble enfoque con detección simple y multicolector). La CIC es una técnica cuantitativa basada en la capacidad de determinadas fuentes espectroquímicas (p.e. plasmas) de proporcionar una respuesta elemental independiente de la estructura química de las moléculas que contienen al elemento a cuantificar. Bajo ciertas condiciones, la respuesta elemental del ICP-MS puede ser directamente proporcional a la cantidad absoluta del elemento introducido. Por tanto, y a diferencia de las técnicas de espectrometría de masas molecular, la señal es independiente de la naturaleza del compuesto. En general, la influencia de la naturaleza de las especies en ICP-MS es pequeña o inapreciable, pero este hecho no se puede asumir y debe ser comprobado, particularmente cuando se utilizan estándares inorgánicos para la cuantificación de biomoléculas [249]. Para ello, se prepararon disoluciones que contenían una mezcla de los compuestos de azufre siguientes: sulfato, cisteína, glutatión y metionina, a diferentes niveles de

concentración (desde 20 ng·g⁻¹ hasta 20 µg·g⁻¹) y se inyectaron en el sistema HPLC-ICP-MS. Para realizar una separación adecuada de estos cuatro compuestos de azufre, se utilizó una cromatografía en fase reversa con un 0,3% de HFBA como agente formador de pares iónicos [250] y un 2% de metanol en la fase móvil, trabajando en modo isocrático a pH 2,5 (ver Figura 34).

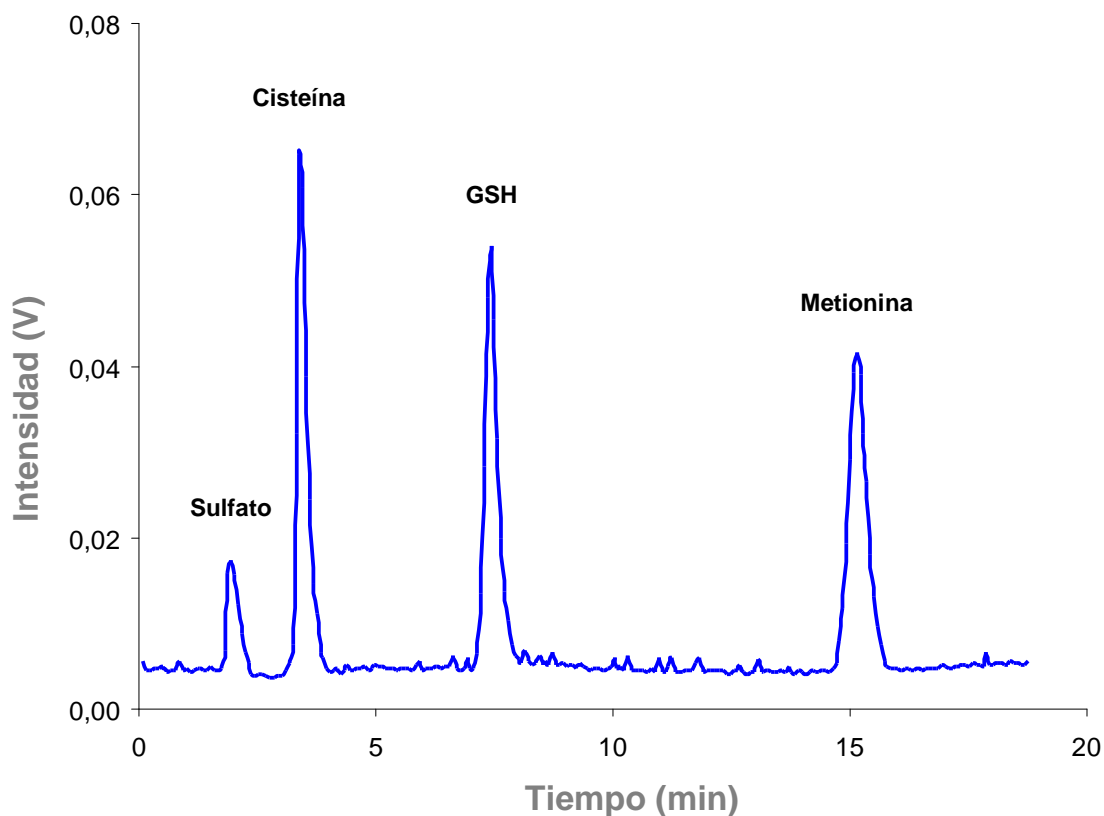


Figura 34. Separación cromatográfica en modo isocrático de los compuestos de azufre sulfato, cisteína, glutatión y metionina detectados por ICP-MS multicolector.

En estas condiciones se observó que para los cuatro equipos ICP-MS utilizados la respuesta analítica (*i.e.* área de pico cromatográfico) frente a la concentración de azufre elemental se ajustaba perfectamente a una recta de calibrado ($r^2 > 0,999$) y por tanto era claramente independiente del compuesto (sulfato, cisteína, glutatión y metionina) dependiendo únicamente de la cantidad total de azufre presente en cada compuesto. De esta manera, se demostró que la CIC se puede aplicar para separaciones cromatográficas en modo isocrático, lo que nos permite cuantificar de forma directa proteínas o péptidos sin derivatización previa utilizando un patrón interno adecuado. Así, se utilizaron estándares inorgánicos de sulfato para el estudio y optimización de las condiciones de hidrólisis de proteínas. Además, se demostró de

esta manera la idoneidad del trazador inespecífico de azufre-33 en forma de sulfato inorgánico para realizar el análisis por dilución isotópica post-columna, ya que la respuesta instrumental para los estándares de sulfato era idéntica que para el resto de estándares de compuestos de azufre ($r^2 > 0,999$), insistiendo otra vez en el hecho de que, bajo las condiciones experimentales estudiadas, la respuesta analítica en el ICP-MS depende únicamente de la cantidad de azufre presente y no de la forma química en la que se encuentre.

En segundo lugar y dado que la eficiencia en la ionización del azufre en la fuente ICP depende de la naturaleza del disolvente utilizado, se comparó, en condiciones de elución en modo gradiente, la estrategia de CIC frente al análisis por dilución isotópica post-columna. La inmensa mayoría de las separaciones por HPLC de péptidos y proteínas en muestras biológicas utilizan gradientes de disolventes orgánicos [251] y por tanto la respuesta de los compuestos que eluyen inicialmente puede ser diferente de la observada en los péptidos y proteínas que eluyen más tarde. En nuestro caso se observó que cuando se trabaja con gradientes de disolventes orgánicos, se producen cambios importantes en la sensibilidad del equipo, y es necesario el uso de IDA post-columna (dichos cambios afectarán en la misma extensión a los isótopos empleados del mismo elemento, por lo que no afectarán a la relación isotópica), ya que utilizando la CIC, incluso en condiciones de gradientes suaves ($2\% \cdot \text{min}^{-1}$ hasta 14% MeOH), se cometieron errores superiores al 10% en la cuantificación exacta de metionina. Sin embargo, los resultados muestran que el uso de IDA con azufre-33 como trazador post-columna se puede emplear para cuantificar de forma absoluta los compuestos de azufre que eluyen de la columna cromatográfica, incluso cuando se trabaja en modo gradiente, al permitir corregir las variaciones en la sensibilidad instrumental y la deriva de la señal. Además, la capacidad inherente de cuantificar especies de estructura desconocida sin la necesidad de utilizar un estándar enriquecido específico para realizar la calibración metodológica, convierte esta estrategia en una herramienta versátil y poderosa para la determinación de péptidos y proteínas en matrices biológicas.

Finalmente, para la caracterización de la levadura marcada con azufre-34, se desarrolló un procedimiento basado en el análisis por dilución isotópica post-columna en combinación con la deconvolución de perfiles isotópicos (IPD) con objeto de separar los perfiles isotópicos de azufre de abundancia natural y azufre-34 enriquecido. Esta tercera estrategia obedeció a que cuando la muestra a analizar contiene composiciones isotópicas de azufre no naturales, como las que se encuentran en los experimentos con trazadores metabólicos, las ecuaciones

tradicionales de la dilución isotópica post-columna [115] no se pueden aplicar. La composición isotópica de los diferentes compuestos de azufre detectados en la muestra puede variar dependiendo de su ruta metabólica. Por tanto, es necesario desarrollar ecuaciones alternativas. En los últimos años, se ha estado aplicando en nuestro grupo de investigación un procedimiento matemático denominado IPD, que es capaz de extraer información sobre las fracciones molares de cada isótopo a partir de las abundancias medidas en el ICP-MS, aislando los diferentes perfiles isotópicos de abundancia natural y de trazadores enriquecidos de una mezcla dada [252]. Para el azufre se pueden medir hasta tres isótopos por ICP-MS (^{32}S , ^{33}S , y ^{34}S). Como utilizamos dos trazadores diferentes marcados isotópicamente, S34 como trazador metabólico y S33 como trazador post-columna para cuantificar, y el flujo másico de azufre-33 post-columna es conocido y las abundancias de cada uno de los isótopos de azufre se miden perfectamente en el ICP-MS, aplicando la ecuación del IPD a cada punto del cromatograma [253], se obtiene inmediatamente el flujo molar de las especies separadas por cromatografía tanto de azufre natural como de azufre-34.

Los resultados obtenidos tras analizar un extracto proteico mediante HPLC-ICP-MS demostraron que la mayor parte del azufre presente en la levadura lo está en forma orgánica y con un enriquecimiento isotópico para el azufre-34 superior al 90% (ver Figura 35). Este hecho es relevante para la realización de estudios en animales de laboratorio utilizando como trazador metabólico la levadura marcada con azufre-34. La combinación del procedimiento de marcaje metabólico (S34) con el procedimiento de IPD post-columna (S33) constituye la base de la metodología cuantitativa desarrollada en esta Tesis Doctoral para estudios de metabolismo de azufre.

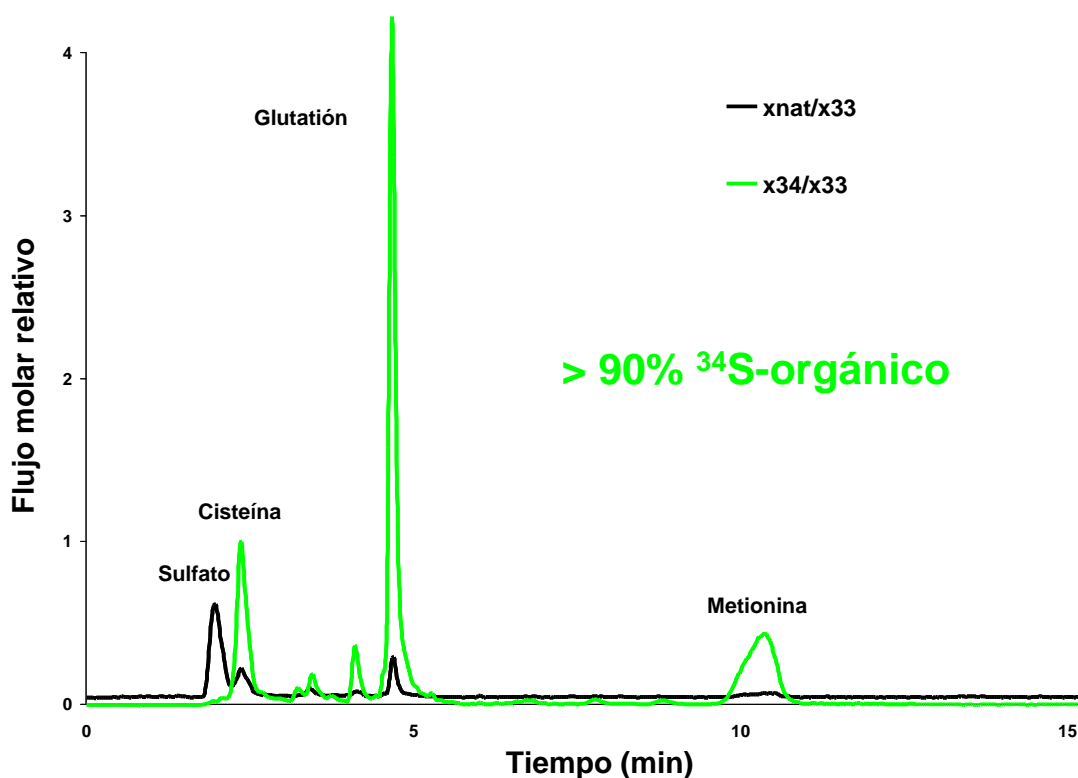


Figura 35. Análisis de un extracto proteico de levadura marcada isotópicamente con azufre-34 mediante HPLC-ICP-MS.

Como punto final de nuestras investigaciones, se abordó la posibilidad de realizar estudios del metabolismo del azufre en animales de laboratorio utilizando isótopos estables enriquecidos, tercer objetivo específico de la presente Tesis Doctoral. Para ello, los resultados obtenidos en los **artículos científicos I y II** fueron muy informativos, estando en consonancia con los publicados por Clough y col. para el estudio de variaciones isotópicas de azufre en muestras de agua mineral embotellada [76], donde la variabilidad natural de la composición isotópica de azufre estaba comprendida entre -12 y +22‰. En nuestros trabajos se encontró un rango de variación más estrecho, entre -0,2 y +13,8‰ para las muestras de cerveza y únicamente 9 unidades en las muestras de pelo humano analizadas.

Si nos basamos en estos datos, se puede calcular la cantidad mínima de trazador metabólico de azufre-34 que será necesaria para un experimento. Por ejemplo, si se asume que aproximadamente el 0,25% de la composición química elemental en el organismo es azufre y del azufre total aproximadamente el 70% estará enlazado a proteínas, un animal de laboratorio pequeño (p.e. una rata Wistar de 100 g) tendrá aproximadamente 0,175 g de azufre proteico. Por tanto, la administración de una dosis única de 1 mg de azufre-34 en forma de levadura marcada isotópicamente,

como la preparada y caracterizada previamente en los **artículos científicos III y IV**, debería cambiar la relación isotópica $^{34}\text{S}/^{32}\text{S}$ del azufre en las proteínas de 0,045 a 0,051, lo que se corresponde con un valor de $\delta^{34}\text{S}$ de aproximadamente +100. Este cambio es mucho más grande que la variabilidad natural esperada para el azufre y además es el mínimo cambio esperado ya que se calcula asumiendo que el azufre enriquecido se incorporará a todas las proteínas del organismo. Como esto es realmente improbable, ya que el organismo no pone en juego todo su azufre de abundancia natural (p.e. proteínas cuya tasa de recambio es muy lenta) cabe esperar que, utilizando esta cantidad de trazador metabólico, el enriquecimiento isotópico del azufre en ciertas proteínas sea fácilmente detectable.

De esta manera, se realizaron los experimentos que se recogen en el **artículo científico V**. En primer lugar, fue necesaria la preparación de un nuevo lote de levadura marcada con azufre-34, dado que para la realización de los estudios previos la levadura marcada se había preparado en tubos de 50 mL y por tanto la cantidad obtenida a pequeña escala no era suficiente para poder llevar a cabo los estudios con animales de laboratorio. Con objeto de obtener una cantidad importante del trazador metabólico, se aumentó la escala de la preparación de la levadura marcada utilizando volúmenes de 2.000 mL, lo que permitió preparar un lote de 15 gramos con un enriquecimiento de 64,5% en azufre-34. Desafortunadamente, se produjo una contaminación significativa con azufre de abundancia natural procedente del reactivo adenina utilizado para fortificar el nuevo medio de cultivo utilizado durante la elaboración de la levadura.

Una vez preparado el nuevo lote de levadura marcada con azufre-34 y previo a su utilización como trazador metabólico en animales de laboratorio, se simuló una digestión gastrointestinal *in vitro*. En una primera aproximación, se comprobó el perfil de las proteínas de la levadura marcada antes y después de la digestión mediante SDS-PAGE. Como se puede observar en la Figura 36, las bandas presentes en el extracto de proteínas de la levadura (calle 1) desaparecen en ambos hidrolizados, tanto en el de la digestión gástrica (calle 2) como en el de la digestión gastrointestinal (calle 3). Únicamente se aprecian las bandas correspondientes a las enzimas añadidas para simular la digestión.

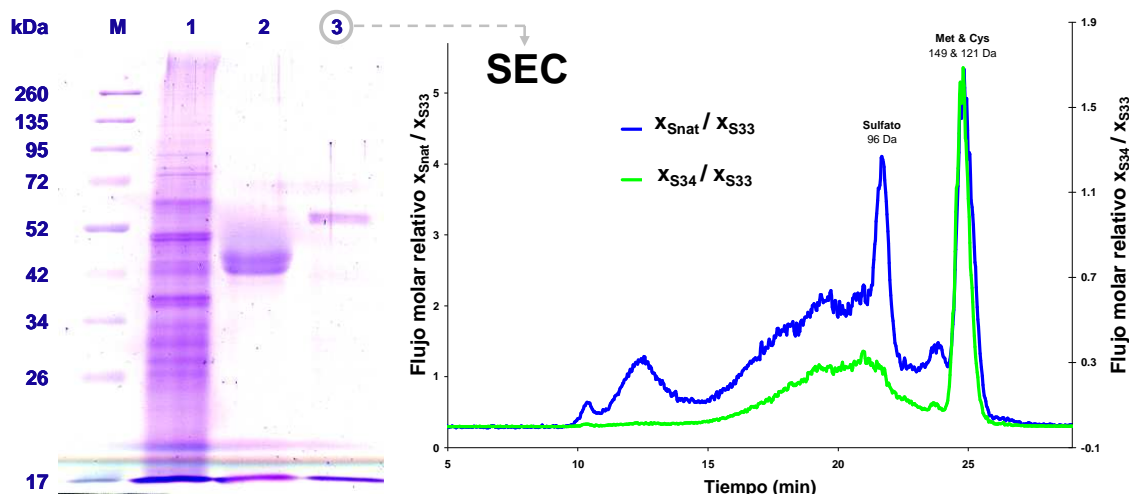


Figura 36. Estudios *in vitro* de digestión gastrointestinal de la levadura marcada con azufre-34 mediante SDS-PAGE y HPLC-ICP-MS.

Estos resultados sugieren la adecuada digestibilidad de las proteínas de la levadura, degradándose a pequeños péptidos y aminoácidos libres, lo que nos permite postular su adecuada absorción e incorporación en mamíferos. Adicionalmente, se llevó a cabo la separación de estas biomoléculas utilizando cromatografía líquida de exclusión por tamaños empleando una columna cromatográfica con un rango óptimo de separación comprendido entre 100 y 7.000 Da. El cromatograma obtenido mediante SEC-ICP-MS para una alícuota del hidrolizado gastrointestinal se muestra en la Figura 36. Como se podía prever, la mayoría del azufre está presente en la levadura en forma orgánica, por lo que las cisteínas y metioninas enriquecidas en azufre-34 procedentes de la digestión de la levadura marcada se deberían incorporar a las proteínas de los animales que las ingieran.

Para verificar esta hipótesis, se realizó un pequeño estudio piloto *in vivo* en la Unidad de Laboratorio Animal de la Universidad de Oviedo utilizando la levadura marcada con azufre-34 como trazador metabólico. Básicamente, a un grupo de cinco ratas Wistar macho se les administró una dosis única de levadura marcada con azufre-34. A continuación se extrajeron los órganos de cada una de las ratas Wistar objeto de estudio (bazo, cerebro, corazón, hígado, intestino delgado, páncreas, pulmón, riñón y testículo) a diferentes tiempos de muestreo (6, 12, 24, 48 y 96 horas) después de la administración de la levadura marcada. De esta manera, se puede estudiar la eficacia de absorción, la acumulación y la cinética del metabolismo del azufre utilizando las metodologías desarrolladas en la presente Tesis Doctoral. En la Figura 37 se recogen los resultados obtenidos mediante DF-ICP-MS con detección simple para los diferentes órganos analizados de las ratas Wistar alimentadas con levadura marcada

con azufre-34. Los valores se representan como relaciones trazador/trazado basadas en las fracciones molares calculadas para S34 (X_{S34}) y Snat (X_{Snat}) mediante IPD (ver procedimientos experimentales). Como se puede observar, se detectó un pequeño enriquecimiento en S34 en todos los tejidos analizados. De esta manera, aunque está fuera del objetivo de este estudio entrar a discutir en detalle el metabolismo del azufre, se pone de manifiesto la posibilidad de obtener resultados metabólicos relevantes utilizando las metodologías desarrolladas en la presente Tesis Doctoral. Asimismo, se determinó la composición isotópica del azufre total en las muestras de orina y heces recogidas de las jaulas metabólicas con el fin de estudiar la cinética de excreción del trazador metabólico (Figura 38). El mayor enriquecimiento se detectó en las heces lo que implica que una gran proporción de S34 no fue absorbida. El enriquecimiento isotópico en orina fue similar al encontrado en los tejidos y disminuyó rápidamente indicando que, tras la absorción, el S34 fue eliminado del organismo de forma veloz.

Una vez demostrado que es posible detectar *in vivo* el enriquecimiento isotópico inducido a través de la levadura marcada, el siguiente paso fue estudiar la forma química en la que está presente el S34 y para ello se utilizó la metodología híbrida HPLC-ICP-MS. Para realizar este estudio se seleccionaron las muestras de suero y orina de las ratas Wistar alimentadas con levadura marcada con azufre-34. Hoy en día, la determinación de péptidos y proteínas en estos fluidos biológicos por técnicas de espectrometría de masas presenta una importancia capital como medio de diagnóstico para la detección, identificación y cuantificación de biomarcadores asociados con estados tanto de salud como de enfermedad [254-256]. Por ejemplo, niveles elevados en suero del antígeno prostático específico (PSA) y del antígeno carbohidrato 125 (CA 125) se utilizan de forma rutinaria para la detección de cáncer de próstata y ovario, respectivamente [257]. Asimismo, está documentado el uso del análisis de orina para el establecimiento de nuevos biomarcadores de diagnóstico de enfermedades renales [258,259] y no renales [260,261].

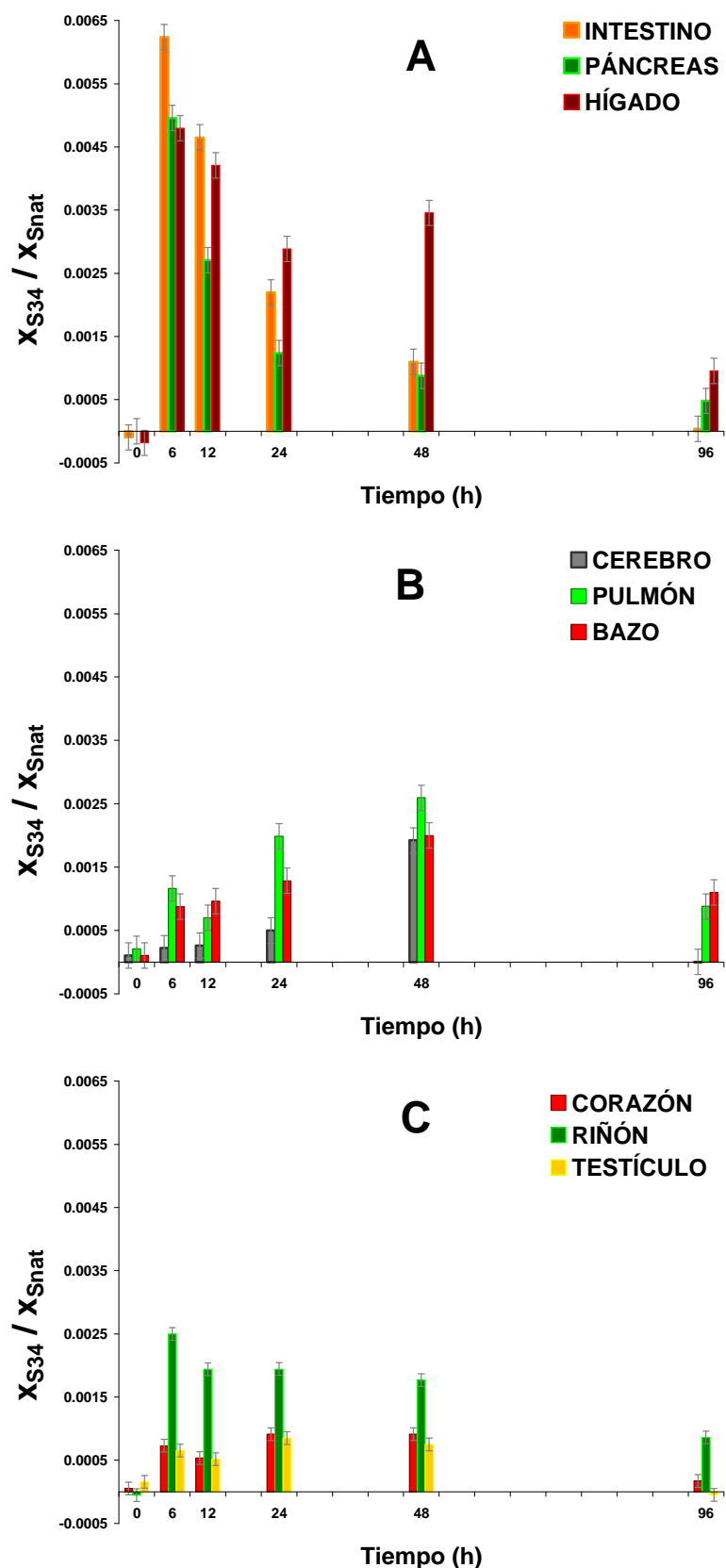


Figura 37. Valores de la relación X_{S34}/X_{Snat} en los tejidos de las ratas Wistar alimentadas con levadura marcada con azufre-34 obtenidos mediante DF-ICP-MS con detección simple.

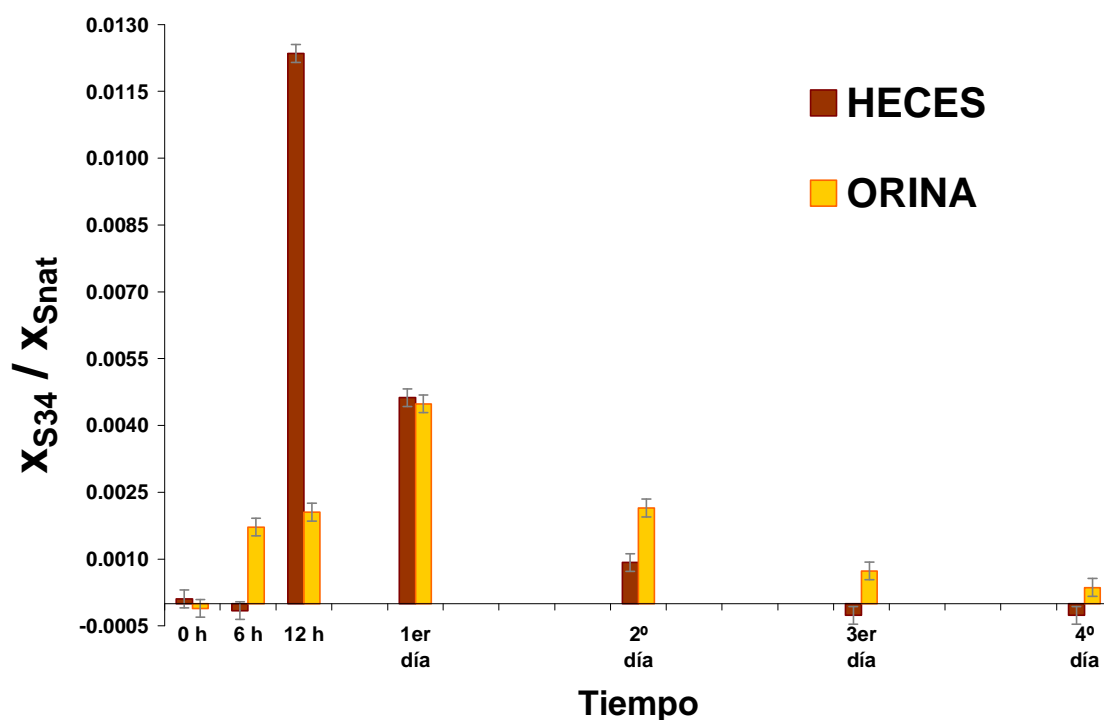


Figura 38. Valores de la relación X_{S34}/X_{Snat} en los productos de desecho (heces y orina) de las ratas Wistar alimentadas con levadura marcada con azufre-34 obtenidos mediante DF-ICP-MS con detección simple.

El análisis del suero constituye un reto analítico debido al intervalo tan alto de concentraciones (más de 10 órdenes de magnitud) de proteínas y péptidos que se encuentra en este fluido biológico, desde la albúmina ($35\text{-}50\text{ mg}\cdot\text{mL}^{-1}$) a la interleucina-6 ($0,5\text{ pg}\cdot\text{mL}^{-1}$) [262]. La mayoría de estas biomoléculas son secretadas a la sangre desde las células y los tejidos y por tanto la determinación de la información histológica contenida en el suero puede ser utilizada para mejorar la detección precoz de enfermedades. Algunas proteínas mayoritarias como la albúmina, inmunoglobulinas, haptoglobinas, antitripsina y transferrina constituyen típicamente más del 90% de la masa total proteica y consecuentemente estas proteínas dominantes pueden interferir en la detección de péptidos o proteínas minoritarias que son de especial interés para el descubrimiento de biomarcadores [263]. De hecho, estas proteínas, péptidos y otras biomoléculas pequeñas que constituyen sólo el 1% del contenido proteico de suero han sido asociadas con determinadas patologías como cáncer, diabetes y enfermedades cardiovasculares e infecciosas [264,265]. Por consiguiente, antes de realizar la inyección en el sistema HPLC-ICP-MS, las muestras de suero se separaron en dos fracciones diferentes mediante la técnica de ultracentrifugación-filtración: proteínas de alto peso molecular (HMW) y bajo peso

molecular (LMW). Las variables más críticas para la eliminación exitosa de las proteínas más abundantes junto con el enriquecimiento de las proteínas/péptidos de bajo peso molecular en suero cuando se utiliza la técnica de ultracentrifugación-filtración son las velocidades de centrifugación, el uso de muestra diluida así como condiciones de desnaturización de la muestra [266]. De este modo, se evaluó la cromatografía líquida de exclusión por tamaños para separar en sus diferentes componentes las fracciones HMW y LMW del suero, empleando columnas cromatográficas con rangos de separación de 10-600 kDa y 100-7.000 Da respectivamente. Al igual que ocurrió para las muestras de tejidos, heces y orina, fue posible detectar el enriquecimiento isotópico inducido a través de la levadura marcada con azufre-34. En general, la relación trazador/trazado expresada como X_{S34}/X_{Snat} encontrada en suero en ambas fracciones varía con el tiempo presentando un máximo a las 6 horas (0,009-0,008) ligeramente superior que el encontrado en los órganos al mismo tiempo de muestreo. Esta relación disminuyó rápidamente por debajo de 0,004 en ambas fracciones de una manera similar al de las muestras de tejidos. A partir de los datos generados para las muestras de suero mediante HPLC-ICP-MS, no se observó un enriquecimiento preferente en ninguna de las dos fracciones HMW y LMW, por lo que no fue posible obtener resultados concluyentes.

A diferencia de la sangre, cuya toma de muestra es invasiva y requiere un meticuloso pretratamiento de la misma, el muestreo de orina es realmente sencillo. Sin embargo, la orina como matriz es uno de los fluidos biológicos más complejos. El rango de concentraciones de péptidos y proteínas en orina cubre varios órdenes de magnitud. La concentración de proteínas en la orina es muy inferior que en el plasma sanguíneo (60 mg·mL⁻¹ aprox.) de tal manera que un individuo adulto sano puede excretar aproximadamente 50-70 g de sólidos por día en la orina de los cuales 50-120 mg corresponden a proteína [267]. La albúmina también es una proteína dominante en la orina. A pesar de su reabsorción desde el filtrado glomerular en el tubo proximal renal, esta proteína se excreta fisiológicamente en cantidades no superiores a 30 mg·día⁻¹ [268]. Un problema adicional consiste en los cambios de volumen relacionados con cambios en la concentración y composición salina que puede variar ampliamente.

Con el objetivo de realizar un tratamiento de las muestras lo más sencillo posible, la orina únicamente se clarificó y se inyectó directamente en el sistema HPLC-ICP-MS. Para la separación de las biomoléculas que contienen azufre presentes en las muestras de orina se evaluaron una cromatografía líquida de exclusión por tamaños (100-7.000 Da) y una en fase reversa. El perfil cromatográfico obtenido mediante SEC-

ICP-MS fue similar al derivado de la fracción LMW del suero, con tres picos principales que presentan un enriquecimiento isotópico similar. La relación trazador/trazado expresada como X_{S34}/X_{S33} encontrada en orina fue siempre inferior a 0,008. Al igual que para las muestras de suero, no se observó un enriquecimiento preferente por lo que no fue posible obtener resultados concluyentes a partir de los datos generados por las muestras de orina mediante SEC-ICP-MS. Finalmente, el perfil cromatográfico de la separación por fase reversa de los compuestos de azufre presentes en las muestras de orina clarificadas se muestra en la Figura 39.

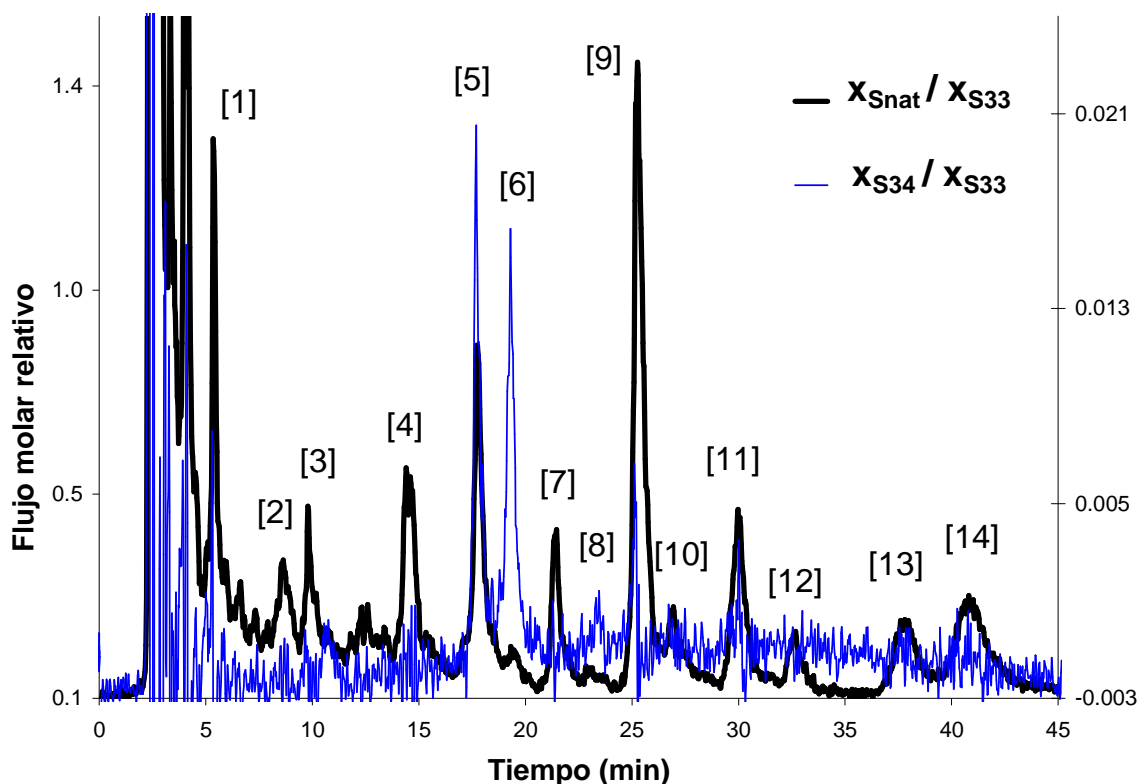


Figura 39. Análisis de orina de una rata Wistar alimentada con levadura marcada con azufre-34 mediante HPLC-ICP-MS (fase reversa).

Como se puede observar en la Figura 39, el perfil cromatográfico obtenido muestra un buen número de picos bien resueltos que corresponden a biomoléculas que contienen azufre en su estructura. Para evaluar la relación trazador/trazado expresada como X_{S34}/X_{S33} en orina se seleccionaron un total de 15 picos cromatográficos (el azufre eluido en cabeza de columna más otros 14 picos). Esta relación se determinó para cada uno de los tiempos de muestreo evaluados y se representó en un diagrama de barras recogido en la Figura 40.

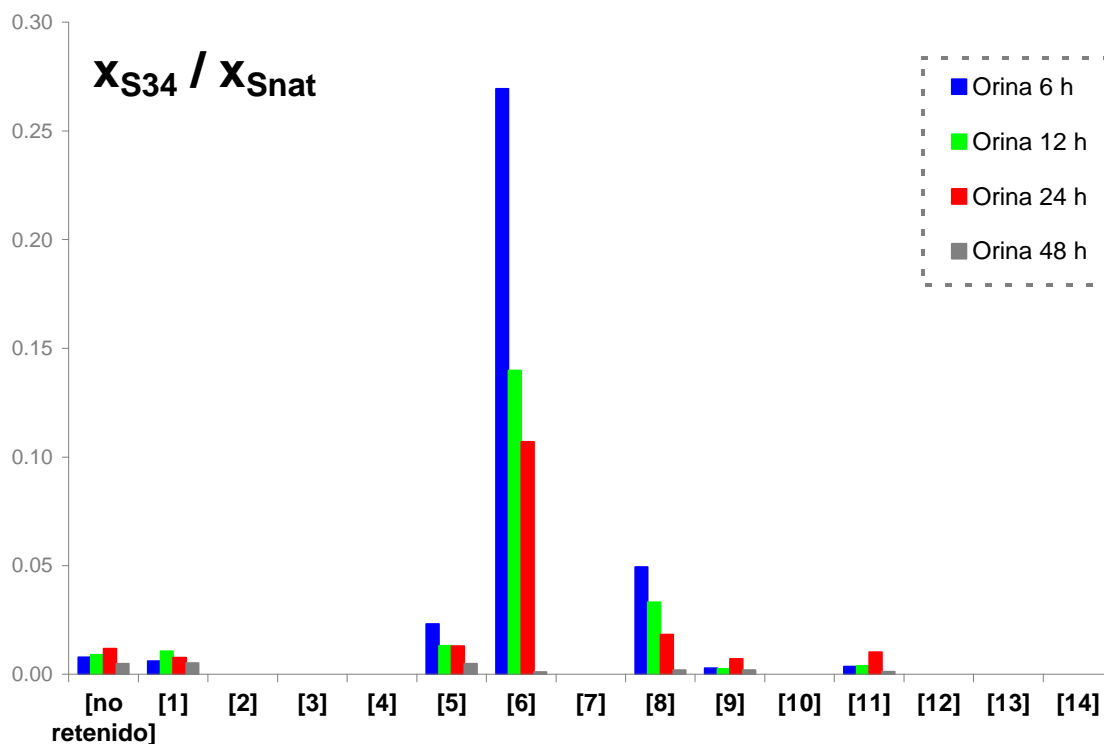


Figura 40. Diagrama de barras de la relación X_{S34}/X_{Snat} detectada en las muestras de orina de ratas Wistar sanas alimentadas con levadura marcada con azufre-34.

A la vista de los resultados obtenidos, se detectó un enriquecimiento isotópico diferencial en las muestras de orina para algunas biomoléculas que contienen azufre (especialmente importante para el compuesto 6). La relación trazador/trazado para este compuesto particular a las 6 h tras la administración de la levadura marcada con azufre-34 fue de 0,270, lo que implica un valor mucho más elevado que el observado para los tejidos e incluso para las heces (0,012). Asimismo se detectó un enriquecimiento isotópico significativo para los picos cromatográficos 1, 5, 8, 9 y 11. En estos dos últimos picos (9 y 11) el máximo enriquecimiento isotópico se observó a las 24 h mientras que para los otros el enriquecimiento máximo se estableció a las 6 y 12 h. De esta manera, se podría exponer que los picos 5, 6 y 8 se corresponden con metabolitos primarios derivados de la levadura marcada con azufre-34 ingerida (quizás metionina y cisteína) mientras que los picos 1, 9 y 11 se corresponden a metabolitos secundarios formados tras la degradación de péptidos o proteínas donde la metionina o cisteína marcadas con azufre-34 habían sido previamente incorporadas.

F.CONCLUSIONES / CONCLUSIONS



Las principales conclusiones derivadas de la presente Tesis Doctoral se pueden resumir en los siguientes puntos:

1. Se ha desarrollado un procedimiento directo para la medida de la variabilidad natural de la composición isotópica de azufre en muestras de cerveza mediante ICP-MS multicolector. Se ha demostrado que el procedimiento de corrección interna de los efectos de matriz utilizando silicio para la medida de relaciones isotópicas de azufre es efectivo en muestras complejas que contienen gran cantidad de materia orgánica disuelta. Los resultados obtenidos en las 26 cervezas estudiadas se expresaron en notación delta relativos a la escala V-CDT, observándose un rango de variación comprendido entre -0,2 y +13,8‰ con una incertidumbre expandida asociada menor del 2‰. La metodología desarrollada permite determinar la variabilidad natural del azufre y podría ser de gran utilidad para la protección de marcas en el campo de autenticidad de bebidas y alimentos utilizando la huella dactilar de azufre.
2. Se ha desarrollado una metodología analítica que permite realizar la medida de variaciones naturales en la composición isotópica de azufre a lo largo de un cabello mediante un sistema de ablación láser acoplado a un ICP-MS multicolector. Los resultados obtenidos nos han permitido estimar la variabilidad natural de las relaciones isotópicas de azufre así como la cantidad mínima de trazador metabólico de azufre-34 que se necesita para poder realizar estudios de metabolismo del azufre utilizando trazadores estables en animales de laboratorio. Asimismo, a raíz de estas investigaciones se abre la posibilidad de utilizar la medida de variaciones isotópicas de azufre en una sola muestra de cabello mediante LA-MC-ICP-MS como un indicador de los movimientos geográficos de un individuo y/o cambios en la dieta.
3. Se han preparado y caracterizado dos trazadores isotópicos de azufre (S33 y S34) mediante ICP-MS multicolector y se ha evaluado el método de la deconvolución de perfiles isotópicos para la determinación simultánea de concentración y composición isotópica de azufre total en muestras biológicas.
4. Se ha preparado levadura marcada isotópicamente con azufre-34 en un medio de cultivo exento de azufre de abundancia natural, con objeto de obtener un enriquecimiento máximo en azufre-34. La levadura marcada se caracterizó tanto en composición isotópica (92,82% en azufre-34) como en concentración total de azufre (700 µg de azufre por gramo de levadura) mediante ICP-MS multicolector.

5. Se han evaluado diferentes estrategias analíticas para la cuantificación de biomoléculas que contienen azufre mediante HPLC-ICP-MS. En primer lugar, se ha demostrado en cuatro equipos ICP-MS diferentes que la calibración independiente del compuesto se puede aplicar para separaciones cromatográficas en modo isocrático, lo que permite cuantificar, a través de la monitorización de azufre, aminoácidos organoazufrados, péptidos y/o proteínas sin derivatización previa utilizando un patrón interno adecuado.
6. Se ha demostrado que el análisis por dilución isotópica utilizando azufre-33 como trazador post-columna se puede emplear para cuantificar de forma absoluta los compuestos de azufre que eluyen de la columna cromatográfica, incluso cuando se trabaja en modo gradiente, lo que convierte esta estrategia en una herramienta versátil y poderosa para la determinación, a través de la monitorización de azufre, de aminoácidos organoazufrados, péptidos y/o proteínas en matrices biológicas. Además, la capacidad inherente de cuantificar especies de estructura desconocida sin la necesidad de utilizar un estándar enriquecido específico para realizar la calibración metodológica, convierten esta estrategia en ideal para su aplicación en estudios metabólicos.
7. Se ha evaluado el método de la deconvolución de perfiles isotópicos para la determinación simultánea de concentración y composición isotópica de azufre en señales transitorias. La metodología desarrollada permite obtener información cuantitativa de las especies individuales presentes en un pico cromatográfico junto con el enriquecimiento isotópico de cada especie y se ha aplicado a la caracterización de levadura marcada con azufre-34. Los resultados obtenidos tras analizar un extracto proteico mediante HPLC-ICP-MS demostraron que la mayor parte del azufre presente en la levadura lo está en forma orgánica y con un enriquecimiento isotópico para el azufre-34 superior al 90%.
8. Se ha simulado *in vitro* una digestión gastrointestinal de la levadura marcada con azufre-34 y el hidrolizado se ha caracterizado mediante SDS-PAGE y HPLC-ICP-MS. Los resultados obtenidos sugieren la adecuada digestibilidad de las proteínas de la levadura, degradándose a pequeños péptidos y aminoácidos libres, lo que nos permite postular su adecuada absorción e incorporación en mamíferos. De esta manera, las cisteínas y metioninas enriquecidas en azufre-34 procedentes de la digestión de la levadura marcada serán presumiblemente incorporadas a las proteínas, lo que conducirá a una

abundancia de azufre-34 alterada, que podría ser detectada con las metodologías analíticas desarrolladas en esta Tesis Doctoral.

9. Se han realizado estudios con trazadores estables de azufre en animales de laboratorio utilizando levadura marcada con azufre-34. Se ha detectado un pequeño enriquecimiento en S34 en todos los tejidos (bazo, cerebro, corazón, hígado, intestino delgado, páncreas, pulmón, riñón y testículo) y en los productos de desecho (heces y orina) de ratas Wistar sanas alimentadas con levadura marcada con azufre-34. De una manera similar, se ha detectado el enriquecimiento isotópico inducido *in vivo* a través de la levadura marcada con azufre-34 en las fracciones HMW y LMW del suero y en la orina de ratas Wistar sanas.
10. El análisis mediante fase reversa HPLC-ICP-MS de las muestras de orina de las ratas Wistar sanas alimentadas con levadura marcada con azufre-34 ha mostrado un perfil cromatográfico con un buen número de picos bien resueltos. Se ha detectado un enriquecimiento isotópico diferencial para algunas biomoléculas que contienen azufre en su estructura.
11. Finalmente, se puede concluir que a lo largo de la presente Tesis Doctoral se han desarrollado metodologías analíticas para el estudio del metabolismo del azufre utilizando isótopos estables enriquecidos. En particular, la combinación del enriquecimiento isotópico en azufre-34 (utilizando S34 como trazador metabólico en forma de levadura) y la cuantificación absoluta de biomoléculas (utilizando S33 como trazador de cuantificación) mediante HPLC-ICP-MS se podría establecer como una estrategia alternativa en estudios metabólicos de compuestos que contengan azufre en su estructura.

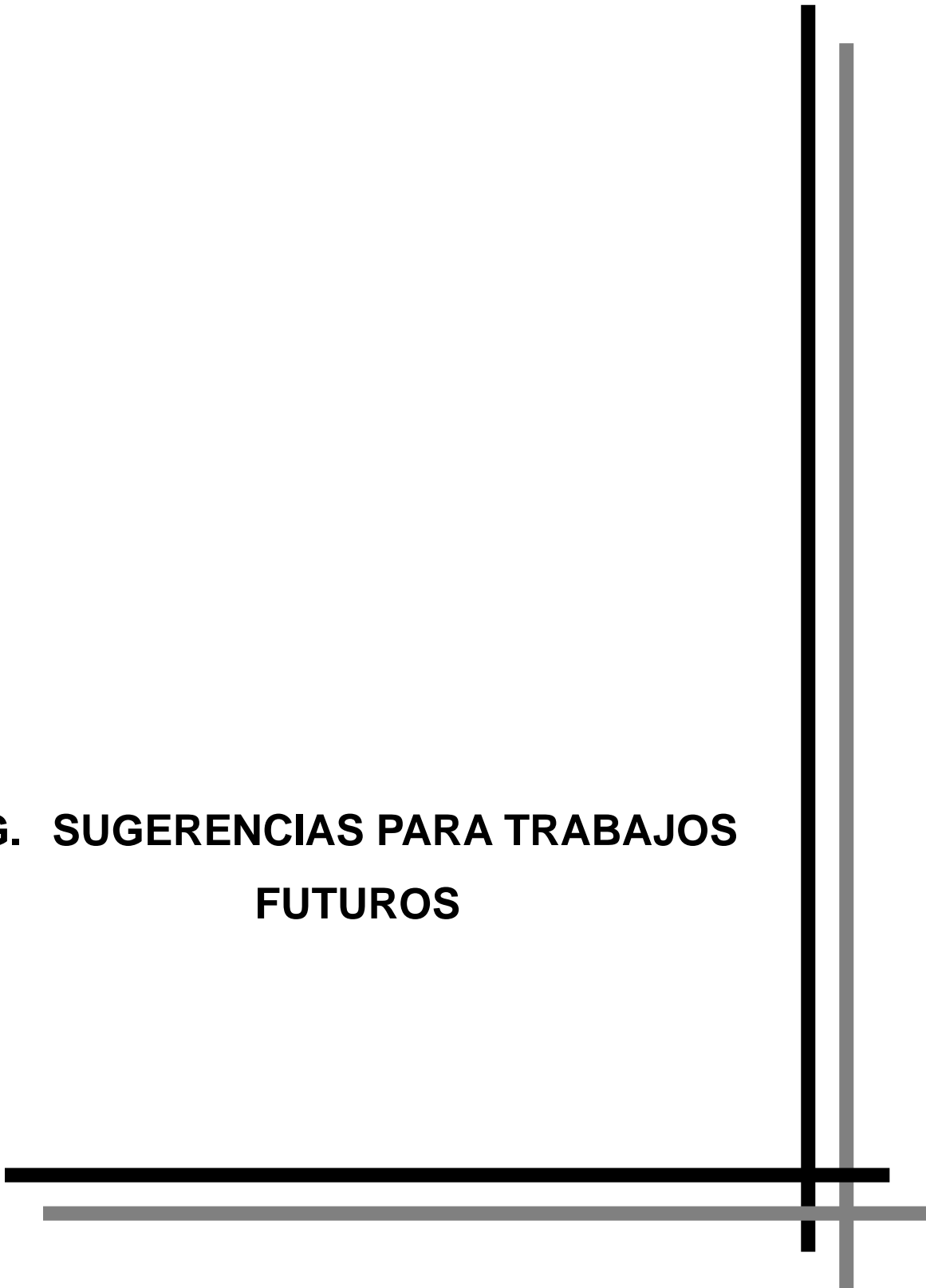
The main conclusions that can be extracted from the present Ph.D. Thesis could be summarized through the following stages:

1. A direct procedure for the measurement of sulfur isotope variability in beer samples by multicollector ICP-MS has been developed. It has been demonstrated that matrix effects on differential sulfur ions transmission could be corrected adequately using silicon internal standardization in samples containing large amounts of dissolved organic matter. The natural isotope variability of sulfur has been evaluated by measuring 26 different beer brands. Measured $\delta^{34}\text{S}_{\text{V-CDT}}$ values ranged from -0.2 to +13.8‰ with typical combined standard uncertainties $\leq 2\%$. The method has therefore great potential to study sulfur isotope variability in foods and beverages.
2. A method for the measurement of longitudinal variations of sulfur isotope ratios in single hair strands using a laser ablation system coupled to a multicollector ICP-MS has been developed. Based on the results obtained, we could calculate the natural variability of sulfur isotope composition in hair samples and the minimum amount of S34 which would be needed for a metabolic tracer experiment using enriched stable sulfur isotopes in laboratory animals. Additionally, sulfur isotopic variations measured in human hair strands could potentially aid prediction of geographical origin and recent movements of subjects or provide information on diet and lifestyle.
3. Two different sulfur spike solutions (S33 and S34) have been characterised with reference to a natural abundance sulfur standard solution by multicollector ICP-MS and the isotope pattern deconvolution approach for the simultaneous determination of natural abundance and ^{34}S -labelled sulfur using the ^{33}S -labelled sulfur as reference has been evaluated.
4. Yeast labelled with sulfur-34 has been prepared by yeast growth on a ^{34}S -enriched, specially prepared, culture medium in the absence of natural abundance sulfur. The final product has been characterised both in isotope composition (92.82% enriched in sulfur-34) and total sulfur concentration (700 μg of sulfur per gram of dry weight of yeast) by multicollector ICP-MS.
5. Different analytical strategies for the quantification of sulfur-containing biomolecules by HPLC-ICP-MS have been evaluated. First of all, compound independent calibration has been demonstrated in four different ICP-MS instruments for isocratic elution allowing the direct quantification of sulfur-

- containing amino acids, peptides and/or proteins without derivatization *via* the determination of sulfur using a suitable internal standard.
6. It has been proved that isotope dilution analysis using S33 as post-column tracer is suitable for the absolute quantification of sulfur-containing compounds eluting from the separation column, even when gradient elution is performed, which makes this strategy a versatile and powerful tool to quantify sulfur-containing amino acids, peptides and/or proteins in complicated biological matrices. Moreover, the inherent capability of quantifying species of unknown structure without the need of using species-specific standards for a methodological calibration makes this methodology an ideal strategy for its application in sulfur metabolism studies.
 7. A procedure based on post-column isotope pattern deconvolution was developed for the simultaneous determination of concentration and isotope composition of sulfur in single compounds rather than in the total element and it has been applied to the characterisation of ^{34}S -labelled yeast. The quantitative results obtained for the protein extract by HPLC-ICP-MS have demonstrated that most of the sulfur is present in yeast in organic form and with isotope enrichment for ^{34}S higher than 90%.
 8. An *in vitro* gastrointestinal digestion of the ^{34}S -labelled yeast has been simulated and the corresponding hydrolysate has been characterised by SDS-PAGE and HPLC-ICP-MS techniques. The results obtained strongly suggest an adequate digestibility of the proteins of the yeast, breaking down to small peptides and free amino acids, and allow us to postulate its further absorption and incorporation. Therefore, ^{34}S -labelled methionines and cysteines coming from the digestion of the labelled yeast will be probably incorporated *in vivo* into proteins, and hence leading to an altered isotope composition of sulfur-containing biomolecules that could be detected using the analytical methodologies that have been developed in this Ph.D. Thesis.
 9. Sulfur stable tracer experiments in laboratory animals using ^{34}S -labelled yeast have been performed. A small S34 enrichment has been detected in all tissues (brain, heart, intestine, kidney, liver, lung, pancreas, spleen and testicle) and in excretion products (faeces and urine) of healthy Wistar rats fed with ^{34}S -labelled yeast by single collector ICP-MS. In a similar way, induced isotopic enrichment has been detected *in vivo* for both HMW and LMW fraction of serum and urine samples by SEC-ICP-MS.

10. Reversed phase HPLC-ICP-MS analysis in urine samples of healthy Wistar rats fed with ^{34}S -labelled yeast has shown a chromatographic profile with a large number of well resolved sulfur-containing peaks. Differential isotope enrichment for several sulfur-containing biomolecules has been detected.
11. Finally, it can be concluded that throughout the present Ph.D. Thesis novel analytical methodologies for the study of sulfur metabolism using enriched stable isotopes have been developed. In particular, the combination of ^{34}S -isotopic enrichment (using S34 as metabolic tracer in the form of yeast) and absolute quantification (using S33 as quantification tracer) after HPLC-ICP-MS could be an alternative strategy for protein turnover or other sulfur-related metabolism studies.

**G. SUGERENCIAS PARA TRABAJOS
FUTUROS**



A partir de los resultados obtenidos a lo largo de la presente Tesis Doctoral y considerando las conclusiones expuestas en el apartado anterior, es posible sugerir algunas líneas de investigación futura, entre las que destacan las siguientes:

1. El procedimiento directo desarrollado para la medida de la variabilidad natural de la composición isotópica de azufre en muestras de cerveza mediante ICP-MS multicolector se podría utilizar para realizar un estudio más completo y general sobre la variabilidad en la composición isotópica de azufre en bebidas. Además se podría extender su aplicación a alimentos previa digestión ácida de las muestras sólidas.
2. La medida de variaciones isotópicas de azufre en una sola muestra de cabello mediante la metodología híbrida LA-MC-ICP-MS podría ser utilizada como un indicador de los movimientos geográficos de un individuo. En este sentido, uno de los primeros pasos sería la creación de una base de datos que se obtendría midiendo las relaciones isotópicas de azufre en una muestra significativa de individuos con diferente dieta y origen geográfico. La información contenida en esta base de datos o mapa mundial de azufre podría combinarse con la información obtenida con otras técnicas más convencionales de modo que pudiera en el futuro convertirse en una herramienta más al servicio de los laboratorios de ensayos químicos y en especial de los de la policía científica.
3. En nuestras investigaciones se utilizó en todos los casos células de una cepa silvestre de la levadura *Saccharomyces cerevisiae*. La concentración total de azufre encontrada en la levadura marcada con azufre-34 fue de 700 µg de azufre por gramo de levadura seca. De esta manera, en trabajos futuros sería muy interesante evaluar la posibilidad de obtener una levadura modificada genéticamente que sobreexpresara alguna proteína con un elevado número de aminoácidos organoazufrados (cisteínas y/o metioninas) para que el contenido total de azufre en la nueva levadura fuera muy superior.
4. A partir de la levadura marcada con azufre-34, se podría llevar a cabo la separación y purificación de (bio)compuestos marcados en azufre-34 (aminoácidos, péptidos, proteínas, etc.) cuya accesibilidad por síntesis química presentaría una mayor dificultad. Estos (bio)compuestos marcados con azufre-34 se podrían utilizar como patrones específicos para realizar la cuantificación de estas mismas especies con abundancia

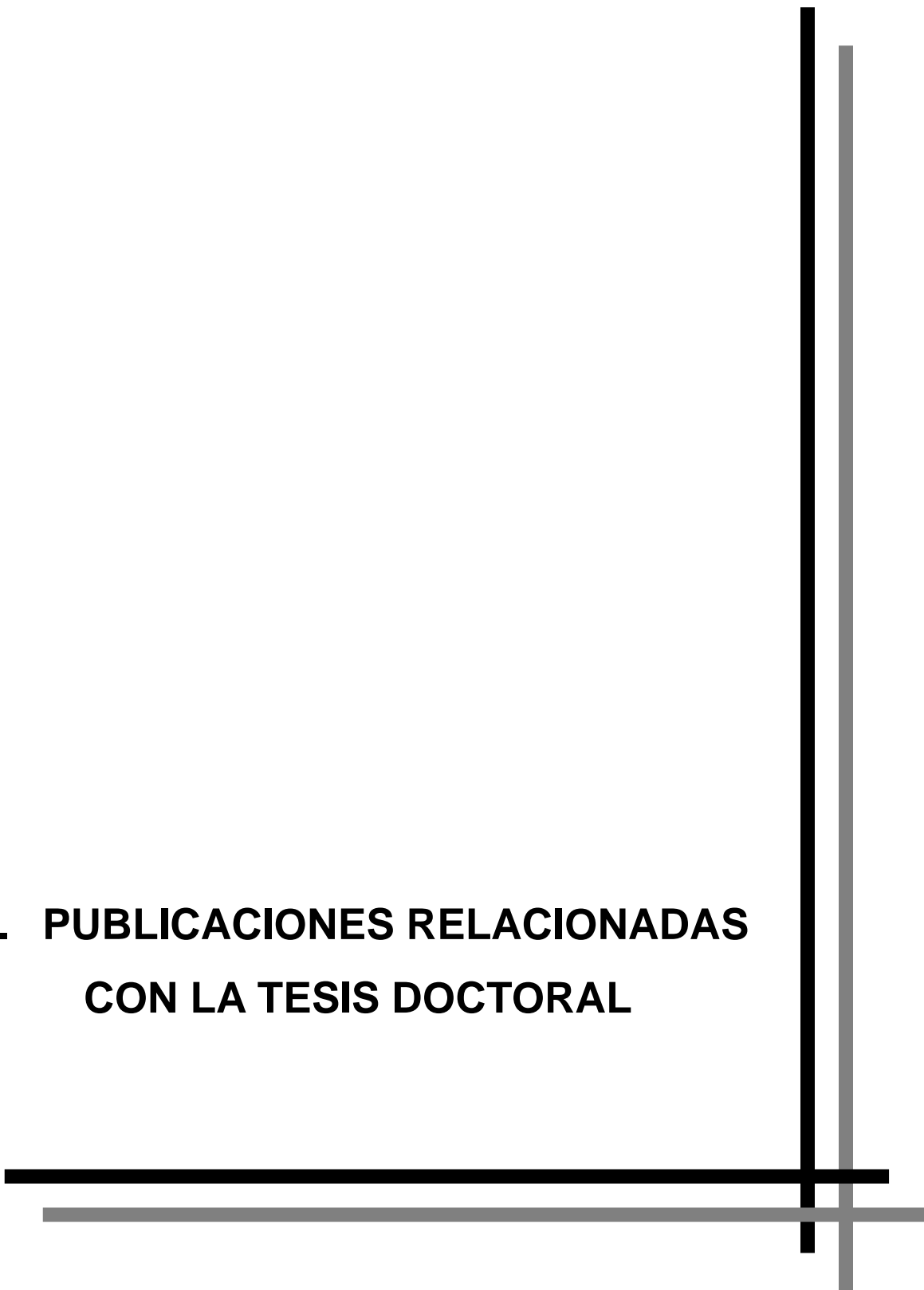
isotópica natural en matrices complejas mediante el análisis por dilución isotópica específica, pudiendo resultar de gran utilidad para la certificación de materiales de referencia y la realización de ejercicios de intercomparación.

5. Por otro lado, resultaría muy interesante evaluar las prestaciones analíticas de un nuevo equipo ICP-MS multicolector que ha sido recientemente instalado en los Servicios Científico Técnico de la Universidad de Oviedo. Este instrumento está equipado específicamente con tres contadores de iones en las posiciones L4-C-H4 lo que permitiría la medida precisa de las abundancias de los tres isótopos de azufre (^{32}S - ^{33}S - ^{34}S) a niveles de concentración muy bajos.
6. El análisis mediante fase reversa HPLC-ICP-MS de las muestras de orina de las ratas Wistar sanas alimentadas con levadura marcada con azufre-34 ha mostrado un perfil cromatográfico con un buen número de picos bien resueltos. Sin embargo, es evidente que se debe profundizar en la mejora de la separación cromatográfica, particularmente para resolver la fracción mayoritaria que eluye en cabeza de columna. El empleo de una cromatografía bidimensional podría resultar muy adecuado en este sentido.
7. El análisis mediante fase reversa HPLC-ICP-MS de las muestras de orina de las ratas Wistar sanas alimentadas con levadura marcada con azufre-34 demuestra el potencial de esta metodología para su aplicación en la búsqueda de nuevos biomarcadores de enfermedades. En trabajos futuros se podría mejorar el enriquecimiento isotópico inducido de los potenciales biomarcadores utilizando una mayor cantidad de levadura marcada con azufre-34 con un enriquecimiento isotópico mayor (>90% azufre-34). Una alternativa interesante para realizar los estudios *in vivo* sería emplear ratones comunes (*Mus musculus*) en lugar de ratas Wistar (*Rattus norvegicus*) ya que son animales de laboratorio más pequeños, con aproximadamente 30 g de peso en la edad adulta.
8. Dado que el ICP-MS no proporciona información estructural de la (bio)molécula de estudio, sería muy adecuado realizar la identificación de los potenciales biomarcadores mediante un análisis adicional, normalmente llevado a cabo con técnicas de espectrometría de masas

molecular, previo aislamiento de la fracción cromatográfica correspondiente.

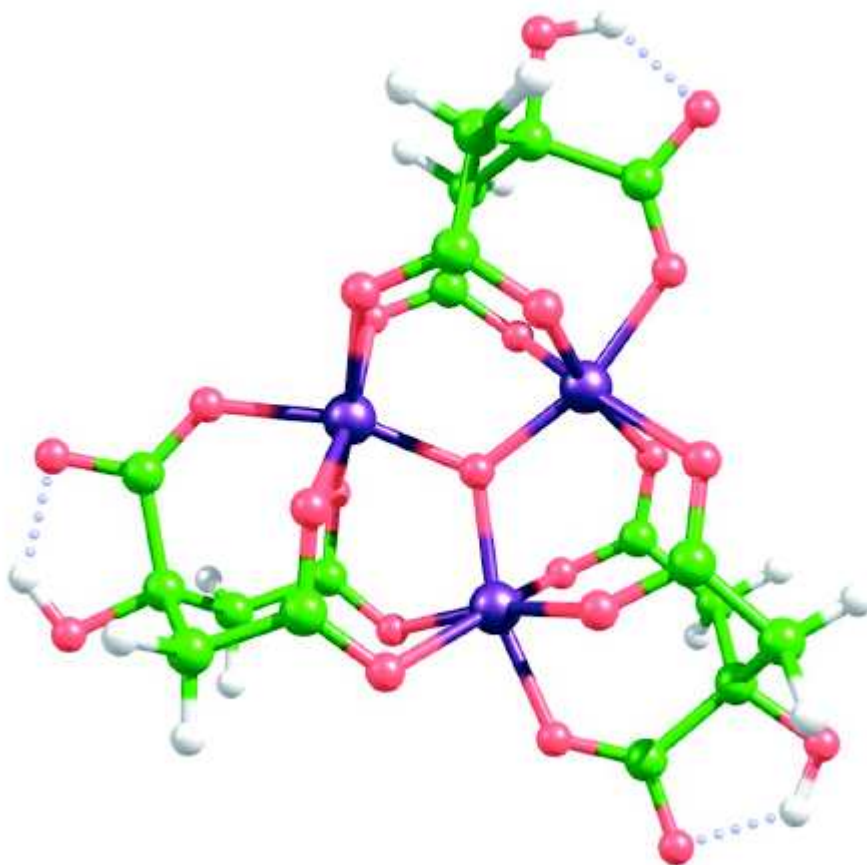
9. Tras establecer la naturaleza de las (bio)moléculas que han presentado un enriquecimiento diferencial en animales de laboratorio sanos, se podrían realizar experimentos similares utilizando levadura marcada con azufre-34 como trazador metabólico y azufre-33 post-columna como trazador de cuantificación con animales de laboratorio (ratas Wistar o ratones) en los que se habrían generado de forma artificial distintos tipos de enfermedades. Se podrían comparar los resultados obtenidos mediante la metodología híbrida HPLC-ICP-MS entre los animales de laboratorio sanos y enfermos. Para ello se deberían elaborar curvas de enriquecimiento isotópico y curvas de concentración para cada potencial biomarcador, aprovechando la doble información proporcionada por la metodología cuantitativa propuesta. La identificación de los potenciales biomarcadores se podría llevar a cabo con técnicas de espectrometría de masas molecular.
10. Por último, en función de los resultados encontrados utilizando los modelos animales, se podrían extender los estudios a seres humanos dada la nula toxicidad de la levadura enriquecida en azufre-34. De esta manera, idealmente se podría desarrollar un nuevo ensayo clínico utilizando isótopos estables enriquecidos de azufre.

**H. PUBLICACIONES RELACIONADAS
CON LA TESIS DOCTORAL**



H.1. ESTUDIOS DEL METABOLISMO DEL HIERRO UTILIZANDO ISÓTOPOS ESTABLES ENRIQUECIDOS

H.1.1. Artículo científico VI: *Plant Cell Physiol.*, 2010, 58, 91-102



Identification of a Tri-Iron(III), Tri-Citrate Complex in the Xylem Sap of Iron-Deficient Tomato Resupplied with Iron: New Insights into Plant Iron Long-Distance Transport

Rubén Rellán-Álvarez¹, Justo Giner-Martínez-Sierra², Jesús Orduna³, Irene Orera¹, José Ángel Rodríguez-Castrillón², José Ignacio García-Alonso², Javier Abadía^{1,*} and Ana Álvarez-Fernández¹

¹Department of Plant Nutrition, Aula Dei Experimental Station, CSIC, PO Box 13034, E-50080 Zaragoza, Spain

²Department of Physical and Analytical Chemistry, University of Oviedo, c/Julian Clavería 8, E-33006 Oviedo, Spain

³New Organic Materials Unit, Institute of Materials Science of Aragón, CSIC-University of Zaragoza, c/Pedro Cerbuna 12, E-50009 Zaragoza, Spain

*Corresponding author: E-mail, jabadia@eead.csic.es; Fax, +34-976716145

(Received September 24, 2009; Accepted November 18, 2009)

The identification of Fe transport forms in plant xylem sap is crucial to the understanding of long-distance Fe transport processes in plants. Previous studies have proposed that Fe may be transported as an Fe–citrate complex in plant xylem sap, but such a complex has never been detected. In this study we report the first direct and unequivocal identification of a natural Fe complex in plant xylem sap. A tri-Fe(III), tri-citrate complex (Fe_3Cit_3) was found in the xylem sap of Fe-deficient tomato (*Solanum lycopersicum* Mill. cv. 'Tres Cantos') resupplied with Fe, by using an integrated mass spectrometry approach based on exact molecular mass, isotopic signature and Fe determination and retention time. This complex has been modeled as having an oxo-bridged tri-Fe core. A second complex, a di-Fe(III), di-citrate complex was also detected in Fe–citrate standards along with Fe_3Cit_3 , with the allocation of Fe between the two complexes depending on the Fe to citrate ratio. These results provide evidence for Fe–citrate complex xylem transport in plants. The consequences for the role of Fe to citrate ratio in long-distance transport of Fe in xylem are also discussed.

Keywords: Iron deficiency • Iron-citrate • Mass spectrometry • Xylem sap • Iron transport.

Abbreviations: B3LYP, hybrid density functional method; DFT, density functional theory; ESI-MS, electrospray ionization-mass spectrometry; EXAFS, extended X-ray absorption fine structure; HILIC, hydrophilic interaction liquid chromatography; HPLC, high performance liquid chromatography; IDA, isotope dilution analysis; IPD, isotope pattern deconvolution; LOD, limits of detection; NA, nicotianamine; Q-ICP-MS, quadrupole-inductively coupled plasma-mass spectrometry; TOF, time of flight; XANES, X-ray absorption near edge structure; SXRF, synchrotron X-ray fluorescence.

This paper is dedicated to the memory of Dr. Arthur Wallace, a pioneer in the study of plant iron nutrition.

Introduction

The mechanisms of long-distance Fe transport in plants have remained elusive until now. In the case of xylem sap, Fe is assumed to be transported as complexed forms, because free ionic forms [Fe(II) and Fe(III)] can be toxic and are also prone to undergo precipitation at the neutral or slightly acidic pH values typical of xylem sap. Increases in carboxylate concentrations in plant xylem exudates with Fe deficiency were reported in several papers published in the 1960s by Brown and co-workers. Iron was first suggested to be transported bound to malate (Tiffin and Brown 1962), but later citrate (Cit), which also increases markedly in stem exudates of many plant species when Fe-deficient (Brown 1966) and co-migrates with Fe during paper electrophoresis (Tiffin 1966a, Tiffin 1966b, Tiffin 1970, Clark et al. 1973), was considered the most likely candidate for Fe transport.

The identity of Fe–Cit complexes in the xylem sap has only been hypothesized by means of *in silico* calculations using total concentrations of possible Fe complexing agents (including carboxylates) and Fe, and the known stability constants of Fe-containing complexes, always assuming that chemical equilibrium was achieved. Using this approach, several Fe–Cit species were predicted to be the most abundant Fe complexes in the xylem sap whereas other potential plant metal chelators such as nicotianamine (NA) were ruled out (von Wirén et al. 1999, Rellán-Álvarez et al. 2008) as possible xylem Fe carriers. NA function as an Fe chelator might be restricted to the cytoplasm and in Fe phloem loading (Curie et al. 2008). Citrate recently has been found by using molecular biology techniques to play a role in long-distance Fe transport. Xylem sap loading

Plant Cell Physiol. 51(1): 91–102 (2010) doi:10.1093/pcp/pcp170, available online at www.pcp.oxfordjournals.org

© The Author 2009. Published by Oxford University Press on behalf of Japanese Society of Plant Physiologists.

All rights reserved. For permissions, please email: journals.permissions@oxfordjournals.org

of Cit is seriously disrupted in two mutants, AtFRD3 (Durrett *et al.* 2007) and OsFRDL1 (Yokosho *et al.* 2009). These mutants display increased Fe-deficiency symptoms that have not been associated with decreased efficiency of Fe translocation into the root vasculature.

Fe–Cit chemistry in aqueous solutions is very complex and a large number of chemical species may occur, depending on many factors (Spiro *et al.* 1967a, Spiro *et al.* 1967b, Pierre and Gautier-Luneau 2000, Gautier-Luneau *et al.* 2005). Direct proof of the presence of Fe–Cit complexes in xylem sap has not been obtained so far. Difficulties in detecting Fe–Cit species in xylem sap may arise for different reasons. First, both pH and Fe: Cit ratio values are known to affect markedly Fe–Cit speciation in standard aqueous solutions (Gautier-Luneau *et al.* 2005). Therefore, when analysis is carried out at pH values too acidic or basic (e.g. during HPLC), the speciation of Fe–Cit complexes could change and species occurring in the original xylem sample may no longer be present after chromatography. Second, analytical techniques such as mass spectrometry (MS), which have been used successfully to identify other metal complexes in the xylem sap (Ouerdane *et al.* 2006, Xuan *et al.* 2006), usually involve ionization steps (with high temperatures and voltages) that may be too harsh for relatively labile compounds such as Fe–Cit complexes. Furthermore, in most plant species the total Fe concentration in the xylem sap is in the μM range, and consequently the concentrations of the possible Fe–Cit complexes are expected to be very low.

Molecular biology approaches have provided a breadth of information about metal, metal chelator and metal complex transporters (Briat *et al.* 2007, Kim and Guerinot 2007, Palmer and Guerinot 2009). However, the elucidation of the molecular identity of metal complexes in plant compartments is still one of the biggest challenges in plant metal transport (Hider *et al.* 2004). The molecular identification of metal complexes has been tackled by two different types of technique. First, the use of highly selective and sensitive molecular and metal-specific techniques such as integrated MS (Meija *et al.* 2006) has been used (Ouerdane *et al.* 2006, Xuan *et al.* 2006), especially in plant fluids (e.g. xylem or phloem) where direct analysis can be carried out. Second, X-ray absorption spectroscopy, extended X-ray absorption fine structure (EXAFS) and X-ray absorption near edge structure (XANES) (Sarret *et al.* 2002, Küpper *et al.* 2004) and synchrotron X-ray fluorescence (SXRF) (Punshon *et al.* 2009) techniques have been applied to study metal speciation in some plant materials. The combination of metal complex elucidation techniques and molecular biology approaches should give a better picture of plant metal transport.

In this study we have used HPLC coupled to electrospray time of flight mass spectrometry (HPLC–ESI–TOFMS) and inductively coupled plasma mass spectrometry (HPLC–ICP–MS) to detect naturally occurring Fe complexes in xylem sap. Analysis conditions were kept as conservative as possible in order to maintain unaltered natural Fe species occurring in the xylem sap. With this approach we have successfully identified a tri-Fe(III), tri-citrate complex (Fe_3Cit_3) in the xylem sap of

Fe-deficient tomato plants after short-term Fe resupply. This complex has been modeled as an oxo-bridged tri-Fe(III) tri-Cit complex. A second Fe–Cit complex, the binuclear Fe(III)–Cit species Fe_2Cit_2 , was only detected in Fe–Cit standard solutions along with the Fe_3Cit_3 complex, with the balance between the two complexes depending on the Fe: Cit ratio.

Results

Analysis of Fe–Cit standard solutions by integrated MS

A method to separate and identify Fe–Cit complexes was developed by analyzing Fe–Cit solutions with Fe and Cit concentrations, Fe: Cit ratios and pH values (5.5) typical of xylem sap, using HPLC and integrated MS (ESI–TOFMS and ICP–MS). In all experiments, ESI–TOFMS spectra were searched for any molecular ion having the characteristic Fe isotopic signatures, including molecular ions previously detected by ESI–MS in high concentration Fe–Cit solutions (100 mM Fe: 1 M Cit) (Gautier-Luneau *et al.* 2005). The four different Fe stable isotopes were determined in the HPLC–ICP–MS runs. The method to determine Fe–Cit complexes was designed by optimizing first the electrospray ionization conditions, and then developing appropriate HPLC separation conditions. Throughout this study we used ^{54}Fe , ^{57}Fe and ^{nat}Fe , the latter being Fe with the natural isotopic composition: 5.85, 91.75, 2.12 and 0.28% of ^{54}Fe , ^{56}Fe , ^{57}Fe and ^{58}Fe , respectively.

Electrospray ionization conditions for Fe–Cit complexes were optimized to avoid in-source fragmentation using direct injection of a 1:10 ^{nat}Fe –Cit solution (100 μM ^{nat}Fe). Optimal ESI values for capillary exit, skimmer 1 and hexapole RF voltages were -57.1 , -39.1 and 145.2 V , respectively. These values correspond to softer ESI conditions than those usually applied to low molecular weight analytes (in the 100–600 m/z range). In all conditions tested, citrate gave a strong signal at the $[\text{CitH}]^-$ mass-to-charge ratio (m/z) of 191.0 (Supplementary Fig. 1A, B; see inset for isotopic signature). With these soft conditions, a 10-fold increase in ionization efficiency was achieved for a m/z 366.4 signal that showed the characteristic isotopic signature of a double charged, three Fe atom-containing molecular ion. This signal can be assigned to the $[\text{Fe}(\text{III})_3\text{Cit}_3\text{H}]^{2-}$ molecular ion (Supplementary Fig. 1A, B; see inset for isotopic signature). Furthermore, a second molecular ion with the characteristic isotopic signature of a double charged, three Fe atom-containing molecular ion was detected at m/z 375.4 (Supplementary Fig. 1B; see inset for isotopic signature). This signal can be assigned to the $[\text{Fe}(\text{III})_3\text{OCit}_3\text{H}_3]^{2-}$ ion. The 9 m/z difference from $[\text{Fe}(\text{III})_3\text{Cit}_3\text{H}]^{2-}$ was assigned to correspond to a labile ligand such as aquo OH_2 , hydroxo OH^- or oxo O^{2-} (Gautier-Luneau *et al.* 2005). Both Fe–Cit molecular ions were previously reported to occur at neutral pH values and at similar Fe: Cit ratios (Gautier-Luneau *et al.* 2005). The relative intensities of the different peaks did not match those found by Gautier-Luneau *et al.* (2005), probably due to differences

in MS devices and solution pH values (at least one pH unit of difference). Conversely, signals at m/z 300.4 and 271.9 appeared under standard ESI conditions (**Supplementary Fig. 1A**) but they were significantly reduced after ESI optimization (**Supplementary Fig. 1B**), suggesting that they may correspond to in-source fragmentation products (mainly due to decarboxylation processes, very common in this kind of compound) of the Fe_3Cit_3 produced at higher voltage values.

HPLC separation conditions were also optimized to obtain a good separation of the Fe–Cit complexes from other matrix components (e.g. Cit) that could interfere in the ESI process. The range of HPLC options available was limited, since: (i) both Cit and Fe–Cit complexes are compounds with a high polarity; (ii) it is mandatory to maintain xylem sap-typical pH values during chromatography; (iii) the method must be suitable for ESI-TOFMS and ICP-MS detection. Different approaches, including several column types, elution programs and eluents—acetonitrile and methanol—were tested. The best results were obtained with a zwitterionic hydrophilic interaction column (ZIC-HILIC; Sequant), previously used to separate polar Fe compounds such as Fe(II)–NA, Fe(III)–deoxymugineic acid [Fe(III)–DMA] and

others (Xuan et al. 2006). Two parallel systems, an HPLC–ICP-MS and an HPLC–ESI-TOFMS, were used to gain knowledge about atomic and molecular identity, respectively. Experiments were carried out with ^{54}Fe –Cit and also with ^{nat}Fe –Cit.

HPLC–ICP-MS experiments were carried out using ^{54}Fe –Cit solutions ($100\ \mu\text{M } ^{54}\text{Fe}$:1 mM Cit) to avoid ^{nat}Fe background from the HPLC system, which could be significant when determining very low concentrations of Fe by ICP-MS. Iron-54 molar flow chromatograms showed only two well-defined Fe peaks at 32.1 and 38.3 min (**Fig. 1A**) that were also observed using UV detection (**Supplementary Fig. 2A**). Using ESI-TOFMS detection, only four molecular ions with characteristic ^{54}Fe isotopic signatures (see below for identification) were found in the chromatogram, two of them at 27.1 min (241.9 and 484.9 m/z) and two more at 32.9 min (363.4 and 372.4 m/z) (**Fig. 1B**), and a UV signal was also found for these peaks (**Supplementary Fig. 2B**). The 5-min differences in retention time between HPLC–ESI-TOFMS and HPLC–ICP-MS analyses are due to the different HPLC devices used (Waters and Agilent, respectively), as judged by the shift in UV detection traces (**Supplementary Fig. 2**). A 5 mM Cit solution was also injected

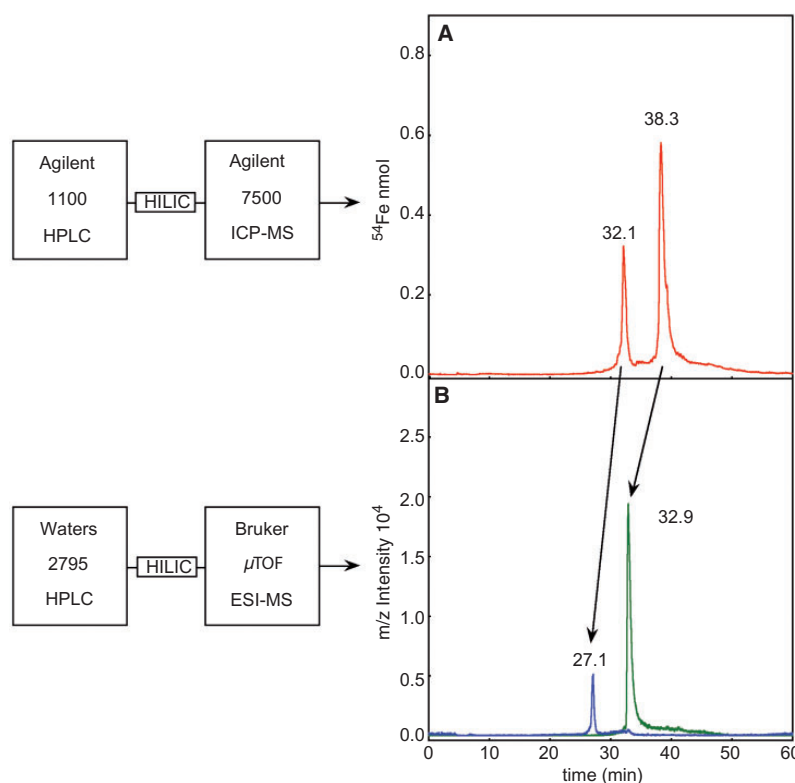


Fig. 1 HPLC–ICP-MS (A) and HPLC–ESI-TOFMS (B) chromatograms of a ^{54}Fe –Cit standard solution (Fe:Cit ratio 1:10, $100\ \mu\text{M } ^{54}\text{Fe}$, pH 5.5, in 50% mobile phase B) showing peaks corresponding to Fe complexes. HPLC–ESI-TOFMS traces (B) are the sum of molecular ions at m/z values 241.93 and 484.87 (± 0.05 ; blue line) and 363.40 and 372.40 (± 0.05 ; green line).

and no Fe–Cit complexes were found in the HPLC–ESI–TOFMS chromatogram, indicating that complexes found were not formed de novo during the chromatographic run.

With this HPLC method a complete separation of Fe–Cit complexes from Cit was reached, since Cit eluted as a broad peak at 5–9 min (m/z trace at 191.1, not included in Fig. 1B; Supplementary Fig. 3A). Other Fe complexes putatively occurring in plant tissues, such as Fe(III)–NA and Fe(III)–DMA, elute at retention times lower than 20 min (Supplementary Fig. 3B, C).

Identification of an Fe_2Cit_2 complex in Fe–citrate standard solutions

When using ^{54}Fe –Cit, the Fe peak at 27.1 min in HPLC–ESI–TOFMS, showed signals at m/z 241.9 and 484.9 (Fig. 1B) with Fe isotopic signatures characteristic of two ^{54}Fe atom-containing molecular ions, the first double charged (Fig. 2A, Table 1) and the second single charged (Supplementary Fig. 4A). Based on these exact mass and isotopic pattern data, the SigmaFit™ algorithm (Ojanperä et al. 2006) proposed $^{54}\text{Fe}_2\text{C}_{12}\text{H}_9\text{O}_{14}$ and $^{54}\text{Fe}_2\text{C}_{12}\text{H}_9\text{O}_{14}$ as the most accurate formulae, corresponding to the two Fe, two Cit molecular ions $[\text{Fe}(\text{III})_2\text{Cit}_2]^{2-}$ and $[\text{Fe}(\text{III})_2\text{Cit}_2\text{H}]^-$, respectively (Table 1); these molecular ions were previously found in concentrated Fe–Cit standards (Gautier-Luneau et al. 2005). The fit of the experimental and theoretical isotopic signatures of the $[\text{Fe}(\text{III})_2\text{Cit}_2]^{2-}$ molecular ion at m/z 241.9 is shown in Fig. 2A and B, respectively. A good fit was also found for the ion $[\text{Fe}(\text{III})_2\text{Cit}_2\text{H}]^-$ at m/z 484.9 (Supplementary Fig. 4A, B).

Further confirmation of the molecular identity of the Fe_2Cit_2 complex was obtained by analyzing $^{\text{nat}}\text{Fe}$ –Cit standard solutions by HPLC–ESI–TOFMS, taking advantage of the characteristic $^{\text{nat}}\text{Fe}$ isotopic signature. The Fe peak at 27.1 min in HPLC–ESI–TOFMS showed signals at m/z 243.9 and 488.9, characteristic of two $^{\text{nat}}\text{Fe}$ atom-containing molecular ions, the first double charged and the second single charged (Fig. 2C, Supplementary Fig. 4C, Table 1). The differences in m/z values found using ^{54}Fe and $^{\text{nat}}\text{Fe}$ (92% ^{56}Fe) were those expected for two Fe atom-containing molecular ions (2 and 4 m/z difference for a double and a single charged ion, respectively). The SigmaFit™ algorithm (Ojanperä et al. 2006) proposed $^{\text{nat}}\text{Fe}_2\text{C}_{12}\text{H}_{18}\text{O}_{14}$ and $^{\text{nat}}\text{Fe}_2\text{C}_{12}\text{H}_9\text{O}_{14}$ as the most accurate formulae corresponding to the molecular ions $[\text{natFe}_2\text{Cit}_2]^{2-}$ and $[\text{natFe}_2\text{Cit}_2\text{H}]^-$ (Table 1). The fit of the experimental and theoretical isotopic signatures of the $[\text{natFe}_2\text{Cit}_2]^{2-}$ molecular ion (for the ^{56}Fe signal at m/z 243.9) is shown in Fig. 2C and D, respectively. A good fit was also found for the molecular ion $[\text{natFe}_2\text{Cit}_2\text{H}]^-$ (for the ^{56}Fe signal at 488.9 m/z ; Supplementary Fig. 4C, D).

Identification of an Fe_3Cit_3 complex in Fe–citrate standard solutions

The Fe peak at 32.9 min in HPLC–ESI–TOFMS analysis of ^{54}Fe –Cit solutions (Fig. 1B) showed signals at m/z 372.4 and 363.4, with isotopic signatures characteristic of three ^{54}Fe atom-containing

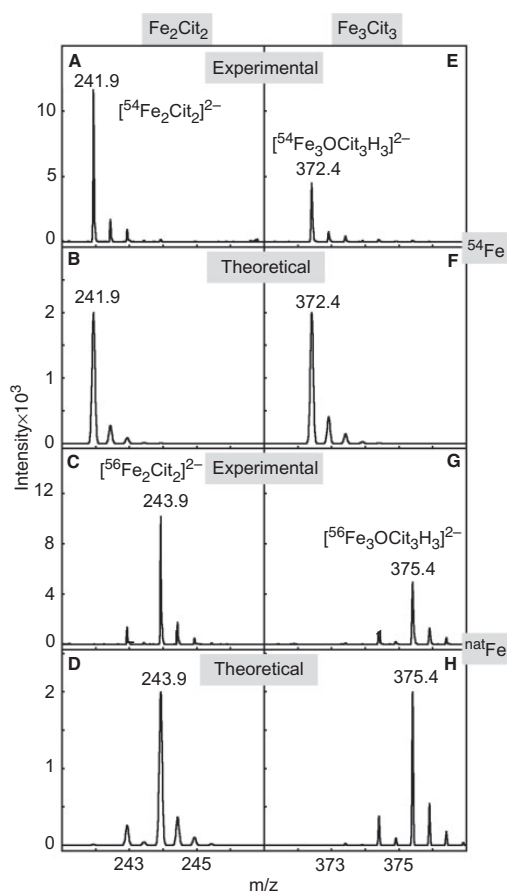


Fig. 2 Experimental (A, C, E, G) and theoretical (B, D, F, H) isotopic signatures of the molecular ions associated with Fe_2Cit_2 and Fe_3Cit_3 , $[\text{Fe}_2\text{Cit}_2]^{2-}$ and $[\text{Fe}_3\text{OCit}_3\text{H}_3]^{2-}$, respectively. Experimental data are zoomed ESI–TOF mass spectra of the Fe_2Cit_2 and Fe_3Cit_3 chromatographic peaks found when using ^{54}Fe (A, E) and $^{\text{nat}}\text{Fe}$ (C, G).

molecular ions, both of them double charged (Fig. 2E, Supplementary Fig. 4E, Table 1). The algorithm proposed $^{54}\text{Fe}_3\text{C}_{18}\text{H}_{15}\text{O}_{22}$ and $^{54}\text{Fe}_3\text{C}_{18}\text{H}_{13}\text{O}_{21}$ as the most accurate formulae, corresponding to the three Fe-, three Cit- molecular ions $[\text{Fe}_3\text{OCit}_3\text{H}_3]^{2-}$ and $[\text{Fe}_3\text{Cit}_3\text{H}]^{2-}$ (Table 1). The fit of the experimental and theoretical isotopic signatures of the $[\text{Fe}_3\text{OCit}_3\text{H}_3]^{2-}$ molecular ion at m/z 372.4 is shown in Fig. 2E and F, respectively. The same occurs with the ion $[\text{Fe}_3\text{Cit}_3\text{H}]^{2-}$ at m/z 363.4 (Supplementary Fig. 4E, F).

Further confirmation of the molecular identity of the Fe_3Cit_3 complex was obtained by analyzing $^{\text{nat}}\text{Fe}$ –Cit standard solutions. The peak at 32.9 min shows signals at m/z 375.4 and 366.4, characteristic of three $^{\text{nat}}\text{Fe}$ atom-containing molecular ions (Fig. 2G, Table 1); these values were 3 m/z higher than those found using ^{54}Fe . The algorithm proposed $^{\text{nat}}\text{Fe}_3\text{C}_{18}\text{H}_{15}\text{O}_{22}$ and

Table 1 Experimental ESI-TOFMS molecular ion data and parameters used to identify the molecular formulae of the Fe–Cit complexes in standard solutions and tomato xylem sap

Measured m/z	$^{56}\text{Fe}/^{54}\text{Fe}$ (Fe atoms) ^a	Charge ^b	Molecular formula	Calculated m/z	Error m/z (ppm)	SigmaFit™ value	Molecular ion
Standard solutions							
241.9362	–	–2	$^{54}\text{Fe}_2\text{C}_{12}\text{H}_8\text{O}_{14}$	241.9359	2.1	0.0234	$[\text{Fe}_2\text{Cit}_2]^{2-}$
484.8781	–	–1	$^{54}\text{Fe}_2\text{C}_{12}\text{H}_9\text{O}_{14}$	484.8790	1.8	0.0157	$[\text{Fe}_2\text{Cit}_2\text{H}]^-$
372.4119	–	–2	$^{54}\text{Fe}_3\text{C}_{18}\text{H}_{15}\text{O}_{22}$	372.4127	2.3	0.0273	$[\text{Fe}_3\text{OCit}_3\text{H}_3]^{2-}$
363.4068	–	–2	$^{54}\text{Fe}_3\text{C}_{18}\text{H}_{13}\text{O}_{21}$	363.4074	1.4	0.0106	$[\text{Fe}_3\text{Cit}_3]^{2-}$
243.9311	7.4 (2)	–2	$\text{natFe}_2\text{C}_{12}\text{H}_8\text{O}_{14}$	243.9311	1.7	0.0165	$[\text{natFe}_2\text{Cit}_2]^{2-}$
488.8705	7.1 (2)	–1	$\text{natFe}_2\text{C}_{12}\text{H}_9\text{O}_{14}$	488.8696	2.6	0.0214	$[\text{natFe}_2\text{Cit}_2\text{H}]^-$
375.4047	5.2 (3)	–2	$\text{natFe}_3\text{C}_{18}\text{H}_{15}\text{O}_{22}$	375.4057	1.7	0.0284	$[\text{natFe}_3\text{OCit}_3\text{H}_3]^{2-}$
366.3994	5.2 (3)	–2	$\text{natFe}_3\text{C}_{18}\text{H}_{13}\text{O}_{21}$	366.4004	2.0	0.0294	$[\text{natFe}_3\text{Cit}_3]^{2-}$
Xylem sap							
372.4097	–	–2	$^{54}\text{Fe}_3\text{C}_{18}\text{H}_{15}\text{O}_{22}$	372.4057	8.2	0.0283	$[\text{Fe}_3\text{OCit}_3\text{H}_3]^{2-}$
375.4045	5.56 (3)	–2	$\text{natFe}_3\text{C}_{18}\text{H}_{15}\text{O}_{22}$	375.4057	6.8	0.0197	$[\text{natFe}_3\text{OCit}_3\text{H}_3]^{2-}$

The parameters used to assess the accuracy of molecular formulae were exact molecular mass and isotopic signatures, with exact mass errors of <10 ppm, and a SigmaFit™ value of <0.03 (Ojanperä et al. 2006) (see Materials and Methods). Data are means of at least three independent HPLC runs.

^aThe $^{56}\text{Fe}/^{54}\text{Fe}$ ratio was used to determine the number of Fe atoms in the molecule. Theoretical $^{56}\text{Fe}/^{54}\text{Fe}$ ratios for molecules containing two or three Fe atoms are 7.9 and 5.3, respectively.

^bThe ion charge was determined by the m/z isotope difference within a given molecule. Differences of 1.0 and 0.5 m/z indicate molecular ion charges of 1 and 2, respectively.

$\text{natFe}_3\text{C}_{18}\text{H}_{13}\text{O}_{21}$ and as the most accurate formulae, corresponding to the three Fe-, three Cit- molecular ions $[\text{natFe}_3\text{OCit}_3\text{H}_3]^{2-}$ and $[\text{natFe}_3\text{Cit}_3]^{2-}$ (Table 1). The fit of the experimental and theoretical isotopic signatures of the $[\text{natFe}_3\text{OCit}_3\text{H}_3]^{2-}$ molecular ion (for the ^{56}Fe signal at m/z 375.4) is shown in Fig. 2G and H, respectively. A good fit was also found for the ion $[\text{natFe}_3\text{Cit}_3]^{2-}$ (for the ^{56}Fe signal at 366.4 m/z; Supplementary Fig. 4G, H).

Iron to citrate ratios drive the balance between Fe_2Cit_2 and Fe_3Cit_3 in standard solutions

To assess the influence of the Fe: Cit ratio on the balance of Fe–Cit complexes, standard solutions with Fe: Cit ratios of 1:1, 1:10, 1:100 and 1:500 (at 100 μM Fe) were analyzed by HPLC–ESI-TOFMS and HPLC–ICP-MS, always at the pH value typical of xylem sap. Both detection systems show that high Fe: Cit ratios favor the formation of Fe_3Cit_3 , whereas lower Fe: Cit ratios lead to the formation of Fe_2Cit_2 (Fig. 3). With Fe: Cit ratios >1:10, Fe_3Cit_3 would account for >75% of the total complexed Fe, whereas with Fe: Cit ratios <1:75, Fe_2Cit_2 would account for >75% of the total. In the range between these ratios both complexes would be present. In all cases, no other Fe-containing peaks different from Fe_2Cit_2 and Fe_3Cit_3 were found by HPLC–ICP-MS or HPLC–ESI-TOFMS (Supplementary Fig. 5).

Quantification of Fe–Cit complexes in Fe–citrate standard solutions

We attempted to quantify the amount of Fe associated with the Fe–Cit complexes found in ^{54}Fe –Cit solutions by using HPLC–ICP-MS ^{54}Fe molar flow chromatograms. The sum of the

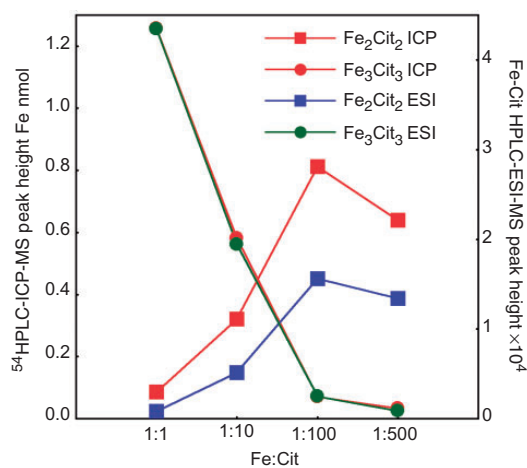


Fig. 3 Effect of the Fe: Cit ratio on the Fe_2Cit_2 and Fe_3Cit_3 balance. Data are chromatographic peak maximum heights obtained with ICP-MS and ESI-TOFMS detection. ^{54}Fe –Cit standard solutions with Fe: Cit ratios of 1:1, 1:10, 1:100 and 1:500 (at 100 μM ^{54}Fe , pH 5.5 in 50% mobile phase B) were used.

Fe–Cit complexes Fe_2Cit_2 and Fe_3Cit_3 accounted for approximately 60% ($n = 4$) of the total injected Fe. However, only 67% of the Fe was eluted from the HPLC. Therefore, the Fe contained in the Fe_2Cit_2 and Fe_3Cit_3 peaks accounted for 91% of the eluted Fe. When the analysis was carried out with longer run times

Table 2 Xylem sap pH, Fe and citrate concentrations, Fe:Cit ratios and Fe₃Cit₃ and Fe₂Cit₂ complexes (in % of the chromatographically eluted Fe), in Fe-sufficient (+Fe), Fe-deficient (-Fe) and Fe-deficient tomato plants resupplied with Fe-*o,o*EDDHA for 12 h (Fe-resupplied)

Fe status	Fe in solution (μM)	pH	Fe (μM)	Cit (μM)	Fe:Cit	Fe ₃ Cit ₃ (%)	Fe ₂ Cit ₂ (%)
+Fe	45	5.8±0.1	19.9±2.6	11.6±6.6	1:0.6	bld ^a	bld
-Fe	0+HCO ₃	5.8±0.1	5.4±4.4	165±9.2	1:31	bld	bld
Fe-resupplied	(0+HCO ₃)+45	5.5±0.1	121.0±13.7	172.2±12.6	1:1.4	71 ^b	bld

Data are means±SE of at least three independent samples.

^abld: below detection limit.

^bSince only 25% of the total injected Fe was eluted from the column, this percentage corresponds to 16% of the total injected Fe.

a broad Fe peak eluted at approximately 70 min, indicating that at least an additional Fe form either occurred in the original sample or was formed from Fe–Cit complexes during the LC run. The UV–visible spectra of this peak suggest that it may correspond to Fe-oxyhydroxides.

The Fe₃Cit₃ complex is present in the xylem sap of Fe-deficient tomato plants resupplied with Fe

We analyzed xylem sap to look for the presence of possible Fe–Cit complexes by the optimized methodology described above. We used xylem of Fe-sufficient, Fe-deficient and Fe-deficient plants resupplied with Fe–ethylenediamine-*N,N'*-bis(*o*-hydroxyphenylacetic) acid (*o,o*EDDHA) for 6, 12 and 24 h, where Fe concentrations were 19.9±2.6, 5.4±4.4, 42.9±3.7, 121.0±13.7 and 43.5±9.1 μM (*n*=4), respectively (Table 2). The xylem sap of plants resupplied for 12 h was chosen for further studies, since they have the highest concentrations of Fe. These xylem sap samples showed a major ⁵⁴Fe peak in HPLC–ICP-MS at 39.5 min (Fig. 4A). When using HPLC–ESI-TOFMS, an Fe peak eluted at 34.1 min and showed signals at *m/z* 372.4 or 375.4 when the Fe source was ⁵⁴Fe-*o,o*EDDHA or ^{nat}Fe-*o,o*EDDHA, respectively (Fig. 4B, C). The retention time difference between HPLC–ICP-MS and HPLC–ESI-TOFMS was due to the use of different HPLC systems as explained above. Based on this exact mass and the isotopic pattern data (see insets of Fig. 4B, C), the algorithm proposed Fe₃C₁₈H₁₅O₂₂ as the more accurate molecular formula (Table 1; ⁵⁶Fe signal *m/z* error 6.8 ppm and SigmaFit™ value 0.0197), corresponding to the Fe₃Cit₃ molecular ion [Fe₃O(Cit)₃H₃]²⁻ also found in the Fe–Cit standards (Figs. 1, 2). The approximately 1-min difference in retention time for Fe₃Cit₃ between xylem sap samples (Fig. 4) and standards (Fig. 1) in both HPLC systems was likely due to matrix effects. It should be noted that although the Fe₃Cit₃ complex was detected in standard solution as a mixture of two ions [Fe₃Cit₃H]²⁻ and [Fe₃OCit₃H₃]²⁻, in xylem sap only the latter was found. No other Fe-containing molecular ions, including Fe–NA, were found in the whole HPLC–ESI-TOFMS run using these HPLC conditions. However, using an HPLC–ESI-TOFMS method designed for Fe-*o,o*EDDHA analysis (Orera *et al.* 2009) a very low concentration of this Fe chelate (0.3±0.1 μM; *n*=4) was found. The Fe₃Cit₃ complex was also found in xylem sap of Fe-deficient plants resupplied with Fe-EDTA for 12 h, as well as in that of plants resupplied

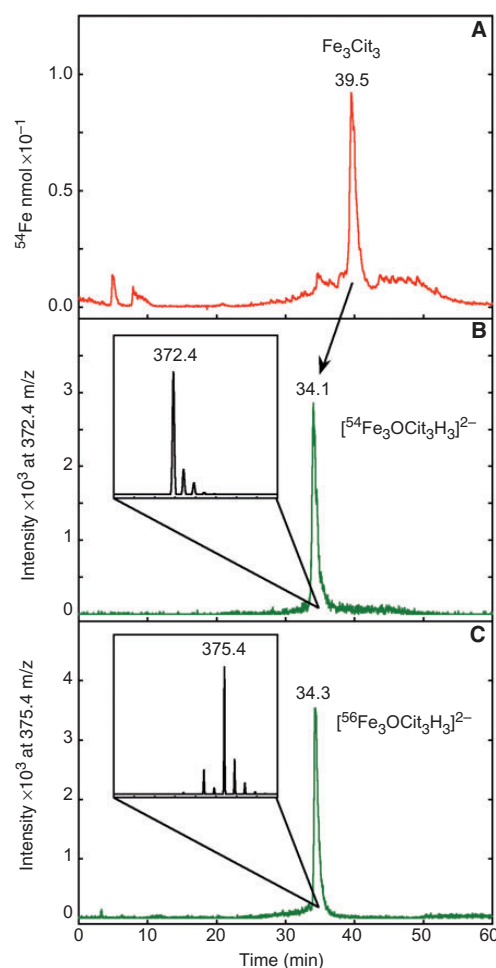


Fig. 4 HPLC–ICP-MS (A) and HPLC–ESI-TOFMS (B, C) typical chromatograms of xylem sap samples from Fe-deficient, 12-h Fe-resupplied tomato plants, showing the peak corresponding to the Fe₃Cit₃ complex. Plants were resupplied with ⁵⁴Fe-*o,o*EDDHA (A, B) or ^{nat}Fe-*o,o*EDDHA (C). HPLC–ESI-TOFMS traces were extracted at *m/z* values 372.40 and 375.40 (±0.05), corresponding to [⁵⁴Fe₃OCit₃H₃]²⁻ and [⁵⁶Fe₃OCit₃H₃]²⁻. Isotopic signatures of both molecular ions are shown in insets in (B) and (C).

with Fe-*o,o*EDDHA for 6 and 24 h (data not shown). However, no Fe-containing compounds could be detected in the xylem of Fe-deficient and Fe-sufficient plants.

We also attempted to quantify the amount of Fe associated with the Fe₃Cit₃ complex found in the xylem of the ⁵⁴Fe-*o,o*EDDHA 12 h-resupplied plants by using HPLC–ICP-MS ⁵⁴Fe molar flow chromatograms (*n* = 3). In these xylem samples >95% of the total Fe was ⁵⁴Fe. Only 25% of the injected Fe eluted from the column. The ⁵⁴Fe₃Cit₃ peak accounted for the 71% of the eluted Fe and 16% of the injected Fe (Table 2).

Method sensitivity for the Fe₃Cit₃ complex

The sensitivity of the HPLC–ESI-TOFMS and HPLC–ICP-MS methods for the detection of the Fe₃Cit₃ complex in xylem sap can be estimated from the signal to noise ratios (*s/n*). Limits of detection and quantification are usually considered as the analyte concentrations giving *s/n* of 3 and 10, respectively. *S/n* found in xylem sap samples with total Fe concentrations of approximately 40 μM were 12 and 6 in HPLC–ESI-TOFMS and HPLC–ICP-MS, respectively. Therefore, in xylem sap with Fe: Cit ratios favouring the formation of Fe₃Cit₃ (>1:10; Fig. 3), an Fe concentration of approximately 25–30 μM will be needed for the Fe₃Cit₃ complex to be detected.

Molecular modeling of the Fe₃Cit₃ complex: an oxo-bridged tri-Fe(III) core complex

Molecular modeling of the Fe₃Cit₃ complex was carried out using the information gained from the molecular identification in xylem sap samples of Fe-deficient plants resupplied with Fe and on the basis of the known basic structure of Fe(III) carboxylates (Lippard 1988). The complex Fe₃Cit₃ has a molecular mass of 750.83 Da, a molecular formula of Fe₃C₁₈H₁₅O₂₂, is composed of three Cit molecules, three Fe atoms and one O atom and has two negative charges. The complex was modeled using Density Functional Theory (DFT), which has become the standard method for quantum chemical modeling of transition metals including those of biological relevance (Deeth et al. 2009 and references therein), as a trinuclear Fe(III) oxo-bridged complex (Fig. 5, Supplementary Fig. 5). The three Fe atoms form an equilateral triangle with an O atom in the center bridging all of them. All Fe atoms have a slightly distorted octahedral configuration. In each of the three Cit molecules, both distal carboxylate groups are bound to two Fe atoms. The four O atoms of the Cit distal carboxylate groups (two from each Cit molecule) are in the same plane of the Fe atom they complex. The two remaining positions of the Fe atom are occupied by the central carboxylate group of a Cit molecule and the O of the oxo-bridged 3-Fe center. This compact molecular geometry is further stabilized by the formation of hydrogen bonds between the hydroxyl groups and the free O atoms in the central carboxylates. Until now, six Fe–Cit complexes (three mononuclear and two dinuclear found in concentrated standard solutions, plus a nonanuclear one) have been isolated and structurally characterized in solid state (Gautier-Luneau et al. 2005 and references therein), and none of them has

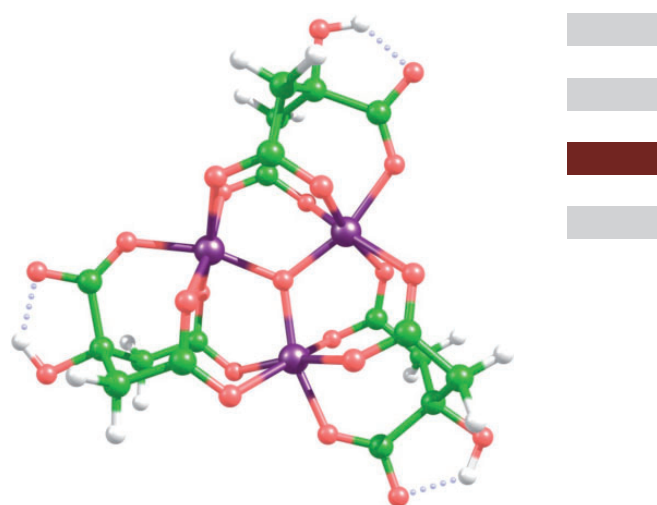


Fig. 5 Proposed structure for the Fe₃Cit₃ found in plant xylem as an oxo-bridged tri-iron–citrate complex. Iron, oxygen, carbon and hydrogen atoms are shown in purple, red, green and white, respectively.

a central μ₃ oxygen coordinated to three Fe atoms. The Fe₂Cit₂ complex found only in Fe–Cit standard solutions was also modeled (see Supplementary Figs. 7, 8, Supplementary Table 3) according to the known structural characteristics found in solid state by Gautier-Luneau et al. (2005) and references therein.

Discussion

We report here the first direct and unequivocal identification of a natural Fe complex in plant xylem sap, Fe₃Cit₃. The complex was modeled as having an oxo-bridged tri-Fe(III) core. This is the first time that an Fe–Cit complex has been identified in biological systems. The Fe₃Cit₃ complex was identified using an integrated MS approach, based on exact molecular mass, isotopic signature, Fe content and retention time. This complex was not predicted to occur in previous *in silico* xylem speciation studies (López-Millán et al. 2000, López-Millán et al. 2001). A second Fe–Cit complex, Fe₂Cit₂, was also found along with Fe₃Cit₃ in standard solutions at xylem-typical pH values, with their respective abundances being tuned by the Fe: Cit ratio. The detection of Fe₃Cit₃ in the xylem sap was made possible by the use of: (i) pH values similar to those of the xylem sap throughout the analysis, (ii) a zwitterionic hydrophilic interaction column that allows for the separation of Cit and Fe–Cit complexes, (iii) high-resolution detection techniques such as ICP-MS and ESI-TOFMS, and (iv) stable Fe isotopes for identification and quantification purposes.

The changes in Fe: Cit ratios in standard solutions drive the balance between the Fe₂Cit₂ and Fe₃Cit₃ complexes, with ratios of >1:10 favoring the formation of Fe₃Cit₃ and ratios of <1:75

favoring the formation of Fe_2Cit_2 (Fig. 3). In the xylem sap of Fe-deficient tomato plants resupplied with Fe for 12 h, where the Fe: Cit ratio was approximately 1:1 (Table 2), the only complex observed was Fe_3Cit_3 . The xylem sap Fe: Cit ratios in Fe-sufficient and Fe-deficient plants were approximately 1:1 and 1:30, and therefore the expected Fe–Cit complexes would be Fe_3Cit_3 and a mixture of the Fe_2Cit_2 and Fe_3Cit_3 complexes, respectively. However, no Fe–Cit complexes could be detected by HPLC–ESI–TOFMS or HPLC–ICP–MS in the xylem of these plants, likely because concentrations were below the limit of detection, estimated as approximately 25–30 μM Fe–Cit. In fact, xylem total Fe concentrations were approximately 20 and 5 μM in Fe-sufficient and Fe-deficient plants, respectively, much lower than the 43–121 μM found in Fe-deficient plants resupplied with Fe where the complex was detected. Limits of detection (LODs) for these Fe–Cit complexes are considerably higher than that reported also in xylem sap and with similar analytical techniques for the synthetic Fe chelate Fe(III)–*o,o*EDDHA, which is <1 μM (Orera *et al.* 2009). This supports that further analytical efforts should be made to improve the LODs for the determination of Fe–Cit complexes in plant fluids, taking into account that Fe–Cit complexes could be very sensitive to external conditions and may decompose during chromatography. Also, since the potential occurrence of other Fe compounds along with Fe–Cit complexes could explain the mass balance results found in both standard solutions and xylem sap, further analytical efforts should be made to completely speciate Fe in xylem sap.

The finding that at least an Fe–Cit complex, Fe_3Cit_3 , participates in long-distance xylem Fe transport in plants is in line with what is known to occur in other organisms. In humans most of the Fe is usually chelated by transferrin, but the serum of patients with Fe overload disorders may have up to 10 μM Fe not bound to transferrin (at pH 7.4, with 100 μM Cit and an Fe: Cit ratio of 1:10) (Evans *et al.* 2008). This Fe fraction was proposed to consist of a mixture of oligomeric, dimeric and possibly monomeric Fe species, using a different approach from that used here. The Fe: Cit ratio in serum has also been proposed to control the balance between Fe–Cit species, with Fe: Cit ratios of >1:10 leading to oligomeric and polymeric Fe species and <1:100 leading to monomeric and dimeric Fe species (Evans *et al.* 2008). This framework is similar to the one we propose here for plant xylem sap, with high Fe: Cit ratios leading to Fe_3Cit_3 and low ratios leading to Fe_2Cit_2 . In the bacterial plasma membrane a Fe_2Cit_2 complex is thought to be transported by the coordinated action of FecABCDE proteins (Mahren *et al.* 2005) where Fe_2Cit_2 binds to FecA in the outer membrane and initiates two independent processes, Fe–Cit transport into the periplasm and transcriptional induction of the *fecABCDE* genes (Yue *et al.* 2003). Fe–Cit transport by proteins of the CitMHS family has also been recently described in bacteria (Lensbouer *et al.* 2008).

The idea that Fe could be transported in the plant xylem by organic acids was first suggested many years ago (Rogers 1932), based on the ability of Fe to form stable complexes with organic

acids and on the increase in these carboxylates with Fe deficiency (see Abadía *et al.* 2002 for a review). Pioneering studies by Brown and co-workers proposed that Fe and Cit were associated in some way, in different plant species, from the co-migration of Fe and Cit during electrophoresis and the increase in xylem Cit concentration with Fe deficiency (Brown and Tiffin 1965, Tiffin 1966a, Tiffin 1966b, Tiffin 1970, Clark *et al.* 1973). The first *in silico* xylem Fe speciation studies also suggested a major role for Cit in the complexation of Fe in tomato and soybean (White *et al.* 1981a, White *et al.* 1981b, Mullins *et al.* 1986). More recently, *in silico* studies incorporating the stability constants of other possible Fe chelators (e.g. NA), also support that Cit, rather than NA, could play a major role in Fe xylem transport (von Wirén *et al.* 1999, López-Millán *et al.* 2000, López-Millán *et al.* 2001, Rellán-Álvarez *et al.* 2008), and this was also supported by ESI–TOFMS direct determination of Fe–NA complexes in standard solutions containing Fe, NA and Cit at typical xylem pH values (Rellán-Álvarez *et al.* 2008). We have reviewed previous studies reporting xylem Fe and Cit concentrations to explore the likelihood of finding the Fe–Cit complexes in xylem sap (Supplementary Table 1). Within a given plant species, Fe: Cit ratios were generally higher in Fe-sufficient than in Fe-deficient plants, and when plants were resupplied with Fe even higher Fe: Cit ratios were found (Supplementary Table 1). A comparison of these Fe: Cit ratios with the threshold values proposed in this study with standard solutions (1:10 for >75% Fe_3Cit_3 and 1:75 for >75% Fe_2Cit_2) suggest that the Fe_3Cit_3 complex may occur in a wide range of species regardless of Fe nutrition status. On the other hand, the Fe_2Cit_2 complex may be prevalent in xylem sap samples with Cit concentrations in the mM range, such as those of some Fe-deficient plant species (Supplementary Table 1).

Recent molecular evidence also supports that Cit may be involved in long-distance Fe transport. Two *Arabidopsis thaliana* and rice mutants with altered root vasculature Cit transporters show decreases in the xylem sap concentrations of Fe and Cit, increased Fe deficiency symptoms and Fe accumulation in the root (Durrett *et al.* 2007, Yokosho *et al.* 2009). Changes found in Fe and Cit concentrations do not support that changes in Fe–Cit speciation may occur, since Fe_3Cit_3 would be expected to occur both in the wild type and mutant genotypes of both species (Supplementary Table 1). The phenotype of these mutants could result from a hampered Fe xylem transport, and/or from the decrease in xylem C transport itself, that may in turn impair the ability of the mutant plants to elicit root responses to Fe deficiency. Carbon fixation in roots by phosphoenolpyruvate carboxylase and export in the xylem have been proposed to play a role in the plant responses when leaf C fixation is decreased by Fe deficiency (López-Millán *et al.* 2000, Zocchi *et al.* 2007).

The central oxo-bridged tri-Fe(III) core bridged by citrate ligands of the Fe_3Cit_3 complex proposed here to occur in the xylem sap is structurally related to the active sites of numerous polyiron–oxo proteins (Tshuva and Lippard 2004). Di-Fe sites are found in a functionally diverse class of proteins which are

activated by oxygen binding and catalyze hydroxylation, desaturation and epoxidation reactions on a variety of alkyl and aryl substrates. A di-Fe site in ribonucleotide reductase, which participates in DNA biosynthesis, is responsible for the formation of organic radicals, whereas ferritins are important for Fe oxidation, storage and transport (see Tshuva and Lippard 2004 and references therein). This is the first time that a small molecule containing an oxo-bridged tri-Fe center has been reported in a biological system. We may speculate that the oxo-bridge structure may confer redox properties to this plant Fe transport form. In fact, the lowest unoccupied molecular orbital of the complex, obtained by DFT calculations, displays an energy of 1.5 eV, which is rather low for a dianionic species and indicates that the reduction of this trinuclear species could be feasible.

The finding of this negatively double charged, relatively large (750.83 Da) Fe_3Cit_3 complex opens new possibilities to re-examine the long-distance transport of Fe in the plant xylem. Very little is still known about the mechanisms of Fe xylem unloading, although it is accepted that a direct flow of Fe could occur through plasmodesmata into xylem parenchyma cells, and a second mechanism could proceed to the leaf mesophyll apoplast (Kim and Guerinot 2007, Palmer and Guerinot 2009). The molecular size of Fe_3Cit_3 , 1.1×0.4 nm, would permit direct passage through plasmodesmata, which usually allows trafficking of molecules < 2 nm. Once in the xylem parenchyma cytoplasm, the prevailing pH change would favor ligand exchange reactions with NA, leading to the formation of Fe–NA complexes (von Wirén et al. 1999, Rellán-Álvarez et al. 2008). Xylem Fe unloading can also proceed directly to the apoplast, where the Fe_3Cit_3 complex is also likely to occur [considering apoplast chemical composition (Kim and Guerinot 2007, Palmer and Guerinot 2009)] and will probably function as a suitable substrate for the mesophyll cell leaf plasma membrane Fe(III) chelate reductase. As mentioned above this complex is likely to have redox activity, and the oxo-bridge may play a role in the interaction with the reductase enzyme. In fact, low Fe: Cit ratios—favoring the presence of Fe_3Cit_3 —seem to be optimal for leaf plasma membrane Fe(III)-chelate reductase activity, since 20-fold increases were observed when Fe: Cit ratios increased from 1:500 to 1:5 (González-Vallejo et al. 1999). Also, the complex may be a natural substrate of the root Fe(III)-chelate reductase, since it is known that root Cit excretion occurs in many plant species under Fe deficiency (Abadía et al. 2002).

Materials and Methods

Plant culture

Tomato (*Solanum lycopersicum* Mill. cv. 'Tres Cantos') plants were grown in a growth chamber with a photosynthetic photon flux density of $350 \mu\text{mol m}^{-2} \text{s}^{-1}$ photosynthetically active radiation, and a 16/8 h photoperiod, 23/18°C day/night temperature regime. Seeds were germinated and grown in vermiculite for

2 weeks. Seedlings were grown for an additional 2-week period in half-strength Hoagland nutrient solution with $45 \mu\text{M}^{\text{nat}}\text{Fe(III)}$ –ethylenediamine tetraacetic acid (EDTA), and then transplanted to 10-liter plastic buckets (18 plants per bucket) containing half-strength Hoagland nutrient solution, pH 5.5, with either 0 (Fe-deficient plants) or $45 \mu\text{M}$ Fe(III)–EDTA (Fe-sufficient plants). Throughout this study we use $^{\text{nat}}\text{Fe}$ to refer to Fe with the natural isotopic composition: 5.85, 91.75, 2.12 and 0.28% of ^{54}Fe , ^{56}Fe , ^{57}Fe and ^{58}Fe , respectively. After 10 d, Fe-deficient plants were resupplied with Fe by transfer to nutrient solution with Fe [$45 \mu\text{M}$ either $^{\text{nat}}\text{Fe(III)}$ –*o,o*EDDHA, $^{54}\text{Fe(III)}$ –*o,o*EDDHA or $^{\text{nat}}\text{Fe(III)}$ –EDTA]. Iron-54 was purchased as Fe_2O_3 (98% Fe, 95% ^{54}Fe ; Cambridge Isotope Labs, Andover, MA, USA). Xylem was sampled from Fe-deficient, Fe-sufficient and Fe-deficient plants resupplied with Fe for 6, 12 and 24 h.

Xylem sap sampling

Tomato xylem sap was sampled using the detopping technique (López-Millán et al. 2009). Plant shoots were cut just below the first true leaf using a razor blade, and xylem sap was left to exude. The sap of the first 5 min was discarded to avoid contamination, the surface was washed with distilled water and blotted dry, and sap was then directly collected for 20 min using a micro-pipet and maintained in Eppendorf tubes kept on ice. Immediately after sample collection, the pH of the samples was measured with a Biotrode pH microelectrode with Idrolyte electrolyte (Metrohm, Herisau, Switzerland), tested for cytosolic contamination as indicated below and kept frozen at -80°C until further analysis. All samples were assessed for cytosolic contamination using *c-mdh* (EC 1.1.1.37) as a cytosolic contamination marker (López-Millán et al. 2000), and no contamination was found. Before analysis, samples were thawed and diluted 2-fold with 10 mM ammonium acetate in methanol at pH 6.8. The actual pH value of this organic mixture is estimated to be 5.5 (Canals et al. 2001). Then, samples were vortexed, centrifuged at $12\,000 \times g$ for 2 min and the supernatant immediately analyzed.

Fe–Cit standard solutions preparation

Iron–Cit standard solutions at different Fe: Cit ratios were prepared by adding the appropriate amounts of Fe ($^{\text{nat}}\text{Fe}$ or ^{54}Fe) to Cit solutions prepared in 10 mM ammonium acetate at pH 5.5. Fe–Cit solutions were gently vortexed, diluted 2-fold with 10 mM ammonium acetate in methanol at pH 6.8 and immediately analyzed. The pH value of this organic mixture is estimated to be 5.5 (Canals et al. 2001).

Analysis of Fe complexes by HPLC coupled to electrospray ionization MS

Chromatographic separation was performed on a modified Alliance 2795 HPLC system (Waters, Mildford, MA, USA). The fluidics system, with the exception of the pump head, was built with PEEK, and a Ti needle was used to minimize metal contamination. Different HPLC conditions were tested, including

several column types, elution programs and organic solvents (acetonitrile and methanol). Final HPLC analysis conditions were as follows. The autosampler was kept at 4°C and the column compartment temperature was set at 30°C. Injection volume was 20 µl, and a ZIC-pHILIC, 150×2.1 mm, 5 µm column (Sequant, Umea, Sweden) was used with a flow rate of 100 µl min⁻¹. The mobile phase was built using two eluents: A (10 mM ammonium acetate in water at pH 5.5) and B (10 mM ammonium acetate in methanol at pH 6.8). All mobile phase chemicals were LC-MS grade (Riedel-de Haën, Seelze, Germany). For separation, an initial equilibration time of 80% B and 20% A (from min 0 to 5) was followed by a linear gradient from 80 to 20% B (from min 5 to 20). This mobile phase composition was held for 15 min, then changed linearly to the initial conditions for 10 min, and kept as such for another 15 min. Total run time per sample was 1 h. The pH values during the HPLC run ranged from 5.3 to 6.2 depending on organic mixture composition of the mobile phase (Canals *et al.* 2001). Injections of 5 mM Cit (20 µl) were carried out between samples to minimize Fe cross-contamination.

High-resolution MS analysis was carried out with a micrOTOF II ESI-TOFMS apparatus (Bruker Daltonik GmbH, Bremen, Germany) in the 50–1000 m/z range. The micrOTOF II was operated in negative mode at 3000 and –500 V capillary and end-plate voltages, respectively. After optimization, capillary exit, skimmer 1 and hexapole RF voltages were set at –57.1, –39.1 and 145.2 V, respectively. Nebulizer gas (N₂) pressure was kept at 2.0 bar and drying gas (N₂) flow was set at 8.0 liter min⁻¹ with a temperature of 180°C. Mass calibration was carried out with 10 mM Li-formate solution using a syringe pump (Cole-Parmer Instruments, Vernon Hills, IL, USA). In each HPLC run mass calibration was carried out by on-line injection of 20 µl of Li-formate at 2 min. Molecular formulae were assigned based on (i) exact molecular mass, with errors <10 ppm, and (ii) the SigmaFit™ algorithm, with a threshold tolerance value of 0.03 SigmaFit™ values (Ojanperä *et al.* 2006). Appropriate isotopic abundances were used for the calculations. The system was controlled with the software packages MicrOTOF Control v.2.2 and HyStar v.3.2 (Bruker Daltonics). Data were processed with Data Analysis v.3.4 software (Bruker Daltonics).

Analysis of Fe and Fe complexes by ICP-MS

ICP-MS analysis was carried out with a Q-ICP-MS instrument (7500ce; Agilent Technologies, Tokyo, Japan). The instrument was fitted with an octapole collision cell system located between the ion lenses and a quadrupole MS analyzer for removal of polyatomic interference. In this study He was used as a collision gas. In addition, O₂ (7%) was added to the plasma by an additional mass flow controller to remove C excess, and to prevent it from condensing on the interface and ion lenses due to the high organic content of the mobile phase during HPLC separation (Woods and Fryer 2007). Platinum interface cones were used to allow the addition of O₂. The Q-ICP-MS instrument was operated with a RF power of 1500 W and cooling, sample and make-up gas flows of 15, 0.9 and 0.2 liter min⁻¹, respectively.

The collision cell was operated with a He gas flow of 4.2 ml min⁻¹ and octapole bias and QP bias voltages of –18.0 and –16.0 V, respectively. The torch position and ion lens voltage settings were optimized daily for maximum sensitivity with a 1 ng g⁻¹ Li, Co, Y, Tl and Ce mixture in 1% (w/w) HNO₃ solution. A solution of 1% (w/w) HNO₃ was also used to check the background level caused by polyatomic Ar interference. The possible contribution of isobaric interference of ⁵⁴Cr and ⁵⁸Ni in the determination of the ⁵⁴Fe and ⁵⁸Fe isotopes was corrected mathematically by measuring the ion signals at masses 52 for Cr and 60 for Ni and assuming natural abundances as reported by IUPAC (De Laeter *et al.* 2003). Mass bias correction was carried out by measuring the isotope ratios of the ^{nat}Fe standard and calculating the mass bias factor (K) with an exponential model (Rodríguez-Castrillón *et al.* 2008). The ICP-MS instrument was controlled with the software packages ICP-MS ChemStation v.B.03.04 and ICP-MS Chromatographic v.B.03.04 (Agilent Technologies).

For the ICP-MS analysis of ⁵⁴Fe–citrate complexes in standard solutions and xylem sap samples, a chromatographic separation was performed on an Agilent 1100 chromatographic system (Agilent Technologies) using the method described for HPLC–ESI-TOFMS analysis. Iron-54 and ^{nat}Fe quantification was carried out by post-column isotope dilution analysis (IDA) (Rodríguez-González *et al.* 2005) with a 20 ng g⁻¹ ⁵⁷Fe in EDTA solution continuously introduced at 0.10 g min⁻¹ through a T piece connected to the end of the column and before the plasma entrance. Iron-57 was purchased as Fe₂O₃ (98% Fe, 95% ⁵⁷Fe; Cambridge Isotope Labs). The ICP-MS intensity chromatograms (counts s⁻¹) were converted into Fe molar flow chromatograms (⁵⁴Fe nmol min⁻¹) using the isotope pattern deconvolution (IPD) equations described elsewhere (Rodríguez-Castrillón *et al.* 2008, González Iglesias *et al.* 2009). Accurate isotope abundances of the ⁵⁷Fe and ⁵⁴Fe enriched solutions were determined by direct ICP-MS injections and used for these calculations. Isotope abundances (% ⁵⁴Fe, ⁵⁶Fe, ⁵⁷Fe and ⁵⁸Fe) were 0.14, 4.74, 94.63 and 0.49 in ⁵⁷Fe-enriched solutions and 99.67, 0.25, 0.01 and 0.06 in ⁵⁴Fe-enriched solutions.

Total ⁵⁴Fe and ^{nat}Fe determinations in xylem sap samples were carried out by direct ICP-MS injections and IDA, spiking known amounts of the characterized ⁵⁷Fe-enriched solution into the samples acidulated with HNO₃. Also, the mathematical IPD procedure described elsewhere (Rodríguez-Castrillón *et al.* 2008, González Iglesias *et al.* 2009) was used.

Other determinations

Citrate was analyzed by HPLC (Waters Alliance 2795) using a Supelcogel H 250×4.6 mm column. Analyses were performed isocratically at a flow rate of 200 µl min⁻¹ and at a temperature of 30°C. The mobile phase was 0.1% formic acid. Detection was performed by ESI-TOFMS (micrOTOF II; Bruker Daltonics) at 191.0 m/z. Quantification was carried out by external calibration with internal standardization (with [¹³C]4-L-malic acid; Cambridge Isotope Laboratories). The Fe(III) chelate of *o,o*EDDHA was determined as described elsewhere (Orera *et al.* 2009).

Iron–citrate complex molecular modeling

All theoretical calculations were performed by using the Gaussian 03 program (Frisch et al. 2003). The molecular geometry of $(\text{Fe}_3\text{OCit}_3)^{2-}$ was optimized assuming C_{3h} symmetry. The chemistry model used consisted in the Becke's three-parameter exchange functional combined with the LYP correlation functional (B3LYP) (Becke 1993) and the LanL2DZ basis set as indicated in the Gaussian 03 program (Frisch et al. 2003). In order to achieve the convergence of the wavefunction, an initial guess was obtained using the same chemistry model on the closed shell $(\text{Fe}_3\text{OCit}_3)^{2-}$ species.

Supplementary data

Supplementary data are available at PCP online.

Funding

This work was supported by the Spanish Ministry of Science and Innovation (grant numbers AGL2006-1416, AGL2007-61948 and CTQ2006-05722, co-financed with FEDER); the European Commission (Thematic Priority 5—Food Quality and Safety, 6th Framework RTD Programme, grant number FP6-FOOD-CT-2006-016279) and the Aragón Government (groups A03 and E39). Acquisition of the HPLC–TOFMS apparatus was cofinanced with FEDER. R.R.-A., J.G.-M.-S., I.O. and J.A.R.-C. were supported by FPI-MICINN, FICYT-MICINN, CONAID-DGA and FPU-MICINN grants, respectively.

Acknowledgments

We thank Ade Calviño and Aurora Poc (Aula Dei Experimental Station–CSIC, Zaragoza, Spain) for growing the plants, Professor Jian Feng Ma (Research Institute for Bioresources, Okayama University, Kurashiki, Japan) for the kind supply of DMA and Dr. Ana-Flor López-Millán (Aula Dei Experimental Station–CSIC, Zaragoza, Spain) for critically reviewing the manuscript and helpful suggestions.

References

- Abadía, J., López-Millán, A.F., Rombolà, A. and Abadía, A. (2002) Organic acids and Fe deficiency: a review. *Plant Soil* 241: 75–86.
- Becke, A.D. (1993) A new mixing of Hartree-Fock and local density-functional theories. *J. Chem. Phys.* 98: 1372–1377.
- Briat, J.F., Curie, C. and Gaymard, F. (2007) Iron utilization and metabolism in plants. *Curr. Opin. Plant Biol.* 10: 276–282.
- Brown, J. (1966) Fe and Ca uptake as related to root-sap and stem-exudate citrate in soybeans. *Physiol. Plant.* 19: 968–976.
- Brown, J.C. and Tiffin, L.O. (1965) Iron stress as related to the iron and citrate occurring in stem exudate. *Plant Physiol.* 40: 395–400.
- Canals, I., Oumada, F.Z., Rosés, M. and Bosch, E. (2001) Retention of ionizable compounds on HPLC. 6. pH measurements with the glass electrode in methanol-water mixtures. *J. Chromatogr. A* 911: 191–202.
- Clark, R.B., Tiffin, L.O. and Brown, J.C. (1973) Organic-acids and iron translocation in maize genotypes. *Plant Physiol.* 52: 147–150.
- Curie, C., Cassin, G., Couch, D., Divol, F., Higuchi, K., Le Jean, M., et al. (2008) Metal movement within the plant: contribution of nicotianamine and yellow stripe 1-like transporters. *Ann. Bot.* 103: 1–11.
- De Laeter, J., Böhlke, J., De Bièvre, P., Hidaka, H., Peiser, H., Rosman, K., et al. (2003) Atomic weights of the elements: review 2000. *Pure Appl. Chem.* 75: 683–800.
- Deeth, R., Anastasi, A., Diedrich, C. and Randell, K. (2009) Molecular modelling for transition metal complexes: Dealing with d-electron effects. *Coord. Chem. Rev.* 253: 795–816.
- Durrett, T.P., Gassmann, W. and Rogers, E.E. (2007) The FRD3-mediated efflux of citrate into the root vasculature is necessary for efficient iron translocation. *Plant Physiol.* 144: 197–205.
- Evans, R.W., Rafique, R., Zarea, A., Rapisarda, C., Cammack, R., Evans, P.J., et al. (2008) Nature of non-transferrin-bound iron: Studies on iron citrate complexes and thalassemic sera. *J. Biol. Inorg. Chem.* 13: 57–74.
- Frisch, M.J., Trucks, G.W., Schlegel, H.B., Scuseria, G.E., Robb, M.A., et al. (2003) Gaussian 03, Revision B.05. Gaussian, Inc., Pittsburgh, PA, USA.
- Gautier-Luneau, I., Merle, C., Phanon, D., Lebrun, C., Biaso, F., Serratrice, G., et al. (2005) New trends in the chemistry of iron(III) citrate complexes: Correlations between X-ray structures and solution species probed by electrospray mass spectrometry and kinetics of iron uptake from citrate by iron chelators. *Chem. Europ. J.* 11: 2207–2219.
- González Iglesias, H., Fernández Sánchez, M.L., Rodríguez-Castrillón, J.A., García-Alonso, J.I., Sastre, J.L. and Sanz-Medel, A. (2009) Enriched stable isotopes and isotope pattern deconvolution for quantitative speciation of endogenous and exogenous selenium in rat urine by HPLC-ICP-MS. *J. Anal. Atom. Spectrom.* 24: 460–468.
- González-Vallejo, E., González-Reyes, J., Abadía, A., López-Millán, A., Yunta, F., Lucena, J., et al. (1999) Reduction of ferric chelates by leaf plasma membrane preparations from Fe-deficient and Fe-sufficient sugar beet. *Aust. J. Plant Physiol.* 26: 601–611.
- Hider, R.C., Yoshimura, E., Khodr, H. and von Wiren, N. (2004) Competition or complementation: the iron-chelating abilities of nicotianamine and phytosiderophores. *New Phytol.* 164: 204–208.
- Kim, S.A. and Guerinot, M.L. (2007) Mining iron: iron uptake and transport in plants. *FEBS Lett.* 581: 2273–2280.
- Küpper, H., Mijovilovich, A., Meyer-Klaucke, W. and Kroneck, P.M. (2004) Tissue- and age-dependent differences in the complexation of cadmium and zinc in the cadmium/zinc hyperaccumulator *Thlaspi caerulescens* (Ganges ecotype) revealed by x-ray absorption spectroscopy. *Plant Physiol.* 134: 748–757.
- Larbi, A., Morales, F., Abadía, J. and Abadía, A. (2003) Effects of branch solid Fe sulphate implants on xylem sap composition in field-grown peach and pear: changes in Fe, organic anions and pH. *J. Plant Physiol.* 160: 1473–1481.
- Lensbouer, J., Patel, A., Sirianni, J. and Doyle, R. (2008) Functional characterization and metal ion specificity of the metal-citrate complex transporter from *Streptomyces coelicolor*. *J. Bacteriol.* 190: 5616–5623.
- Lippard, S.J. (1988) Oxo-bridged polyiron centers in biology and chemistry. *Angew. Chem. Int. Ed.* 27: 344–361.
- López-Millán, A., Morales, F., Gogorcena, Y., Abadía, A. and Abadía, J. (2009) Metabolic responses in iron deficient tomato plants. *J. Plant Physiol.* 166: 375–384.
- López-Millán, A.F., Morales, F., Abadía, A. and Abadía, J. (2000) Effects of iron deficiency on the composition of the leaf apoplasmic fluid and

- xylem sap in sugar beet. Implications for iron and carbon transport. *Plant Physiol.* 124: 873–884.
- López-Millán, A.F., Morales, F., Abadía, A. and Abadía, J. (2001) Iron deficiency-associated changes in the composition of the leaf apoplastic fluid from field-grown pear (*Pyrus communis* L.) trees. *J. Exp. Bot.* 52: 1489–1498.
- Mahren, S., Schnell, H. and Braun, V. (2005) Occurrence and regulation of the ferric citrate transport system in *Escherichia coli*, *Klebsiella pneumoniae*, *Enterobacter aerogenes*, and *Photobacterium luminescens*. *Arch. Microbiol.* 184: 175–186.
- Meija, J., Montes-Bayón, M., Caruso, J. and Sanz-Medel, A. (2006) Integrated mass spectrometry in (semi-) metal speciation and its potential in phytochemistry. *Trends Anal. Chem.* 25: 44–51.
- Mullins, G.L., Sommers, L.E. and Housley, T.L. (1986) Metal speciation in xylem and phloem exudates. *Plant Soil.* 16: 377–391.
- Nikolic, M. and Römheld, V. (1999) Mechanism of Fe uptake by the leaf symplast: Is Fe inactivation in leaf a cause of Fe deficiency chlorosis? *Plant Soil* 215: 229–237.
- Ojanperä, S., Pelander, A., Pelzing, M., Krebs, I., Vuori, E. and Ojanperä, I. (2006) Isotopic pattern and accurate mass determination in urine drug screening by liquid chromatography/time-of-flight mass spectrometry. *Rapid Commun. Mass Spectrom.* 20: 1161–1167.
- Orera, I., Abadía, A., Abadía, J. and Álvarez-Fernández, A. (2009) Determination of α,ρ EDDHA—a xenobiotic chelating agent used in Fe fertilizers—in plant tissues by liquid chromatography/electrospray mass spectrometry: Overcoming matrix effects. *Rapid Commun. Mass Spectrom.* 23: 1694–1702.
- Ouerdane, L., Mari, S., Czernic, P., Lebrun, M. and Lobinski, R. (2006) Speciation of non-covalent nickel species in plant tissue extracts by electrospray Q-TOFMS/MS after their isolation by 2D size exclusion-hydrophilic interaction LC (SEC-HILIC) monitored by ICP-MS. *J. Anal. Atom. Spectrom.* 21: 676–683.
- Palmer, C. and Guerinot, M.L. (2009) Facing the challenges of Cu, Fe and Zn homeostasis in plants. *Nat. Chem. Biol.* 5: 333–340.
- Pierre, J.L. and Gautier-Luneau, I. (2000) Iron and citric acid: a fuzzy chemistry of ubiquitous biological relevance. *BioMetals* 13: 91–96.
- Punshon, T., Guerinot, M.L. and Lanzirotti, A. (2009) Using synchrotron X-ray fluorescence microprobes in the study of metal homeostasis in plants. *Ann. Bot.* 103: 665–672.
- Rellán-Álvarez, R., Abadía, J. and Álvarez-Fernández, A. (2008) Formation of metal-nicotianamine complexes as affected by pH, ligand exchange with citrate and metal exchange. A study by electrospray ionization time-of-flight mass spectrometry. *Rapid Commun. Mass Spectrom.* 22: 1553–1562.
- Rodríguez-Castrillón, J.A., Moldován, M. and Encinar, J.R. (2008) Isotope pattern deconvolution for internal mass bias correction in the characterisation of isotopically enriched spikes. *J. Anal. Atom. Spectrom.* 23: 318–324.
- Rodríguez-González, P., Marchante-Gayón, J., García Alonso, J. and Sanz-Medel, A. (2005) Isotope dilution analysis for elemental speciation: a tutorial review. *Spectrochim. Acta B* 60: 151–207.
- Rogers, C. (1932) Factors affecting the distribution of iron in plants. *Plant Physiol.* 7: 227–252.
- Sarret, G., Saumitou-Laprade, P., Bert, V., Proux, O., Hazemann, J.L., Traverse, A., et al. (2002) Forms of zinc accumulated in the hyperaccumulator *Arabidopsis halleri*. *Plant Physiol.* 130: 1815–1826.
- Spiro, T., Bates, G. and Saltman, P. (1967a) Hydrolytic polymerization of ferric citrate. II. Influence of excess citrate. *J. Am. Chem. Soc.* 89: 5559–5562.
- Spiro, T., Pape, L. and Saltman, P. (1967b) Hydrolytic polymerization of ferric citrate. I. Chemistry of the polymer. *J. Am. Chem. Soc.* 89: 5555–5559.
- Tiffin, L.O. (1966a) Iron translocation. I. Plant culture exudate sampling iron-citrate analysis. *Plant Physiol.* 41: 510–514.
- Tiffin, L.O. (1966b) Iron translocation. II. Citrate/iron ratios in plant stem exudates. *Plant Physiol.* 41: 515–518.
- Tiffin, L.O. (1970) Translocation of iron citrate and phosphorus in xylem exudate of soybean. *Plant Physiol.* 45: 280–283.
- Tiffin, L.O. and Brown, J.C. (1962) Iron chelates in soybean exudate. *Science* 135: 311–313.
- Tshuva, E. and Lippard, S. (2004) Synthetic models for non-heme carboxylate-bridged diiron metalloproteins: Strategies and tactics. *Chem. Rev.* 104: 987–1012.
- von Wirén, N., Klair, S., Bansal, S., Briat, J.F., Khodr, H., Shioiri, T., et al. (1999) Nicotianamine chelates both FeIII and FeII. Implications for metal transport in plants. *Plant Physiol.* 119: 1107–1114.
- White, M.C., Baker, F.D., Chaney, R.L. and Decker, A.M. (1981a) Metal complexation in xylem fluid: II. Theoretical equilibrium and computational computer program. *Plant Physiol.* 67: 301–310.
- White, M.C., Decker, A.M. and Chaney, R.L. (1981b) Metal complexation in xylem fluid: I. Chemical composition of tomato and soybean exudate. *Plant Physiol.* 67: 292–300.
- Woods, G.D. and Fryer, F.I. (2007) Direct elemental analysis of biodiesel by inductively coupled plasma-mass spectrometry. *Anal. Bioanal. Chem.* 389: 753–761.
- Xuan, Y., Scheuermann, E.B., Meda, A.R., Hayen, H., von Wirén, N. and Weber, G. (2006) Separation and identification of phytosiderophores and their metal complexes in plants by zwitterionic hydrophilic interaction liquid chromatography coupled to electrospray ionization mass spectrometry. *J. Chromatogr. A* 1136: 73–81.
- Yokosho, K., Yamaji, N., Ueno, D., Mitani, N. and Ma, J.F. (2009) OsFRDL1 is a citrate transporter required for efficient translocation of iron in rice. *Plant Physiol.* 149: 297–305.
- Yue, W.W., Grizot, S. and Buchanan, S. (2003) Structural evidence for iron-free citrate and ferric citrate binding to the TonB-dependent outer membrane transporter FecA. *J. Mol. Biol.* 332: 353–368.
- Zocchi, G., De Nisi, P., Dell'Orto, M., Espen, L. and Gallina, P.M. (2007) Iron deficiency differently affects metabolic responses in soybean roots. *J. Exp. Bot.* 58: 993–1000.

H.1.2. Información suplementaria del artículo científico VI

Supplementary Table I. Xylem sap pH, Fe and citrate concentrations, and Fe:Cit ratios found in previous studies under different Fe status. The most likely Fe-Cit forms are indicated with ● symbols.

	Fe status ^a	Fe in solution (μM) ^b	pH	Fe (μM)	Cit (μM)	Fe:Cit	Fe ₃ Cit ₃ ^c	Fe ₂ Cit ₂ ^c
Sunflower (Tiffin, 1966)	+Fe	10 + 10	-	2	30	1:15	●	●
	-Fe/+Fe	0.01 + 10	-	31	890	1:29	●	●
Sunflower (Tiffin, 1966)	-Fe	1 + 1	-	8	200	1:25	●	●
	-Fe/+Fe	1 + 50	-	465	460	1:1.0	●	
Tomato (Tiffin, 1966)	-Fe	1 + 2	-	28	72	1:2.6	●	
	-Fe/+Fe	1 + 10	-	131	135	1:1.0	●	
Soybean (Tiffin, 1966)	-Fe	1 + 0.5	-	10	400	1:40	●	●
	-Fe/+Fe	1 + 10	-	290	710	1:2.5	●	
Soybean (Tiffin, 1970)	-Fe	1 + 2.5	-	34	120	1:3.6	●	
<i>Zea mays</i> L WF9 (Clark et al., 1973)	-Fe	18 + 0	-	57	120	1:2	●	
<i>Zea mays</i> L ys1/ys2 (Clark et al., 1973)	-Fe		-	9	430	1:48	●	●
Soybean (White et al., 1981)	+Fe	10	6.1	6	1700	1:283		●
Tomato (White et al., 1981)	+Fe		6.4	7	300	1:43	●	●
Faba bean (Nikolic and Römheld, 1999)	+Fe	100	5.5	12	100	1:8	●	
	-Fe	2	5.5	4	2600	1:650		●
	-Fe	1 + HCO ₃ ⁻	5.5	3	2300	1:767		●
Sugar beet (López-Millán et al., 2000)	+Fe	45	6.0	6	200	1:36	●	●
	-Fe	0 + HCO ₃ ⁻	5.7	2	4700	1:2474		●
Pear trees (Larbi et al., 2003)	-Fe	field-grown	6.8	3	780	1:260		●
	-Fe/+Fe		6.5	4	470	1:118		●
Peach trees (Larbi et al., 2003)	-Fe	field-grown	6.6	2	250	1:125		●
	-Fe/+Fe		6.4	5	40	1:8	●	
<i>A. thaliana</i> WT (Durrett et al., 2007)	+Fe	100	-	11	90	1:8	●	
<i>A. thaliana frd3-1</i> (Durrett et al., 2007)	+Fe		-	5	55	1:11	●	●
<i>O. sativa</i> WT (Yokosho et al., 2009)	-Fe	2	-	6	185	1:31	●	●
	+Fe	10	-	13	135	1:10	●	●
<i>O. sativa FRDL1 KO</i> (Yokosho et al., 2009)	-Fe	2	-	5	80	1:16	●	●
	+Fe	10	-	9	55	1:65	●	●

^aIron-sufficient, Fe-deficient and Fe-deficient, Fe-resupplied plants are labeled as +Fe, -Fe and -Fe/+Fe.

^bWhen plants were precultured in a different nutrient solution the Fe concentration is indicated as A + B, where A is the Fe concentration in the preculture solution and B is the Fe concentration in the final one. Citrate, Fe and pH xylem sap values correspond to plants grown in the final nutrient solution.

^cIron to citrate concentration ratios higher than 1:10 will lead to Fe₃Cit₃, ratios lower than 1:75 will lead to Fe₂Cit₂, and ratios between 1:10 and 1:75 will lead to both complexes.

Supplementary Table II. Atom coordinates of the Fe₃Cit₃ complex. The center numbers are indicated in Supplementary Fig. 6. All values are expressed in Amstrongs.

Center number	Atomic number	Coordinates		
		X	Y	Z
1	8	0.000000	0.000000	0.000000
2	26	1.910259	0.007702	0.000000
3	26	-0.948460	-1.658184	0.000000
4	26	-0.961800	1.650482	0.000000
5	8	-2.478861	1.197270	1.251661
6	8	-1.916080	-0.994839	1.526843
7	6	-2.789751	-0.038554	1.417397
8	8	-2.478861	1.197270	-1.251661
9	8	-1.916080	-0.994839	-1.526843
10	6	-2.789751	-0.038554	-1.417397
11	8	0.096485	2.156794	1.526843
12	8	2.276297	1.548122	1.251661
13	6	1.361487	2.435272	1.417397
14	8	2.276297	1.548122	-1.251661
15	8	0.096485	2.156794	-1.526843
16	6	1.361487	2.435272	-1.417397
17	8	0.202565	-2.745392	1.251661
18	8	1.819596	-1.161955	1.526843
19	6	1.428264	-2.396718	1.417397
20	8	0.202565	-2.745392	-1.251661
21	8	1.819596	-1.161955	-1.526843
22	6	1.428264	-2.396718	-1.417397
23	6	2.561794	-3.405276	1.309731
24	1	3.240187	-3.292325	2.161717
25	1	2.181368	-4.430083	1.274604
26	6	2.561794	-3.405276	-1.309731
27	1	3.240187	-3.292325	-2.161717
28	1	2.181368	-4.430083	-1.274604
29	6	3.411223	-3.161585	0.000000
30	6	1.668158	3.921217	1.309731
31	1	1.231144	4.452247	2.161717
32	1	2.745881	4.104162	1.274604
33	6	1.668158	3.921217	-1.309731
34	1	1.231144	4.452247	-2.161717
35	1	2.745881	4.104162	-1.274604
36	6	1.032402	4.534998	0.000000
37	6	-4.229952	-0.515941	1.309731
38	1	-4.927249	0.325922	1.274604

H. PUBLICACIONES RELACIONADAS CON LA TESIS DOCTORAL

39	1	-4.471331	-1.159922	2.161717
40	6	-4.443624	-1.373413	0.000000
41	6	-4.229952	-0.515941	-1.309731
42	1	-4.927249	0.325922	-1.274604
43	1	-4.471331	-1.159922	-2.161717
44	6	4.288980	-1.772224	0.000000
45	8	3.822713	-0.553188	0.000000
46	8	5.545710	-2.022058	0.000000
47	8	4.404176	-4.226855	0.000000
48	1	5.277408	-3.731650	0.000000
49	6	-3.679281	-2.828253	0.000000
50	8	-2.390431	-3.033973	0.000000
51	8	-4.524009	-3.791697	0.000000
52	8	-5.862652	-1.700701	0.000000
53	1	-5.870407	-2.704545	0.000000
54	6	-0.609699	4.600477	0.000000
55	8	-1.432282	3.587160	0.000000
56	8	-1.021702	5.813755	0.000000
57	8	1.458476	5.927556	0.000000
58	1	0.592999	6.436194	0.000000

Supplementary Table III. Atom coordinates of the Fe₂Cit₂ complex. The center numbers are indicated in Supplementary Fig. 8. All values are expressed in Amstrongs.

Center number	Atomic number	Coordinates		
		X	Y	Z
1	26	-0.649031	-1.269867	0.345147
2	8	-2.273378	-2.137284	-0.205427
3	8	0.365552	-2.585555	-0.668604
4	8	0.95098	-0.285869	0.693017
5	8	-0.95193	0.285427	-0.695264
6	8	-1.678777	-0.343245	1.678666
7	8	1.791792	-4.35806	-0.40878
8	8	-4.352662	-2.257098	-1.131281
9	8	-3.451755	1.12418	1.784734
10	6	-3.328889	-1.594025	-0.806204
11	6	-3.296482	-0.082957	-1.15242
12	6	-2.288066	0.78429	-0.363277
13	6	-2.387041	2.278805	-0.694062
14	6	1.471176	-3.157399	-0.190886
15	6	-2.522466	0.551273	1.173632
16	26	0.648976	1.270087	-0.344755
17	6	-1.471616	3.157646	0.187817
18	6	2.385836	-2.279492	0.692795
19	6	2.287712	-0.784723	0.363143
20	8	2.27388	2.137016	0.206819
21	8	-0.366502	2.585828	0.666859
22	8	1.680033	0.344148	-1.678471
23	8	-1.791055	4.359045	0.403416
24	6	3.295229	0.081948	1.153975
25	6	2.523537	-0.550281	-1.173588
26	6	3.328066	1.593477	0.809266
27	8	3.453849	-1.122397	-1.783827

H. PUBLICACIONES RELACIONADAS CON LA TESIS DOCTORAL

28	8	4.351311	2.256054	1.137158
29	1	-3.057366	-0.00083	-2.221894
30	1	-4.312482	0.29819	-1.002936
31	1	-2.105865	2.434717	-1.744268
32	1	-3.413489	2.627254	-0.54769
33	1	3.412414	-2.627896	0.54719
34	1	2.103544	-2.436238	1.742562
35	1	4.311288	-0.299075	1.004555
36	1	3.055736	-0.001408	2.223267
37	8	0.667394	2.723017	-1.802866
38	8	-0.665955	-2.723827	1.802424
39	1	1.096799	3.434919	-1.276741
40	1	1.331386	2.256401	-2.364666
41	1	-1.330323	-2.257944	2.364365
42	1	-1.094422	-3.436212	1.276321

Supplementary Figure Legends.

Supplementary Figure 1. ESI-TOFMS mass spectra of a ^{nat}Fe -Cit standard solution (Fe:Cit ratio 1:10, 100 μM ^{nat}Fe , pH 5.5, in 50% mobile phase B) before (A) and after electrospray ionization optimization (B). Isotopic signatures of the $[\text{CitH}]^-$, $[\text{Fe}_3\text{Cit}_3\text{H}]^{2-}$ and $[\text{Fe}_3\text{OCit}_3\text{H}_3]^{2-}$ molecular ions are shown in the panel insets.

Supplementary Figure 2. HPLC-UV chromatograms obtained with Agilent 1100 (A) and Waters 2795 (B) HPLC systems of an Fe-Cit standard solution (Fe:Cit ratio 1:10, 100 μM Fe, pH 5.5 diluted in 50% mobile phase B) showing peaks corresponding to Fe_2Cit_2 and Fe_3Cit_3 complexes.

Supplementary Figure 3. HPLC-ESI-TOFMS chromatograms of 5 mM citrate (A), 100 μM Fe (III)-NA (B) and 100 μM Fe(III)-DMA (C) standard solutions. Chromatograms show the $[\text{CitH}]^-$ (A), $[\text{Fe(III)-NA+Cl}]^-$ (B) and $[\text{Fe(III)-DMA}]^-$ (C) ions at m/z values 191.0, 391.0 and 356.0 (± 0.1), respectively.

Supplementary Figure 4. Experimental (A, C, E and G) and theoretical (B, D, F and H) isotopic signatures of the molecular ions associated to Fe_2Cit_2 and Fe_3Cit_3 , $[\text{Fe}_2\text{Cit}_2\text{H}]^-$ and $[\text{Fe}_3\text{Cit}_3\text{H}]^{2-}$, respectively. Experimental data are zoomed ESI-TOF mass spectra of the Fe_2Cit_2 and Fe_3Cit_3 chromatographic peaks found when using ^{54}Fe (A, E) and ^{nat}Fe (C, G).

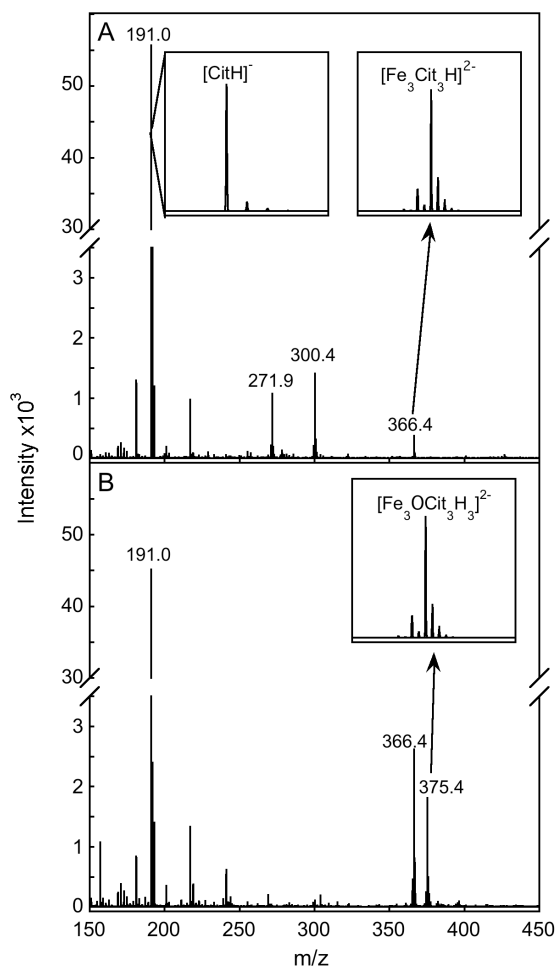
Supplementary Figure 5. Effect of the Fe:Cit ratio on the Fe_2Cit_2 and Fe_3Cit_3 balance, HPLC-ICP-MS (A-D) and HPLC-ESI-TOFMS (E-H) chromatograms of ^{54}Fe -Cit standard solutions with Fe:Cit ratios 1:1, 1:10, 1:100 and 1:500 (100 μM ^{54}Fe , pH 5.5 in 50% mobile phase B) showing peaks corresponding to Fe_2Cit_2 and Fe_3Cit_3 complexes. HPLC-ESI-TOFMS traces were extracted at m/z values 241.93 and 484.87 (± 0.05), corresponding to $[\text{Fe}_2\text{Cit}_2]^{2-}$ and $[\text{Fe}_2\text{Cit}_2\text{H}]^-$, respectively, (for Fe_2Cit_2 , solid line) and 363.40 and 372.40 (± 0.05), corresponding to $[\text{Fe}_3\text{Cit}_3\text{H}]^{2-}$ and $[\text{Fe}_3\text{OCit}_3\text{H}_3]^{2-}$, respectively, (for Fe_3Cit_3 , dotted line).

Supplementary Figure 6. Proposed structure for the Fe_3Cit_3 indicating the center numbers (See atom coordinates in Supplementary Table I). Iron, oxygen, carbon and hydrogen atoms are shown in purple, red, green and white, respectively.

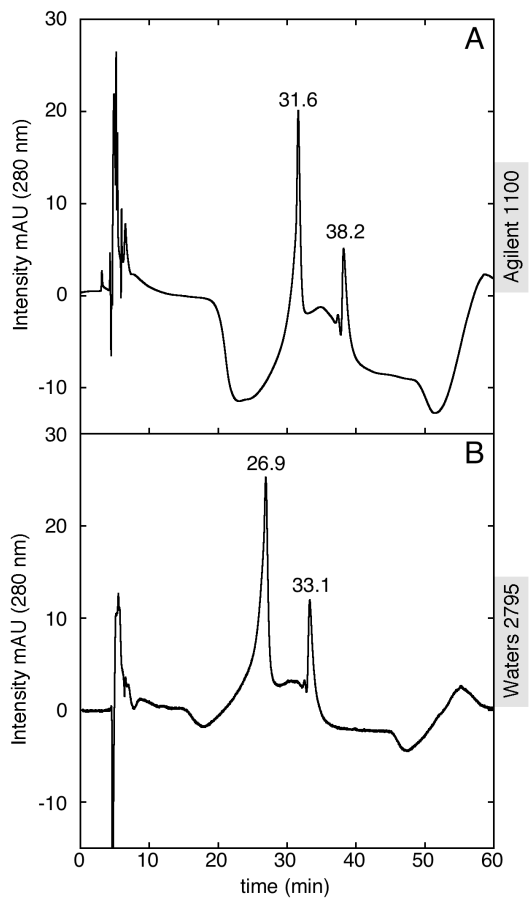
Supplementary Figure 7. Proposed structure for the Fe_2Cit_2 complex. Iron, oxygen, carbon and hydrogen atoms are shown in purple, red, green and white, respectively.

Supplementary Figure 8. Proposed structure for the Fe_2Cit_2 indicating the center numbers (See atom coordinates in Supplementary Table III). Iron, oxygen, carbon and hydrogen atoms are shown in purple, red, green and white, respectively.

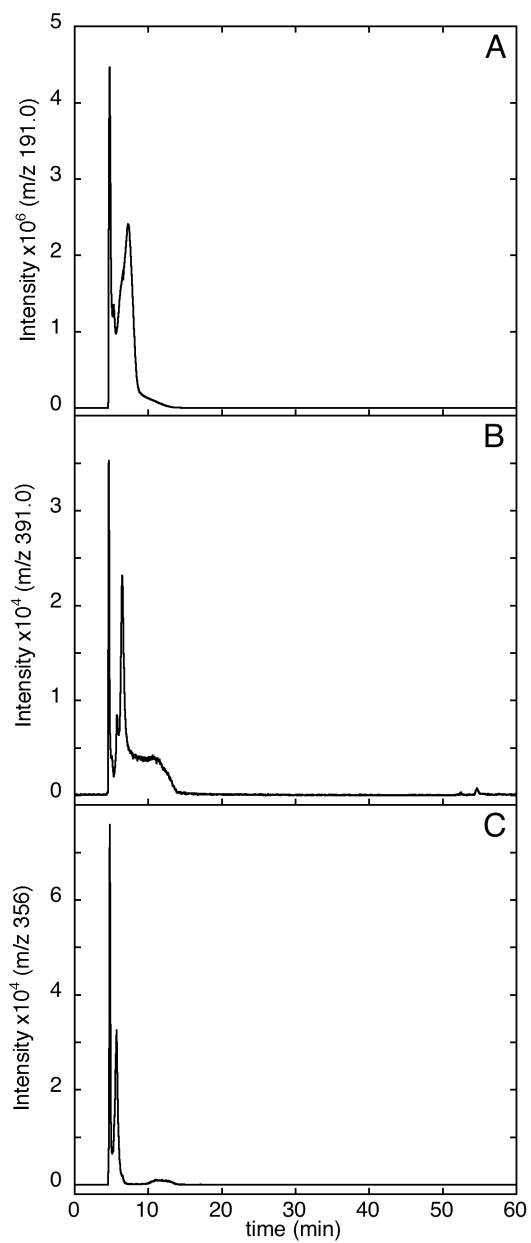
Supplementary Figure 1



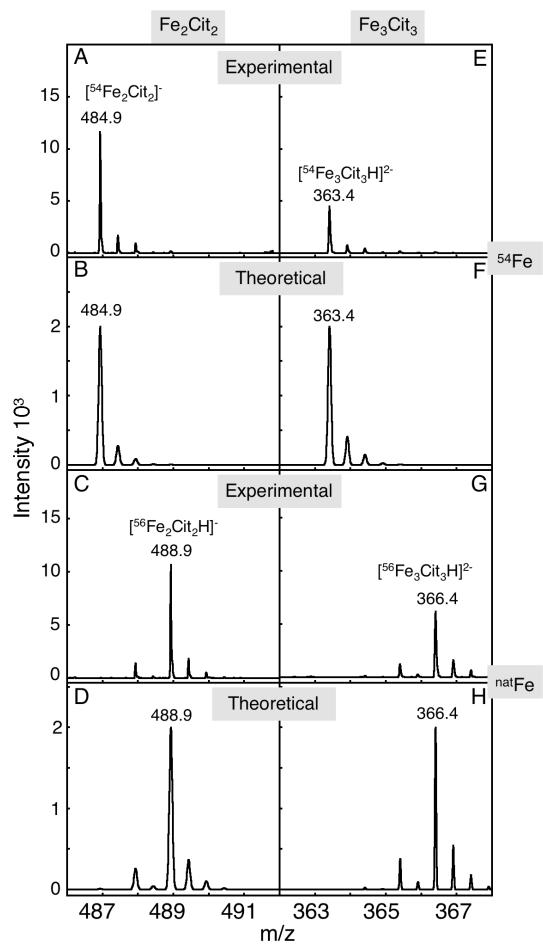
Supplementary Figure 2



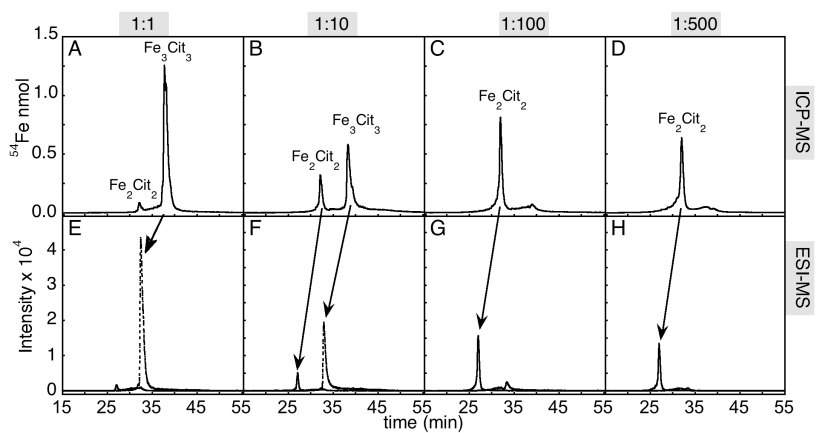
Supplementary Figure 3



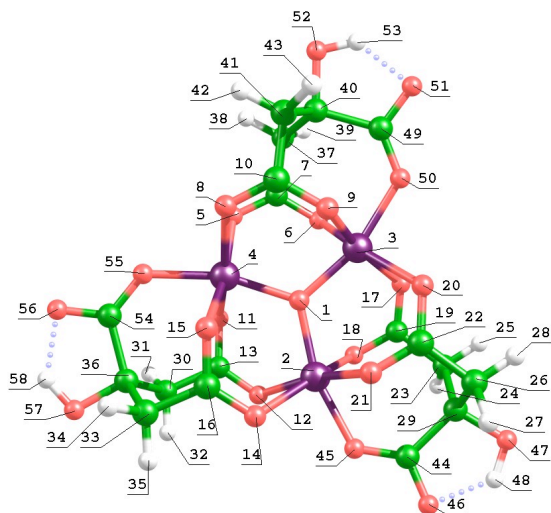
Supplementary Figure 4



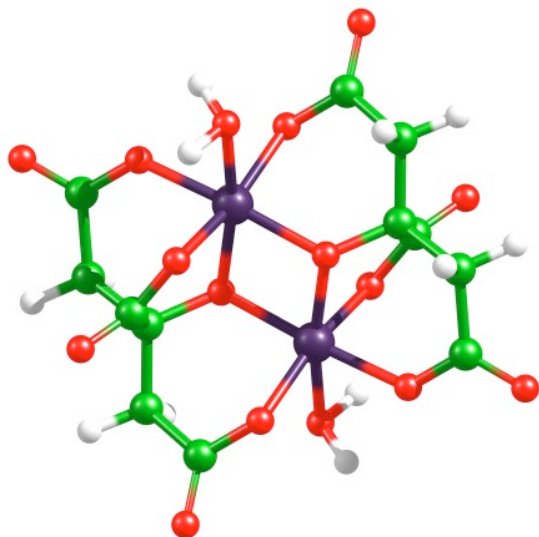
Supplementary Figure 5



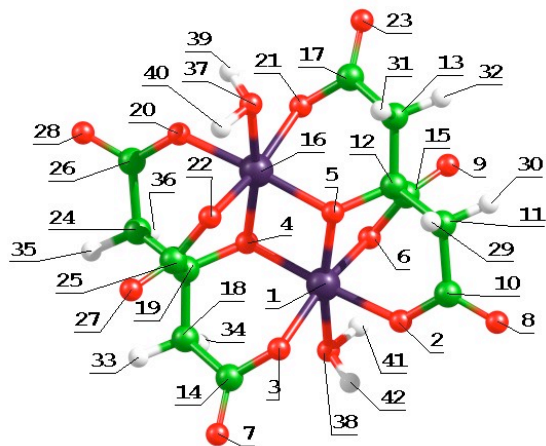
Supplementary Figure 6



Supplementary Figure 7

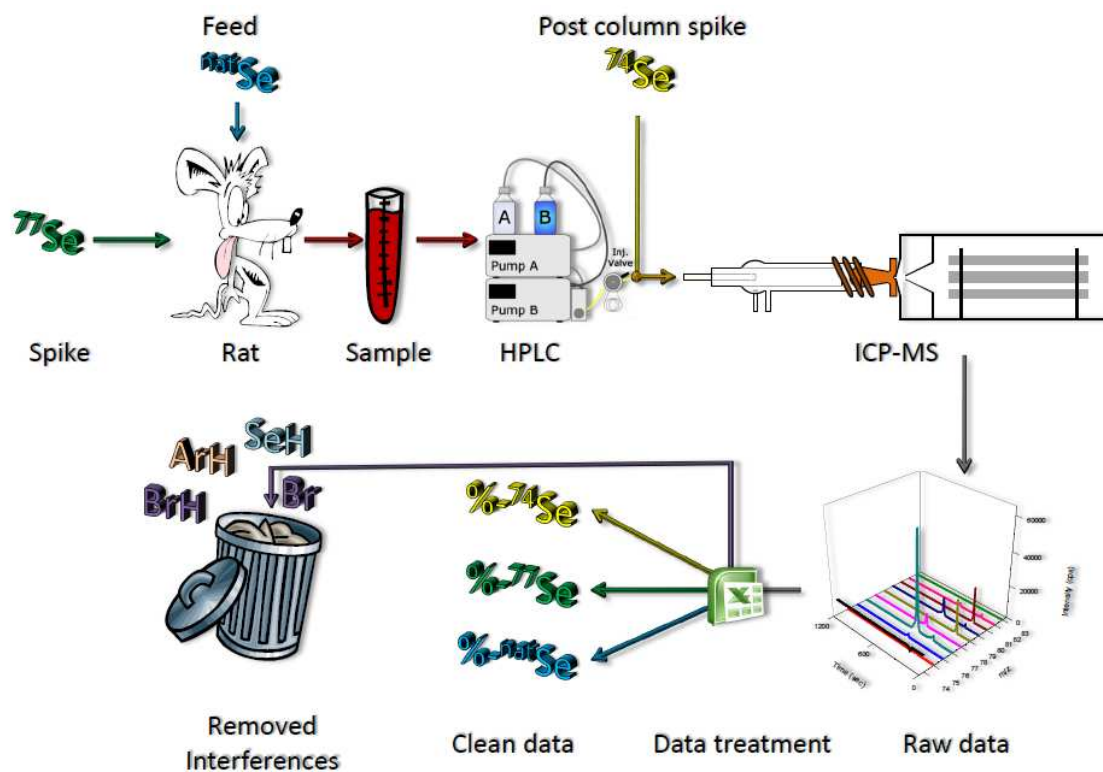


Supplementary Figure 8



H.2. ESTUDIOS DEL METABOLISMO DEL SELENIO UTILIZANDO ISÓTOPOS ESTABLES ENRIQUECIDOS

H.2.1. Artículo científico VII: Anal. Bioanal. Chem., 2012, 402, 2749-2763



Anal Bioanal Chem (2012) 402:2749–2763
DOI 10.1007/s00216-012-5747-7

ORIGINAL PAPER

Internal correction of spectral interferences and mass bias for selenium metabolism studies using enriched stable isotopes in combination with multiple linear regression

Kristoffer Lunøe · Justo Giner Martínez-Sierra ·
Bente Gammelgaard · J. Ignacio García Alonso

Received: 13 October 2011 / Revised: 12 January 2012 / Accepted: 13 January 2012 / Published online: 10 February 2012
© Springer-Verlag 2012

Abstract The analytical methodology for the *in vivo* study of selenium metabolism using two enriched selenium isotopes has been modified, allowing for the internal correction of spectral interferences and mass bias both for total selenium and speciation analysis. The method is based on the combination of an already described dual-isotope procedure with a new data treatment strategy based on multiple linear regression. A metabolic enriched isotope (^{77}Se) is given orally to the test subject and a second isotope (^{74}Se) is employed for quantification. In our approach, all possible polyatomic interferences occurring in the measurement of the isotope composition of selenium by collision cell quadrupole ICP-MS are taken into account and their relative contribution calculated by multiple linear regression after minimisation of the residuals. As a result, all spectral interferences and mass bias are corrected internally allowing the fast and independent quantification of natural abundance selenium (^{nat}Se) and enriched ^{77}Se . In this sense, the calculation of the tracer/tracee ratio in each sample is straightforward. The method has been applied to study the time-related tissue incorporation of ^{77}Se in male Wistar rats while maintaining the ^{nat}Se steady-state conditions. Additionally, metabolically relevant information such as selenoprotein synthesis and selenium elimination in urine could be studied using the proposed methodology. In this case, serum proteins were separated by affinity chromatography while reverse phase

was employed for urine metabolites. In both cases, ^{74}Se was used as a post-column isotope dilution spike. The application of multiple linear regression to the whole chromatogram allowed us to calculate the contribution of bromine hydride, selenium hydride, argon polyatomics and mass bias on the observed selenium isotope patterns. By minimising the square sum of residuals for the whole chromatogram, internal correction of spectral interferences and mass bias could be accomplished. As a result, the tracer/tracee ratio could be calculated for each selenium-containing species and a time relationship for synthesis and degradation established. Both selenite and selenized yeast labelled with ^{77}Se were employed for comparative purposes.

Keywords Mass spectrometry · ICP-MS · Speciation · Biological samples


Introduction

Selenium is both an essential and a toxic element and has furthermore shown cancer-protective properties. Neither the mechanisms behind the cancer-protective properties nor the general metabolism are fully elucidated yet. The chemical forms of selenium are of key importance and speciation studies are therefore needed to gather knowledge as to the species transformation occurring in the organism; selenium speciation and metabolism have recently been reviewed [1].

Studies aimed at clarifying the selenium metabolism and cancer-protective effect need the ability to trace the selenium from administration to excretion. By use of enriched stable isotopes, radioactive tracers, formerly employed for this type of study, are avoided. Enriched stable isotopes of selenium have been employed by different research groups [2–9] both for the total determination and speciation analysis of selenium

K. Lunøe · B. Gammelgaard
Department of Pharmaceutics and Analytical Chemistry,
Faculty of Pharmaceutical Sciences, University of Copenhagen,
2100 Copenhagen, Denmark

J. G. Martínez-Sierra · J. I. G. Alonso (✉)
Department of Physical and Analytical Chemistry,
University of Oviedo,
33006 Oviedo, Spain
e-mail: jiga@uniovi.es

 Springer

in biological materials and/or for metabolism purposes [10–14]. In most cases, final quantitative measurements are performed by ICP-MS using a collision/reaction cell instrument. The accurate determination of total selenium in biological materials by isotope dilution analysis has been described [1]. Additionally, speciation methodologies combining affinity separations and post-column isotope dilution analysis were developed [2] and further improved [3–6] for the determination of Glutathione peroxidase (GPX3), Selenoprotein P (SePP1) and Selenoalbumin (SeAlb) in blood serum. For *in vivo* metabolism studies, two general isotopic procedures were described: (a) the saturation of the animals with an enriched isotope of selenium [10–14] or (b) the use of a double isotope procedure without prior isotopic saturation [8, 9]. In all cases, severe polyatomic interferences from bromine hydride (BrH), selenium hydride (SeH) and argon polyatomics (Ar₂ and Ar₂H) needed to be corrected for. Generally, external correction based on natural abundance bromine or selenium standards was employed for the elimination of spectral interferences [2, 3, 8, 9]. So, the SeH/Se and the BrH/Br factors were measured externally and applied for the correction in the measured samples. Rodriguez-Castrillon *et al.* [15] showed that the values of SeH/Se and BrH/Br in the real samples could be different from those measured in the standards and developed an internal correction procedure in the determination of total selenium in biological materials based on multiple linear regression. However, the method was developed for total determinations and when only one enriched isotope of selenium was employed. For speciation analysis in metabolic studies, and when more than one enriched isotopes were used, the classical external correction procedure was applied [8]. In the paper of Gonzalez-Iglesias *et al.* [8] for selenium speciation in urine samples, the bromine peak eluted at the same time as the inorganic selenium peak. Under those circumstances a very good estimation of the BrH/Br factor is required because slight over- or under-correction of the interference will provide variable signals of the inorganic selenium peak at mass 80. So, it is important to calculate the correction factors to be applied in the real samples and not in standard solutions as those have been observed to change [15]. Also, the internal correction procedure is much faster than the previous method as it not requires the measurement of any external standard.

In this paper, we extend the internal correction procedure developed by Rodriguez-Castrillon *et al.* [15] for selenium metabolic studies including speciation analysis and when two selenium enriched isotopes are used. The multiple linear regression procedure allows the automatic and internal correction of all possible spectral interferences (BrH, SeH, Ar₂, Ar₂H) and the calculation of the instrumental mass bias to be applied for the correction of the selenium isotope abundances. The method was developed for the case when two enriched isotopes of selenium are employed (⁷⁷Se as metabolic tracer and ⁷⁴Se as

quantitation tracer) both for total selenium determination in biological fluids and tissues and for speciation studies in blood serum and urine. To illustrate the advantages of the proposed procedure the method was applied for the study of the time related tissue incorporation and selenoprotein synthesis in male Wistar rats fed with ⁷⁷Se-enriched selenite and selenized yeast.

Experimental

Instrumentation

The ICP-MS used was an Agilent 7500ce (Agilent Technologies, Kyoto, Japan). For interference suppression, the collision cell was employed in the helium mode with 4 mL/min He. Other relevant operating parameters are given in Table 1. Masses measured were 74, 75, 76, 77, 78, 79, 80, 81, 82 and 83 for all samples. Speciation analyses were performed with a Shimadzu LC-20AD UFLC system (Shimadzu, Duisburg, Germany) comprising two LC pumps and a system controller directly coupled to the nebulizer of the ICP-MS instrument. Tissue samples were digested using a microwave oven from CEM (Matthews, North Carolina, USA). All sample preparation was done gravimetrically.

Reagents and materials

Enriched isotopes of selenium ⁷⁴Se and ⁷⁷Se were obtained in solid form from Cambridge Isotope Laboratories (Andover, MA, USA) and dissolved in nitric acid. These selenium standards were in the form of Se(IV) and were already characterised in isotope composition and concentration [8, 9]. Selenized yeast labelled with ⁷⁷Se was generously supplied by PharmaNord (Vejle, Denmark). This selenized yeast has been previously characterised both in isotopic composition and selenium concentration [16]. The isotope composition of all enriched isotopes employed together with the natural selenium abundance is included in Table 2. Please note that the isotopic composition of the inorganic and yeast ⁷⁷Se was slightly different.

Table 1 Typical operating parameters for the ICP-MS used for the selenium measurements

Agilent 7500ce ICP-MS		
Parameter	Value	Unit
RF Power	1,500	W
Carrier Gas	1.15	L/min
QP Focus	-10	V
QP Bias	-16	V
OctP Bias	-18	V
He Gas	4	mL/min

Table 2 Selenium isotopic patterns used in the calculations for natural abundance selenium (^{nat}Se), ^{74}Se enriched selenium (^{74}Se) and ^{77}Se enriched selenium (^{77}Se) both as labelled yeast or inorganic selenium

Mass	^{nat}Se	^{74}Se	^{77}Se (yeast)	^{77}Se (inorganic)
74	0.0089	0.9967	0.0003	0.0006
76	0.0937	0.0006	0.0007	0.0103
77	0.0763	0.0003	0.9933	0.911
78	0.2377	0.0007	0.002	0.039
79	0.0000	0.0000	0.0000	0.0000
80	0.4961	0.0015	0.002	0.034
81	0.0000	0.0000	0.0000	0.0000
82	0.0873	0.0003	0.002	0.0054
83	0.0000	0.0000	0.0000	0.0000

Animal experiments

Animal experiments were carried out following the guidelines established by The Animal Experiments Directive (86/609/EEC) on the protection of animals used for experimental and other scientific purposes. Male Wistar rats were kept in separate metabolic cages and exposed to 12-h light–dark cycles. A number of 11 rats were employed in this experiment. Rats were fed *ca.* 10 μg of ^{77}Se either as selenite or selenized yeast and faeces and urine samples were collected after 0, 6, 12, 18, 24 and 48 h. Drinking water and standard maintenance feed were available *ad libitum*. At each time interval, a corresponding ^{77}Se labelled rat from each group was anesthetized using an isoflurane–oxygen mixture and the blood extracted by heart puncture. Afterwards the rats were killed by severing the spinal cord. Different tissues (brain, testes, kidney, spleen, pancreas–intestine, liver, lungs and heart) were collected.

Sample preparation

For tissue samples representative, accurately weighed (wet weight) cuts from the extracted tissue were taken and these were microwave digested in 1 mL sub-boiled nitric acid. Total selenium determination was carried out after spiking with a known amount of ^{74}Se . The blood of the rat was allowed to clot and afterwards centrifuged 5 min at 3,000 rpm, the supernatant transferred to a clean tube and centrifuged again. The resulting supernatant was portioned out in Eppendorf tubes and frozen at $-20\text{ }^{\circ}\text{C}$ until analysis. The serum was diluted 1+1 with mobile phase A before injection. The red blood cells were digested as for the tissue samples. The urine samples were centrifuged and the supernatant portioned into Eppendorf tubes and frozen at $-20\text{ }^{\circ}\text{C}$ until analysis. Faeces samples were digested as for tissue samples.

Chromatographic procedures

For serum speciation, the affinity chromatography setup was an adapted version of the method originally developed by Reyes *et al.* [2] and since refined by Jitaru *et al.* [4–7]. The applied method made use of unmodified 1 mL HiTrap[®] Blue and 1 mL HiTrap[®] Heparin columns (GE Healthcare, Barcelona, Spain). Mobile phase A was 0.05 mol/L ammonium acetate and mobile phase B was 1.5 mol/L ammonium acetate. Injection volume was 100 μL . The post-column isotope dilution solution was 20 ng/g ^{74}Se in 1% HNO_3 and was introduced into the LC flow at 0.3 g/min by a peristaltic pump. For urine speciation we employed the same reverse phase chromatography setup used by González Iglesias *et al.* [8] and the same post-column spike used for the affinity separation. An injection volume of 50 μL was employed for the urine analysis.

Data treatment procedures

Two data treatment procedures based on multiple linear regression were developed either for total selenium analysis or speciation analysis. It was assumed that all intensities measured were originating from five different isotopic signatures in the sample: natural abundance selenium (^{nat}Se), ^{77}Se labelled selenium (^{77}Se) used as metabolic tracer, ^{74}Se labelled selenium (^{74}Se) added for quantification, natural abundance bromide (^{nat}Br) present in all samples and natural abundance argon (^{nat}Ar) present as polyatomic interferences not completely eliminated by the collision cell. The theoretical isotope signatures employed were calculated taking into account the possible formation of hydrides for all components. For selenium, a single SeH/Se factor was applied to all isotopic signatures considered. For total selenium analysis, the raw intensity data at masses 74, 76, 77, 78, 79, 80, 81, 82 and 83 were first corrected for mass bias using the exponential mass bias correction equation:

$$I_i = I_i^{\text{exp}} e^{-k\Delta M} \quad (1)$$

Where I_i are the corrected intensities and I_i^{exp} the measured intensities. The mass bias factor k was given an initial value of 0 and was then optimised by the least square procedure. All ΔM values were the nominal mass differences *versus* mass 80 of selenium which was used as reference. Then, all corrected intensities were converted into relative abundances, A_i , using the equation:

$$A_i = \frac{I_i}{\sum_{i=74}^{i=83} I_i} \quad (2)$$

These relative abundances were subjected to multiple linear regression using the five component isotope matrix

corresponding to ^{nat}Se , ^{77}Se , ^{74}Se , ^{nat}Br and ^{nat}Ar . Finally, the residuals of the multiple linear regression were minimised by changing the mass bias factor, k , and the SeH/Se , BrH/Br and $\text{Ar}_2\text{H}/\text{Ar}_2$ factors employed to calculate the theoretical isotope abundances in the multiple linear regression. For this purpose, the SOLVER application in Excel was used. As a result, the molar fractions and their uncertainties corresponding to the three selenium isotope signatures in the sample were calculated. The concentrations of ^{nat}Se and ^{77}Se were then calculated using the equations:

$$N_{nat\text{Se}} = N_{74\text{Se}} \frac{X_{nat\text{Se}}}{X_{74\text{Se}}} \quad (3)$$

and

$$N_{77\text{Se}} = N_{74\text{Se}} \frac{X_{77\text{Se}}}{X_{74\text{Se}}} \quad (4)$$

Where N_{nat} , N_{74} and N_{77} are the moles of natural abundance selenium and selenium enriched in either ^{74}Se or ^{77}Se , respectively. The known weights of sample and spike taken together with the corresponding atomic weights then enable the calculation of the individual concentrations.

For speciation analysis, a similar procedure was employed. First, all intensities in the chromatogram were corrected for mass bias as indicated above. For every time interval, a multiple linear regression calculation was performed and a “reconstructed” chromatogram was calculated for all masses. The intensity differences between the experimental chromatogram and the reconstructed chromatogram are the residuals at each mass. The sum of squared residuals was then calculated for all measured masses and for the whole chromatogram and minimised by changing the mass bias and the hydride factors. As a result, the molar fractions for ^{nat}Se , ^{77}Se and ^{74}Se were obtained. From those molar fractions, a relative molar flow chromatogram was obtained. The integration of the peaks in the molar flow chromatogram produced the amounts of ^{nat}Se and ^{77}Se in the corresponding peaks as explained previously [8, 9].

Results and discussion

Development of the calculation procedure for total selenium determination

The measurement of selenium isotopes by ICP-MS is hindered by several spectral interferences. Argon polyatomics (Ar_2^+ and Ar_2H^+) are present mainly at masses

76, 78, 80 and 81 while bromine hydrides affect masses 80 and 82 of selenium. Additionally, selenium can also form hydrides which will be observed as low signals at masses 75, 77, 78, 79, 81 and 83. Argon polyatomics can be reduced or even eliminated in collision cell quadrupole instruments by using helium, hydrogen or mixtures of both as collision gas [2, 3]. Dynamic Reaction Cell quadrupole instruments most often use methane as reaction gas to eliminate the polyatomic argon interferences [16–18]. Bromine and selenium hydrides cannot be eliminated by the cell technologies and their contribution needs to be corrected for. When performing isotopic measurements on selenium, these spectral interferences are usually corrected by an external procedure in which bromine and selenium standards are used to calculate the BrH/Br and SeH/Se factors [2, 3, 8, 9]. However, it has been observed that these factors may not be the same for samples and standards and an internal correction procedure based on multiple linear regression was developed [15]. The internal correction procedure was only developed for a single enriched isotope of selenium and for total analysis. This procedure is extended here to metabolism studies both for total analysis and speciation where two enriched isotopes of selenium are considered: a metabolic isotope and a quantitation isotope. The internal correction procedure is particularly important when the retention time of the selenium species is similar to that of bromine as it occurs for inorganic selenium in urine samples and for Glutathione peroxidase in serum samples.

The procedure is based on multiple linear regression in which the intensities measured at masses 74, 76, 77, 78, 79, 80, 81, 82 and 83 are deconvoluted by multiple least squares into the molar fractions of five different isotope patterns. These five isotope patterns considered are those of natural abundance selenium (^{nat}Se), enriched ^{77}Se (^{77}Se), enriched ^{74}Se (^{74}Se), natural abundance bromine (^{nat}Br) and natural abundance argon (^{nat}Ar). The theoretical isotope patterns considered in the multiple linear regression fitting were those of the expected species in the plasma. For selenium, the theoretical patterns included the contribution of Se^+ and SeH^+ with a given SeH/Se ratio which was the same for all isotopic forms of selenium considered. For bromine the theoretical patterns included both Br^+ and BrH^+ at a given BrH/Br ratio. Finally, for argon the theoretical patterns included Ar_2^+ and Ar_2H^+ at a given $\text{Ar}_2\text{H}/\text{Ar}_2$ ratio. It was necessary to include the argon pattern to improve the fit of the multiple linear regression even when this contribution was small in the collision cell instrument. We did not consider the possibility of ArCl interferences at masses 75 and 77 as these are readily removed by the collision cell instrument.

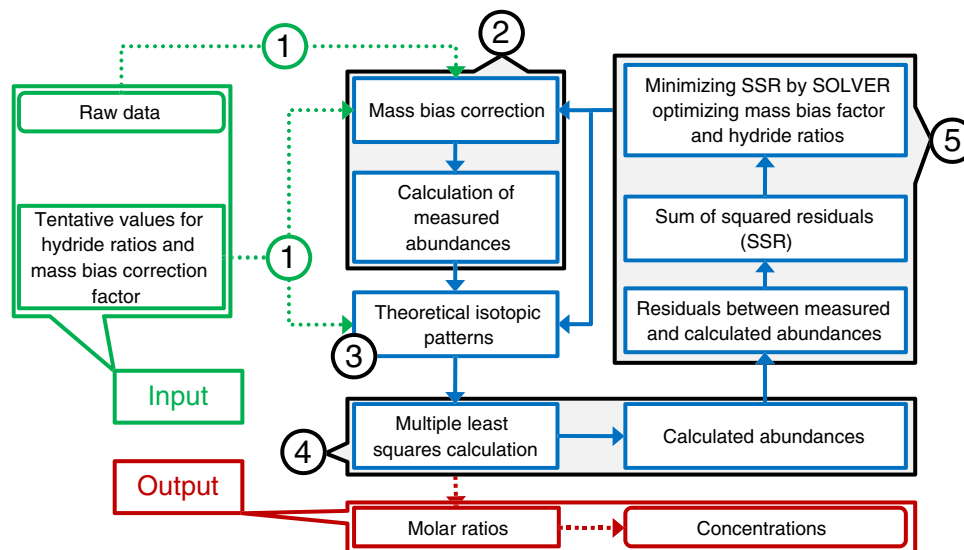


Fig. 1 Flow diagram of the calculation procedure. (1) Input raw data along with tentative values for hydride ratios and the mass bias correction factor (*k*). (2) Correct for mass bias using tentative *k* value and calculate abundances. (3) Calculate theoretical isotopic patterns based on tentative hydride ratios. (4) Apply multiple least squares

calculations and find calculated abundances. (5) Calculate residuals between measured and calculated abundances and let the SOLVER function minimize the sum of squared residuals by changing the hydride ratios and mass bias

The multiple linear regression equation used is shown below:

$$\begin{bmatrix} A_{74} \\ A_{76} \\ A_{77} \\ A_{78} \\ A_{79} \\ A_{80} \\ A_{81} \\ A_{82} \\ A_{83} \end{bmatrix} = \begin{bmatrix} A_{natSe} & A_{77Se} & A_{74Se} & A_{natBr} & A_{natAr} \\ A_{74} & A_{74} & A_{74} & A_{74} & A_{74} \\ A_{76} & A_{76} & A_{76} & A_{76} & A_{76} \\ A_{77} & A_{77} & A_{77} & A_{77} & A_{77} \\ A_{78} & A_{78} & A_{78} & A_{78} & A_{78} \\ A_{79} & A_{79} & A_{79} & A_{79} & A_{79} \\ A_{80} & A_{80} & A_{80} & A_{80} & A_{80} \\ A_{81} & A_{81} & A_{81} & A_{81} & A_{81} \\ A_{82} & A_{82} & A_{82} & A_{82} & A_{82} \\ A_{83} & A_{83} & A_{83} & A_{83} & A_{83} \end{bmatrix} \times \begin{bmatrix} x_{natSe} \\ x_{77Se} \\ x_{74Se} \\ x_{natBr} \\ x_{natAr} \end{bmatrix} + \begin{bmatrix} e_{74} \\ e_{76} \\ e_{77} \\ e_{78} \\ e_{79} \\ e_{80} \\ e_{81} \\ e_{82} \\ e_{83} \end{bmatrix} \tag{5}$$

The measured abundances at masses 74 to 83 are deconvoluted into five theoretical isotope patterns, *j*, and the contribution of each isotope pattern to the observed abundances, *x_j*, calculated. As we have more equations (*i*=9) than unknowns (*j*=5), we have to include an error vector in the equation. The squared sum of all *e_i* values is the square sum of residuals of the multiple linear regression. This square sum of residuals is important as it can be employed for the correction of systematic errors in the regression such as spectral interferences or mass bias [15].

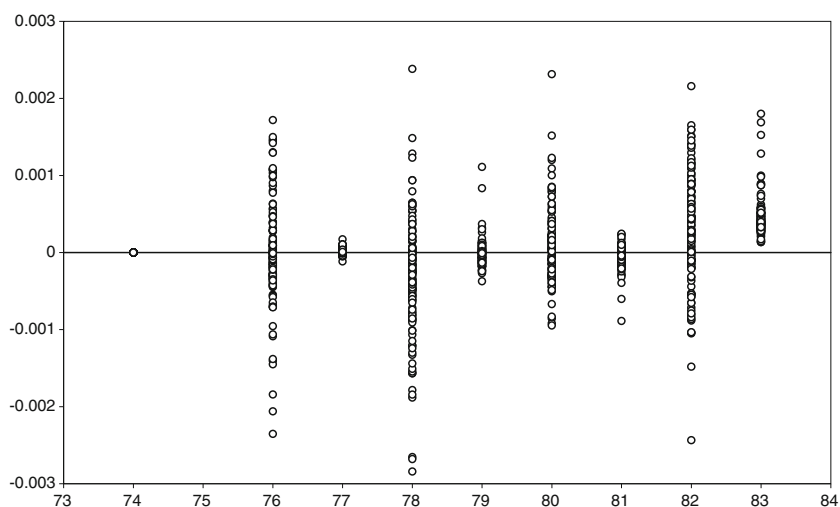
An important source of systematic errors in multiple linear regression is mass bias. The transport and detection efficiency of different isotopes of an element normally increases with mass in ICP-MS. So, when fitting several theoretical isotope patterns to one observed convoluted pattern the effect of mass bias needs to be considered. Mass bias is usually defined for a

single element. In this paper we have considered that the different transmission of all measured masses (arising either from Se, Br or Ar species) could be modelled with a single mass bias factor. So, the original intensities measured were corrected for mass bias using Eq. (1) regardless of the originating species. The reference isotope was taken as mass 80 for convenience but any other isotope could have been taken without affecting the results. Once mass bias corrected intensities are calculated, the measured isotope abundances to be used in Eq. (5) are determined using Eq. (2): each corrected intensity is divided by the sum of all intensities.

Table 3 Example of the theoretical isotope patterns calculated for the five components after optimisation of the hydride factors. In this case SeH/Se=0.030, BrH/Br=0.128 and Ar₂H/Ar₂=4.06

Mass	Natural Se	⁷⁴ Se	⁷⁷ Se (yeast)	Natural Br	Natural Ar
74	0.00864	0.96782	0.00029	0.00000	0.00000
76	0.09099	0.00058	0.00068	0.00000	0.00132
77	0.07680	0.00031	0.96454	0.00000	0.00538
78	0.23302	0.00069	0.03072	0.00000	0.00025
79	0.00689	0.00002	0.00006	0.44944	0.00101
80	0.48173	0.00146	0.00194	0.05746	0.19595
81	0.01437	0.00004	0.00006	0.43721	0.79607
82	0.08477	0.00029	0.00194	0.05589	0.00000
83	0.00253	0.00001	0.00006	0.00000	0.00000

Fig. 2 Residuals of the multiple linear regression for the 132 samples analysed for total selenium determination



For the calculation of the multiple linear regression, it is important to take into account that the theoretical patterns to be used in Eq. (5) can be optimised as well. Depending on the SeH/Se, BrH/Br and Ar₂H/Ar₂ factors considered, different theoretical patterns can be generated. Obviously, the “right” hydride factors to be employed when building the theoretical patterns will be those producing a minimum in the sum of squared residuals of the multiple linear regression. If we take into account that, for each sample, five contribution factors, x_j , need to be calculated, and four parameters optimised, it was found necessary to gain degrees of freedom by assuming that the four parameters to be optimised (k , SeH/Se, BrH/Br and Ar₂H/Ar₂) remained

constant for the group of samples analysed on the same run. So, the minimisation of the sum of squared residuals was made for a group of samples rather than for individual samples. For example, for the 132 samples analysed on the same run, 664 parameters needed to be calculated ($5 \times 132 + 4$) with 1188 data points (9 masses \times 132) resulting in 524 degrees of freedom. It was observed that the optimisation procedure using the SOLVER application in Excel was straightforward when many samples were optimised simultaneously.

The flow diagram of the calculation procedure employed is shown in Fig. 1. First, tentative values are given to the four parameters to be optimised for all samples: k , SeH/Se, BrH/

Fig. 3 Variation of the optimized hydride factors SeH/Se and BrH/Br (*left axis*) and the mass bias factor k (*right axis*) for the 11 serum samples analysed by LC-ICP-MS. Average and standard deviation values are also shown

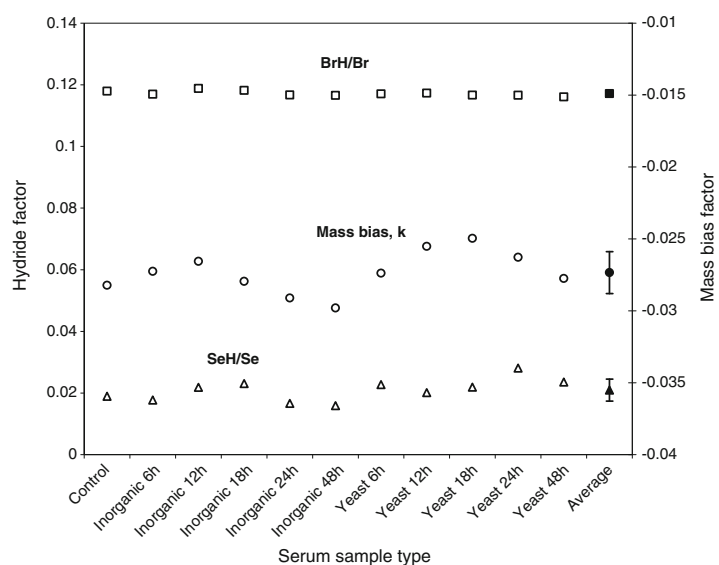


Fig. 4 Steps in the calculation for the affinity chromatographic method (6 h after yeast ^{77}Se administration), see the “Experimental” section for details. **(a)** Experimental (red line) and reconstructed (black dashed line) chromatograms at mass 80 together with the residuals obtained (circles, right axis). **(b)** Contribution factors for $^{\text{nat}}\text{Br}$, $^{\text{nat}}\text{Se}$, ^{77}Se and ^{74}Se . **(c)** Pattern-specific relative molar flow chromatogram

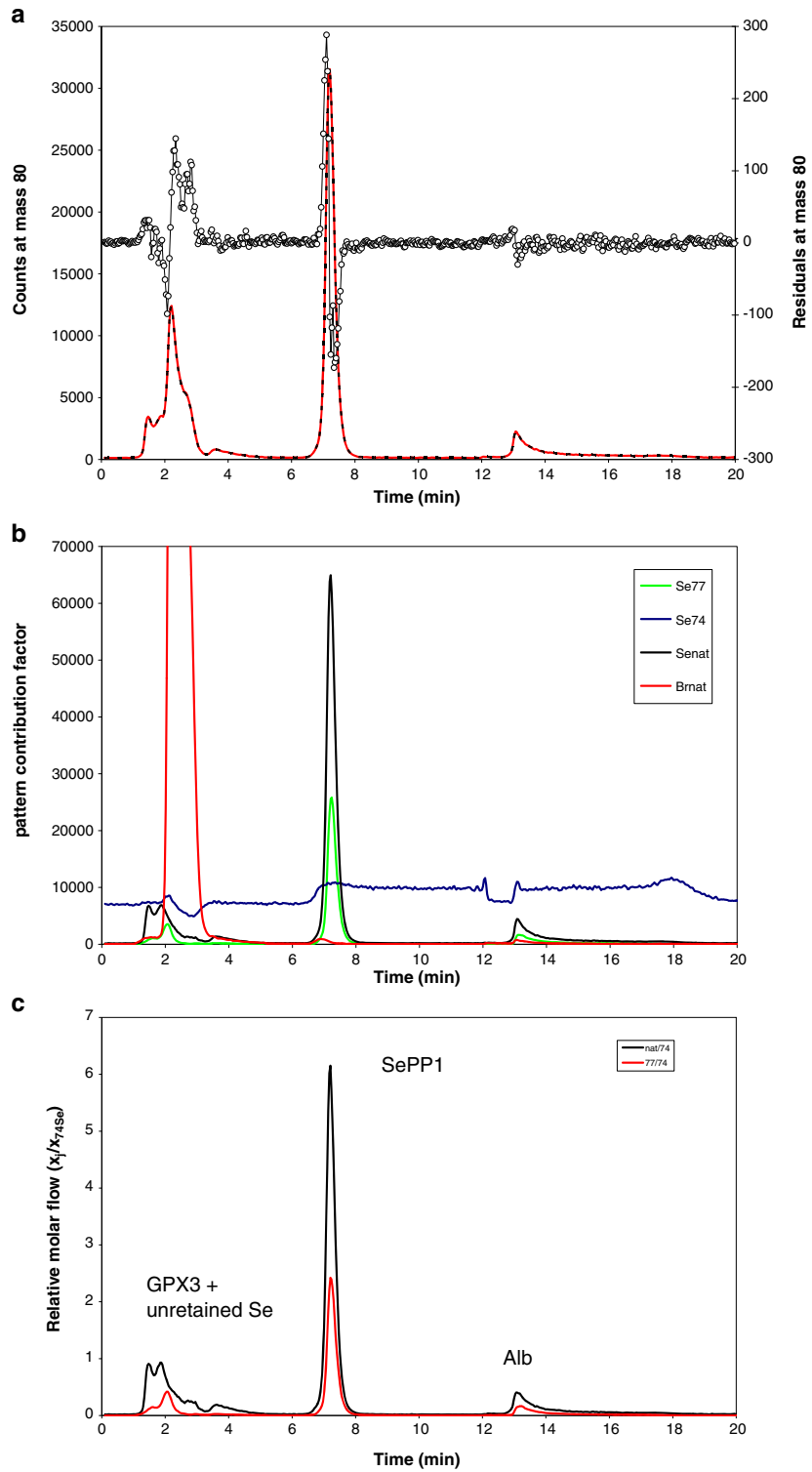


Table 4 Total selenium results obtained for the experiments with ⁷⁷Se in inorganic form

Sample	Control (76 g)		6 h (94 g)		12 h (143 g)		18 h (134 g)		24 h (135 g)		48 h (120 g)	
	natSe	⁷⁷ Se	natSe	⁷⁷ Se	natSe	⁷⁷ Se	natSe	⁷⁷ Se	natSe	⁷⁷ Se	natSe	⁷⁷ Se
Brain	134.5±1.3	-0.2±0.8	176.6±6.9	20.0±4.1	166.2±2.6	7.3±1.5	166.4±3.3	7.5±1.9	170.1±3.7	10.4±2.2	161.0±1.8	5.0±1.1
Testes	683.5±3.7	-1.6±2.1	543.2±4.1	41.7±2.4	687.0±7.9	23.4±4.6	561.0±9.0	29.8±5.3	584.5±8.9	38.0±5.2	717±12	38.3±6.9
Kidney	847±10	-3.2±5.5	869.4±4.9	444.4±2.9	730.0±6.0	247.9±3.4	825.5±5.3	241.2±3.1	778.3±8.8	211.7±5.1	867±10	134.1±5.7
Spleen	335.4±2.8	-2.7±2.8	350.3±5.8	115.0±3.4	325.7±4.2	44.9±2.5	313.9±5.3	65.4±3.1	334.6±3.7	50.8±2.2	416.0±7.6	47.7±4.5
Pancreas-intestine	303.1±4.1	-2.9±2.4	243.8±4.1	150.8±2.4	204.9±4.1	70.1±2.4	217.6±4.2	38.3±2.5	210.1±5.6	49.9±3.3	228.1±4.2	22.1±2.5
Liver	702.9±2.9	-2.8±1.7	556.5±9.4	532.3±5.6	781±12	336.0±7.2	512.9±6.8	132.3±4.0	573±10	116.2±5.8	535.9±9.4	69.3±5.5
Lungs	285.3±5.0	0.0±2.9	300.9±5.3	155.2±3.1	267.7±5.2	63.1±3.0	302±10	59.4±6.0	291.4±8.5	55.6±5.0	345±10	39.8±5.8
Heart	340.3±8.6	2.6±5.1	216.2±6.2	68.2±3.7	275.7±4.2	30.2±2.5	287.9±3.9	39.2±2.3	283.8±3.7	35.3±2.2	292.1±3.1	20.9±1.8
Red blood cells	331.7±8.2	-2.4±4.9	312.3±7.0	60.8±4.1	277.6±4.3	36.0±2.5	333.2±8.9	38.2±5.3	283.7±5.5	30.8±3.2	289.9±6.1	26.1±3.6
Serum	293.1±3.9	-0.8±2.1	223.3±2.3	122.3±1.3	244.6±1.9	97.6±1.1	237.3±1.2	90.8±0.7	247.3±3.3	75.4±1.9	291.6±2.6	51.7±1.5
Urine	63.2±1.6	-0.8±0.9	51.1±0.9	193.8±0.5	147.1±1.7	478.0±1.4	268.8±2.9	508.8±2.4	259.5±3.6	540.1±3.1	228.7±3.8	164.5±2.3
Faeces	111.1±9.0	0.0±5.3	109±10	6.6±5.7	134.3±6.6	37.9±3.9	149.8±7.8	183.3±4.6	129.1±5.8	255.8±3.4	141.2±5.0	23.0±2.9

Concentrations in ng/g wet weight except serum and urine. Uncertainties are indicated as standard uncertainties. The weights of the rats are indicated in parentheses

Br and Ar₂H/Ar₂. Second, the measured abundances in the samples are calculated using Eqs. (1) and (2). Third, the theoretical isotope patterns are computed based on the given SeH/Se, BrH/Br and Ar₂H/Ar₂ factors and, fourth, the contribution of the different components is calculated by multiple linear regression (function LINEST in Excel) using Eq. (5) for all samples considered. Finally, an iterative procedure is initiated (SOLVER in Excel) in which the sum of squared residuals, pooled for all samples considered, is minimised by changing the four correction parameters. Typical values of the theoretical isotope patterns generated taking into account

the hydride contribution are given in Table 3. Please compare these theoretical patterns generated taking into account the hydride contribution with the pure selenium isotope patterns given in Table 2 and those for bromine published by the IUPAC (0.5069 for ⁷⁹Br and 0.4931 for ⁸¹Br) [19]. The observed hydride factors for SeH/Se and BrH/Br, 0.030 and 0.128 respectively, were typical of those determined in the same instrument [2, 3, 15].

Figure 2 shows the goodness of fit for the multiple linear regression. All residuals for the 132 samples measured are plotted for the different measured masses. As can be

Table 5 Total selenium results obtained for the experiments with ⁷⁷Se in organic form (yeast)

Sample	6 h (129 g)		12 h (161 g)		18 h (127 g)		24 h (90 g)		48 h (120 g)	
	natSe	⁷⁷ Se	natSe	⁷⁷ Se	natSe	⁷⁷ Se	natSe	⁷⁷ Se	natSe	⁷⁷ Se
Brain	162.4±3.9	17.6±2.1	156.6±4.2	14.6±2.3	153.4±1.9	22.7±1.1	181.7±3.3	21.1±1.8	171.9±5.4	11.0±3.0
Testes	690.0±4.6	34.5±2.5	767.4±4.4	32.7±2.3	763.8±8.1	44.4±4.3	532.7±8.1	65.5±4.4	725.9±6.0	37.4±3.2
Kidney	822.4±5.0	225.3±2.7	945±10	262.8±5.1	829.0±9.3	282.4±5.0	850.0±7.0	254.3±3.8	910.8±6.7	140.8±3.6
Spleen	348.1±5.0	90.7±2.7	314.7±4.0	65.8±2.1	342±13	91.0±6.9	382.9±3.5	88.1±1.9	382.9±5.1	44.2±2.7
Pancreas-intestine	193.6±3.3	110.2±1.8	240.6±3.2	105.6±1.7	249.3±4.9	138.0±2.6	216.5±6.4	80.4±3.5	287.9±4.2	48.2±2.3
Liver	611.2±4.6	244.2±2.4	707.5±5.4	152.9±2.9	639.1±8.5	168.6±4.6	569.8±4.7	178.5±2.6	644.2±2.9	92.2±1.6
Lungs	338.9±5.4	86.6±2.9	244.6±8.1	54.9±4.4	290.0±8.1	84.5±4.4	305.2±7.4	75.3±4.0	317.8±3.7	37.8±2.0
Heart	293.2±3.1	40.1±1.7	274.1±4.4	32.1±2.4	291.1±2.1	50.7±1.1	305.8±7.5	48.4±4.1	295.0±2.1	24.9±1.1
Red blood cells	281.1±8.0	26.0±4.4	315.8±6.3	40.9±3.4	290±11	36.8±6.1	288.0±8.8	41.5±4.8	325±10	27.2±5.3
Serum	235.8±2.1	70.6±1.1	265.5±2.5	83.8±1.3	267.6±1.6	109.3±0.8	251.0±2.4	90.3±1.3	307.3±1.3	55.8±0.7
Urine	266.7±4.4	711.6±4.5	163.2±1.5	147.9±0.9	316.6±5.4	618.5±4.9	366.9±4.8	641.4±4.4	140.1±3.8	65.2±2.1
Faeces	118.9±5.9	-0.5±3.2	180.3±5.3	71.1±2.9	152.4±5.6	197.8±3.0	86.2±3.2	45.6±1.8	123.3±7.4	17.3±4.0

Concentrations in ng/g wet weight except serum and urine. Uncertainties are indicated as standard uncertainties. The weights of the rats are indicated in parentheses

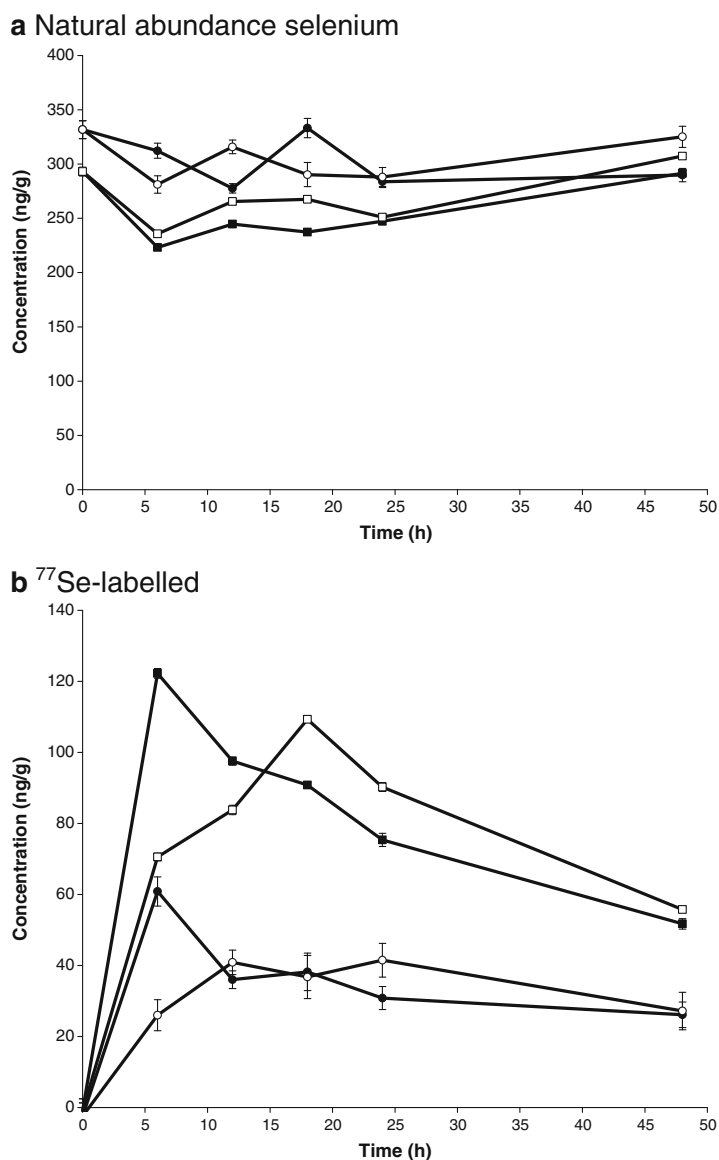
observed, all residuals were lower than ± 0.003 and showed a uniform distribution between positive and negative values. No influence of the sample type (i.e. tissues, urine, blood, etc.) on the residual distribution was observed.

Once the contribution factors for ^{nat}Se ($x_{nat\text{Se}}$), ^{77}Se ($x_{77\text{Se}}$) and ^{74}Se ($x_{74\text{Se}}$) are calculated for all samples, Eqs. (3) and (4) are applied to compute independently the concentrations of ^{nat}Se and labelled ^{77}Se in all samples. The tracer/tracee ratio is obtained directly by the ratio $x_{77\text{Se}}/x_{nat\text{Se}}$.

Development of the calculation procedure for selenium speciation

For selenium speciation, a similar calculation procedure was employed. In this case, every point in the chromatogram at all measured masses (here including mass 75 for a better definition of the SeH/Se factor using ^{74}Se added post-column) was subjected to multiple linear regression. A sixth theoretical pattern for natural abundance arsenic (100% ^{75}As) had to be included in Eq. (5) as this element could be present in some of

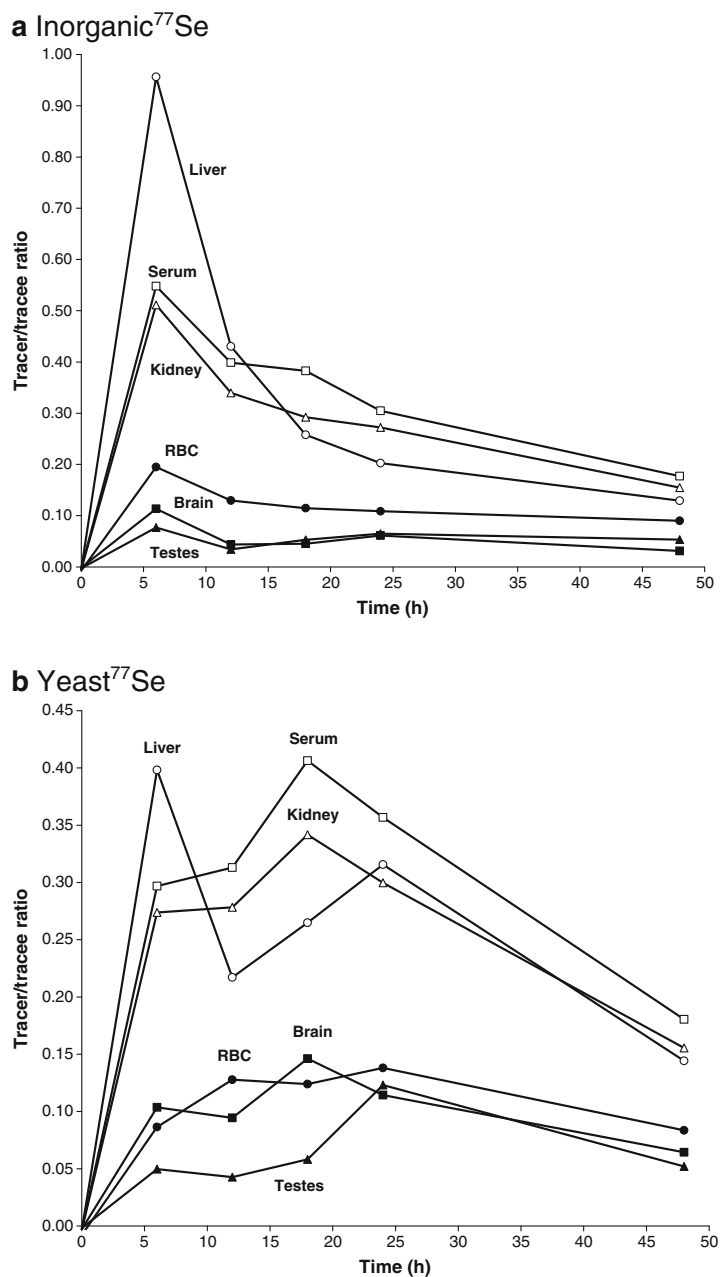
Fig. 5 Concentrations of selenium vs. time in serum (squares) and red blood cells (circles) for ^{nat}Se (a) and ^{77}Se (b) when administering inorganic selenium (black symbols) or organic selenium (white symbols). Error bars indicate standard uncertainties. (a) Natural abundance selenium. (b) ^{77}Se -labelled



the samples analysed such as urine. The square sum of residuals was calculated for every point in the chromatogram and the sum of all squared residuals for the chromatogram used in the optimisation procedure. For each chromatogram, an independent optimisation was performed. A typical chromatogram for serum or urine speciation contained *ca.* 800–900 data

points obtained every 2 s at 10 different masses (0.2 s integration time per mass). In all cases (11 urine samples and 11 serum samples) the optimised mass bias and hydride values were very similar and close to those obtained by total analysis. For example, Fig. 3 shows the optimised values for the BrH/Br and the SeH/Se factors together with the mass bias factors *k*

Fig. 6 Tracer/tracee ratios ($^{77}\text{Se}/^{\text{nat}}\text{Se}$) for inorganic selenium administration (a) and organic selenium (b). Tissues indicated are liver, serum, kidney, rbc, brain and testes. (a) Inorganic ^{77}Se . (b) Yeast ^{77}Se



calculated for the 11 serum samples. As can be observed, reasonable and reproducible values were obtained by the internal multiple linear regression procedure. For the BrH/Br factor the average value was 0.117 ± 0.001 (1 s) which is very close to that obtained for the 132 samples for total selenium (0.128). For the SeH/Se factor, the average value was 0.021 ± 0.004 (1 s) which was also close to the selenium hydride factor calculated for the 132 samples analysed for total selenium (0.030). In conclusion, the multiple linear regression procedure applied with internal optimisation of the hydride factors and mass bias provided chemically meaningful results of the mass bias and hydride factors. Finally, the average mass bias factor k calculated for the 11 chromatograms was -0.027 ± 0.001 (1 s) which was also similar to the best fit value for the 132 samples of $k = -0.025$.

The only problem observed with this calculation procedure was due to spectral skew. For some masses the fit was limited by the sequential nature of the quadrupole measurements. For example, Fig. 4a shows the experimental and the fitted chromatogram at mass 80 together with the residuals calculated in one of the serum chromatograms. As can be observed, during peak elution, a series of positive/negative residuals are obtained and this is clearly seen for the SePP1 peak at ca. 7.5 min. The small differences in the times in which all masses are measured during peak elution (spectral skew) produced this trend of positive residuals before the peak and negative residuals after the peak. Anyway, the maximum value of the residuals (ca. 300 counts) was less than 1% of the absolute count values at this mass so the reconstructed chromatogram fitted very well to the measured chromatogram. Apart from these minor problems of spectral skew all chromatograms obtained at all masses could be reconstructed adequately by the proposed multiple linear regression procedure.

The variation of the contribution factors, x_j , with time are given in Fig. 4b for the same serum sample shown

in Fig. 4a. These contribution factors can be seen here as the sum of all intensities at the different masses that can be ascribed to a certain isotope pattern. As can be observed, a large peak between 2 and 3 min was ascribed to the natural abundance bromine pattern. Once the contribution of bromine is computed all other selenium patterns are free from spectral interferences and show the real contribution of each selenium pattern to the observed intensities.

For the calculation of the concentrations of ^{nat}Se and ^{77}Se we have only to divide, point by point, the contribution of the ^{nat}Se or ^{77}Se by the contribution of ^{74}Se added post-column. In that way we obtain the relative molar flow chromatogram shown in Fig. 4c where the first peak corresponds to GPX3 and other unknown selenium species, and the second peak to SePP1 and the third small peak to SeAlb. The y -axis represents the ratio of molar flows $^{nat}\text{Se}/^{74}\text{Se}$ or $^{77}\text{Se}/^{74}\text{Se}$. As we know the molar flow of ^{74}Se (added post-column), we can calculate the molar flows of the other selenium isotopic patterns. Finally, the integration of the molar flow chromatograms provides directly the mols of each selenium pattern in each peak. So, pattern specific quantitative information can be obtained by this procedure. Obviously, the tracer/tracee ratio can be obtained for each peak obtaining species-specific metabolic data.

Time-related selenium incorporation and elimination in tissues

To test the mathematical procedure developed, a very simple metabolic experiment was carried out. Five male Wistar rats were fed $10.8 \mu\text{g}$ of ^{77}Se in the form of Se(IV) in water and another five $10.0 \mu\text{g}$ of ^{77}Se in the form of selenized yeast in a suspension. An untreated rat was used as control. Solid

Table 6 Results for selenium speciation in serum obtained for the experiments with ^{77}Se in inorganic and organic (yeast) forms. Concentrations in ng/g

Fraction	Control		6 h		12 h		18 h		24 h		48 h	
	^{nat}Se	^{77}Se	^{nat}Se	^{77}Se	^{nat}Se	^{77}Se	^{nat}Se	^{77}Se	^{nat}Se	^{77}Se	^{nat}Se	^{77}Se
Inorganic ^{77}Se												
GPX3	27	nd	53	30	32	6	35	4	46	7	50	7
SePP1	127	nd	124	85	71	48	106	55	132	52	149	28
SeAlb	6	nd	17	13	12	4	11	4	14	4	17	4
Total	160	–	193	128	115	58	151	63	191	63	216	39
Yeast ^{77}Se												
GPX3	–	–	65	16	64	13	68	12	51	11	50	7
SePP1	–	–	139	54	145	64	143	82	135	60	162	30
SeAlb	–	–	20	9	22	7	18	7	16	7	17	4
Total	–	–	224	79	232	85	229	100	202	78	229	42

samples were microwave digested, while liquid samples were diluted and all samples measured by ICP-MS as indicated in the procedures. Data on concentrations of ^{nat}Se and ^{77}Se as well as $^{77}\text{Se}/^{nat}\text{Se}$ (tracer/tracee ratios) could be obtained together with their standard uncertainties (from the multiple linear regression calculations). Tables 4 and 5 summarise all concentration results obtained for inorganic selenium (Table 4) and organic selenium (Table 5). All

results are expressed in ng/g on a wet weight basis except for serum and urine where a simple dilution with water and ^{74}Se spiking was performed. In order to better understand the results a graphic representation is more suitable. Figure 5 shows the data obtained for serum and red blood cells both for natural abundance selenium (Fig. 5a) and ^{77}Se enriched (Fig. 5b). As can be observed in Fig. 5a, the concentrations of natural abundance selenium are relatively constant with

Fig. 7 Tracer/tracee ratios ($^{77}\text{Se}/^{nat}\text{Se}$) for inorganic selenium administration (a) and organic selenium (b) for selenium species in serum. (a) Inorganic ^{77}Se . (b) Yeast ^{77}Se

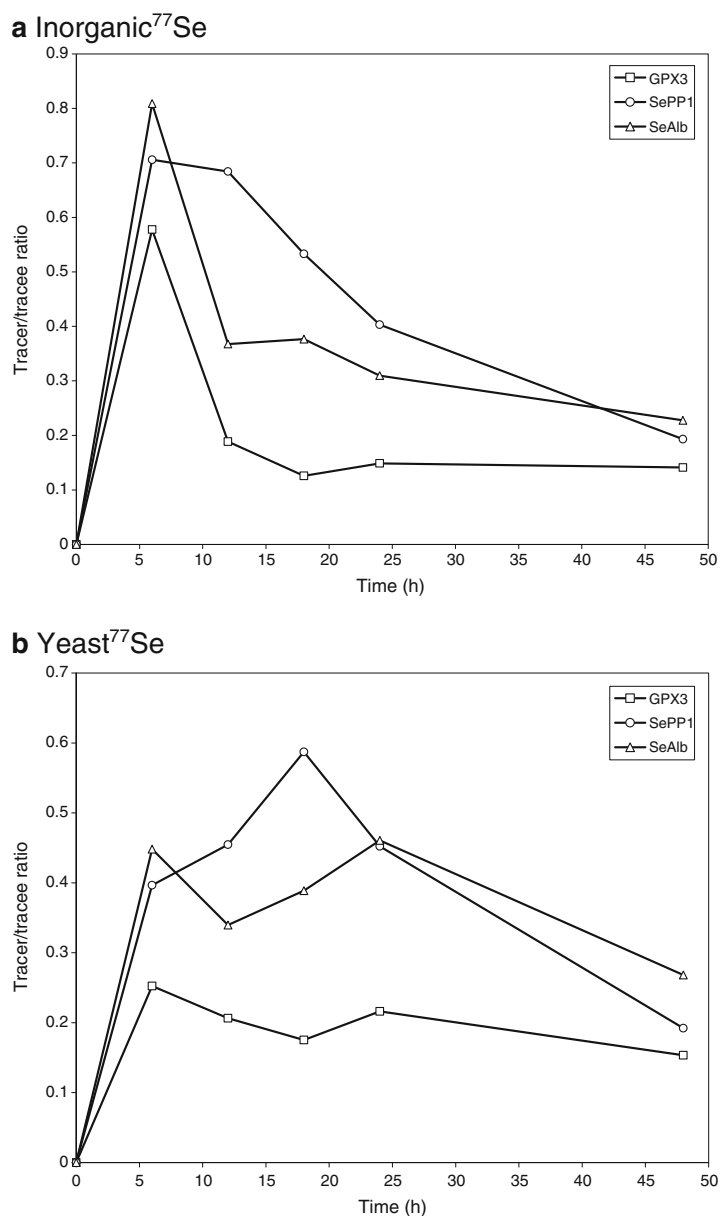
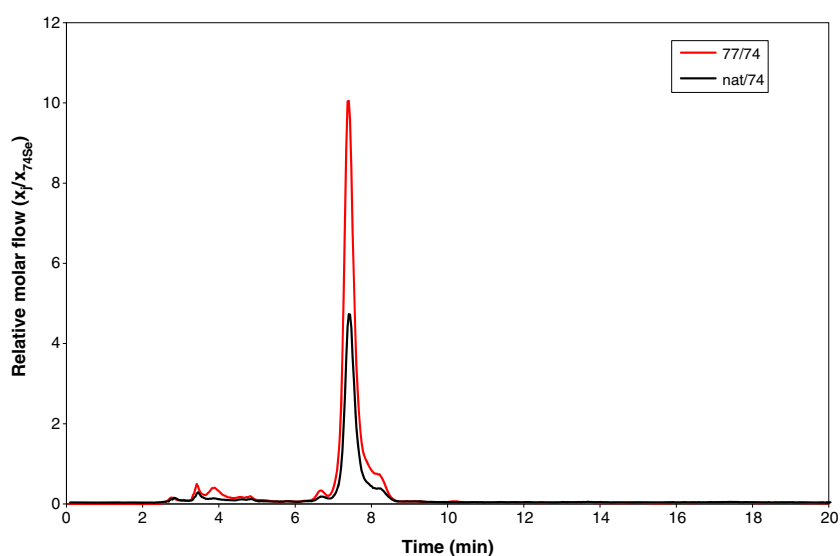


Fig. 8 Typical relative mass flow chromatogram of a urine sample (Yeast ^{77}Se administration after 18 h). Reverse phase chromatographic procedure, see the “Experimental” section



time for both samples and both forms of supplementation (inorganic and organic ^{77}Se). No corrections based on the weights of the rats were performed here. So, steady state conditions for natural abundance selenium seemed to have been achieved for this experiment. Similar results were obtained for all sample types. The results for labelled ^{77}Se are given in Fig. 5b. Here it can be observed that incorporation of inorganic ^{77}Se is progressing faster than for yeast ^{77}Se . Inorganic selenium peaks at 6 h while organic selenium peaks at 18 h. The results are similar for the other tissues. When comparing serum and red blood cells it is clear that the relative amount of ^{77}Se incorporated in serum is much higher than the relative incorporation in the red blood cells. However, these comparative incorporation

data is better seen as tracer/tracee ratios as these ratios should not be strongly affected by rat weight or biological variability between individuals.

Figure 6 shows the tracer/tracee ratios for selected tissues and inorganic selenium administration (Fig. 6a) or organic selenium administration (Fig. 6b). As can be observed, the time profiles for tissue incorporation are completely different for both selenium sources. Inorganic selenium is rapidly incorporated in all tissues (6 h) with a continuous decay afterwards. On the other hand, organic selenium peaks between 18 and 24 h except for the liver that shows a mixed behaviour with two peaks at 6 and 24 h. For both tracer forms, there is a distinct behaviour between liver, serum and kidney on the one

Table 7 Results for selenium speciation in urine

Type	Control		6 h		12 h		18 h		24 h		48 h	
	nat ⁷⁷ Se	⁷⁷ Se	nat ⁷⁷ Se	⁷⁷ Se	nat ⁷⁷ Se	⁷⁷ Se	nat ⁷⁷ Se	⁷⁷ Se	nat ⁷⁷ Se	⁷⁷ Se	nat ⁷⁷ Se	⁷⁷ Se
Inorganic ^{77}Se												
Peak 1	5.1	nd	8.1	28.4	10.8	32.4	32.5	64.8	19.3	45.3	22.5	19.1
Peak 2	21.8	nd	17.8	101.2	74.7	291.8	135.6	283.8	149.2	363.4	127.7	122.4
Total Se	26.9	nd	25.9	129.6	85.5	324.1	168.0	348.5	168.6	408.7	150.2	141.5
Yeast ^{77}Se												
Peak 1	–	–	22.7	75.3	9.0	17.9	24.7	54.6	43.0	111.7	17.3	11.9
Peak 2	–	–	144.7	403.5	77.8	55.4	242.0	503.4	252.9	437.3	57.7	30.2
Total Se	–	–	167.4	478.8	86.8	73.3	266.6	557.9	295.8	549.0	75.0	42.1

Peak 1 corresponds to the sum of all peaks between 2 and 5 min retention time. Peak 2 corresponds to the selenosugar plus the two small satellite peaks. Total selenium is the sum of peaks 1 and 2. Concentrations in ng/g

hand and RBC, brain and testes on the other hand. Much lower tracer/tracee ratios are obtained for these last three tissues.

It is not the objective of this work to discuss in detail selenium metabolism but to show that relevant metabolic results can be obtained easily by combining the double isotope approach with advanced data treatment methodologies. It is clear that a larger number of animals would be needed to conclude on the metabolic information.

Time related incorporation of selenium into serum proteins

For the study of selenium incorporation into serum proteins, the affinity procedure developed by Reyes *et al.* [2] was applied. As can be observed in Fig. 4c, three fractions were isolated by affinity chromatography. The first fraction corresponded to GPX3 and other non retained selenium compounds, the second fraction corresponded to SePP1 and the third fraction to SeAlb. Based on the relative molar flow chromatograms obtained for all samples, the concentrations of natural abundance selenium (^{nat}Se) and isotopically labelled selenium (^{77}Se) could be calculated for all three fractions. The results obtained are summarised in Table 6 both for inorganic ^{77}Se and organic (yeast) ^{77}Se respectively. The sum of all fractions should be similar to the total concentrations shown in Tables 4 and 5 for serum. Speciation recoveries (column recoveries) were, on average, $80 \pm 16\%$ from those of total analysis.

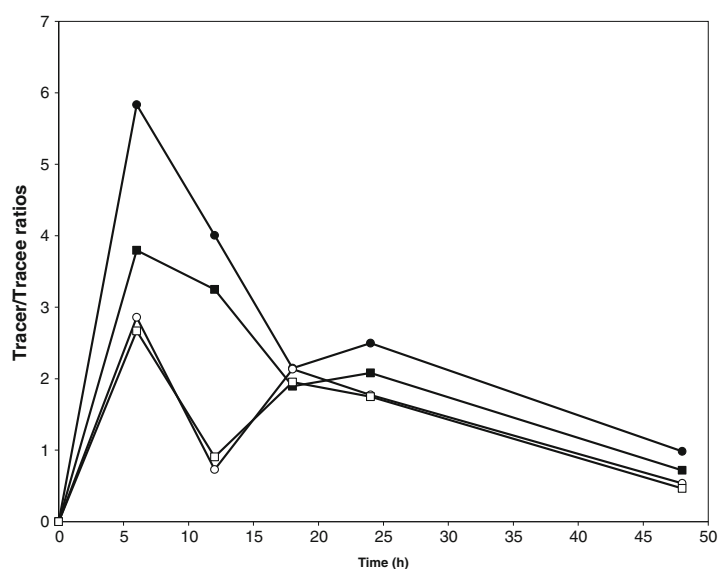
The tracer/tracee ratios for each selenium fraction and type of ^{77}Se label are shown in Fig. 7 for inorganic

^{77}Se (Fig. 7a) and yeast ^{77}Se (Fig. 7b). As can be observed, all selenoproteins show different tracer/tracee ratios and different apparent rates of synthesis and degradation. Fast turnover is observed for inorganic ^{77}Se administration while a slower turnover was observed for yeast ^{77}Se with SePP1 peaking after 18 h of administration and SeAlb with a double peak at 6 and 24 h. It is remarkable to observe that SePP1 has a synthesis–degradation profile similar to that of total selenium in the kidney (Fig. 6), while SeAlb (and perhaps also GPX3) has a synthesis–degradation profile similar to total selenium in liver (Fig. 6) for both ^{77}Se sources. This behaviour fits reasonably well with SePP1 being a transport protein synthesized primarily in the liver where albumin is also synthesized [20]. The liver takes up the selenium after gastrointestinal uptake and synthesizes SeAlb and SePP1 [21]. Both proteins enter the bloodstream and as SePP1 is the Se-transport protein it is selectively taken up by the kidney, thereby increasing the Se content of the organ, and the kidney utilizes the selenium from SePP1 to synthesize GPX3 [22, 23].

Time related urinary excretion of selenium

Figure 8 shows a typical reverse phase relative molar flow chromatogram for ^{nat}Se and ^{77}Se in urine. The main peak at *ca.* 7.5 min corresponds to the selenosugar [8, 9]. The other small peaks were not identified. All urine chromatograms obtained had the same profile with varying contribution from ^{nat}Se or ^{77}Se . It was decided to integrate the chromatograms in two parts. The first peak (peak 1) corresponded to

Fig. 9 Tracer/tracee ratios for the selenosugar peak (peak 2) in urine (circles) and for total selenium (squares). Yeast ^{77}Se is shown as white symbols and inorganic ^{77}Se as black symbols



the small peaks with retention times between 2 and 5 minutes. The second peak (peak 2) corresponded to the main selenosugar peak and the two small satellite peaks on both sides. The sum of all urine peaks could be compared with the results obtained for the total selenium concentrations found for the same urine samples to check for selenium recovery. The average recovery (column recovery) was 67% with a standard deviation of 13%. Also, the tracer/tracee ratios in the selenosugar peak (peak 2) for the two ^{77}Se sources could be calculated. The concentration results found are shown in Table 7 and the tracer/tracee ratios for peak 2 represented in Fig. 9 in comparison with the results for total selenium (Tables 4 and 5). As can be observed in Fig. 8, the tracer/tracee ratios for the selenosugar are close to those observed for total selenium in urine, particularly for the rats administered with yeast ^{77}Se . It is again remarkable that the synthesis–degradation profile obtained for the selenosugar is very similar to that obtained for total selenium in liver (Fig. 6) indicating that this organ is responsible for the synthesis of the selenosugar in agreement with the results of Ogra *et al.* [24].

Conclusion

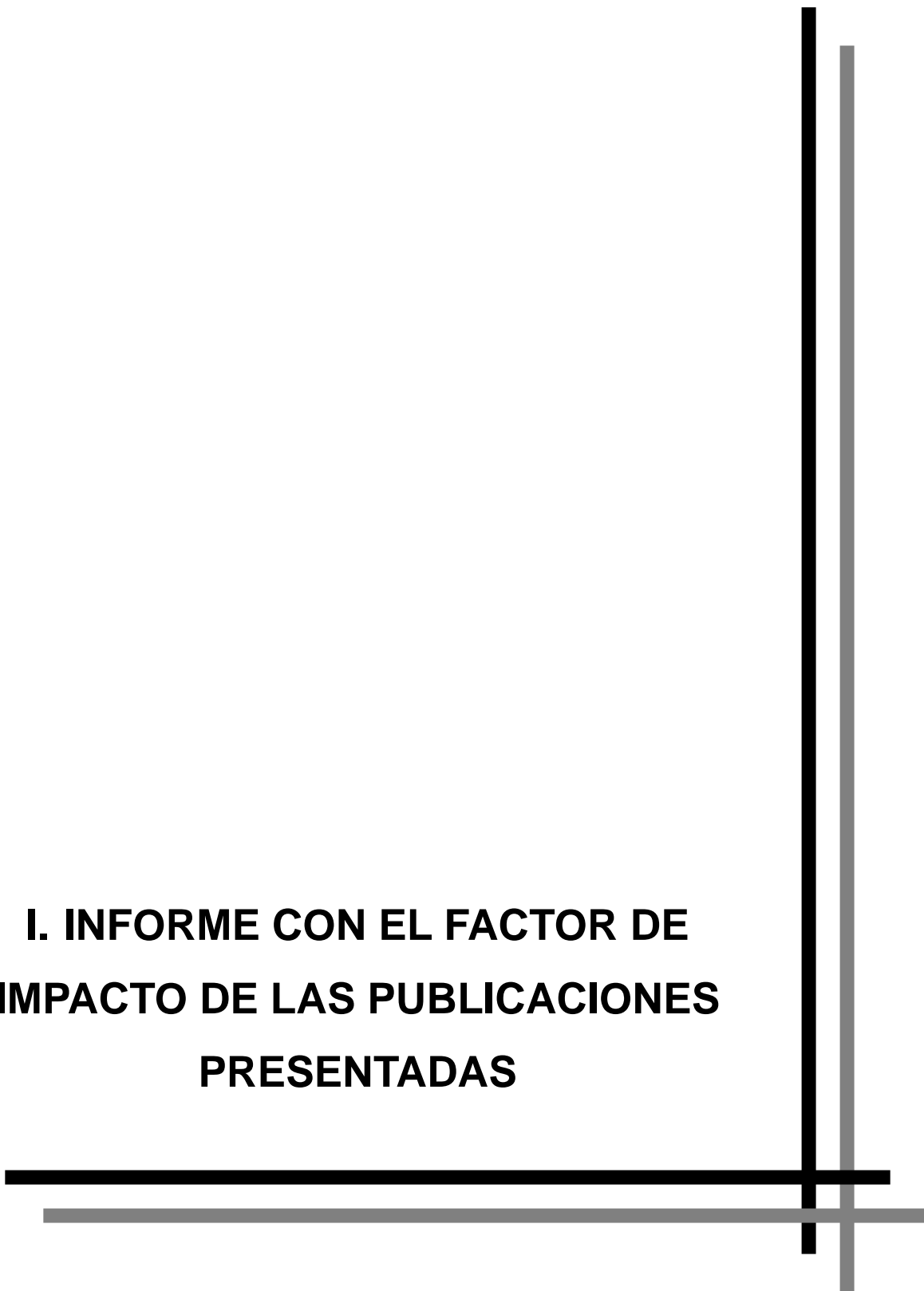
The mathematical procedure developed here allows the fast and reliable study of selenium metabolism. The examples given here with only 11 rats should not be considered as a metabolic study but only to indicate that comprehensive total elemental and speciation information can be obtained by combining this dual isotope procedure [8, 9] with advanced data treatment in which all intensity data are treated simultaneously. This methodology should also be easily transferrable to human trails as no radioactivity is used and a single bolus dose of enriched selenium is employed.

Acknowledgements We would like to thank PharmaNord for supplying of the ^{77}Se enriched yeast, Marisa Fernández Sánchez for the supply of the ^{74}Se spike and Teresa Fernández and Agustín Brea from the Biotery of the University of Oviedo for their help regarding animal experiments. Funding from the Spanish Ministry of Science and Innovation through project number CTQ2009-12814 and the Education and Science Council of the Principado de Asturias (grant BP07-059) are gratefully acknowledged.

References

1. Gammelgaard B, Jackson M, Gabel-Jensen C (2011) *Anal Bioanal Chem* 399:1743–1763
2. Reyes LH, Marchante-Gayon JM, García Alonso JI, Sanz-Medel A (2003) *J Anal At Spectrom* 18:1210–1216
3. Reyes LH, Marchante Gayon JM, García Alonso JI, Sanz-Medel A (2003) *J Anal At Spectrom* 18:11–16
4. Jitaru P, Goenaga-Infante H, Vaslin-Reimann S, Fiscaro P (2010) *Anal. Chim Acta* 657:100–107
5. Jitaru P, Roman M, Cozzi G, Fiscaro P, Cescon P, Barbante C (2009) *Microchim Acta* 166:319–327
6. Jitaru P, Prete M, Cozzi G, Turetta C, Cairns W, Seraglia R, Traldi P, Cescon P, Barbante C (2008) *J Anal At Spectrom* 23:402–406
7. Jitaru P, Cozzi G, Gambaro A, Cescon P, Barbante C (2008) *Anal Bioanal Chem* 391:661–669
8. González Iglesias H, Fernández Sánchez M, Rodríguez-Castrillón JA, García Alonso JI, López Sastre J, Sanz-Medel A (2009) *J Anal At Spectrom* 24:460–468
9. González Iglesias H, Fernández Sánchez M, García Alonso JI, Sanz-Medel A (2007) *Anal Bioanal Chem* 389:707–713
10. Suzuki KT, Tsuji Y, Ohta Y, Suzuki T (2008) *Toxicol Appl Pharmacol* 227:76–83
11. Suzuki KT, Ohta Y, Suzuki N (2006) *Toxicol Appl Pharmacol* 217:51–62
12. Suzuki KT, Somekawa L, Kurasaki K, Suzuki N (2006) *J Health Sci* 52:590–597
13. Suzuki KT, Somekawa L, Suzuki N (2006) *Toxicol Appl Pharmacol* 216:303–308
14. Suzuki KT, Doi C, Suzuki N (2006) *Toxicol Appl Pharmacol* 217:185–195
15. Rodríguez-Castrillón JA, Reyes LH, Marchante-Gayon JM, Moldovan M, Alonso JIG (2008) *J Anal At Spectrom* 23:579–582
16. Larsen EH, Sloth JJ, Hansen M, Moesgaard S (2003) *J Anal At Spectrom* 18:310–316
17. Sloth JJ, Larsen EH (2000) *J Anal At Spectrom* 15:669–672
18. Sloth JJ, Larsen EH, Bugel SH, Moesgaard S (2003) *J Anal At Spectrom* 18:317–322
19. Berglund M, Wieser ME (2011) *Pure Appl Chem* 83:397–410
20. Schomburg L, Schweizer U, Holtmann B, Flohe L, Sendtner M, Kohrle J (2003) *Biochem J* 370:397–402
21. Kato T, Read R, Rozga J, Burk RF (1992) *Am. J Physiol* 262:G854–G858
22. Avissar N, Ornt DB, Yagil Y, Horowitz S, Watkins RH, Kerl EA, Takahashi K, Palmer IS, Cohen HJ (1994) *Am. J Physiol* 266:C367–C375
23. Hill KE, Zhou JD, McMahan WJ, Motley AK, Atkins JF, Gesteland RF, Burk RF (2003) *J Biol Chem* 278:13640–13646
24. Ogra Y, Ishiwata K, Takayama H, Aimi N, Suzuki KT (2002) *J Chromatogr B Analyt Technol Biomed Life Sci* 767:301–312

**I. INFORME CON EL FACTOR DE
IMPACTO DE LAS PUBLICACIONES
PRESENTADAS**



De acuerdo con el Reglamento de los Estudios de Doctorado aprobado por el Consejo de la Universidad de Oviedo el 21 de julio de 2011 (Boletín Oficial del Principado de Asturias, núm. 197 de 25-VIII-2011) para poder presentar una Tesis Doctoral como compendio de publicaciones (artículo 26) se deberá incluir en la memoria de tesis un apartado en el que figure un informe con el factor de impacto de las publicaciones presentadas. Por ello, a continuación, se comentará brevemente este punto.

Los trabajos que se recogen en el apartado de estudios de variabilidad natural de la composición isotópica de azufre mediante ICP-MS multicollector (artículos científicos I y II) han surgido fruto de la colaboración con el grupo de investigación de Espectrometría de Masas Inorgánica del Laboratorio Nacional de Metrología Química del Reino Unido (LGC Limited), dirigido por la Dra. Ruth Hearn, donde el doctorando realizó dos estancias predoctorales en los años 2007 y 2008. Así, el **artículo científico I** ha sido publicado en la prestigiosa revista científica **Journal of Agricultural and Food Chemistry**, situada en el primer cuartil dentro de las revistas de la categoría de Agricultura multidisciplinar (2 de 55), Química Aplicada (8 de 70) y Ciencia y Tecnología de los Alimentos (10 de 126), con un **índice de impacto de 2,816** (fuente: JCR 2010). Adicionalmente, los resultados de esta investigación han sido presentados en forma de comunicación oral en las *12^{as} Jornadas de Análisis Instrumental* celebradas en Barcelona (España) en octubre de 2008, y en forma de comunicación tipo póster en el congreso internacional *14th Biennial National Atomic Spectroscopy Symposium*, celebrado en Brighton (Inglaterra) en julio de 2008.

Por su parte, los resultados recogidos en el **artículo científico II** han sido publicados en la prestigiosa revista científica **Analytical and Bioanalytical Chemistry**, situada en el primer cuartil dentro de las revistas de la categoría de Química Analítica (6 de 70), con un **índice de impacto de 3,480** (fuente: JCR 2009). Esta publicación fue seleccionada entre los 3 artículos finalistas nominados a “*2009 Best Paper Award*” por los editores de la revista. Los resultados de esta investigación fueron recogidos por el Servicio de Información y Noticias Científicas (SINC) lo que originó una gran repercusión en los medios de comunicación nacionales e internacionales tanto de interés general como especializados. De esta manera, se publicaron dos reseñas bibliográficas en las revistas especializadas *Optics and Photonics Focus* (2010, 8, story 6) y *National Measurement News* (2010, issue 3, pag 4). Asimismo, prensa nacional escrita y la edición digital de periódicos nacionales e internacionales así como plataformas nacionales e internacionales especializadas en divulgación y difusión científica se hicieron eco de nuestros resultados. Además, este

artículo científico fue galardonado con el **XXII Premio San Alberto Magno para Trabajos de Investigación y Desarrollo Tecnológico** otorgado por el Colegio Oficial de Químicos de Asturias y León y la Asociación de Químicos del Principado de Asturias. Adicionalmente, los resultados de esta investigación han sido presentados en forma de comunicación oral en los congresos internacionales *2009 European Winter Conference on Plasma Spectrochemistry*, celebrado en Graz (Austria) en febrero de 2009; *2010 Winter Conference on Plasma Spectrochemistry*, celebrado en Florida (USA) en enero de 2010 y *Fourth FIRMS Network Conference*, celebrado en Washington DC (USA) en abril de 2010.

Los trabajos que se recogen en el apartado de preparación y caracterización de levadura marcada isotópicamente con azufre-34 (artículos científicos III y IV) así como el estudio con trazadores estables de azufre en animales de laboratorio utilizando levadura marcada con azufre-34 (artículo científico V) han sido realizados en colaboración con el grupo de investigación de Biología Molecular y Biotecnología de Levaduras, del Departamento de Bioquímica y Biología Molecular de la Facultad de Medicina de la Universidad de Oviedo, dirigido por el Prof. Fernando Moreno Sanz. De esta manera, el **artículo científico III** se publicó en la prestigiosa revista científica **Journal of Analytical Atomic Spectrometry**, situada en el primer cuartil dentro de las revistas de la categoría de Química Analítica (9 de 70) y Espectroscopía (6 de 39), con un **índice de impacto de 3,269** (fuente: JCR 2007). Además, esta publicación científica fue seleccionada como “**Hot article**” por los editores de la revista y clasificada como “**Top 10 paper**” durante el periodo comprendido entre los meses de septiembre-2007 y julio-2008 al encontrarse entre los diez artículos más descargados desde la página web de la revista. Adicionalmente, los resultados de esta investigación han sido presentados en forma de comunicación tipo póster en la *III Reunión de la Sociedad Española de Espectrometría de Masas (SEEM)*, celebrada en Oviedo en septiembre de 2006 y en el congreso internacional *2007 European Winter Conference on Plasma Spectrochemistry*, celebrado en Taormina (Italia) en febrero de 2007.

El **artículo científico IV** ha sido publicado en la prestigiosa revista científica **Journal of Analytical Atomic Spectrometry**, situada en el primer cuartil dentro de las revistas de la categoría de Química Analítica (5 de 73) y Espectroscopía (4 de 42), con un **índice de impacto de 4,372** (fuente: JCR 2010). Adicionalmente, los resultados de esta investigación han sido presentados en forma de comunicación tipo póster en los congresos internacionales *14th Biennial National Atomic Spectroscopy Symposium*, celebrado en Brighton (Inglaterra) en julio de 2008 y *2009 European Winter*

Conference on Plasma Spectrochemistry, celebrado en Graz (Austria) en febrero de 2009.

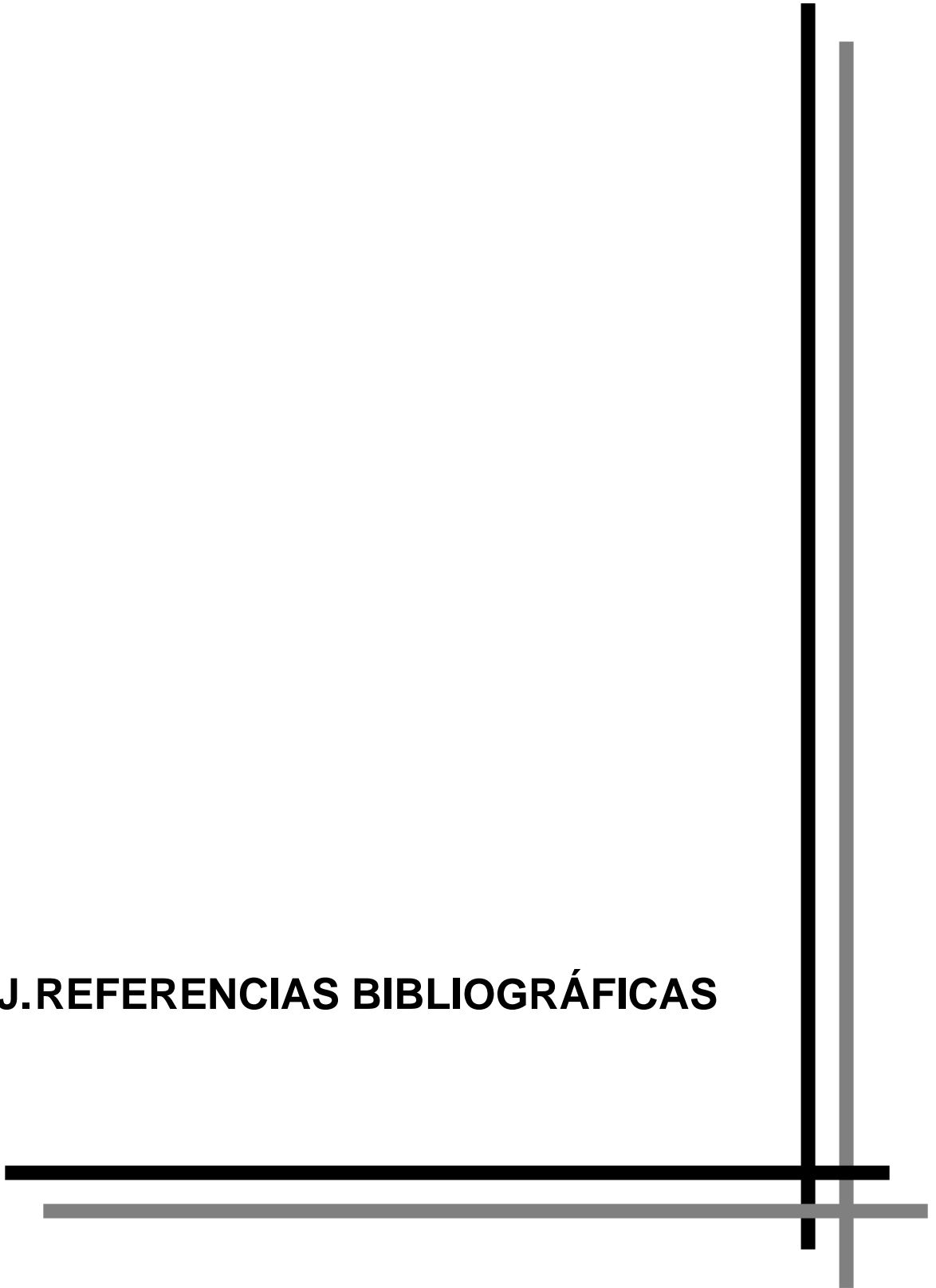
Por su parte, los resultados recogidos en el **artículo científico V** han sido publicados en la prestigiosa revista científica **Analytical and Bioanalytical Chemistry**, situada en el primer cuartil dentro de las revistas de la categoría de Química Analítica (13 de 73), con un **índice de impacto de 3,778** (fuente: JCR 2011). Además, este trabajo fue galardonado con el **1^{er} Premio de Espectrometría de Masas, 2009** otorgado por la Sociedad Española de Espectrometría de Masas (SEEM), tras ser presentado como comunicación oral en la *IV Reunión de la SEEM*, celebrada en Castellón (España) en octubre de 2009 [269]. Adicionalmente, los resultados de esta investigación han sido presentados en forma de comunicación oral en el congreso internacional *2011 European Winter Conference on Plasma Spectrochemistry*, celebrado en Zaragoza (España) en febrero de 2011 y en forma de comunicación tipo póster en el *Third International Symposium on Metallomics (Metallomics 2011)*, celebrado en Münster (Alemania) en junio de 2011.

En último lugar, se han incluido dos publicaciones relacionadas con la Tesis Doctoral (artículos científicos VI y VII). El trabajo recogido en el **artículo científico VI** surge de la colaboración iniciada con el grupo de investigación de Fisiología de Estrés Abiótico en Plantas, del Departamento de Nutrición Vegetal del Instituto de Ciencias Agrarias (Estación Experimental de Aula Dei) del Consejo Superior de Investigaciones Científicas (CSIC) de Zaragoza, dirigido por el Prof. Javier Abadía. Los resultados de esta investigación han sido publicados en la prestigiosa revista científica **Plant and Cell Physiology**, situada en el primer cuartil dentro de las revistas de la categoría de *Plant Sciences* (15 de 187), con un **índice de impacto de 4,257** (fuente: JCR 2010). Adicionalmente, los resultados de esta investigación han sido presentados en forma de comunicación oral en la *XVIII Reunión de la Sociedad Española de Fisiología Vegetal (SEFV)* y *XI Congreso Hispano-Luso de Fisiología Vegetal*, celebrado en Zaragoza (España) en septiembre de 2009.

Para finalizar, el **artículo científico VII** surge fruto de la colaboración con el grupo de investigación de Química Analítica y Bioinorgánica del Departamento de Farmacología y Química Analítica de la Universidad de Ciencias Farmacéuticas de Copenhague (Dinamarca), dirigido por la Prof. Bente Gammelgaard. Este trabajo de investigación ha sido publicado en la prestigiosa revista científica **Analytical and Bioanalytical Chemistry**, situada en el primer cuartil dentro de las revistas de la categoría de Química Analítica (13 de 73), con un **índice de impacto de 3,778** (fuente: JCR 2011). Los resultados de esta investigación fueron recogidos por el

Servicio de Información y Noticias Científicas (SINC) lo que originó una gran repercusión en plataformas nacionales e internacionales especializadas en divulgación y difusión científica. Asimismo, los resultados de esta investigación han sido presentados en forma de comunicación oral en el congreso internacional *2011 European Winter Conference on Plasma Spectrochemistry*, celebrado en Zaragoza (España) en febrero de 2011.

J.REFERENCIAS BIBLIOGRÁFICAS



- [1] Komarnisky LA, Christopherson RJ, Basu TK. **Sulfur: its clinical and toxicologic aspects.** *Nutrition*, 2003, 19, 54-61.
- [2] Brosnan JT, Brosnan ME. **The sulfur-containing amino acids: an overview.** *The Journal of Nutrition*, 2006, 136, 1636-1640.
- [3] Tesseraud S, Coustard SM, Collin A, Seilliez I. **Role of sulfur amino acids in controlling metabolism and cell functions: implications for nutrition.** *British Journal of Nutrition*, 2009, 101, 1132-1139.
- [4] Shoveller AK, Stoll B, Ball RO, Burrin DG. **Nutritional and functional importance of intestinal sulfur amino acid metabolism.** *The Journal of Nutrition*, 2005, 135, 1609-1612.
- [5] Stipanuk MH. **Sulfur amino acid metabolism: Pathways for production and removal of homocysteine and cysteine.** *Annual Review of Nutrition*, 2004, 24, 539-577.
- [6] Wang WW, Qiao SY, Li DF. **Amino acids and gut function.** *Amino Acids*, 2009, 37, 105-110.
- [7] Finkelstein JD. **Homocysteine: A history in progress.** *Nutrition Reviews*, 2000, 58, 193-204.
- [8] Stipanuk MH. **Metabolism of sulfur-containing amino-acids.** *Annual Review of Nutrition*, 1986, 179-209.
- [9] Townsend DM, Tew KD, Tapiero H. **Sulfur containing amino acids and human disease.** *Biomedicine and Pharmacotherapy*, 2004, 58, 47-55.
- [10] Giles GI, Jacob C. **Reactive sulfur species: An emerging concept in oxidative stress.** *Biological Chemistry*, 2002, 383, 375-388.
- [11] Métayer S, Seilliez I, Collin A, Dechêne S, Mercier Y, Geraert PA, Tesseraud S. **Mechanisms through which sulfur amino acids control protein metabolism and oxidative status.** *Journal of Nutritional Biochemistry*, 2008, 19, 207-215.
- [12] Lyons J, Rauh-Pfeiffer A, Yu YM, Lu XM, Zurakowski D, Tompkins RG, Ajami AM, Young VR, Castillo L. **Blood glutathione synthesis rates in healthy adults receiving a sulfur amino acid-free diet.** *Proceedings of the National Academy of Sciences PNAS*, 2000, 97, 5071-5076.
- [13] Lu SC. **Regulation of glutathione synthesis.** *Molecular Aspects of Medicine*, 2009, 30, 42-59.
- [14] Nimni ME, Han B, Cordoba F. **Are we getting enough sulfur in our diet?** *Nutrition and Metabolism*, 2007, 4, 24-36.
- [15] Vuong GL, Weiss SM, Kammer W, Priemer M, Vingron M, Nordheim A, Cahill MA. **Improved sensitivity proteomics by postharvest alkylation and radioactive labeling of proteins.** *Electrophoresis*, 2000, 21, 2594-2605.
- [16] Stipanuk MH, Ueki I. **Dealing with methionine/homocysteine sulfur: cysteine metabolism to taurine and inorganic sulfur.** *Journal of Inherited Metabolic Disease*, 2011, 34, 17-32.
- [17] Garlick PJ. **Toxicity of methionine in humans.** *The Journal of Nutrition*, 2006, 136, 1722-1725.

- [18] Griffith OW. **Mammalian sulfur amino-acid metabolism - An overview.** *Methods in Enzymology*, 1987, 143, 366-376.
- [19] Anderson JW, **Assimilation of inorganic sulfate into cysteine**, in *The Biochemistry of Plants*, eds. Stumpf PK and Conn EE, Academic Press, New York, USA, 1980, vol. 5, p. 203.
- [20] Thomas D, Surdin-Kerjan Y. **Metabolism of sulfur amino acids in *Saccharomyces cerevisiae*.** *Microbiology and Molecular Biology Reviews*, 1997, 61, 503-532.
- [21] Porro D, Sauer M, Branduardi P, Mattanovich D. **Recombinant protein production in yeasts.** *Molecular Biotechnology*, 2005, 31, 245-259.
- [22] Libby WF. **Measurement of radioactive tracers - particularly C-14, S-35 and other longer-lived low-energy activities.** *Analytical Chemistry*, 1947, 19, 2-6.
- [23] Sloper JC, Arnott DJ, King BC. **Sulphur metabolism in the pituitary and hypothalamus of the rat - a study of radioisotope-uptake after the injection of S-35 DL-cysteine, methionine, and sodium sulphate.** *Journal of Endocrinology*, 1960, 20, 9-23.
- [24] Johnson WH, Goodrich RD, Meiske JC. **Metabolism of radioactive sulfur from elemental sulfur, sodium sulfate and methionine by lambs.** *Journal of Animal Science*, 1971, 32, 778-783.
- [25] Seligman AM, Fine J. **The production of radioactive plasma protein from amino acids containing radioactive sulfur.** *Journal of Clinical Investigation*, 1943, 22, 265-273.
- [26] Gerner C, Vejda S, Gelbmann D, Bayer E, Gotzmann J, Schulte-Hermann R, Mikulits W. **Concomitant determination of absolute values of cellular protein amounts, synthesis rates, and turnover rates by quantitative proteome profiling.** *Molecular and Cellular Proteomics*, 2002, 1, 528-537.
- [27] Walkenstein SS, Seifter J. **Fate, distribution and excretion of S-35 promazine.** *Journal of Pharmacology and Experimental Therapeutics*, 1959, 125, 283-286.
- [28] Symchowicz S, Peckham WD, Eisler M, Perlman PI. **The distribution and excretion of radioactivity after administration of ³⁵S-labeled perphenazine (trilafon).** *Biochemical Pharmacology*, 1962, 11, 417-422.
- [29] Alexande WD, Evans V, MacAulay A, Gallagher TF, Londono J. **Metabolism of ³⁵S-labelled antithyroid drugs in man.** *British Medical Journal*, 1969, 2, 290-291.
- [30] Allègre CJ. **Isotope geology.** *Cambridge University Press*, 2008.
- [31] Baskaran M. **Handbook of environmental isotope geochemistry.** Springer-Verlag Berlin Heidelberg, 2011.
- [32] Kelly S, Heaton K, Hoogewerff J. **Tracing the geographical origin of food: The application of multi-element and multi-isotope analysis.** *Trends in Food Science and Technology*, 2005, 16, 555-567.

- [33] Luykx DMAM, Van Ruth SM. **An overview of analytical methods for determining the geographical origin of food products.** *Food Chemistry*, 2008, 107, 897-911.
- [34] Cordella C, Moussa I, Martel AC, Sbirrazzuoli N, Lizzani-Cuvelier L. **Recent developments in food characterization and adulteration detection: Technique-oriented perspectives.** *Journal of Agricultural and Food Chemistry*, 2002, 50, 1751-1764.
- [35] Rossmann A. **Determination of stable isotope ratios in food analysis.** *Food Reviews International*, 2001, 17, 347-381.
- [36] Neufeld JD, Wagner M, Murrell JC. **Who eats what, where and when? Isotope-labelling experiments are coming of age.** *ISME Journal*, 2007, 1, 103-110.
- [37] Evershed RP, Dudd SN, Copley MS, Berstan R, Stott AW, Mottram H, Buckley SA, Crossman Z. **Chemistry of archaeological animal fats.** *Accounts of Chemical Research*, 2002, 35, 660-668.
- [38] Bentley AR. **Strontium isotopes from the earth to the archaeological skeleton: a review.** *Journal of Archaeological Method and Theory*, 2006, 13, 135-187.
- [39] Montgomery J. **Passports from the past: investigating human dispersals using strontium isotope analysis of tooth enamel.** *Annals of Human Biology*, 2010, 37, 325-346.
- [40] Meier-Augenstein W. **Applied gas chromatography coupled to isotope ratio mass spectrometry.** *Journal of Chromatography A*, 1999, 842, 351-371.
- [41] Preston T. **The measurement of stable isotope natural abundance variations.** *Plant Cell and Environment*, 1992, 15, 1091-1097.
- [42] Benson S, Lennard C, Maynard P, Claude R. **Forensic applications of isotope ratio mass spectrometry - A review.** *Forensic Science International*, 2006, 157, 1-22.
- [43] Criss RE. **Principles of stable isotope distribution.** *Oxford University Press*, 1999.
- [44] De Laeter JR, Bohlke JK, De Bièvre P, Hidaka H, Peiser HS, Rosman KJR, Taylor PDP. **Atomic weight of the elements: Review 2000.** *Pure and Applied Chemistry*, 2003, 75, 683-800.
- [45] Jensen ML, Nakai N. **Sulfur isotope meteorite standards, results and recommendations.** In *Biochemistry of sulfur isotopes*, NSF Symposium, 1962, 30.
- [46] Beaudoin G, Taylor BE, Rumble D, Thiemens M. **Variations in the sulfur isotope composition of troilite from the Canon Diablo iron meteorite.** *Geochimica et Cosmochimica Acta*, 1994, 58, 4253-4255.
- [47] Robinson BW. **Sulphur isotope standards.** In: Reference and intercomparison materials for stable isotopes of light elements. *Proceedings of a Consultants Meeting held in Vienna (A)*, 1-3 December, 1993. IAEA-TECDOC-825, IAEA, Vienna, 39-45.
- [48] Krouse HR, Coplen TB. **Reporting on relative sulfur isotope-ratio data.** *Pure and Applied Chemistry*, 1997, 69, 293-295.
- [49] Platzner IT. **Modern isotope ratio mass spectrometry.** *John Wiley and Sons Ltd*, 1997.

- [50] Werner RA, Brand WA. **Referencing strategies and techniques in stable isotope ratio analysis.** *Rapid Communications in Mass Spectrometry*, 2001, 15, 501-519.
- [51] Muccio Z, Jackson GP. **Isotope ratio mass spectrometry.** *Analyst*, 2009, 134, 213-222.
- [52] Mann JL, Vocke RD, Kelly WR. **Revised delta S-34 reference values for IAEA sulfur isotope reference materials S-2 and S-3.** *Rapid Communications in Mass Spectrometry*, 2009, 23, 1116-1124.
- [53] Gao X, Thiemens MH. **Variations on the isotopic composition of sulfur in enstatite and ordinary chondrites.** *Geochimica et Cosmochimica Acta*, 1993, 13, 3171-3176.
- [54] Strauss H. **The isotopic composition of sedimentary sulfur through time.** *Palaeogeography Palaeoclimatology Palaeoecology*, 1997, 132, 97-118.
- [55] Farquhar J, Savarino J, Jackson TL, Thiemens MH. **Evidence of atmospheric sulphur in the Martian regolith from sulphur isotopes in meteorites.** *Nature*, 2000, 404, 50-52.
- [56] Farquhar J, Wing BA, McKeegan KD, Harris JW, Cartigny P, Thiemens MH. **Mass-independent sulfur of inclusions in diamond and sulfur recycling on early earth.** *Science*, 2002, 298, 2369-2372.
- [57] Tachibana S, Huss GR. **Sulfur isotope composition of putative primary troilite in chondrules from Bishunpur and Semarkona.** *Geochimica et Cosmochimica Acta*, 2005, 69, 3075-3097.
- [58] Rai VK, Jackson TL, Thiemens MH. **Photochemical mass-independent sulfur isotopes in achondritic meteorites.** *Science*, 2005, 309, 1062-1065.
- [59] Ohmoto H, Watanabe Y, Ikemi H, Poulson SR, Taylor BE. **Sulphur isotope evidence for an oxic archaean atmosphere.** *Nature*, 2006, 442, 908-911.
- [60] Ono S, Wing B, Johnston D, Farquhar J, Rumble D. **Mass-dependent fractionation of quadruple stable sulfur isotope system as a new tracer of sulfur biogeochemical cycles.** *Geochimica et Cosmochimica Acta*, 2006, 70, 2238-2252.
- [61] Boner M, Forstel H. **Stable isotope variation as a tool to trace the authenticity of beef.** *Analytical and Bioanalytical Chemistry*, 2004, 378, 301-310.
- [62] Rossmann A, Haberhauer G, Holz S, Horn P, Pichlmayer F, Voerkelius S. **The potential of multielement stable isotope analysis for regional origin assignment of butter.** *European Food Research and Technology*, 2000, 211, 32-40.
- [63] Pillonel L, Badertscher R, Froidevaux P, Haberhauer G, Holz S, Horn P, Jakob A, Pfammatter E, Piantini U, Rossmann A, Tabacchi R, Bosset JO. **Stable isotope ratios, major, trace and radioactive elements in emmental cheeses of different origins.** *Food Science and Technology*, 2003, 36, 615-623.
- [64] Qi HP, Coplen TB. **Evaluation of the $^{34}\text{S}/^{32}\text{S}$ ratio of Soufre de Lacq elemental sulfur isotopic reference material by continuous flow isotope-ratio mass spectrometry.** *Chemical Geology*, 2003, 199, 183-187.

- [65] Coleman ML. **Data corrections for mass-spectrometer analysis of SO₂**. *Handbook of stable isotope analytical techniques*, 2004, vol I, Elsevier, Amsterdam, 14pp.
- [66] Mason PRD, Kaspers K, van Bergen MJ. **Determination of sulfur isotope ratios and concentrations in water samples using ICP-MS incorporating hexapole ion optics**. *Journal of Analytical Atomic Spectrometry*, 1999, 14, 1067-1074.
- [67] Stürup S, Bendahl L, Gammelgaard B. **Optimization of LC-DRC-ICP-MS for speciation of selenotrisulfides with simultaneous detection of sulphur and selenium as oxides combined with determination of elemental and isotope ratios**. *Journal of Analytical Atomic Spectrometry*, 2006, 21, 201-203.
- [68] Wang M, Feng W, Lu W, Li B, Wang B, Zhu M, Wang Y, Yuan H, Zhao Y, Chai Z. **Quantitative analysis of proteins via sulfur determination by HPLC coupled to isotope dilution ICP-MS with hexapole collision cell**. *Analytical Chemistry*, 2007, 79, 9128-9134.
- [69] Prohaska T, Latkoczy C, Stingeder G. **Precise sulfur isotope ratio measurements in trace concentration of sulfur by high resolution inductively coupled plasma sector field mass spectrometry (HR-ICP-SFMS)**. *Journal of Analytical Atomic Spectrometry*, 1999, 14, 1501-1504.
- [70] Boulyga SF, Heilmann J, Heumann KG. **Isotope dilution ICP-MS with laser assisted sample introduction for direct determination of sulfur in petroleum products**. *Analytical and Bioanalytical Chemistry*, 2005, 382, 1808-1814.
- [71] Rehkamper M, Schonbachler M, Stirling CH. **Multiple collector ICP-MS: Introduction to instrumentation, measurement techniques and analytical capabilities**. *Geostandards Newsletter-The Journal of Geostandards and Geoanalysis*, 2001, 25, 23-40.
- [72] Yang L. **Accurate and precise determination of isotopic ratios by MC-ICP-MS: A review**. *Mass Spectrometry Reviews*, 2009, 28, 990-1011.
- [73] Vanhaecke F, Balcaen L, Malinovsky D. **Use of single-collector and multi-collector ICP mass spectrometry for isotopic analysis**. *Journal of Analytical Atomic Spectrometry*, 2009, 24, 863-886.
- [74] Santamaria-Fernandez R, Hearn R. **Systematic comparison of delta(34)S measurements by multicollector inductively coupled plasma mass spectrometry and evaluation of full uncertainty budget using two different metrological approaches**. *Rapid Communications in Mass Spectrometry*, 2008, 22, 401-408.
- [75] Santamaria-Fernandez R, Hearn R, Wolff JC. **Detection of counterfeit tablets of an antiviral drug using $\delta^{34}\text{S}$ measurements by MC-ICP-MS and confirmation by LA-MC-ICP-MS and HPLC-MC-ICP-MS**. *Journal of Analytical Atomic Spectrometry*, 2008, 23, 1294-1299.
- [76] Clough R, Evans P, Catterick T, Evans EH. **$\delta^{34}\text{S}$ measurements of sulfur by multicollector inductively coupled plasma mass spectrometry**. *Analytical Chemistry*, 2006, 78, 6126-6132.
- [77] Craddock PR, Rouxel OJ, Ball LA, Bach W. **Sulfur isotope measurement of sulfate and sulfide by high-resolution MC-ICP-MS**. *Chemical Geology*, 2008, 253, 102-113.

- [78] Rai VK, Thiemens MH. **Mass independently fractionated sulfur components in chondrites.** *Geochimica et Cosmochimica Acta*, 2007, 71, 1341-1354.
- [79] Moldovan M, Krupp EM, Holliday AE, Donard OFX. **High resolution sector field ICP-MS and multicollector ICP-MS as tools for trace metal speciation in environmental studies: a review.** *Journal of Analytical Atomic Spectrometry*, 2004, 19, 815-822.
- [80] Viteri FE, Warren R. **Considerations on the use of radioisotopes in human nutrition research.** *Food and Nutrition Bulletin*, 2002, 23, 7-16.
- [81] Roth E. **Critical evaluation of the use and analysis of stable isotopes.** *Pure and Applied Chemistry*, 1997, 69, 1753-1828.
- [82] Schoenheimer R, Rittenberg D. **Deuterium as an indicator in the study of intermediary metabolism.** *Journal of Biological Chemistry*, 1935, 111, 163-168.
- [83] Schoenheimer R, Rittenberg D. **The application of isotopes to the study of intermediary metabolism.** *Science*, 1938, 11, 221-226.
- [84] Dainty JR. **Use of stable isotopes and mathematical modelling to investigate human mineral metabolism.** *Nutrition Research Reviews*, 2001, 14, 295-315.
- [85] Patterson KY, Veillon C. **Stable isotopes of minerals as metabolic tracers in human nutrition research.** *Experimental Biology and Medicine*, 2001, 226, 271-282.
- [86] Stürup S. **The use of ICPMS for stable isotope tracer studies in humans: a review.** *Analytical and Bioanalytical Chemistry*, 2004, 378, 273-282.
- [87] Stürup S, Hansen HR, Gammelgaard B. **Application of enriched stable isotopes as tracers in biological systems: a critical review.** *Analytical and Bioanalytical Chemistry*, 2008, 390, 541-554.
- [88] Mutlib AE. **Application of stable isotope-labeled compounds in metabolism and in metabolism-mediated toxicity studies.** *Chemical Research in Toxicology*, 2008, 21, 1672-1689.
- [89] Singher HO, Marinelli L. **Distribution of radioactive sulfur in the rat.** *Science*, 1945, 101, 414-415.
- [90] Davies DV, Young L. **The distribution of radioactive sulfur (³⁵S) in the fibrous tissues, cartilages and bones of the rat following its administration in the form of inorganic sulphate.** *Journal of Anatomy*, 1954, 88, 174-83.
- [91] Zhao FJ, Verkampen KCJ, Birdsey M, Blake-Kalff MMA, McGrath SP. **Use of the enriched stable isotope ³⁴S to study sulphur uptake and distribution in wheat.** *Journal of Plant Nutrition*, 2001, 24, 1551-1560.
- [92] Jensen BP, Smith C, Wilson ID, Weidolf L. **Sensitive sulphur-specific detection of omeprazole metabolites in rat urine by high-performance liquid chromatography/inductively coupled plasma mass spectrometry.** *Rapid Communications in Mass Spectrometry*, 2004, 18, 181-183.

- [93] Hu VW, Heikka DS. **Radiolabeling revisited: metabolic labeling with ^{35}S -methionine inhibits cell cycle progression, proliferation, and survival.** *FASEB Journal*, 2000, 14, 448-454.
- [94] Griffin IJ. **Using stable isotopes and isotope ratio mass spectrometry to study mineral metabolism in humans.** *Journal of Analytical Atomic Spectrometry*, 2002, 17, 1186-1193.
- [95] Rodríguez-Cea A, Fernández de la Campa MR, García Alonso JI, Sanz-Medel A. **The use of enriched ^{111}Cd as tracer to study *de novo* cadmium accumulation and quantitative speciation in *Anguilla anguilla* tissues.** *Journal of Analytical Atomic Spectrometry*, 2006, 21, 270-278.
- [96] Sievers E, Dorner K, Garbe-Schonberg D, Schaub J. **Molybdenum metabolism: Stable isotope studies in infancy.** *Journal of Trace Elements in Medicine and Biology*, 2001, 15, 185-191.
- [97] Quinn TJ. **Primary methods of measurement and primary standards.** *Metrología*, 1997, 34, 61-65.
- [98] Vogl J. **Characterisation of reference materials by isotope dilution mass spectrometry.** *Journal of Analytical Atomic Spectrometry*, 2007, 22, 475-492.
- [99] Vogl J, Pritzkow W. **Isotope dilution mass spectrometry – A primary method of measurement and its role for RM certification.** *Journal of Metrology Society of India*, 2010, 25, 135-164.
- [100] Careri M, Mangia A. **Validation and qualification: the fitness for purpose of mass spectrometry-based analytical methods and analytical systems.** *Analytical and Bioanalytical Chemistry*, 2006, 386, 38-45.
- [101] Heumann KG. **Isotope-dilution ICP-MS for trace element determination and speciation: from a reference method to a routine method?** *Analytical and Bioanalytical Chemistry*, 2004, 378, 318-329.
- [102] Heumann KG. **Isotope dilution mass spectrometry (IDMS) of the elements.** *Mass Spectrometry Reviews*, 1992, 11, 41-67.
- [103] Heumann KG. **Isotope dilution mass spectrometry.** *International Journal of Mass Spectrometry and Ion Processes*, 1992, 118, 575-92.
- [104] Becker JS, Dietze HJ. **Inorganic trace analysis by mass spectrometry.** *Spectrochimica Acta Part B-Atomic Spectroscopy*, 1998, 53, 1475-1506.
- [105] Deleenheer AP, Thienpont LM. **Applications of isotope-dilution mass-spectrometry in clinical-chemistry, pharmacokinetics and toxicology.** *Mass Spectrometry Reviews*, 1992, 11, 249-307.
- [106] Chace DH. **Mass spectrometry in the clinical laboratory.** *Chemical Reviews*, 2001, 101, 445-477.
- [107] Heumann KG, Rottmann L, Vogl J. **Elemental speciation with liquid-chromatography inductively-coupled plasma isotope-dilution mass-spectrometry.** *Journal of Analytical Atomic Spectrometry*, 1994, 9, 1351-1355.
- [108] Heumann KG, Gallus SM, Rädlinger G, Vogl J. **Accurate determination of element species by on-line coupling of chromatographic systems with ICP-MS using isotope dilution technique.** *Spectrochimica Acta Part B: Atomic Spectroscopy*, 1998, 53, 273-287.

- [109] Kot A, Namiesnik J. **The role of speciation in analytical chemistry.** *TRAC-Trends in Analytical Chemistry*, 2000, 19, 69-79.
- [110] Szpunar J. **Bio-inorganic speciation analysis by hyphenated techniques.** *Analyst*, 2000, 125, 963-988.
- [111] Hill SJ, Pitts LJ, Fisher AS. **High-performance liquid chromatography-isotope dilution inductively coupled plasma mass spectrometry for speciation studies: an overview.** *TRAC-Trends in Analytical Chemistry*, 2000, 19, 120-126.
- [112] Clough R, Belt ST, Evans EH, Fairman B, Catterick T. **Isotope dilution ICP-MS for speciation studies.** *Applied Spectroscopy Reviews*, 2003, 38, 101-132.
- [113] Szpunar J, Lobinski R, Prange A. **Hyphenated techniques for elemental speciation in biological systems.** *Applied Spectroscopy*, 2003, 57, 102-112.
- [114] Waddell R, Lewis C, Hang W, Hassell C, Majidi V. **Inductively coupled plasma mass spectrometry for elemental speciation: Applications in the new millennium.** *Applied Spectroscopy Reviews*, 2005, 40, 33-69.
- [115] Rodríguez-González P, Marchante Gayón JM, García Alonso JI, Sanz-Medel A. **Isotope dilution analysis for elemental speciation: a tutorial review.** *Spectrochimica Acta Part B: Atomic Spectroscopy*, 2005, 60, 151-207.
- [116] Schaumlöffel D, Lobinski R. **Isotope dilution technique for quantitative analysis of endogenous trace element species in biological systems.** *International Journal of Mass Spectrometry*, 2005, 242, 217-223.
- [117] Rodríguez-González P, García Alonso JI. **Recent advances in isotope dilution analysis for elemental speciation.** *Journal of Analytical Atomic Spectrometry*, 2010, 25, 239-259.
- [118] García Alonso JI. **Determination of fission products and actinides by inductively coupled plasma mass spectrometry using isotope dilution analysis: a study of random and systematic errors.** *Analytica Chimica Acta*, 1995, 312, 57-78.
- [119] Feldmann I, Jakubowski N, Stuewer D. **Application of a hexapole collision and reaction cell in ICP-MS Part I: Instrumental aspects and operational optimization.** *Fresenius' Journal of Analytical Chemistry*, 1999, 365, 415-421.
- [120] Tanner SD, Baranov VI, Vollkopf U. **A dynamic reaction cell for inductively coupled plasma mass spectrometry (ICP-DRC-MS). Part III. Optimization and analytical performance.** *Journal of Analytical Atomic Spectrometry*, 2000, 15, 1261-1269.
- [121] Bandura DR, Baranov VI, Tanner SD. **Reaction chemistry and collisional processes in multipole devices for resolving isobaric interferences in ICP-MS.** *Fresenius' Journal of Analytical Chemistry*, 2001, 370, 454-470.

- [122] Tanner SD, Baranov VI, Bandura DR. **Reaction cells and collision cells for ICP-MS: a tutorial review.** *Spectrochimica Acta Part B-Atomic Spectroscopy*, 2002, 57, 1361-1452.
- [123] Koppenaal DW, Eiden GC, Barinaga CJ. **Collision and reaction cells in atomic mass spectrometry: development, status, and applications.** *Journal of Analytical Atomic Spectrometry*, 2004, 19, 561-570.
- [124] Giessmann U, Greb U. **High-resolution ICP-MS - A new concept for elemental mass-spectrometry.** *Fresenius Journal of Analytical Chemistry*, 1994, 350, 186-193.
- [125] Jakubowski N, Moens L, Vanhaecke F. **Sector field mass spectrometers in ICP-MS.** *Spectrochimica Acta Part B-Atomic Spectroscopy*, 1998, 53, 1739-1763.
- [126] Reed NM, Cairns RO, Hutton RC, Takaku Y. **Characterization of polyatomic ion interferences in inductively-coupled plasma-mass spectrometry using a high-resolution mass-spectrometer.** *Journal of Analytical Atomic Spectrometry*, 1994, 9, 881-896.
- [127] Montes Bayón M, García Alonso JI, Sanz Medel A. **Enhanced semiquantitative multi-analysis of trace elements in environmental samples using ICP-MS.** *Journal of Analytical Atomic Spectrometry*, 1998, 13, 277-282.
- [128] Begley IS, Sharp BL. **Characterisation and correction of instrumental bias in inductively coupled plasma quadrupole mass spectrometry for accurate measurement of lead isotope ratios.** *Journal of Analytical Atomic Spectrometry*, 1997, 12, 395-402.
- [129] Evans P, Wolff-Briche C, Fairman B. **High accuracy analysis of low level sulfur in diesel fuel by isotope dilution high resolution ICP-MS, using silicon for mass bias correction of natural isotope ratios.** *Journal of Analytical Atomic Spectrometry*, 2001, 16, 964-969.
- [130] Baker J, Peate D, Waight T, Meyzen C. **Pb isotopic analysis of standards and samples using a ^{207}Pb – ^{204}Pb double spike and thallium to correct for mass bias with a double-focusing MC-ICP-MS.** *Chemical Geology*, 2004, 211, 275-303.
- [131] Hayes JM, Schoeller DA. **High precision pulse counting: limitations and optimal conditions.** *Analytical Chemistry*, 1977, 49, 306-311.
- [132] Russ GP, Bazan JM. **Isotopic ratio measurements with an inductively coupled plasma source mass spectrometer.** *Spectrochimica Acta Part B: Atomic Spectroscopy*, 1987, 42, 49-62.
- [133] Heilmann J, Heumann KG. **Development of a species-specific isotope dilution GC-ICP-MS method for the determination of thiophene derivatives in petroleum products.** *Analytical and Bioanalytical Chemistry*, 2008, 390, 643-653.
- [134] Rottmann L, Heumann KG. **Development of an on-line isotope dilution technique with HPLC-ICP-MS for the accurate determination of elemental species.** *Fresenius Journal of Analytical Chemistry*, 1994, 350, 221-227.

- [135] Rodríguez-González P, Rodríguez-Cea A, García Alonso JI, Sanz-Medel A. **Species-specific isotope dilution analysis and isotope pattern deconvolution for butyltin compounds metabolism investigations.** *Analytical Chemistry*, 2005, 77, 7724-7734.
- [136] Castillo A, Rodríguez-González P, Centineo G, Roig-Navarro AF, García Alonso JI. **Multiple spiking species-specific isotope dilution analysis by molecular mass spectrometry: simultaneous determination of inorganic mercury and methylmercury in fish tissues.** *Analytical Chemistry*, 2010, 82, 2773-2783.
- [137] Houk RS, Fassel VA, Flesch GD. **Inductively coupled argon plasma as an ion-source for mass-spectrometric determination of trace-elements.** *Analytical Chemistry*, 1980, 52, 2283-2289.
- [138] Hill SJ. **Inductively Coupled Plasma Spectrometry and Its Applications.** *Blackwell Publishing Ltd. 2nd Ed., Oxford, Reino Unido*, 2007.
- [139] Szpunar J. **Advances in analytical methodology for bioinorganic speciation analysis: metallomics, metalloproteomics and heteroatom-tagged proteomics and metabolomics.** *Analyst*, 2005, 130, 442-465.
- [140] Sanz-Medel A, Montes-Bayon M, de la Campa MDRF, Encinar JR, Bettmer J. **Elemental mass spectrometry for quantitative proteomics.** *Analytical and Bioanalytical Chemistry*, 2008, 390, 3-16.
- [141] Lobinski R, Schaumlöffel D, Szpunar J. **Mass spectrometry in bioinorganic analytical chemistry.** *Mass Spectrometry Reviews*, 2006, 25, 255-289.
- [142] Gammelgaard B, Jensen BP. **Application of inductively coupled plasma mass spectrometry in drug metabolism studies.** *Journal of Analytical Atomic Spectrometry*, 2007, 22, 235-249.
- [143] Rao RN, Talluri MVNK. **An overview of recent applications of inductively coupled plasma-mass spectrometry (ICP-MS) in determination of inorganic impurities in drugs and pharmaceuticals.** *Journal of Pharmaceutical and Biomedical Analysis*, 2007, 43, 1-13.
- [144] Carr JE, Dill AE, Kwok K, Carnahan JW, Webster GK. **LC-ICP-MS for nonmetal selective detection of pharmaceuticals.** *Current Pharmaceutical Analysis*, 2008, 4, 206-214.
- [145] Balcaen L, Moens L, Vanhaecke F. **Determination of isotope ratios of metals (and metalloids) by means of inductively coupled plasma mass spectrometry for provenancing purposes – A review.** *Spectrochimica Acta Part B*, 2010, 65, 769-786.
- [146] Ingle CP, Sharp BL, Horstwood MSA, Parrish RR, Lewis DJ. **Instrument response functions, mass bias and matrix effects in isotope ratio measurements and semi-quantitative analysis by single and multi-collector ICP-MS.** *Journal of Analytical Atomic Spectrometry*, 2003, 18, 219-229.
- [147] West RC, Astle MJ, Beyer WH. **CRC Handbook of chemistry and physics 64th Ed.** *Boca Raton Eds., Florida*, 1988.
- [148] Tan SH, Horlick G. **Background spectral features in inductively coupled plasma/mass spectrometry.** *Applied Spectroscopy*, 1986, 40, 445-460.

- [149] Wildner H. **Application of inductively coupled plasma sector field mass spectrometry for the fast and sensitive determination and isotope ratio measurement of non-metals in high-purity process chemicals.** *Journal of Analytical Atomic Spectrometry*, 1998, 13, 573-578.
- [150] Yu LL, Kelly WR, Fassett JD, Vocke RD. **Determination of sulphur in fossil fuels by isotope dilution electrothermal vaporization inductively coupled plasma mass spectrometry.** *Journal of Analytical Atomic Spectrometry*, 2001, 16, 140-145.
- [151] Naka H, Grégoire DC. **Determination of trace amounts of sulfur in steel by electrothermal vaporization - inductively coupled plasma mass spectrometry.** *Journal of Analytical Atomic Spectrometry*, 1996, 11, 359-363.
- [152] Resano M, Verstraete M, Vanhaecke F, Moens L, Claessens J. **Direct determination of sulfur in Bisphenol A at ultratrace levels by means of solid sampling-electrothermal vaporization-ICP-MS.** *Journal of Analytical Atomic Spectrometry*, 2001, 16, 793-800.
- [153] Kwok K, Carr JE, Webster GK, Carnahan JW. **Determination of active pharmaceutical ingredients by heteroatom selective detection using inductively coupled plasma mass spectrometry with ultrasonic nebulization and membrane desolvation sample introduction.** *Applied Spectroscopy*, 2006, 60, 80-85.
- [154] Bluemlein K, Krupp EM, Feldmann J. **Advantages and limitations of a desolvation system coupled online to HPLC-ICPqMS/ES-MS for the quantitative determination of sulfur and arsenic in arseno-peptide complexes.** *Journal of Analytical Atomic Spectrometry*, 2009, 24, 108-113.
- [155] Menegario AA, Gine MF. **On-line removal of anions for plant analysis by inductively coupled plasma mass spectrometry.** *Journal of Analytical Atomic Spectrometry*, 1997, 12, 671-674.
- [156] Menegario AA, Gine MF, Bendassolli JA, Bellato ACS, Trivelin PCO. **Sulfur isotope ratio ($^{34}\text{S}:$ ^{32}S) measurements in plant material by inductively coupled plasma mass spectrometry.** *Journal of Analytical Atomic Spectrometry*, 1998, 13, 1065-1067.
- [157] Divjak B, Goessler W. **Ion chromatographic separation of sulfur containing inorganic anions with an ICP-MS as element specific detector.** *Journal of Chromatography A*, 1999, 844, 161-169.
- [158] Bandura DR, Baranov VI, Tanner SD. **Detection of ultratrace phosphorus and sulfur by quadrupole ICPMS with dynamic reaction cell.** *Analytical Chemistry*, 2002, 74, 1497-1502.
- [159] Bradshaw N, Hall EFH, Sanderson NE. **Inductively coupled plasma as an ion source for high-resolution mass spectrometry.** *Journal of Analytical Atomic Spectrometry*, 1989, 4, 801-803.
- [160] Makishima A, Nakamura E. **Determination of total sulfur at microgram per gram levels in geological materials by oxidation of sulfur into sulfate with in situ generation of bromine using isotope dilution high-resolution ICPMS.** *Analytical Chemistry*, 2001, 73, 2547-2553.
- [161] Bendall C, Lahaye Y, Fiebig J, Weyer S, Brey GP. **In situ sulfur isotope analysis by laser ablation MC-ICP-MS.** *Applied Geochemistry*, 2006, 21, 782-787.

- [162] Mason PRD, Kosler J, de Hoog JCM, Sylvester PJ, Meffan-Main S. **In situ determination of sulfur isotopes in sulfur-rich materials by laser ablation multiple-collector inductively coupled plasma mass spectrometry (LA-MC-ICP-MS).** *Journal of Analytical Atomic Spectrometry*, 2006, 21, 177-186.
- [163] Ammann AA. **Inductively coupled plasma mass spectrometry (ICP-MS): a versatile tool.** *Journal of Mass Spectrometry*, 2007, 42, 419-427.
- [164] de Leon CAP, Montes-Bayon M, Caruso JA. **Elemental speciation by chromatographic separation with inductively coupled plasma mass spectrometry detection.** *Journal of Chromatography A*, 2002, 974, 1-21.
- [165] Popp M, Hann S, Koellensperger G. **Environmental application of elemental speciation analysis based on liquid or gas chromatography hyphenated to inductively coupled plasma mass spectrometry - A review.** *Analytica Chimica Acta*, 2010, 668, 114-129.
- [166] Sanz-Medel A, Montes-Bayón M, Sanchez MLF. **Trace element speciation by ICP-MS in large biomolecules and its potential for proteomics.** *Analytical and Bioanalytical Chemistry*, 2003, 377, 236-247.
- [167] Bettmer J, Montes-Bayón M, Encinar JR, Fernández Sánchez ML, Fernández de la Campa MR, Sanz Medel A. **The emerging role of ICP-MS in proteomic analysis.** *Journal of Proteomics*, 2009, 72, 989-1005.
- [168] Prange A, Schaumlöffel D. **Hyphenated techniques for the characterization and quantification of metallothionein isoforms.** *Analytical and Bioanalytical Chemistry*, 2002, 373, 441-453.
- [169] Sarioego Muñoz C, Marchante-Gayón JM, García Alonso JI, Sanz-Medel A. **Speciation of essential elements in human serum using anion-exchange chromatography coupled to post-column isotope dilution analysis with double focusing ICP-MS.** *Journal of Analytical Atomic Spectrometry*, 2001, 16, 587-592.
- [170] Krachler M. **Environmental applications of single collector high resolution ICP-MS.** *Journal of Environmental Monitoring*, 2007, 9, 790-804.
- [171] Huang JQ, Hu X, Zhang JR. **The application of inductively coupled plasma mass spectrometry in pharmaceutical and biomedical analysis.** *Journal of Pharmaceutical and Biomedical Analysis*, 2006, 40, 227-234.
- [172] Bouyssiére B, Szpunar J, Lobinski R. **Gas chromatography with inductively coupled plasma mass spectrometric detection in speciation analysis.** *Spectrochimica Acta Part B*, 2002, 57, 805-828.
- [173] Bouyssiére B, Leonhard P, Pröfrock D, Baco F, Garcia CL, Wilbur S, Prange A. **Investigation of the sulfur speciation in petroleum products by capillary gas chromatography with ICP-collision cell-MS detection.** *Journal of Analytical Atomic Spectrometry*, 2004, 19, 700-702.
- [174] Heilmann J, Heumann KG. **Development of a species-unspecific isotope dilution GC-ICP-MS method for possible routine quantification of sulfur species in petroleum products.** *Analytical Chemistry*, 2008, 80, 1952-1961.

- [175] Pröfrock D, Leonhard P, Wilbur S, Prange A. **Sensitive, simultaneous determination of P, S, Cl, Br and I containing pesticides in environmental samples by GC hyphenated with collision-cell ICP-MS.** *Journal of Analytical Atomic Spectrometry*, 2004, 19, 623-631.
- [176] St. Remy RR, Montes-Bayón M, Sanz-Medel A. **Determination of total homocysteine in human serum by capillary gas chromatography with sulfur-specific detection by double focusing ICP-MS.** *Analytical and Bioanalytical Chemistry*, 2003, 377, 299-305.
- [177] Amrani A, Sessions AL, Adkins JF. **Compound-specific $\delta^{34}\text{S}$ analysis of volatile organics by coupled GC-multicollector-ICP-MS.** *Analytical Chemistry*, 2009, 81, 9027-9034.
- [178] Rodríguez-Fernández J, Montes-Bayón M, Pereiro R, Sanz-Medel A. **Gas chromatography double focusing sector-field ICP-MS as an innovative tool for bad breath research.** *Journal of Analytical Atomic Spectrometry*, 2001, 16, 1051-1056.
- [179] Alvarez-Llamas G, de la Campa MD, Sanz-Medel A. **ICP-MS for specific detection in capillary electrophoresis.** *TRAC-Trends in Analytical Chemistry*, 2005, 24, 28-36.
- [180] Yeh CF, Jiang SJ, His TS. **Determination of sulfur-containing amino acids by capillary electrophoresis dynamic reaction cell inductively coupled plasma mass spectrometry.** *Analytica Chimica Acta*, 2004, 502, 57-63.
- [181] Prange A, Schaumlöffel D, Bratter P, Richarz AN, Wolf C. **Species analysis of metallothionein isoforms in human brain cytosols using capillary electrophoresis hyphenated to inductively coupled plasma – sector field mass spectrometry.** *Fresenius Journal of Analytical Chemistry*, 2001, 371, 764-774.
- [182] Schaumlöffel D, Prange A, Marx G, Heumann KG, Brätter P. **Characterisation and quantification of metallothionein isoforms using capillary electrophoresis – inductively coupled plasma isotope dilution mass spectrometry.** *Analytical and Bioanalytical Chemistry*, 2002, 372, 155-163.
- [183] Wang Z, Prange A. **The use of surface modified capillaries in the separation and characterisation of metallothionein isoforms by capillary electrophoresis inductively coupled plasma mass spectrometry.** *Analytical Chemistry*, 2002, 74, 626-631.
- [184] Pröfrock D, Leonhard P, Prange A. **Determination of sulfur and selected trace elements in metallothionein-like proteins using capillary electrophoresis hyphenated to inductively coupled plasma mass spectrometry with an octopole reaction cell.** *Analytical and Bioanalytical Chemistry*, 2003, 377, 132-139.
- [185] Montes-Bayon M, DeNicola K, Caruso JA. **Liquid chromatography-inductively coupled plasma mass spectrometry.** *Journal of Chromatography A*, 2003, 1000, 457-476.
- [186] Wang T. **Liquid Chromatography - Inductively Coupled Plasma Mass Spectrometry (LC-ICP-MS).** *Journal of Liquid Chromatography and Related Technologies*, 2007, 30, 807-831.
- [187] Wang M, Feng WY, Zhao YL, Chai ZF. **ICP-MS-based strategies for protein quantification.** *Mass Spectrometry Reviews*, 2010, 29, 326-348.

- [188] Yates JR. **Mass spectrometry and the age of the proteome.** *Journal of Mass Spectrometry*, 1998, 33, 1-19.
- [189] Schaumlöffel D. **Capillary liquid separation techniques with ICP-MS detection.** *Analytical and Bioanalytical Chemistry*, 2004, 379, 351-374.
- [190] Schaumlöffel D. **New ways in qualitative and quantitative protein analysis: Nano chromatography coupled to element mass spectrometry.** *Journal of Trace Elements in Medicine and Biology*, 2007, 21, 18-22.
- [191] Wind M, Eisenmenger A, Lehmann WD. **Modified direct injection high efficiency nebulizer with minimized dead volume for the analysis of biological samples by micro- and nano-LC-ICP-MS.** *Journal of Analytical Atomic Spectrometry*, 2002, 17, 21-26.
- [192] Todoli JL, Mermet JM. **Sample introduction systems for the analysis of liquid microsamples by ICP-AES and ICP-MS.** *Spectrochimica Acta, Part B*, 2006, 61, 239-283.
- [193] Giusti P, Lobinski R, Szpunar J, Schaumlöffel D. **Development of a nebulizer for a sheathless interfacing of nanoHPLC and ICP-MS.** *Analytical Chemistry*, 2006, 78, 965-971.
- [194] Bendahl L, Stürup S, Gammelgaard B, Hansen SH. **UPLC-ICP-MS – A fast technique for speciation analysis.** *Journal of Analytical Atomic Spectrometry*, 2005, 20, 1287-1289.
- [195] Thompson DF, Michopoulos F, Smith CJ, Duckett CJ, Wilkinson RW, Jarvis P, Wilson ID. **Profiling biological samples using ultra performance liquid chromatography-inductively coupled plasma-mass spectrometry (UPLC-ICP-MS) for the determination of phosphorus and sulfur-containing metabolites.** *Molecular Biosystems*, 2011, 7, 1149-1157.
- [196] Evans EH, Wolff JC, Eckers C. **Sulfur-specific detection of impurities in Cimetidine drug substance using liquid chromatography coupled to high resolution inductively coupled plasma mass spectrometry and electrospray mass spectrometry.** *Analytical Chemistry*, 2001, 73, 4722-4728.
- [197] Jiang SJ, Houk RS. **Inductively coupled plasma mass spectrometric detection for phosphorus and sulfur compounds separated by liquid chromatography.** *Spectrochimica Acta Part B: Atomic Spectroscopy*, 1988, 43, 405-411.
- [198] Wind M, Wegener A, Eisenmenger A, Kellner R, Lehmann WD. **Sulfur as the key element for quantitative protein analysis by capillary liquid chromatography coupled to element mass spectrometry.** *Angewandte Chemie International Edition*, 2003, 42, 3425-3427.
- [199] Hann S, Koellensperger G, Obinger C, Furtmüller PG, Stingeder G. **SEC-ICP-DRC and SEC-ICP-SFMS for determination of metal-sulfur ratios in metalloproteins.** *Journal of Analytical Atomic Spectrometry*, 2004, 19, 74-79.
- [200] Hann S, Obinger C, Stingeder G, Paumann M, Furtmüller PG, Koellensperger G. **Studying metal integration in native and recombinant copper proteins by hyphenated ICP-DRC-MS and ESI-TOF-MS: capabilities and limitations of the complementary techniques.** *Journal of Analytical Atomic Spectrometry*, 2006, 21, 1224-1231.

- [201] Zinn N, Krüger R, Leonhard P, Bettmer J. **µLC coupled to ICP-SFMS with post-column isotope dilution analysis of sulfur for absolute protein quantification.** *Analytical and Bioanalytical Chemistry*, 2008, 391, 537-543.
- [202] Schaumlöffel D, Giusti P, Preud'Homme H, Szpunar J, Lobinski R. **Precolumn isotope dilution analysis in nano HPLC-ICP-MS for absolute quantification of sulfur-containing peptides.** *Analytical Chemistry*, 2007, 79, 2859-2868.
- [203] Prange A, Proßrock D. **Chemical labels and natural element tags for the quantitative analysis of bio-molecules.** *Journal of Analytical Atomic Spectrometry*, 2008, 23, 432-459.
- [204] Rappel C, Schaumlöffel D. **The role of sulfur and sulfur isotope dilution analysis in quantitative protein analysis.** *Analytical and Bioanalytical Chemistry*, 2008, 390, 605-615.
- [205] Ogra Y, Kitaguchi T, Suzuki N, Suzuki KT. **In vitro translation with [S-34]-labeled methionine, selenomethionine, and telluromethionine.** *Analytical and Bioanalytical Chemistry*, 2008, 390, 45-51.
- [206] Pfeffer M, Maurer M, Köllensperger G, Hann S, Graf AB, Mattanovich D. **Modeling and measuring intracellular fluxes of secreted recombinant protein in *Pichia pastoris* with a novel 34S labeling procedure.** *Microbial Cell Factories*, 2011, 10:47.
- [207] Meermann B, Sperling M. **Hyphenated techniques as tools for speciation analysis of metal-based pharmaceuticals: developments and applications.** *Analytical and Bioanalytical Chemistry*, 2012, 403, 1501-1522.
- [208] Russo RE, Mao XL, Liu HC, Gonzalez J, Mao SS. **Laser ablation in analytical chemistry – a review.** *Talanta*, 2002, 57, 425-451.
- [209] Mokgalaka NS, Gardea-Torresdey JL. **Laser ablation inductively coupled plasma mass spectrometry: Principles and applications.** *Applied Spectroscopy Reviews*, 2006, 41, 131-150.
- [210] Niemax K. **Laser ablation - Reflections on a very complex technique for solid sampling.** *Fresenius Journal of Analytical Chemistry*, 2001, 370, 332-340.
- [211] Gunther D, Jackson SE, Longerich HP. **Laser ablation and arc/spark solid sample introduction into inductively coupled plasma mass spectrometers.** *Spectrochimica Acta Part B: Atomic Spectroscopy*, 1999, 54, 381-409.
- [212] Durrant SF, Ward NI. **Recent biological and environmental applications of laser ablation inductively coupled plasma mass spectrometry (LA-ICP-MS).** *Journal of Analytical Atomic Spectrometry*, 2005, 20, 821-829.
- [213] Becker JS, Boulyga SF, Becker JS, Pickhardt C, Damoc E, Przybylski M. **Structural identification and quantification of protein phosphorylations after gel electrophoretic separation using Fourier transform ion cyclotron resonance mass spectrometry and laser ablation inductively coupled plasma mass spectrometry.** *International Journal of Mass Spectrometry*, 2003, 228, 985-997.

- [214] Becker JS, Zoriy MV, Dehnhardt M, Pickhardt C, Zilles K. **Copper, zinc, phosphorus and sulfur distribution in thin section of rat brain tissues measured by laser ablation inductively coupled plasma mass spectrometry: possibility for small-size tumor analysis.** *Journal of Analytical Atomic Spectrometry*, 2005, 20, 912-917.
- [215] Günther D, Heinrich CA. **Enhanced sensitivity in laser ablation-ICP mass spectrometry using helium-argon mixtures as aerosol carrier.** *Journal of Analytical Atomic Spectrometry*, 1999, 14, 1363-1368.
- [216] Taylor PDP, de Bièvre P, Walder AJ, Entwistle A. **Validation of the analytical linearity and mass discrimination correction model exhibited by a MC-ICP-MS by means of a set of synthetic uranium isotope mixtures.** *Journal of Analytical Atomic Spectrometry*, 1995, 10, 395-398.
- [217] Nelms SM, Quétel CR, Prohaska T, Vogl J, Taylor PDP. **Evaluation of detector dead time calculation models for ICP-MS.** *Journal of Analytical Atomic Spectrometry*, 2001, 16, 333-338.
- [218] Vanhaecke F, Wannemacker G, Moens L, Dams R, Latkoczy C, Stingeder G. **Dependence of detector dead time on analyte mass number in inductively coupled plasma mass spectrometry.** *Journal of Analytical Atomic Spectrometry*, 1998, 13, 567-571.
- [219] Sariego Muñoz C, Marchante Gayón JM, García Alonso JI, Sanz-Medel A. **Accurate determination of iron, copper and zinc in human serum by isotope dilution analysis using double focusing ICP-MS.** *Journal of Analytical Atomic Spectrometry*, 1999, 14, 1505-1510.
- [220] Ruiz Encinar J, García Alonso JI, Sanz-Medel A, Main S, Turner PJ. **A comparison between quadrupole, double focusing and multicollector ICP-MS instruments.** *Journal of Analytical Atomic Spectrometry*, 2001, 16, 315-321.
- [221] Valles Mota JP, Ruiz Encinar J, Fernández de la Campa MR, García Alonso JI, Sanz-Medel A. **Determination of cadmium in environmental and biological reference materials using isotope dilution analysis with a double focusing ICP-MS: a comparison with quadrupole ICP-MS.** *Journal of Analytical Atomic Spectrometry*, 1999, 14, 1467-1473.
- [222] Meija J. **Mathematical tools in analytical mass spectrometry.** *Analytical and Bioanalytical Chemistry*, 2006, 385, 486-499.
- [223] Hughes PS, Baxter ED. **Beer: Quality, safety and nutritional aspects.** *The Royal Society of Chemistry*, Cambridge, Reino Unido, 2001, capítulos 1, 3 y 5.
- [224] Landaud S, Helinck S, Bonnarne P. **Formation of volatile sulfur compounds and metabolism of methionine and other sulfur compounds in fermented food.** *Applied Microbiology and Biotechnology*, 2008, 77, 1191-1205.
- [225] Hill PG, Smith RM. **Determination of sulphur compounds in beer using headspace solid-phase microextraction and gas chromatographic analysis with pulsed flame photometric detection.** *Journal of Chromatography A*, 2000, 872, 203-213.

- [226] Cortacero-Ramírez S, Hernáinz-Bermúdez de Castro M, Segura-Carretero A, Cruces-Blanco C, Fernández-Gutiérrez A. **Analysis of beer components by capillary electrophoretic methods.** *TRAC – Trends in Analytical Chemistry*, 2003, 22, 440-455.
- [227] Rodushkin I, Axelsson MD. **Application of double focusing sector field ICP-MS for multielemental characterization of human hair and nails. Part II. A study of the inhabitants of northern Sweden.** *Science of the Total Environment*, 2000, 262, 21-36.
- [228] Legrand M, Lam R, Jensen-Fontaine M, Salin ED, Man Chan H. **Direct detection of mercury in single human hair strands by laser ablation inductively coupled plasma mass spectrometry (LA-ICP-MS).** *Journal of Analytical Atomic Spectrometry*, 2004, 19, 1287-1288.
- [229] Legrand M, Lam R, Passos CJ, Mergler D, Salin ED, Chan HM. **Analysis of mercury in sequential micrometer segments of single hair strands of fish-eaters.** *Environmental Science and Technology*, 2007, 41, 593-598.
- [230] Elish E, Karpas Z, Lorber A. **Determination of uranium concentration in a single hair strand by LA-ICP-MS applying continuous and single pulse ablation.** *Journal of Analytical Atomic Spectrometry*, 2007, 22, 540-546.
- [231] Stadlbauer C, Reiter C, Patzak B, Stingeder G, Prohaska T. **History of individuals of the 18th/19th centuries stored in bones, teeth, and hair analyzed by LA-ICP-MS. A step in attempts to confirm the authenticity of Mozart's skull.** *Analytical and Bioanalytical Chemistry*, 2007, 388, 593-602.
- [232] Stadlbauer C, Prohaska T, Reiter C, Knaus A, Stingeder G. **Time-resolved monitoring of heavy-metal intoxication in single hair by laser ablation ICP-DRCMS.** *Analytical and Bioanalytical Chemistry*, 2005, 383, 500-508.
- [233] Sela H, Karpas Z, Zoiry M, Pickhardt C, Becker SJ. **Biomonitoring of hair samples by laser ablation inductively coupled plasma mass spectrometry (LA-ICP-MS).** *International Journal of Mass Spectrometry*, 2007, 261, 199-207.
- [234] Rodushkin I, Axelsson MD. **Application of double focusing sector field ICP-MS for multielemental characterization of human hair and nails. Part I. Analytical methodology.** *Science of the Total Environment*, 2000, 250, 83-100.
- [235] Bermejo-Barrera P, Moreda-Pineiro A, Romero-Barbeito T, Moreda-Pineiro J, Bermejo-Barrera A. **Traces of cadmium in human scalp hair measured by electrothermal atomic absorption spectrometry with the slurry sampling technique.** *Clinical Chemistry*, 1996, 42, 1287-1288.
- [236] Karpas Z, Lorber A, Sela H, Paz-Tal O, Hagag Y, Kurttio P, Salonen L. **Measurement of the $^{234}\text{U}/^{238}\text{U}$ ratio by MC-ICPMS in drinking water, hair, nails, and urine as an indicator of uranium exposure source.** *Health Physics*, 2005, 89, 315-321.
- [237] Bol R, Marsh J, Heaton THE. **Multiple stable isotope (^{18}O , ^{13}C , ^{15}N and ^{34}S) analysis of human hair to identify the recent migrants in a rural community in SW England.** *Rapid Communications in Mass Spectrometry*, 2007, 21, 2951-2954.

- [238] Macko SA, Engel MH, Andrusevich V, Lubec G, O'Connell TC, Hedges RE. **Documenting the diet in ancient human populations through stable isotope analysis of hair.** *Philosophical Transactions of the Royal Society of London. Series B, Biological Sciences*, 1999, 354, 65-75.
- [239] Khalique A, Ahmad S, Anjum T, Jaffar M, Shah MH, Shaheen N, Tariq SR, Manzoor S. **A comparative study based on gender and age dependence of selected metals in scalp hair.** *Environmental Monitoring Assessment*, 2005, 104, 45-57.
- [240] Fraser I, Meier-Augenstein W. **Stable ^2H isotope analysis of modern-day human hair and nails can aid forensic human identification.** *Rapid Communications in Mass Spectrometry*, 2007, 21, 3279-3285.
- [241] Fraser I, Meier-Augenstein W, Kalin RM. **The role of stable isotopes in human identification: a longitudinal study into the variability of isotopic signals in human hair and nails.** *Rapid Communications in Mass Spectrometry*, 2006, 20, 1109-1116.
- [242] Petzke KJ, Feist T, Fleig WE, Metges CC. **Nitrogen isotopic composition in hair protein is different in liver cirrhotic patients.** *Rapid Communications in Mass Spectrometry*, 2006, 20, 2973-2978.
- [243] O'Connell TC, Hedges REM. **Investigations into the effect of diet on modern human hair isotopic values.** *American Journal of Physical Anthropology*, 1999, 108, 409-425.
- [244] Petzke KJ, Boeing H, Metges CC. **Choice of dietary protein of vegetarians and omnivores is reflected in their hair protein ^{13}C and ^{15}N abundance.** *Rapid Communications in Mass Spectrometry*, 2005, 19, 1392-1400.
- [245] Bol R, Pflieger C. **Stable isotope (^{13}C , ^{15}N and ^{34}S) analysis of the hair of modern humans and their domestic animals.** *Rapid Communications in Mass Spectrometry*, 2002, 16, 2195-2200.
- [246] Ehleringer JR, Bowen GJ, Chesson LA, West AG, Podlesak DW, Cerling TE. **Hydrogen and oxygen isotope ratios in human hair are related to geography.** *Proceedings of the National Academy of Sciences of the United States of America*, 2008, 105, 2788-2793.
- [247] Robbins CR. **Chemical and physical behaviour of human hair.** *Springer, 4th Edition, New York*, 2002.
- [248] Barnett JA. **Beginnings of microbiology and biochemistry: the contribution of yeast research.** *Microbiology*, 2003, 149, 557-567.
- [249] Svantesson E, Pettersson J, Markides KE. **The use of inorganic elemental standards in the quantification of proteins and biomolecular compounds by inductively coupled plasma mass spectrometry.** *Journal of Analytical Atomic Spectrometry*, 2002, 17, 491-496.
- [250] Cecchi T. **Ion pairing chromatography.** *Critical Reviews in Analytical Chemistry*, 2008, 38, 161-213.

- [251] Quian WJ, Jacobs JM, Liu T, Camp II DG, Smith RD. **Advances and challenges in liquid chromatography - mass spectrometry - based proteomics profiling for clinical applications.** *Molecular and Cellular Proteomics*, 2006, 5, 1727-1744.
- [252] Rodríguez-Castrillón JA, Moldovan M, García Alonso JI, Lucena JJ, García-Tomé ML, Hernández-Apaolaza L. **Isotope pattern deconvolution as a tool to study iron metabolism in plants.** *Analytical and Bioanalytical Chemistry*, 2008, 390, 579-590.
- [253] González Iglesias H, Fernández Sanchez ML, Rodríguez-Castrillón JA, García Alonso JI, López Sastre J, Sanz-Medel A. **Enriched stable isotopes and isotope pattern deconvolution for quantitative speciation of endogenous and exogenous selenium in rat urine by HPLC-ICP-MS.** *Journal of Analytical Atomic Spectrometry*, 2009, 24, 460-468.
- [254] Villar-Garea A, Griese M, Imhof A. **Biomarker discovery from body fluids using mass spectrometry.** *Journal of Chromatography B*, 2007, 849, 105-114.
- [255] Apweiler R, Aslanidis C, Deufel T, Gerstner A, Hansen J, Hochstrasser D, *et al.* **Approaching clinical proteomics: current state and future fields of application in fluid proteomics.** *Clinical Chemistry and Laboratory Medicine*, 2009, 47, 724-744.
- [256] Silberring J, Ciborowski P. **Biomarker discovery and clinical proteomics.** *TRAC-Trends in Analytical Chemistry*, 2010, 29, 128-140.
- [257] Shau H, Chandler GS, Whitelegge JP, Gornbein JA, Faull KF, Chang HR. **Proteomic profiling of cancer biomarkers.** *Briefings in functional genomics and proteomics*, 2003, 2, 147-158.
- [258] Wittke S, Fliser D, Haubitz M, Bartel S, Krebs R, Hausadel F, Hillmann M, Golovko I, Koester P, Haller H, Kaiser T, Mischak H, Weissinger EM. **Determination of peptides and proteins in human urine with capillary electrophoresis – mass spectrometry, a suitable tool for the establishment of new diagnostic markers.** *Journal of Chromatography A*, 2003, 1013, 173-181.
- [259] Haubitz M, Wittke S, Weissinger EM, Walden M, Rupprecht HD, Floege J, Haller H, Mischak H. **Urine protein patterns can serve as diagnostic tools in patients with IgA nephropathy.** *Kidney International*, 2005, 67, 2313-2320.
- [260] Theodorescu D, Wittke S, Ross MM, Walden M, Conaway M, Just I, Mischak H, Frierson HF. **Discovery and validation of new protein biomarkers for urothelial cancer: a prospective analysis.** *Lancet Oncology*, 2006, 7, 230-240.
- [261] Kaiser T, Kamal H, Rank A, Kolb HJ, Holler E, Ganser A, Hertenstein B, Mischak H, Weissinger EM. **Proteomics applied to the clinical follow-up of patients after allogeneic hematopoietic stem cell transplantation.** *Blood*, 2004, 104, 340-349.
- [262] Tirumalai RS, Chan KC, Prieto DA, Issaq HJ, Conrads TP, Veenstra TD. **Characterisation of the low molecular weight human serum proteome.** *Molecular and Cellular Proteomics*, 2003, 2, 1096-1103.
- [263] Shou M, Conrads TP, Veenstra TD. **Proteomic approaches to biomarker detection.** *Briefings in Functional Genomics and Proteomics*, 2005, 4, 69-75.

- [264] Luque-Garcia JL, Neubert TA. **Sample preparation for serum/plasma profiling and biomarker identification by mass spectrometry.** *Journal of Chromatography A*, 2007, 1153, 259-276.
- [265] Martorella A, Robbins R. **Serum peptide profiling: identifying novel cancer biomarkers for early disease detection.** *Acta Biomedica*, 2007, 78, 123-128.
- [266] Linke T, Doraiswamy S, Harrison EH. **Rat plasma proteomics: Effects of abundant protein depletion on proteomic analysis.** *Journal of Chromatography B*, 2007, 849, 273-281.
- [267] Khan A, Packer NH. **Simple urinary sample preparation for proteomic analysis.** *Journal of Proteome Research*, 2006, 5, 2824-2838.
- [268] Magagnotti C, Fermo I, Carletti RM, Ferrari M, Bachi A. **Comparison of different depletion strategies for improving resolution of the human urine proteome.** *Clinical Chemistry and Laboratory Medicine*, 2010, 48, 531-535.
- [269] Hernández F, Sancho JV, Barceló D. **Mass spectrometry: fourth conference of the Spanish Society of Mass Spectrometry (SEEM).** *Analytical and Bioanalytical Chemistry*, 2010, 397, 2761-2762.